AD-A268 344

REPORT DOCUMENTATION PAGE

Form Approved
OBM No. 0704-0188

1. Agency Use Only *(Leave blank)*.	2. Report Date.	3. Report Type and Dates Covered.
	March 1993	Final

4. Title and Subtitle.
Forecasters Handbook for the Bering Sea, Aleutian Islands, and Gulf of Alaska

5. Funding Numbers.

Program Element No.	O&M,N
Project No	---
Task No.	---
Accession No.	DN656794
Work Unit No	O&M,N-1

6. Author(s).
R.W. Fett, R.E. Englebretson*, D.C. Perryman

7. Performing Organization Name(s) and Address(es).
Naval Research Laboratory
Marine Meteorology Division
Monterey, CA 93943-5006

8. Performing Organization Report Number.
NRL/PU/7541--93-0006

9. Sponsoring/Monitoring Agency Name(s) and Address(es).
Naval Oceanography Command
Stennis Space Center, MS 39529-5000

10. Sponsoring/Monitoring Agency Report Number.

11. Supplementary Notes.
*Authors' affiliation: Science Applications International Corp., Monterey, CA 93940

12a. Distribution/Availability Statement.
Approved for public release; distribution is unlimited.

12b. Distribution Code.

13. Abstract *(Maximum 200 words).*

Weather conditions in the Bering Sea, Aleutian Islands, and Gulf of Alaska region are described. Rules of thumb and other quick reference materials are provided for use by operational forecasters. Background information is included to enhance understanding of regional conditions. Case studies utilizing satellite imagery are provided to examine a wide variety of regional weather phenomena. Also included are relevant portions of the previously published "Forecasters Handbook for the Arctic" (NEPRF TR 89-12, October 1989, DTIC AD A238424), which did not address the Bering/Aleutian region because of its size and complexity and because this present stand-alone volume was intended.

93-19154

14. Subject Terms.
Adak, Alaska, Aleutian Islands, Attu, Bering Sea, Bering Strait, Gulf of Alaska, pack ice, polar lows, Unimak

15. Number of Pages.
302

16. Price Code.

17. Security Classification of Report.	18. Security Classification of This Page.	19. Security Classification of Abstract.	20. Limitation of Abstract.
UNCLASSIFIED	UNCLASSIFIED	UNCLASSIFIED	Same as report

Contents

FOREWORD

The Forecasters Handbook for the Bering Sea, Aleutian Islands, and Gulf of Alaska is one of a series of regional forecaster handbooks produced by the Naval Research Laboratory, Marine Meteorology Division (formerly Naval Oceanographic and Atmospheric Research Laboratory (NOARL), Atmospheric Directorate). The publication has been developed in response to a request by the Commander in Chief, U.S. Pacific Fleet (CINCPACFLT) and validated by the Chief of Naval Operations (OP-096) as PACMET 87-16. The objective of this publication is to provide fleet forecasters with a single, comprehensive reference guide on environmental conditions in the Bering Sea-Aleutians Islands region. Particular effort has been made to provide weather satellite examples and numerical model forecasts of environmental effects over the region and to relate these to known or suggested analyses and forecast rules. This handbook should be regarded as a flexible document capable of being updated or revised based on new data, concepts, or understandings. Fleet users having direct experience through operations in the region are urged to submit suggestions for revisions and/or additions so that this handbook can be updated as required for increased usefulness.

ACKNOWLEDGMENTS

The support of the sponsors, Naval Oceanography Command, Stennis Space Center, Mississippi, and Fleet Numerical Oceanography Center, Monterey, California (Program Element O&M, N), is gratefully acknowledged. Several reviewers in the field contributed many insightful comments to help us ensure a final version as error free and accurate as possible. Many thanks to those who participated in the draft review.

RECORD OF CHANGES

CHANGE NUMBER	DATE OF CHANGE	DATE ENTERED	PAGE NUMBER	ENTERED BY

1. GENERAL INTRODUCTION

The Armed Forces of the United States have a long history of operation in the Bering Sea, Aleutian Islands, and Gulf of Alaska region. In particular, during the final decades of the 20th century, the U.S. Navy Third Fleet conducted increased land, sea, and air operations over the entire area. The diversity and harshness of observed environmental conditions make the Bering Sea an extremely difficult operating area. Known as the "Land of the Smoky Sea" by the Aleutian natives, this is a generally treeless region typified in its weather by persistent fog and intermittent storms, often exceeding hurricane intensity.

1.1 Objective

Individual Navy and Air Force stations in the Aleutian Islands have published studies, guides, and even handbooks for individual locations. An excellent "Climatological Guide to Alaskan Weather" was published by the Air Force (Grubbs and McCollum, 1968). The objectives of this handbook are twofold: (1) to draw upon, examine, and present pertinent information contained in the above-mentioned studies integrated into one volume; and (2) to update the material presented as much as possible through correlation of the earlier results with high quality satellite data, conventional data, and numerical forecasts.

1.2 Approach

The effort to develop this handbook involved three tasks:

- Obtaining and review of existing publications concerning weather analysis and forecast procedures over the Bering Sea, Aleutian Islands, and Gulf of Alaska.
- Review of suggested procedures through correlation with satellite data, conventional data, and numerical model output.
- Assembling of pertinent information in a high quality volume dedicated to the needs of the present-day Fleet forecaster operating in the Bering Sea, Aleutian Islands, and Gulf of Alaska region.

Manuscript approved March 9, 1993.

1.3 Organization

This handbook first provides general information concerning the physical characteristics and climatology of the region. General analysis and forecasting rules are then presented in a series of studies in which weather satellite data, conventional analysis, and numerical model forecasts play a prominent role in establishing validity of concept. Finally, unique aspects associated with ship and aircraft icing, refractive effects, and numerical model forecast errors are described.

2. PHYSICAL CHARACTERISTICS OF THE REGION

This handbook is designed to provide weather analysis and forecast guidance concentrating on the region between latitudes 50 to 60 °N and 150 °W westward to and including the Kamchatka Peninsula. Figure 2-1 shows the region in a larger perspective. The larger perspective is important to consider since many of the storms affecting the Aleutian Islands and Bering Sea region originate far to the southwest near Japan. These storms are further influenced in their movement and intensity changes by the synoptic pattern to the east, from Hawaii (near 20 °N, 155 °W) to the Gulf of Alaska. It is not unusual for a storm center over 1000 n mi (1850 km) away, just east of Japan, to move over the Aleutians and dominate weather conditions in the Bering Sea within a 24- to 36-hr period.

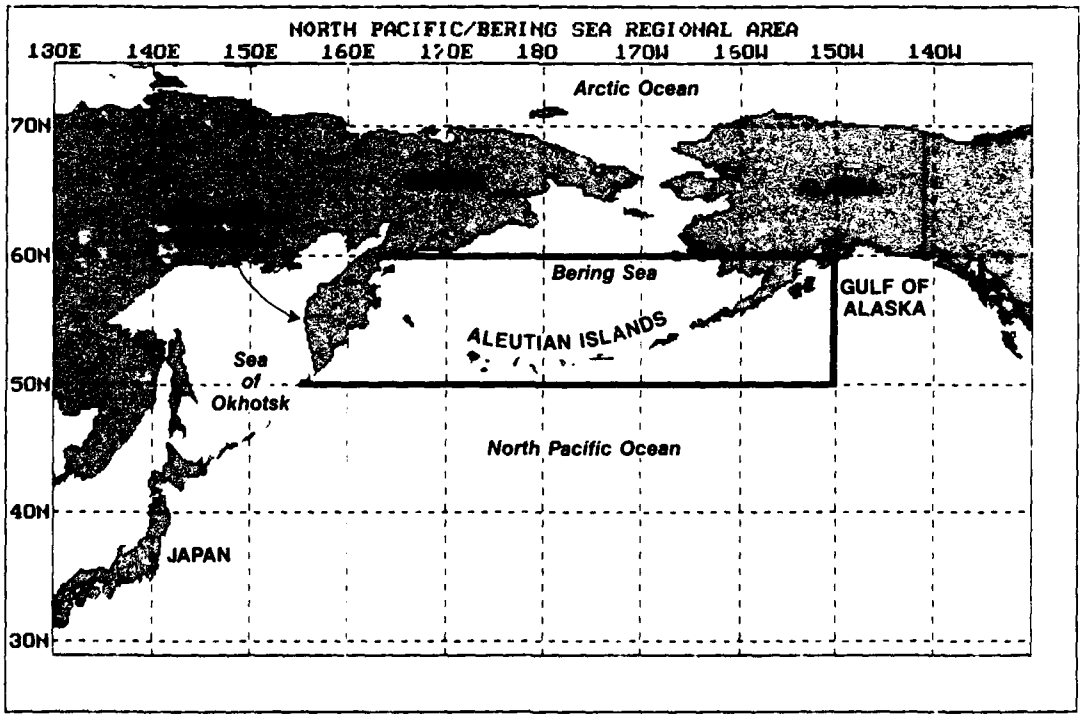

Figure 2-1. Locator chart. North Pacific and Bering Sea regional area.

2.1 Bering Sea and Aleutian Islands

The Aleutian Islands extend 1700 n mi (3150 km) westward from the Alaskan Peninsula in a saucer-shaped pattern. The Aleutian chain approaches within 500 n mi (925 km) of the Kamchatka Peninsula at Attu (near 173 °E), the westernmost island (Fig. 2-2). In so doing the islands separate the Bering Sea to the north from the North Pacific Ocean to the south.

2.1.1 Geography

First discovered by Vitus Bering in 1741, the Aleutian Islands were inhabited by a native population estimated at 25,000. Mass murder and enslavement followed. By 1867, when the Aleutians became part of the United States with the purchase of Alaska, fewer than 2500 native Aleuts remained. This number was further reduced through flu and smallpox epidemics, reaching a low of 1400 at the commencement of World War II.

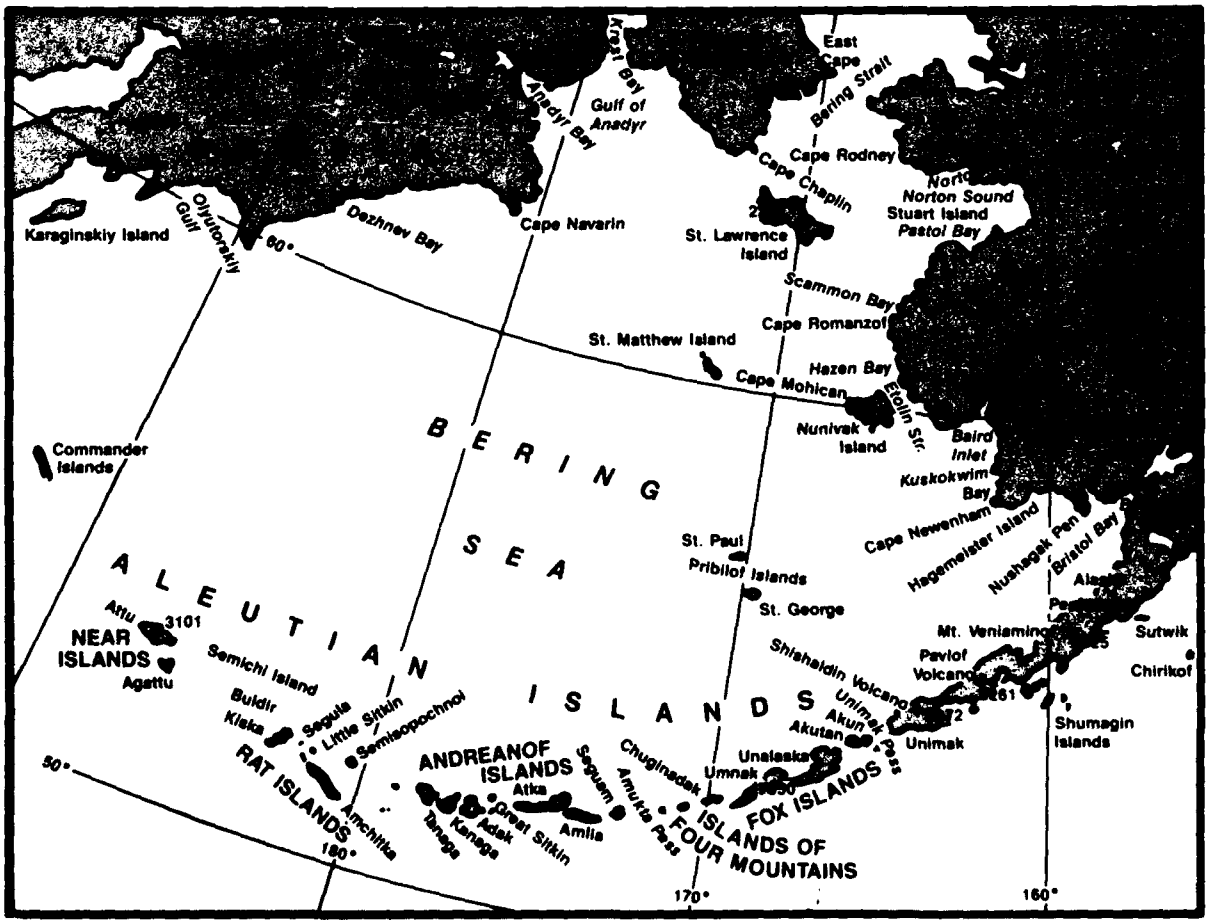

Figure 2-2. Locator chart. Bering Sea and Aleutian Islands.

Military interest in the islands was firmly established by 1940 when the U.S. Navy built a base at Dutch Harbor on Unalaska Island, one of the few good harbors (aside from Adak) in the entire chain. Most of the other islands are surrounded by reefs that make nearby navigation hazardous. The islands are of great strategic interest, made clear on June 3, 1942, when the Japanese bombed Dutch Harbor and followed this with the occupation of Attu and Kiska.

The United States counterattacked, regaining Attu and control of the Aleutians in 1943, and built additional bases on Umnak (169 °W), Atka (174.5 °W), Amchitka (179 °E), and Shemya (Semichi Islands) (174 °E). Shemya Air Force Base and Adak Naval Station remain active today. A Coast Guard station is also active on Kodiak Island. Other bases have converted from military to civilian use over the years.

2.1.2 Topography

The topography of much of the land areas related to this handbook is mountainous and contains some active volcanoes. The ground throughout the Aleutians beyond the Alaskan Peninsula is spongy and marshlike during warm periods and completely frozen during winter. Layers of volcanic ash are usually prevalent below the surface. Very few trees exist except for "Adak National Forest" (a small clump of manually maintained trees). Surface vegetation is abundant, however, and hundreds of varieties of flowers provide a colorful display in summer.

The Fox Islands (Fig. 2-3) extend southwestward starting with Unimak near 164 °W, to Umnak near 169 °W. The Fox Islands received their name from Russian fur traders

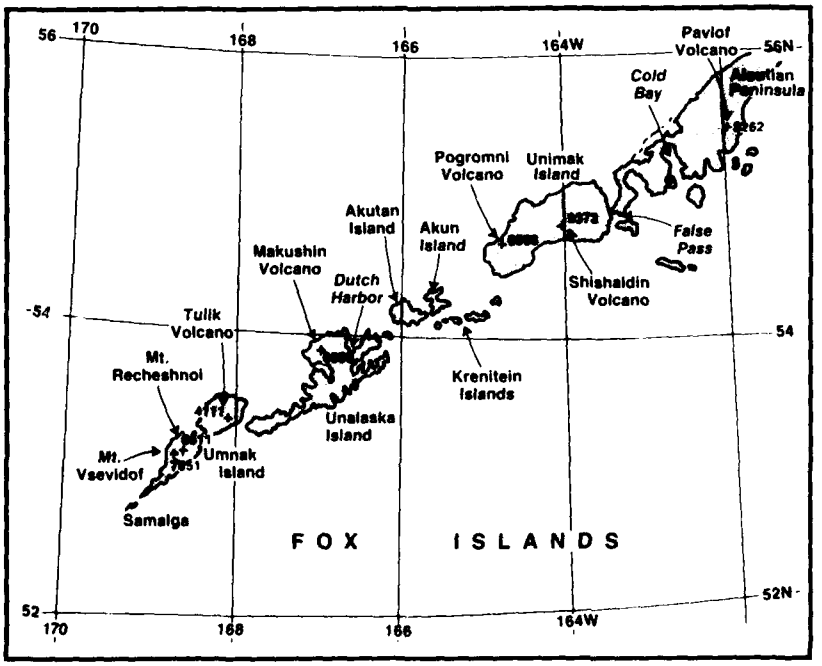

Figure 2-3. Locator chart. Fox Islands.

because of the large fox population of earlier years. The group is distinguished in topography by the highest Aleutian volcano, Shishaldin on Unimak Island, which extends to an elevation of 9372 ft (2857 m). Pogromni volcano (6568 ft or 2002 m) on the southwestern end of the island is another prominent feature. Makushin volcano (6680 ft or 2036 m) is found on Unalaska Island, near Dutch Harbor. Another volcano, Tulik (4111 ft or 1253 m), is found on Uninak, the westernmost island of the Fox group. Mt. Recheshnoi (6511 ft or 1985 m) and Mt. Vsevidof (7051 ft or 2149 m) are also located on Umnak Island.

These topographic features are often apparent in weather satellite images because of their snow-covered domes and high elevation. Figure 2-4 shows a Defense Meteorological Satellite Program (DMSP) infrared example on 8 January 1990 at 0445 GMT. In this image the cold peaks of Veniaminof volcano and Pavlof volcano are clearly visible. Shishaldin volcano is located along a flat east-west oriented ridge that appears as a similarly-oriented narrow white dash in the DMSP image. Gravity waves in the form of "ship wake" patterns are apparent in the region, generated by turbulent effects induced by the topography. The "ship wake" pattern implies a well-mixed lower level with stability maximized at the inversion interface near cloud top level (see NTAG Vol. 1, Sec. 2C).

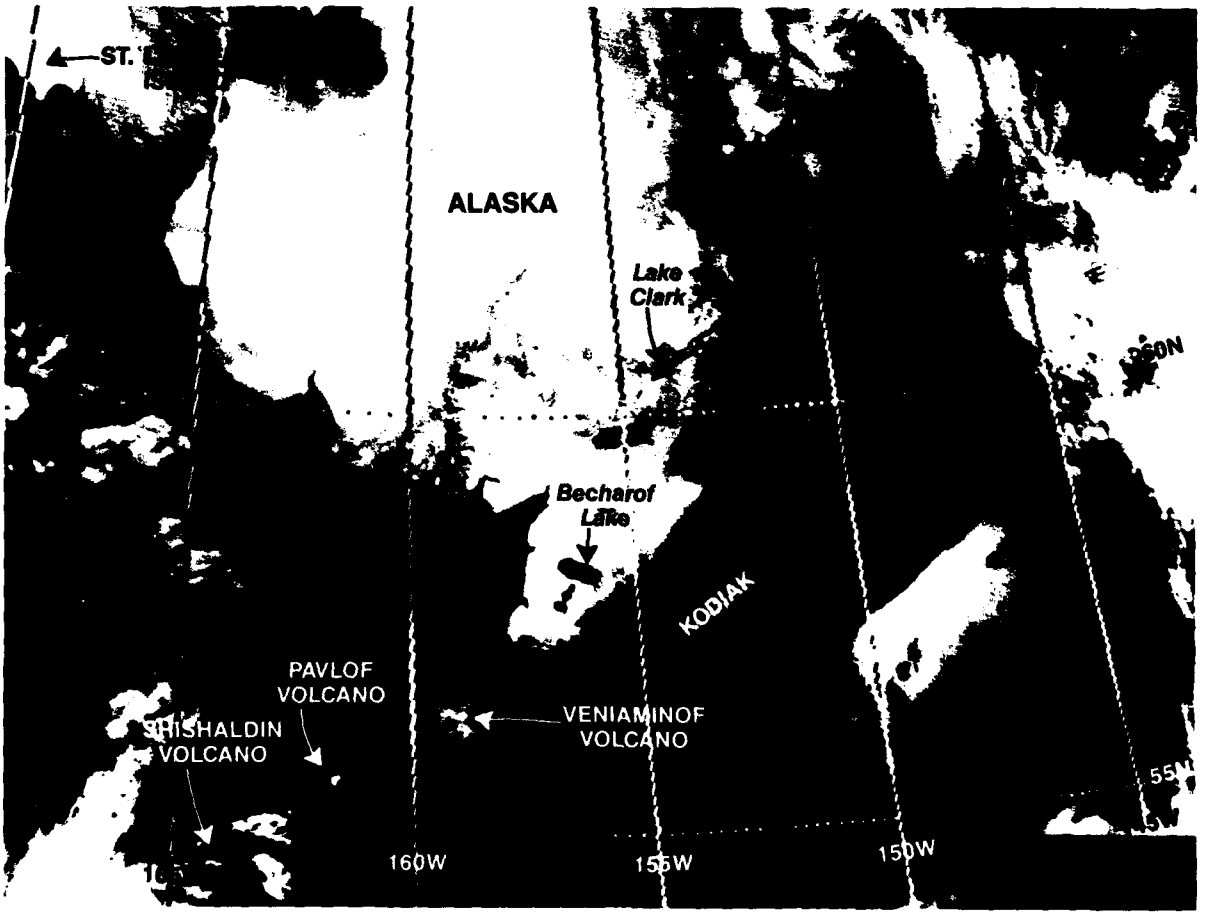

Figure 2-4. DMSP infrared imagery 0445 GMT 8 January 1990.

Figure 2-5 shows the next three groups of islands further west—the islands of the Four Mountains, the Andreanof Islands, and the Delarof Islands. The Islands of the Four Mountains consist of a small group of five islands clustered near 170°W. The tallest of the mountains in this group lies on Chuginadak Island and has an elevation of 5675 ft (1730 m). Yunaska, Chugulak, and Seguam Islands, unnamed as a group, then lead westward to the Andreanof Islands. These islands were explored by a Russian named Andrean Tolstykh in the 1760s and were named after him based on the account he wrote of his explorations. The group includes the island of Adak, present site of a U.S. Navy air strip and port facility (Adak Naval Station). Mount Moffett (3917 ft or 1194 m) is the highest mountain on the island, but mountainous terrain of lesser elevation still acts to provide a blocking action to moderate wind flow from the south. Topography is a key element and influences all forecasts at Adak and, indeed, all locations within the Aleutian chain.

The two final groups of islands in the Aleutian chain are the Rat Islands and the Near Islands. These are shown in Fig. 2-6.

The Rat Islands, so named because of a large rodent population, include Semisopochnoi, Amchitka, Kiska, and Buldir, which lies at the western extremity. Amchitka has a weather service office that provides hourly surface observations and radiosonde data on a routine basis. These observations are monitored very carefully by forecasters at Adak since Amchitka's present weather often becomes Adak's present weather in a matter of a few hours. Problems in applying this concept occur, however, during blocking situations when flow over the Adak-Amchitka area becomes more meridional rather than zonal. In such

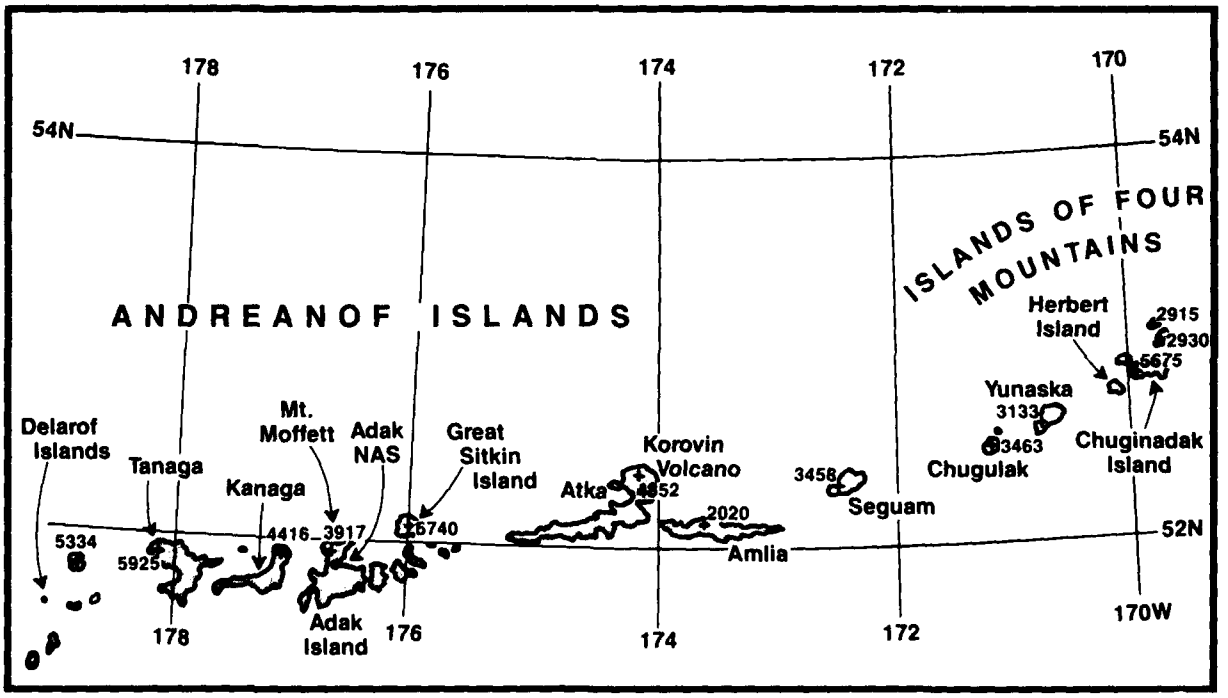

Figure 2-5. Locator chart. Islands of the Four Mountains and Andreanof Islands.

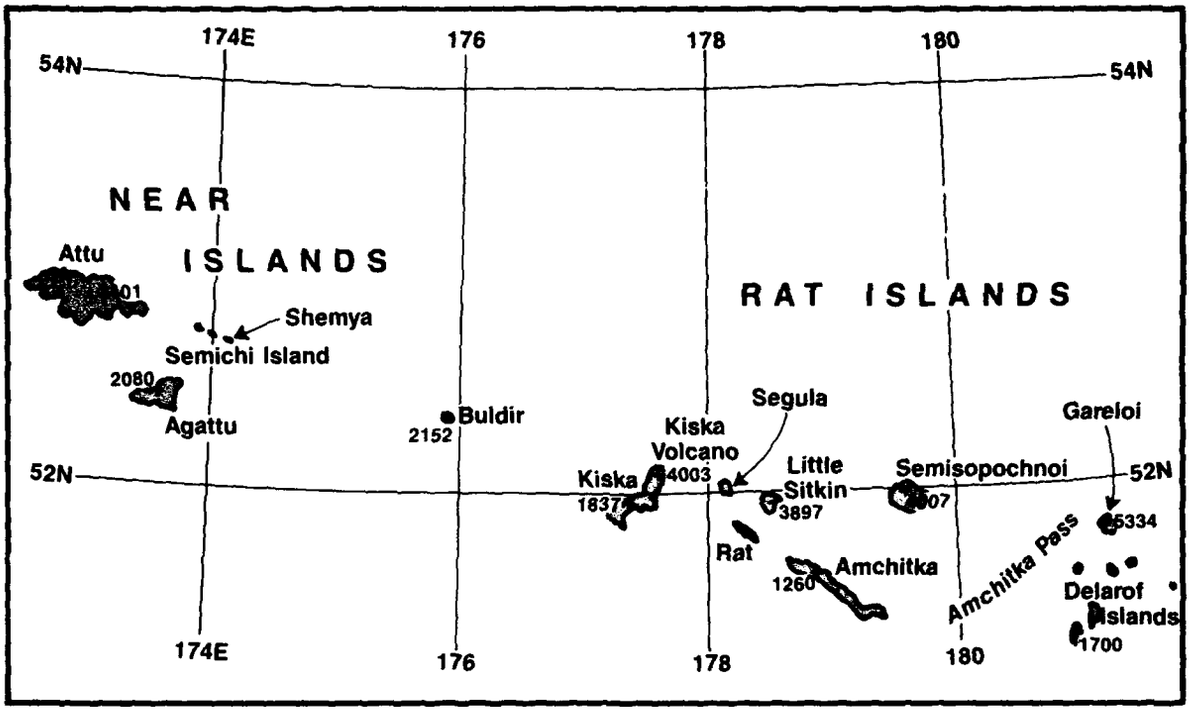

Figure 2-6. Locator chart. Rat Islands and Near Islands.

circumstances the north-south-oriented frontal zone may stall in the region or even slip northward and dissipate. Amchitka's weather and winds at such times cannot be reliably forecast for Adak.

The Kiska volcano (4003 ft or 1220 m) is a prominent topographical feature of the area. Other peaks of about equal height exist on Little Sitkin Island (3897 ft or 1188 m) and on Semisopochnoi Island (4007 ft or 1221 m). Under northerly or southerly flow through the area funneling effects will considerably enhance wind speed in the passages between the mountains, especially when this flow is confined below a strong low-level inversion.

The Near Islands consist of the Semichi group, which includes Attu, Agattu, and Shemya, the site of an U.S. Air Force Base. The group was named because of the relative "nearness" of these islands to the Russian homeland at the time of discovery. The Semichi group is quite flat; however, peaks of 3101 ft (945 m) and 2080 ft (634 m) exist on Attu and Agattu, respectively. The Russian Islands to the west (Commander Islands), although a logical extension of the Aleutian chain, are omitted from this discussion.

2.1.3 Bathymetry

The bathymetry of the Bering Sea and Aleutian Islands region is shown in Fig. 2-7. The Aleutian trench, with depths in excess of approximately 20,000 ft (6000 m), runs parallel to the islands on the south side and continues in its eastward extremity into the northern portion of the Gulf of Alaska. Figure 2-8 shows some of the region's more prominent submarine and physiographic features.

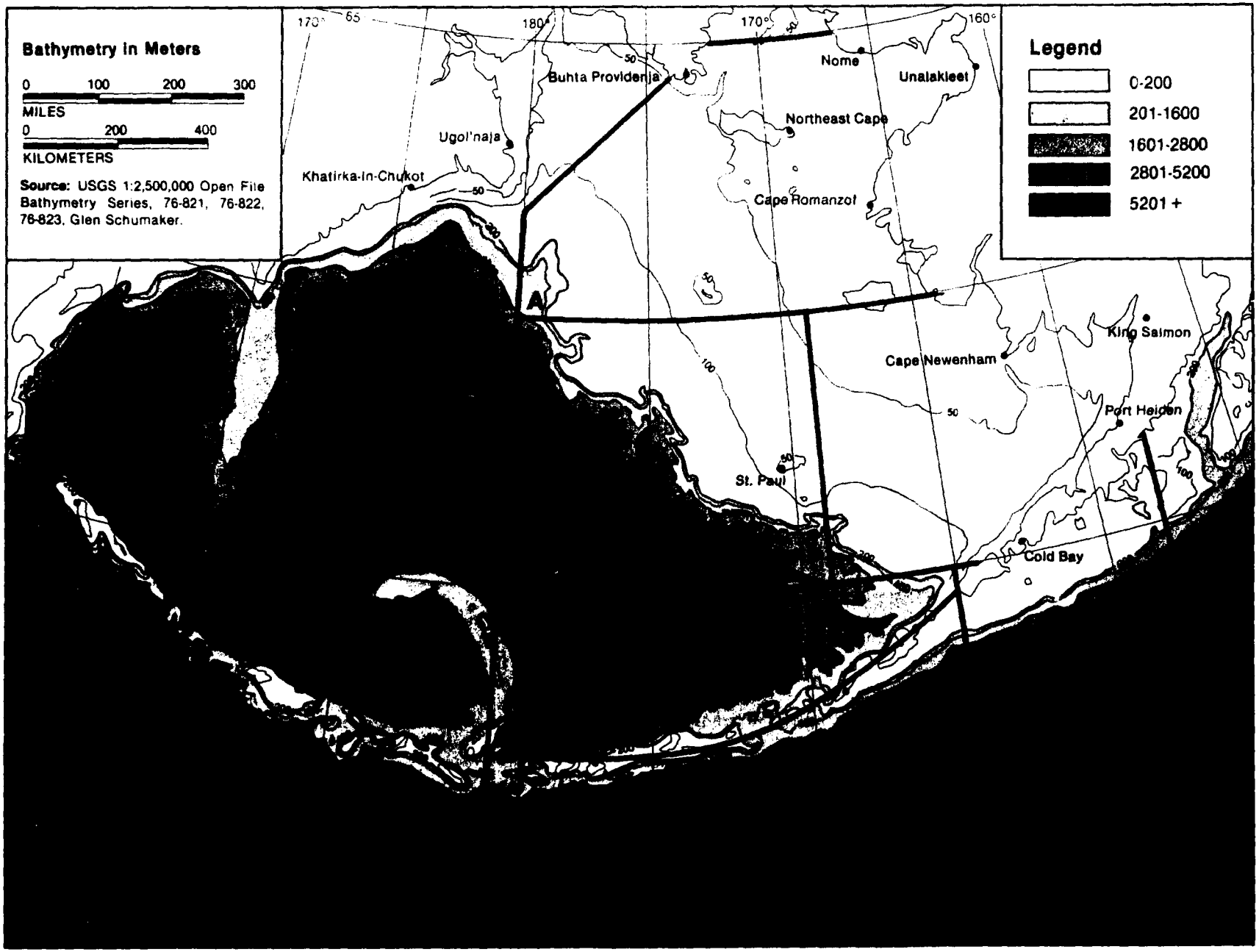

Figure 2-7. Bathymetry of the Bering Sea and Aleutian Island area (Brower et al., 1988).

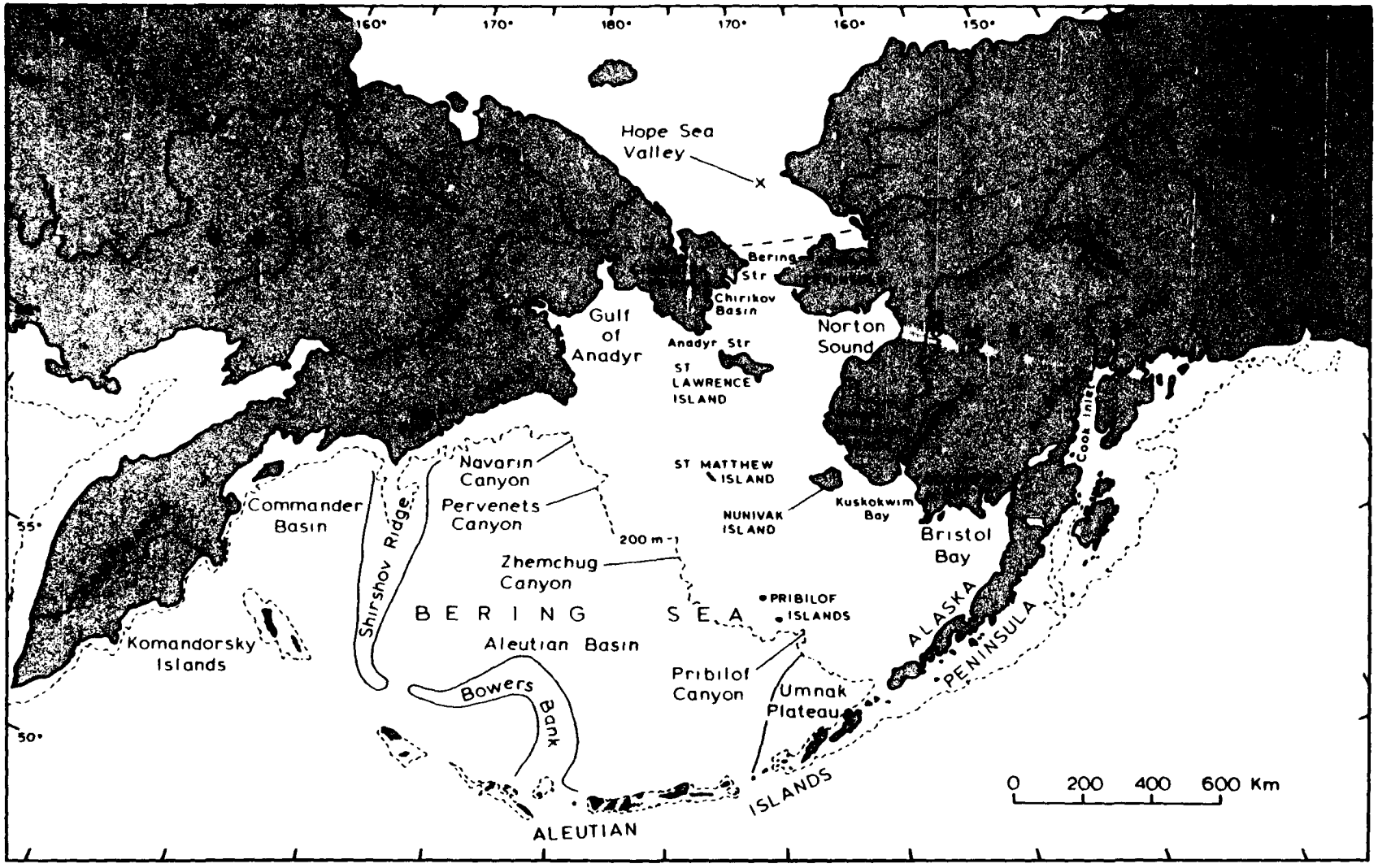

Figure 2-8. Submarine and continental physiographic features of the Bering Sea region (Nelson et al., 1974).

In general, the depth and area of the major openings in the Aleutian-Commander island chain are not large. Of the 39 openings in this chain only 14 have an area greater than 0.3 n mi² (1 km²) and a sill depth of at least 655 ft (200 m). Table 2-1 provides the statistics of these 14 passes on straits. The water is shallowest from the Alaskan Peninsula westward to Amukta Pass near 170 °W (Fig. 2-2). Amchitka Pass near 179 °E is the only pass east of 172 °E having a water depth exceeding 3280 ft (1000 m).

Figure 2-9 is a schematic showing a vertical section of the island passes and straits. From this schematic one can see that the Commander-Near Island Strait and the Kamchatka Strait are the major deep-water passes of the Aleutian chain.

TABLE 2-1. DEPTH AND AREA OF THE MAJOR OPENINGS IN THE ALEUTIAN-COMMANDER ISLAND CHAIN (FAVORITE, 1974)

General Opening	Pass/Strait	Depth (m)	Area (km²)	
East Aleutian group	Samalga	200	3.9	
	Cuginadak	210	1.0	
	Herbert	275	4.8	
	Yunaska	457	6.6	
	Amukta	430	19.3	
	Seguam	165	2.1	37.7
Central Aleutian group	Tanaga	235	3.6	
	Amchitaka	1155	45.7	49.3
West Aleutian	Kiska	110	6.8	
	Buldir	640	28.0	
	Semichi	105	1.7	36.5
Commander-Near St.	Near	2000	239.0	
	Commander	105	3.5	242.5
Kamchatka Strait		4420		335.3
			Total area	701.3

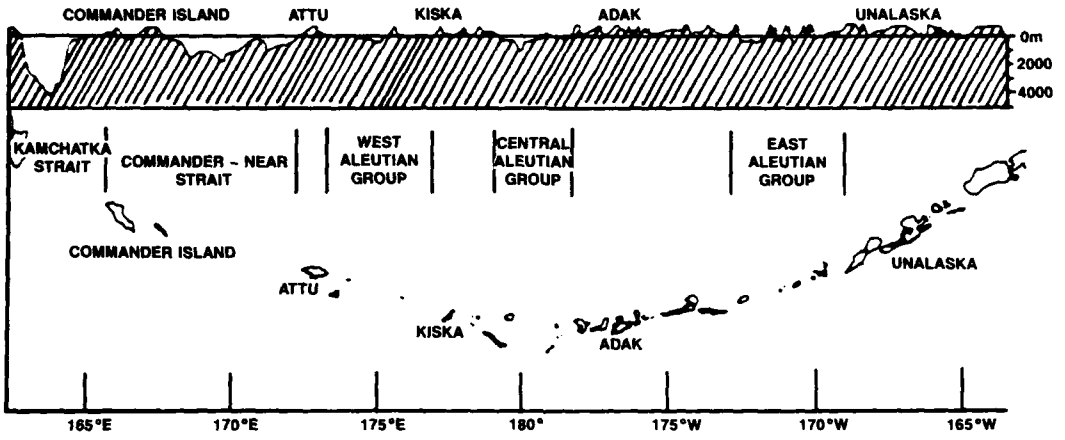

Figure 2-9. Aleutian-Commander island arc and a schematic vertical section of island passes and straits (Favorite, 1974).

2.1.4 Currents

It was originally thought, based on data from the NORPAC (Northern Pacific) Expedition in 1955, that the primary flow of water into the Bering Sea was through Unimak Pass (Fig. 2-2). This source is even suggested in the work by Brower et al. (1988), which provides ocean and atmospheric summaries for the region. However, this viewpoint has been challenged as a physical impossibility since the sill depth for Unimak Pass is only 200 ft or 60 m (Favorite, 1974), which is not of sufficient depth, based on ocean current strength, to permit a large volume of water to enter the region. Actual flow through the various passes in the Aleutian arc is known to be so variable that both north and south flows have been found simultaneously within a single pass.

In such circumstances data are generally inadequate to determine net flow in either direction. The best estimate at the present time is that no net annual exchange occurs through the eastern Aleutian passes, and the westward flowing Alaska Stream provides the major impetus with flow entering the Bering Sea through Amchitka Pass and the Commander-Near Strait. Figure 2-10 shows a diagram of the suggested flow pattern and water mass characterization. Note the clockwise eddies bringing southerly flow through Amchitka Pass near 180° and through the Commander-Near Island pass near 170°E. Major outflow occurs far to the west in the East Kamchatka Current.

The surface circulation pattern is still open to various interpretations because of conflicting results from various data sources. Summer and winter surface circulation patterns are shown in Figs. 2-11 and 2-12, respectively (Brower et al., 1988).

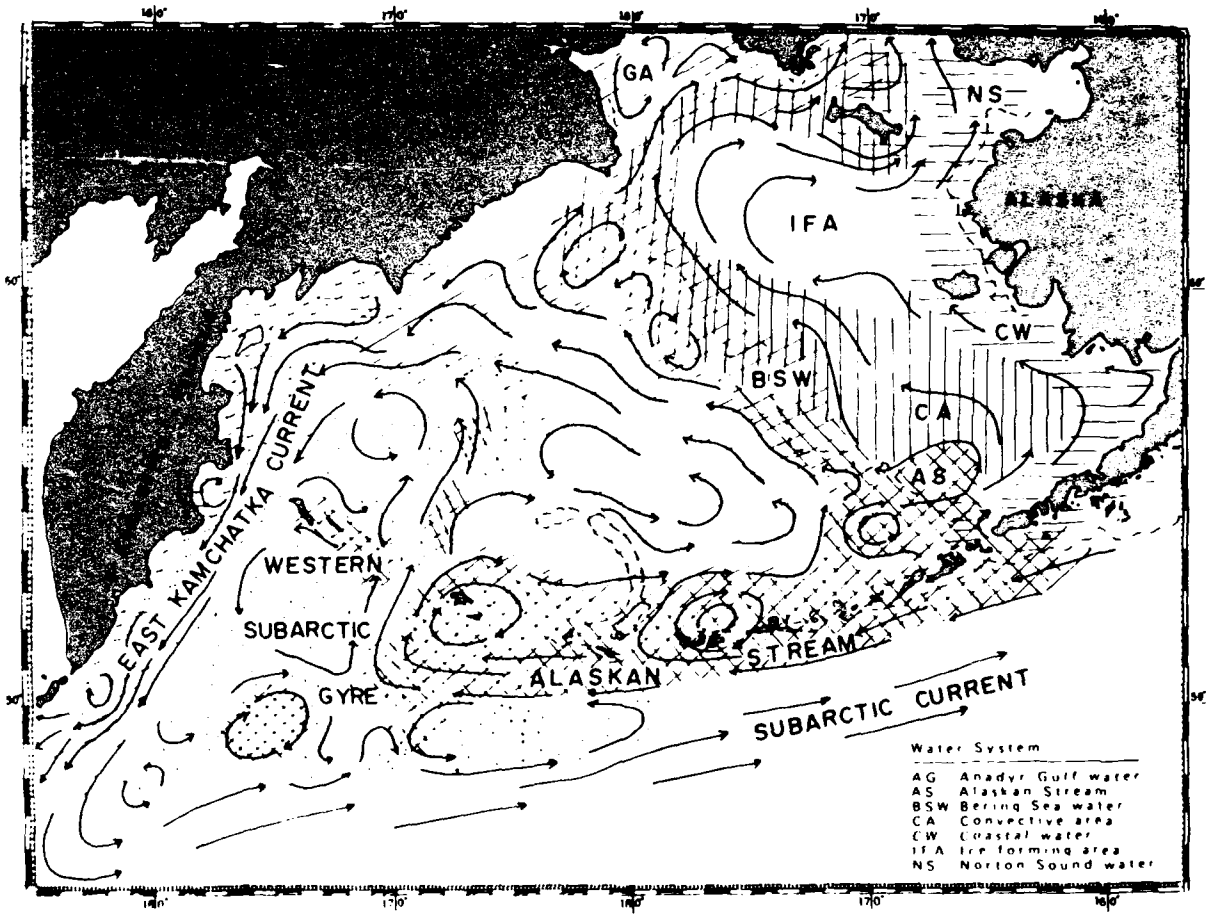

Figure 2-10. Schematic diagram of circulation and extent of water masses in the Bering Sea and northwestern Pacific Ocean (Takenouti and Ohtani, 1974).

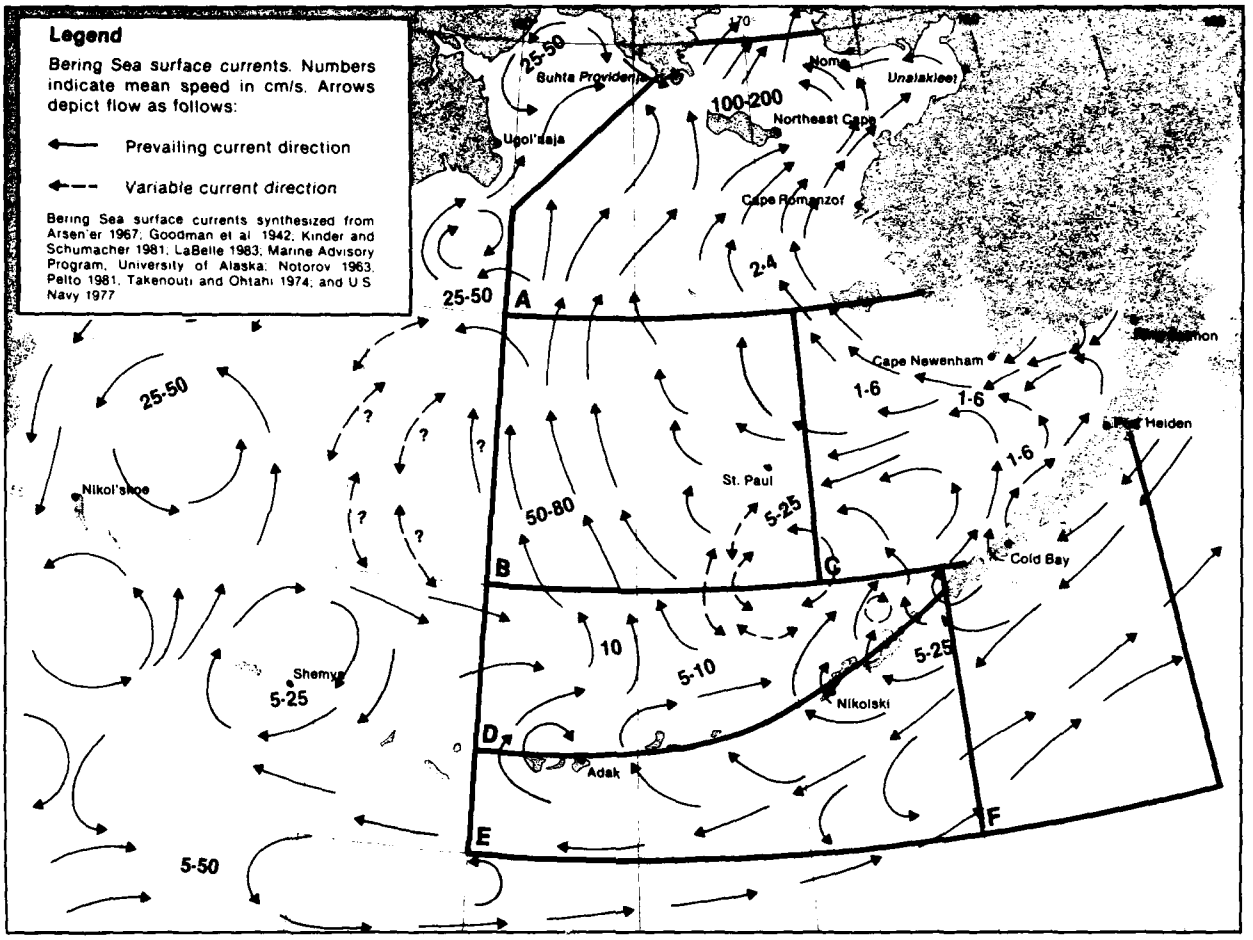

Figure 2-11. Bering Sea currents—summer (Brower et al., 1988).

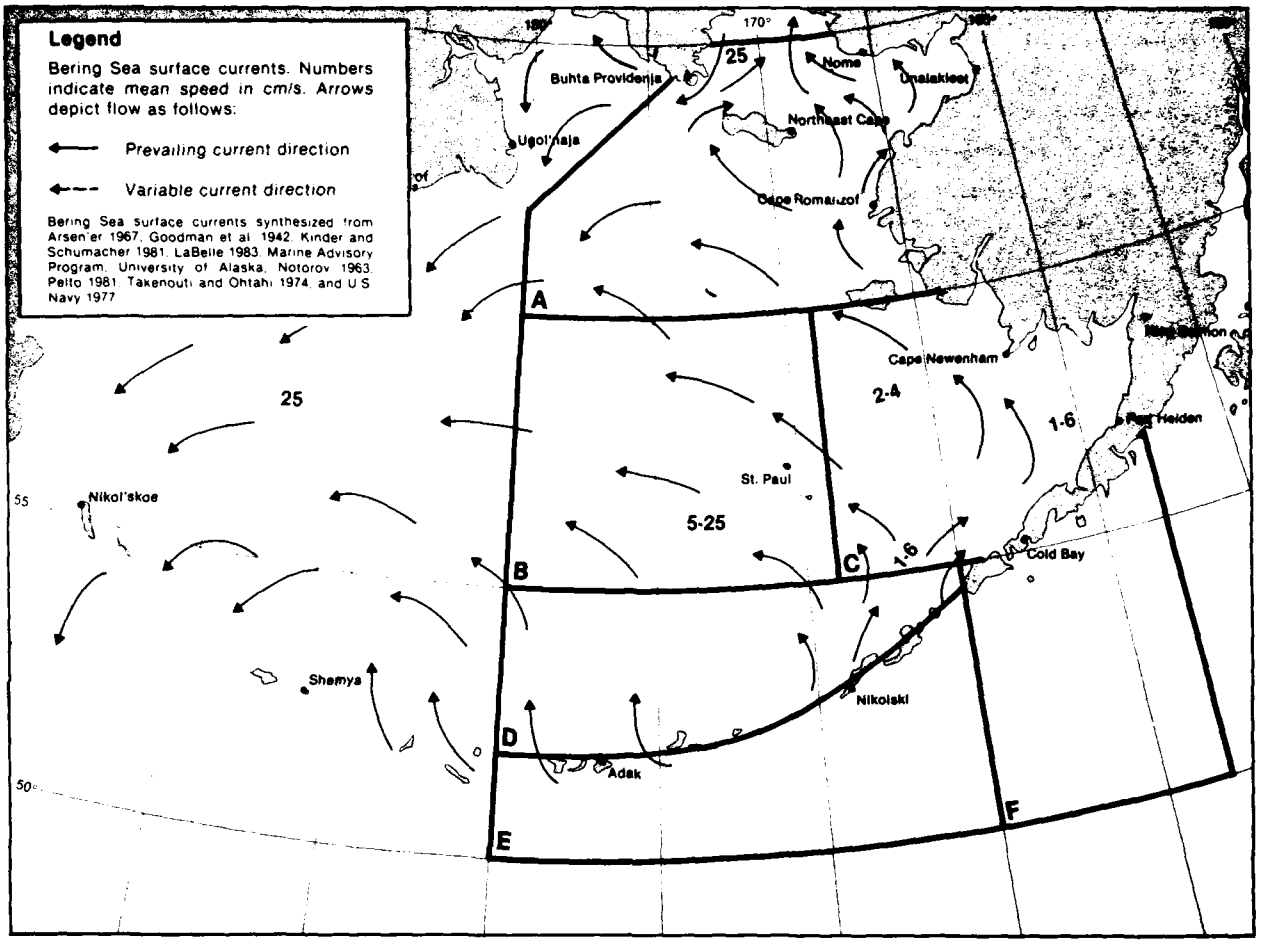

Figure 2-12. Bering Sea currents—winter (Brower et al., 1988).

2.1.5 Tides

The Moon is about twice as effective as the Sun in producing tides. Together they bring about a change in sea level at a given location about every 6 hr. High tide usually occurs twice a lunar day (24 hr, 50 min) at a fixed interval following the Moon's meridional passage. The height difference between high and low tides is called the range of the tide. It is generally greatest during the period of full moon (spring tide) and smallest at half moon or quadrature (neap tide) when the Sun and Moon's overhead longitudes differ by 90°. The range can vary, worldwide, from essentially 0 to over 60 ft (18 m). Figure 2-13 illustrates positioning and tidal effect of the Sun, Moon, and Earth during spring and neap tides. Spring and neap tides occur at approximately 2-week intervals and not seasonally as their names might imply.

Secondary variations include an increase in tidal range when the moon is closest to the Earth (perigee) and a similar decrease when the Moon is furthest from the Earth (apogee).

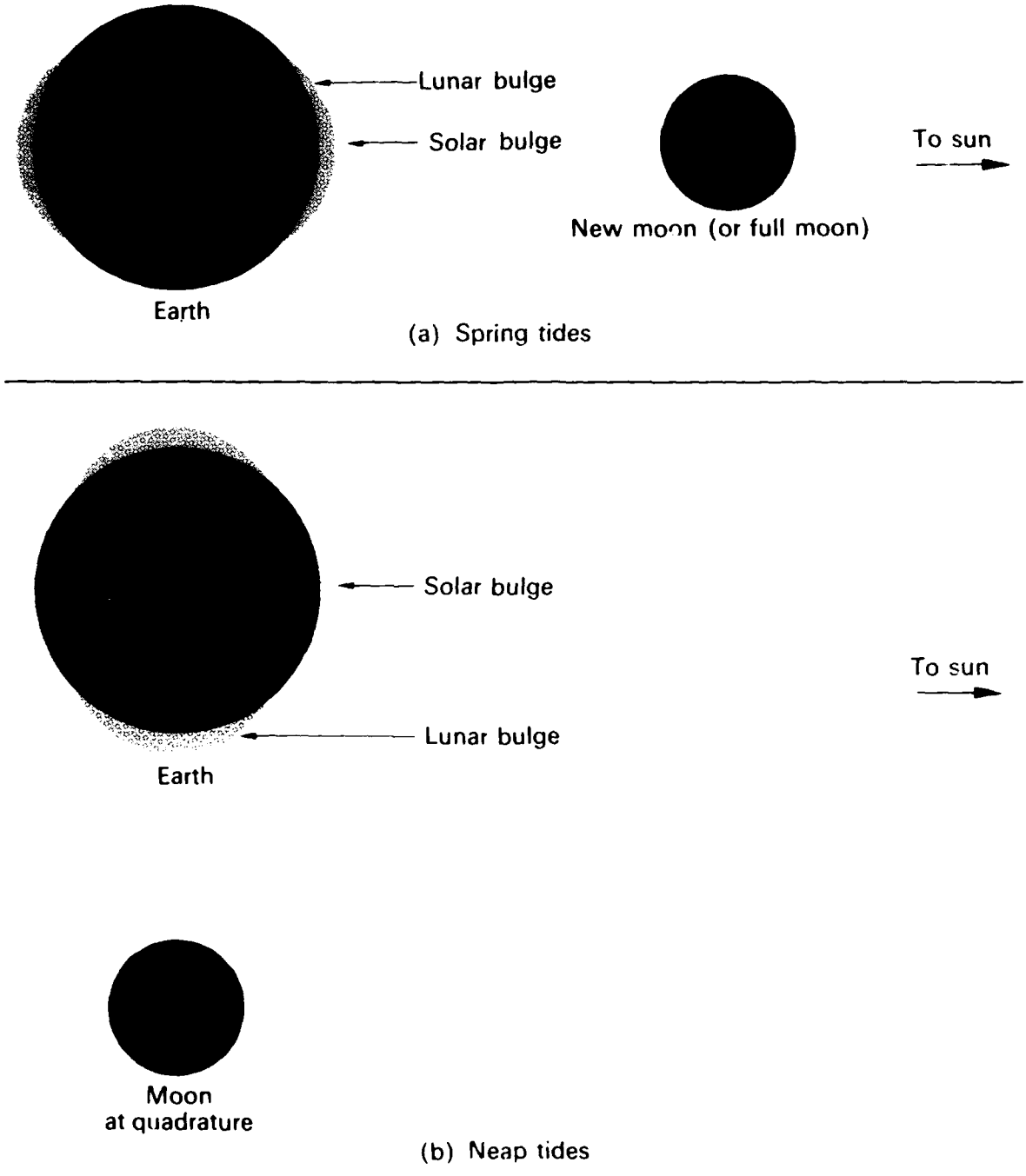

Figure 2-13. (a) Sun, Moon, and Earth aligned to produce spring tides. (b) Sun and Moon acting at right angles to each other to produce neap tides (after Bascom, 1980).

The season of the year also influences the magnitude of high and low water levels with the maximum range occurring at the time of the solstice, during June and December.

A complete discussion of tidal behavior is beyond the scope of the general background material presented here. However, it should be understood that a variety of combinations of forces are involved at any particular time and location, including effects of friction and bottom topography. The complexity of the topic has resulted in defining three types of tides to cover the variations: the semidiurnal tide, the diurnal tide, and the mixed tide. The semidiurnal tide is most common, producing successive high and low tides twice a day about 6 hr apart. The diurnal tide occurs at some locations where only one high tide and one low tide are observed, roughly 12 hr apart. Finally, the mixed tide refers to tides where one of the two maxima is higher than the other. The effect is called diurnal inequality. In this situation a location may experience a high-water level, a highest-high level, a low and a lowest-low level, not in this order of course.

Tidal action in the Bering Sea contains complicated distributions of the three tidal types. Figure 2-14 is a recent assessment of tidal types (Brower et al., 1988) showing the range from high to low tide over the region. Figure 2-15 lists tidal statistics for the Bering Sea at a number of locations. According to Brower et al.:

> "The tide wave enters the Bering Sea as a progressive wave from the North Pacific Ocean, mainly through the central and western passages of the Aleutian-Komandorski Islands (Commander Islands). The Arctic Ocean is a minor secondary source of tides that propagate southward into the north Bering Sea where they complicate the tidal distributions.
>
> Tides in the Bering Sea are considered to be the result of co-oscillation with large oceans. Once inside the Bering Sea, each tidal constituent propagates as a free wave subject to Coriolis effect and bottom friction.
>
> The tide wave propagates rapidly across the deep western basin. Part of it propagates onto the southeast Bering shelf where large amplitudes are found along the Alaska Peninsula and in Kvichak and Kuskokwim Bays (Fig. 2-14). Another part propagates north, eastward past St. Lawrence Island and into Norton Sound. Over most of the eastern Bering shelf region the tide is mainly semi-diurnal, but in Norton Sound diurnal tides predominate. Over the remainder of the Bering tides tend to be mixed. In the Aleutians diurnal rather than semi-diurnal components are stronger."

The influence of the Moon and Sun on ocean tides creates tidal currents of three categories: (a) the rotary type characteristic of currents in the open ocean and along coastal regions; (b) the rectilinear or reversing type, found in inland bodies of water and in bay regions; and (c) the hydraulic type typified by current flow through straits connecting the two independent bodies of water. Tidal currents are much weaker than wind driven currents except in shallow coastal areas. They repeat themselves as regularly as the tidal motions from which they are derived. Tidal currents are strongly influenced by the Coriolis force. For example, in broad estuaries during flood tide in the Northern Hemisphere, the Coriolis force causes a piling up of the water along the shore on one side of the basin during ebbtide.

The Bering Sea is characterized by an open shelf south of St. Lawrence Island. Mean currents are variable in direction and range from 0.02 to 0.08 kt (1 to 4 cm/s), and the

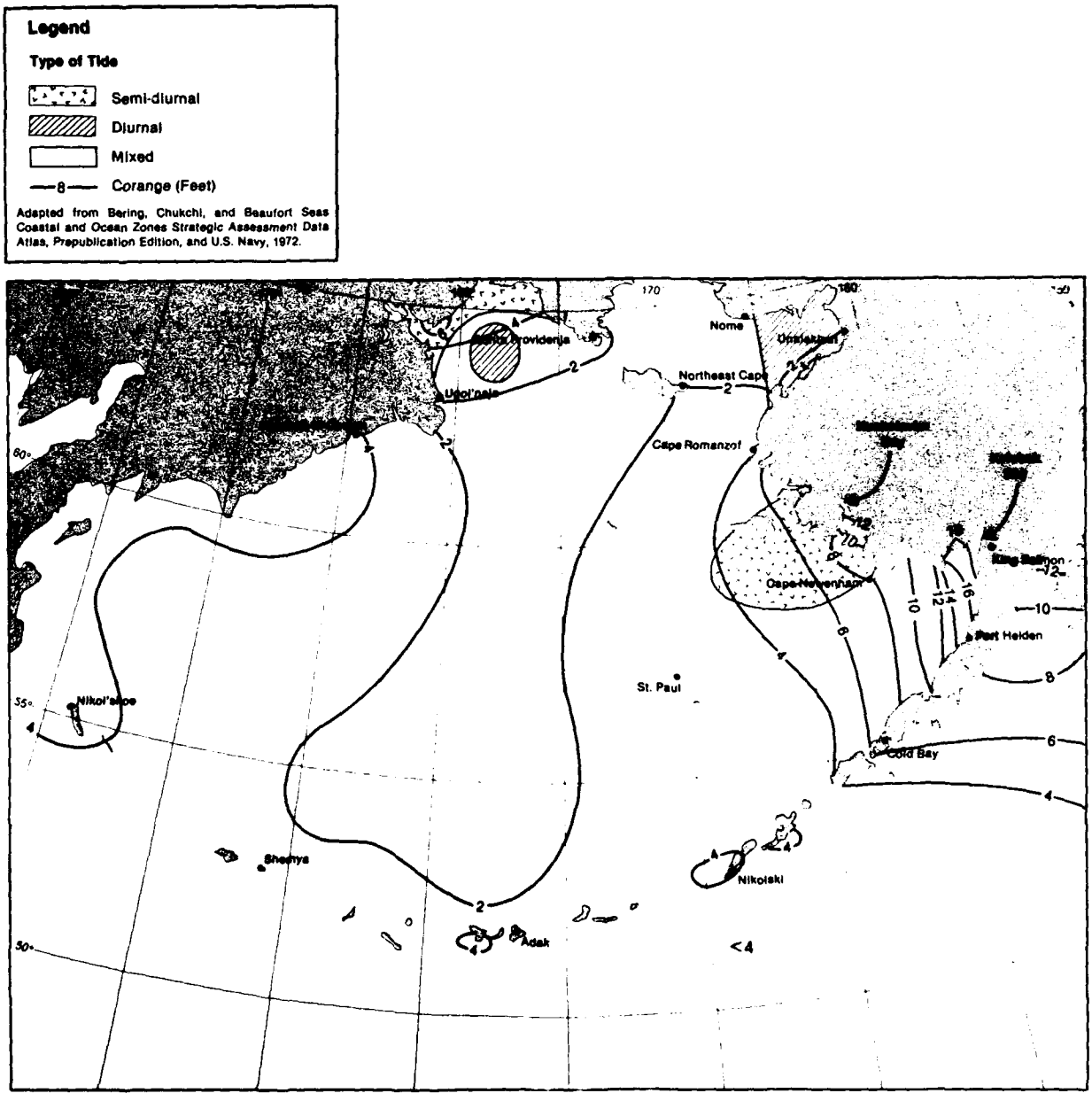

Figure 2-14. Tide types of the Bering Sea (Brower et al., 1988).

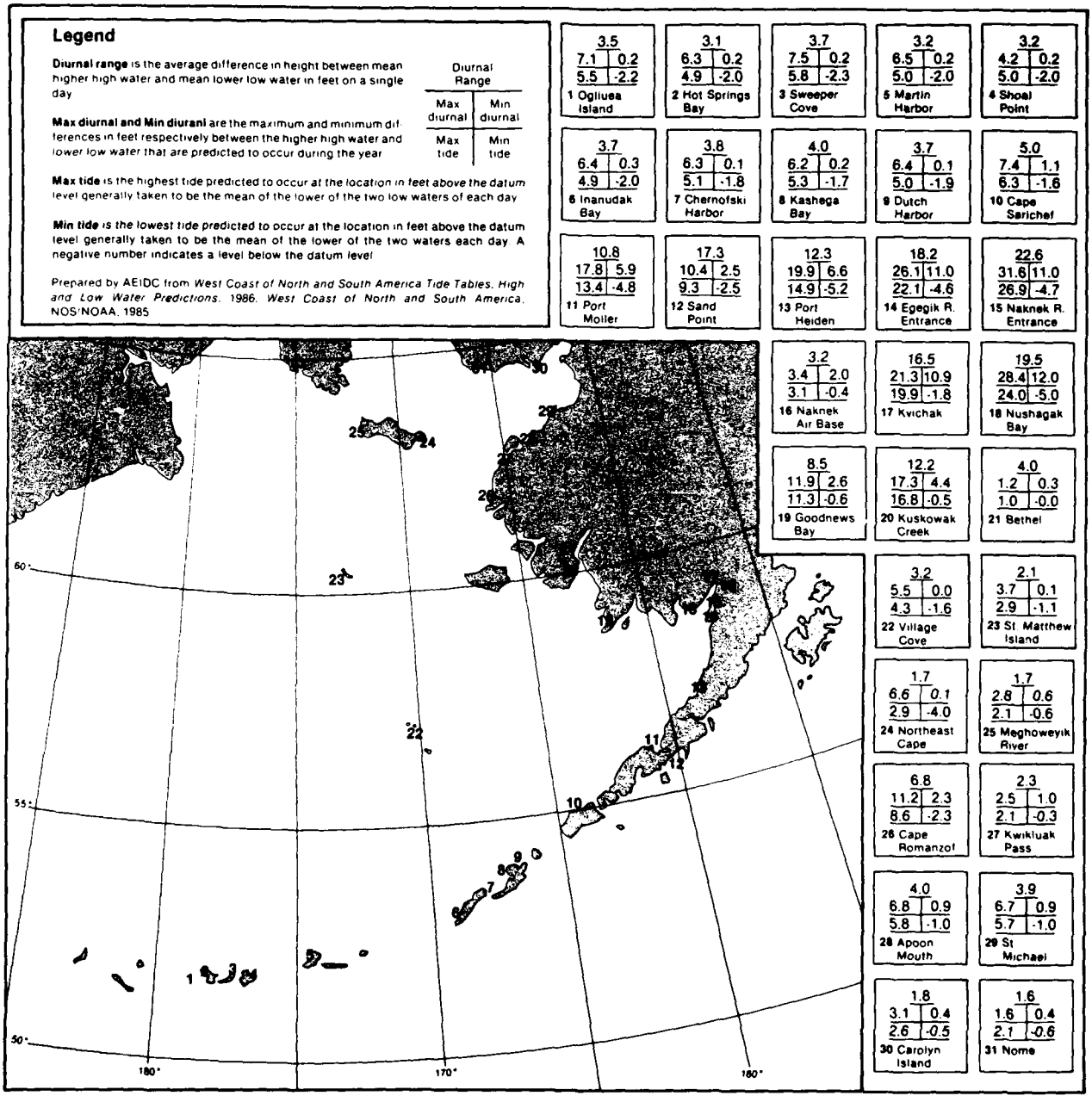

Figure 2-15. Tide statistics for various locations in the Bering Sea (Brower et al., 1988).

tidal current accounts for 55 (± 31)% of the fluctuation (Salo et al., 1983). Near St. Lawrence Island, the Bering Sea narrows into two straits: the Shpanberg to the east and the Anadyr to the west. North of the island the two straits merge to form the Bering Strait. Circulation here is dominated by a northward mean flow ranging from 0.08 to 0.3 kt (4 to 15 cm/s), varying 11% to 37% due to tidal influences (Salo et al., 1983). Flow in both the Anadyr and the Shpanberg is to the north, approximately parallel to the local bathymetry contours. The flow appears to come from around both ends of St. Lawrence Island. Frequent reversals are coincidental with meteorological events. These reversals can affect the flow over vast regions covering thousands of square kilometers. The presence of ice appears to dampen the impact of wind stress forcing. The major driving force for the northward flow through Bering Strait is the sea surface sloping down to the north (Coachman and Aagaard, 1981). The normal condition is one in which sea level in the southern Chukchi Sea (in summer) is about 1.5 ft (0.5 m) lower than in the northern Bering Sea. A major cause of variations in the sea level difference can be traced to fluctuations of the regional wind distribution. It is also possible that the atmospheric pressure field may itself directly modify the oceanic pressure field (Coachman et al., 1975).

2.2 Gulf of Alaska

2.2.1 Geography

The Gulf of Alaska lies between 50 to 60 °N and 130 to 155 °W in the extreme northeast sector of the Pacific Ocean (Fig. 2-16). The region was officially first explored by the Russians in the mid 1700s. Captain Cook, on his third and final voyage sailed from his newly discovered Hawaiian Islands in 1788 to the Pacific Northwest and entered what is now called "Cook's Inlet," leading to Anchorage.

2.2.2 Topography

The Gulf of Alaska is ringed in its northern semicircle by very mountainous terrain. In fact the world's highest coastal range extends from Mount Fairweather (15,310 ft or 4666 m) near Glacier Bay (58.6 °N, 136 °W) to the Chugach Mountains, leading to Prince William Sound, just southeast of Anchorage. Mt. Fairweather has possibly the greatest "sea level to peak" slope of any mountain on Earth. The entire coastal range forms a wall and literally "makes its own weather." The Alaska Range and the Aleutian Range form additional significant barriers. Denali (Mt. McKinley), North America's highest mountain (20,320 ft or 6194 m) is located north of Anchorage in the Alaska Range. Figure 2-17 is a map of the region listing some important places and features.

Heavily wooded mountains are found on the Kenai Peninsula, Afognak Island, Kodiak Island, and on the southeastern portion of the Alaska Peninsula (Fig. 2-18). These mountains provide a block to northwesterly winds that often flow with hurricane force through a gap over Kamishak Bay, then past the Barren Islands, at the entrance to Cook Inlet, and out into the Gulf of Alaska. Low terrain leads from near King Salmon across the Alaskan Peninsula to Kamishak Bay. This gap is referred to as the Kamishak Gap. Gap winds also flow through Shelikof Strait when, with high pressure inland, isobars are aligned parallel to the Shelikof Strait axis. Figure 2-19 is a mesoscale analysis showing aircraft-measured winds at 260 ft (80 m) during such an event. Northerly winds at the strait entrance veered southeasterly a short distance into the strait. It was also noted that wind speed increased through the strait from about 10 kt (5 m/s) at the entrance to 25 kt (13 m/s) near the exit.

The Alaskan Peninsula is typified by a flat tundra region on the northwest side, numerous mountains of the Aleutian Range on the southeast side, and the Pavlof volcano (8262 ft or 2518 m) near 162 °W (Fig. 2-3). The Veniaminof volcano (8225 ft or 2507 m) near 159.5 °W is a dominant feature of the southwest portion of the peninsula. The peninsula terminates just southeast of Cold Bay where a narrow channel (False Pass) separates it from Unimak Island (Fig. 2-3).

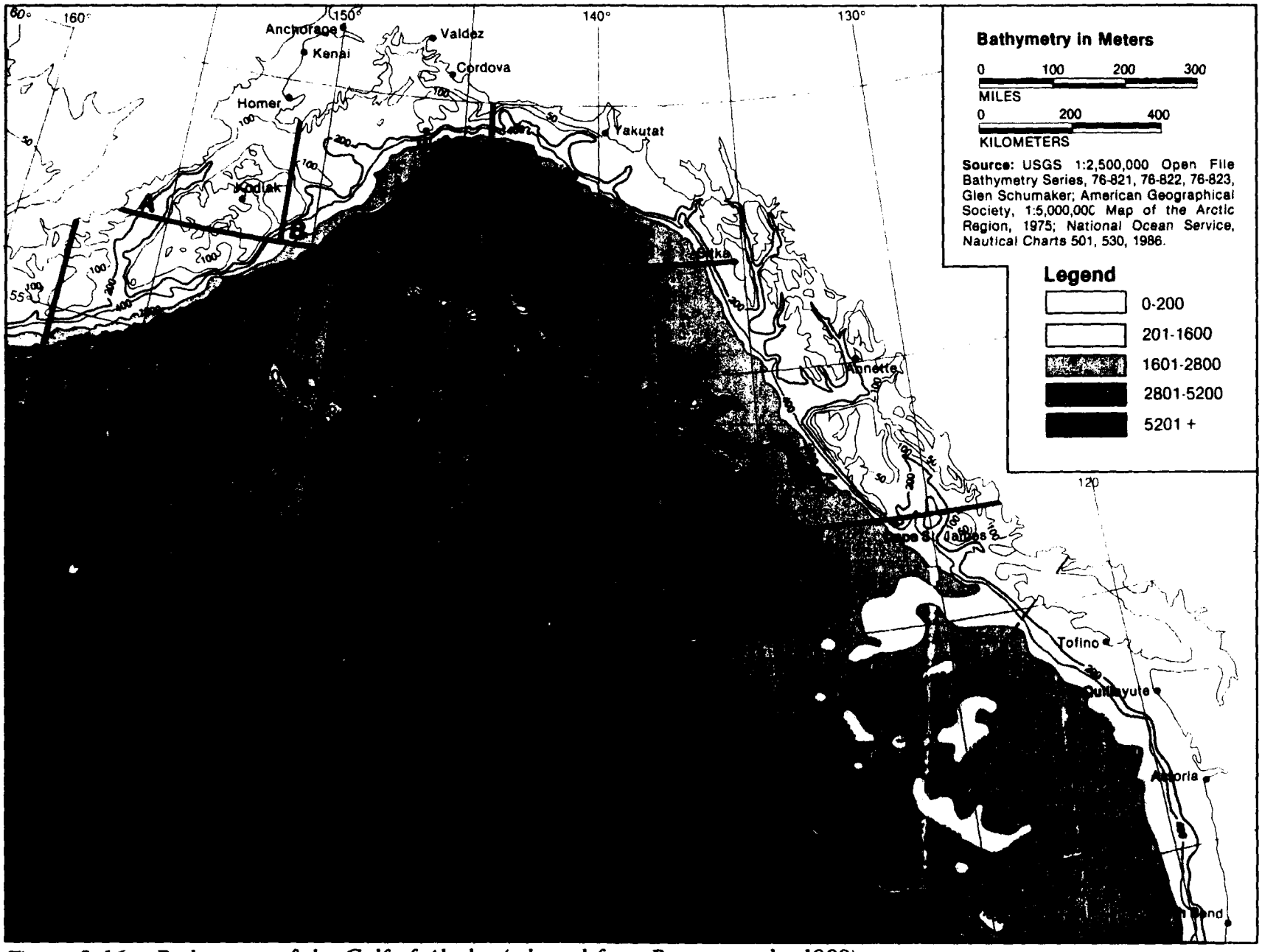

Figure 2-16. Bathymetry of the Gulf of Alaska (adapted from Brower et al., 1988).

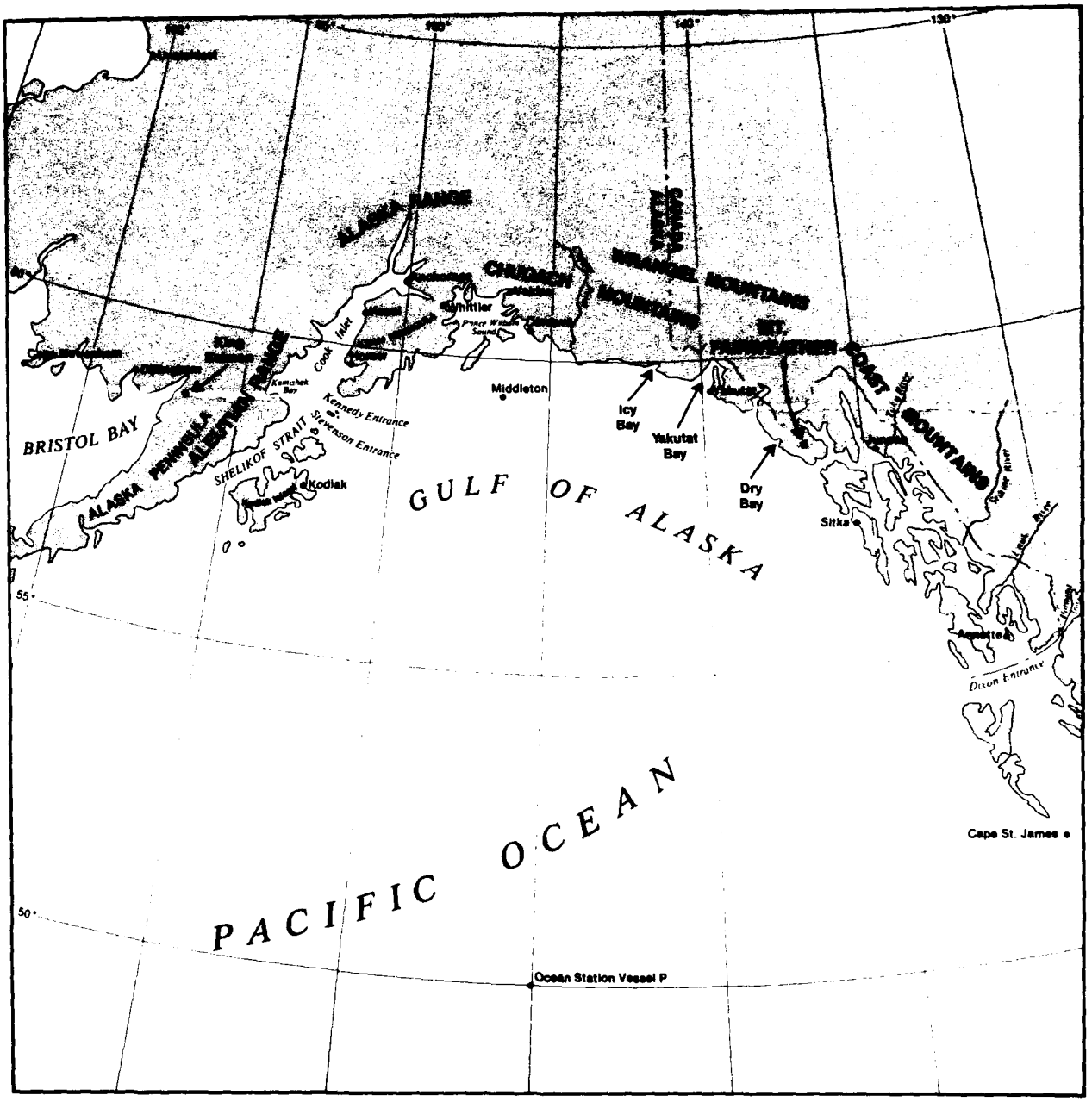

Figure 2-17. Locator map for the Gulf of Alaska (adapted from Brower et al., 1988).

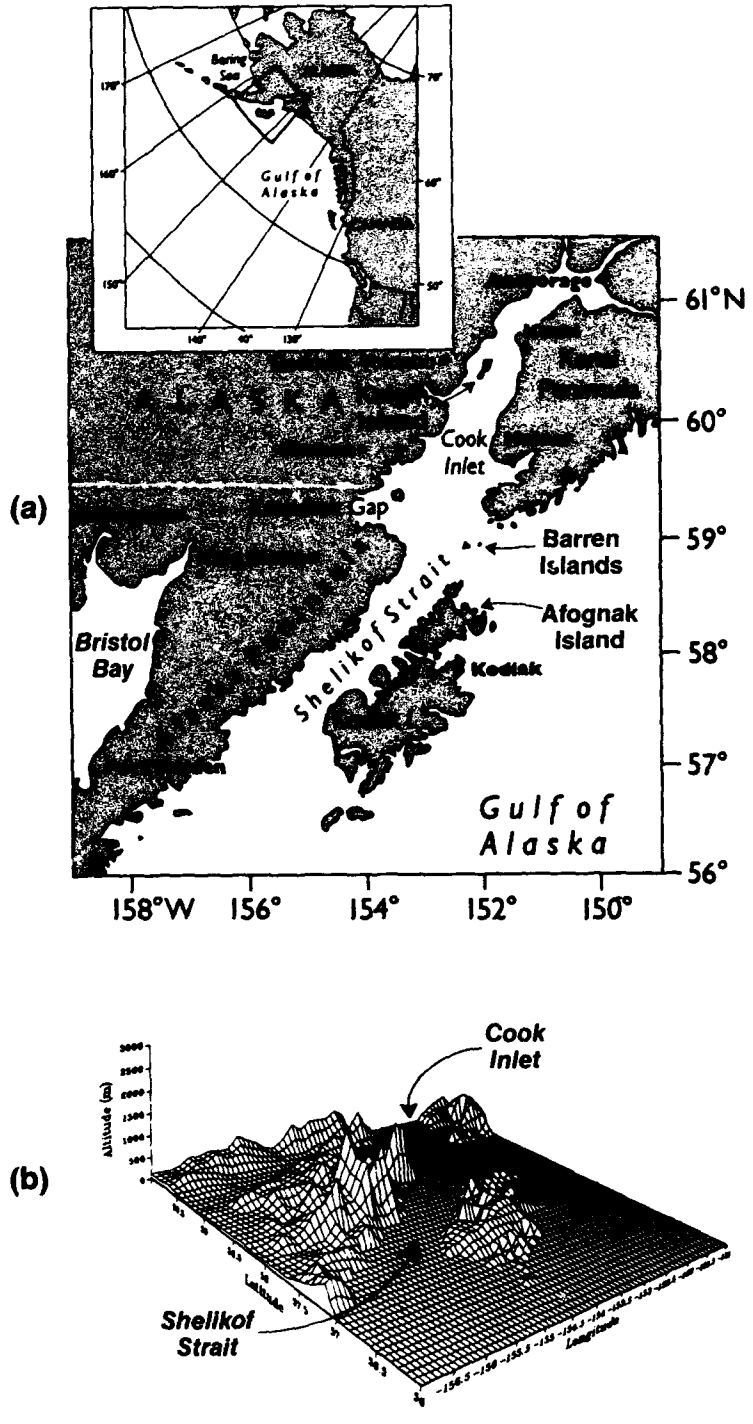

Figure 2-18. (a) Shelikof Strait region; (b) Topography of the Shelikof Strait region. Horizontal grid spacing is 5 min, vertical scale exaggerated 50 times (adapted from Lackmann and Overland, 1989).

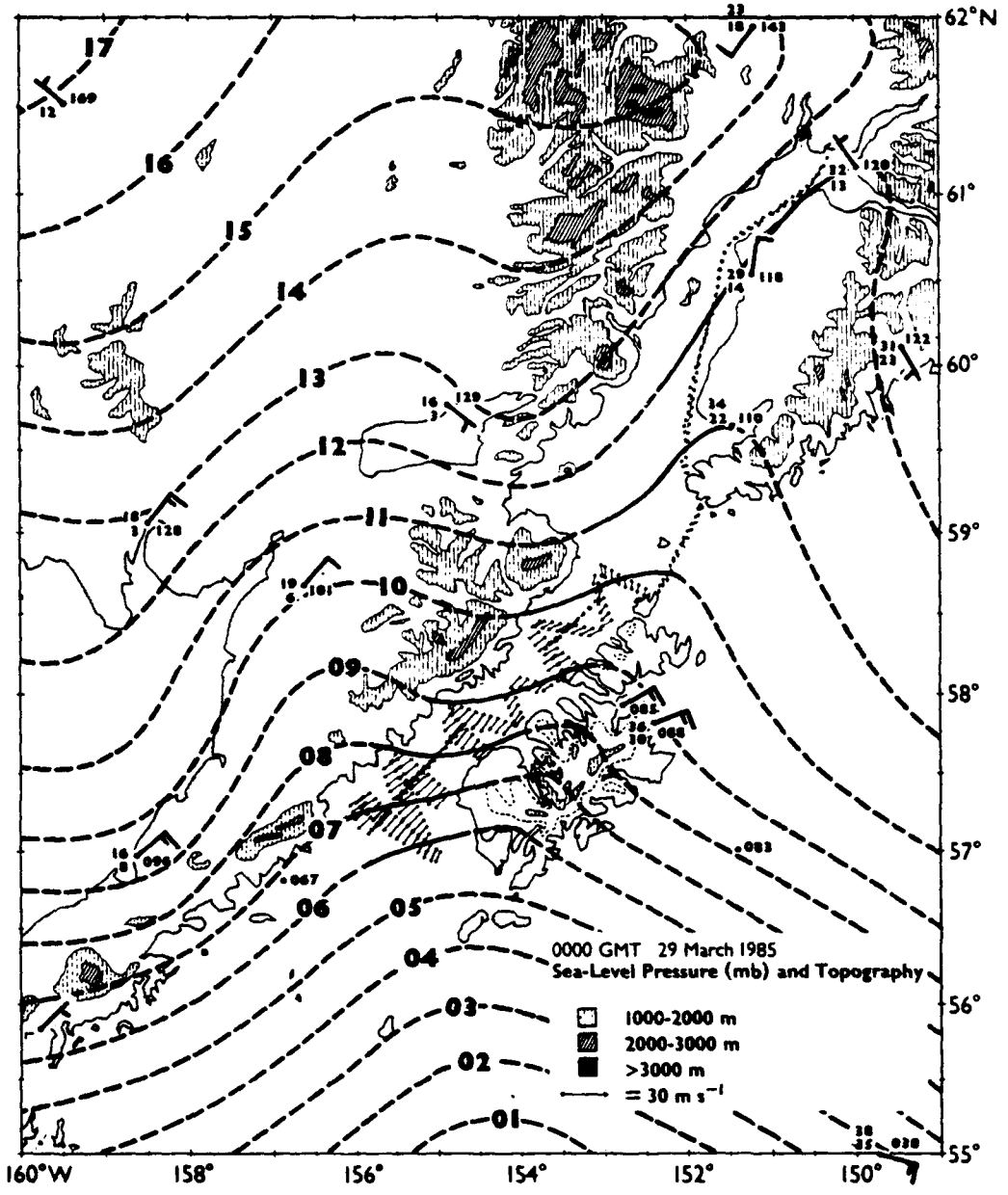

Figure 2-19. Mesoscale sea-level pressure analysis and topography. Isobars are dashed outside of areas where aircraft data were collected and over topography to indicate a higher degree of uncertainty. Station temperatures and dewpoints are in °F, pressures are in mb – 1000 (Lackmann and Overland, 1989).

2.2.3 Bathymetry

The bathymetry of the Gulf of Alaska is shown in Fig. 2-16. It can be seen that the shallowest water is to the southeast, and the deepest water is in the trench that parallels the south side of the entire Aleutian chain and extends eastward to an area just south of Kodiak Island.

2.2.4 Currents

The North Pacific Current, an eastward extension of the Kuroshio Current crosses the ocean near 45 °N. It then splits into two branches offshore of Washington and Oregon. The southward flowing branch is called the California Current and the northward flowing branch, the Alaska Current. In the region of the Gulf of Alaska the system describes a huge cyclonic gyre, centered near 52 °N, 140 to 145 °W during both winter and summer. Figure 2-20 is a depiction of the summer sea surface currents in that area (Brower et al.,

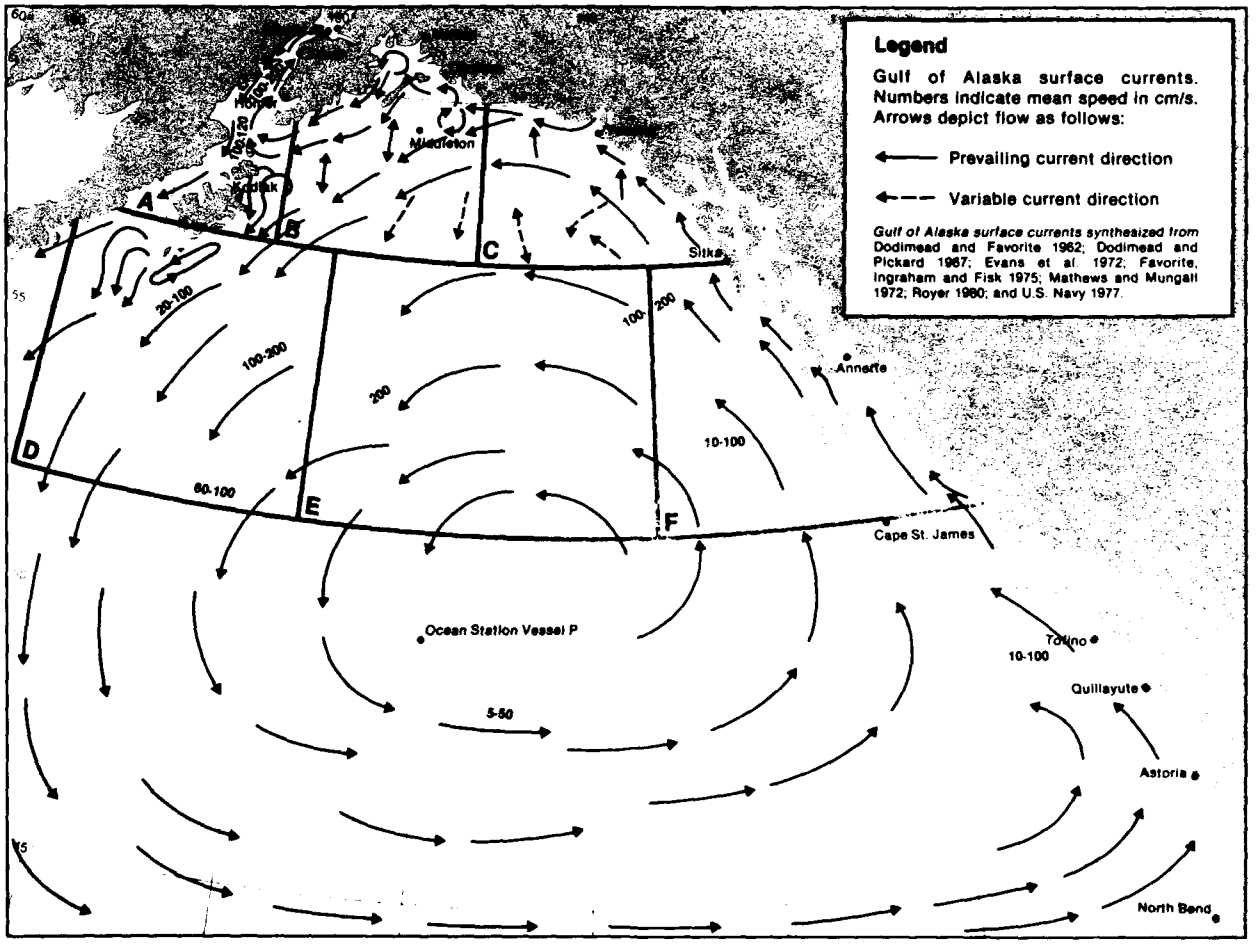

Figure 2-20. Gulf of Alaska sea surface currents: Summer (Brower et al., 1988).

1988). The companion winter pattern is shown in Fig. 2-21. No appreciable seasonal shift is apparent in the position of the current.

The current narrows with maximum speed along the shelf break near Kodiak (Fig. 2-21). In this region the current is referred to as the "Alaska Stream." Maximum current velocities in the region of 4 kt (2 m/s) have been noted.

The circulation near the shelf break contains frequent meanders and eddies, associated with changes in bathymetry (See Section 6 for related case study). Eddy formation is most notable in the fall. The eddies propagate eastward on the north (shoreward) side of the Alaska Current, moving onto the continental shelf with rotational speeds of up to 1 kt (0.5 m/s). Troughs or trenches extend from the shelf break into Yakutat Bay and Icy Bay. In these regions flow is often diverted anticyclonically toward shore in an easterly flow.

A small anticyclonic eddy called the Kayak Island eddy is located just south of Cordova (Fig. 2-20). The eddy circulates in a typical speed of 0.6 kt (0.3 m/s).

The Kenai Current or the Alaska Coastal Current, a narrow intense current associated with fresh water runoff, extends from Prince William Sound through the Shelikof Strait

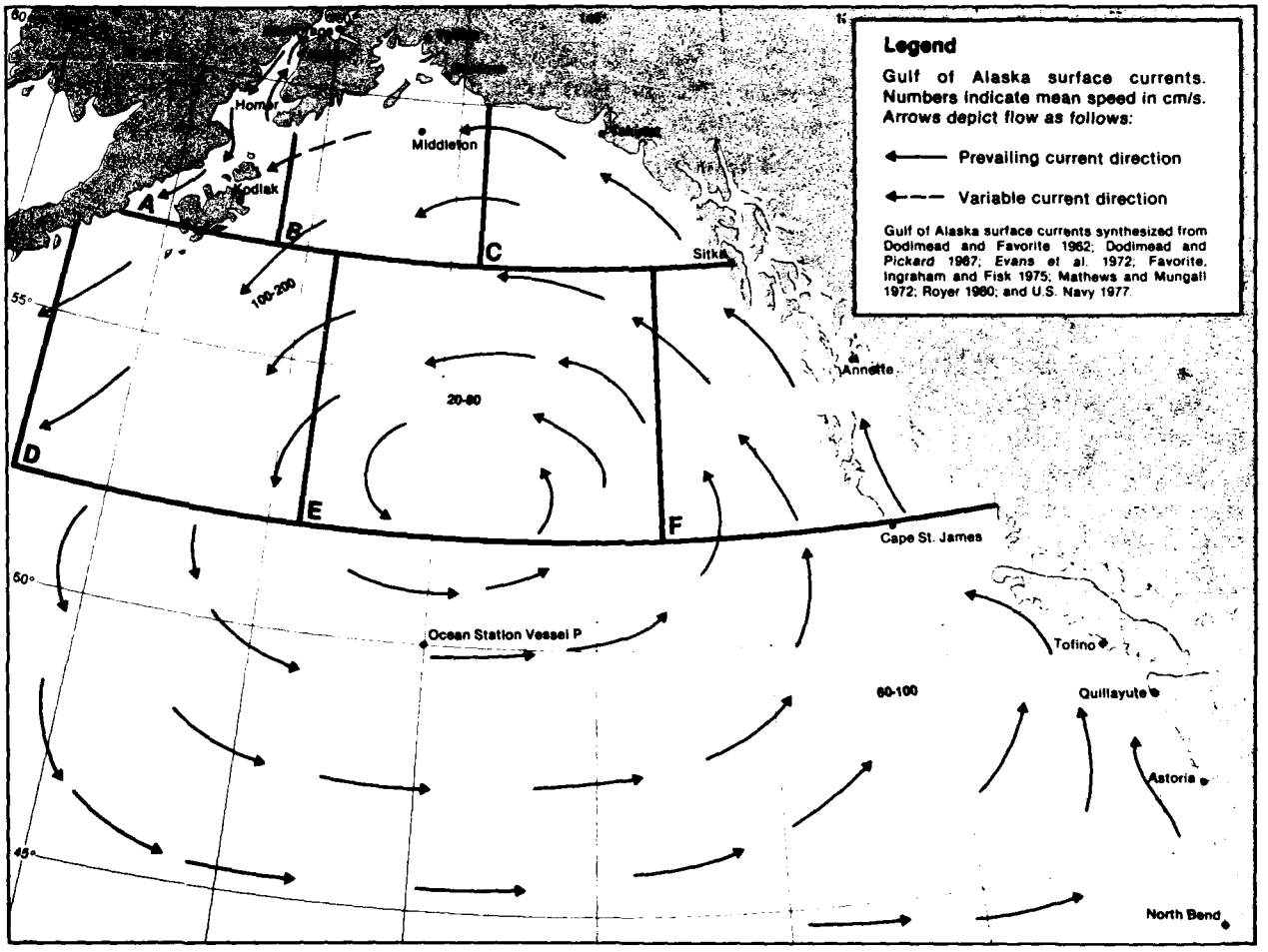

Figure 2-21. Gulf of Alaska sea surface currents: Winter (Brower et al., 1988).

to the western end of the Alaska Peninsula. The current is quite narrow with widths estimated from 2.7 to 13.5 n mi (5–25 km). Speed can be quite high reaching 2 to 3 kt (1–1.5 m/s) in some areas. Maximum speeds are usually noted in mid to late autumn.

Observations have shown that flow entering the Kennedy Entrance (between Barren Islands and Kenai Peninsula) to Cook Inlet is stronger and more persistent than flow entering the Stevenson Entrance (between Kodiak Island and Barren Islands). Speeds of 0.6 kt (0.3 m/s) are commonly observed, being stronger near the Kenai Peninsula. Superimposed on the current speed are tidal speeds reaching 1 kt (>0.5 m/s) in the Kennedy Entrance.

The current flow in Cook Inlet is interesting in that clear oceanic water enters the inlet from the southeast on the south side of the inlet during floodtide and departs as turbid water along the north and west coast during ebbtide. Currents near Kalgin Island, just east of the Redoubt Volcano (Fig. 2-18), are complex. In this region ebbtides and floodtides meet, speeds are higher, and occasional strong cross-inlet currents are observed. Peak velocities of 6 to 8 kt (3–4 m/s) occur during tidal extremes.

2.2.5 Tides

Figure 2-22 shows the range from high to low tide typical of the Gulf region. The tides are of the mixed type with two highs and two lows per day in most locations. It can be seen that a very high tidal range of 30 ft (9 m) is characteristic of the Anchorage area. Secondary maximum tides occur in Nushagak and Kvichak Bay at the northeast end of Bristol Bay.

2.2.6 Sea Ice and Sea Surface Temperature

February and March are typified by the coldest sea surface temperatures in the Gulf of Alaska. A bulging of the isotherms northward along the southeast coast of Alaska reflects the warming influence of the Alaska Current in that region. Figure 2-23 shows the mean sea surface temperature for February. The Gulf of Alaska is ice free throughout the year. However, Cook Inlet has appreciable ice amounts (shown as percentage of coverage in Fig. 2-23) during the winter. Floating glacial ice, calved from glaciers, and winter bay ice is found in most of the bays and inlets from Annette, Alaska (Fig. 2-16), northward. A listing of calving tidewater glaciers in Alaska is given in Table 2-2 (Brower et al., 1988).

Figure 2-24 shows the Gulf of Alaska sea surface temperatures in August, which are about the warmest of the year. Again, the northward bulge of isotherms along the coast reflects the influence of the warm Alaska Current. Although Fig. 2-24 indicates "no ice of any kind reported in the area," this refers only to the open waters of the gulf. The bays and inlets of Alaska usually have bergs and growlers calved from glaciers at some locations throughout the year. Note that the Exxon Valdez ran aground while "dodging" Prince William Sound growlers (April 1989), resulting in an ecological disaster. Obviously bergs and growlers can be extremely hazardous to navigation.

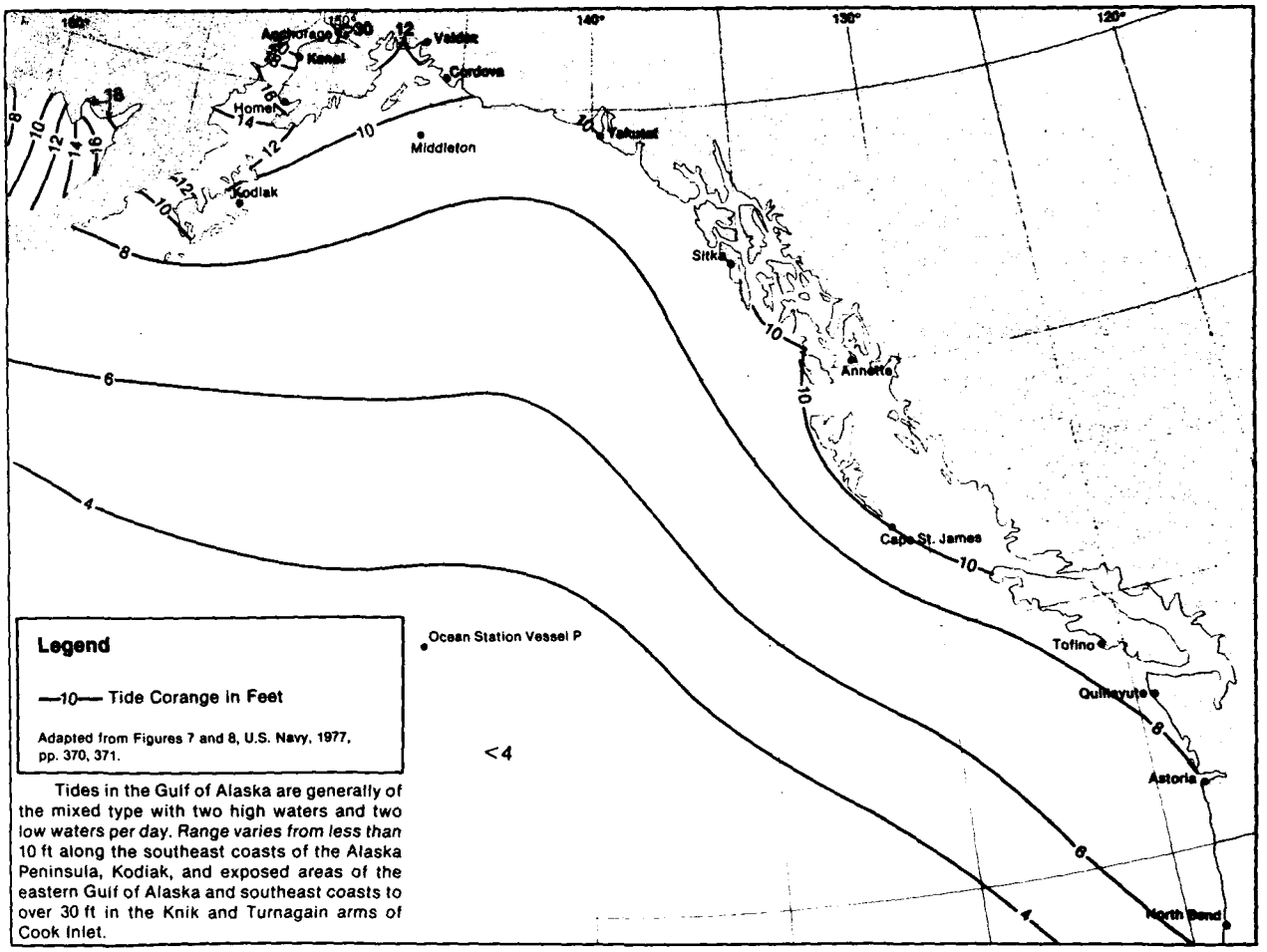

Figure 2-22. Gulf of Alaska tide corange (Brower et al., 1988).

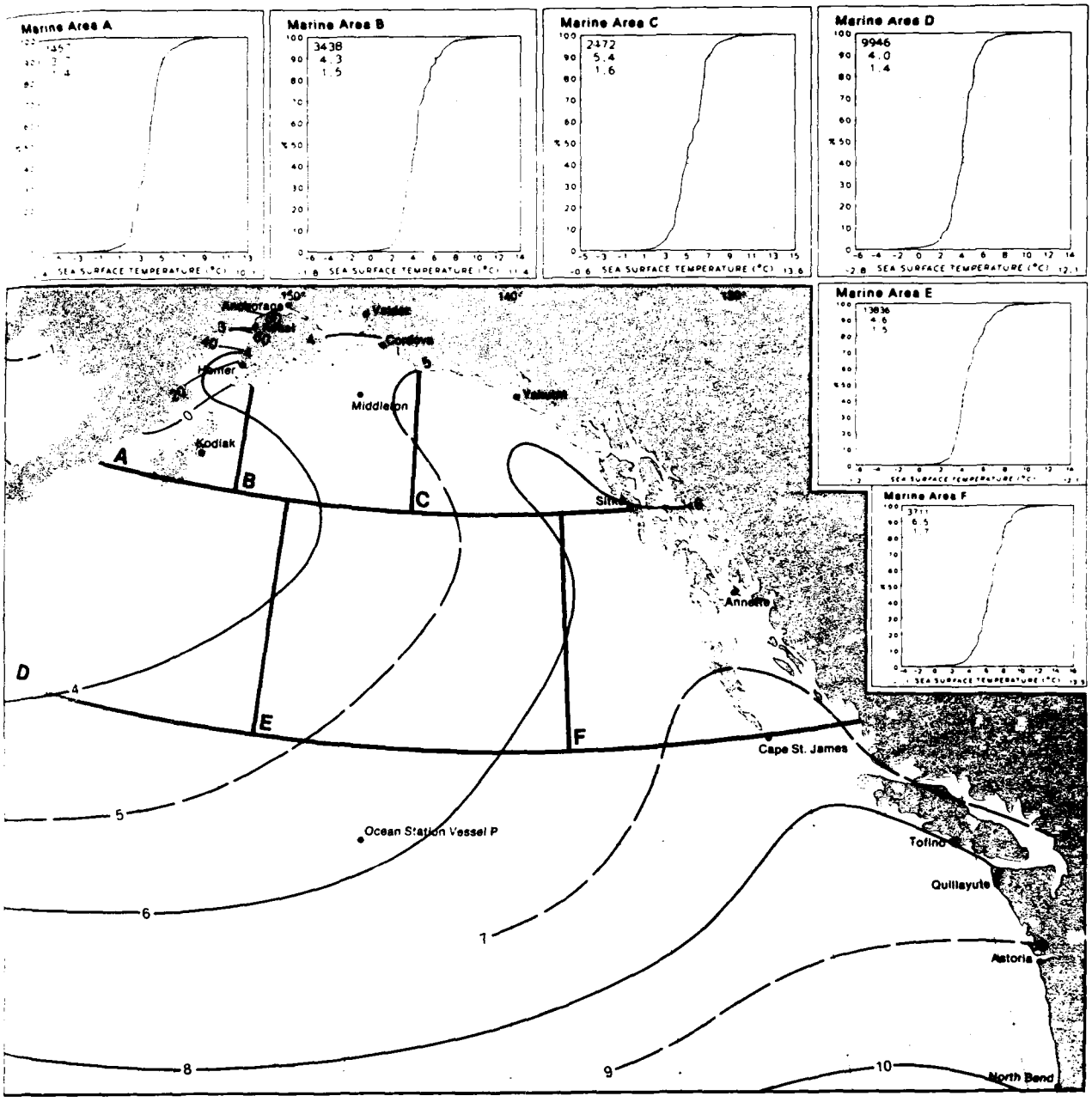

Figure 2-23. Gulf of Alaska mean sea surface temperature (°C) for February and ice of any kind (%) (Brower et al., 1988).

TABLE 2-2. CALVING TIDEWATER GLACIERS IN ALASKA, NUMBERED FROM SOUTH TO NORTH (BROWER ET AL., 1988)

Frederick Sound
1. Le Conte Glacier, in Le Conte Bay

Stevens Passage
2. Dawes Glacier, in Endicott Arm
3. South Sawyer Glacier, in Tracy Arm
4. Sawyer Glacier, in Tracy Arm
5. Taku Glacier, in Taku Inlet

Glacier Bay
6. McBride Glacier, in Muir Inlet
7. Riggs Glacier, in Muir Inlet
8. Muir Glacier, in Muir Inlet
9. Plateau Glacier, in Wachusett Inlet
10. Grand Pacific Glacier, in Tarr Inlet
11. Margerie Glacier, in Tarr Inlet
12. Toyatte Glacier, in Johns Hopkins Inlet
13. Johns Hopkins Glacier, in Johns Hopkins Inlet
14. Gilman Glacier, in Johns Hopkins Inlet
15. Hoonah Glacier, in Johns Hopkins Inlet
16. Kashoto Glacier, in Johns Hopkins Inlet
17. Lamplugh Glacier, in Johns Hopkins Inlet
18. Reid Glacier, in Reid Inlet

Cross Sound
19. Brady Glacier, in Taylor Bay

Northeast Gulf of Alaska
20. La Perouse Glacier

Lituya Bay
21. North Crillon Glacier
22. Cascade Glacier
23. Lituya Glacier

Yakutat Bay
24. East Nunatak Glacier, in Nunatak Fiord
25. Hubbard Glacier, in Disenchantment Bay
26. Turner Glacier, in Disenchantment Bay

Icy Bay
27. Tyndall Glacier
28. Yahtse Glacier
29. Guyot Glacier

Prince William Sound
30. Shoup Glacier, in Shoup Bay on Port Valdez
31. Columbia Glacier, in Columbia Bay
32. Meares Glacier, in Unakwik Inlet
33. Yale Glacier, in College Fiord on Port Wells
34. Harvard Glacier, in College Fiord on Port Wells
35. Smith Glacier, in College Fiord on Port Wells
36. Wellesley Glacier, in College Fiord on Port Wells
37. Coxe Glacier, in Barry Arm on Port Wells
38. Barry Glacier, in Barry Arm on Port Wells
39. Cascade Glacier, in Barry Arm on Port Wells
40. Serpentine Glacier, in Harriman Fiord on Port Wells
41. Surprise Glacier, in Harriman Fiord on Port Wells
42. Harriman Glacier, in Harriman Fiord on Port Wells
43. Blackstone Glacier, in Blackstone Bay
44. Beloit Glacier, in Blackstone Bay
45. Nellie Juan Glacier, in Derickson Bay on Port Nellie Juan
46. Chenega Glacier, in Nassau Fiord on Icy Bay
47. Tiger Glacier, in Icy Bay

Alalik Bay
48. Alalik Glacier
49. Holgate Glacier, in Holgate Arm

Harris Bay
50. Northwestern Glacier, in Northwestern Lagoon

Nuka Bay
51. McCarty Glacier, in McCarty Fiord
52. Dinglestadt Glacier (eastern tongue), in McCarty Fiord

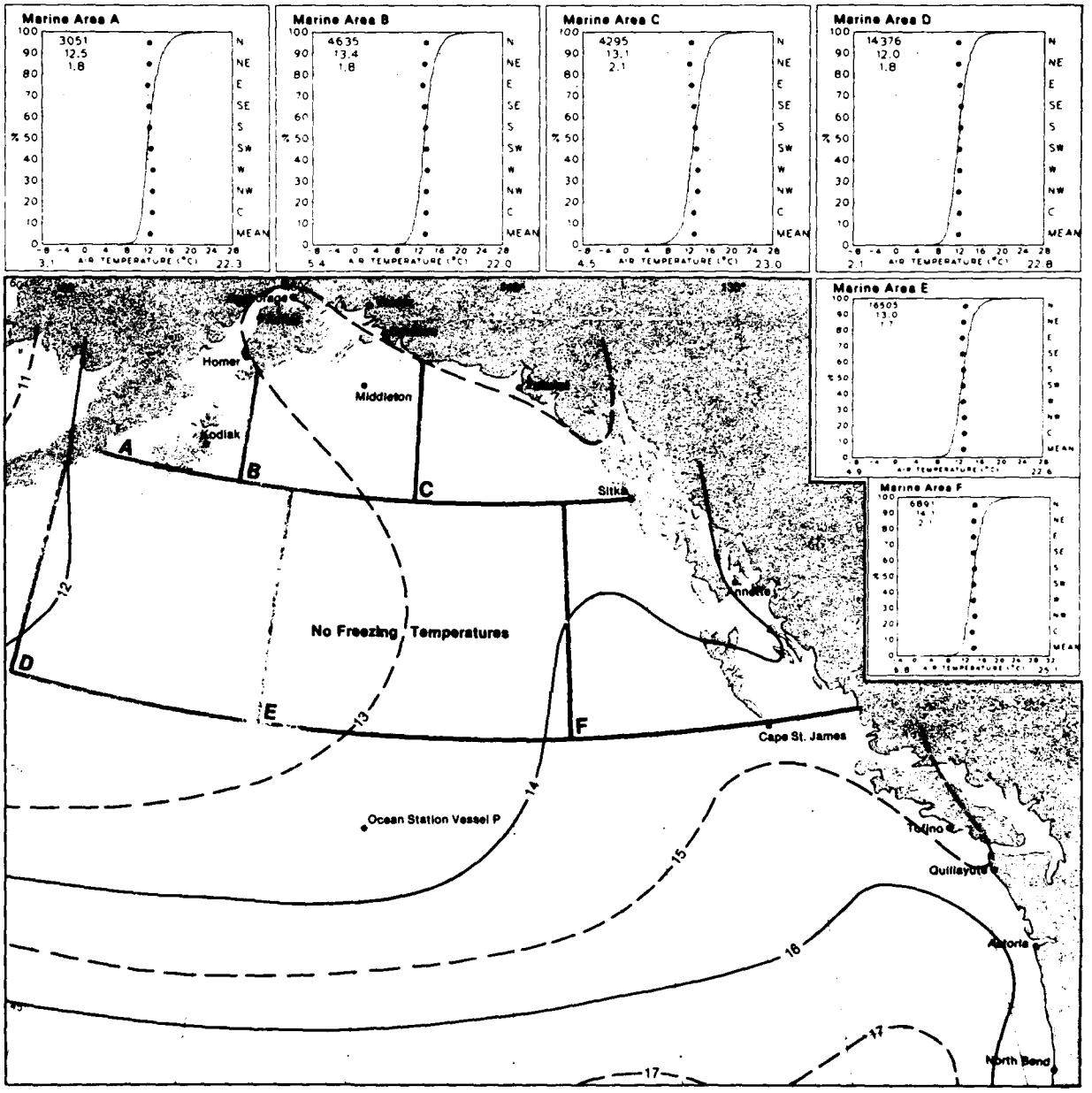

Figure 2-24. Gulf of Alaska mean sea surface temperature (°C) for August and ice of any kind (%) (Brower et al., 1988).

3. CLIMATOLOGY OF THE REGION

Various climatological phenomena are examined for the three subregions, the Bering Sea, Aleutian Islands, and Gulf of Alaska. Some of the elements examined are precipitation, temperature, humidity, wind, and sea ice.

3.1 Bering Sea

The Bering Sea ice pack has an extremely important influence on the climate of the region, forming in October as fast ice along the shores of the Seward and Chukotsk peninsulas. The coastal climate at this time changes from maritime to continental in nature as both temperature and moisture in the air decrease. Ice begins moving south over the open sea in November, and by February through April there is at least a 10% chance that it will extend as far south as St. Paul Island in the Pribilofs. In the western portion of the Bering Sea ice begins forming as fast ice in late October or early November along the Siberian coastline to the central portion of the Kamchatka Peninsula. This ice gradually extends southeastward almost reaching Nikol'skoe in the Commander Islands by January. The ice limit arches northward from this location and then drops southward toward the Pribilof Islands. The position of the limit of ice is quite changeable, moving southward at speeds approaching 30 to 100 n mi (56–185 km) in one day under northerly flow, and contracting 20 to 30 n mi (37–56 km) under southerly flow. Ice is continuously melting at the southern edge and forming to the north. The Bering Sea is almost completely free of ice from July through most of October.

During winter, in the absence of sunlight, the loss of heat from the Arctic latitudes is continuous because of long-wave radiation to space. As a consequence, huge masses of cold, dense air accumulate over the area. Eventually this air moves southward toward less dense air over the Bering Sea and Aleutian Island region. A principal factor in promoting this imbalance is the Aleutian Low, centered close to the western end of the Aleutians during January through April. Warm air brought into the Bering Sea by this system is eventually displaced by cold Arctic air moving through the region of the Bering Strait.

It is important to understand that the Aleutian Low is a climatological feature reflecting the high frequency of lows in the area. However, on a day-to-day basis the low can be located

anywhere from Kamchatka to Kodiak or even not appear at all, as ridging or high pressure develops to dominate the region.

The Aleutian Low characteristically has an elongated east-west axis and most storm developments move from west to east through the area. As noted by Grubbs and McCollum, 1968, "The most frequent track trajectory is along the Aleutian chain and into the Gulf of Alaska in winter, and along the same general path to the west but curving northward into the Bering Sea during summer." The winter storm track, eastward along the Aleutian chain, is in response to the expanding dome of cold Arctic air and resulting high pressure over Siberia and Alaska. A deviation from this pattern, permitting meridional north-to-northeast movement of lows into the Bering Sea, occurs when long-wave ridging develops over the eastern Bering Sea and Alaska. This usually happens a couple of times for extended periods during the winter, most frequently during late January to mid-February.

The storms moving through the Aleutian chain are associated with frontal zones separating airmasses with distinctive qualities related to lapse rate and stability, cloudiness, cloud type, precipitation, visibility, and wind flow. Cold Arctic air moving southward contrasts with warm Pacific air moving northward creating baroclinic frontal zones and often very intense cyclogenesis. Along the frontal zone and to the northeast of the low center, overcast multilayer cloud conditions and showers or steady rain and/or snow prevail. Wind speed can be very intense in the frontal zone and around the low center.

It has been noted (Grubbs and McCollum, 1968) that "normally, cloudiness associated with frontal passages in winter is confined to much lower levels than in summer, but even in winter clouds may extend to altitudes of 12,000 to 15,000 ft (3660–4574 m).

The temperature of the water in the Bering Sea is another important influence on weather developments, and it is cold, ranging from about 37 to 30 °F (+3 to −1°C) from January through April, warming to about 43 to 50 °F (+6 to 10 °C) during the summer through September, and then gradually cooling during October and November, when ice again begins to form.

Advective fog is common. Southerly flow brings warm, moist air northward, which is cooled by the underlying water. Such fog may persist for extended periods (days at a time), dependent upon the rapidity of movement of weather systems through the area. During summer, fog or stratus prevails, and clearing occurs only following the low pressure center and/or cold frontal passage.

The major currents affecting the Bering Sea and the Aleutian Islands are the eastward flowing Aleutian or Subarctic Current containing a mixture of the warm water of the Kuroshio Current and the cold water of the Oyashio Current, the westward flowing Alaskan Current or Alaskan Stream (actually a branch of the Aleutian Current), and the southward flowing East Kamchatka Current (the Oyashio Current) (see Chapter 2; Fig. 2-10). Although the water is quite cold, there are large air-sea temperature differences. Colder Arctic air flows over the relatively warmer water, producing significant heat and moisture fluxes from the sea to the air. These fluxes make an integral contribution to cyclogenesis, including explosive polar low development favored in the region southeast of coastal Siberia.

3.1.1 Precipitation

The heaviest precipitation in the Bering Sea occurs during the months of November through April with peak amounts in the central Bering Sea. In this region 30% to more than 40% of all observations report precipitation, primarily in the form of snow or snow pellets. A tendency exists in this region for most precipitation to occur with enhanced cloud streets and open-celled convective patterns that accompany northerly flow. This flow is produced as low pressure systems move in a northeasterly direction near the southern portion of the region, exposing all except the southeastern portion of the area to northerly winds. Liquid precipitation, when it occurs during the November to April period, is often in the form of freezing rain or drizzle. Island locations such as the Pribilofs tend to have more frequent precipitation than over the open waters as a result of orographic lifting of the air over the islands.

By May the frequency of precipitation drops fairly drastically in the southern Bering Sea and is most often of the liquid variety. In the more northerly latitudes greater than 25% of all observations indicate precipitation, and 60% to as much as 85% of the precipitation occurs in the form of snow.

July and August are the only months when frozen precipitation becomes a rarity. During these months a minimum of observations indicate precipitation in the northern Bering Sea, with a greater number in the central and eastern regions of the Bering Sea. A minimum also occurs in the western Bering Sea ($< 10\%$). This summer season precipitation pattern is related to the northward migration of the North Pacific anticyclone to a position just south of the Gulf of Alaska (near 40 °N, 150 °W). Storm tracks are steered from southwest to northeast through the central Aleutian chain toward Bristol Bay and western Alaska.

A general decrease in total annual precipitation is found from the south to the north over the Bering Sea because of the ice pack influence; decreasing temperatures, increasing continentality, less open ocean, increased land area, an increase in ice cover over ocean areas, and decreasing moisture sources. As an example the Seward Peninsula has an average annual precipitation of 15 inches (38 cm), whereas the southern region experiences a precipitation amount of about 25 inches (63 cm). Heaviest rainfall occurs in summer when 24-hr amounts may exceed 2 inches (5 cm) in severe storm events.

3.1.2 Snowfall and Snow Cover

Snow occurs more frequently in the northern Bering Sea than in the southern Bering Sea. Because of lower temperatures in the north, the snow is a light, fine type that may drift and pile up to depths of 2 to 3 feet (1 m). Snow can occur as early as September. In the southern portion of the Bering Sea the snow is often wet and heavy. Accumulations generally do not exceed 1 ft (30 cm); however these can occur very rapidly. The wet snow packs very easily and is often melted by rainfall that may follow the snow event. Snow can be expected on a periodic basis from October through April.

Snow showers can be anticipated throughout the region. It is not unusual for a single open cell to cause an accumulation of 1/4 inch (0.6 cm) of snow as it moves over a given

location. Snow from such events is frequently in the form of snow pellets rather than snow flakes. Cold troughs or upper cold lows can be located in satellite data by the accompanying, underlying fields of enhanced open-celled cumulus or cumulonimbus.

3.1.3 Thundershowers

The cold waters of the Bering Sea generally have a stabilizing influence on airmasses that move over them in summer. Even in winter, when the water can be relatively warm in comparison to Arctic airmasses, modification of air occurs fairly rapidly so that potential instability is rapidly lessened, particularly if upper level conditions are unfavorable.

Thundershowers, therefore, are a relatively rare event, occurring mainly in late winter in conjunction with synoptic scale disturbances, such as polar lows (which can achieve synoptic scale), polar or Arctic fronts, or upper level cold troughs on cold low features. The northwestern portion of the Bering Sea produces most of these events.

3.1.4 Temperature

The significant north-south extent of the Bering Sea gives rise to a latitudinal variation in temperature, particularly noticeable in winter. The presence of the Aleutian Low in winter tends to cause warmer temperatures in the central and southeastern portions of the region; colder temperatures are experienced to the northwest where Arctic airmasses flow from off the Siberian mainland. Freezing temperatures are experienced more than 50% of the time for the area just north of the Aleutians from December through May. The frequency of freezing temperatures increases to over 90% of the time from the edge of the pack ice northward. From May through July temperatures warm considerably, with the coldest pocket of air centered over the central Bering Sea. In this region, by July, freezing temperatures are experienced about 8% of the time, and the southward limit of freezing temperatures lies just north of the Aleutians. From June through October warmer temperatures are found near the coasts. This situation reverses during the winter and spring months when colder temperatures occur near the coasts.

August is the warmest month of the year over the Bering Sea. Temperatures range from about 44 °F (7 °C) in the north to 50 °F (10 °C) in the south. By late October freezing temperatures (daily minimums) again move into the northern Bering Sea and gradually extend southward to the Pribilofs by December, as the ice pack is reestablished.

3.1.5 Humidity

The main factors affecting humidity over the Bering Sea are season and direction of wind flow. Humidity is generally high in summer. In winter the central and southeastern portions of the Bering Sea tend to have higher humidities, whereas the northern Bering Sea coastal areas have lower humidities. This difference relates to flow around the Aleutian Low when southerly winds tend to promote moister conditions in the southeastern Bering

Sea due to saturation effects as air is cooled from below. To the north and northwest in northerly cold air outbreaks, cold air over relatively warmer water leads to considerable vertical mixing, which brings about reduced humidities at lower levels.

3.1.6 Cloudiness

The Bering Sea, like the Aleutians, is one of the cloudiest areas in the Northern Hemisphere. During the winter the central Bering Sea experiences broken to overcast conditions more than 85% of the time, averaging only 1 or 2 days per month in which the cloudiness is less than or equal to two-eighths coverage. The cloudiness situation becomes even worse in summer when as many as 95% of the days are overcast.

During both seasons the situation improves from the central Bering Sea toward the Russian and Alaskan coastlines, where during winter as many as 9–12 days per month may be essentially clear. During summer such days occur about half as often. Ceilings are low throughout the year. Cloud tops tend to extend much higher in summer.

It is important to stress the marked change in average cloud top height experienced as one moves from typical midlatitude expectations to conditions over the Bering Sea. In winter even intense cyclones are usually confined to altitudes below 15,000 ft (4572 m). Similarly cloud bases are much lower than normally seen at lower latitudes. A stratocumulus broken to overcast conditions may frequently exist with a base at 800 ft (244 m) or less compared to midlatitude expectations of 1500 ft (457 m) or higher. Cirrus cloudiness in summer and winter is frequently found well below the 20,000 ft (6096 m) level, and the rare thunderstorm events may be topped at 15,000 ft (4572 m) or lower. Cloud tops are often twice as high over islands, however, as over the open water, due to orographic uplifting.

3.1.7 Wind, Visibility, and Cloudiness

Combined optimum factors important for aircraft operations include a ceiling of at least 5000 ft, a visibility ≥ 5 n mi (≥ 9 km), and a moderate wind speed of 11 to 21 kt (6–11 m/s). During winter such optimum conditions prevail only about 2 to 3 days a month. Conditions improve to as much as 6 days per month along the Russian coastal area and west coast of Alaska. Best flying conditions occur following storm passages. Post-frontal cyclonic flow gives rise to open-celled convection and a higher mixed layer depth with improved low level visibility. Although cloud coverage is frequently broken with ceilings < 5000 ft, this is typically the best condition experienced. The situation deteriorates rather drastically from May through August when optimum conditions occur less than 2 days per month in the central Bering Sea and 3 or 4 days per month near the coastal areas. Surface visibility is better during winter than summer as fog is frequent during June, July, and August.

3.1.8 Storm Tracks and Surface Winds

Surface winds over the Bering Sea are closely related to the track of storms through the region. Generally in winter this track is further south approaching from the west or southwest and passing to the east or northeast. In these conditions easterly, northeasterly, and northerly flow is experienced over the lower portion of the Bering Sea. Blocking conditions are favored for extended periods along longitude 140 °W, forcing the Aleutian Low to be centered well to the west near the Kamchatka Peninsula. Under such circumstances meridional flow develops and storms move from south to north through the central Aleutians into the Bering Strait region and into northwestern Alaska. During blocking regimes northerly or northeasterly flow is experienced over the western Bering Sea and southerly or southeasterly flow over the eastern portion. Occasionally (not mentioned in most climatological studies of the region), storms recurve and dissipate as they move northwestward toward Siberia. The strength of the surface wind is closely related to the frontal position and often drops rapidly immediately following passage of the trailing edge of the frontal cloudiness. Frequent satellite views of the region facilitate excellent wind forecasts using the above observation.

During summer the frequency and intensity of storms is considerably reduced. Because of the northward and westward extension of the North Pacific, high warm moist air is advected northward along the western boundary of the high and then turns anticyclonically producing westerly or southwesterly flow over the region. Cooling by the underlying cold water gives rise to extensive prolonged periods of low overcast cloudiness and fog. West to east storm tracks also tend to move to a more northerly latitude producing westerly flow in the southern Bering Sea and northerly or northeasterly flow in the northern regions.

Major weather producers in the fall are the recurving, extra-tropical storms. When tropical, these storms normally track westerly toward southeast Asia, then, as they recurve, track northerly east of Japan and northeasterly into the Bering Sea or easterly into the Gulf of Alaska. These storms are often intense with gale winds a frequent occurrence. Heavy rainfall is generally present because of the high moisture content still remaining from the storm's tropical origin.

3.1.9 Bering Sea Ice

The ice pack coverage of the Bering Sea has an important influence on the climate of the region. The ice distribution in the Bering Sea is closely related to both the seasonal cycle and shorter term circulation regimes and synoptic patterns. Interseasonal variations of prevailing long-wave patterns are reflected in the timing of onset of fall freezeup, spring breakup or melt, and winter extent and character of the ice pack. On a year-to-year basis the mean location of the winter months ice edge may vary by as much as 150 n mi (278 km) (Barnes and Bowley, 1979). During the growth and retreat the ice edge position or areal coverage may vary by a couple hundred nautical miles (300–400 km) over a day or two under reversals of strong northerly and southerly winds or vise versa.

The winter ice pack acts to extend the area of continental type climate southward over the Bering Sea by significantly reducing the source of heat and moisture flux from the sea surface. The prevailing northerly flow from off the high pressure dominated landmasses and out *over* the Bering Sea results in the pack-ice-covered areas remaining generally cloud free. However, extensive areas of convective type cloud streets form *off* the ice edge and extend hundreds of nautical miles (hundreds of kilometers) seaward under strong off-ice flow. Small scale cyclones, referred to as polar lows, frequently form within a couple hundred nautical miles (300–400 km) of the ice edge. With certain upper air patterns, polar lows can persist for several days while migrating eastward across the Bering Sea parallel to the ice edge.

The formation and growth of the ice during the freezeup season are governed by the air and water temperatures and the prevailing wind regime. The breakup, or melting, of the pack is largely controlled by the timing of the northward shift of the storm track. Shorter term fluctuations of the ice edge location are determined by the track and intensity of individual synoptic highs and lows. The initial development and ultimate extent of the ice pack is strongly influenced by the proximity of cold landmasses and local ocean depths. The wide relatively shallow continental shelf area of the eastern portion of the Bering Sea results in much greater areal coverage of sea ice in that region than over the deeper waters south of Siberia (Ahlnäs and Wendler, 1979).

The shallow coastal areas of northern Bristol Bay experience ice formation as early as September and as late as June. Extensive ice coverage occurs throughout Bristol Bay from December through April. The harbor of Cold Bay, located near the southwestern end of the Alaska Peninsula, may be closed by ice for a month or more from January into April. Bays, inlets, and harbors of the Aleutian chain west of Unimak Pass (about 165 °W) will experience some ice cover during the coldest periods of winter (December through March).

Freezeup starts in Norton Bay in eastern Norton Sound by late October and proceeds rapidly southward along the shallow coastal zones that are cooled by flow off the landmasses. Around the first of November the Bering Strait and Gulf of Anadyr on the Siberian side become ice covered. Ice extends southward beyond eastern St. Lawrence Island to Nunivak Island. By early to mid-December the ice edge reaches St. Matthew Island and extends into Bristol Bay. The last area to freeze is south of St. Lawrence Island in the central Bering Sea.

The southward advance of ice coverage over the Bering Sea occurs quite rapidly from early November through late January. The maximum areal coverage is typically reached during late March or early April. Retreat of the ice edge is also quite rapid, occurring mostly during June. By July the Bering Sea is basically ice free and remains so until early October when coastal ice begins to form in coastal bays and inlets along the shores of the Seward and Chukotsk peninsulas. Table 3-1 provides average dates for southward advances and retreats of the ice edge ($\geq$ one-tenth coverage) through the Bering Strait.

It should be noted, however, that sea ice generally develops in Norton Sound and the Gulf of Anadyr and other coastal areas of bays and inlets before ice edge passage through the Bering Strait. Ice also tends to persist in those same regions after the retreat of ice through the Bering Strait. In fact, most of the Bering Sea ice is formed along the shores

TABLE 3-1. WEEK OF THE YEAR OF ICE EDGE (≥ ONE-TENTH COVERAGE) ADVANCE AND RETREAT PASS 65.5°N AT 169°W, APPROXIMATE CENTER OF THE BERING STRAIT, FOR THE PERIOD 1972 THROUGH 1986

	Earliest	Average	Latest
Southward advance	week 45 (1975)	week 47	week 51 (1978)
Northward retreat	week 18 (1979)	week 24	week 27 (1973)

of the Seward and Chukotsk peninsulas and advected southward across the Norton Sound and Gulf of Anadyr over the northern and central Bering Sea.

The mean southern winter limits of sea ice are closely related to the edge of the continental shelf (see Chapter 2; Fig. 2-7) and closely bounds the 100 to 200-m depth contour interval. The 200-m contour marks the edge of the continental shelf where depths drop off rapidly to 2000 m, frequently within 50 to 100 n mi (93–185 km). The entire northeastern sector of the Bering Sea overlies a continental shelf, but only a very narrow shelf exists along the Siberian coast from Cape Navarin southwestward.

The ice forms in situ during a typical ice year in the shallow (<100 ft or <30 m) waters of Norton Sound and the eastern Bering Sea where isothermal water of 29°F (−1.8°C) develops. Under prevailing northerly to easterly wind the ice is advected southward into regions of warmer water.

Pease (1980) described the Bering Sea ice advance characteristics as those of a "conveyor belt," growth occurring in the north and advection by the wind to the south. The leading edge ice melts and cools the water column, thereby enhancing the wind-forced advance of the ice edge. Because of this southward advection of ice, persistent polynyi are formed in the lee (southern side) of islands such as St. Lawrence, St. Matthew, and Nunivak. Because of the conveyor belt action persistent leads also form seaward of the land-fast ice along south-facing coastlines.

The exact location and configuration of the ice edge is very sensitive to wind patterns. The location of the edge can fluctuate rapidly under reversing northerly or southerly winds. With the onset of winter the combination of high pressure development over the Siberian landmass and resulting southward shift of the cyclonic storm track to south of the Aleutian chain results in prevailing north-to-northeast flow over the ice-covered portion of the eastern Bering Sea. Under this forcing the ice edge advances southward where the leading edge encounters warmer water and on-ice swell action. The interactions of off-ice wind, on-ice swell, and increasing sea surface termperatures to the south result in recurring ice edge configuration characteristics, which are described in the following paragraphs.

The leading portion of the ice divides into three zones referred to as the edge, transition, and interior zones (Squire and Moore, 1980) during periods of off-ice flow. A schematic diagram showing both the horizontal and vertical dimensions of ice in the three zones is shown in Fig. 3-1. The edge zone is characterized by formation of long, linear bands of

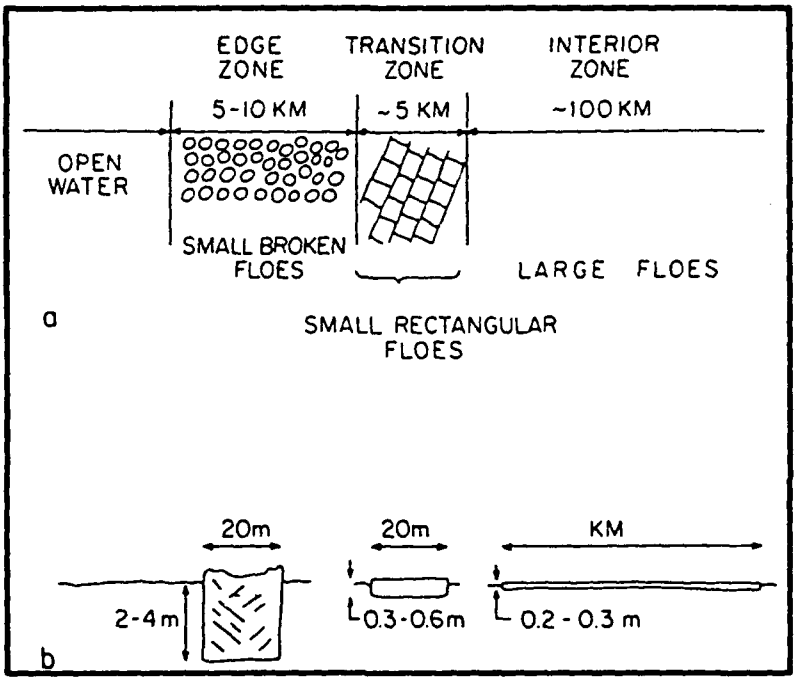

Figure 3-1. Schematic diagram of the three kinds of ice that occur near the ice edge, proceeding inward from open water. The upper part of the figure shows the ice in plan view; the lower part, in side view (Bauer and Martin, 1980).

ice up to 5 to 10 n mi (9–19 km) long and 1/2 n mi (0.9 km) or so wide (Bauer and Martin, 1980). These bands become nearly perpendicular to the wind and move southwestward faster than the main body of pack ice. The edge zone consists of small broken floes that are heavily rafted and ridged with increasing sail heights and keel depths. The rafting and ridging result from opposing wind and swell interactions. The edge zone ice moves faster downwind, probably due to the increased aerodynamic roughness, and tends to separate from the rest of the pack. This advanced location leads to rapid melting, exposure of the trailing pack to undampened southerly swell, and development of a new edge zone. Because of the reduced swell amplitude (damped by the edge zone) the waves fracture the ice in the transition zone into small rectangular floes but do not heavily raft or ridge it. The interior zone is marked by an abrupt transition to a region of large floes measuring miles in extent.

During on-ice wind flow, the ice edge becomes compact with only widely scattered ice seaward from the compact ice edge. Under persistent strong on-ice flow during the freezeup season the edge can make dramatic retreats of hundreds of miles. In general, polynyi will form on the reverse sides of islands and coastal areas under on-ice flow. Thus, the polynyi change location from the prevailing south facing sides to the north facing sides.

The ice pack of the Bering Sea is composed of nearly 100% first year ice. The sea becomes free of sea ice each summer, and advection of multiyear ice from the Arctic Ocean basin region is rare. Ice pack thickness varies from 1.6 to 6.5 ft (0.5–2 m), and most of the area is covered by 3.3 ft (1 m) or less thick ice.

A persistent north setting current flows through the Bering Strait, which, in general, cuts off advection of any multiyear ice out of the Arctic Basin (Pritchard et al., 1979). Only under particular circulation patterns, characterized by strong high pressure over northeast Siberia and a deep low in the Gulf of Alaska, will the northerly winds become strong enough to advect multiyear ice southward through the Bering Strait. Pritchard et al. (1979) determined that a pressure difference of 20 mb must be created between Cape Schmidt, Siberia (higher pressure), and Nome, Alaska, to reverse the flow through the Bering Strait. This results in an outbreak of Arctic basin ice from the Chukchi Sea, which may contain thicker multiyear ice, into the northern Bering Sea. The circulation pattern resulting in these outbreaks may occur a couple times each winter and remain for a day to a week or so each. The pattern is characterized by an intense high pressure cell over northeastern Siberia and a deep low pressure cell in the Gulf of Alaska. High pressure and strong northeasterly flow will dominate the eastern Bering Sea in the steep gradient zone between the two cells.

The evolution of mean ice coverage, illustrated in Figs. 3-2 through 3-5, provides frequencies of occurrence of ice of any kind (land fast or pack and first year or multiyear). By November (Fig. 3-2) ice prevails in the coastal regions of the Seward and Chukchi peninsulas as denoted by the 60% or greater frequencies of occurrence. All coastal bays and inlets of Alaska and Siberia from northern Bristol Bay northward to St. Lawrence Island and then southwestward to the Kamchatka Peninsula experience ice cover from 10% to 70% of the time in November. The continental influence is strongly evident in the ice coverage pattern during the autumn freezeup period.

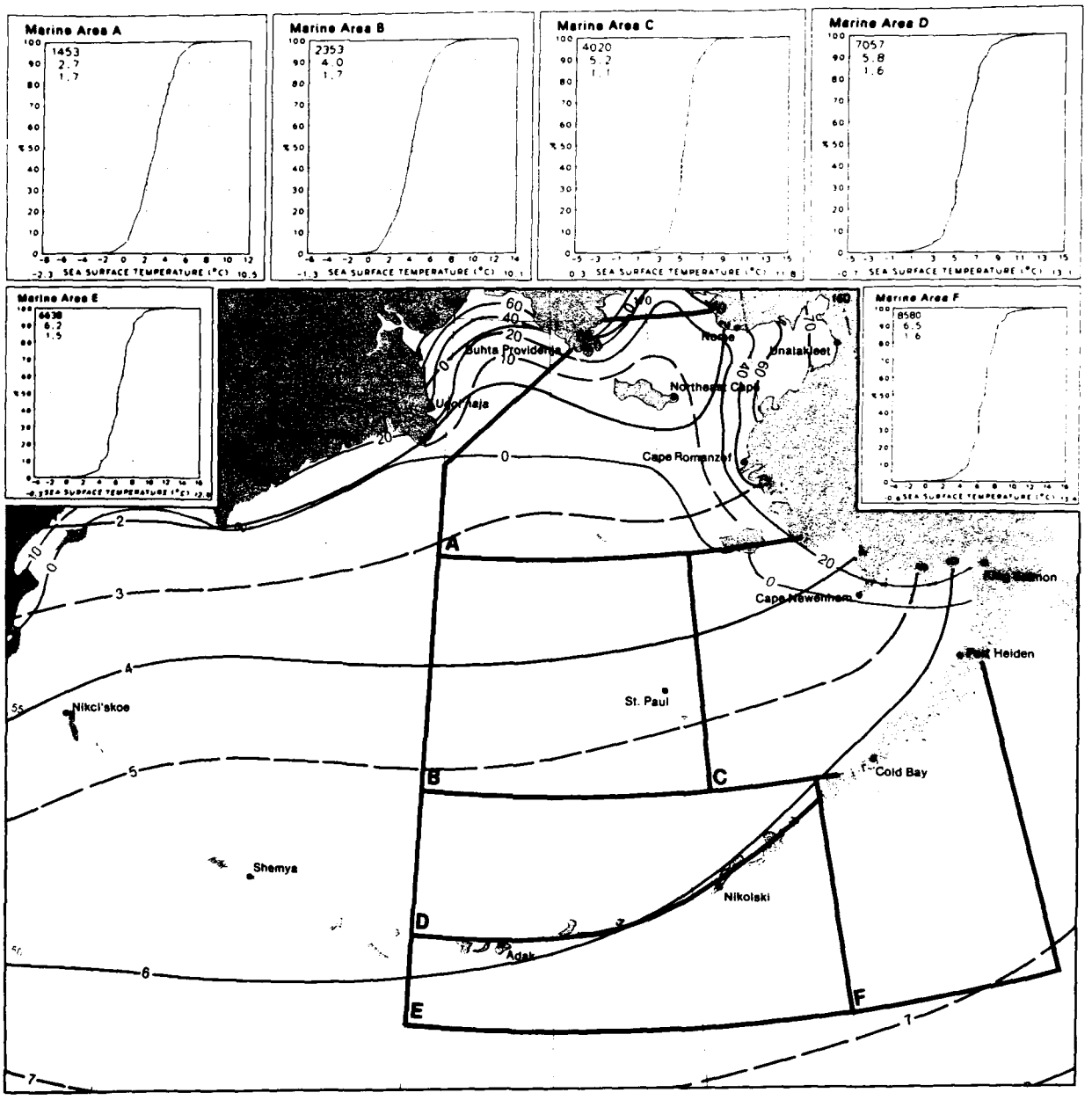

Figure 3-2. Mean sea surface temperature (°C) and ice of any kind—November (Brower et al., 1988).

By January (Fig. 3-3) the 100% frequency ice coverage reaches St. Lawrence Island and extends southeastward along the Alaskan coast and southwestward along the Siberian coast to northern Kamchatka. The ice coverage frequencies continue to reflect the continental influence as well as the bathymetry pattern of the extensive shallow continental shelf of the eastern Bering Sea. It is during this freezeup and general advancing ice period that rapid advances of the ice edge by hundreds of miles can occur in a matter of days. These

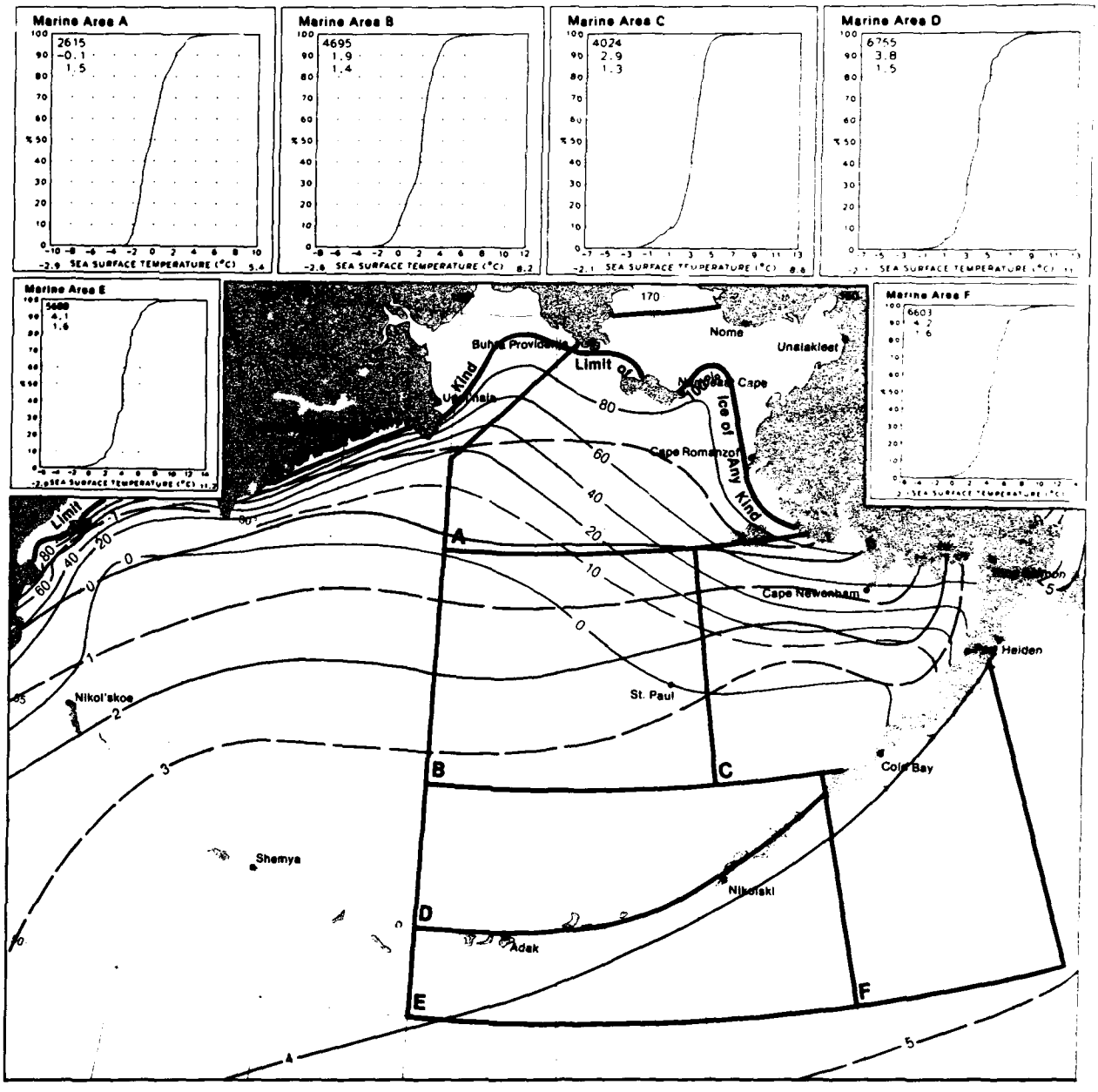

Figure 3-3. Mean sea surface temperature (°C) and ice of any kind—January (Brower et al., 1988).

large advances typically occur following periods of temporary retreat (northward advection) of the ice under strong southerly flow. Because the shallow water column has been preconditioned to near isothermal 29 °F (−1.8 °C) temperature, the return to northerly flow results in combined wind advection of ice and in situ freezing of ice. The result is an advance of ice coverage at much greater speeds than possible from ice advection alone.

The maximum coverage of ice typically occurs in late March or early April. Figure 3-4 shows the March coverage, which on average includes the maximum area of 100% coverage

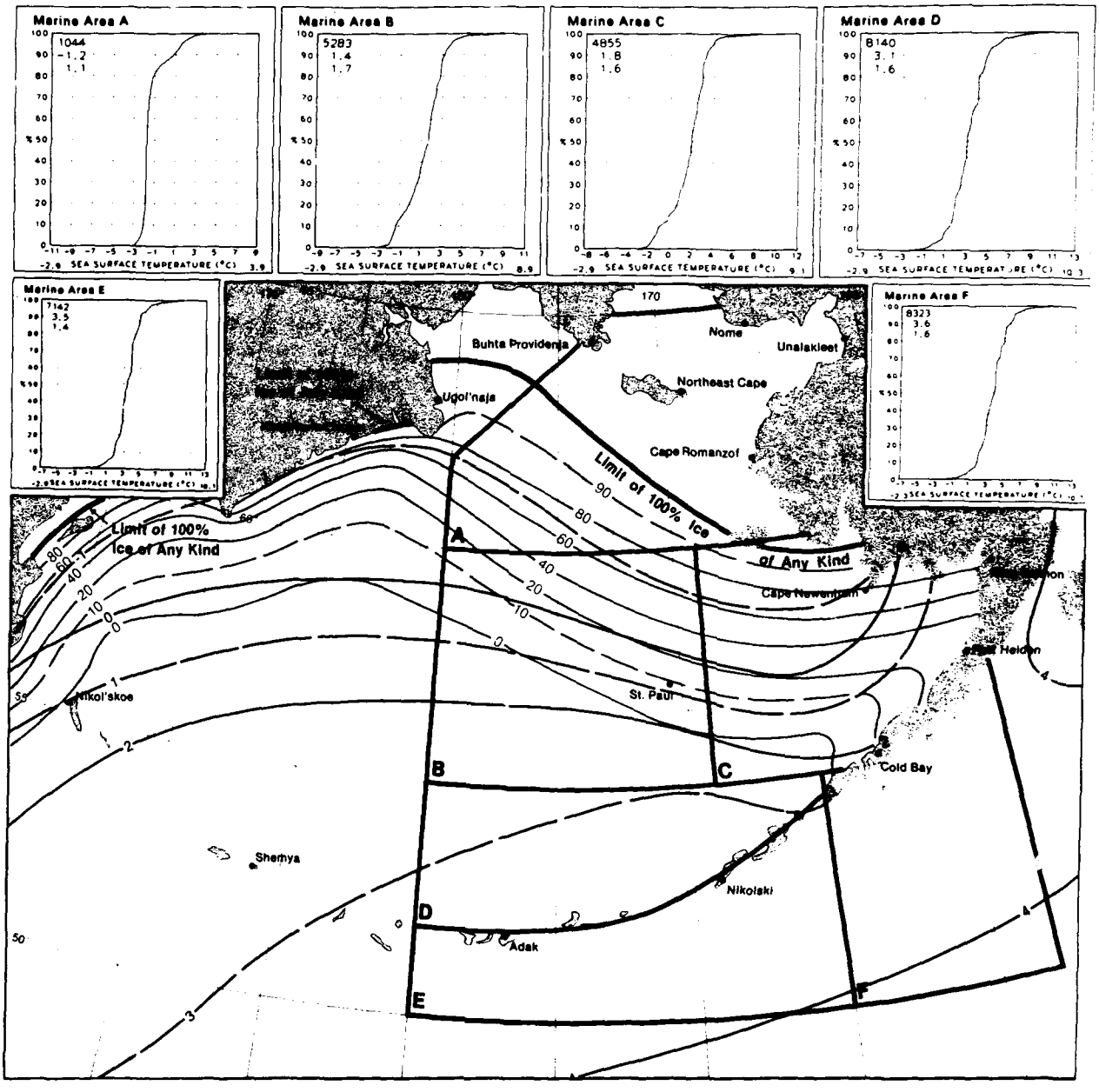

Figure 3-4. Mean sea surface temperature (°C) and ice of any kind—March (Brower et al., 1988).

as well as extreme advances of lesser frequencies over the eastern Bering Sea. The mean April conditions (not shown) show slightly greater advances of the lower frequencies over the western Bering Sea, but lesser advances over the eastern portion.

By June (Fig. 3-5) a rapid retreat has occurred. The retreat occurs largely during the month of June. The spring retreat is usually not as dynamic as the autumn advance. This results from the weakening storm systems of spring into early summer compared to intensifying systems of late fall into winter. The delay of the marine ice season as compared to continental seasons contributes to these differences in freezeup and breakup (melt) time and intensity. By early July the Bering Sea becomes ice free and remains so until late September when the first small bays and inlets along extreme northern Bering Sea coasts experience the start of freezeup.

Table 3-2 provides information on the advance, retreat, interannual variability, and extremes of ice edge location for the period 1972 through 1987 along the 171 to 167 °W longitude corridor. Data are presented for the "ice year" at 2-week intervals starting in mid-November (week 46) and ending in late June (week 26). The corridor extends southward from the midpoint of the Bering Strait (65.5 °N, 169 °W) to the southern limit of ice coverage, 56 °N for this data set.

The general variability as well as seasonal traits of Bering Sea ice coverage is evident in several of the statistics in Table 3-2. The mean edge location values show a steady advance southward until late February (58.14 °N), then a small retreat by early March (58.40 °N) that may reflect the period of southerly flow associated with the "February thaw" event, noted as a singularity of that region. Following the retreat, an advance to 58.05 °N, maximum mean extent for the corridor, occurs by late March. The means for the 10-week period of early February through mid-April are all between 58.05 and 58.97 °N. This is the ice "winter" period when the coverage is maximum and the interannual variations, as reflected by the smaller standard deviations, are smallest. The larger standard deviations during the preceding ice growth and following retreat periods reflect the atmospheric wind and ice coverage tendencies for warm southerly or ice retreat and cold northerly or ice advance conditions. The interannual variations between extreme northern and southern locations also tend to be largest during the early and late "ice year" periods, with variations that approach 400 n mi (741 km) during the early retreat (mid and late May, weeks 20 and 22 having up to 6.5 ° of latitude difference). There is a strong indication of persistence within a given year of maximum or minimum coverage. Persistent maximum coverage is indicated in 1976 and minimal coverage in 1979. Both years record extreme conditions in 7 of the 17 biweekly periods in Table 3-2. Also of interest, no cases of change occurred from one extreme to the other within an "ice year," which reflects a strong tendency for interyear persistence. This does not preclude events of large week-to-week changes. The following events of large changes in ice edge location during the period covered in Table 3-2 illustrate this fact:

1972 week 1 to 2	62.00 ° to 59.88 °N
1974 week 2 to 3	61.00 ° to 58.75 °N
1979 week 4 to 5	63.88 ° to 59.50 °N
1976 week 25 to 26	60.75 ° to 64.88 °N

The years of 1972, 1974, and 1976 had greater than normal coverage, and 1979 was generally the year of minimum coverage for the 1972--87 period.

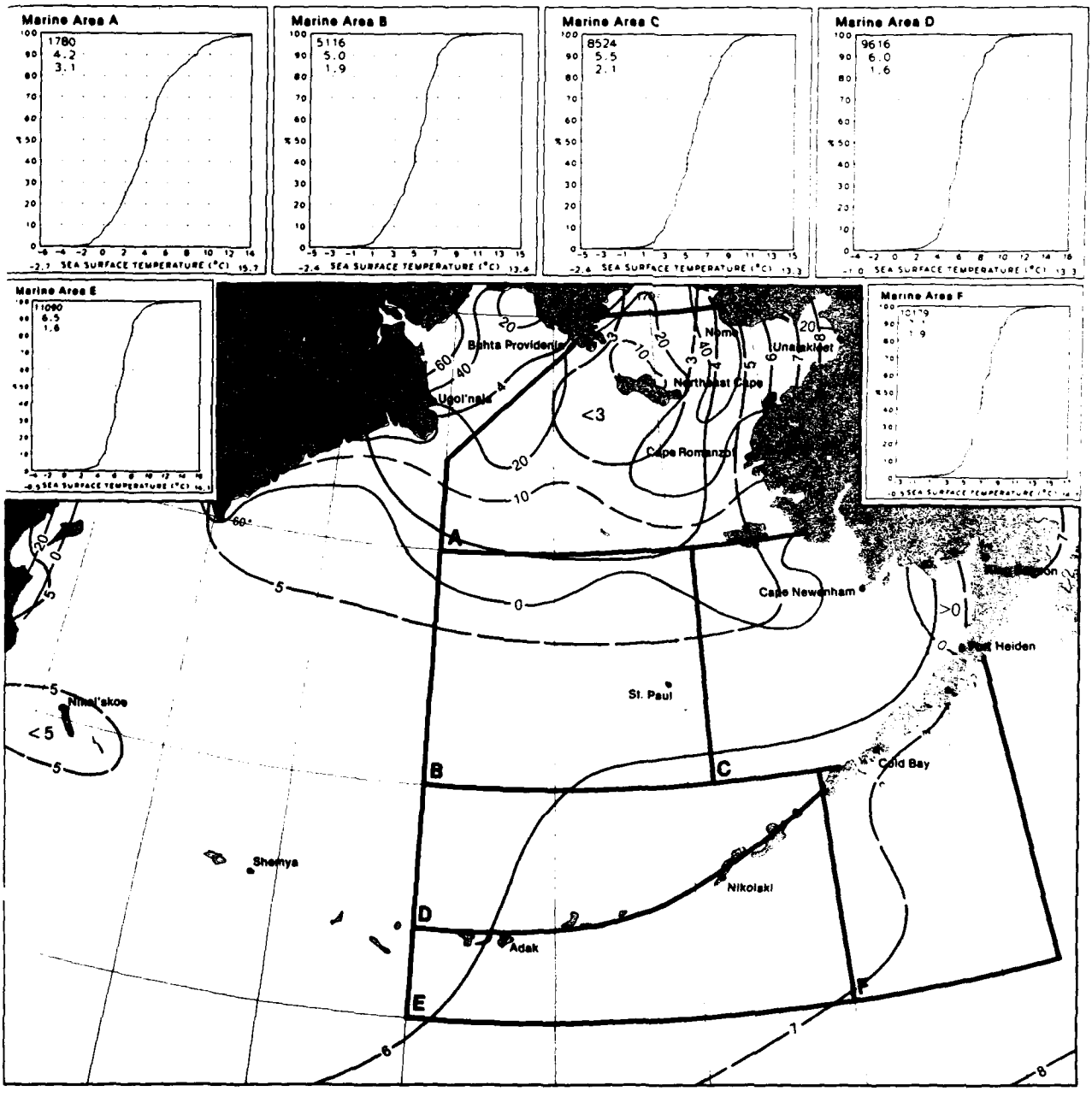

Figure 3-5. Mean sea surface temperature (°C) and ice of any kind—June (Brower et al., 1988).

TABLE 3-2. ICE EDGE LOCATION BETWEEN 171°W AND 167°W FROM MID-NOVEMBER THROUGH JUNE AT TWO-WEEK INTERVALS FOR THE PERIOD 1972–1987. DATA SOURCE: DIGITIZED WEEKLY JIC, SUITLAND ICE CONDITION CHARTS

Time of Year	Mean Latitude	Extremes (year)
Week No.	Standard Deviation	Northern and Southern
Mid Nov	65.04	65.50 (several)
Week #46	1.08	62.76 (1975)
Early Dec	63.49	65.50 (several)
Week #48	1.85	61.26 (1976)
Mid Dec	61.87	65.32 (1978)
Week #50	1.93	59.32 (1974)
Late Dec	60.89	63.69 (1984)
Week #52	1.66	58.63 (1974)
Mid Jan	60.27	62.75 (1979)
Week #2	1.69	57.94 (1983)
Late Jan	59.47	63.69 (1979)
Week #4	1.66	57.94 (1980)
Early Feb	58.97	62.88 (1985)
Week #6	1.40	59.94 (1976)
Late Feb	58.14	60.69 (1979)
Week #8	1.10	56.63 (1975)
Early Mar	58.40	60.19 (1982)
Week #10	0.93	56.63 (1984)
Late Mar	58.05	59.44 (1981)
Week #12	0.95	56.38 (1976)
Early Apr	58.28	61.50 (1979)
Week #14	1.36	56.00 (1976)
Mid Apr	58.75	62.63 (1981)
Week #16	1.76	56.32 (1974)
Apr - May	59.23	64.57 (1979)
Week #18	2.34	56.69 (1976)
Mid May	60.55	64.00 (1979)
Week #20	2.05	57.50 (1972)
Late May	61.54	65.00 (1981)
Week #22	2.06	58.50 (1976)
Mid Jun	63.03	65.50 (1979 and 1982)
Week #24	2.03	60.13 (1975)
Late Jun	63.93	65.50 (several)
Week #26	1.57	61.19 (1976)

Notes to Table 3-2:

1. The ice edge latitude values represent an average of conditions between 171 °W and 167 °W at quarter degree intervals.
2. By week 28 (mid-July) the Bering Sea is basically ice free.
3. Location 65.5 °N, 169 °W is considered center of Bering Strait in this study.
4. During this 16-yr period all minimum coverages occurred in 1978 and following years; all but three maximum coverages were in the 1972 through 1976 period.
5. The sequence of standard deviations reflect large interannual variations during freezeup and melt, and less variability during the period of maximum coverage.

3.2 Aleutian Islands

The Aleutian Islands have received a reputation for having a climate considered to be one of the world's worst. However from a standpoint of temperature and precipitation extremes, this is certainly an exaggeration. Winter's cold winds from the north are rapidly warmed through heat flux from the water, whereas summer's warmer winds from the south are cooled from the same source. Therefore, winters are mild and summers are cool, avoiding the harsh extremes of either the Arctic or desert environment. Precipitation is predominantly accumulated in the winter as a result of the frequent passage of storms, and throughout the year it is more than ample to support a vigorous development of flora and fauna. Few trees exist, however, because of the volcanic nature of the islands' soils. The variety of smaller plants, flowers, and wildlife thriving in this environment make it a "dream world" for the biologist.

From the point of view of the Navy sailor or aviator, however, the Aleutians' reputation for foul weather can hardly be exaggerated. Storms passing the Aleutians usually arrive from the west as deep occluded systems, sometimes as transformed versions of typhoons that have "gone extratropical." Winds at sea and exposed regions on the islands often exceed hurricane force, sometimes further strengthened as a result of venturi effects through mountain passes or ocean gaps between islands. It has been reported that at Shemya Air Force Base the local wind indicator is a log attached to a chain hanging vertically, suspended above the ground from a horizontal beam. When the log and chain are blown by the wind to a position horizontal to the ground it is generally considered unsafe to venture out-of-doors.

Visibilities are frequently severely restricted by fog, which can persist for days without improvement and for lesser periods on the islands and at sea through intense precipitation in cyclone activity. The tendency for extended consecutive days of bad conditions can be very frustrating for operations at sea, in the air, and at naval and air installations on the islands.

3.2.1 Precipitation

The most frequent precipitation period ($>30\%$ of all observations) occurs mainly from December through April. More than 50% of the time during this period precipitation is

of the frozen form, and the frequency of frozen precipitation increases gradually to the west from about 50% near Cold Bay to 90% or more over the Commander Islands. During May and June precipitation is the lightest of the year, when only about 15% of the stations report precipitation, all of which is in liquid form.

Convective showers produce rainfall on a 15 to 20% frequency from July through September, and by October and November snow begins reappearing at similar frequencies.

3.2.2 Snowfall and Snow Cover

During winter snow frequently covers the ground but the depth of coverage rarely exceeds 1 ft (30 cm). High winds, however, cause snow to drift so that depth at an individual location is highly dependent on topography. Some depressions may fill to depths exceeding 6 ft (1.8 m), and other areas remain relatively free of snow. Because of the relatively mild temperatures the snow is frequently of the wet, heavy type. Annual rainfall for the islands averages 40 to 50 inches (102–152 cm), and, again is heavily influenced by topography so that individual locations may have quite different rainfall amounts even though they are separated by only a short distance.

3.2.3 Thundershowers

Thundershowers are a rarity in the Aleutian Islands region with an expected frequency of only 1 or 2 thundershowers per year at a given location. These usually occur during the winter months in association with frontal activity and orographic uplifting effects, or with unusually cold temperatures and an upper cold low or trough aloft. The cumulonimbus clouds are not of the giant variety found in the tropics and midlatitudes where tops reach 50,000 ft (15.2 km) or higher. Lightning and/or thunder has been observed in the Aleutians with cloud tops at 10,000 ft (3 km). Effects on the ground resulting from convective cells are also less dramatic compared to more southerly regions. Strong winds, heavy downbursts, and heavy precipitation are usually not observed.

3.2.4 Temperature

The modifying influence of the water surrounding the Aleutians causes air flow in cold winter surges to be warmed as the air moves over the water. Conversely, warm air moving northward is cooled due to the loss of heat to the colder water. This event results in a relatively small annual temperature range. Winter temperatures are near or slightly below freezing, and summer temperatures rarely exceed 65 °F (18 °C). Average temperatures show little variation from the Alaska Peninsula out to Adak, during winter, but then drop by 7 to 12 F° (4–6 C°) westward along the island chain to Nikol'shoe in the Commander Islands. During May through October little longitudinal variation in temperature occurs along the entire chain.

3.2.5 Humidity

Relative humidity along the chain is high in summer with values of 90% or more about 50% of the time. In winter relative humidity is also high, especially during frequent storm episodes. The overall winter average value is close to 80%.

3.2.6 Cloudiness

The Aleutian chain is considered to be one of the cloudiest regions in the Northern Hemisphere. More than 90% of the time broken to overcast conditions exist during the summer; the figure improves to about 50% during the fall and winter. According to Grubbs and McCollum (1968), "throughout the year the islands of the Aleutians experience only 2 to 4 clear days per month."

Satellite data yield some useful relationships for predicting clear sky scenarios. With low pressure to the east giving cold surge effects, and northerly flow across the Bering Sea, expect clear skies up to 60 n mi (111 km) to the lee (southside) of the islands resulting from topographical blocking. Figure 3-6 shows an example typical of such conditions on 12 April 1985. Von Karmen vortex effects, apparent to the lee of a few of the islands, indicate that low level inversion conditions existed over those islands and that the islands protruded above the inversion in the local area (see NTAG Vol. 1, Sec. 2C).

During winter decreased cloud cover is favored in col regions between pressure centers. When a col region is predicted to move over a given location a partly cloudy sky forecast can be made with some confidence.

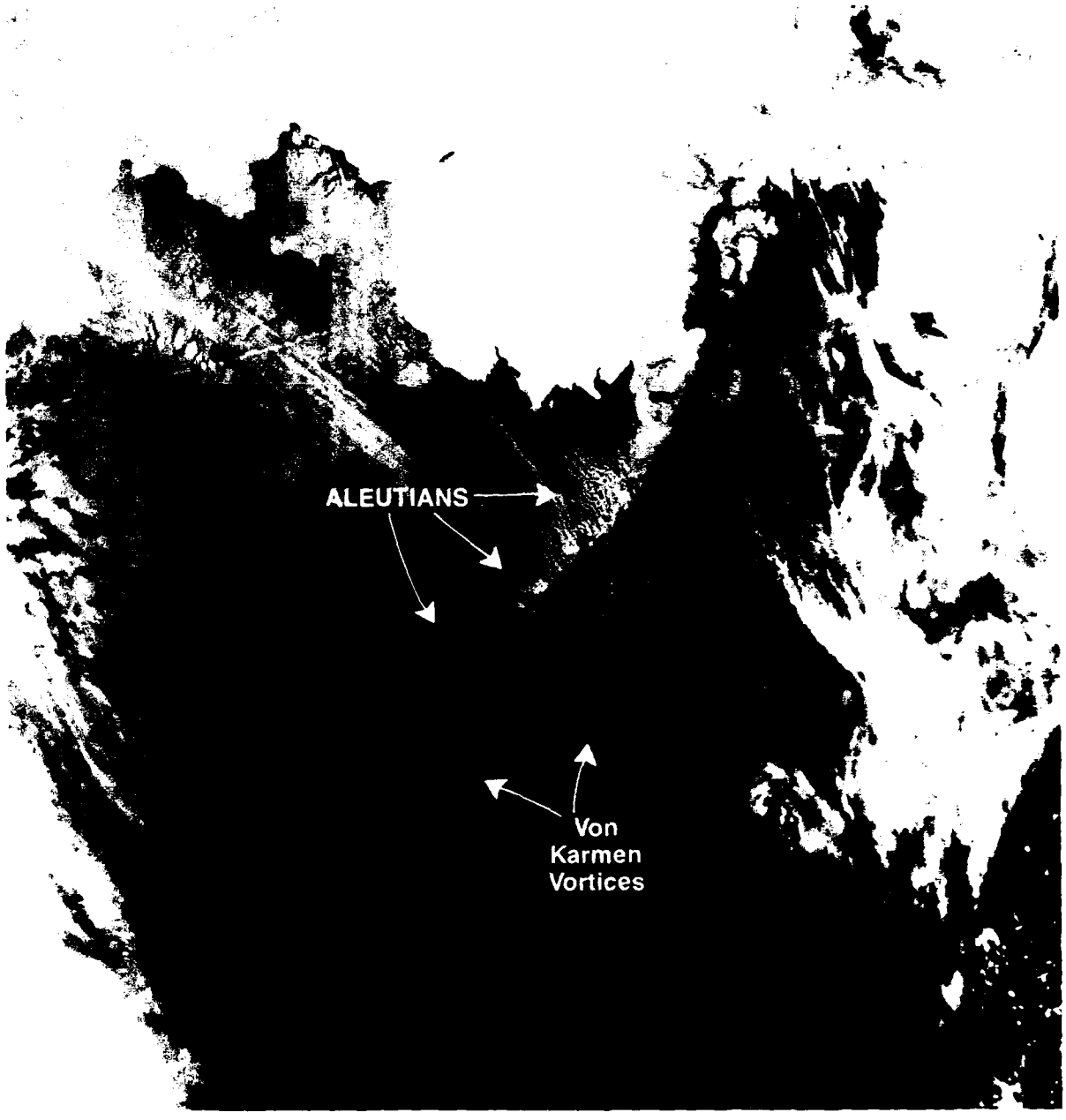

Figure 3-6. DMSP infrared imagery 0551 GMT 12 April 1985.

During the summer period the location of high pressure centers is the key to cloud cover forecasts. The high center itself and ridge lines emanating from the high tend to be overcast in low stratus or fog. When the high center is south of the islands and flow around the high extends over the islands into the Bering Sea, low overcast cloudiness conditions are often found in southerly flow on the west side of the high. Clearer conditions are evident east of the high center and particularly in northerly flow south of the island chain east of the high center. Figure 3-7 shows an example of such a condition on 17 July 1989. Drying of air lifted over the island chain and the normal condition of subsidence in a southward trajectory of northerly (anticyclonic or straight-line) flow over the ocean contribute to the clearing effect. Cloudiness reappears when flow changes from anticyclonic or straight-line flow to flow with cyclonic curvature.

3.2.7 Visibility

July and August are the months with the poorest visibility; 30% of the time visibility is less than 1 n mi (1.9 km) and the ceiling is less than 1000 ft. The rest of the year such conditions occur only about 10% to 15% of the time. Fog and precipitation, frozen and liquid, are the most common obstructions to vision. The Alaska Peninsula enjoys better visibility than the Aleutian Island chain, especially in the interior and on the northwest coast.

3.2.8 Storm Tracks and Surface Winds

Storms generally track from southwest to northeast through the Aleutians into the Bering Sea where eventually they impinge on the coastline of western Alaska. A secondary storm track causes a diversion of the storm center into the Gulf of Alaska. Such storms may originate northeast of Japan, and occasionally as polar low developments off the coast of Siberia where they begin a trajectory to the southeast. During periods of blocking (frequently in January and February) storms move through the islands from the south to the north, occasionally recurving westward toward the Siberian coastline.

Winds on the islands are routinely from the north to northwest during winter and from the southwest during summer. Actual direction varies drastically at different locations on the islands due to effects of topography. Highest speeds, of course, are normally in association with intense storm development during the winter. Speeds of 85 kt (44 m/s) and higher are common on all of the islands, often exaggerated by venturi effects in gap regions and in channels between islands. When a jet stream crosses the islands, producing winds in excess of 50 kt (26 m/s) at the 850-mb level, low-level turbulence can be extreme, as gusty winds reach the surface in terrain-induced eddy formations. Cancellation of flights into Adak, as an example, is frequently caused by such effects with strong winds from the south.

The Aleutian chain is famous for intense northerly down-slope winds called "williwaws." These winds result from a release of cold dense air that builds on the windward slopes of the mountains and then falls and gathers momentum due to gravity on the leeward side. Speeds of gale force and higher are common. Such winds occur most frequently in the winter when the land is coldest relative to the surrounding water. When snow is on the

Figure 3-7. DMSP visible imagery 1634 GMT 17 July 1989.

ground, intermittent gusting winds may cause an immediate deterioration in visibility as snow is lifted and blown about. The characteristic of repetitive sequences of onset and cessation make winds of this type extremely hazardous.

3.3 Gulf of Alaska

Weather in the Gulf of Alaska is modulated by several factors. Very important is the warm oceanic Alaska Current that moves northward along the coast until forced to turn cyclonically westward by the terrain of southern Alaska. The cyclonic rotation continues so that a huge gyre is created centered near 50 to 53 °N, 140 to 145 °W throughout the year. The relatively warm temperature of the water greatly modifies the climate of coastal regions so that mild temperatures are generally experienced.

Atmospheric cyclogenetic events are also quite common over the gulf. The surrounding mountainous terrain and blocking effect of the coastal area significantly affect weather systems that are forced to slow down from previous speeds over open water. Occasionally, cyclone centers appear trapped over the gulf and linger before being forced to move onshore, or simply dissipate in place, having spent much of their life cycle in the region. It is also the site of significant cyclogenesis, often occurring when cold, winter surges plunge southward into the region and merge with warmer air coming up from the south. The cold continental climate of interior Alaska is felt at times in coastal regions, especially in mountain gap areas where cold dense air is accelerated with jet stream force from land to the offshore waters.

3.3.1 Precipitation

Precipitation is maximized along the coastal regions and averages from 30 to 60 inches (76–152 cm) annually with some individual locations recording as much as 231 inches (587 cm) (Grubbs and McCollum, 1968). Heaviest precipitation occurs during the fall and winter when all observations report precipitation 15% to 30% of the time—again, tending to be much heavier along the coast. Frozen precipitation occurs most frequently further north in the Anchorage, Homer, Kenai, and Valdez areas, for example; but even in January, most of the precipitation over the gulf is in the form of rain or wet snow. These conditions do imply a serious aircraft icing hazard at low altitudes. The driest conditions in the gulf occur May through August. However, occasional cyclone activity still brings 8 to 12 days per month of significant rainfall to coastal regions, lessened considerably in terms of frequency and amount in the middle of the gulf.

3.3.2 Snowfall and Snow Cover

Snowfall occurs fairly frequently during fall, winter, and spring. Amounts can be heavy in coastal regions and along frontal zones and low pressure regions. Snow depths along the coast generally average from 2 to 3 ft (1 m), but commonly drifts of 6 ft (2 m) or

higher are found in local areas. Because of the relatively mild temperatures snow is often of the heavy, wet variety, which does not attain great depth and frequently melts completely even in the middle of winter or during periods of rain. Heads of inlets and other protected areas may experience especially heavy snowfall; snow cover at Valdez is among the greatest for sea level stations worldwide. Heavy snowfall and avalanches commonly occur in the mountainous terrain (the "wall") surrounding the gulf. Snow is a rarity in the gulf from June through September.

3.3.3 Thundershowers

Because of increased offshore activity in and around the Gulf of Alaska, thundershower sightings appear to be more common than hitherto perceived; they also occur frequently along the coastal mountain ranges that surround the gulf. In winter cold air moving southeastward over the gulf from western Alaska gathers much moisture that is actively released in thundershowers when the air is uplifted over the mountains of southeastern Alaska. "Sea breeze fronts" will also produce thundershowers along the gulf coast, especially when coupled with a slight upper level short-wave feature. Frontal thundershowers are common in extreme southeastern Alaska especially during the summer months. Also, with easterly 700-mb flow, thundershowers can be advected from British Columbia into the southeastern Alaska region. Coastal thundershowers in this area are normally accompanied by low ceilings, heavy precipitation, and violent or gusty surface winds, in contrast to much more benign conditions experienced in thundershowers over the Aleutians and Bering Sea where vertical development is suppressed.

3.3.4 Temperature

The mean air temperature in the central gulf ranges from about 41 °F (5 °C) in January to 55.4 °F (13 °C) in August. Coldest temperatures are found along the coast of Alaska. Figure 3-8 shows the mean air temperatures and frequency of days with below 32 °F (0 °C) readings during January. The August temperature distribution is shown in Fig. 3-9. The winter continental effect is drastic. It implies that on an average winter day a ship entering Cook Inlet would experience an outside air temperature of 35.6 °F (2 °C). A few hours later on arrival at Anchorage the temperature would drop to 17.6 °F (−8 °C). Add to this a northeast wind of 16 kt (8 m/s) and a wind chill of −20.2 °F (−29 °C) would be experienced. This is not an uncommon event!

3.3.5 Humidity

Relative humidity over the gulf is highest in the early morning and lowest by midday. It increases again with nightfall. Coastal areas show the greatest variation, being subject to episodes of relatively dry offshore flow. Cold interior air holds very little moisture, hence, when north or northeast winds blow offshore, very low humidity results.

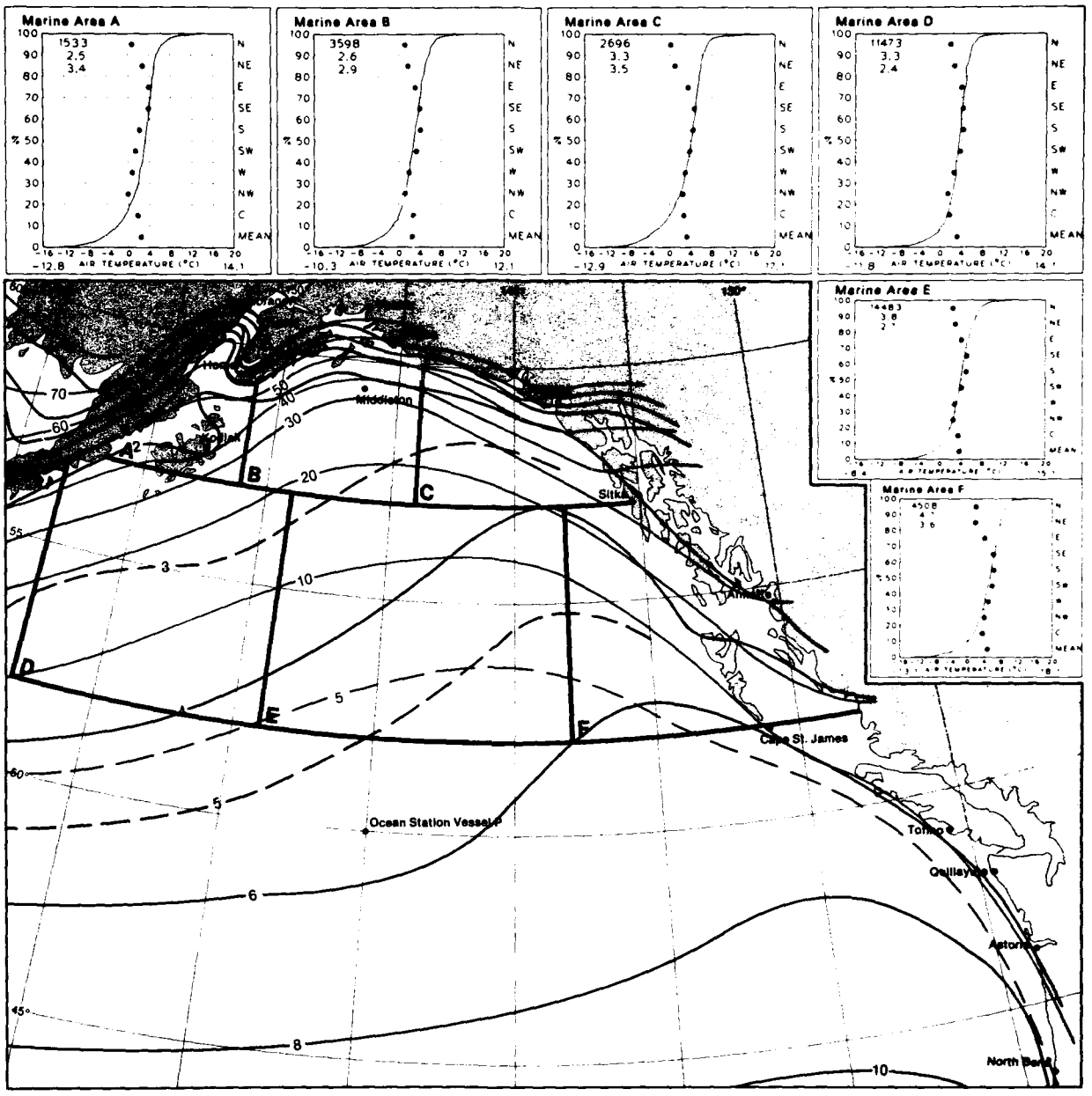

Figure 3-8. Air temperature mean and frequency (≤0°C) for January (Brower et al., 1988).

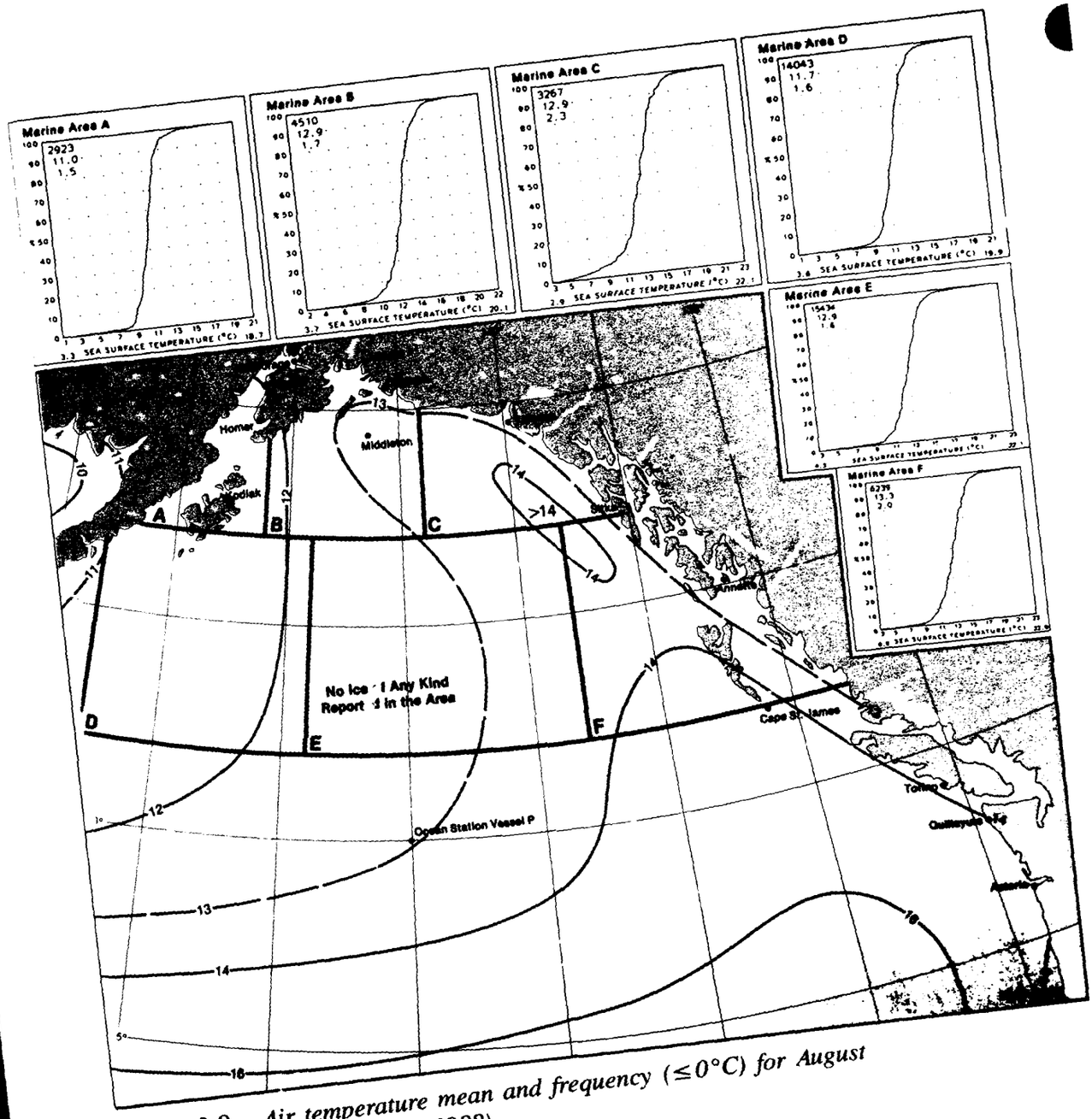

Figure 3-9. Air temperature mean and frequency (≤0°C) for August (Brower et al., 1988).

3.3.6 Cloudiness

The Gulf of Alaska, like the Bering Sea, is a very cloudy area throughout the year. Fall tends to be the period of least cloudiness in the central gulf, but even then 70% or more of all observations indicate five-eighths or more of low cloud coverage. During summer, close to 90% of all observations indicate five-eighths or more of low cloud coverage. The upper level ridge axis has an excellent correlation with the eastern edge of the sea stratus over the gulf. Forecasters can track the ridge advancement and hence, track the stratus edge. Coastal locations fare better because of occasional periods of offshore flow. In such areas clear to scattered cloudiness days are fairly frequent. Grubbs et al. noted that "along the coastal sections, most of the days are either clear or overcast, with broken skies occurring only infrequently." Much of the cloudiness in the gulf is due to low pressure systems that regularly find their way into this area.

Cloud bases in the gulf are normally higher in summer than in winter. Unlike the Bering Sea, cloud tops often extend to very high altitudes.

3.3.7 Visibility

The best visibilities in the gulf occur during the fall. Combined climatologies of ceilings less than 300 ft and/or visibilities less than 1 n mi (1.6 km) indicate poorest conditions in the central gulf and generally marked improvement in coastal regions. Such conditions prevail about one-third of the time in the gulf and only 10% to 15% of the time along the coast.

When winds over the gulf show a long fetch from the south, development of sea fog and poor visibilities are optimized. Statistics from ship observations in the gulf show that this relationship holds true about 50% to 60% of the time. Such winds often develop in the region between low and high pressure centers. A typical scenario producing such effects follows: Southerly winds move northward around the North Pacific High cell, turn southwest into the central gulf, and then converge into a low center near the eastern Aleutians. Fog and low stratus are observed in the strong southerly current over the Gulf of Alaska.

3.3.8 Storm Tracks and Surface Winds

Storms regularly track into the Gulf of Alaska from the region south of the Aleutians and extend westward as far as the Kuril Islands. On occasion (notably during the summer) storms may move into the region from the west-northwest, crossing into the area from the Bering Sea after moving southward across the Alaska Peninsula.

The barrier effect of the mountains bordering the Gulf of Alaska act to impede the further movement of storms that often "stall-out" in the Gulf. When this occurs the analyzed pressure gradient along coastal southeastern Alaska is not a reliable indicator of actual wind speeds in those regions. As a result, National Weather Service (NWS) forecasters at Anchorage double the wind speed normally expected from a given gradient to arrive at more realistic estimates of actual values.

Another important phenomenon occurring along the south coast of Alaska as a result of the mountains is the "mountain gap" wind. Especially strong winds roar through the mountain gaps and offshore at the Copper River exit near Cordova (50.3°N, 145.7°W); at Icy Bay (50°N, 141.7°W); at Yakutat Bay (49.5°N, 140°W); at Dry Bay (59.2°N, 138.3°W); and at Cross Sound near Cape Spencer in southeastern Alaska. Many other gap winds are present in the numerous channels in Southeast Alaska; terrain primarily dictates the weather along the eastern gulf coast and inland waters. Further west strong winds, as a result of mountain effects, occur through the Kamishak Gap at the entrance to Cook Inlet and through Shelikof Strait between Kodiak and the Alaska Peninsula (see related case study in Section 6.4). Winds in Shelikof Strait from the northeast or southwest are usually 4 times the gradient across the strait. A 4-mb gradient produces 16-kt (8 m/s) winds. For the Kamishak Gap, with low pressure in the Gulf of Alaska, the pressure difference between King Salmon and Kodiak or Homer is multiplied by 6 to get an estimate of the strength of the northwesterly Kamishak Gap wind. As an example, a 6-mb difference would be expected to produce a 36-kt (19 m/s) northwest wind through the gap. Several of the bays along the Alaska Peninsula are also known for strong northwesterly gap wind effects.

When temperatures are below freezing these gap winds can cause severe structural icing on ships in the region. An oil rig in Kamishak Bay suffered an unusual accumulation of structural icing during one significant event. Fishing vessels, especially those of 60 ft (18 m) or less are severely troubled by combined waves of 6 ft (2 m) or more. When icing and high winds exist at the same time such vessels are in extreme danger. (Chapter 7 of this guide describes an example of a ship lost with all onboard because of this problem.) A local rule to reduce superstructure icing is to "run with wind." Better yet, if at all possible, seek immediate refuge in sheltered bays or harbors. When available the immediate lee of an island often provides a topographical blocking effect, which reduces both winds and sea state. The leesides of the Barren Islands in the Kamishak Gap, for example, often have a reduced sea state during strong northwest wind events. The reduced sea-state effect extends from the immediate lee of the island more than 60 n mi (111 km) southeastward out into the gulf.

One of the problem forecasts in the Gulf of Alaska concerns the rapid development of atmospheric waves along a north-south oriented cold front. (This is also true of such fronts during blocking episodes in the Aleutian region.) Such developments are normally not captured in numerical forecast products nor in synoptic analyses until after development. By this time ships in the region, not being forewarned, may already be in trouble. The key method to detect and monitor such developments are high quality satellite images received at least every 3 hr. Figure 3-10 shows an example of a north-south oriented front in the central Gulf of Alaska on 23 February 1991 at 0753 GMT. Figure 3-11, over the same area on 24 February at 0505 GMT, less than 24 hr later, reveals four wave developments along the front. Significant weather including heavy rain, strong winds, wind shifts, out-of-phase wind, and swell waves are associated with such developments. The especially dangerous factor is that such waves can intensify further into significant cyclones in a short time interval, giving little time for adequate warning.

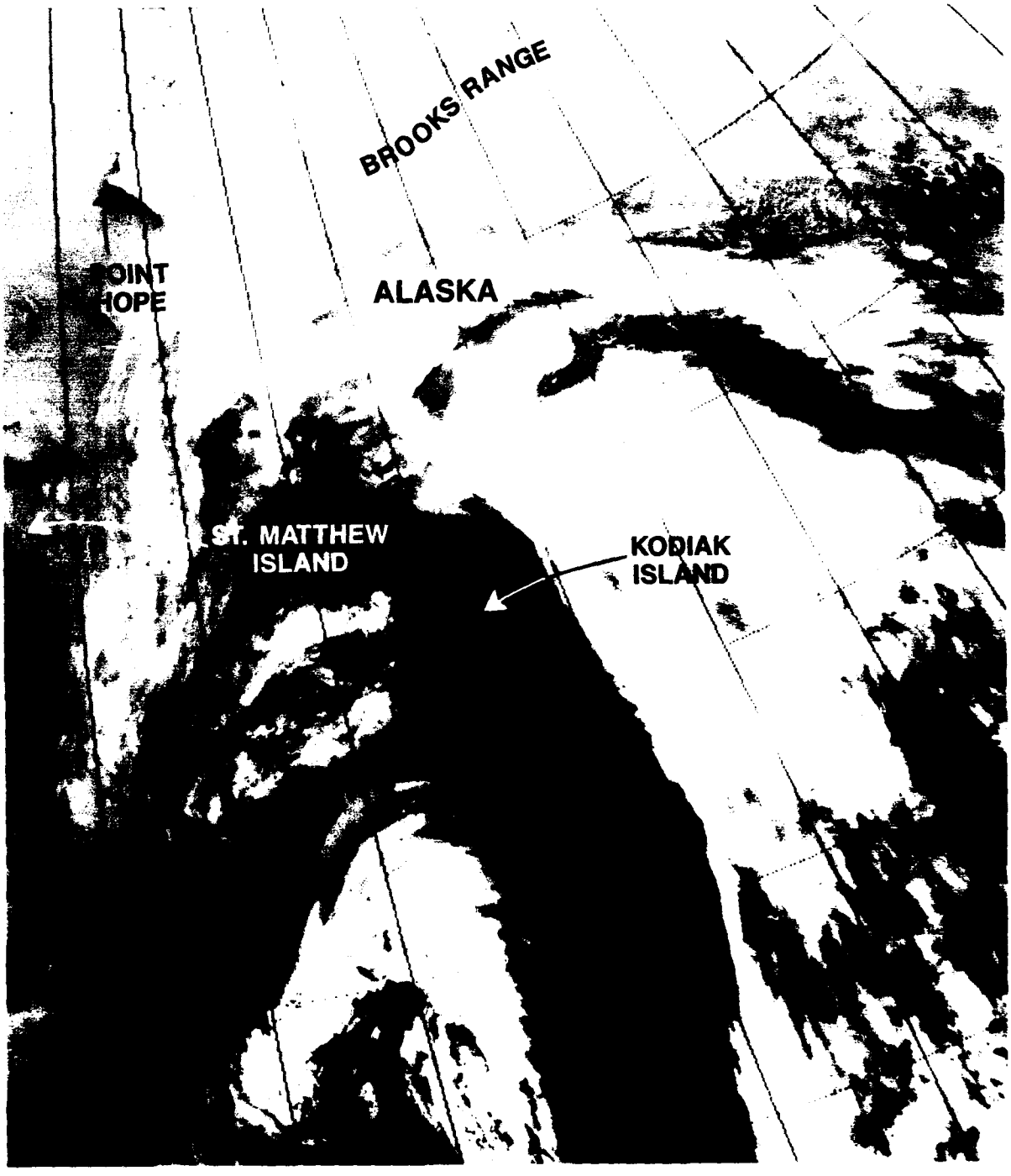

Figure 3-10. DMSP infrared imagery 0753 GMT 23 February 1991.

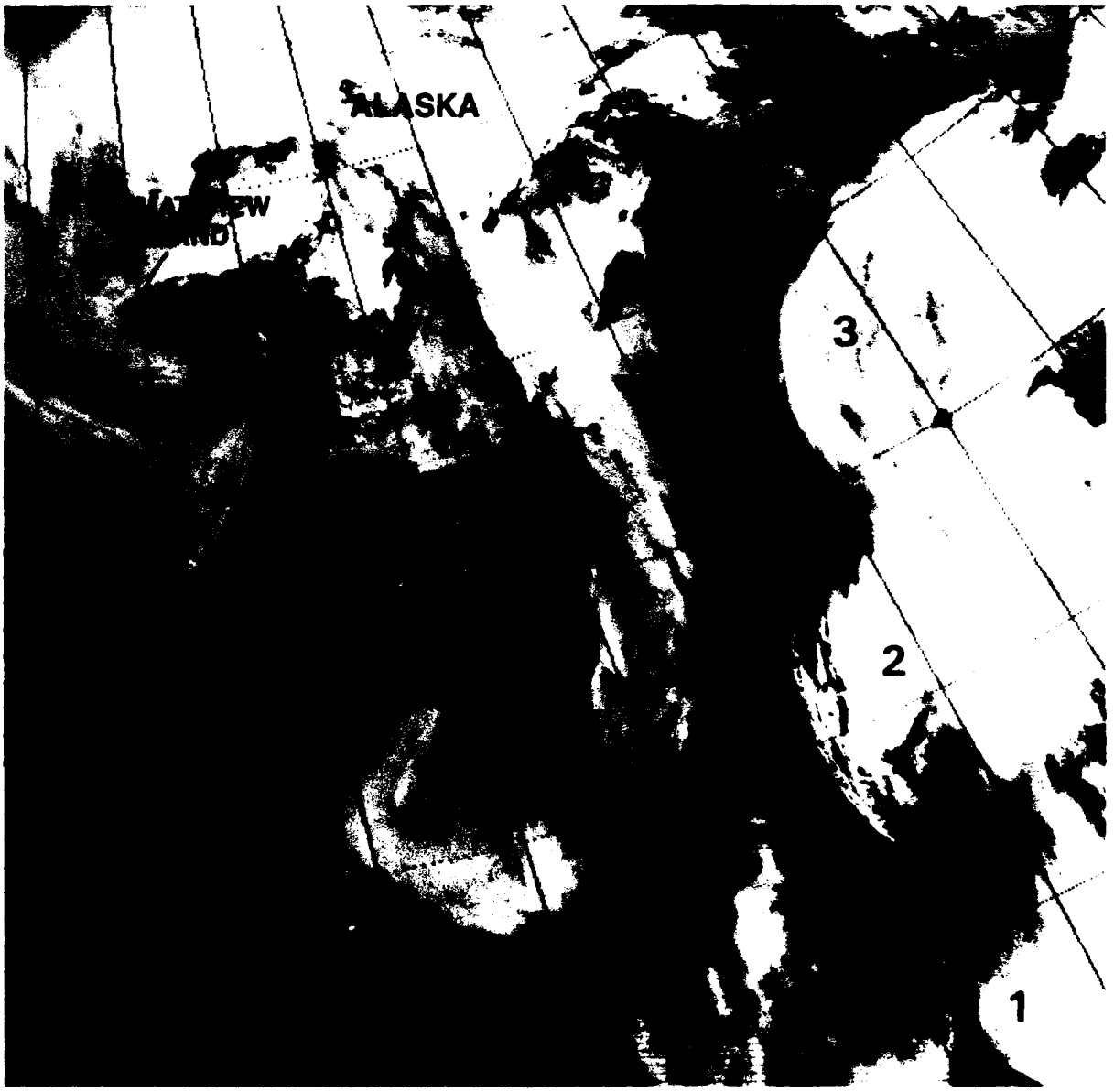

Figure 3-11. DMSP infrared imagery 0505 GMT 24 February 1991.

3.3.9 Gulf of Alaska Ice

Winter temperatures of the water in the gulf are between 35 and 45 °F (+2 and +7 °C), and the area is ice free except in near coastal regions during the entire winter. Summer temperature of the water varies from 50 to 55 °F (10–13 °C). For details see Section 2.2.6).

4. BASIC WEATHER REGIMES OF THE ALEUTIAN ISLANDS

The Aleutian Islands have two distinct weather regimes: one for the western Aleutians and one for the eastern Aleutians. Material describing typical seasonal synoptic patterns occurring in the western Aleutians was adapted from the "Local Area Forecaster's Handbook for Adak Alaska." Material describing nine weather regimes typically occurring in the eastern Aleutians was adapted from 11th Weather Squadron Pamphlet 105-5 (March 1990).

4.1 Western Aleutians

The forecaster's handbook for Adak Alaska contains a description of four winter-type situations and one each for the spring, summer, and fall, as noted by forecasters at that location. The material includes a discussion of specific weather effects at Adak, much of which is also germane to other islands of the Aleutian chain. It is additionally noted that most of the weather patterns described could occur at any time of the year but these effects are more frequently encountered during the specified seasons. The winter storms are listed in order of greatest frequency of occurrence.

It is noted that:

> "Proper forecasting of the onset of any of the deep cyclonic storms of the winter season depends on the effective correlation of the surface chart, upper air charts, and satellite photos of the areas concerned. Falling surface pressure, wind shift, increase in wind speed, and precipitation occur almost simultaneously. The storms which originate off the coast of Japan, being warm frontal type occlusions, are preceded by warm frontal types clouds and large scale warm air advection aloft. These signs first appear 12 to 24 hr in advance of the falling surface pressure and accompanying weather; however, the usual prevailing low cloudiness often prevents the observation of the approaching warm frontal type clouds. There are not any advance clouds or warm air advection aloft ahead of the cold type occlusions which move out of Siberia into the Aleutian region. Forecasting the approach of this situation is dependent upon a complete review of the surface chart, surface and aircraft reports to the west of Adak, together with the upper air charts and satellite photos."

4.1.1 Type I Winter Low

Figure 4-1 shows the Type I winter low synoptic situation. This configuration is most frequently encountered during January through March when "deep, strong lows (pass) south of or directly over Adak moving easterly and recurving northeasterly into the Gulf of Alaska."

Type I lows follow the main storm track that begins to the east of Japan, where the lows form, and extends northeastward passing south of Shemya and Adak, then eastward into the Gulf of Alaska, where the lows recurve to the northeast. These lows develop and deepen considerably as they approach Adak. As they near Adak, they slow in movement and bring strong southeasterly to easterly flow over Adak. The fronts in Type I lows are fully occluded and cause considerable snowfall at Adak. The amount of snowfall is generally not heavy by most standards; however, the high winds associated with these storms cause drifting and blowing snow, which greatly reduces visibility and hampers aircraft operations. As these lows gradually leave the local area, they pick up speed and move into the Gulf of Alaska at 20 to 30 kt (10–15 m/s) where they stagnate and eventually die out. Occasionally these lows recurve abruptly to the north, moving into the Bering Sea just east of Adak, where they frequently stagnate for periods of up to 4 days resulting in northeasterly winds up to gale force in the Adak area. This situation is particularly detrimental to Adak in that a strong northeasterly swell entering Kuluk Bay and Sweeper Cove (both of which open to the northeast) seriously hampers or halts ship operations.

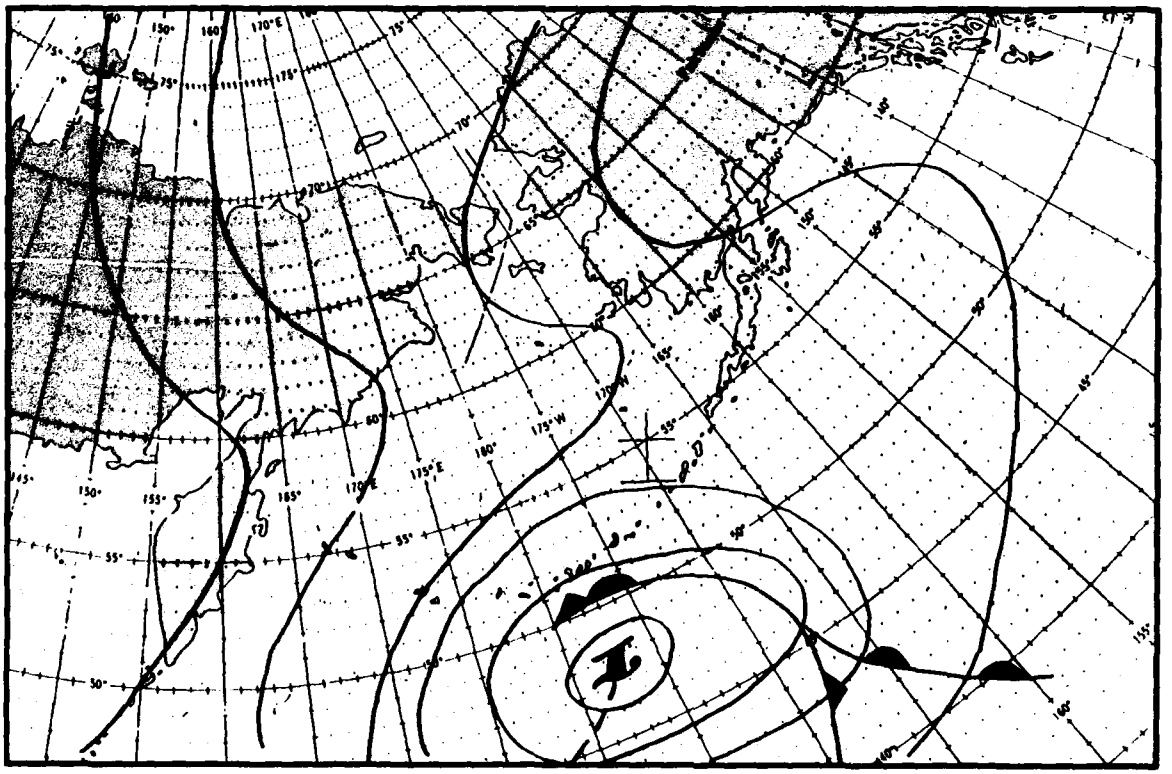

Figure 4-1. Type I winter low synoptic situation.

4.1.2 Type II Winter Low

Figure 4-2 shows the Type II winter low synoptic situation. Type II lows form to the west and southwest of Adak and then move northerly into the Bering Sea passing to the west of Adak.

Type II lows initially follow the main storm track east-northeastward from Japan, but when these lows are 500 to 800 n mi (925–1500 km) southwest of Shemya, they begin to move northward. As they move northward into the Bering Sea and pass to the west of Adak, clear cut frontal passages are observed at Adak. These storms consist of a sharply bent back, warm frontal occlusion centered in a deep low. The precipitation associated with these fronts is generally mixed rain and snow or wet snow, during the southerly flow associated with this synoptic situation. Precipitation ahead of the surface occlusion consists of light snow and rain, becoming moderate or heavy as the upper cold front approaches, and then ceasing after passage of the upper cold front. Drizzle and light rain is often encountered behind the surface occlusion or warm front. Temperatures rise, and much of the fallen snow melts, particularly if the southerly to southwesterly winds are high. After passage of the cold front, which is never as clearly evident as a cold frontal passage at a continental station, the winds veer to the west or northwest. These lows usually pass to the west of Adak and move northward into the Bering Sea. Once into the Bering Sea, the lows either continue moving northward or recurve to the east or northeast and begin to dissipate as they reach the Alaskan mainland.

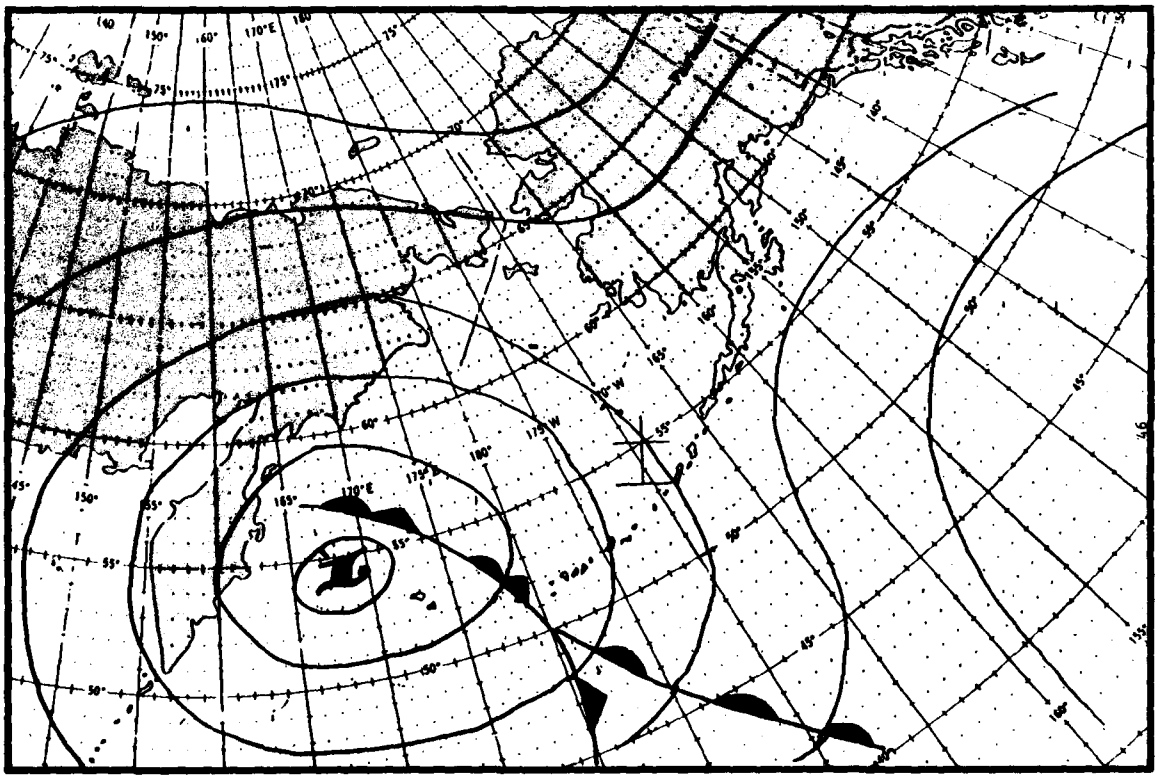

Figure 4-2. Type II winter low synoptic situation.

4.1.3 Type III Winter Low

Figure 4-3 shows the typical Type III winter low synoptic situation. Type III lows occur infrequently. The Type III low is a variation of the Type I low, which, having passed Adak, begins to curve in a counterclockwise direction across the Aleutian chain and eventually recurves over Adak again. This type of low will tend to move very slowly after it has passed Adak and moving toward the east. It will stagnate and begin moving erratically, but in a general northwesterly direction. The second passage of this type is usually not as violent as the first passage, since the fronts associated with the system usually continue moving eastward out of the low center. These storms can stagnate for periods up to 4 days, and the associated strong winds, usually northeasterly in direction, generate a strong northeasterly swell that greatly hampers ship operations in Sweeper Cove, which opens to the northeast. Snow occurs with the greater majority of these storms, but as this type of low stagnates east of Adak, the precipitation becomes drizzle or very light rain. However, the precipitation is not heavy enough nor the temperature high enough to melt any appreciable amount of snow on the ground. Rather it adds to the weight of the snow and increases snow removal problems. If the system is very slow moving after passing Adak, it is likely to be a stagnating and retrograding low.

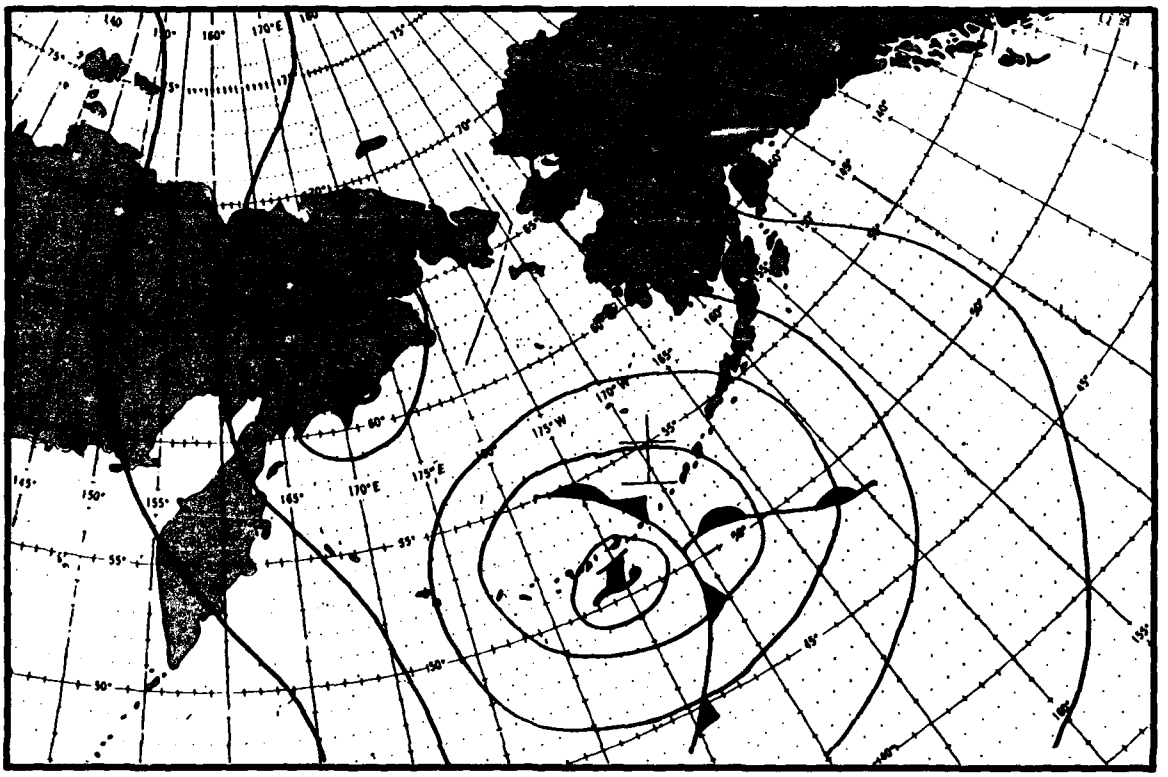

Figure 4-3. Type III winter low synoptic situation.

4.1.4 Type IV Winter Low

Figure 4-4 shows the typical Type IV winter low synoptic situation. In the Type IV configuration high pressure areas form to the east of Japan and become sandwiched between two low pressure centers. This development causes the high to move slowly over Adak, with the best weather generally found in the eastern half of the high.

Type IV situations are infrequent and difficult to forecast. When high pressure ridges from either the Siberian or Alaskan mainland occasionally push into the Bering Sea, the time is favorable for formation of a high over Adak. High pressure areas that form to the east of Japan occasionally push northward and eastward, sandwiched between two low pressure systems, eventually passing slowly over Adak. The best weather in these highs is generally found in the eastern half of the high.

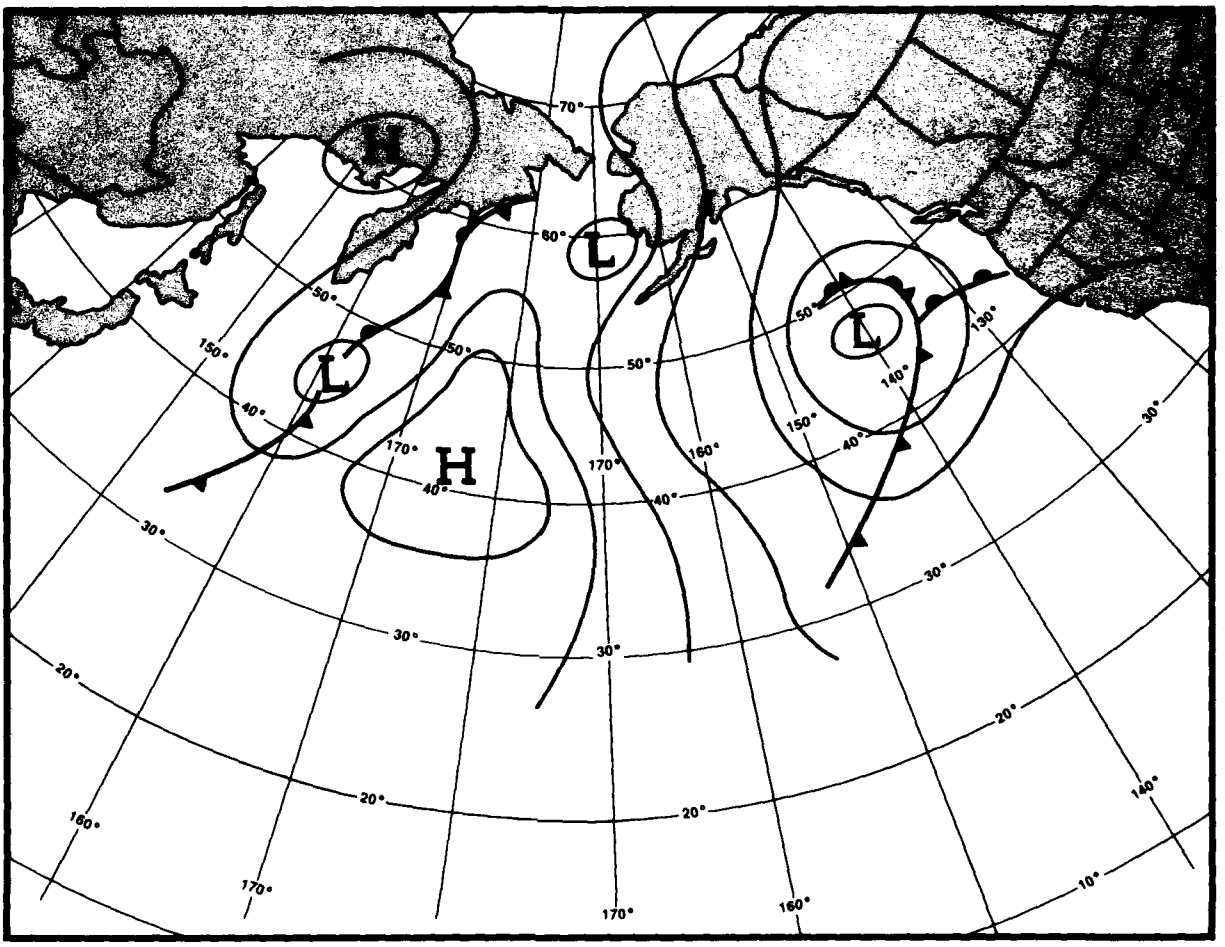

Figure 4-4. Type IV winter low synoptic situation.

4.1.5 Winter Variations

In addition to these four main types of weather situations several other situations are worthy of mention. Once or twice during the winter a low center will move into the Pacific out of Siberia, passing north of Hokkaido. Usually the cyclonic center will stagnate north of Shemya, and the Aleutian chain as far east as Adak will experience the passage of a sharply bent cold-type occlusion. The pressure pattern shows packing of the isobars ahead of the occlusion, bringing winds in excess of 65 kt (33 m/s). The precipitation pattern consists of heavy snowfall at the time of the occluded frontal passage and frequent snow showers behind the front. Also of importance is the formation of active waves on the cold front trailing occlusions. Frequently these active waves will form over the ocean region to the southwest of Adak, intensify swiftly, and move onto the Aleutian chain with little warning. On the back (west) side of lows after they have passed to the east of Adak, Adak experiences northerly to northwesterly flow and scattered to broken clouds accompanied by scattered snow showers. These conditions occasionally last for 2 to 3 days at a time.

4.1.6 Spring Pattern

Figure 4-5 depicts a typical spring (April-June) synoptic pattern. The following paragraphs describe some observations valid during the spring season.

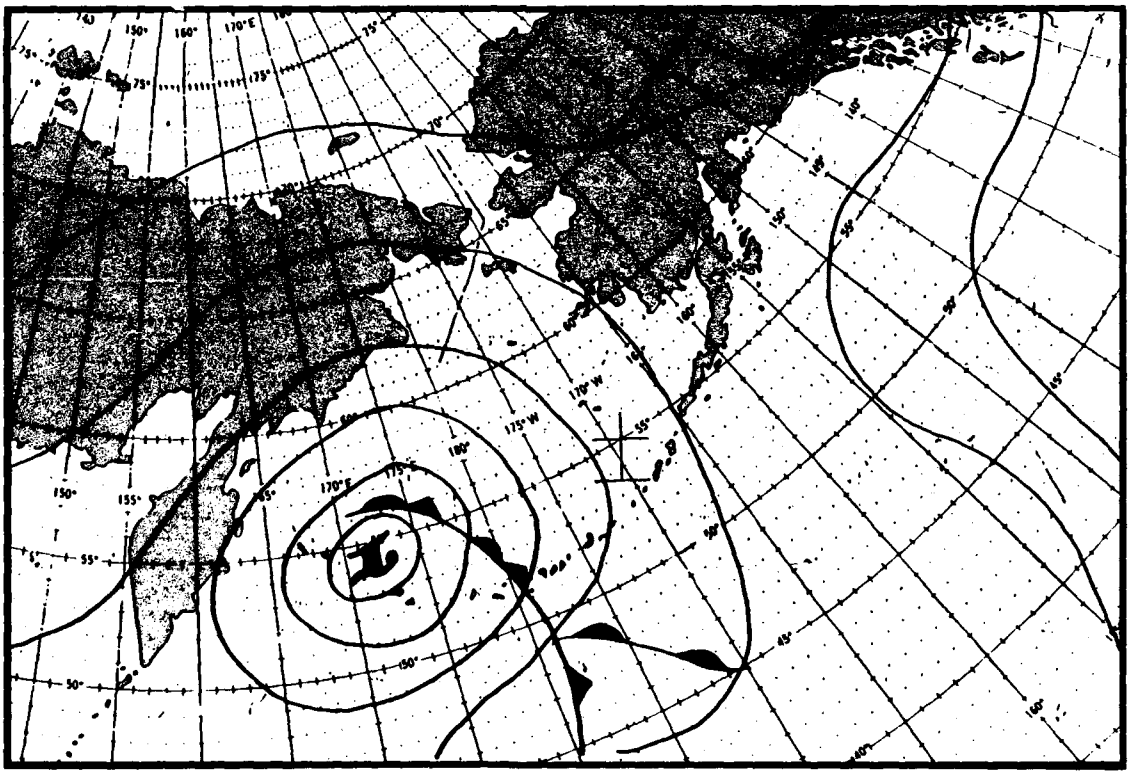

Figure 4-5. Synoptic situation for spring season.

(1) The spring season brings a gradual transition from the strong, high index, east-west orientation flow of the winter season to a weaker north-south flow. Ridges of high pressure frequently extend northward from the Pacific High cell into the Bering Sea. Frontal waves occlude rapidly, and deep storm centers are the main synoptic development. Movement of these low centers is much slower than during the winter season and is generally more northeasterly, becoming north-northeasterly as the spring season progresses. The systems that form off the east coast of Japan during the spring season usually pass just east of the Kamchatka Peninsula into the Bering Sea area.

(2) The waves that form along the front between the two cells of the split Pacific High seldom affect the Adak area, generally passing well to the south or southeast.

(3) As the frontal waves occlude, the deep storm centers tend to stagnate, and the associated frontal systems continue to move around the periphery of the low until they reach a point east or southeast of the center where frequently a new center will form. This center, along with the fronts, then moves eastward and in turn stagnates. The fronts, however, continue eastward, and frequently a third center will form by the same process.

(4) During the spring season two main storm tracks affect the Aleutian chain. The more important track is from the east coast of Japan, passing west of the Kamchatka Peninsula and into the Bering Sea. Surface winds of 40 kt (21 m/s) and gusts to 60 kt (31 m/s) are often recorded along the Aleutian chain as the storms move over this track. Since most of the Aleutian chain is east of the storm center, the winds are generally southerly in direction. Frontal passage of a sharply bent back, warm type occlusion occurs along the Aleutian chain with surface wind maximums recorded before the passage of both the upper cold front and the surface warm front. Precipitation in the form of rain occurs and reaches a peak during the passage of the upper cold front, after which the precipitation changes to drizzle and fog and the sky lightens considerably. After passage of the surface warm front, winds veer southwesterly and rapidly drop to 20 kt (10 m/s) or less. After entering the Bering Sea, the storm center usually will drift slowly eastward, and a packing of the isobars will result in high westerly winds to the south and southwest of the storm center. Winds generally will reach up to gale force in this sector. Often these storm centers will drift northeast into the Bering Straits or Norton Sound rather than east along the Aleutian chain, and in this case the high westerly winds do not occur.

(5) The second important storm track extends from Siberia across the southern tip of the Kamchatka Peninsula and along the Aleutian chain, usually just north of the chain. These storms are not particularly deep as a rule, and the associated frontal system is generally in the form of an open wave or a cold type occlusion. Precipitation associated with these storms is either rain or mixed rain and snow. Surface winds seldom exceed 30 kt (15 m/s). These storms generally move east along the Aleutian chain and fill fairly rapidly.

(6) Each spring several storms form on the trailing cold fronts of the storms that have passed into the Bering Sea area. These storms generally form in the area

southwest of Adak and cross the Aleutian chain as an open wave. During the spring season this type of development does not present as severe a problem as during the winter months, and the main weather consists of the rainfall associated with the fronts.

(7) A frequent occurrence in spring is the combination of a complex low elongated north and south with a blocking high to the east. The resulting isobaric pattern produces a band of high winds with velocities up to 40 kt (21 m/s). This band frequently is 40 n mi (75 km) or more in width and 1200 n mi (2225 km) or more in length. The flow is south to north or southeast to northwest and brings very warm, moist air over the cold waters of the Aleutian area, resulting in overcast skies with ceilings of 1000 ft or less and intermittent light drizzle. This situation may persist for 48 hr or more.

(8) In general the spring storms give more advance warning than do the storms of the winter season. Falling pressure and a shift of the wind usually occur 8 to 12 hr before the precipitation and high winds begin. Warm air advection aloft and typical warm frontal cloudiness also forewarn the forecaster of the approaching warm frontal occlusion. However, as in all seasons, the prevailing low cloudiness of the Aleutian area usually prevents the observation of the higher warm frontal clouds.

4.1.7 Summer Pattern

The synoptic pattern shown in Fig. 4-6 is one of two summer regimes; one is of weak lows as shown and the other of weak ridges. The major summer problem is fog forecasting.

(1) Although fog occurs on an average of 151 days a year, it occurs most frequently during the months of June through September. The weather maps of the summer season show the Adak area dominated by weak lov centers and weak ridges for long periods. The fog in the Aleutian area is mainly the advection type, formed either south of the chain or in the Bering Sea by warm, moist air being imported from tropical waters to the cooler waters in the Northwest Pacific and Bering Sea by elongated pressure systems; the fog is then advected or blown in by local winds. Conversely, cooler air from Asia or the Arctic basin is not conducive to fog formation.

(2) Fog occurs approximately 32% of the time (32 out of 100 hr) at the Naval Air Station, Adak, with a higher percent frequency on the surrounding waters. The fog will generally occur during the early morning hours and lift by early afternoon, except in cases of unusually intense fog or fog associated with passing frontal systems. Because of the rugged terrain of Adak and the relatively high average wind velocity, the visibility seldom drops below 3 mi (5 km).

(3) Whereas this fog is caused by advection, the relationship of surface winds to topography is of primary importance. It has been noted that 47% of all fog occurring on the Naval Air Station, Adak, is accompanied by winds from a west-to-southwest direction (the prevailing winds during this period). One can expect that winds blowing from this direction will be accompanied by fog at least 36%

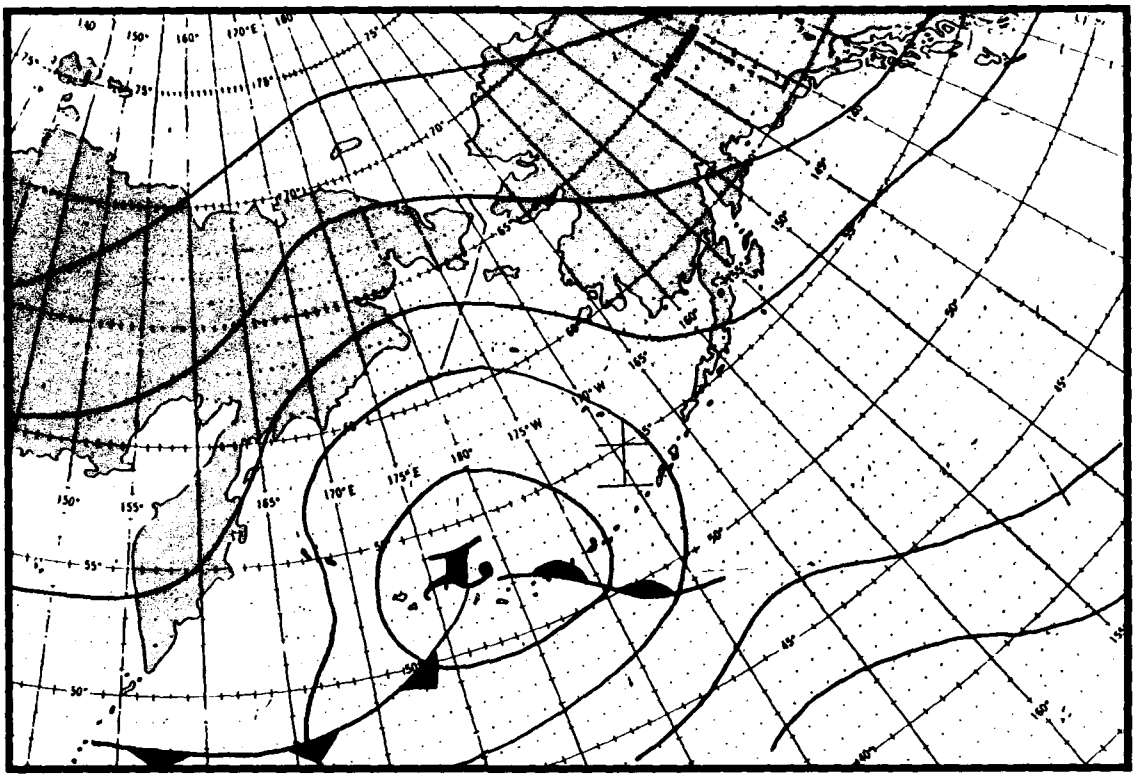

Figure 4-6. Synoptic situation for summer season.

of the time. Winds from the north to northeast result in a little over 20% of Adak's fog and indicate fog in the Bering Sea. A little more than 29% of the winds from this direction will advect fog over the island. Winds from the southeast to south are the third significant source of wind direction (about 14% of the total Adak fog). These winds will be accompanied by fog 35% of the time. About 18% of Adak's fog will occur with all other wind directions and calm winds. Fog on Adak can also occur with wind speeds of up to 20 kt (10 m/s) if the wind is from the west to southwest.

(4) Whether the curvature of the isobars at the surface is cyclonic or anticyclonic over Adak is not important since this is an advection fog, although it will be important in the source area. Fog will occur at Adak with both types of curvature. More important is the isobaric pattern and the source of air being advected over the island. The most severe fog conditions occur on the west side of anticyclones or in advance of warm fronts.

(5) Winds from the south to southeast will normally leave the field with a 500- to 1000-ft ceiling because of the terrain, even if fog banks are present south of Adak. Fog associated with these wind directions is normally of the frontal type. The fog over the water will usually be advected ashore in the form of stratus, causing a significant number of low ceilings at the approach end of instrument runway 23. The remainder of the field has fewer low ceilings because of terrain features.

(6) Winds from the southwest to west associated with the anticyclonic circulation from a high pressure center located south of Adak and having a moderate to long over-the-water trajectory are conducive to fog formation. When advected over the station, these winds are usually accompanied by light drizzle or light rain. With velocities in access of 25 kt (13 m/s), the fog will be patchy and the ceilings will be variable, but generally near 100 ft. With velocities of less than 10 kt (5 m/s), the fog will frequently remain on the seaward side of the low hills to the west of the runways. Winds from these directions will not advect fog over the station when the source of air is the Asian Continent or the Arctic basin.

(7) Northwest winds do not frequently occur over the Naval Air Station at low speeds because of the blocking effect of Mount Moffett. However, a northwest flow over the island will usually be associated with good ceilings since the source of air will probably be the Asian Continent or the Arctic basin.

(8) To forecast fog associated with north-to-northeast winds, one must be able to forecast fog in the Bering Sea. An isobaric pattern that brings warm, tropical air into the Bering Sea and causes northerly winds over Adak will result in fog, which is occasionally very intense.

(9) A close scrutiny of the topography to the east of the island will show why little fog, except frontal fog, is associated with winds from easterly directions.

(10) The paths and weather associated with cyclonic storms during the summer season closely parallel those found during the spring months, though frequency of cyclonic storms falls off during July and August. On occasion, late in the season, a fairly strong storm, which originates as a recurving tropical storm, will affect the Aleutian area (also see discussion on fall weather). The characteristics of these storms are the same as those of the storms that originate off the coast of Japan, as described in the spring season. Particularly, the storms are associated with heavy rainfall and southerly winds with peak gusts to 65 or 70 kt (33 or 36 m/s). One problem is determining exactly when they will begin to move with the 500-mb flow. Satellite photos are an invaluable aid to prediction. Forecasting the summer cyclonic storms follows the same general rules as forecasting for the spring season.

4.1.8 Fall Pattern

Figure 4-7 shows one of the typical synoptic patterns observed during fall (October-December). The following paragraphs describe some observations valid during the fall season.

(1) In general the fall season in the Aleutian area is similar to the winter season. The cloud forms are predominantly cumuliform, accompanied by frequent periods of extremely squall-like weather. Electrical activity, not generally common in the Aleutian area, is observed during this season particularly in October and early November. Although only a few observations of lightning or thunder

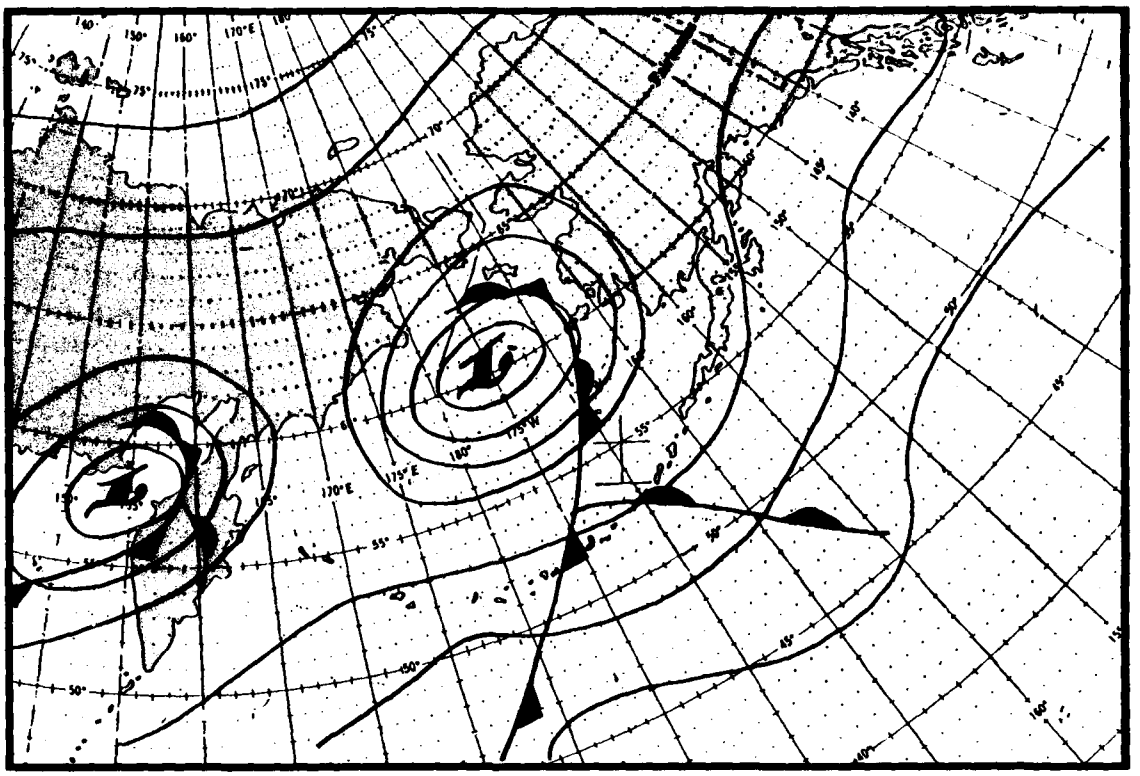

Figure 4-7. Synoptic situation for fall season.

at Adak have been reported, scattered cumulonimbus are frequent during this season.

(2) The fall season is characterized by cyclonic circulation with the passage of one deep cyclonic storm after another through the Aleutian area. In the winter seasons these storms stagnate in the Aleutian area, however, during the fall they move through the Aleutian area and stagnate against the Alaskan mainland or in the northern reaches of the Bering Sea. The wind flow around the low centers brings cold air from the mainland of Siberia or Alaska across the Bering Sea and the Aleutians, resulting in squall-like weather.

(3) The surface winds during these squall-like periods often are northwesterly at 35 to 40 kt (18–21 m/s), with gusts of 60 to 70 kt (31–36 m/s) for as long as 4 or 5 days. Precipitation is usually heavy with rain or mixed rain and snow in October, becoming snow, usually in the form of snow pellets, in November and December.

(4) Ceiling and visibility in the snow showers drop to zero. The showers generally last from 10 to 20 min, and sky conditions are scattered to broken for 30 to 60 min between showers. This brief restriction to ceiling and visibility has only a temporary effect on air operations, but the sustained high velocity winds from the northwest, resulting in dangerous cross runway flow over both runways, can prohibit the use of the field for extended periods.

(5) A second weather feature peculiar to the fall season is the large number of deep cyclonic systems that move out of Siberia north of Japan and into the Aleutian area. As the system moves out of Siberia over the Sea of Okhotsk, the cooler air passes over warmer water causing intensification of the system. Also, tropical air moving around the western side of the Pacific High enters into the system, and further intensification occurs as the system moves across the Kamchatka Peninsula and into the Aleutian area. Frequently one of these lows from Siberia will merge with a low from Japan or with a wave formation moving up the cold front trailing the main low center. This type of development will form a very deep and complex system. Generally these systems move across the Bering Sea north of the chain. Winds in advance of the system may reach 40 to 50 kt (21–26 m/s). Behind the system the winds are usually gale force accompanied by the squall-like weather described. Occluded frontal systems are usually of the cold type. Precipitation occurs along the fronts: generally rain in October, and snow in November and December. If Adak enters the warm sector of the system, considerable melting may occur, which will freeze after the passage of the cold front.

(6) Forecasting the onset of the squall-like condition typical of the fall season is dependent upon forecasting the continued movement of a deep low system to a position so that the Aleutian area will be in an air flow originating over either the Siberian or Alaskan mainland. To forecast this movement it is necessary to know the storm's maturity and the general surface pressure pattern, and to have the pressure tendency reports from stations in the Aleutian chain and along the west coast of Alaska. Generally the low center will move directly through the Aleutian area at 20 to 30 kt (35–55 km/hr), although stagnation and recurvature typical of the winter season may be expected in December.

(7) Particular attention must be paid during extended periods of northwesterly flow to trough lines, which will bring snowfall and accompanying low ceilings and visibilities for longer periods than during the typical showers. The movement of these troughs is indicated by wind shifts and a slight pressure drop and rise.

(8) Forecasting the end of this situation is more difficult. The end of the situation is usually caused by the filling of the old low as it moves eastward accompanied by the movement of either a high or another low center into the area from the southwest. If a high pressure system or ridge moves in behind the filling low, the wind will remain strong and from the northwest at stations on the Aleutian chain. If another low moves into the area, the wind can be expected to decrease in velocity temporarily and gradually back to a southwesterly direction.

(9) Forecasting the approach of a deep low pressure system moving out of Siberia into the Aleutian area is dependent upon knowledge of the surface winds and weather to the west of Adak and a proper correlation with the upper air flow.

(10) On about one occasion each year in the fall, a storm with tropical origins will affect the region. Forecasters tracking an ex-tropical storm in the area should be alerted to the possibility of high winds and heavy precipitation amounts. Extensive flooding has occurred in the region during previous encounters with this type of storm. These storms are relatively easy to track using satellite imagery.

4.2 Eastern Aleutians

During World War II the Air Force maintained many stations throughout the Aleutians including Adak, Shemya, Amchitka, Umnak, Atka, Cold Bay, Port Heiden, King Salmon, and others. Air Weather Service forecasters gained a wealth of experience concerning weather in the Aleutians, and they maintained an active program to document this experience for the benefit of forecasters to follow. Much of this experience can be found in 11th Weather Squadron Pamphlet 105-5 (March 1990), which summarizes the nine weather regimes typical of that area. The regimes were developed and refined based on years of Aleutian and Alaskan forecasting experience and are shown in this section directly derived from that pamphlet.

4.2.1 Strong Ridge South and Southwest Flow Regime

Figure 4-8 is an illustration of what is termed the "strong ridge south-southeast flow regime," pattern. Listed below is a description of typical upper air and surface conditions found in this type of regime.

Upper Air (above 850 mb). A very strong, stable ridge pattern aloft exists northward through western Canada into Yukon territory. This pattern can remain more than a week and occurs 6 to 12 times a year, mainly in the warmer half of the year.

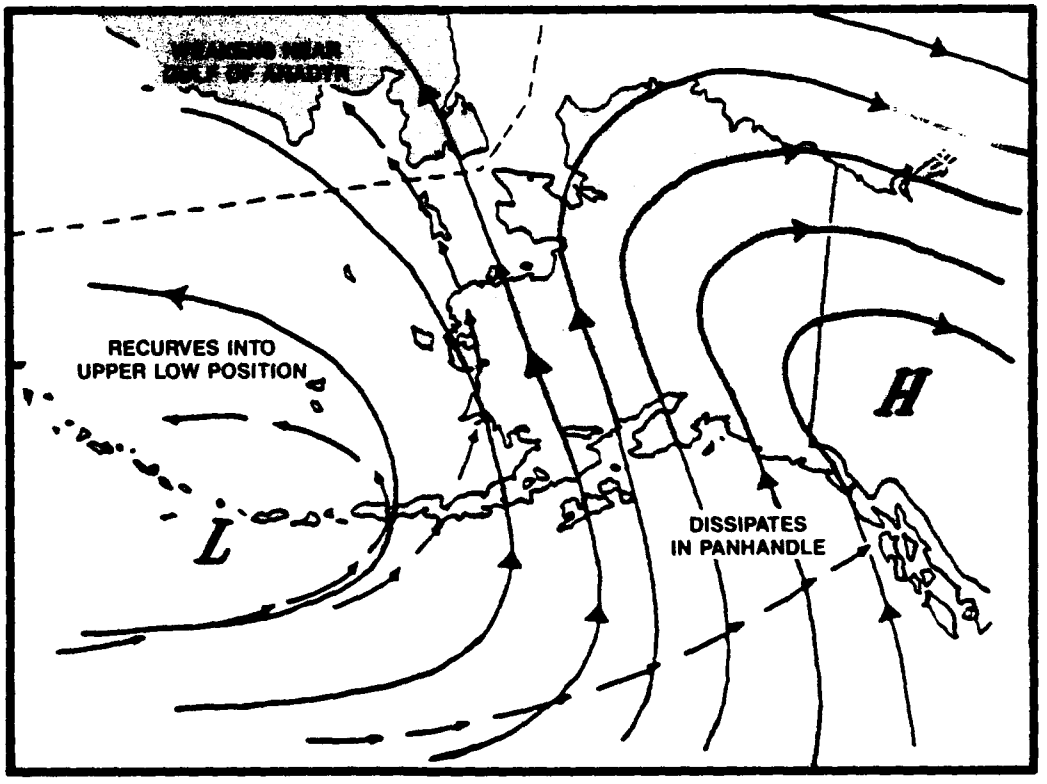

Figure 4-8. Strong ridge south-southeast flow regime.

Surface. Surface lows tend to stay to the west of the mainland usually over the Aleutian Islands and Bering Sea.* A second low pressure track through the Gulf of Alaska dissipates near the Panhandle region.** When the south or southeasterly flow aloft across the mainland is strong (40–60 kt or 21–31 m/s), gusty surface winds can be expected in south central Alaska and significant turbulence over the Chugach and Alaska ranges. A weaker flow (<25 kt or 13 m/s) produces summertime thundershower activity over the interior.

Forecaster notes from King Salmon (PAKN) with respect to this regime are listed below:

"This regime is an important weather producer for King Salmon, especially in terms of warming criteria winds. The upper level jet stream will normally track over the area as the surface low moves into the Bering Sea or Bristol Bay. Progging the track of the jet is most important. Usually, Cold Bay and Port Heiden will experience strong winds before PAKN. Ceilings and visibilities will lower as the front moves through. PAKN has experienced winds of 50 kt (26 m/s) during this regime."

* Many west coast lows remain weak. The "strong" west coast storm regime is discussed in Section 4.2.2.

** Associated occluded fronts approaching the west coast weaken as they move northward. Gulf of Alaska occlusions tend to dissipate inland as they move northward over the Alaska Range. Shower activity can be expected ahead of the occlusion before it dissipates.

4.2.2 Moderate to Strong Southwest Flow Regime

Typical upper level and surface conditions associated with the moderate to strong southwest flow regime are illustrated in Fig. 4-9. Regime attributes are listed below.

Upper Air (above 850 mb). This moderate to strong southwest flow pattern aloft across Alaska is the most widespread precipitation producer of all the regimes. Although mainly a fall and winter season phenomenon, it occurs during all seasons, about 10 times a year.

Surface. Since the jet stream crosses Alaska, low pressure tracks traverse the Bering Sea into the state, or they curve into the upper low usually northwest of Barrow. Once or twice a year, during autumn, western Bering Sea surface lows can develop into deep powerful storms. As the system tracks northward across the eastern tip of Siberia, associated very strong winds and rain cause coastal flooding along portions of western Alaska. Another low pressure area redevelops south of the Alaska Peninsula and tracks northeastward across the Gulf of Alaska. Even though low pressure systems tracking into Alaska usually dissipate once they make landfall, the associated frontal systems and precipitation bands continue northeastward through the state.

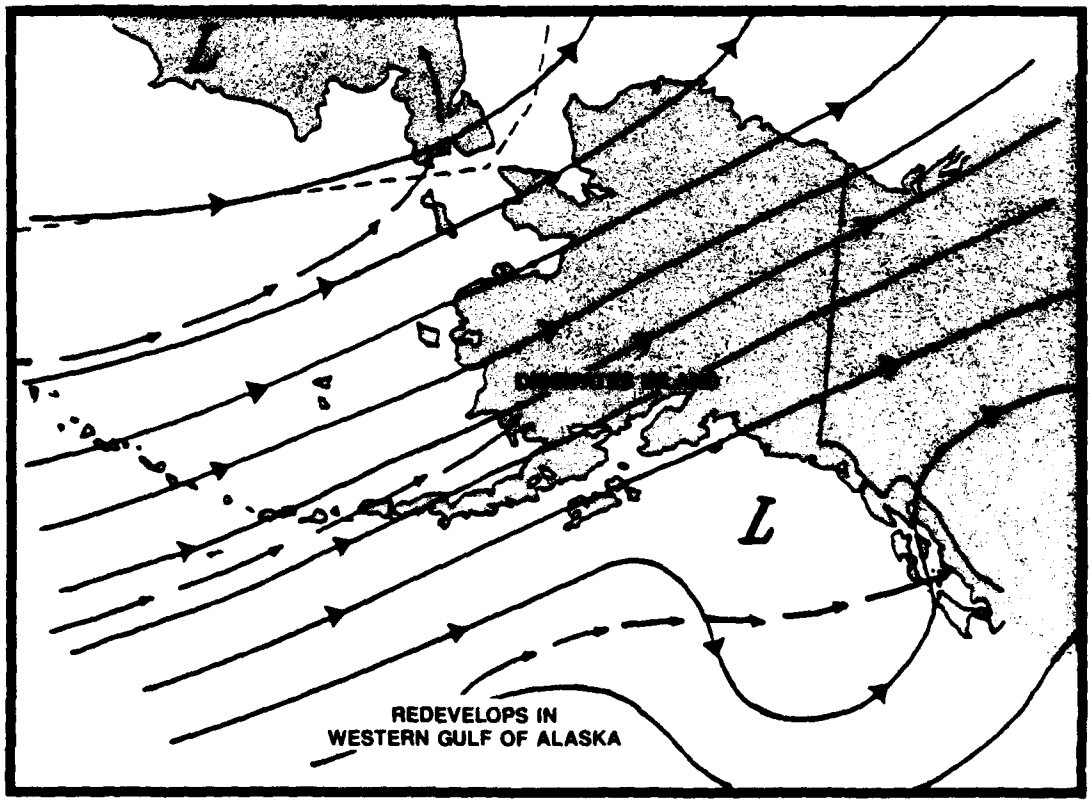

Figure 4-9. Moderate to strong southwest flow regime.

Forecasters at King Salmon note: "This system can also produce gusty winds. If the surface low crosses the Alaska Peninsula, expect gusty easterly winds ahead of the front and extensive periods of low ceilings and visibilities after frontal passage. If the low passes south of the area, however, ceiling and visibility conditions will not be as poor."

4.2.3 The Fair Weather Regime

The fair weather regime is illustrated in Fig. 4-10. Listed below are the attributes of this regime.

Upper Air (above 850 mb). A sharp north-south-oriented ridge of high pressure along or west of Alaska's west coast sets up a stable cold fair weather pattern across the state. This is mainly a winter season phenomenon occurring 3 to 6 times a year. If a low aloft develops over the eastern Gulf of Alaska, the resulting "omega block" situation can remain 1 to 2 weeks. During February 1979, it persisted the whole month bringing record-breaking cold to much of the state.

Surface. Surface lows tend to remain over the western Aleutians and western Bering Sea and track into Siberia. Any weak surface lows forming in the Gulf of Alaska will move away from the mainland. At times, an upper level low will form in the

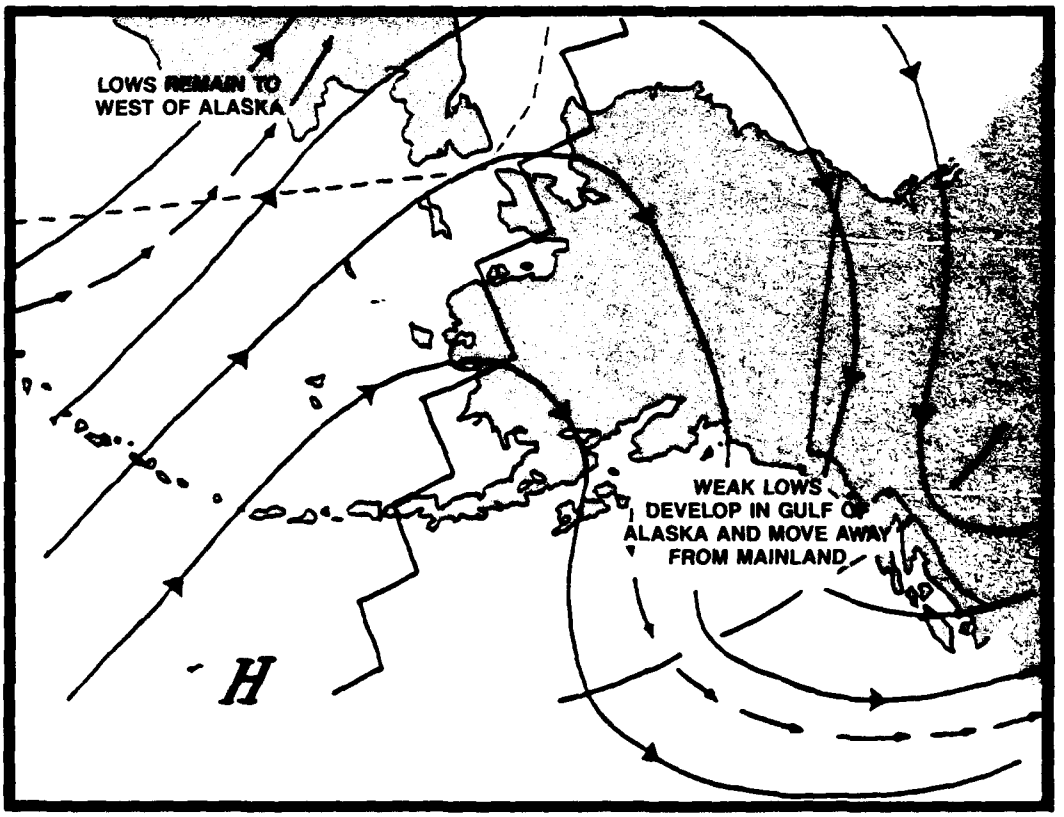

Figure 4-10. Fair weather ridge regime.

eastern Gulf of Alaska and support development of a stronger vertically stacked surface low. The resulting tight low level pressure gradient across southern coastal Alaska will cause very strong northerly winds through channels and passes, accompanied by freezing spray and clear skies.

Forecaster notes from King Salmon indicate that, "this is a very cold weather regime for most of Alaska. PAKN must remain on the eastern side of the ridge line to experience cold, clear weather. Otherwise, with Bristol Bay virtually unfrozen, moisture from onshore flow will cause IFR (instrument flight rules) conditions to occur under a strong subsidence inversion."

4.2.4 Broad Long-Wave Trough

The broad long-wave trough regime is illustrated in Fig. 4-11. Characteristics of this regime at upper and lower levels are described below.

Upper Air (above 850 mb). This broad but weak north-south long-wave trough pattern aloft over Alaska is a rather common feature. It develops a dozen or more times a year, mainly during the winter. Winds aloft are cyclonic but light. More often than not, the trough line remains nearly stationary, or eventually retrogrades

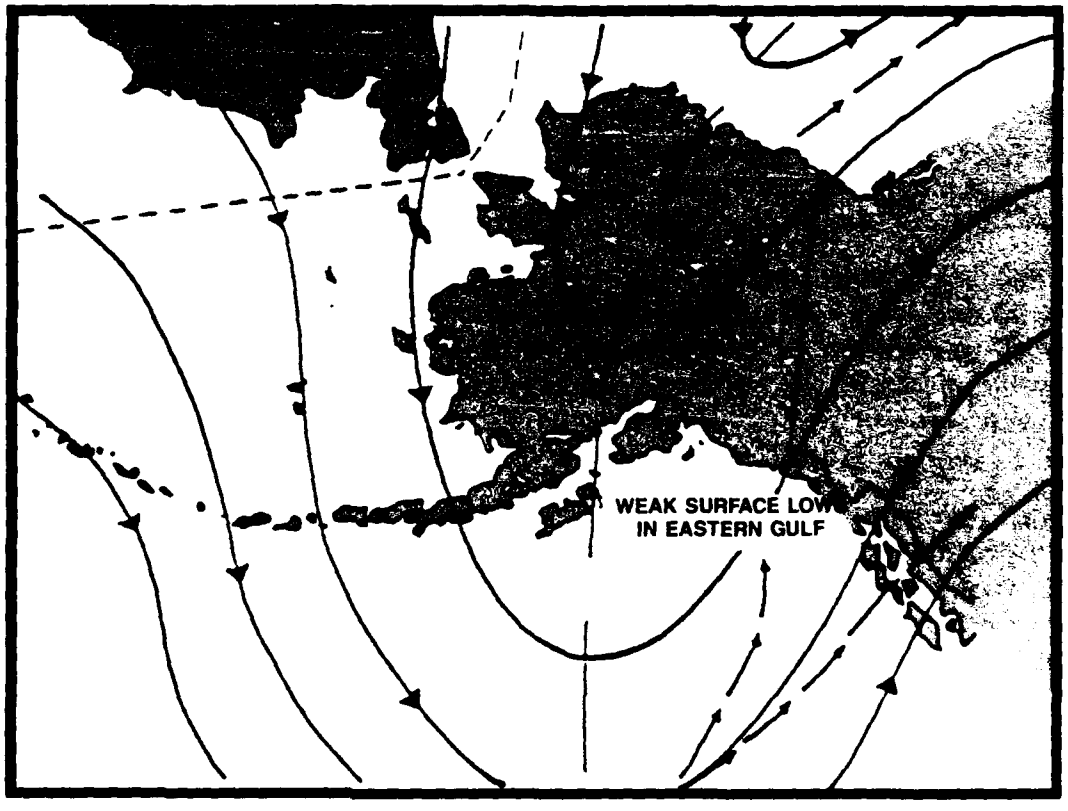

Figure 4-11. Broad long-wave trough regime.

westward. Once established, this broad trough type flow pattern tends to remain a week or more.

Surface. Surface lows tend to be restricted to the eastern Gulf of Alaska and track inland, redeveloping in the Yukon Territory. Weather over Alaska is unsettled to the east of the trough line with rather disorganized areas of clouds and precipitation and very little movement. West of the trough line, weather conditions are predominately VFR (visual flight rules). A secondary low pressure track across the Arctic Ocean is of little consequence south of the Brooks Range.

Forecasters at King Salmon note: "If PAKN remains west of the trough, good weather should persist. Should the trough begin to retrograde, check the weather at stations ILI, Z30, and MCG. These stations will give an indication of the conditions associated with the trough. Weather conditions at PAKN tend to remain slightly better than those at these other locations, however."

4.2.5 Transient Short-Wave Low Within Long-Wave Trough Regime

The transient short-wave low regime is illustrated in Fig. 4-12. Upper and surface level characteristics of this regime are listed below.

Upper Air (above 850 mb). This "transient" short-wave low aloft pattern in a stationary long-wave trough regime is among the most common over Alaska. It can occur during any and all seasons. Variations of this regime can be expected from 15 to 20 times a year. Essentially, a small short wave upper level low or vorticity center passes through the stationary open long-wave trough position moving from the Bering Sea toward Alaska. Most frequently, the low settles into the Gulf of Alaska on its way eastward.

Surface. Surface weather undergoes frequent changes with passage of the frontal system associated with each surface low pressure area. In rare instances, a "closed isobar" surface low, accompanied by a closed low circulation aloft, may actually traverse interior Alaska. When this happens (only 1 to 3 times a year), IFR conditions in the vicinity of the low are virtually assured—especially in winter. Filling Prince William Sound lows also occur in this regime.

Forecaster notes concerning effects of this regime at King Salmon are listed below:
"This regime will produce widespread IFR conditions at PAKN as the low moves into the area. Poor conditions will persist until the low weakens and drifts northeastward. Since the jet stream with this regime is usually well to the south, strong winds are normally not a problem."

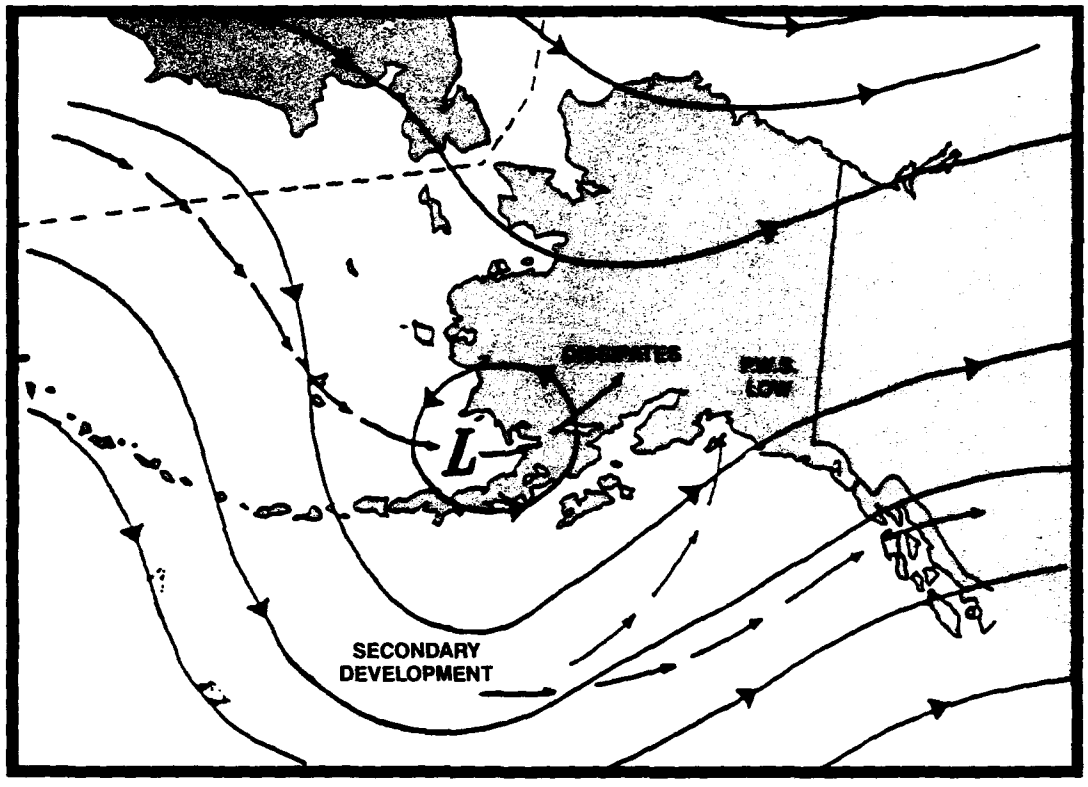

Figure 4-12. Transient short-wave low with long-wave trough regime.

4.2.6 Polar Northeasterly Flow Regime

The polar northeasterly flow regime is illustrated in Fig. 4-13. Attributes of this regime at upper and surface levels are listed below.

Upper Air (above 850 mb). Deep low pressure aloft over the Gulf of Alaska is a winter season pattern. It occurs 3 to 6 times a year and remains anywhere from 4 to 7 days per episode. The resultant induced ridge of high pressure aloft across northern Alaska produces a dry rather cold polar northeasterly flow over the whole interior. Ordinarily, only coastal regions of southern Alaska experience any precipitation.

Surface. Surface storms track into the Gulf of Alaska and become quite extensive as they curve into the low position aloft before weakening. Clouds and snowfall are restricted to areas south and east of the Alaska Range. Occasionally, "back-door" snowfall is carried into the upper Tanana Valley from the southeast.

Forecasters at King Salmon note that "this system will produce little weather in the PAKN area. Usually, the Arctic boundary will remain north of PAKN."

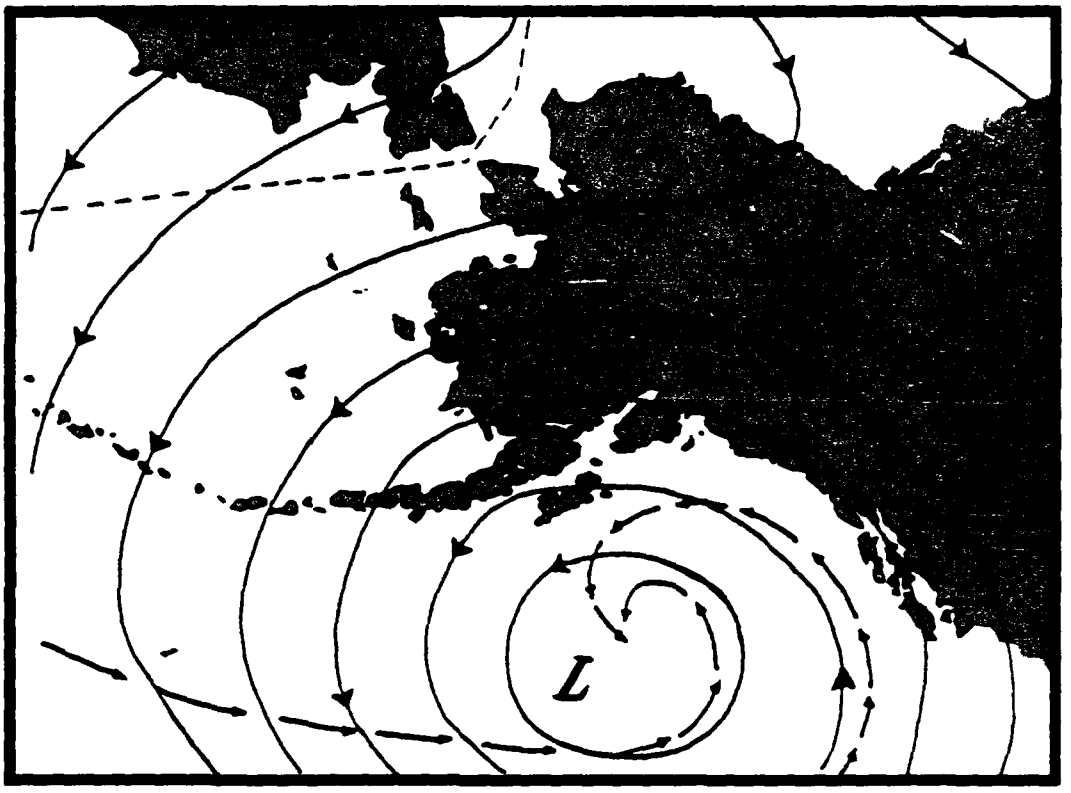

Figure 4-13. Polar northeasterly flow regime.

4.2.7 Rapid Building North Pacific Ridge Regime

The regime called the rapid building North Pacific ridge regime is illustrated in Fig. 4-14. Attributes of this infrequent but important region at upper and surface levels are listed below.

Upper Air (above 850 mb). From 2 to 4 times during a normal year, a tight gradient type ridge aloft will build rapidly northward through the Gulf of Alaska into the state. Just as rapidly, after only 1 to 3 days, it can recede southward back into the Pacific Ocean. Note how it differs from the fair weather ridge regime (Fig. 4-10). Here the strong 75 to 100 kt (39–51 m/s) upper level jet stream rapidly advects moisture from the North Pacific straight into mainland Alaska. The anti-cyclonic curvature is unable to "dry things out" owing to the flatness of the ridge.

Surface. Although infrequent, this upper flow pattern is accompanied by a remarkable transition in surface weather. Low pressure systems are absent, but there is a rapid advection of moisture into Alaska, especially if the ridge amplitude remains fairly flat. During winter it coincides with very sharp warming over the interior. Temperature increases of 40 to 50 Fahrenheit degrees (22–28 Celsius degrees) in 24 hr are not uncommon, accompanied by areas of heavy snow inland and rain along the coast.

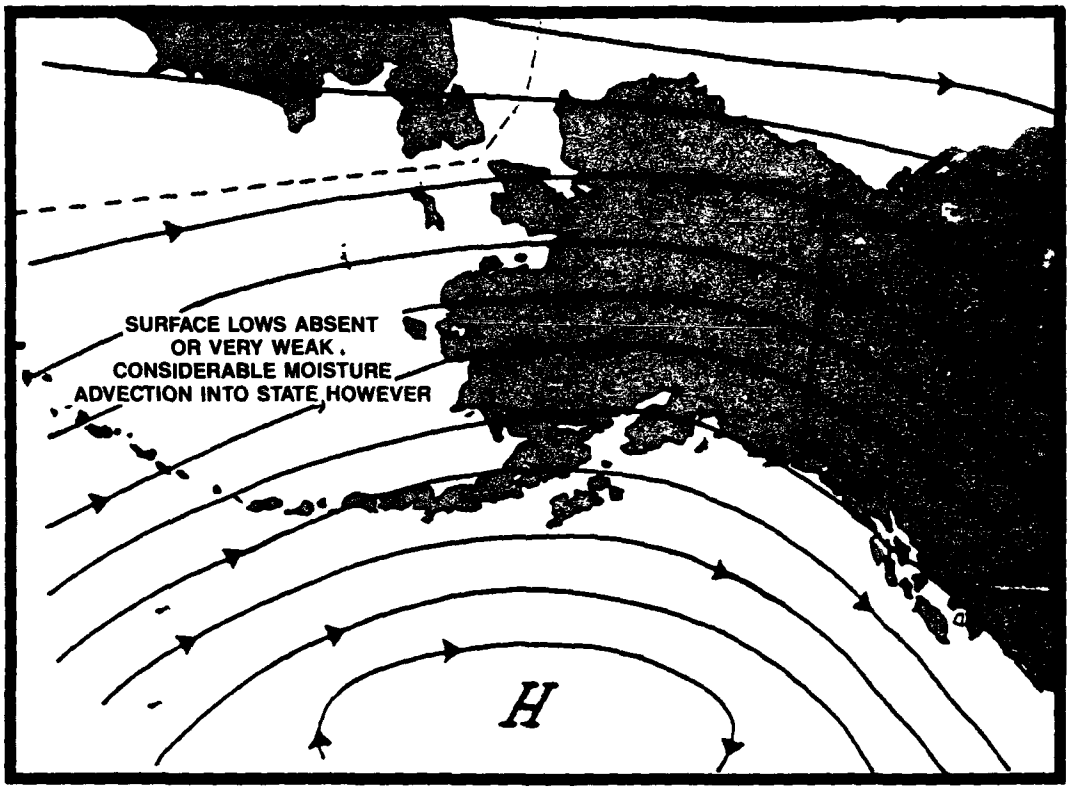

Figure 4-14. Rapid building North Pacific ridge regime.

Forecasters at King Salmon note that "this regime may produce IFR conditions at PAKN. Low ceiling and visibility conditions are most likely during the early morning hours. By mid to late morning, conditions should improve."

4.2.8 No Flow Regime

The no flow regime is shown in Fig. 4-15. Its characteristics at upper and surface levels are described below.

Upper Air (above 850 mb). Generally speaking, the jet stream remains south of the Alaskan mainland a good portion of the year. One important case is the light and variable or "no-flow" wind regime aloft, which can be expected over the state 10 to 20 times a year. These episodes last from 3 to 5 days. Satellite imagery is the only useful nowcasting and forecasting tool under this regime.

Surface. Surface lows track rapidly eastward, but remain well south of the mainland. During winter, patchy areas of clouds and snow can be found almost anywhere in the state. Any synoptic features are ill defined at best, and sporadic precipitation will occur in regions of upward vertical motion. During summer airmass type

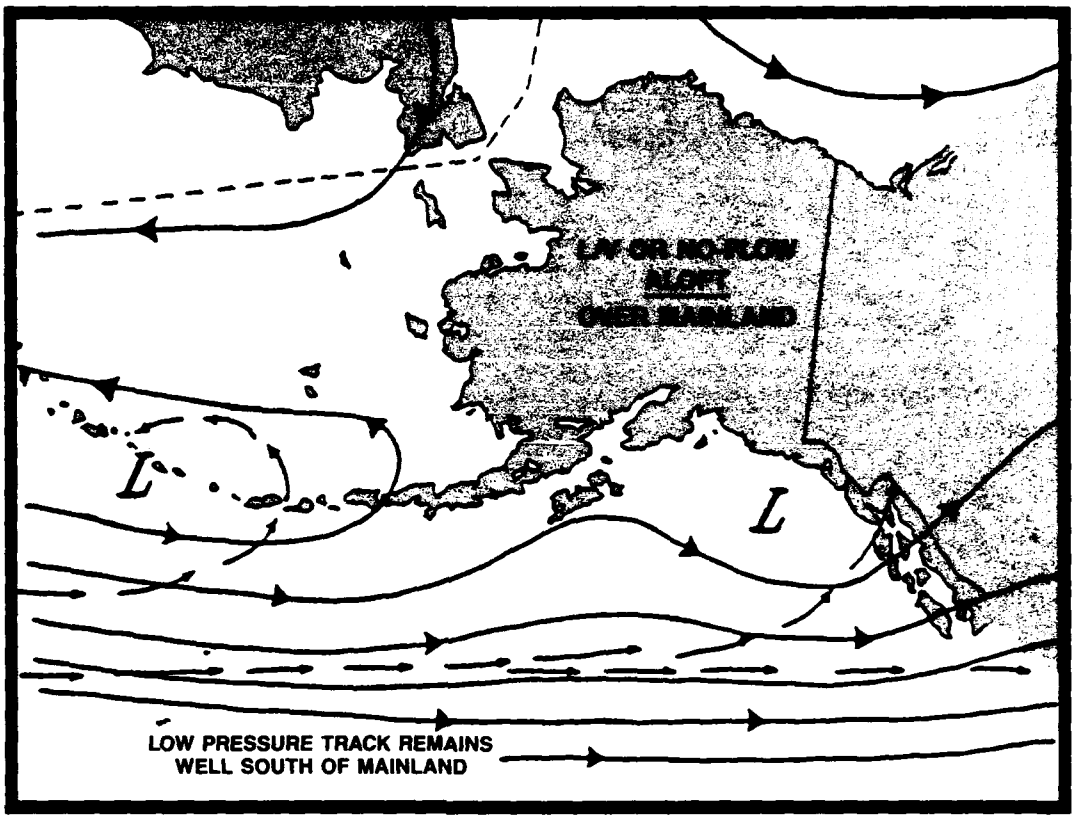

Figure 4-15. No flow regime.

showers and thundershowers will break out if weak divergence aloft (weak ridging) exists.

Forecasters at King Salmon note that "this can be a very unpredictable situation at PAKN. Check the SKEW-T and instability charts in the warmer months for possible convective activity."

Thunderstorms very rarely occur at the station but will develop in the area around PAKN. The Arctic boundary will frequently "dip" south in the colder months; low ceilings and light snow can be expected on its north side.

4.2.9 West Coast Storm Regime

The west coast storm regime is illustrated in Fig. 4-16. Characteristics of this regime at upper and lower levels are listed below.

Upper Air (above 850 mb). Low pressure circulation aloft somewhere over the Bering Sea is fairly common. About 3 to 6 times during a typical fall-winter stretch, such a low aloft over the west central Bering Sea will support a powerful winter

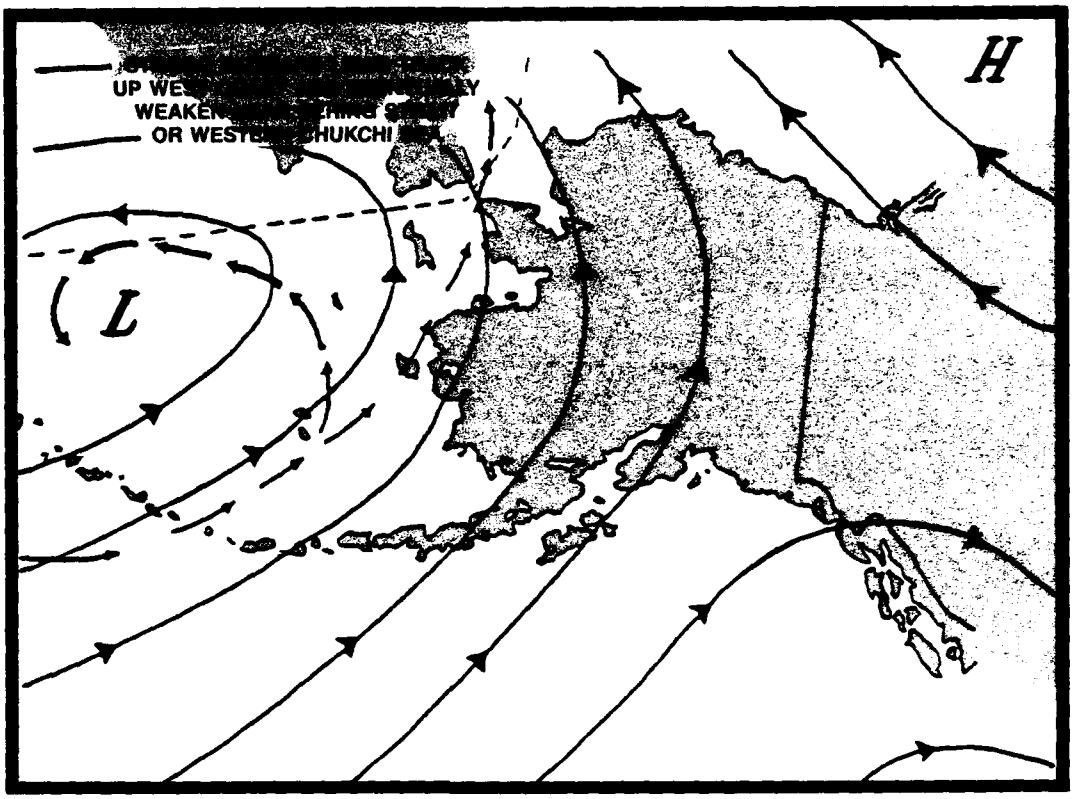

Figure 4-16. West coast storm regime.

storm tracking toward southwest Alaska. A ridge aloft over the eastern Arctic Ocean and/or a ridge over the eastern Gulf of Alaska will then curve the storm northward toward the Bering Strait before it eventually weakens. Note how the position of the upper low and extent of cyclonic curvature into Alaska differs from the regime in Fig. 4-8.

Surface. The storm at the surface normally attains its maximum intensity between the Pribilofs and Nunivak Island. The low will then weaken as it tracks either northward, or recurves slowly westward into the upper low while slowly dissipating. Blizzard conditions are almost assured along the west coast in advance of the system's northward moving occluded front. Since prevailing surface winds are easterly (a dry interior source), snowfall is normally restricted to extreme southwest and western Alaska.

Forecaster notes from King Salmon indicate at that location "this system can cause heavy rain and snow. Strong winds are normally not a problem since strong ridging is absent in eastern Alaska" (as opposed to the strong ridge south-southeast flow regime of Fig. 4-8, when very strong winds are experienced).

5. LOCAL THUMB RULES AND OBSERVATIONS

The forecasters handbooks for Adak, Amchitka, Shemya, King Salmon, Cold Bay, Port Heiden, and Kodiak were perused for local rules and observations made by forecasters at those locations and for their thoughts on area forecasts over the entire region. These guidelines are given below either in direct quotes or paraphrased for the purposes of this handbook. Note that many of these rules were developed years ago and although still valid, may be supplanted by current, reliable numerical guidance. Where numerical products are not available, these rules will prove invaluable. Credit for this section must be given to the many forecasters who contributed their knowledge and background in the development of those handbooks for the benefit of all the military forecasters to follow.

5.1 Bering Sea

Cold airmasses, both polar continental and Arctic, move into this area with regularity during the winter months. These airmasses become unstable as they modify rapidly over water and intense low pressure systems form on the fronts between these airmasses. Snow squalls frequently occur with a situation of this type, and the associated cumulus and altocumulus clouds appear as perfect thunderstorm formations although they lack the extreme violence of such. The tops of these clouds are often observed to be as high as 12,000 ft (3660 m) mean sea level.

When the Pacific High advances to the north, low pressure cells and the associated fronts move over Sakhalin Island, across the Sea of Okhotsk, over the Kamchatka Peninsula, northeast along the Siberian coast and across Alaska. The warm fronts affect Attu, but they do not cause weather at Amchitka.

5.2 Alaska Peninsula and Aleutian Islands

a. Under the influence of the expanding Pacific High southwesterly winds prevail as part of the summer circulation. Having originated far to the south in the warm, humid area of the Pacific Ocean, the air is cooled rapidly during its passage over

the North Pacific. Becoming saturated, it gives rise to the fog and low stratus that envelop the Aleutian Islands during this season. Since vertical circulation is practically nonexistent in such a stable airmass, only the lower levels are influenced by the colder water surface.

b. When the Pacific High recedes to the south, an area of frontogenesis develops southwest of Attu. The resulting waves move east-northeast and pass slightly to the south of the Aleutian chain or over the chain, causing precipitation but no appreciable wind velocities. Since the prevailing fog during the summer prevents observations of cloud formations, forecasting the approach of these disturbances becomes difficult. Pressure changes, wind direction and velocity, satellite data, and pilot reports serve to locate the fronts fairly accurately.

c. Partially occluded waves moving in behind an old occlusion have been observed to break up over the westernmost Aleutian Islands while the old occlusion continues in a northeasterly direction. The young waves may regenerate and move eastward along the Aleutians.

d. When a low pressure cell exists in the Sea of Okhotsk and a large cell of high pressure has built up over the central Pacific and the Aleutian Islands, observations have shown that the main storm track will reorient itself southwest-northeast through the western Aleutians and will cause low cells to stagnate in the Attu area.

e. Observations have shown that with the passage along the chain of a high pressure wedge originating in Siberia (1015 mb or higher), the low pressure cell following this wedge will deepen and slow down, causing very high winds and heavy precipitation along the western end of the Aleutian Islands.

f. The Aleutian Islands have a significant impact on oceanic wave heights in the vicinity. Wave heights can dramatically increase between the islands as the waves are funneling through the straits and passes. However, wave heights on the leeward side of the Aleutians are substantially diminished as the islands block the traveling wave trains.

5.2.1 King Salmon

a. When early morning fog or stratus is present and there are very few clouds, an increase of 4 to 6° after 15 GMT will be enough to dissipate the fog or stratus.

b. When the jet stream is not forecast to move over PAKN, pressure-gradient-induced winds should be forecasted to "max out" near 28 to 32 kt (14–15 m/s).

c. For warning criteria winds (35–49 kt or 18–25 m/s), the jet must pass over PAKN. Orientation is not important.

d. Gusts to 50 kt (26 m/s) are extremely rare at PAKN and should be forecasted only when an intense system is approaching the area, the low crosses the chain near Cold Bay, and the jet is very strong over PAKN. Even with this situation gusts of 50 kt (26 m/s) or more will endure only 1 to 2 hr. Gusts of 38 to 45 kt (20–23 m/s) will endure for several hours, or until the synoptic situation changes as the jet moves out of the PAKN area.

e. A survey of surface analyses for the period January 1969 through February 1970 and discussions with experienced forecasters indicated that three general wind conditions occurred at King Salmon and that each of these was associated with a distinct synoptic situation.

1. North wind (direction 320° to 050°). The north wind is associated with a low in the Gulf of Alaska moving northward or northwestward, along with a southward outbreak of cold air west of the Alaska-Aleutian mountain range. It appears that the strongest winds occur when the low is east of Kodiak Island at about 150°W longitude. As the low moves further west, the band of maximum wind shifts to the west of King Salmon. Furthermore, maximum winds are frequently associated with the period of strongest warm advection at 850 mb over King Salmon. The advent of cold air advection at 850 mb, which indicates that the low is filling and the cold air is becoming dominate, signals a decrease in wind speed at the surface.
2. East wind (direction 060° to 130°). The east wind occurs when an intense low is moving eastward or northeastward south of the Alaska Peninsula and crosses 50°N when still west of King Salmon. This is the most frequent strong wind situation at King Salmon. If the low continues to move with an easterly component into the Gulf of Alaska, the wind at King Salmon will back and decrease as the low passes south of the station. However, the strongest winds experienced at King Salmon occur when the low turns northward and moves across the Alaska Peninsula into Bristol Bay somewhere east of Cold Bay (winds as high as 82 kt or 42 m/s have been recorded). In most cases, an east wind will continue above 35 kt (18 m/s) as long as warm advection is occurring at 850 mb, but with the advent of cold advection, it will tend to decrease fairly rapidly. Extreme cross-isobaric flow is not unusual with east winds because of the effect of the mountains east of the airport. Occasionally, after the winds decrease to less than 35 kt (18 m/s), they will again increase from the south to over 35 kt (18 m/s).
3. South wind (direction 140° to 270°). The south wind occurs when an intense low moves northward or northeastward into western Bristol Bay, crossing the Aleutian chain between Adak and Cold Bay. If the low curves toward the northwest and does not cross the coast of the Alaska mainland, strong winds at King Salmon will usually be of short duration. The situation will be "touch and go" whether the winds exceed 35 kt (18 m/s). However, if the low continues to move northeastward into interior Alaska, an extended period of winds greater than 35 kt (18 m/s) may occur. Unlike east and north winds, the strongest southerly winds are associated with cold advection at 850 mb.

5.2.2 Port Heiden

a. The topography in the Port Heiden area exerts a moderate orographic influence upon the airmasses that reach this vicinity. To the southeast a pass is formed between the plateaulike hills to the east and the mountains to the south and

southwest producing a venturi effect on the winds from the southeast. Since this funnellike effect adds to the normal velocity of the winds, most of the extreme velocities recorded are from the southeast. Except during frontal activity southerly and easterly winds usually bring good weather since stability from latitudinal cooling is combined with the downslope effect of air traveling over the mountains to the south and east of the field.

b. Accompanying the establishment of a high pressure cell to the north over the Alaskan mainland, a northeasterly wind develops over Port Heiden. The airmass thus introduced with a trajectory over the mainland is a product of cold, dry air, and clear skies. In the fall and winter, when a ridge extends from the south over the field as a protuberance of the Pacific High, divergence will cause clear to scattered skies to prevail. This situation, however, is infrequent and of short duration.

c. When a high pressure cell exists over eastern Siberia and the western Bering Sea, much of the trajectory of the air over the station will have been over water. Winds will be north to northwesterly, and clouds will be broken cumuliform at 2000 to 3000 ft (610–915 m). With winds from the north or northwest bringing unstable air originating far to the north of Nome and a long trajectory over the Bering Sea, squalls and instability showers will develop. These showers and squalls are of moderate intensity and are frequent, occurring about two each hour and lasting from 3 to 5 min.

d. During the fall months when low centers stagnate in the Bering Sea and Pribilof-Nunivak areas, excellent flying conditions with light southwesterly winds exist at Port Heiden. In the winter months when the polar front is to the south of this area, a low cell persisting in the Gulf of Alaska and a high cell over the mainland of Alaska will cause fresh polar air to envelop the station. Winds will be northeasterly with temperatures ranging from 0° to −20°F (−18° to −29°C). As the occlusion moves in an easterly direction south of the station, moderate to heavy snowfall will reduce the visibility and ceiling to zero, and strong winds will continue. In the absence of frontal weather, blowing and drifting snow will often reduce the visibility to zero. The station will open as soon as the cold air recedes to the north.

e. In the late fall and winter, lows ordinarily pass to the south of Port Heiden. When the occlusion is to the southwest, broken to overcast clouds at 5000 to 8000 ft (1525–2440 m) will ordinarily prevail and winds will be light to moderate southeasterly. As the occlusion moves eastward to a position south of the station, the overcast will become solid with the ceiling lowering to 2000 to 3000 ft. Within 2 to 3 hr the ceiling will lower to 800 to 1000 ft, winds will become northeasterly, and precipitation will reduce the visibility to 3 to 6 mi (5–10 km) when falling as rain and 1 to 3 mi (1.6–4.8 km) when falling as snow. After the low center has moved east of the Kodiak area, precipitation will cease, ceiling and visibility will improve, and sky coverage will be overcast-to-broken.

f. During the late summer and early fall a low passing to the north will bring overrunning air from the warm front with the formation of an overcast 6 to 12 hr preceding the passage of the front. Drizzle and rain with poor visibilities will

begin just before frontal passage and will prevail through the warm sector. After passage of the cold front a northwesterly wind and cumuliform overcast will occur with frequent showers and squalls. Ceilings are usually from 1000 to 1500 ft, and visibilities lower to 3 to 6 mi (5–10 km) in precipitation. Winds are 17 to 26 kt (9–13 m/s) with gustiness of 30 to 35 kt (15–18 m/s).

g. When a low system proceeds along the chain and passes over Port Heiden, good weather will precede the occlusion, especially in the fall, and winds will be light to moderate from the southeast and northeast. About 3 to 6 hr before the arrival of the occlusion, flying conditions will become unfavorable with low ceilings, poor visibility, and considerable precipitation. In the immediate center of the low the weather will be calm and practically clear, but with the passage of the upper trough line closed conditions with moderate northwesterly surface winds will prevail.

h. In the fall a weak, slow-moving occlusion may move over the station while a high pressure area is situated over Canada and eastern Alaska. With the trajectory of the air behind the occlusion from the south or southwest over the Pacific Ocean, fog and low stratus will prevail for approximately 24 hr after the occlusion has passed. Occasional drizzle and fog will reduce the visibility to 0 to 1 n mi (0–2 km) and the ceiling to 0 to 100 ft. In the late fall and winter, warm front type occlusions with marked upper cold fronts frequently pass. With the passage of the upper cold front, strong, gusty, southeasterly winds and moderate precipitation will be observed. Immediately to the rear of the upper cold front clearing will be rapid and the winds will decrease sharply. Although the station is not closed preceding the passage of this portion of the storm, flight is hazardous because of heavy turbulence and strong gusts at the surface of the field. Moderate to severe icing is usually prevalent with the passage of an upper cold front. As the occlusion passes the station only slight gustiness will occur, but closed conditions will exist for 6 to 12 hr.

i. Southeasterly winds of gale force with williwaw effect will occur when a low from the west or northwest passes over or north of the station. Wind velocities will be 9 to 17 kt (5–9 m/s) higher than the general circulation around the approaching low. An intense low deepening to the southeast through southwest will cause northerly winds with velocities somewhat lower than the general circulation. Northerly and westerly winds are usually associated with overcast skies, but frequent breaks and a minimum of precipitation occur except during frontal activity. Northeasterly winds blowing from a high pressure area located over the Alaskan mainland tend to produce clear skies. In midwinter northeasterly winds envelop the station with fresh polar air and cause the temperature to fall as low as 0° to −20°F (−18° to −29°C).

j. In winter, especially after a snowfall, moderate to strong winds from the west through the northeast may cause moderate to heavy drifting snow. In the late spring and summer when the station is dry and free of snow, southeasterly winds of 17 kt (9 m/s) or more will cause blowing dust, and velocities over 35 kt (18 m/s) may restrict visibility by a condition of severe blowing dust.

k. In summer with cyclonically curved isobars and light circulation from the northwest, west, or southwest, fog and low stratus will prevail. With a ridge of the Pacific High extending into the Bristol Bay area, fog will lie offshore during the day and move inland at sunset.

l. In the spring months certain ideal conditions for the formation of fog have been noted. A filling low and a frontal occlusion in Bristol Bay give rise to a gradual change in wind direction from the southeast or south to the west with a velocity of 4 to 10 kt (2–5 m/s). Fog will envelop the station shortly after the wind change. This fog will persist for an extended period or until the wind backs to an easterly direction. With winds from the northwest fog will develop about 4 to 5 hr after the frontal passage. However, northeasterly winds will give rise to low ceilings, but the visibility will remain comparatively good.

5.2.3 Cold Bay

a. The topography in the vicinity of Cold Bay exerts a pronounced effect on the strength and direction of the wind recorded at the surface. Good protection is afforded by the mountains to the east and west, and as a consequence, winds from these directions are light, rarely exceeding 9 to 13 kt (5–7 m/s).

b. A low centered near the airfield results in a southwest to southeast circulation producing south-southeast winds of supergradient velocities. North winds are representative and are not altered in velocity and direction.

c. When a low pressure system moves south of the Alaska Peninsula and then into the Gulf of Alaska, with the Siberian High situated over the Bering Sea area and across the western Aleutians, the winds at Cold Bay are from a northwesterly direction and are moderately strong in intensity. The ceiling and visibility will be near zero for the first 24 to 48 hr, improving thereafter, but snow squalls and showers will continue throughout the following few days. This situation is usually noted in the winter months.

d. A situation that occurs rather frequently during the fall, winter, and spring months causes well defined weather conditions that are not too difficult to forecast. When a ridge of high pressure from the Pacific High is oriented from south to north near or just east of Cold Bay, the station will have ceilings of about 2000 ft and southerly winds. When a fairly deep low center approaches Adak, which has an occlusion extending to the southeast approaching Cold Bay, the station will experience increasing wind velocities of 26 to 43 kt (13–22 m/s) from the southeast. Lowering ceilings and precipitation will also accompany the frontal approach. If the high pressure ridge remains near Cold Bay, the winds will increase to 60 kt (31 m/s) or more with increasing precipitation and very low visibilities. The eastward movement of the occlusion will become almost stationary near the station, whereas the northern portion of the occlusion will proceed around the low center to the north. With this situation Cold Bay will have winds of 35 kt (18 m/s) or higher continue for 24 to 48 hr, depending upon the intensity of the low center

and the occlusion associated with it. The strong southeasterly winds will begin to decrease a few hours after the pressure starts to rise.

e. In summer a strong cyclone still deepening over the western half of the chain will be retarded and stop completely whenever a similar low occurs in the Gulf of Alaska, and it will not start moving until the low in the Gulf fills. At the same time a col or weak high ridge is always present over the peninsula, and Cold Bay is usually in the center of the col or ridge. Under these conditions the ceilings are usually higher than at neighboring stations, i.e., 1500 to 2000 ft (460–610 m). A col or high pressure wedge over the peninsula in summer results in warm polar maritime air being brought onto the peninsula, causing drizzle and fog that are most dense at night.

f. Fronts, usually occlusions, that travel along the chain stations normally move with a fairly constant speed until they pass Umnak. Frequently they will decelerate rapidly between Umnak and Cold Bay, particularly when the Alaska Peninsula has pressures of 1015 mb or higher and the pressure is continuing steady or is falling very slowly.

g. The lows that frequently stagnate and fill in the Bristol Bay area north and northeast of Cold Bay cause weather that comes in a more or less routine sequence. Immediately after passage of the front the winds will shift from southeast to west-southwest to west-northwest. The frequent squalls and showers will lower the ceilings and visibilities for the next 2 hr after frontal passage. The second day will show a pronounced clearing to low scattered or broken clouds. On the third day the cloud cover will be overcast, but ceilings will remain favorable for flying. Such a sequence will not, of course, hold true if another front moves in after the stagnating low. A northwest surface wind after passage of a frontal system or an outbreak of cold air will give the Cold Bay area strong winds and instability showers for the first 24 to 36 hr. In summer when a front passes, which is oriented in such a manner that postfrontal winds are south-southeast at Cold Bay, a day of favorable weather may be expected with good ceilings and no precipitation.

h. Because of the orography at this station the strongest winds are from the south-southeast. The maximum velocity is attained when a low pressure system is approaching from the west. These winds usually endure for only a few hours. Strong surface winds that continue for 24 to 48 hr are noted after the pressure begins to rise. A northwesterly gradient brings southeast winds and a stable type of weather. Frontal approaches cause well defined wind shifts from south-southwest that back slowly to southeast and increase in velocity. The frontal shift will then be to west-southwest, and the winds will be nearly calm if the low center is nearby.

i. In August when the first deep lows start to move across the chain with any regularity, the winds behind the low center seem to be directly proportional to the rate of rise of pressure. This isallobaric influence seems to have as great an effect as the actual pressure gradient itself. The faster the pressure rises at the station the higher the winds will be over the gradient velocity.

j. Southwesterly winds bring improving conditions and clear weather after a period of 24 to 48 hr when a frontal system has passed or from the circulation of a high

pressure system south of Cold Bay. Occasionally, light fog and drizzle are associated with southwesterly to southeasterly winds, depending upon the synoptic situation.

k. In summer with scattered low stratus or fog over the Bering Sea in a warm air-mass, the westerly circulation will cause the stratus to blow into the bay area. At this time the fog area has moved north of Amchitka across the Bering Sea and is found all along the coast of Bristol Bay. The sky may be overcast for days at a time until a low system to the west causes southeasterly winds.

l. Diurnal heating, although of small range, is nevertheless of sufficient influence to have some regulatory effect upon the formation of stratus and stratocumulus clouds. During a synoptic situation that favors the development of stratus throughout the Cold Bay region, the diurnal increase of temperature will, with light winds, ordinarily cause the ceiling to rise by noon. It is noted, however, that the areas adjacent to the Bering Sea (north and west of the station) on the instrument landing approach to the airfield usually have ceilings one-half the height of those reported at the station. However, if the ceiling over the field is greater than 2000 ft this condition is negligible. When light north and west winds (less than 17 kt or 9 m/s) are present, a greater tendency exists for fog and drizzle to occur in that quadrant. If the wind is south-southeast at the surface, the ceiling is also lower near the narrowest part of the station. In winter, synoptic situations that give rise to outbreaks of polar continental air are normally conducive to the extensive development of stratocumulus formations. This cloud cover during the day usually completely covers the land areas but dissipates entirely during the night.

m. Difficulty arises when forecasting the formation of lower cloud layers and cirrostratus without associated frontal activity. The unexpected formation of a high overcast makes the forecasting of the lifting or breaking of the summer stratus uncertain. At times the higher overcast may be due to cyclonic waves south of the Aleutian chain. In general, the high overcasts are attributed to the overrunning of warm air.

n. A synoptic situation in which a low is centered in the Gulf of Alaska and a high in the Bering Sea is conducive to advection type fog. During the early summer, advection type fog exists at Cold Bay with a south-southeast surface wind of fairly light intensity. The dissipating time of this type of fog is dependent upon the upper cloud cover. During summer in the bay area sea fog and stringers of stratus, which stream through the passes in the mountains, should not be mistaken for fronts.

o. During the summer months when most of the Aleutian chain has considerable fog from the southwesterly flow of the Pacific High cell, Cold Bay usually has flyable weather. When Cold Bay is in the area of a light westerly gradient at the ridge of the high, surface winds will be light and vary from south-southwest to west. Frosty Peak to the southwest causes some dissipation of the fog, and as a result ceilings may be 100 to 400 ft, whereas visibilities will be variable from near 0 to 2 to 3 mi (0–3–5 km) in fog and drizzle. When the gradient wind from the Pacific High is definitely southwest, Frosty Peak will cause improved conditions only over the base. At such times Cold Bay will have ceilings of approximately 500 to 1000 ft though surrounded by low stratus and fog lying 2 or 3 mi (3–5 km) from the field.

p. During most of the year when a low center passes nearly north of the chain or along the chain, the clearing behind an occlusion or warm front is slow because the prefrontal fog and drizzle are carried around the low center. By carefully drawing the fog area around the occlusion, the forecaster may calculate, with good verification, the time required for the fog to be completely blown around the low.

5.2.4 Adak

a. Certain synoptic patterns do presage certain events. The most reliable and striking are
   1. A blocking upper level ridge over the central and eastern Bering Sea and Alaska will steer surface cyclones into the western Bering Sea or south of Adak into the Gulf of Alaska.
   2. The cyclones that move north will bring dissipating frontal weather into Adak as the fronts continue eastward into the block. The weather is all warm frontal or occluded type with rain predominating, followed 12 to 24 hr later by broken conditions with little or no precipitation.
   3. The cyclones that move south of Adak bring light easterly winds with light rain or drizzle if the center is north of 45 °N. This type of cyclone may very well cut under the block. Unless the block shows eastward movement it will reestablish itself after cyclone passage.
   4. When the block retrogrades so that the ridge axis is near Adak, overcast conditions with light winds and no precipitation predominate. In spite of the strong subsidence aloft, a residual surface trough persists across the western Aleutians as the successive cyclone frontal systems dissipate in the block.

b. True northwest winds seldom reach any velocity over 15 kt (8 m/s) regardless of the gradient, as Mount Moffett will block and funnel wind around it to become west to west-northwest. Winds from 120° to 190° will generally be about one-third of the gradient wind due to the mountainous terrain south of the field, unless the gradient exceeds 50 kt (26 m/s). Winds from 190° to 250° will normally be representative ot the area gradient (though gusty), unless the pressure gradient shows signs of strengthening, at which time the winds will be about one-third more than the gradient flow due to lower mountainous terrain and a more favorable orientation of passes that lead away from the airfield. Winds in any direction will be gusty when in excess of 15 kt (8 m/s). Gale force winds may have gusts frequently as high as double their velocity.

c. An intense low center passing 60 n mi (111 km) west of Adak will produce storm force southerly flow, whereas the same low passing over Adak or east of Adak will seldom produce storm force winds.

d. The marine environment and mountainous terrain guarantee persistent orographically induced low cloud coverage. It averages two-tenths to three-tenths more than normally would be expected; however, increased ceiling heights usually keep Adak in VFR conditions.

e. Storms may occur in any season but are most numerous and severe in winter.

Winter is a season of intense cyclonic storms, gusty winds, rain, snow, or rain and snow mixed. Between storms, however, Adak has some of its best flying weather in winter. Basically, convective conditions prevail with good visibility and high broken or even scattered skies. During the summer season, the frequency and intensity of storms is much less. The warm air being advected up the back side of the North Pacific High over the cool local waters gives rise to extensive areas of advection fog and low stratus, which frequently drift over the station, although rarely bringing the visibility below minimum.

f. Nearly all forms of precipitation occur on Adak; mixed rain and snow showers are quite common throughout winter, and snow and ice pellets occur mostly in late fall and winter. A few thunderstorms have been recorded, mostly in late winter just before sunrise. They are usually of short duration and are accompanied by snow or ice pellets rather than hail. Besides heavy frontal precipitation, cold air-masses move from Asia behind cold fronts over the warmer waters of the Northwest Pacific during the winter, causing frequent snow showers to dominate the local weather. Because the Pacific High extends south of Adak in the summer, warm moist air is trajected over the cooler waters producing widespread drizzle and fog.

g. In the spring and summer, fog is the prevalent situation through most of the North Pacific and the Bering Sea because of the warm moist air flowing north over colder water. Although the conditions over the ocean may be near zero, Adak is normally VFR. When the wind direction is from the south to the west, the stratus and fog will be lifted by orographic effects, the degree of which is determined by the wind speed. With calm winds or winds of less than 5 kt (2.5 m/s) from the north-northeast, ceilings and visibility will be at or near zero. Normally around dusk, they will improve as a result of either an increase in wind speed and/or heating of land surfaces.

h. The precipitation type is predominantly showery. Showers are brief and frequent due to island characteristics and topography. Steady precipitation occurs only with advancing warm fronts and occluded fronts associated with cyclones moving along or south of the Aleutian chain. Snow showers occur in winter and early spring, whenever the predominate flow is from the northwest to northeast and a lowering of the freezing level occurs.

i. Rain and snow mixed generally accompanies any system moving around the southwest periphery of Adak in the winter; showers are heavier than normal. The steady rain associated with a warm front usually extends out to about 300 n mi (555 km) ahead of the front. Many times, however, passages of warm fronts are very difficult to distinguish. A slight rise in temperature and a shift of the wind to a more southwesterly direction may be the only indicators.

j. Some of the most useful rules for forecasting (particularly in the autumn season) are
   1. A blocking high centered near 40 °N, 160 °W will cause all lows in the Adak area to move northeast.
   2. The strongest winds are usually in advance of lows, associated with isobar packing immediately in advance of frontal systems, except when an occlusion moves over the central Aleutians. Because of topography, Adak's strongest winds, which are north to northeasterly, will occur after frontal passage.

3. The strongest diurnal winds occur near 1500 to 1600 LST, and the minimum occurs from 2300 to 0600 LST.
4. With a freezing level:
   above 2500 ft (762 m)—forecast rain
   800 to 2500 ft (244–762 m)—forecast snow pellets
   0 to 800 ft (0–244 m)—forecast snow

k. Additional rules that may be of assistance include
1. With a temperature above 25 °F (−4 °C) a wet snow will fall and not drift as badly as a powdery snow, which typically occurs at temperatures below 25 °F (−4 °C).
2. Partly cloudy conditions and calm winds will produce the most extreme minimum temperatures.
3. High pressure over Siberia in February will keep lows south of the Adak area.
4. Lows that remain south of 45 °N will seldom have a cloud shield and never have a rain shield that affects Adak.
5. In summer, with a high over the Shemya area moving eastward, the lowering of subsidence inversion and development of either fog or extremely low stratus should be expected.
6. With a southerly wind at Shemya near zero conditions at Adak should be expected.
7. The warm and cold advection pattern at the 500-mb level should be watched to determine rain versus snow. During the winter, frontal precipitation may begin as snow, changing to rain with the crossing of the line of warm advection at the 500-mb level. After frontal passage, rain showers may predominate until the leading edge of cold advection at 500-mb passes, and then snow showers will prevail.

l. Ceiling and visibility forecasts during the summer can be determined with the aid of the following thumb rules:
1. With a wind speed of 10 to 20 kt (5–10 m/s) from the south through west, the ceiling will usually be between 300 and 600 ft and the visibility less than 1 n mi (2 km).
2. When the speed decreases to less than 10 kt (5 m/s), the ceiling may drop to 100 to 200 ft and the visibility to 0.5 n mi (1 km).
3. With a wind speed below 10 kt (5 m/s) from the northwest to north, fog is brought in through the passes to the north of the field, dropping ceilings to 200 to 500 ft and visibility down near 0.5 n mi (1 km).
4. Field conditions will be near zero-zero with calm winds, or winds less than 5 kt (2.5 m/s) from the north-northeast.
5. With winds less than 12 kt (6 m/s) from the east-southeast to south-southeast, ceilings will normally be 200 to 600 ft and visibility between 0.5 to 2 n mi (1–4 km). Conditions will improve with higher winds, which normally do not exceed 25 kt (13 m/s) with this weather pattern.
6. Whenever any strong flow (20 kt or 10 m/s, or more) tends to cross the Aleutian chain from north to south or vice versa, low-level turbulence (due to speed and directional shear in the vertical and horizontal) can be expected.

m. Studies have generally shown that the clear area associated with the center of a migratory anticyclone remains in the same position relative to the high pressure center, even though the clear area decreases in size with the collapse of the ridge.

n. When it can be definitely ascertained from the satellite image that a formerly clear area associated with a surface high cell has become filled with clouds (excluding stratus), the forecaster may anticipate complete collapse of the anticyclone in 24 hr.

o. Variable fog conditions occur over Adak during the year: from infrequent fog during the winter to frequent fog moving over the field in spring and summer. On the average, fog occurs 151 days per year. A long trajectory of warm moist air, extending sometimes to Japan, is carried over the cooler waters of the Northwest Pacific High during these months. This results in large areas of advection fog. Because of the rugged terrain of Adak and the relatively high average velocity, ceilings seldom lower below FAA minimums. When the winds are calm or a light north-to-east wind is blowing, the stratus and fog approach the airfield causing the ceiling and visibility to be near zero. After several hours the visibility and ceilings will rise above the FAA minimums, and the winds will increase to 5 to 10 kt or with normal daytime heating.

p. During most of the entire year, icing is a significant hazard for small aircraft, and in the ascent and descent patterns of large aircraft because of the large number of frontal passages, the predominance of a cold airmass, and convective type clouds over Adak. Icing depends on many parameters including temperature, humidity, size, and stability of the water droplet present, and the speed, altitude, and geometry of the aircraft. The orographic lifting of conditionally unstable air because of the rough terrain of Adak also contributes much to the ice-forming process.

q. The most significant type of turbulence at Adak is mechanical. With certain wind speeds and directions near the ground, small eddies and gusts are produced by wind shear. This turbulence is very significant in takeoffs and landings at Adak. Its intensity depends on the wind direction and is directly proportional to the wind speed. Southwesterly winds produce the most mechanical turbulence at Adak. Zeto Point, when using runway 23, is a particularly turbulent area that has northeasterly flows. For strong winds between 2000 ft (610 m) and 6000 ft (1829 m) from the west, severe to extreme turbulence to 8000 ft (2438 m) is very common. Also, with winds of a southerly component of 20 kt (10 m/s) or higher, severe to extreme turbulence to 10,000 ft (3048 m) should be expected because of mountain waves.

5.2.5 Amchitka

a. Because of the frequency of snow squalls associated with modified polar continental air, the weather conditions over Amchitka may change very rapidly, sometimes going from unlimited to zero-zero within a few minutes. This condition ordinarily will last for only 10 to 15 min during each intense squall or shower, but it may be expected to occur rather frequently during the coldest months.

b. High pressure cells rarely dominate the Amchitka area during summer; however, when they do occur and Amchitka is near the western rim of the high cell, a layer of stratocumulus will develop with the base at 2000 to 2500 ft (610–762 m) and a thickness of approximately 1000 ft (305 m). When the station is on the eastern rim of the high pressure cell, cloudiness will decrease and become cumulus type with shower activity throughout the area.

c. Frontal passages through Amchitka are frequent and intense during the winter months. Through the early part of the winter period the storms move south of the western Aleutians. When the Pacific High dominates the Gulf of Alaska, the low cells are deflected and move along a general south-north path, crossing the chain very near Amchitka and stagnating over the Bering Sea. This situation produces little or no frontal weather over the extreme western end of the Aleutians, but it results in the fronts passing Amchitka with their full force. When the low stagnates over the Bering Sea, Amchitka will experience overcast skies at 1000 to 1500 ft (305–457 m) for a period of 18 to 24 hr.

d. When a storm path is oriented east-west and a frontal system approaches this station, the precipitation shield will be approximately 200 to 250 n mi (370–465 km) in advance of the front, and one can estimate a 9- to 10-hr elapse time from the beginning of precipitation until frontal passage. For a storm with this orientation, a reliable forecast of the time of frontal passage can be made by computing the time required for movement of the shield from Shemya or to Amchitka. The forecast is more difficult when the system passes south of the Aleutians and forms a bent-back occlusion just south of this station. In this case the precipitation shield may reach Amchitka within a few hours after Shemya reports precipitation and lowering ceiling.

e. Throughout the winter the predominant type of front is the warm type occlusion. When these fronts pass through Amchitka, rapid clearing will result, followed about 2 to 3 hr later by quite extensive shower activity that may continue for 24 to 36 hr. The velocity of the accompanying winds, if from the northwest or north, will often equal and sometimes exceed the velocity recorded prior to frontal passage. When the low pressure center moves north of the Aleutians and stagnates north of Amchitka, a series of secondary cold fronts may develop and move over the western Aleutians at intervals of approximately 10 hr. If a low pressure cell passes 200 to 400 n mi (370–740 km) south of the station, a solid deck of altostratus clouds will form at an average of 7500 ft (2286 m) with a few stratocumulus below 3000 ft (914 m). As fronts pass to the south within 150 n mi (278 km) of Amchitka, continuous precipitation will prevail over the area for a period of 18 to 24 hr. It has been noted that if the pressure begins to fall before the appearance of high clouds, the storm center will pass to the north; whereas, if the high clouds appear and the pressure begins to fall simultaneously, the low center will pass over or very near the station.

f. Indications of a secondary cold front formation and movement within the area of influence of this station are limited, but some general indications have been noted as follows:

1. With returning circulation behind a deep, stagnant low in the central Bering Sea, a secondary cold front passage may be expected within 18 to 24 hr after the low cell stagnates in this position.
2. The pressure will hold steady until a front is within 50 to 75 n mi (93–140 km) of Amchitka, at which time the pressure will begin to drop slowly.
3. Low pressure cells centered in the south central portion of the Bering Sea have a tendency to generate secondary cold fronts oriented along an east-west axis. These secondary cold fronts result in the entire western Aleutians coming under the influence of the system almost simultaneously. Amchitka is usually affected 3 to 4 hr after the extreme western islands.
4. Low pressure cells centered in the southwestern portion of the Bering Sea tend to generate secondary cold fronts oriented along a northeast-southwest axis. Under these conditions the time of passage over Amchitka may be determined by assuming a movement of 22 kt (11 m/s) after passage over Shemya.

g. Cold fronts that affect this area during summer have their origin over the landmasses of eastern Asia. They follow a path over the Island of Sakhalin, across the Sea of Okhotsk, over the Kamchatka Peninsula, and then east-northeast along or north of the Aleutian Islands. Since these systems are very weak, they are important to Amchitka only because of the circulation they bring to the area. Summer frontal systems do not constitute a hazard to flying in this area except for the fog and low stratus that result from a southerly flow.

h. The forecasting of strong winds in winter at Amchitka is as important as forecasting summer fog and usually can be done with considerably more accuracy. Winds above 30 kt (15 m/s) are a common occurrence during the winter, and frequently winds above 90 kt (46 m/s) are recorded when an intense low cell passes through this area. In almost all types of synoptic situations the wind is very gusty: at times the gusts are 20 to 30 kt (10–15 m/s) higher than the constant wind velocity. The winds that accompany a winter snow squall may, within a very short time, increase in intensity by 25 to 30 kt (13–15 m/s). The accuracy of wind direction and velocity forecasts depends upon the degree of accuracy to which the forecaster is able to plot the paths of the intense winter cyclones.

i. Forecasting wind direction during the summer months is important only in relation to fog formation. Winds above 25 kt (13 m/s) are rare for this period even when low centers pass over or very near the station.

j. During winter the dominant cloud type is stratocumulus, although altocumulus is the prevalent middle cloud type associated with the passage of frontal systems. The clouds that appear with the winter squalls are not the typical cumulus type generally found over landmasses but appear to be formed by the joining of the stratocumulus and altocumulus layers. A continuous southerly flow for a long period prior to the approach of a deep low cell from the southwest or west will bring in low stratus cloud.

k. The prevailing cloud type during summer is low thin stratus. Stratocumulus type clouds will develop with the passage of a cold front that brings modified polar continental air into this area.

l. Although Amchitka Island is rather narrow, the surface area is quite large and may at times be heated sufficiently to form a cumulus cloud deck. This condition, as observed from aircraft, exists mainly over the island; the surrounding water area is free of clouds or has only scattered cumulus. The heating, however, is insufficient to produce extensive vertical buildup, and the clouds remain quite shallow throughout the day. Clouds produced under such conditions prevail until sunset and dissipate, leaving clear to scattered skies.

m. Fog is the most important restriction to visibility during the summer months, while light rain or drizzle constitutes a minor restriction to visibility. During the summer season fog is associated with practically all surface synoptic situations, but the actual forecasting of the time of formation and dissipation is indeed difficult. Close observation of airmasses and storm paths to determine a flow pattern is imperative for accurate forecasting of fog conditions. This is made difficult because of the small number of reporting stations in this area.

n. Two types of fog have been observed at Amchitka, a wet type and a dry type. The wet type fog is associated with fine drizzle that falls continuously, forming water on vehicles, buildings, and the ground. The number of water droplets correlates closely with the thickness of the fog layer (thick layer-large droplets) and with the trajectory of the airmass over water. The dry type fog will not cause condensation on ground objects and is subject to rather rapid dissipation by surface heating. Both types of fog are formed by the advection of warm air over cold water.

o. The plotting of airmass trajectory is helpful in forecasting fog formation, especially when the tongue of warm air has come around a low center and approaches the island from the north. Such a condition is extremely difficult to forecast without satellite imagery because of the lack of accurate reports that are necessary to trace the boundaries of an airmass. A good example of this is found in one situation where a low pressure cell at Atka produced a northerly flow at Amchitka that resulted in scattered to broken clouds at 500 to 800 ft (152–244 m). A pilot report obtained several days later indicated that a stream of fog approximately 100 n mi (185 m) wide had extended from Tanaga to Kiska with a north-south orientation. This observation provides an excellent example of how airmass trajectory affects fog forecasting. During the months of May through September when a southerly flow of air is observed, fog can be expected within 2 to 4 hr, depending on the proximity of the fog bank. Pilot reports are helpful in determining the northern boundaries of fog banks.

p. When Amchitka is under the influence of a southerly flow accompanied by advection fog, the following deductions concern its influence on the field. As the air moves north from one runway toward the other runway, it crosses land that slopes gently downward. Adiabatic heating then usually maintains a ceiling of 100 to 200 ft (31–61 m) with visibility 0.5 to 1 n mi (1–2 km).

q. Some of the conditions producing fog-free weather or causing the dissipation of fog are as follows:

   1. When a wedge of high pressure builds up from the Pacific High over the Sea of Okhotsk and Siberia, returning tropical maritime air that has had a trajectory north of the 60° latitude dominates the area.

2. In many instances, with the approach of a well defined warm front having a widespread cloud pattern, fog has been observed to clear for a period of 3 to 6 hr preceding the precipitation shield. This clearing is especially true if the precipitation shield arrives over the island during the late evening.
3. Fog-free weather may result when the station is on the back side of a low that has passed far enough north to give circulation from above 65 °N latitude.
4. If fog of the dry variety is 1500 ft (457 m) or less in thickness, no upper clouds exist, and if the surface wind is greater than 13 kt (7 m/s), fog will flow over the field and cause variable ceiling and visibility conditions on the runways. However, under these conditions the clouds will be broken 1 n mi (2 km) north of the runway.
5. A synoptic situation resulting in northwest winds at the surface and cold air advection up to 10,000 ft (3048 m) will generally produce fog-free weather and cumulus cloud formations instead of stratus. This rule has worked quite well for Amchitka on many occasions but has not been thoroughly tested.

r. Some of the elements to be observed during periods of fog-free weather for indications of fog moving in or forming are as follows:
1. When the wind is from a southerly direction with a velocity below 10 kt (5 m/s), a definite tendency toward increased velocity may be an indication of fog.
2. When the wind is from any direction other than south with a velocity less than 15 kt (8 m/s) and the air has a short trajectory over the Pacific, an increase in wind velocity to over 18 kt (9 m/s) may be an indication of fog.
3. If a bulge of high pressure extends north of the Aleutians and gives fog-free weather at Amchitka, fog may be expected to form again when the wind shifts from northwest to southwest.
4. The formation of vapor trails from fast moving aircraft may be observed for indications of the amount of saturation.
5. A few thin wisps of fog drifting over the station often give 15 to 30 min warning before zero-zero conditions prevail.

s. On 23 August 1948 a low pressure cell passed north of this station and a thunderstorm of moderate intensity was reported with the passage of an occluded front. Zero-zero conditions prevailed at the surface during the entire period of frontal activity. This is the only thunderstorm activity ever reported at Amchitka. It is indeed a rare phenomenon! (This statement was made in 1949.)

t. Light rain and drizzle during the summer months can be considered a daily occurrence. This precipitation is usually continuous during long periods of southerly flow. Although of long duration, the precipitation reported for a 24-hr period seldom exceeds 0.2 inch (0.5 cm).

u. The temperature is very stable during the summer months, and the diurnal variation is usually less than 3 Fahrenheit degrees (1.5 Celsius degrees). The free air temperature is an important factor during this period since the extensive fog formations are a direct result of the warm air in the lower levels passing over the colder surface of the North Pacific.

5.2.6 Shemya

a. The moist property of the air around Shemya is indicated by the fact that almost every day in the year has at least a trace of precipitation.

b. When a low occurs to the east or southeast of Shemya accompanied by a strong southeastward movement of the Siberian High cell, a tight pressure gradient often develops with resultant high winds. This movement of the Siberian High can be predicted by a rapid filling of pressure in the quasi-stationary low cell off the east coast of the Kamchatka Peninsula. During the transitional period precipitation is, for the most part, in the form of rain and snow pellets.

c. When a storm passes to the south of Shemya and high pressure builds to the north, strong east-to-northeasterly winds and heavy precipitation will occur. Strongest winds are observed when a low passes to the south of Shemya. A strong easterly wind may continue for 24 hr, gradually swinging toward the north after the system has moved past. The best weather in this period is usually found on the first day of a northerly wind flow after the system has moved to the east. By the second day air temperature falls sufficiently to cause numerous clouds and squalls.

d. A low coming from the west, associated with a slowly falling barometer, usually comes in slower and stays longer than a low from the southwest.

e. When a storm center approaches from the south or southwest, the intense frontal weather, low ceilings, poor visibilities, precipitation, and gusty winds will begin approximately 9 hr after the first appearance of cirrus or cirrostratus clouds. These southwest lows usually pass Shemya from 12 to 16 hr after the barograph begins its downward trace. Lows from the southwest have the characteristics of an open wave with rapid movement, far reaching overrunning, and fairly rapid clearing. However, it is usually not possible to distinguish the passing of both fronts.

f. In summer the polar front lies well to the north of the western portion of the chain, and storms passing north of Shemya are weak and of little consequence. Winds at Shemya veer from southeast to southwest. If a summer frontal passage does occur it is usually of the warm type.

g. When a front is approaching Shemya, attending weather will usually commence at the front of the trough as soon as the barograph trace starts down. After the passage of a strong front, if the barograph fails to rise and a complete windshift does not occur, the approach of a secondary cold front is indicated and continued heavy winds and precipitation may be expected. When the secondary front passes, the winds will gradually decrease and veer to the northwest. Precipitation will be in the form of scattered rain and snow squalls, and cloudiness will decrease. After passage of a warm front or warm front type occlusion, clearing may be rapid and the flight weather may sometimes become scattered to unlimited immediately after the wind shift. However, rapid clearing does not occur when the tips of occluded fronts pass or when the frontal trough is wide and diffuse.

h. The speed of frontal passage depends mainly upon conditions to the east. With a deep system in the central or eastern Aleutians, a storm passage through Shemya is rapid with clearing between storms. If, however, a ridge of high pressure develops

over the central Aleutians, a storm at Shemya will stagnate and a prolonged period of heavy precipitation and winds will maintain itself for several days.

i. The period of highest winds is dependent upon the strength of frontal passage. With strong fronts the highest winds seem to prevail 4 to 6 hr after passage; after a weak frontal passage the strongest winds occur within 1 hr. Moderate gusts begin with winds at 22 to 26 kt (11–13 m/s), and winds above 30 kt (15 m/s) are nearly always accompanied by strong gusts. However, winds of high velocity are not nearly as turbulent as those of equal strength that are encountered on islands with rugged topography, such as nearby Attu.

j. Precipitation during frontal activity from November through April is in the form of large wet flakes mixed with rain, and storm passage in the winter is characterized by heavy snow squalls. Following frontal passage, snow falling in frequent squalls is lighter and drier.

k. Fog associated with cyclonic disturbances is relatively infrequent at Shemya; however, with a storm center to the north and the passage of a warm front at Shemya, fog may occur.

l. A period of summer fog prevails at Shemya from June through early September. The southwesterly flow of air from the Pacific High across the Aleutians brings air cooled to the saturation point during its passage over the North Pacific; consequently low lying fog banks envelop the Aleutians. At Shemya this stable layer of fog may build up to as high as 4000 ft (1219 m). Because of the stability of the air this fog can exist with any wind speed, and no relationship between high or low velocities and fog has been found. Comparison of the temperature of the sea surface with the dew point has proved useful in forecasting the formation of fog. The colder the sea surface temperature in comparison with the dew point of the air, the greater is the probability of fog. The converse also applies.

m. The dispersal of summer fog at Shemya is most probable when a synoptic situation occurs that will give rise to an extended period of northerly flow and thus introduces a drier, cooler airmass. Dissipation of fog at the surface may be caused by the southward movement of air from the circulation set up by waves on the diffused polar front to the north. The resulting instability at the surface will ordinarily not cause complete dissipation of clouds, and the height of the ceiling will depend upon the extent to which this circulation continues. With a warm front passage the surface temperature may rise 2 to 3 Fahrenheit degrees (1–1.5 Celsius degrees), and visibility will temporarily improve and then lower again after a few hours. In this season if a significant trough aloft moves over the Aleutians, the polar front may move south and frontal passage in the form of an occlusion may cross Shemya. If showers occur at the passage of the occlusion, a broken sky with ceilings of 1500 to 2000 ft may be expected for 6 to 12 hr; if few or no showers are present, breaking up may not occur or will be of very short duration.

n. Surface and pilot reports from Shemya indicate that in spite of its small area the island has better conditions than the surrounding body of water. Reports from both Shemya and Attu may indicate ceilings of 800 to 1000 ft, though the ceiling over the water as reported by pilots is 0 to 100 ft. Quite frequently the main runway at Shemya may have a ceiling of 50 to 200 ft, though the higher part of the island

to the north and often the east end of the runway are completely enveloped in fog.

o. The surface wind at Shemya is at all times representative of the gradient wind direction.

p. In the fall, a calm wind will usually become a southerly wind indicating the approach of a frontal system.

q. With a west to southwest flow at both Casco Cove and Shemya, the sequence of weather at Shemya will follow that of Casco Cove in 3 to 6 hr, depending upon wind velocity. Ceilings may vary because of topographic effects at Casco Cove. This relationship between Casco Cove and Shemya is most reliable from September through March when storms are well defined. If both stations are free of fog and Casco Cove is closed, Shemya will follow.

r. During days of zero conditions in fog, a useful aid in forecasting the dissipation of fog, or the lifting of the ceiling, is the observation of a steaming effect of the fog close to and at the surface of the ground. This usually occurs in late morning.

s. Because orographic effects are absent, Shemya is nearly free of squall and shower activity caused by mechanical lifting, which is so characteristic of the winter weather at the more mountainous Aleutian Islands.

t. The "Attu effect" refers to a clearing of low cloudiness over Shemya as a result of a clearing of clouds in the lee of Attu under west-northwesterly wind conditions. The clearing occurs under strong, low level inversion conditions with cloud tops below the level of the highest mountains on Attu. Turbulent mixing effects of dry air above the inversion into the moist boundary layer result in a lee clearing from Attu extending over Shemya. Figure 5-1 is a DMSP example showing such an effect on 21 August 1989. The Attu effect is an excellent example of how local

Figure 5-1. DMSP visible imagery 2020 GMT 21 August 1989.

terrain can have a significant influence over the local weather and why synoptic scale forecasting must be tailored to a specific location for accurate forecasts.

u. Prevailing surface winds during the summer are westerly and generally range between 10 and 20 kt (5–10 m/s). Although gusty surface winds are not as prevalent during this season, gusts up to 60 kt (31 m/s) have been reported each month. Crosswinds of greater than 25 kt (13 m/s) only occur about 1.5% of the time during this season; therefore, this potential hazard to flight operations does not tend to be a major problem.

v. Thunderstorms are so rare at Shemya that they do not present a problem for the forecaster. Rainshower activity, however, will occasionally present problems with reduced visibility.

w. Icing is very rare in the summer at Shemya. Very stable airmasses occur during this season, and the freezing level is generally from 6000 to 12,000 ft (1830–3660 m). The tops of the low stratus are between 1000 and 3000 ft (305–914 m); consequently, the potential source of icing is generally well below the freezing level. Light rime icing may occur in the stratocumulus type clouds that appear with the infrequent frontal systems passing across the island during the summer.

x. To forecast precipitation type, the latest Shemya radiosonde observation (RAOB) should be used to determine the 1000- to 500-mb thickness and the 1000- to 700-mb thickness, and then the following guide should be used:

1000–500-mb Thickness (m)	Type
≤5200	Snow
5201 to 5269	Mixed
≥5270	Rain

1000–700-mb Thickness (m)	
≤2665	Snow
2666 to 2862	Mixed
≥2835	Rain

The 1000- to 700-mb thickness has been suggested as the better guide.

y. The following are various suggestions and/or observations pertaining to precipitation forecasts for Shemya:

1. Advection and trajectory of air are important factors in forecasting type and character of precipitation. Northerly flow will favor showers.
2. Surface air temperature has little effect on the precipitation forecast.
3. Snow showers have a tendency to remain over the water (as a result of heating and/or obstructed flow) during daylight hours. Then during the late afternoon and night they tend to move over the island. "Showers in the vicinity" is a good descriptive forecast when an occasional shower occurs at the station, or most anywhere under the cloud street, observed as W2X 1/2 SW (see related case study 6.1.1). High winds will normally prevent the accumulation of a measurable amount of snow, although 4 to 6 inches (10–15 cm) of snow overnight is not uncommon.

4. Depth of moisture or clouds will influence the precipitation forecast. Clouds from the 950- to 850-mb layer or above favor showers or a combination of precipitation types for prevailing forecast conditions. Low stratiform, below 900 mb, favors steady rain or drizzle.
5. Accurate evaluation of satellite data as to type and depth of clouds should provide an additional tool for forecasting type and character of precipitation.

z. Fog forecast rules:
1. Fog forms as soon as the dew point depression decreases to 1.5 Fahrenheit degrees (0.8 Celsius degrees) and continues to decrease, provided the dewpoint temperature is not 2 Fahrenheit degrees (1.1 Celsius degrees) or more colder than the water temperature.
2. Fog forms suddenly after the air temperature starts to fall, if the dewpoint is more than 1 Fahrenheit degree (0.6 Celsius degree) above the sea surface temperature.
3. Fog does not form as long as the dewpoint is 2 Fahrenheit degrees (1.1 Celsius degrees) or more colder than the water temperature, if the cloud cover is seven-tenths or more, and in only rare cases even when the cloud cover is less than seven-tenths.
4. After a rain, the visibility generally will be better than that normally associated with similar conditions of air temperature, dewpoint, and water temperature because the number of hygroscopic nuclei in the atmosphere is reduced.
5. With falling pressure, the entire airmass is being cooled through expansion, and fog formation and persistence is more likely than with rising pressure, which may dissipate the fog.

5.3 Gulf of Alaska

a. Extrapolation can be used with modest success over the open ocean where an adequate history exists based on a correct analysis. It should not be used with systems approaching land. In this case, surface centers should be anticipated to either decelerate or jump the land barrier, then redevelop on the leeside. A system is more apt to jump when strong upper flow exists across the mountain barrier. The best use of extrapolation is with short-wave troughs.

b. Upper air steering is a good tool for forecasting direction of movement of systems as long as they remain under the vicinity of a jet maximum. This technique is most useful with mid-ocean polar front cyclones under strong zonal flow. If the flow becomes meridional, recurvature should be anticipated.

c. The analysis of warm and cold advection patterns at 700 mb will give good qualitative information as to the movement and intensification of polar front cyclones. Basic rules available in current literature should be applied. Advection analysis at 850 mb will assist in the determination of the development and movement of Arctic airmasses and fronts.

d. A low over the interior of Alaska and a strong northwesterly flow aloft over the Alaska Peninsula will frequently result in the low moving rapidly southeast between charts or jumping into the Gulf of Alaska where rapid deepening then occurs.

Strong northwest surface winds and williwaw conditions will develop almost simultaneously at Kodiak.

e. When a jet maximum at 500 mb passes over or near Kodiak from the northwest, it can be expected to plunge southward and develop a strong trough off the west coast of the United States. This trough often becomes a cut-off low that persists off the California coast.

f. When the jet is farther south and the northwesterly jet passes near 50 °N, 145 °W, the trough usually forms on the coastline or slightly inland, and the formation of a cut-off low is less frequent.

g. A deepening of a 500-mb trough in mid-Pacific will tend to build a downstream ridge in the Gulf of Alaska. A preexisting low in the Gulf of Alaska both at the surface and aloft will fill rapidly.

h. Upper lows in the Gulf of Alaska seldom move inland and maintain themselves as separate centers, but instead, stagnate in the Gulf and fill, with a short-wave trough continuing into the North American Continent.

i. An alternate situation under (h) above occurs when a strong short-wave trough approaches the low from the west or northwest. This trough will deepen the low and cause it to retrograde.

j. The ring of mountains around the Gulf of Alaska forms a natural barrier to the movement of low pressure systems entering the area. As a result, the progress of a low is retarded, and several days may elapse while the low fills in a nearly stationary position. This condition occurs frequently in the winter and transitional periods. In conjunction with a moderate or strong ridge to the west and northwest, this situation accounts for lengthy periods of strong northwesterly winds at Kodiak. In summer a storm occasionally moves through a break in the barrier at a point between Seward and Middleton Island. In such cases, it reforms as a moderate center in the Copper River Valley and then drifts eastward into the Yukon Territory.

5.3.1 Kodiak

a. Persistence is a poor technique to use in the Kodiak area because of the rapidly changing conditions most always present. It can be used as a last resort with stagnant cold lows and blocks, and with limited success on short range terminal forecasts.

b. A forecast method uses the 500 to 1000-mb thickness as a predictor for the probability of occurrence of rain and/or snow. It has an excellent theoretical basis, but two conditions weaken this method as a forecast tool. The thickness value must be a forecast value, and favorable precipitation conditions must be assumed or forecast such as presence of moisture, vertical upward motion, and positive vorticity advection. The thickness value of 17,200 ft (5243 m) as "equal probability thickness" provides a basis for stating whether or nor snow or rain is more likely to occur. Again its chief advantage lies in its ease of determination, but it must be considered as a supplemental aid.

c. Trajectories of the air flowing over Kodiak and the expected changes in trajectory during the forecast period are of prime importance to the Kodiak forecaster. In

general, flow from the east will produce rain; from the southwest, partly cloudy to cloudy with scattered showers; from the northwest, clear to partly cloudy.

d. Air flowing from easterly quadrants having long trajectories and/or dwell time over the water will acquire low level moisture. If subsidence occurs aloft (as occurs in conjunction with 500-mb ridging), the low level moisture will be capped by an inversion with dry, relatively clear air aloft. The result will be extensive fog and drizzle over and to the east of Kodiak.

e. Local northwesterly winds are often the result of the terrain features altering the otherwise northeasterly or easterly surface flow.

f. Reported winds are representative of gradient winds only from the easterly quadrants.

g. Winds seldom prevail from due north or south for more than brief periods of time. When gradient winds are north, south, east, or west, observed surface directions will be northwest, southeast, northeast, or southwest, respectively.

h. When the gradient wind is north or northwest: (1) surface winds are generally light if 2000- and 3000-ft (610 and 914 m) levels have winds less than 30 kt (15 m/s); (2) surface winds are strong with higher gusts when winds exceeding 30 kt (15 m/s) are observed at these levels; and (3) when the wind at these levels is 35 to 40 kt (18–21 m/s) and the airmass is cold, the surface gusts may reach 50 to 60 kt (26–31 m/s) and low level turbulence will be moderate to severe.

i. Observed winds from the southwest quadrant are rarely of long duration and are usually much below gradient speed except when associated with convective activity. It normally takes a gradient speed of more than 40 kt (21 m/s) to produce sustained speeds in excess of 10 kt (5 m/s). Wind speeds over adjacent water areas of 30 to 40 kt (15–21 m/s) may be reached. Moderate turbulence is observed from the surface to 6000 ft (1830 m) under these conditions.

j. Gradient winds from south and north quadrants usually exhibit a 45 to 90° backing at the local station due to topography, i.e., cross-isobar flow may be as great as 90°.

k. It has been found that for the situation where a low is in the Gulf of Alaska and a ridge of high pressure to the west and northwest, the simultaneous pressure difference between Cold Bay and Cordova gives a rough value for average hourly wind speed at Kodiak. Multiplying the difference in millibars by a factor of 1.4 gives a value of average gustiness. A factor of 2 applied to the difference gives maximum possible gusts. By anticipating pressure tendencies, this rule gives fair results for the following 3 to 6 hr. The pressure gradient between Kodiak and Cold Bay may also be used as an index. However, in many instances the Cordova-Cold Bay comparison will prove to be the more accurate predictor.

l. During periods of high winds from the north to northwest at the station, winds of 10% higher speed should be expected in the hangar area.

m. During periods of high winds from the west to northwest at Kodiak, winds should be from the west to south in the hangar area with strong eddy motions. In addition, peak gusts should be expected to be 20 to 30 kt (10–15 m/s) higher in the hangar area.

n. During periods of high winds from easterly quadrants at Kodiak, wind speeds in the hangar area should be lower than at the weather facility.

o. During the months of May through August, sea-breeze components are generated in the local area when solar heating permits. Westerly winds tend to be dampened by the sea breeze, whereas easterly winds tend to be reinforced. The forecaster is advised to consider that easterly gradient flow, a high daytime temperature maximum over land, and a low sea surface temperature are all factors supporting the development of a sea breeze, whereas the opposite conditions will have an inhibiting effect.

p. Cumulonimbus clouds form infrequently, but they will sometimes be observed in the strong flow around a low situated in the Bering Sea after the occlusion has passed Kodiak. In the above synoptic situation cumulus clouds almost always form; it is a function of the stability of the airmass whether or not they progress to towering cumulus or cumulonimbus. As a result of the prevailing southwest flow, however, the shielding effect of the terrain causes most of the convective activity to remain offshore. Precipitation will consist of showers of rain, snow, snow pellets, or small hail, and surface winds will gust often as high as 40 kt (21 m/s).

q. When a low center passes to the south of Kodiak and surface winds change to northwest, extensive shower activity, low ceilings, and low visibilities will persist until upper winds change from northeast to northwest. The duration will be extended if (1) extensive troughing exists at upper levels to the rear (westward) of the surface low, or (2) an active Arctic front is drawn into the cyclonic circulation from the northwest.

r. The appearance of a cirrostratus cloud shield from the southwest will be followed by precipitation in 12 hr or less.

s. In winter, cloud formations due to convergence usually extend to about 6000 to 8000 ft (1830–2440 m/s) over water, whereas cloud tops over Kodiak Island may extend to twice this altitude.

t. The cause of a heavy snowfall (accumulation of several inches) is usually low tropospheric convergence around a low in the Gulf of Alaska that is situated such that the maritime polar air from the south is brought into juxtaposition with Arctic or continental polar air along the Gulf coast, and a northeasterly flow aloft over Kodiak results. Surface winds will be northeast through northwest. Care must be taken to determine whether or not a land trajectory below 700 mb terminates over Kodiak. If not, precipitation will most likely be rain, or snow changing to rain.

u. Southwest gradient winds, despite moisture content, tend to leave Kodiak open, with ceilings of 2500 ft or higher and visibilities of 10 n mi (19 km) or more except in widely scattered showers.

v. The poorest flying conditions associated with a cyclonic system from the standpoint of ceilings, visibilities, and surface winds are immediately prior to frontal passage. Frequently partial clearing will occur for 1 to 3 hr following an occluded frontal passage followed by lowering again of ceilings and visibilities.

w. Advection fog occurs in spring and summer only. Offshore fog banks will drift toward the shore when winds are from the easterly quadrants. However, if the winds are less than 10 kt (5 m/s) the fog will stop at the beach and will not obscure

the runways. If the sky has been clear or scattered for 2 or 3 hr after sunrise a southeast or east wind of 10 to 15 kt (5–8 m/s) will not bring fog over the field. A southerly gradient wind will usually leave the field open but with an east to southeast wind and a fog bank remaining offshore. Under these conditions fog will frequently be observed to drift over Long Island, Woody Island, and Near Island in that order. With westerly gradient winds of 12 kt (6 m/s) or less and scattered to broken skies, a southeast sea breeze will occur between 1000 and 1400 LST. Seaward fog banks will not move over the field under these conditions because of the dissipating effects of surface heating. However, the sea-breeze effect will flatten the diurnal temperature profile and lower the daily maximum temperature. These consequences must be taken into account when issuing the forecast.

x. When low pressure areas stagnate southwest of Kodiak and cause surface winds from the southeast to the northeast, the ceiling will be about 500 ft and visibility will average 2 to 6 n mi (4–11 km) in light fog. Such conditions prevail from 18 to 24 hr even though the barometer is rising due to the filling of the low.

y. As low centers move past Kodiak to the southeast and into the northern Gulf of Alaska, surface winds at the station will become northwest, and lower cloud layers will become broken to scattered. With this same condition but extreme low level convergence, the sky will remain overcast.

z. When a low approaches Kodiak from the southwest, the wind will generally remain light and variable until the center is between 200 and 400 n mi (370–740 km) from Kodiak. The winds then become easterly, increasing to gale force. In most cases the winds increase at the same time the first precipitation occurs; although in winter, with Arctic air over the station, the easterlies will commence sometime later than the onset of precipitation (snow).

5.3.2 Additional Rules and Observations for Kodiak

(a) With a northwest to north gradient, supergradient (williwaw) winds are brought about by funneling through the mountain passes. With 30 to 40 kt (15–21 m/s) (or higher, in williwaw conditions) west to northwest winds, gusts in the hangar area adjacent to Women's Bay will be 10 to 20 kt (5–10 m/s) greater than the gusts over the runway. In addition, the direction in the hangar area will back to south or southwest. This local effect is of vital interest to the forecaster because aircraft parked in the hangar area are vulnerable to wind damage during these conditions. The character of the wind under these conditions is extremely variable in terms of both direction and velocity.

(b) Because of the mountainous terrain southwest of Women's Bay, a subgradient local wind results from a southwesterly gradient wind. Empirical data indicates that an established southwest gradient of 30 to 40 kt (15–21 m/s) will yield a wind over the field that is 10 to 20 kt (5–10 m/s) lower.

(c) Winds from due north or south are seldom observed at Kodiak because of the topography. When observed, these winds exist for short periods only, usually during a transition from westerly to easterly flow.

(d) Ceilings and visibilities are lower over the station than over the water when the wind is from the east quadrant. The reverse is true with winds from the southwest or northwest quadrants.

(e) Kodiak is considered to have a marine climate. The evidence of this is apparent from the limited daily and annual temperature ranges. For instance, the mean annual temperature range is about 25 Fahrenheit degrees (14 Celsius degrees).

(f) The mean monthly temperature is less than 32 °F (0 °C) for the 4 months December through March, although no month has a mean temperature less than 30 °F (−1 °C). Only 3 months (July, August, and September) have mean temperatures of 50 °F (10 °C) or greater.

(g) During the summer, the mean air temperature closely approximates the mean sea surface temperature; the air temperature rises slightly above the sea surface temperature during August, but falls below again in September. In winter, the mean maximum air temperature more closely resembles the mean sea surface temperature curve.

(h) Because of the proximity of a large landmass to Kodiak, the overall temperature range is 95 Fahrenheit degrees (53 Celsius degrees), regardless of the marine influence. Records show a low of −9 °F (−23 °C) in January 1917 and a high of 86 °F (30 °C) in June 1953.

(i) Even with a northerly air flow, Kodiak's surrounding waters and mountain barriers to the northwest temper the climate considerably. For example, temperatures at Naknek (King Salmon), only 155 n mi (287 km) to the northwest, are frequently 20 Fahrenheit degrees (11 Celsius degrees) lower in winter than those at Kodiak. Naknek, a near sea level station like Kodiak, has a mean annual temperature only 6 Fahrenheit degrees (3.5 Celsius degrees) below this station. However, Naknek's absolute minimum temperature is 34 °F (19 °C).

(j) In summer, maximum temperatures will vary 10 to 20 Fahrenheit degrees (5 °–11 Celsius degrees), depending on whether the northwest gradient is strong enough to maintain a flow of air from over the island, or whether it is weak enough that the sea breeze predominates. The highest daily maximum temperatures occur with northwest winds in summer.

(k) Precipitation is normally abundant throughout the year. Maximums do occur in September and October, and again in May. March and July are the driest months. All months, however, have a wide variation in the amount of precipitation fall. The mean annual precipitation is about 55 inches (140 cm) but ranges between 40 and 80 inches (102 and 203 cm). A very high percentage of the annual precipitation falls when northeast to southeast winds prevail.

(l) Small amounts of snow may fall as late as May or as early as September. Substantial amounts (e.g., a good ground cover) may be anticipated in November and April, but the bulk of the snowfall arrives in the period December through March. The mean annual fall for the 19 yr of complete records is 74.8 inches (190 cm). Here again, a wide yearly variation is seen. In 1956 a total of 178.1 inches (452 cm) of snow fell at Kodiak, but in 1945 only 15.9 inches (40 cm) was recorded.

(m) The proximity of mature occlusions accounts for most of the precipitation, but large-scale areas of upward vertical motion and airmass instability are also contributing factors. Twenty-four hour amounts usually do not exceed 1 or 2 inches (2.5–5 cm) (water equivalent), but may reach 4.5 inches (11 cm) on rare occasions. Precipitation intensity is usually light, but occasionally becomes moderate or (infrequently) heavy in cases of extreme vertical motion or when a strong front is close to the station.

(n) Although the prevailing wind direction is northwesterly every month of the year except May, June, and July, and the average speed is about 10 kt (5 m/s), these data may be misleading to the newly arrived forecaster because of the extreme variability in both direction and speed. The maximum gust recorded at the Naval Station was 92 kt (47 m/s) in 1948. Gusts of over 50 kt (26 m/s) have occurred during each month of the year but are most likely to occur in the winter months. A study of maximum monthly gusts shows occurrence from the northwest 45% of the time and that the average maximum gust from this direction is 46 kt (24 m/s). When the maximum monthly gust occurs from the northwest quadrant during the period from September through March, it is usually greater than 50 kt (26 m/s). An average of eight storms each year bring winds in excess of 55 kt (28 m/s). The average duration of gusts in excess of 55 kt (28 m/s) is about 8 hr per storm.

(o) The criteria established for flying conditions are (1) VFR: 1000 ft and 3 mi, or better; (2) IFR: between 1000 ft and 3 mi, and 200 ft and 1 mi; and (3) CLOSED: below 200 ft and 1 mi. The VFR conditions occur about 91% of the time. Climatically, July is the worst month with respect to flying conditions, averaging only 88% VFR. October is the best month, being VFR 96% of the time. A greater frequency of closed conditions exists in summer than in any other season. This is due to the occurrence of advection fog and low stratus in summer. In winter, low clouds and precipitation are more likely to result in IFR rather than closed conditions.

(p) In the Kodiak area a high frequency of "marginal" conditions occur: ceilings between 1000 and 3000 ft, visibilities between 3 and 5 n mi (6–19 km), strong winds from unfavorable directions, and restrictions due to the adjacent high terrain.

(q) Extensive aircraft icing occurs in advance of frontal systems, near fronts, in areas of extensive upward vertical motion, in turbulent buildups over mountainous areas, and in freezing rain at the surface and lower levels. However, moderate to severe rime icing has been experienced in areas where none of the conditions listed above were apparent. Pilot reports have indicated much higher buildups over Kodiak Island than anywhere over the surrounding water. Both turbulence and icing can be severe in these clouds.

(r) During periods of strong northwesterly flow, moderate to severe turbulence will be encountered over Kodiak Island and in the vicinity of the Alaska-Aleutian Range. Pilot reports indicate areas of strong downdrafts in the lee of the Alaska-Aleutian Range in such situations, similar to the "sierra" or standing wave. Magnitudes of as much as 2500 ft per min (762 m) have been reported.

(s) In summer, the freezing level is generally high enough that aircraft icing presents little problem. During the period from October through May, however, the average height of the freezing level is below 6000 ft (1830 m). Consequently, the possibility of aircraft icing should be mentioned in every flight briefing and forecast issued during these months, particularly in frontal and prefrontal weather.

(t) Ice forms on Women's Bay during the winter when the air temperature falls to about 27 °F (−3 °C) and the wind is calm. A light breeze is sometimes sufficient to prevent the formation of ice or to dissipate a thin cover. When ice does form, it is usually not of sufficient thickness to hamper operations other than small boats. However, there have been occasions when substantial portions of the bay have been covered with ice up to 36 inches (91 cm) thick.

(u) It should be noted that williwaw conditions pose a hazard to aircraft in flight as well as on the ground. Turbulence can be severe for 20 mi (32 km) or more downwind of the mountain barriers, and the only visible evidence outside the aircraft is the agitated state of the sea with surges of spray observed. The severe turbulence may also extend a few thousand feet (few hundred meters) above the mountain crests with strong updrafts and downdrafts.

6. SATELLITE DATA EXAMPLES

This chapter presents satellite case studies on a variety of topics. Examples of the features described include a winter storm track, a blocking ridge, summer cyclones, polar vortices, formation of boundary layer fronts, wind pattern in sunglint, and local wind-induced clouds.

6.1 Cyclogenesis

The Aleutian Low is recognized, along with the Icelandic Low and the eastern Pacific and Bermuda highs, as one of the major Northern Hemisphere large scale atmospheric circulation features. The Aleutian Low, however, is largely a climatological feature. It is reflected in climatology because of the frequent migration of cyclones into the area and the tendency for the mature synoptic scale cyclones to stall and dissipate in the region. The Aleutian Low climatic feature is thereby the summation of numerous migratory lows rather than the persistence of an individual cell such as is the case for the eastern Pacific High. This nonpersistent aspect of the Aleutian Low complicates the task of forecasting in the region. Because nearly every day of the year, especially during the cold seasons, one or more cyclones are influencing the weather somewhere over the Bering Sea and Gulf of Alaska, there is an endless variety of storm tracks, storm sizes, stages of development, and interactions to consider. The examples contained in this section are provided as illustrations of some of the many cyclonic events unique to this region. Each example provides snapshots of the circulation pattern as depicted by the surface and 500-mb analyses, cloud patterns as seen in DMSP imagery, and selected surface and upper air observations. Forecasting aids and references to various regional forecast thumb rules are also provided when available.

6.1.1 Winter Storm Track into the Bering Sea

Climatic Background

During January the primary storm track across the North Pacific extends from east of Japan north-northeastward to the Gulf of Alaska passing south of the Aleutian chain. At times high pressure develops over the western North Pacific and the storm track shifts northward into the Bering Sea. Synoptic patterns of this latter type, although generally

occurring more frequently in spring through summer than in winter, are characteristic of a regional climate singularity known as the midwinter thaw. Synoptically the midwinter thaw is characterized by blocking high pressure over the Gulf of Alaska. The southerly flow around the western side of the blocking high results in warm air advection over the eastern Bering Sea region and at times northward into the Arctic basin.

Climate Forecast Aids

1. Knowledge of the variability of regional circulation patterns will aid forecasters in recognizing changing and/or anomalous weather scenarios.
2. Monitoring the existing 500-mb circulation pattern relative to climatological mean patterns will provide insights to changing storm tracks.

Synoptic Scenario 0000 GMT 11 January Through 1200 GMT 13 January 1989

Preceding 11 January 1989 strong ridging had developed over the eastern North Pacific. By 1200 GMT 11 January, the 500-mb, 18,300-ft (5580-m) height contour was north of 50 °N over the Gulf of Alaska, with ridging extending northward across Alaska (Fig. 6-1). Surface high pressure systems with center pressures greater than 1036 mb were located near 40 °N in the western and eastern North Pacific (Fig. 6-2). Surface lows were being steered into the Bering Sea.

Three synoptic scale lows influenced the Bering Sea weather during the 0000 GMT 11 January through 1200 GMT 13 January 1989 period. The 970-mb low (low 1), located 150 n mi (278 km) north of Unimak Pass (Fig. 6-2), moved northeastward at 25 kt (45 km/hr) for 24 hr, then slowed and filled while dropping southeastward into the Gulf of Alaska by 0000 GMT 13 January (Fig. 6-3). Low 2, located 300 n mi (556 km) west of Kamchatka (Fig. 6-2), moved slowly over the peninsula to a position in the extreme western Bering Sea by 0000 GMT 13 January (Fig. 6-3). Low 3, not apparent in Fig. 6-2, formed just east of Japan on 11 January, then moved northeastward crossing the Aleutian chain to its position in Fig. 6-3 on 13 January. Over the following 24 hr, low 2 and low 3 merged. Low 2, near the Siberian coast of the northwestern Bering Sea at 1200 GMT 13 January (Fig. 6-4), deepened slightly to 990.2 mb while low 3 evolved into an elongated trough extending southeastward over the central Bering Sea and about 600 n mi (1112 km) beyond the Aleutian chain.

Scenario Specific Climate and Synoptic Forecast Aids

1. When winter 500-mb ridging develops over the eastern North Pacific, surface lows tend to track north of the principal storm track and enter the Bering Sea.
2. Under this synoptic pattern, northward-moving developing surface lows, while over the Pacific, will on average move a little slower (25–35 kt or 45–65 km/hr) than the typical east-northeast moving lows (35–45 kt or 65–85 km/hr). However, they maintain a higher speed of advance, track to higher latitudes, and occlude at higher latitudes.

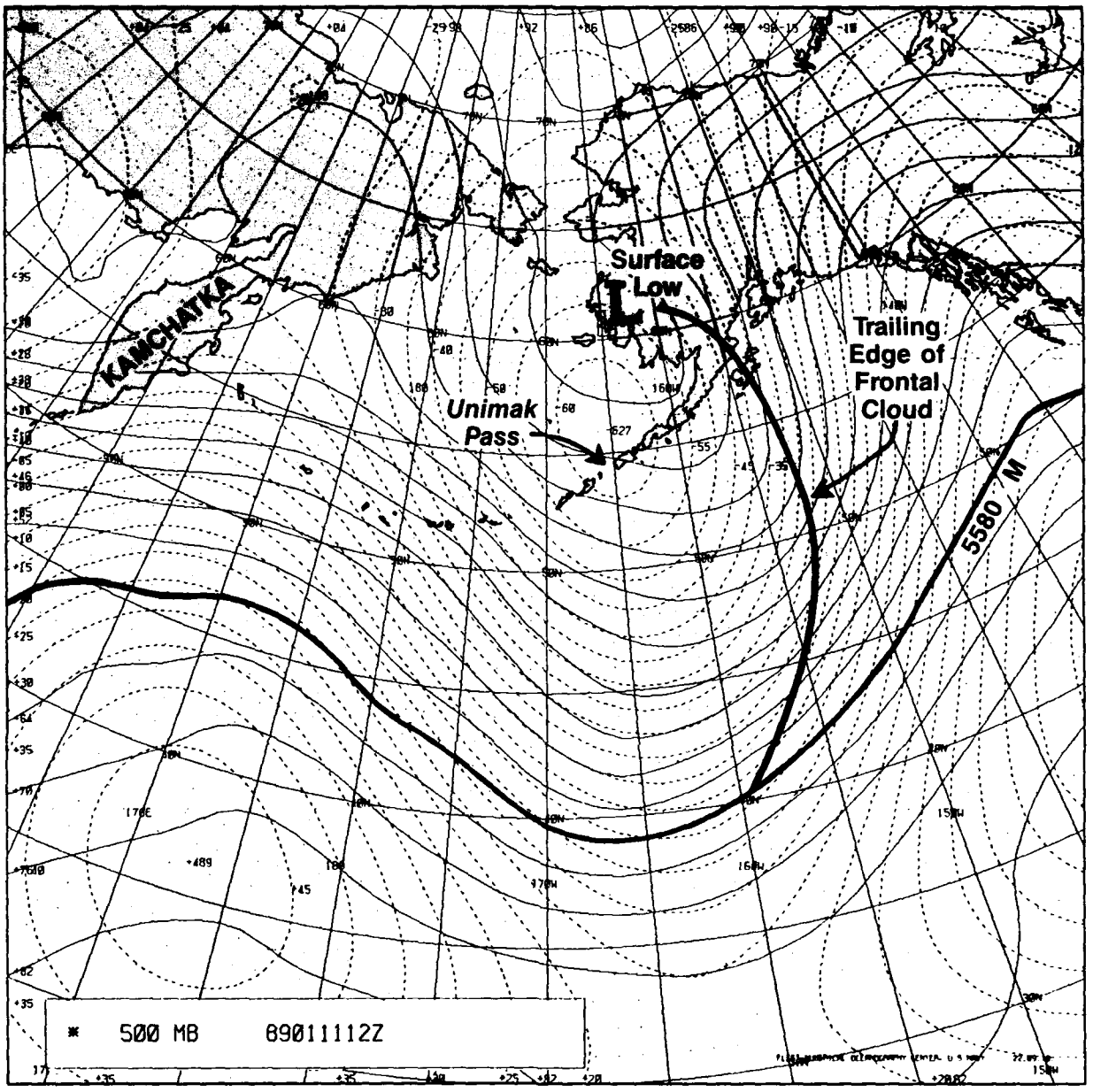

Figure 6-1. FNOC 500-mb analysis 1200 GMT 11 January 1989.

3. When high pressure extends westward across the Pacific, as in this case, lows formed off Japan will move northward, as low 3 did in this example.

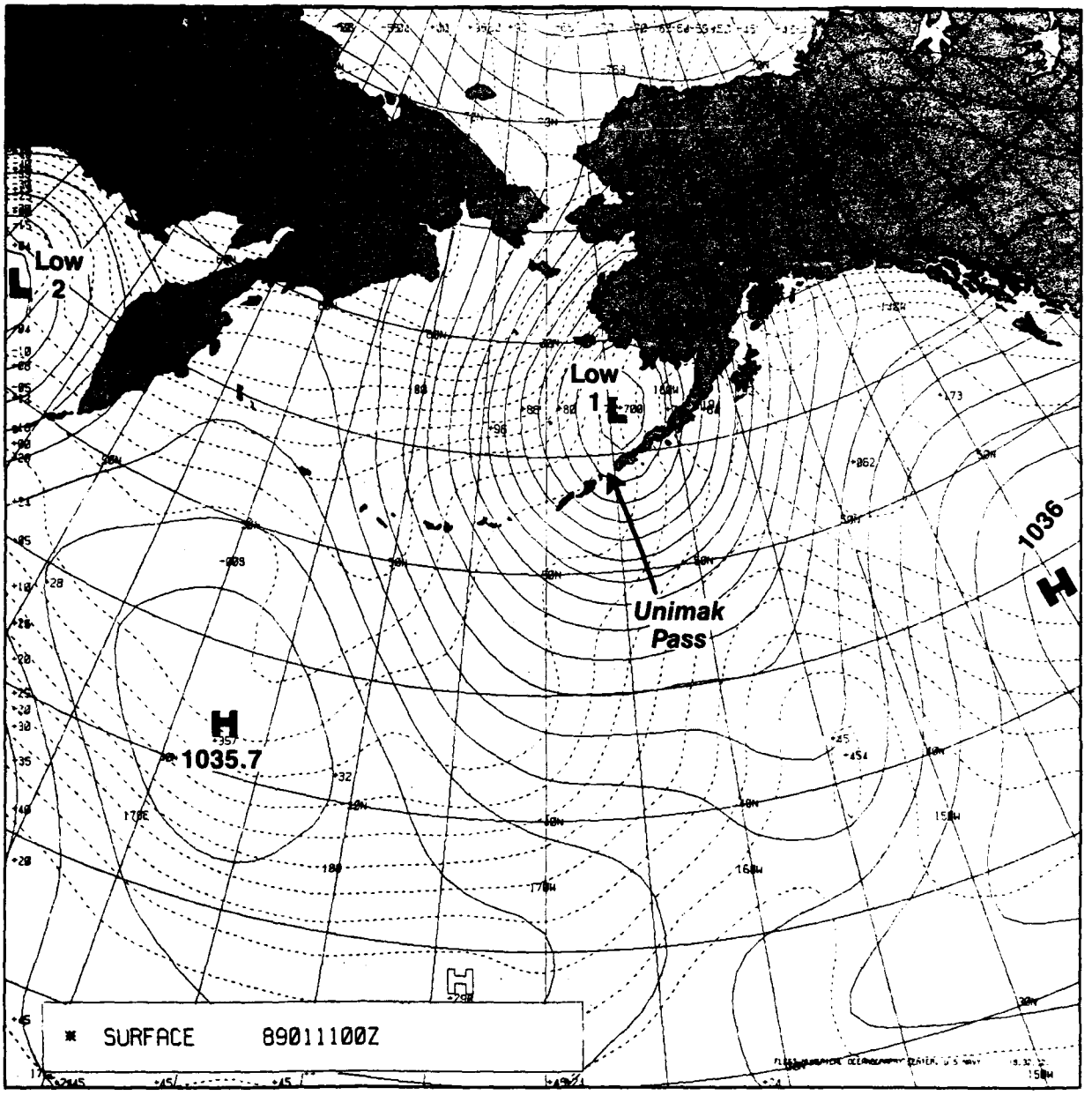

Figure 6-2. FNOC surface analysis 0000 GMT 11 January 1989.

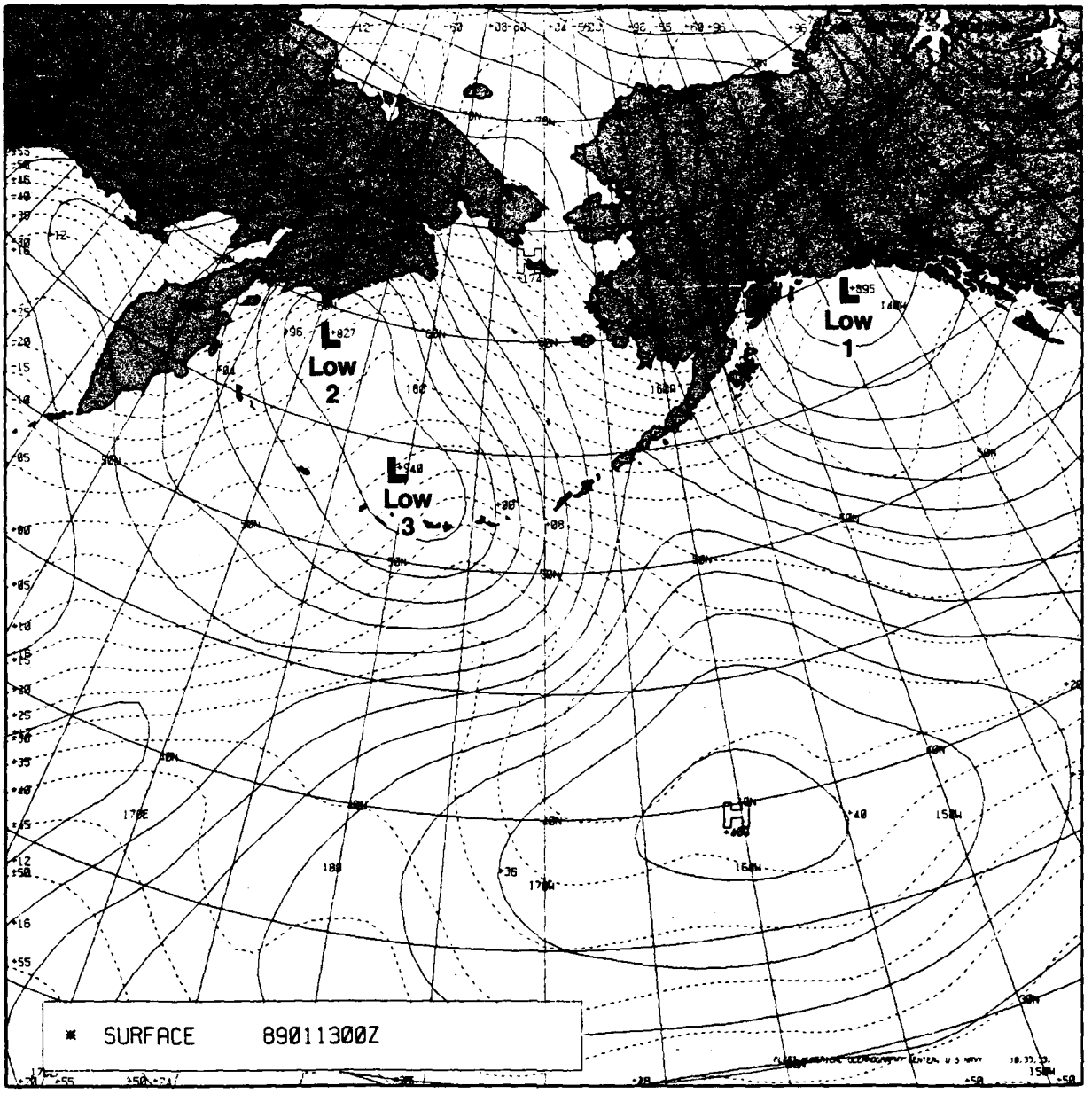

Figure 6-3. FNOC surface analysis 0000 GMT 13 January 1989.

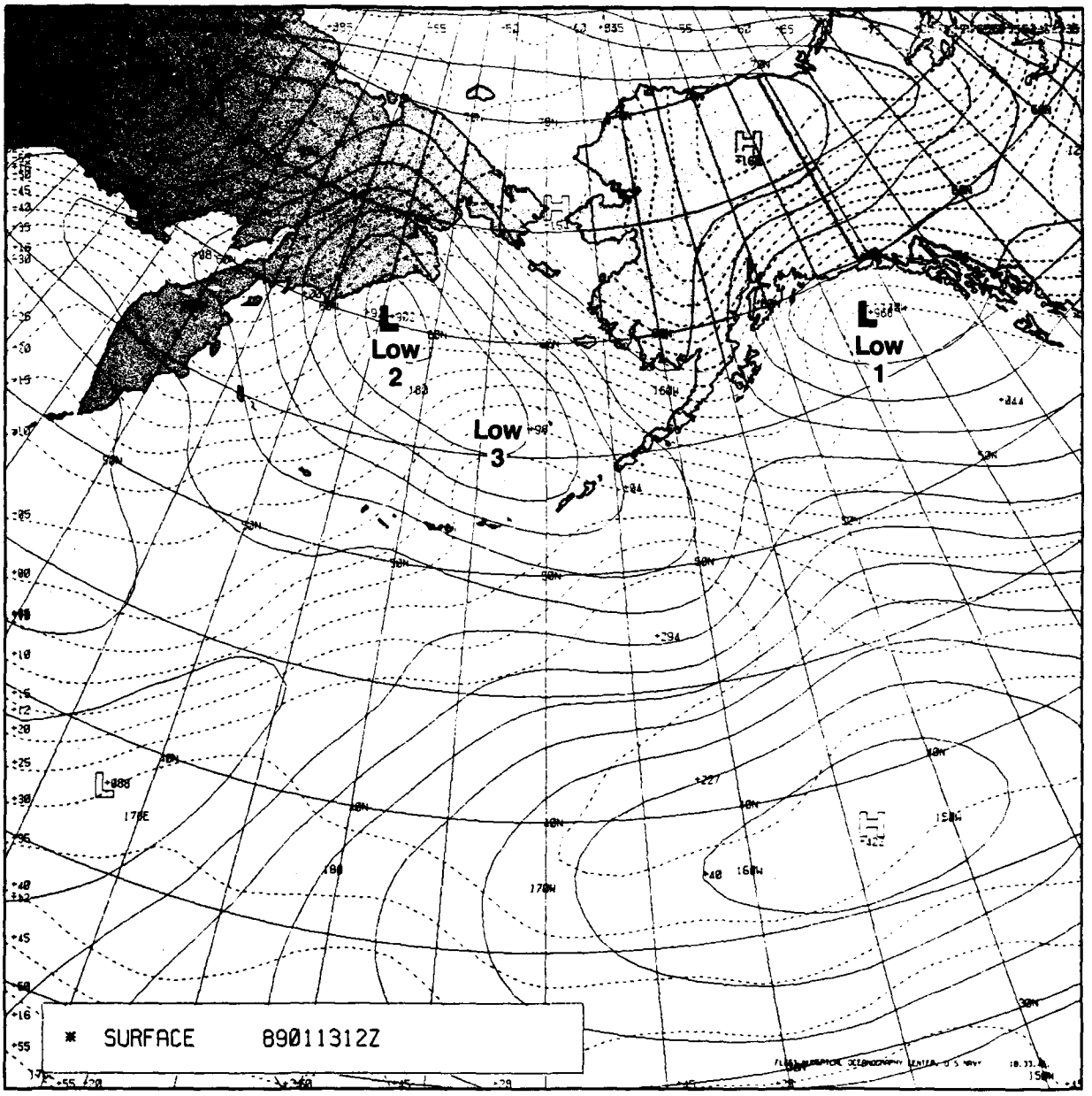

Figure 6-4. FNOC surface analysis 1200 GMT 13 January 1989.

Satellite Imagery Features

Figure 6-5 (0937 GMT 11 January 1989) shows the cloud pattern associated with the 970-mb low (low 1). Selected 500-mb wind and temperature values, surface freezing line, and surface low position and pressure are indicated for 1200 GMT 11 January. Classical image and flow relationships that are evident include

1. Coldest temperature (lightest gray shades) in the anticyclonic outflow region of the frontal band indicates the upper level divergence or low level convergence necessary to maintain the surface low intensity. The 970-mb center pressure reflecting no change from 12 hr earlier (Fig. 6-2), even though the center has moved over land, is evidence of the effective maintenance of this system.

Figure 6-5. DMSP infrared imagery 0937 GMT 11 January 1989 and 500-mb data for 1200 GMT.

2. The bright cloud plume seen near 60 °N, 147 °W indicates orographic lifting (across the Kenai Mountains) in strong southerly winds. Under areas of bright cloud plumes surface winds are strong and gusty with moderate to severe low level turbulence. Wind speed and related turbulence drop off rapidly to the west of cloud plumes that are caused by strong southerly flow. Wind speed increases are more uniform (less turbulence) when approaching the plume area from the east.
3. The clear area (dark band) immediately behind the frontal band reflects strong subsidence. This subsidence, coupled with the sharp trailing edge of the bright frontal band clouds, is indicative of a strong frontal system.
4. The southern extension of the low level cold air outbreak behind the front is indicated by the extension of cloud streets where the air flows off the ice pack and over the "relatively warm" Bering Sea water and the region of open-celled cumulus beyond the cloud street regime. The surface air temperature 32 °F (0 °C) isotherm, labeled on Fig. 6-5, extends about 300 n mi (556 km) south of the Aleutian chain. Snow showers were reported as far south as the vicinity of 46 °N under this outbreak. The cloud streets extend to and beyond the Aleutian chain and evolve into an open celled convective pattern downstream from the chain. Weather observations of the southeastern Bering Sea under the cloud streets indicate conditions of 25- to 35-kt (13–18 m/s) northwesterly wind, air temperatures of 5 °F or −15 °C (near ice edge) to 25 °F or −4 °C north of the chain, near 0 to 3 n mi (6 km) visibility in snow showers, and broken to overcast skies with ceiling heights of a few hundred feet in showers.
5. The lack of cloud streets over the Bristol Bay area (57 °N, 160 °W) in Fig. 6-5 indicates the presence of warm air wrapping around the low center during the occlusion process.
6. Two particular areas of enhanced cloud development of interest are outlined in Fig. 6-5. Enhanced clouds, those of greater vertical development and therefore colder tops, are indicated in infrared imagery by lighter gray shades. Area 1 is centered near 48 °N, 158 °W just behind the frontal cloud band. Area 2 is located over the central Bering Sea. The movement and interaction of these areas will be tracked throughout this case.

Figure 6-6 (1946 GMT 11 January) reflects the cloud conditions 10 hr after Fig. 6-5. The occluded position of the frontal band is beginning to align east-west, which indicates the center was stalling while the cold front moved more rapidly northeastward. Some anti-cyclonic outflow is still evident, and little change in the center pressure occurs until 1200 GMT 12 January (982 mb), some 16 hr after this view. Image and flow relationships evident in Fig. 6-6 include

1. The occluding process was progressing (compare cloud patterns to those in Fig. 6-5). The slowing of the forward motion of the center was occurring and is reflected by the occluded front cloud band becoming east-west aligned.
2. The cloud pattern was becoming complex as the higher level cirrus and cold front cloud band moved out ahead of the clouds wrapped around the stalling pressure center.

Figure 6-6. DMSP infrared imagery for 1946 GMT 11 January 1989 and surface data for 1800 GMT.

3. Small scale vortices formed west and south of the center in the baroclinic zone between the cold air in the northerly flow on the back side of the low and the warm air wrapping around the low.
4. Enhanced cumulus area 1 immediately behind the frontal subsidence zone moved northeastward toward the low center; area 2 of enhanced cumulus intensified over and south of the chain.

5. Cloud streets continue to dominate the eastern half of the Bering Sea.
6. Stratiform clouds over the Bering Sea, seen on the left edge of the image, reflect the induced ridge line between the mature low over Alaska and lows approaching from the west and south. Weather conditions over the eastern Bering Sea are dominated by cloud streets with below freezing temperature, strong northwesterly winds, and periods of low ceiling and visibility in snow showers. Hazardous shipping conditions caused by high winds and seas are occurring throughout this region and well to the south of the Aleutian chain.

Figure 6-7 (0511 GMT 12 January 1989) shows the cloud patterns over the eastern Bering Sea, Alaska, and the Gulf of Alaska about 10 hr after Fig. 6-6 imagery. The surface low has moved to the interior of Alaska (near 63 °N, 150 °W) while maintaining its central pressure (972-mb closed contour at 0600 GMT). The track and intensity of this low is somewhat anomalous and results from the strong ridging over the eastern Gulf of Alaska (Fig. 6-1). The normal winter storm track is into the Gulf of Alaska from south of the Aleutians with lows filling rapidly as they move over the mountains of south central Alaska. Image and flow relationships evident in Fig. 6-7 include

1. The east-to-west alignment of the occluded portion of the frontal cloud band is extending in length with time (compare to Fig. 6-6).
2. Enhanced cumulus area 1 has moved northward around the center and interacted with the coastal mountain range of south central Alaska, resulting in an east-to-west band of convective clouds extending from the Kenai Peninsula (60 °N, 150 °W) to Yakatat Bay (59 °N, 140 °W).
3. Enhanced cumulus area 2 interacted with the front resulting in frontal wave development. The wave development is indicated by the area of anticyclonic curvature in the frontal band seen near 53 °N, 138 °W.
4. The transformation from cloud streets to stratiform clouds over the eastern Bering Sea (left center of Fig. 6-7) reflects a weakening of the cold air outbreak over that region. The 0600 GMT surface analysis (not shown) indicates that the ridge between the mature low over Alaska and lows approaching from the west and south has moved eastward to near 175 °W (extreme left edge of Fig. 6-7).

By 0458 GMT 13 January 1989 (Fig. 6-8) the only remaining significant cloud feature associated with the now rapidly dissipating mature low is the large area of enhanced cumulus (area 2) along the coast of southeast Alaska. This area of enhanced cumulus reflects the evolution of the frontal wave development previously seen in Fig. 6-7 and its further interaction with the mountains of southeastern Alaska and British Columbia. The old low and clouds have largely dissipated over the interior of eastern Alaska and northwestern Canada. The clear area over the Alaska Peninsula region reflects the ridge line between the dissipating low to the east and the trough line over the central Bering Sea (Fig. 6-3). By 1800 GMT 13 January at St. Paul Island (station 70308) the air temperature reached 36 °F (2 °C), warming up some 25 Fahrenheit degrees (14 Celsius degrees) from the 10 °F (−12 °C) at 1800 GMT 11 January.

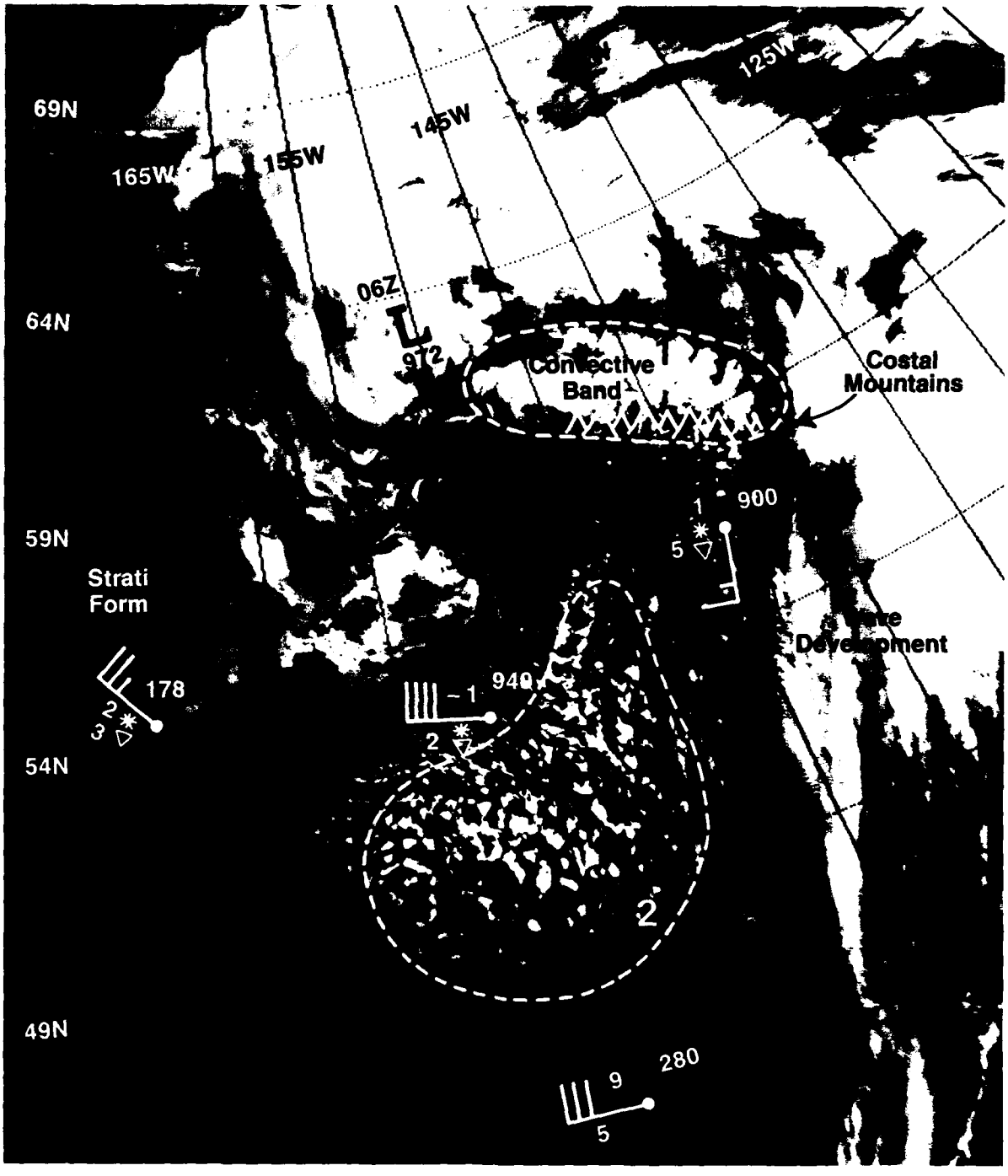

Figure 6-7. DMSP infrared imagery 0511 GMT 12 January 1989 with surface data for 1800 GMT.

Figure 6-8. DMSP infrared imagery 0458 GMT 13 January 1989.

Satellite Imagery Forecast Aids

1. Cold anticyclonically curved clouds indicate upper level divergence and intensification or maintenance of surface low pressure systems.
2. Clearly defined frontal and vortex cloud features indicate that system intensity or development is being maintained.
3. During the occlusion process warm air wrapping around the vortex results in formation of baroclinic zones to the west and south of the vortex. Internal small scale vortices frequently develop in these baroclinic zones (see Fig. 6-6 near 58 °N, 162 °W).
4. When the forward motion of the low center begins to slow, the occluded portion of the front takes on an east-west alignment.
5. Cloud streets form during winter when the sea surface temperature is at least 39 to 41 Fahrenheit degrees (21–22 Celsius degrees) warmer than the air. The streets are aligned with the low level wind and may extend a couple hundred nautical miles (300–400 km) downstream with only a gradual increase in cloud height and cloud linewidth. The clouds are identified as stratocumulus from below and are topped by an inversion. Weather under cloud lines includes extensive areas of steam fog, particularly within 100 n mi (185 km) or so of the ice edge, and scattered snow showers with ceiling and visibility restrictions from near zero-zero to a few hundred feet (meters) and a nautical mile or two (1–2 km).
6. Cloud street patterns typically transform to an open celled cumulus pattern a couple hundred nautical miles (300–400 km) downstream where the shower activity becomes more intense, but the time between showers increases to 30 to 60 min for a stationary point.
7. During winter, under cloud street patterns, surface air temperatures over the Bering Sea will range from 5 °F (−15 °C) or lower near the ice edge to 32 °F (0 °C) as much as 400 n mi (741 km) south of the Aleutian chain. The extension of open celled cumulus downstream from the cloud streets is a good indicator of the extent of cold air. Ship superstructure icing and extreme wind chill temperatures occur under winter cloud street patterns.
8. Winds will be intensified through island and mountain passes thereby increasing wave heights, spray, superstructure icing, and wind-chill hazards. When cloud streets extend over the Aleutian chain, extreme conditions will be experienced when air temperatures are at or below freezing.
9. The western boundary of a cold air outbreak is indicated by a change from cloud street patterns to stratiform clouds. The induced ridge line between successive lows may be indicated by a cloud-free area, which will be maintained and move eastward as long as the relative spacing of the lows is maintained. If the lead low stalls, the southerly flow ahead of the following low will cover the clear area with prefrontal stratiform clouds.

6.1.2 Cyclogenesis Under Zonal Flow

On 16 and 17 January 1989 zonal flow prevailed over the Bering Sea region. Migratory cyclones approaching from the midlatitudes were steered to the east into the Gulf of Alaska. During periods of zonal flow the cloud patterns over the northern portion of migratory lows, generally the occluded front portion, tend to be sheared off from the lower latitude portions of the front. The lower portions are advected rapidly eastward, and the higher latitude portion of the frontal cloud band becomes aligned east-west and gradually dissipates. As the major cyclogenetic features move rapidly off to the east, small scale cyclogenetic features will form and propagate along the dissipating portion of the "hang-back" front. Figures 6-9 through 6-11 are DMSP images that show a hang-back front and embedded small scale cyclogenetic features under a zonal flow regime. Figure 6-9 shows a frontal band extending southeastward out of the central Bering Sea with frontal shearing indicated by a cross-over cirrus shield near 48 °N, 170 °W. Figure 6-10, from the next orbit, provides

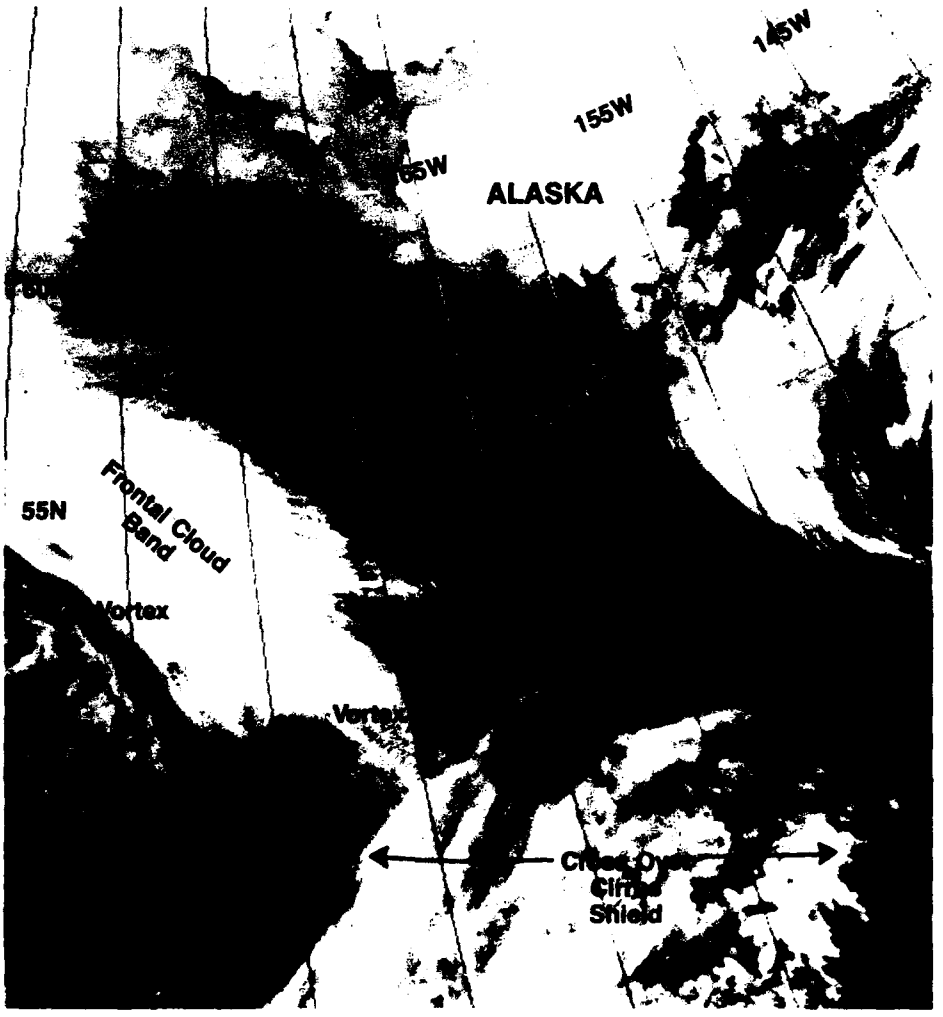

Figure 6-9. DMSP infrared imagery 0512 GMT 16 January 1989.

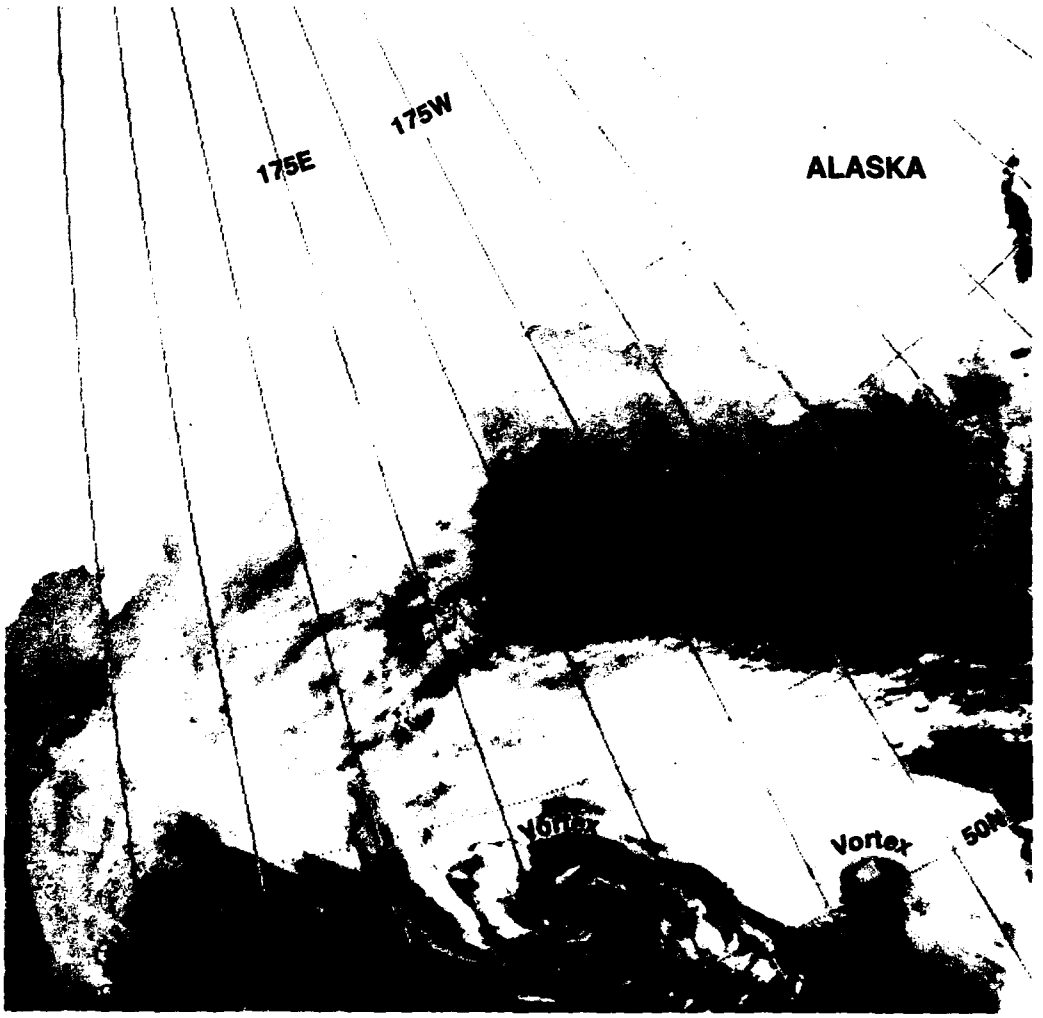

Figure 6-10. DMSP infrared imagery 0654 GMT 16 January 1989.

overlapping coverage and an extended view to the west. Two obvious vortices are seen in the nearly east-west aligned hang-back portion of the frontal band. Figure 6-11, from about 24 hr later, indicates that the lower latitude portion of the frontal system, that part south of the shear area, has moved off to the east. The western part of the hang-back portion of the front has actually moved westward and is influencing the weather over the extreme western Bering Sea and Kamchatka Peninsula. In general, the hang-back portion of the front tends to become nearly stationary and dissipates in place. However, it will continue to cause unsettled weather conditions, which, along with an irregular motion, will create some unique hang-back front forecast problems.

Forecast reasoning, if based on the characteristics of midlatitude behavior of frontal systems, (i.e., generally northeastward movement at 25 to 35 kt, or 45–65 km/hr producing 6 to 12 hr of weather at a given location followed by rapidly improving conditions after frontal passage), must be modified greatly when dealing with hang-back front situations.

Prolonged variable conditions with gradual improvement over a day or two is the rule. The fact that individual cells or cloud features are likely to approach from an easterly quadrant further complicates the forecast problem. It should be noted that the low level flow will generally be easterly in the poleward portions of hang-back fronts and westerly on the midlatitude side.

Figure 6-11. DMSP infrared imagery 0641 GMT 17 January 1989.

The 500 mb (Fig. 6-12) and surface (Fig. 6-13) analyses for 1200 GMT 16 January 1989 show the synoptic scale flow during this hang-back front event. South of 50 °N strong zonal flow prevails at the 500-mb level with light winds of variable direction over the Bering Sea. The surface analysis reflects one large west-northwest to east-southeast elongated low, which is nearly vertically stacked under a similarly shaped 500-mb trough. Note that although at least two distinct vortices are evident in the satellite imagery (Figs. 6-9, 6-10, and 6-11)

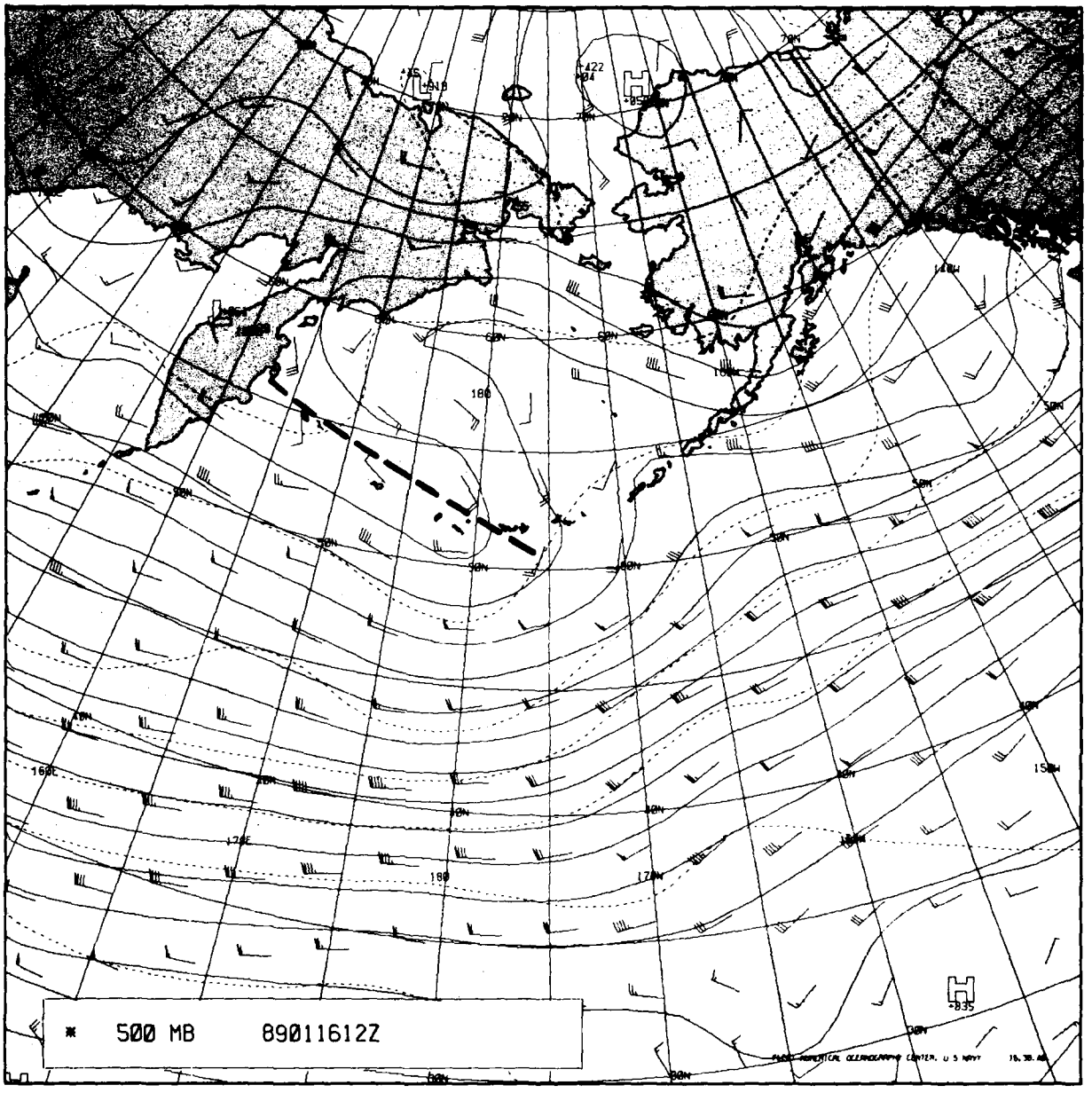

Figure 6-12. FNOC 500-mb analysis 1200 GMT 16 January 1989.

they are not resolved in the surface analysis at 1200 GMT, and not until 0600 GMT 17 January 1989 in following analyses (not shown) is there any indication of multiple vortices along the frontal band. The coarse numerical model resolution, coupled with the probable lack of conventional observation data, is the likely reason for limitations in numerical analysis depiction of these subsynoptic vortices. The numerical analyses do, however, reflect the favorable synoptic scale pattern, and this information, coupled with satellite imagery, will provide the necessary information for accurate short-term (0-24 hr) forecasts.

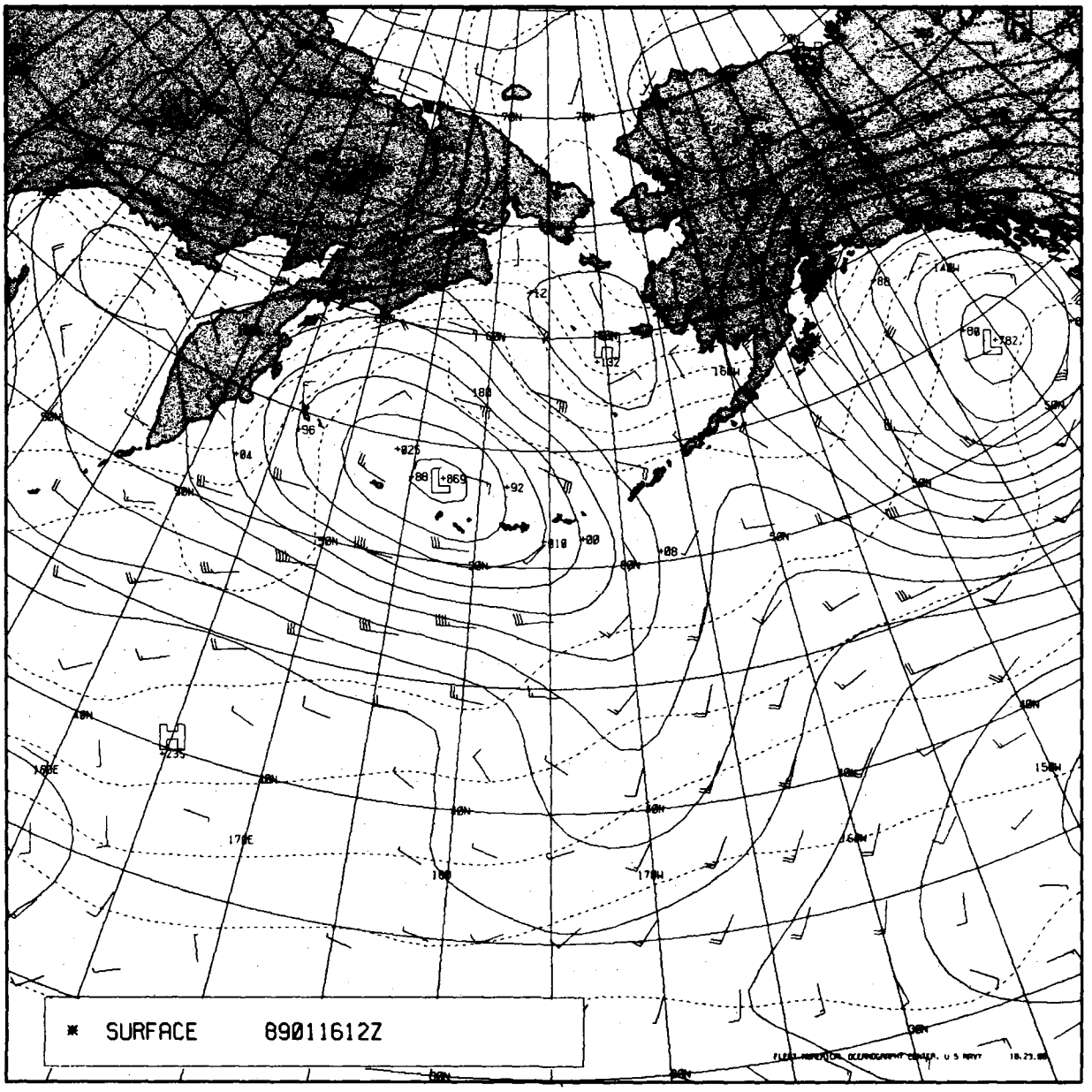

Figure 6-13. FNOC surface analysis 1200 GMT 16 January 1989.

Forecast Aids

1. During periods of strong zonal flow at 500 mb, hang back frontal zones are likely to develop poleward of the zonal flow pattern.
2. The area poleward of the strong 500-mb zonal flow will exhibit light and variable winds aloft.
3. The frontal zone will become elongated nearly east-west and subsynoptic vortices may slowly retrograde westward along with the entire frontal cloud band.
4. This so-called hang back frontal zone will not exhibit the typical behavior of migratory midlatitude frontal systems. It will likely remain nearly stationary for a couple of days with embedded vortices that may also be stationary or move slowly either eastward or westward along the frontal zone.

6.1.3 Triple Point Cyclogenesis South of the Chain

Triple point cyclogenesis refers to cyclogenesis near the apex of the warm, cold, and occluded fronts. This is a fairly frequent event in the area south of the eastern Aleutian chain and Alaska Peninsula. Triple point cyclogenesis occurs following the occlusion process and after the parent low becomes vertically stacked and begins to stall. As the parent low stalls, the frontal systems continue to move eastward around its southern periphery. The parent low tends to take on an elongated east-west configuration, and a secondary cyclogenesis occurs in the extreme eastern portion of the elongated pattern. Following the secondary development the new low becomes the primary center as the original low slowly fills. The Adak Forecaster's Handbook reports that during the spring season this sequence may be repeated where a third low forms in the vicinity of the secondary low's triple point.

Lows that approach the Bering Sea region from the ocean sector rather than from off the Siberian landmass typically exhibit warm type occlusions. These lows reflect the cold airmass over the Bering Sea in advance of the warm front, in comparison to the cool airmass behind the cold front that has been modified over the western North Pacific. With warm type occlusions extensive overrunning by warm air occurs, resulting in an extensive cloud shield that typically provides about 24 hr advance indication of an approaching storm. However, the precipitation shield only extends 300 to 400 n mi (556–741 km) northward from the warm front in advance of the low. The duration of precipitation will vary with the movement of the parent low and secondary low.

This example shows a warm type occluded frontal system associated with an intense winter low that moves east-northeastward from the western Pacific to near 45 °N, 180 °, where it stalls. Secondary cyclogenesis occurs about 600 n mi (1112 km) to the east of the stalling area. Both the primary and secondary lows generally remain 300 to 400 n mi (556–741 km) south of the Aleutian chain and Alaska Peninsula.

25–26 January 1989

Figure 6-14 (1654 GMT 25 January) shows the cloud pattern associated with a triple point cyclogenesis event in January 1989. Four particular aspects of the cloud patterns seen in Fig. 6-14 are noted: (1) a mature low centered near 45 °N, 170 °E with its associated occluded front extending around it to the north; (2) a bright anticyclonically curved cloud shield across the frontal cloud band seen near 42 °N, 176 °W; (3) an extensive cloud street pattern over much of the Bering Sea; and (4) nearly cloud-free conditions over Siberia, the Bering Sea pack ice, and western Alaska. Each of these four aspects can provide insight into the atmospheric conditions that if integrated into decision making should lead to better forecasts for the Bering Sea region over the next day or so.

Figure 6-14. DMSP infrared imagery 1654 GMT 25 January 1989.

The nearly cloud-free land and pack ice area, coupled with the implied strong northerly flow off the ice (indicated by the cloud street area), implies that high pressure dominates the region. Figure 6-15, the surface analysis at 1800 GMT 25 January 1989, shows a strong high pressure system centered over Siberia. These factors, combined with the east-west alignment of the occluded front and the apparent shearing of the frontal band near 41 °N, imply that the main westerly steering current is some distance south of the Aleutian chain. All these factors point toward the likelihood that any new cyclogenesis and primary frontal activity will remain south of the chain with the original low stalling and filling in the vicinity of the chain. When lows move eastward south of the Aleutian chain and into the Gulf of Alaska, they tend to steepen the pressure gradient over the northern Bering Sea area and enhance low level cold air outbreaks. Such outbreaks result in cloud street development such as that seen in Fig. 6-14.

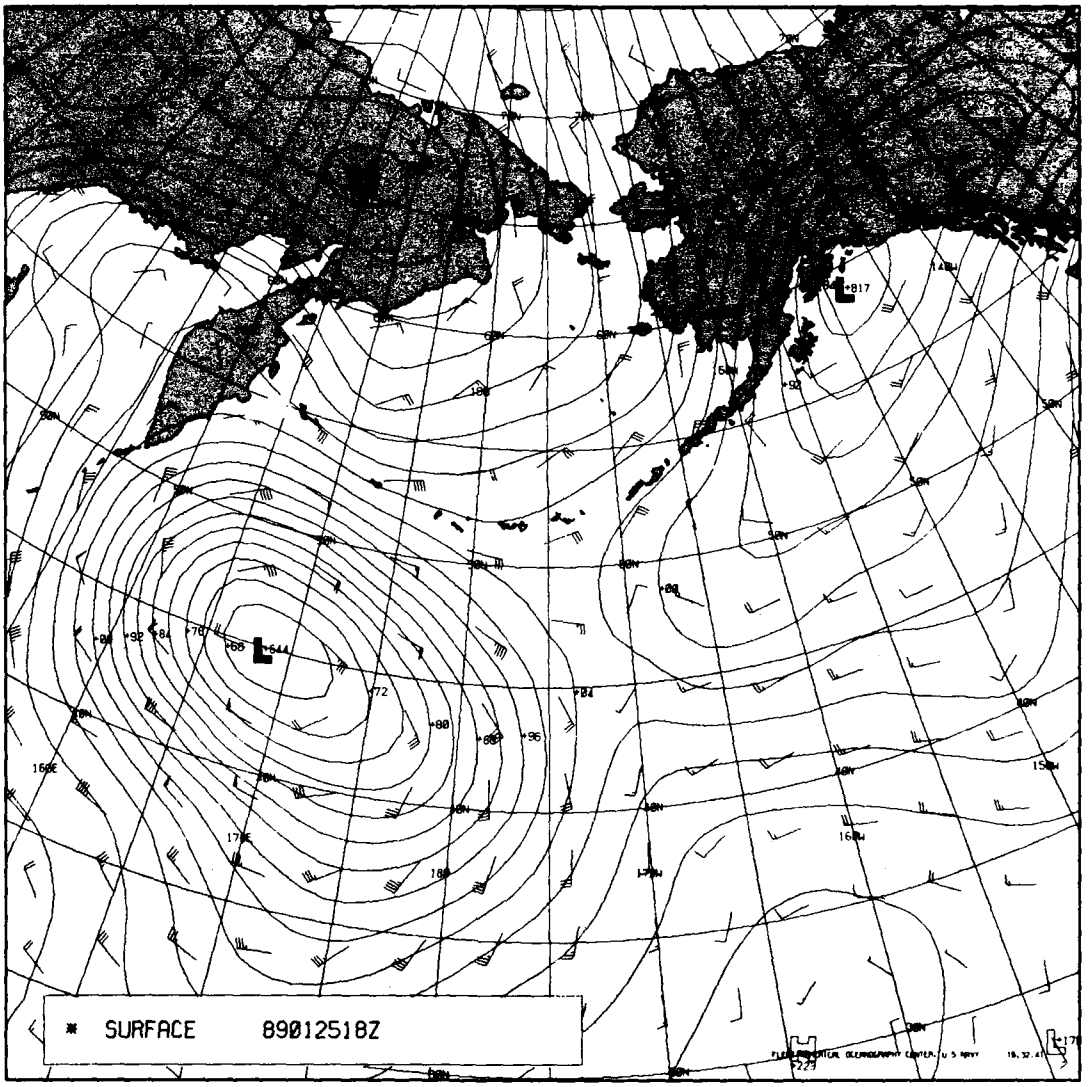

Figure 6-15. FNOC surface analysis 1800 GMT 25 January 1989.

Figure 6-16 (1900 GMT 26 January 1989) shows the cloud conditions about 26 hr after Fig. 6-14. Several characteristics of the frontal cloud pattern seen south of the Aleutian chain imply active cyclogenesis. A large bright portion of the frontal cloud bands capped by anticyclonically curved cirrus outflow, a sharp clearly defined trailing edge of the frontal band, and a relatively clear area behind the front are indicators of frontal wave development on a strong front. The cloud street pattern over the northeastern Bering Sea remains well

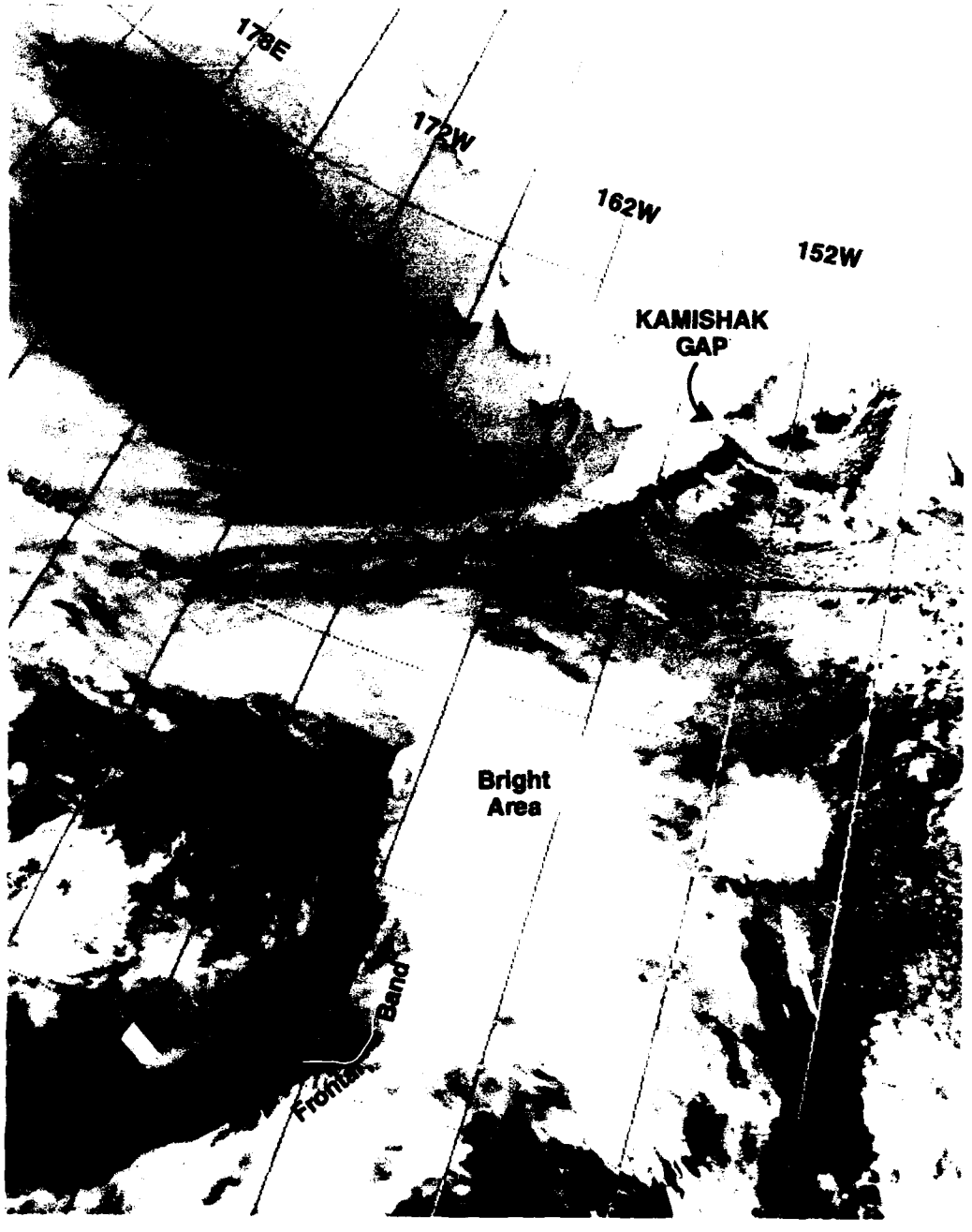

Figure 6-16. DMSP infrared imagery 1900 GMT 26 January 1989.

defined, and, with low pressure prevailing over the western Gulf of Alaska (Fig. 6-17), the cold outflow has spread across the Alaska Peninsula and Kodiak Island area. Initiation of the Kamishak Gap wind regime is implied by the cloud lines streaming eastward through the passage way between Kodiak Island and the Kenai Peninsula (Fig. 6-16). This particular storm track and related events reflect a frequent winter time condition over the Bering Sea and Gulf of Alaska regions.

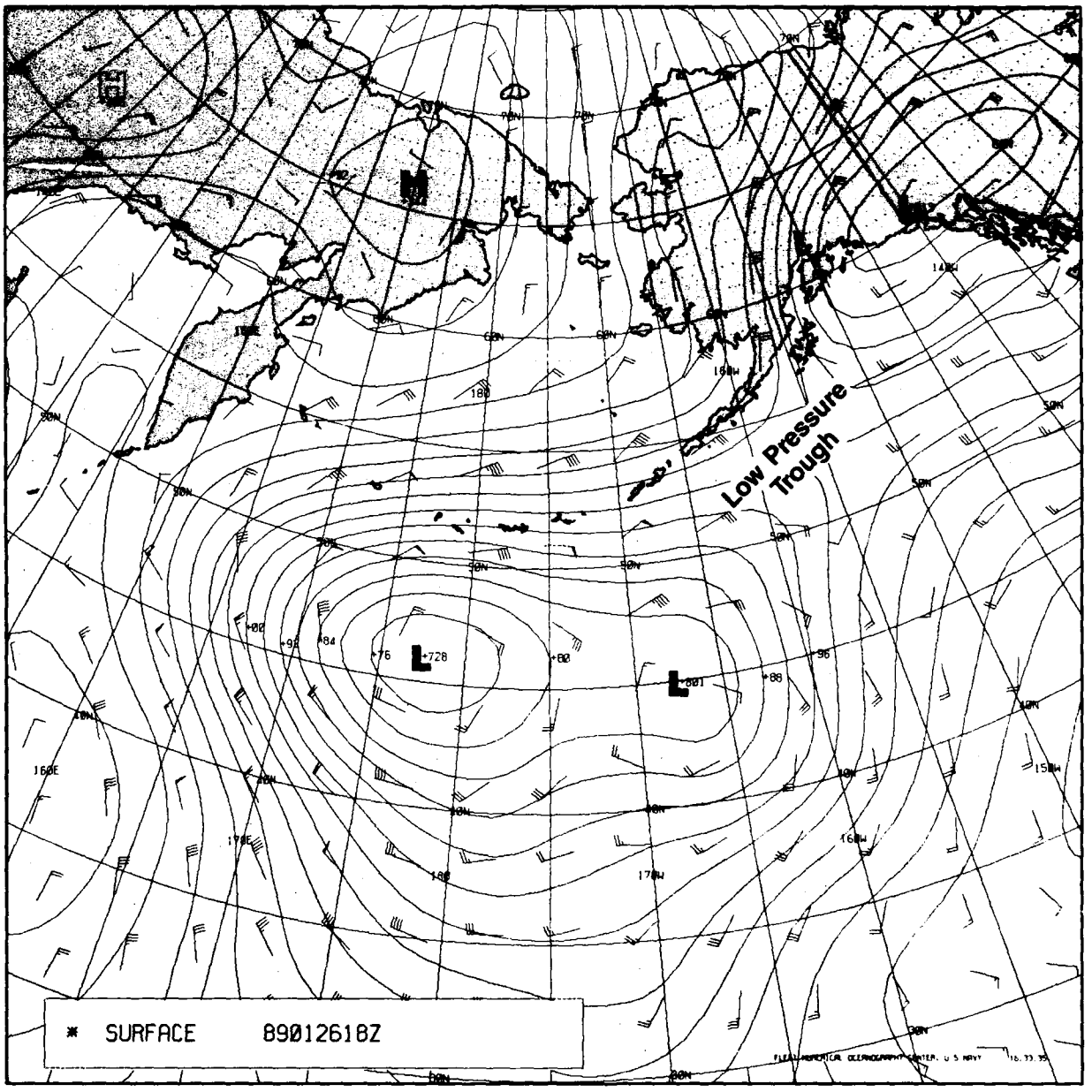

Figure 6-17. FNOC surface analysis 1800 GMT 26 January 1989.

Forecast Aids

1. When the high pressure ridge from Siberia to Alaska, north of the Bering Sea, is well developed it blocks the northward movement of western Pacific cyclones, and they tend to be steered into the Gulf of Alaska.
2. A typical scenario under these conditions is for the original occluding low to become vertically stacked from the surface to 500 mb, then stall and dissipate, with cyclogenesis occurring near the cold, warm, or occluded front apex somewhere south of the Aleutian chain. The new cyclone then tracks eastward into the Gulf of Alaska.
3. Under these synoptic conditions a cold air outbreak typically occurs over the northeastern Bering Sea and is revealed by the cloud street pattern indicating off-ice flow.
4. As the developing low tracks eastward, the cold air outbreak and strong low level winds follow its movement, resulting in deteriorating conditions well to the north and west of the actual frontal weather associated with the low.

6.1.4 Blocking Ridge over the Bering Sea

When blocking patterns occur over the Bering Sea-Gulf of Alaska region meridional circulation is established. The southerly flow on the west side of the blocking pattern advects frontal moisture and clouds, and warm air into the Arctic basin. Under the ridge a subsidence-induced inversion caps an extensive area of low stratus and fog. Blocking patterns are typically nearly stationary or may slowly progress either east or west. In all cases the weather and cloud conditions associated with the blocking pattern become quite persistent, more like the summer pattern than the normal rapidly changing winter conditions.

23–26 April 1990

Three images and various concurrent 500-mb and surface analyses spanning about a 76-hr period are shown to illustrate this April 1990 blocking event. Figure 6-18 (2038 GMT 23 April 1990) shows a frontal cloud band that extends northward from an area just west of the Sea of Okhotsk to near the northern coast of Siberia. The island barrier effects of the western Aleutian chain and the widespread fog and stratus over the region imply high pressure with a probable ridge line extending from west of Attu northeastward toward the Bering Strait. Arrows are plotted on Fig. 6-18 to depict the cloud feature implied low level wind directions and relative speeds. Figures 6-19 and 6-20 show the 500-mb and surface analyses for 0000 GMT 24 April 1990. The ridge and light wind pattern implied by the satellite cloud features are clearly shown.

The sector of the Arctic basin north of Siberia at this time is generally cloud free indicating the current lack of meridional flow into that area. Figure 6-19 (500 mb) supports this interpretation. The central and eastern Bering Sea is dominated by a stratus cloud deck and light surface winds. The low level light wind condition and anticyclonic flow pattern are clearly indicated by the distribution of island barrier and wave cloud features. The island

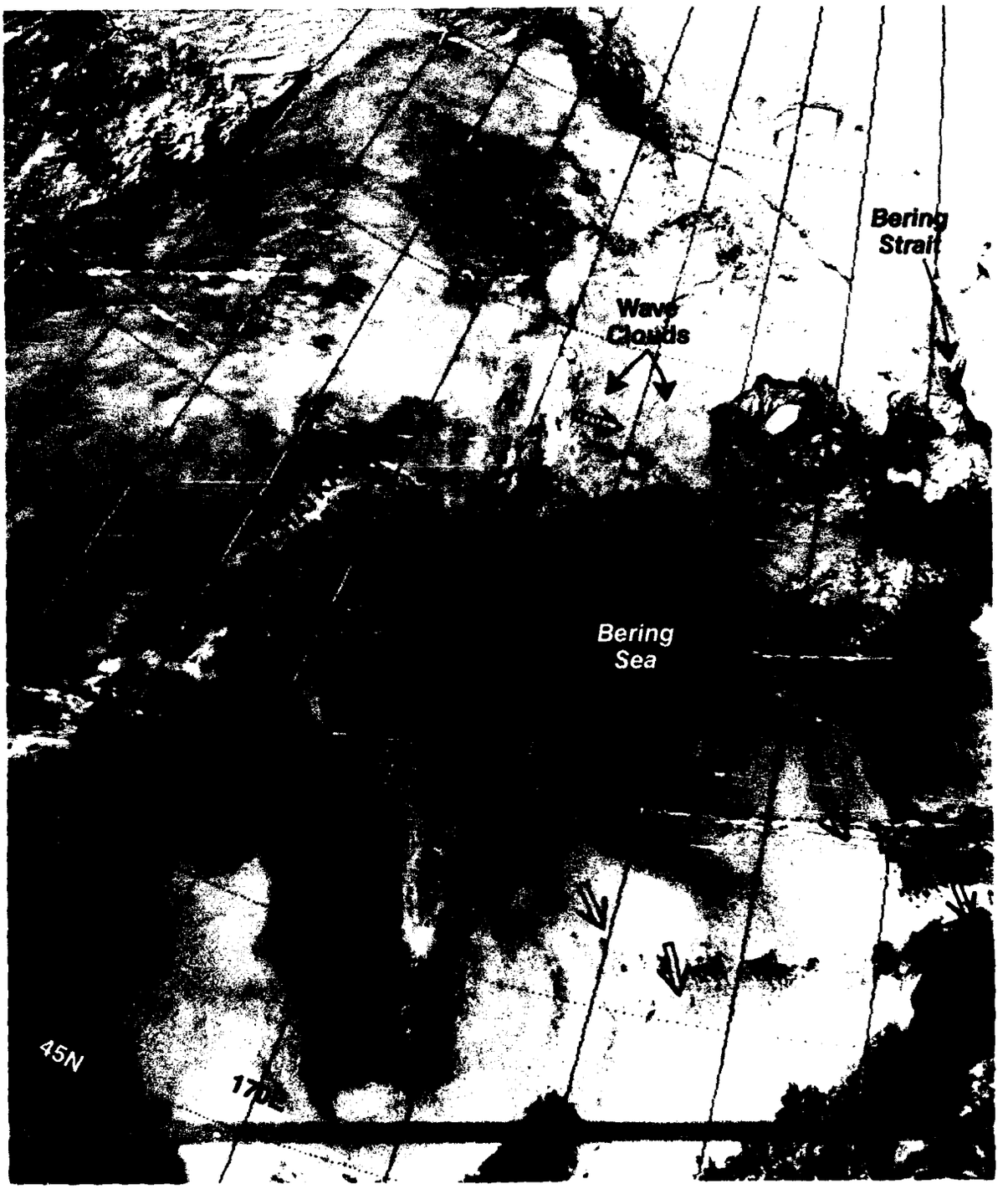

Figure 6-18. DMSP infrared imagery 2038 GMT 23 April 1990.

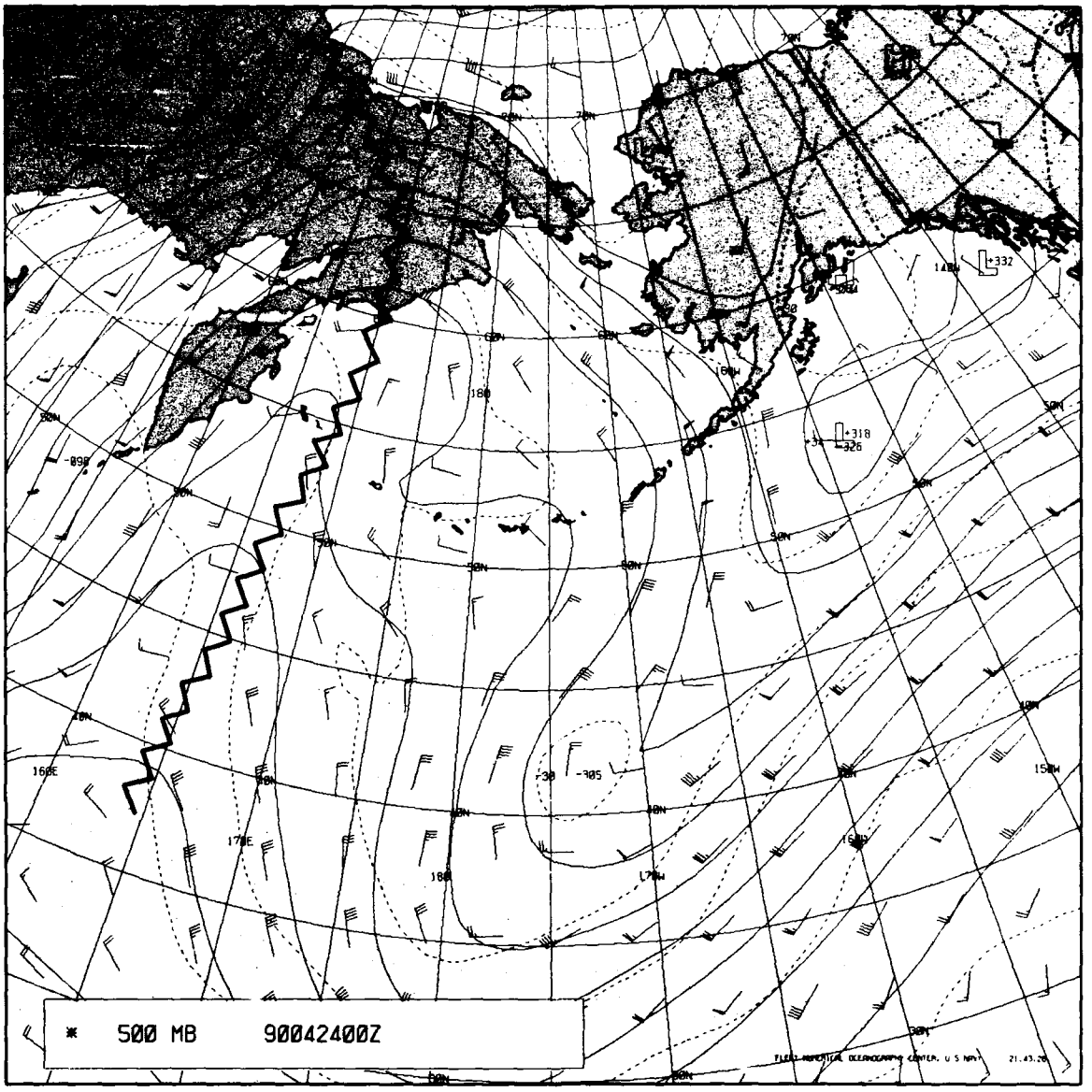

Figure 6-19. FNOC 500-mb analysis 0000 GMT 24 April 1990.

barrier features (clearing to leeward) seen in Fig. 6-18 indicate veering wind directions (clockwise shifting) from about 270° over the Commander Islands (near 167°E) to about 350° over Unimak Island (near 165°W). Note that the island barrier effects in the vicinity of 180° are very small, implying very light winds near the center of the ridge line. The various wave cloud signatures support the same general ridge configuration with indications of westerly winds over Siberia (near 63°N, 175°E), becoming northwesterly over western Alaska (near 60°N, 165°W). Wave clouds typically form at or above the elevation of the terrain features with which they are associated, thereby providing evidence of wind conditions at various elevations.

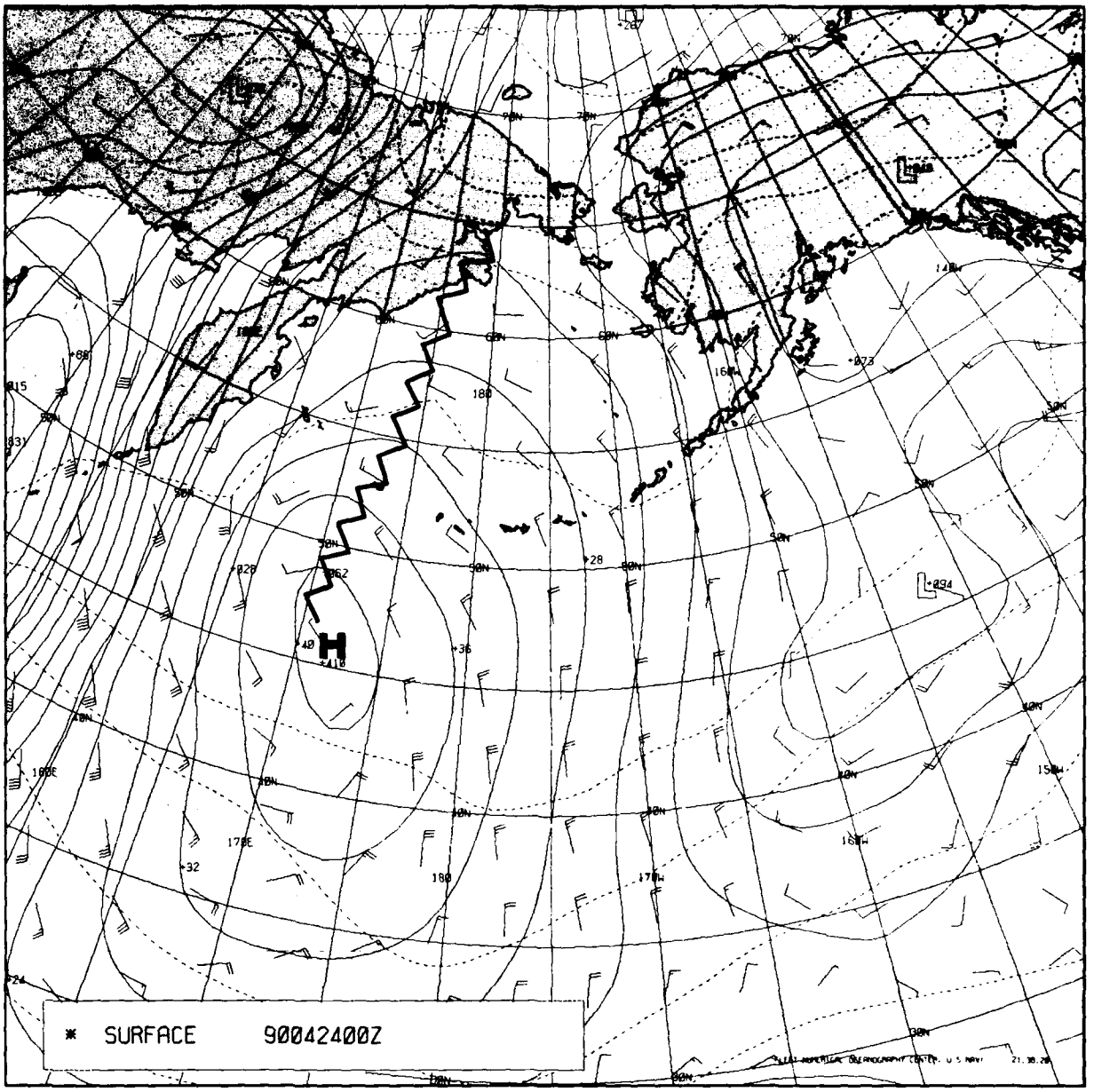

Figure 6-20. FNOC surface analysis 0000 GMT 24 April 1990.

The extent of the southerly meridional flow to the west of the blocking ridge is reflected in Fig. 6-21 (2017 GMT 24 April) by the advection of the frontal clouds well into the central Arctic basin. The onset of increasing southerly winds in advance of the front is indicated by the large leeside clearing to the north of Attu Island (near 173 °E). Westward from Attu Island a general breaking up of the low level stratus clouds is seen with increasing frontal clouds yet further to the west. The breakup of the low stratus deck is likely in response to vertical mixing associated with increasing southerly winds. The surface ridge appears to have narrowed in comparison to the condition seen approximately 20 hr earlier (Figs. 6-19 and 6-20), apparently as a result of the eastward movement of the frontal band. However, over the Aleutian chain the ridge line appears to have moved only slightly eastward to near 180°. An increase in northerly low level winds over the eastern Bering Sea is implied by the enlarged clear areas associated with flow off the land and ice as well as the clearing to lee of the eastern Aleutian Islands and Alaska Peninsula.

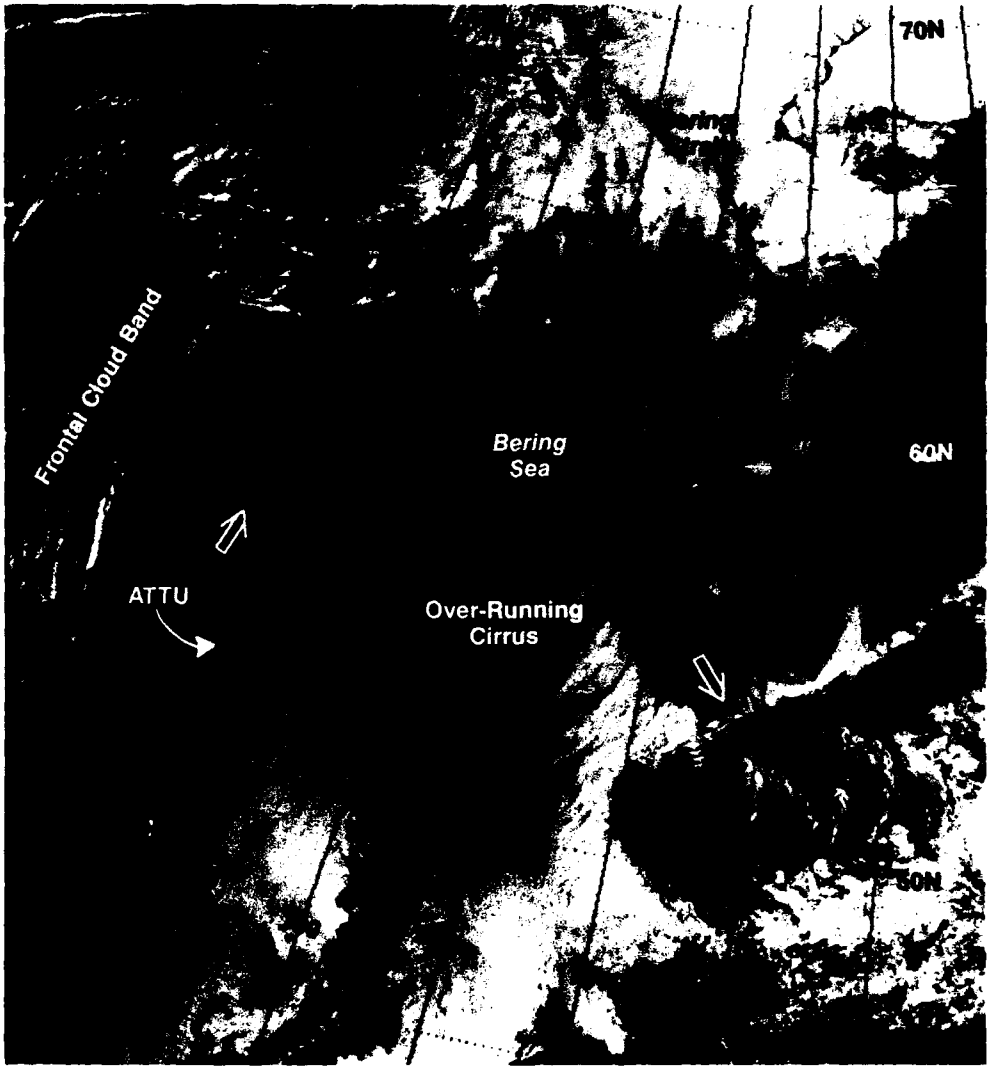

Figure 6-21. DMSP visible imagery 2017 GMT 24 April 1990.

Two days later (Fig. 6-22) some remnant of the ridge remains over the eastern Bering Sea, judging from the fog and stratus in that region. The surface ridge line appears to be west of 170 °W since northerly flow is apparent near 169 °W where Von Karmen vortices appear south of the islands. The frontal cloud streaks imply a rapid transition to strong southerly flow near 178 °W, west of the ridge line. The wave clouds extending northward from the vicinity of Attu Island (173 °E) indicate that strong southerlies extend westward to that longitude. The clearing seen further west off Kamchatka and wave clouds over Kamchatka imply westerly flow behind the front. The rapid decrease of strong southerly

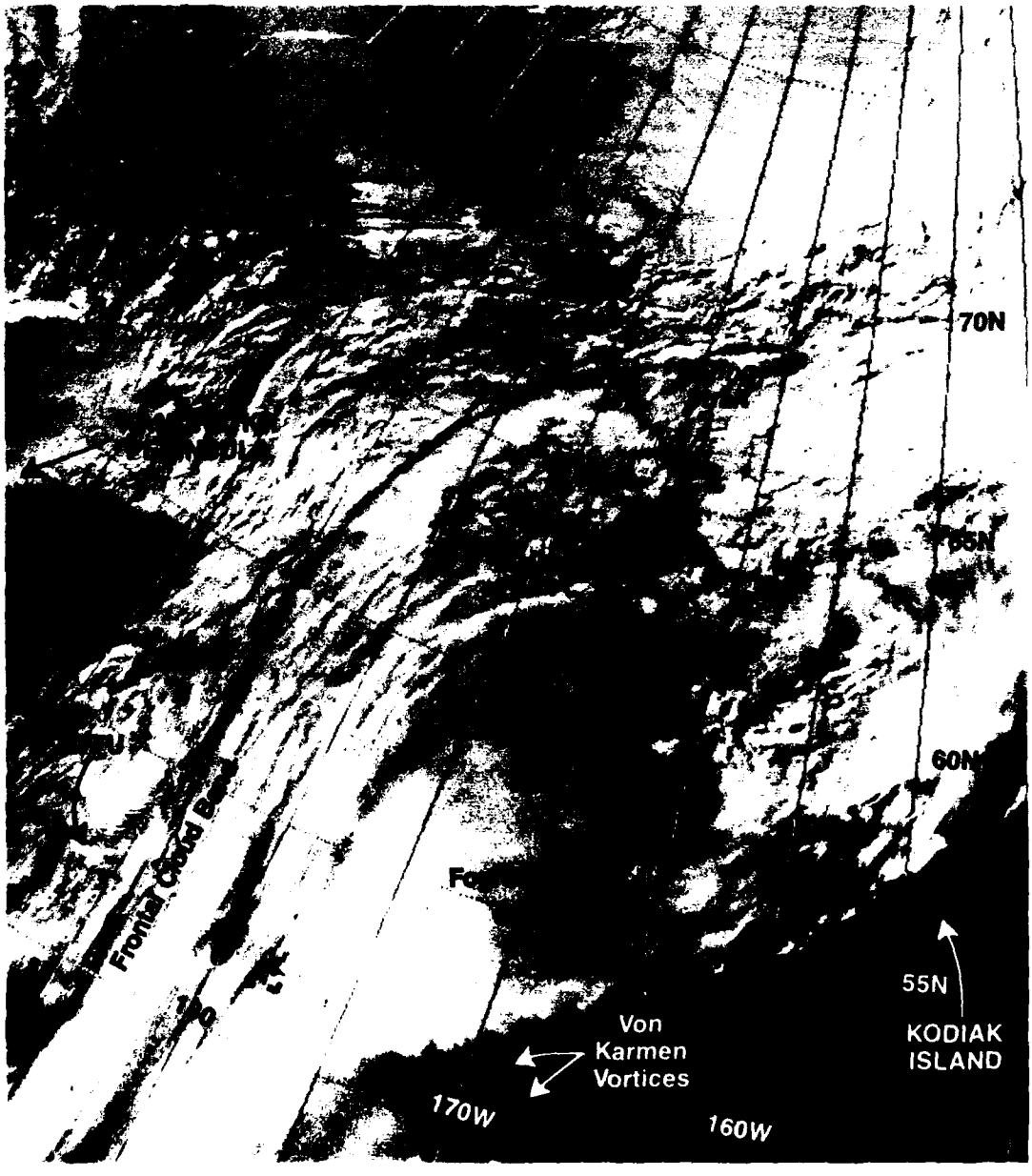

Figure 6-22. DMSP visible imagery 1935 GMT 26 April 1990.

winds with the passage of frontal cloud bands has been noted at various Aleutian chain observation stations. Figures 6-23 (500 mb) and 6-24 (surface) show the analyses at 0000 GMT 27 April 1990 shortly after the image seen in Fig. 6-22. The surface analysis (Fig. 6-24) indicates that the front at this time has moved past Attu, as winds are shown to shift from southerly to northwesterly. The narrowing ridge over the southeastern Bering Sea and onset of northwesterly flow over the western Bering Sea are shown in these analyses.

Forecast Aids

1. Blocking patterns result in large areas of relatively unchanging cloud and weather conditions over periods of several days, a significant variation from the rapid changes typically experienced during the cold season.

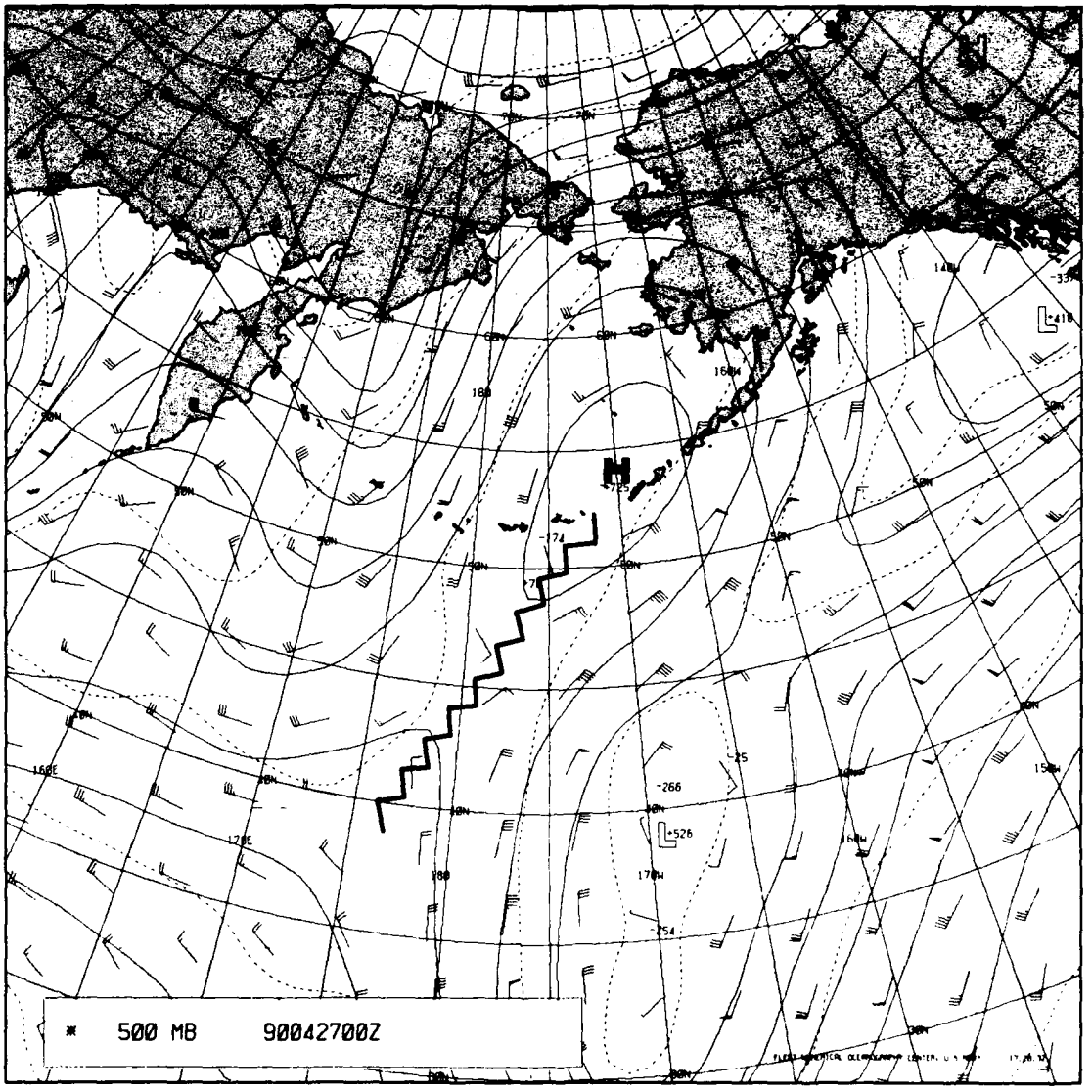

Figure 6-23. FNOC 500-mb analysis 0000 GMT 27 April 1990.

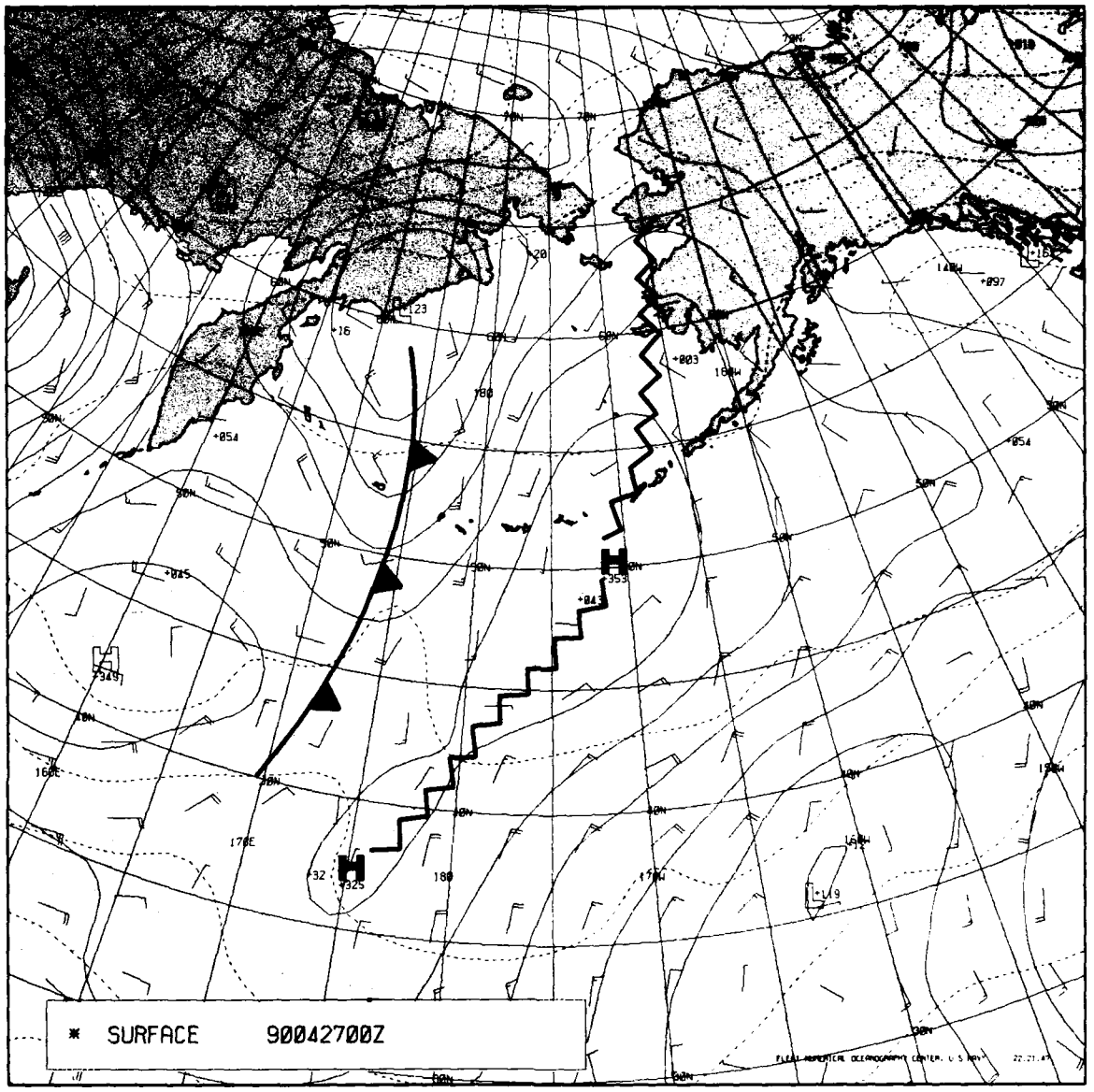

Figure 6-24. FNOC surface analysis 0000 GMT 27 April 1990.

2. Island barrier effects can be used to analyze the low level wind direction and speed.
3. Although the west-to-east movement of synoptic features under blocking patterns is very slow, large changes in wind, cloud, and weather conditions can occur over relatively short horizontal distances (<200 n mi or <370 km) on the periphery of high pressure areas.
4. During strong blocking patterns relatively warm moist air is typically advected deep into the Arctic basin.
5. Indication of blocking circulations as depicted by the location, alignment, and features of cloud patterns is clearly evident in satellite imagery.

6.1.5 Summer Cyclone over the Bering Sea

During summer the primary storm track of the North Pacific shifts northward over the Bering Sea. Although summer cyclones tend to be less intense than winter ones, with the possible exception of ex-typhoons (see Section 4.1.8), they can be disruptive to surface and air operations. One positive effect of summer cyclones is that they temporarily break up the persistent summer fog and low stratus regimes. For a day or two improved ceiling and visibility conditions will be found over various sections of the Bering Sea region.

This case illustrates the passage of a summer cyclone over the Aleutian chain and into the central Bering Sea where the cyclone stalls and dissipates. Small synoptic scale cyclones are seen further north as they pass from over the Siberian landmass into the Arctic basin. These higher latitude cyclones frequently intensify as they move over the open water of the Arctic Ocean that exists during summer and early fall between the Siberian and Alaskan coasts and the pack ice to the north.

20–21 July 1990

Figure 6-25 (2020 GMT 20 July 1990) shows the northern portion of a frontal cloud band located over the central Bering Sea. Although the frontal band appears to be wrapped at least half way around an assumed low center, the clouds in the vicinity of the suspected low do not clearly define the center. The general cyclonic circulation is, however, clearly depicted by the frontal cloud band as well as peripheral cloud features. To the west, low clouds are seen stacking against the western slopes of the Kamchatka Peninsula terrain, and leeside clearing is seen extending eastward over the extreme western Bering Sea. These observations imply general westerly flow over the peninsula. Northwesterly flow over the extreme western Bering Sea is implied by both the general configuration of the leeside clearing pattern and the partial clearing, seen under close inspection extending south of the Commander Islands. Moving eastward along the Aleutian chain to the vicinity of 180°, a well defined pattern of wave clouds can be seen extending eastward from various islands reflecting the low level westerly flow over that area. Further east the packing of clouds against the southern coastline of the Alaska Peninsula, the clouds extending northward through the channel openings of the eastern Aleutian Islands, exhibiting Von Karmen vortex lee effects, and the general leeside clearing over the Bristol Bay indicate southerly flow in that region. These barrier type cloud features, plus the frontal cloud band, quite clearly define the large scale cyclonic circulation over the Bering Sea.

The cloud vortex is more clearly depicted in Fig. 6-26, approximately 24 hr after Fig. 6-25. The frontal system appears to have weakened significantly. The inconspicuous nature of wave cloud patterns along the Aleutian chain at this time implies weaker winds than for the previous day. The northerly flow to the west of the cyclone has resulted in a general clearing over the western Bering Sea. The fairly rare cloud-free condition of that area provides a clear view of the Commander Islands seen near 55°N, 166°E. The reestablishment of high pressure over the area is indicated both by the stratus deck near 50°N, 170°E and ship track cloud lines seen in the stratus southwest of the vortex. Both of these cloud signatures imply that a stable atmospheric layer exists near the level where they form.

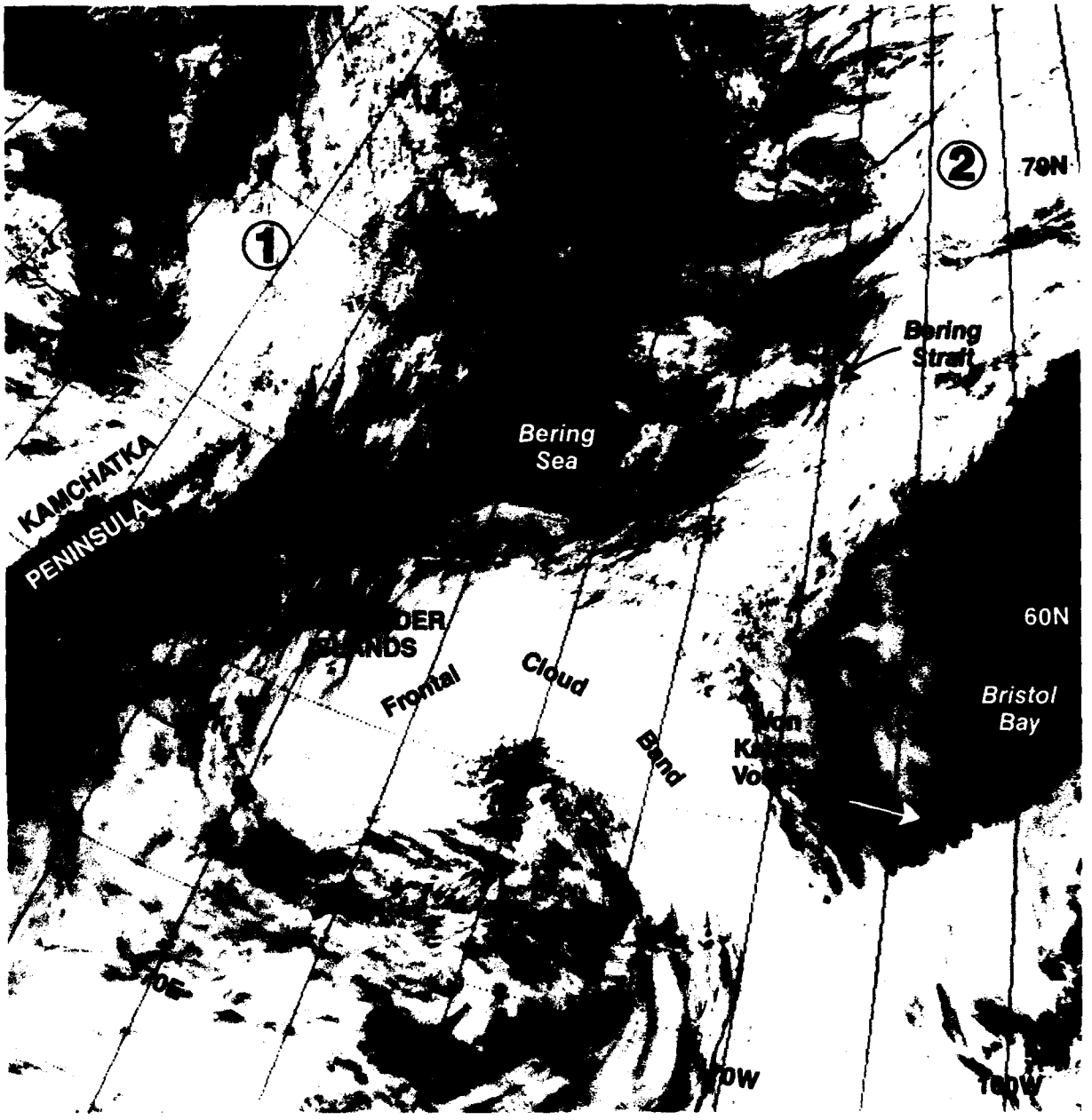

Figure 6-25. DMSP visible imagery 2020 GMT 20 July 1990.

Small synoptic scale, baroclinic cloud features can be seen in both Figs. 6-25 and 6-26 over the area north of the Bering Sea. Two disturbances are seen in Fig. 6-25, the first over the northern sector of Kamchatka Peninsula (labeled 1) and the second over the eastern Chukchi Sea near 70 °N, 165 °W (labeled 2). By the time of the DMSP imagery in Fig. 6-26 the first system is nearing the northern coast of Siberia around 165 °E, and only a general nondescript cloudmass off the northern coast of Alaska can be seen in relation to the second feature.

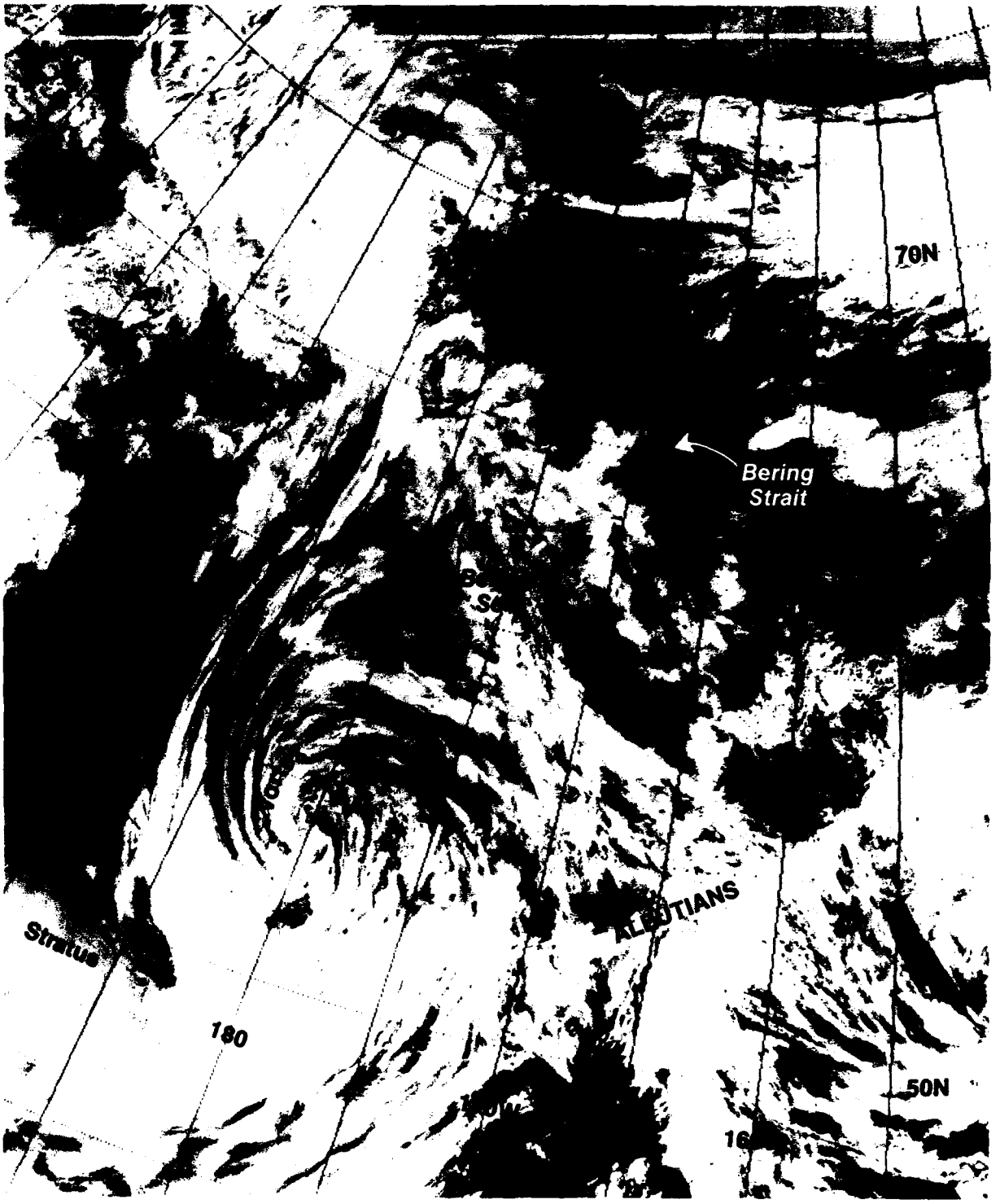

Figure 6-26. DMSP visible imagery 1959 GMT 21 July 1990.

16 July 1990, Typical Summer Cloud Pattern

Figure 6-27 (2003 GMT 16 July 1990), a separate but similar example from the preceding case, shows a seemingly chaotic cloud pattern over the Bering Sea. Review of a number of years of Bering Sea region imagery from the summer periods found patterns of this type to have a high frequency. The cloud patterns tend not to show any prominent synoptic scale signature. However, closer inspection yields a number of clues providing insight into the synoptic situation. A cloud eddy north of the Aleutian chain near Bristol Bay reveals southerly flow into the area. General cloud striations suggest an upper level low near 55 °N, 178 °E. Wave clouds over Wrangel Island and the De Long Mountains show strong westerly to southwesterly flow over those regions with probable frontal action over northwest Alaska. Cloud types east of the upper level low have a high probability of consisting of low stratus and fog because of the southerly flow over increasingly colder water in that region. When satellite data are supplemented by conventional data at low and high levels a very accurate analysis and assessment of prevailing conditions can be obtained.

Forecast Aids

1. Summer cyclones track through the Bering Sea and also over Siberia and into the Arctic basin.
2. Summer cyclones bring mixed conditions of heavier frontal weather, but also a break in the typical summer low stratus and fog regime.
3. Both ship-stack cloud features and widespread wave-cloud patterns imply atmospheric stable conditions and likely inversions at or above the level at which they are formed.
4. Cyclones moving out of Siberia quite often intensify as they move over the open waters north of Siberia and Alaska. Because the Chukchi Sea region typically has the largest open water area in this sector of the Arctic, the potential for cyclogenesis over that area is high.

6.1.6 Summer Cyclones or Fronts Disturbing Dominant High Pressure

The northward extension of the Pacific High over the Bering Sea and Gulf of Alaska dominates the summer circulation pattern. Migratory lows and associated frontal systems do, however, pass through the region and result in temporary breaks in the summer fog and stratus regimes.

This case illustrates the cloud patterns associated with both the prevailing high pressure and the migratory lows and fronts. The tendency for rapid return to the high pressure cloud patterns is also shown. When under the influence of high pressure and general light southwesterly flow the Bering Sea cloud patterns reflect many local effects, such as island induced wave clouds, leeside clearing, and flow through gaps in the island chain. Ship track cloud lines are also quite prevalent, particularly under the influence of the stronger and more persistent high pressure systems where strong low level inversions are common.

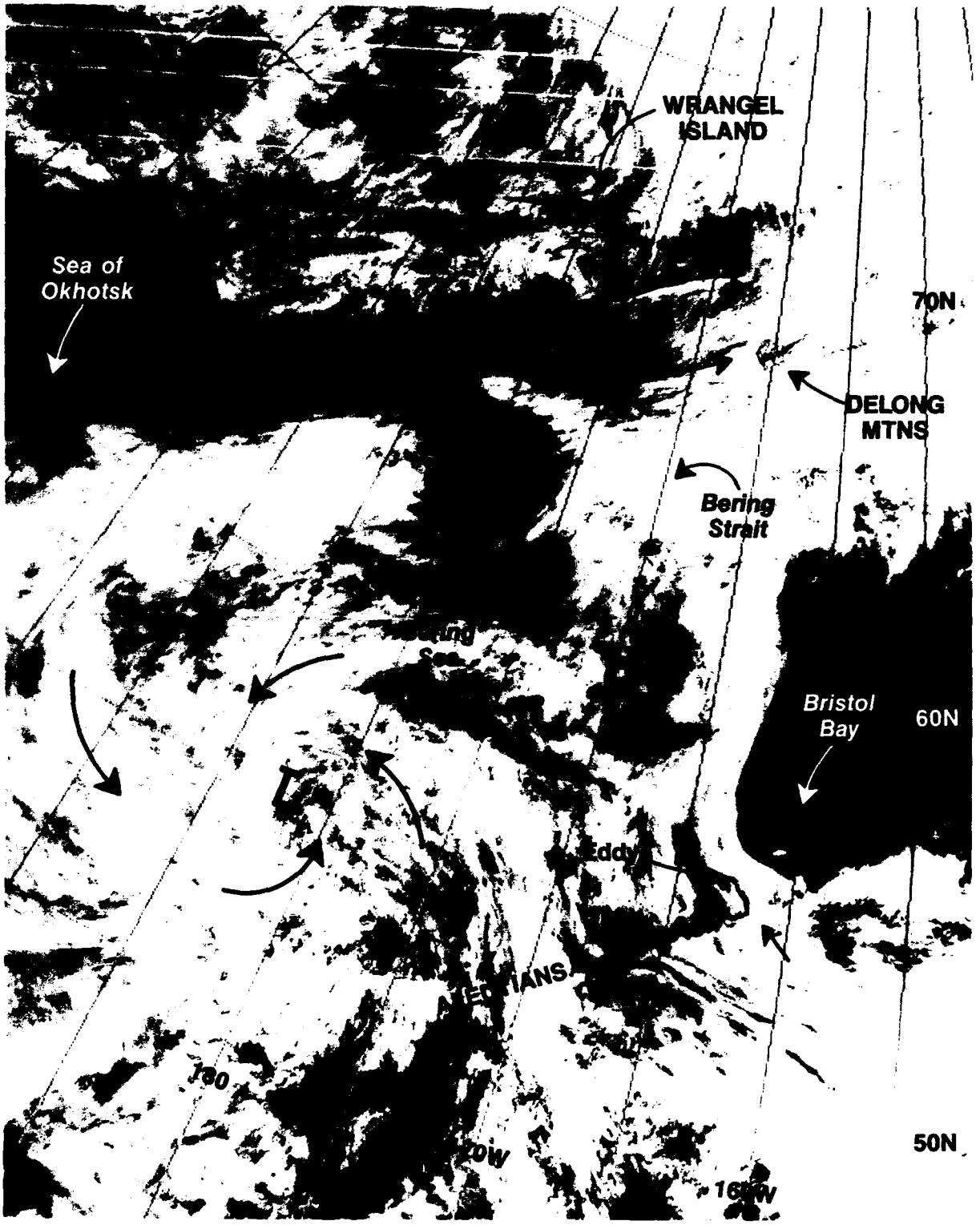

Figure 6-27. DMSP visible imagery 2003 GMT 16 July 1990.

24–29 August 1990

This sequence of images starts on the 24th of August 1990 (Fig. 6-28), at which time a small, short wave, cyclonic disturbance, reflected by enhanced cloud development, is located over the central Bering Sea. Some enhanced southerly flow is indicated by the wave clouds extending northward from the Aleutian chain between about 176°W to 167°W. This wind indication, plus the enhanced clouds seen north of the area, implies the existence of a weak frontal zone. The surface front appears to be located near Adak (about 177°W). East of the frontal zone, where ridging would be expected, an area of low stratus and/or fog covers the oceanic area south of the Aleutian chain. The low level anticyclonic flow

Figure 6-28. DMSP visible imagery 1956 GMT 24 August 1990.

configuration over the ridge line is indicated by stratus or fog streaming northward through the Unimak Pass (165 °W), the change of leeside conditions from the north to the south side of Alaska Peninsula, and the wave clouds extending southward from Kodiak Island, Alaska Peninsula, and smaller islands to the south.

The frontal cloud band is more distinct in Fig. 6-29, taken about 24 hr after Fig. 6-28. The general appearance of the entire cloud pattern associated with the front and apparent developing cyclone is one of intensification. However, the cloud patterns seen to both the east and the west of the frontal band appear dominated by high pressure systems. The general disturbance of the summer cloud pattern by the cyclone feature is reflected in the obscuration of local effect cloud features in Fig. 6-29 and dominance of the synoptic scale frontal system.

Figure 6-29. DMSP visible imagery 1935 GMT 25 August 1990.

Figure 6-30 (1853 GMT 27 August 1990) shows the cloud pattern about 48 hr after Fig. 6-29. Summer type local effect cloud features once more dominate the view. A weak remnant of the frontal cloud band extends diagonally from the lower left portion of the image, extending northeastward to Kodiak Island (near 57 °N, 154 °W) and beyond to southern Alaska. East of the weak front the large area of diffuse low clouds exhibiting crisscrossing ship track plume cloud lines implies strong high pressure ridging and a large area covered by a subsidence induced low level inversion. Extensive fog is normally found in association with such features. The fine featured wave clouds extending generally eastward

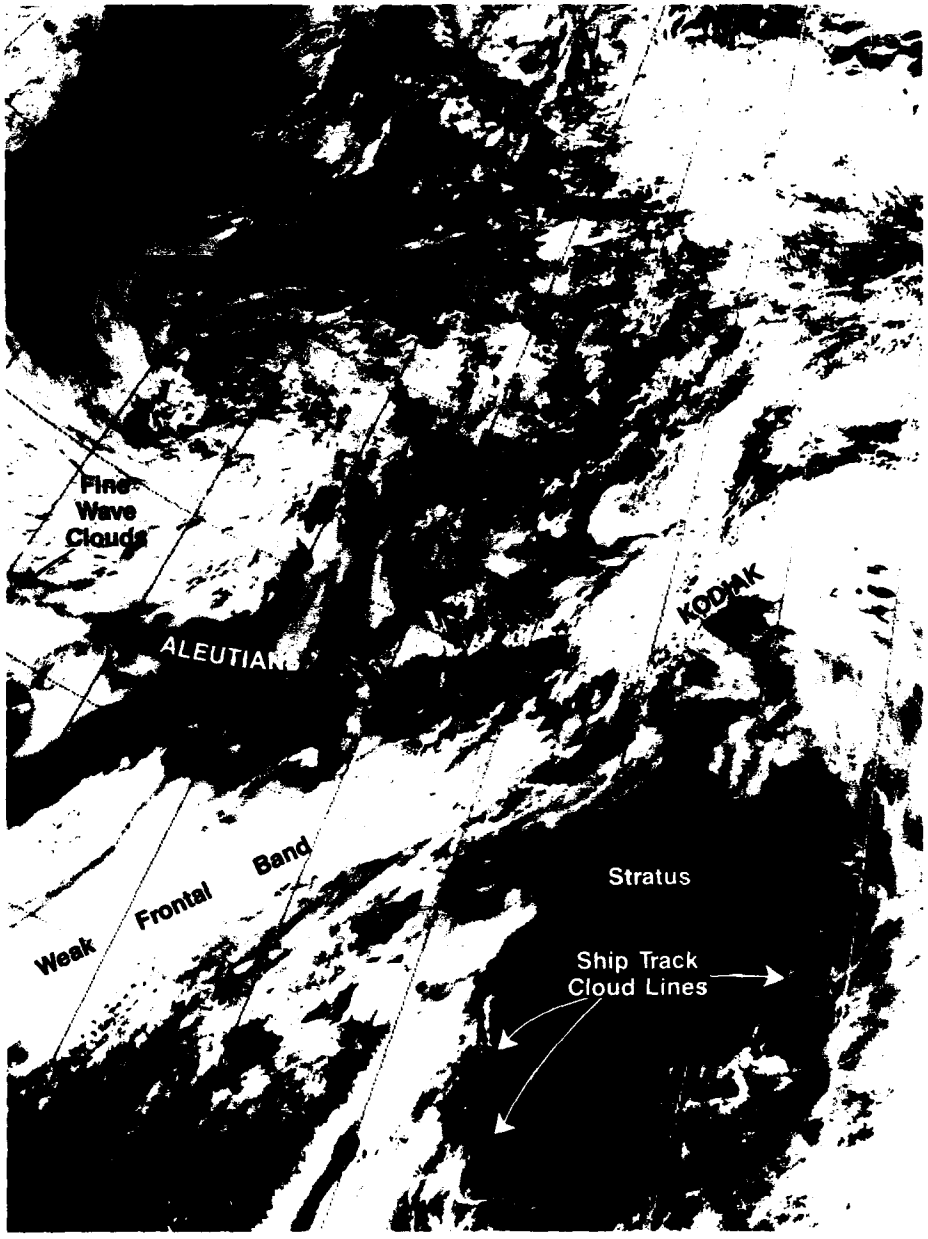

Figure 6-30. DMSP visible imagery 1853 GMT 27 August 1990.

from various islands along the Aleutian chain indicates a stable layer over them with light westerly winds. Another weak cyclonic vortex is reflected in the clouds over the west central Bering Sea near 58 °N, 178 °W.

The condition 2 days later, seen in Fig. 6-31 (1952 GMT 29 August 1990), shows a weak disturbance over the eastern Bering Sea and stratus and fog dominating the western Bering Sea. Areas of leeside clearing are seen extending some 30 n mi (55 km) or so northeastward from both Ostrow Island of the Commander Islands (near 55 °N, 166 °E) and Attu Island (near 53 °N, 173 °E). Note that the gridding on Fig. 6-31 is offset about 1 ° north and west. This is evident from the location of the cross point of 60 °N, 170 °E, which should be right at the southern tip of Mys Olyutorskiy rather than as it is shown off to the northwest.

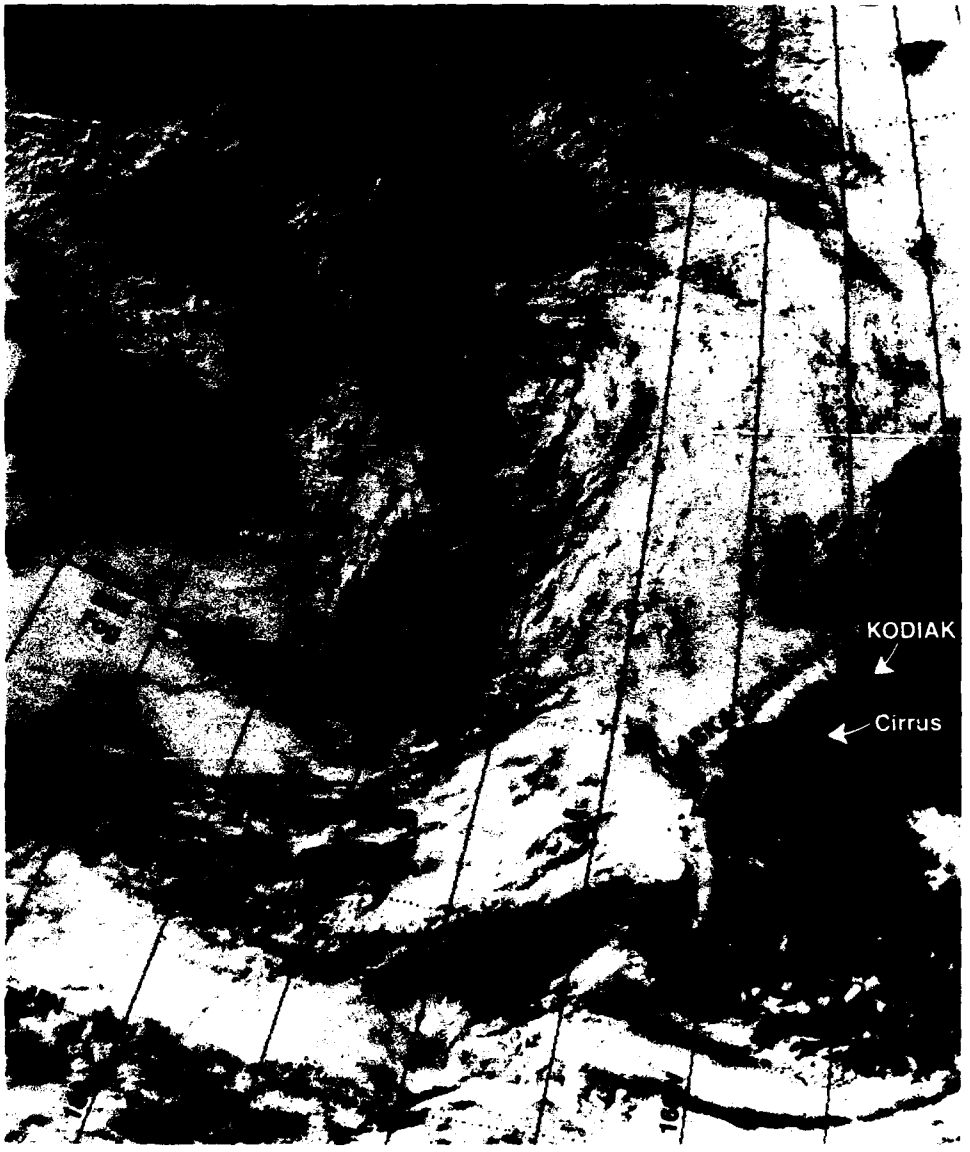

Figure 6-31. DMSP visible imagery 1952 GMT 29 August 1990.

Some indication of the relative shallowness of frontal clouds over these latitudes can be recognized by the blocking effect of the Alaska Peninsula west of Kodiak Island. Except for some thin cirrus to the south of Kodiak, all the frontal clouds are effectively blocked to the west of the peninsula, which generally has elevations of 6000 ft (1830 m) or less. Nonetheless, airfield conditions along the entire peninsula, Aleutian chain, and western Alaska are likely to be marginal IFR under this combined weak front and following ridging regime.

Forecast Aids

1. The more evident local effect cloud features are reflected in satellite imagery over the Bering Sea region during summer, the more likely are the occurrence and persistence of low ceilings and visibility.
2. Migratory cyclonic systems and associated fronts may, if strong enough, provide some breaks in the near zero-zero ceiling and visibility conditions that prevail during summer.
3. Cyclone and frontal cloud systems of these high latitudes are typically limited in vertical development to 10,000 to 12,000 ft (3048–3658 m). Weak systems are likely to top out below 8000 ft (2440 m).
4. Local effects are likely to result in lower visibility and ceiling through the straits and passes, and clearing conditions to the lee of islands.
5. The extent of leeside clearing is related to the strength of the low level flow and height and strength of the inversion. Stronger winds and strong low inversions will result in enhanced leeside clearing.
6. Under near calm conditions, typically near ridge lines and centers of highs, leeside effects will be minimal.

6.2 Polar Lows

The term "polar low" has been applied to various subsynoptic Arctic disturbances. Both the theory of polar low systems and an unambiguous definition of a polar low are evolving. Small cloud vortices have a tendency to develop in regions where cyclonic vorticity is maximized. These may occur along trough lines extending from closed lows or in regions of cyclonic horizontal shear in wind speed. In such regions, despite the cloud vortex, a closed wind circulation implying a pressure minimum does not exist; hence, the term polar low seems inappropriate for the description of such features. At the same time, it is agreed that these types of cloud features may evolve into polar lows. The distinction is similar to that made in tropical meteorology, of an easterly wave that has not yet evolved into a tropical depression (a closed tropical circulation having a wind speed of less than 34 kt or 17 m/s). For the purposes of this publication, using similar logic, a cloud vortex in the cold air behind a frontal system in the Arctic will be referred to as only a polar vortex or cloud vortex until the forecaster can ascertain that (1) a closed circulation and pressure minimum exists, and (2) that wind speeds of 35 kt (18 m/s) or more have been attained.

At that point, the polar vortex or cloud vortex will be referred to as a polar low. This seems especially fitting since the term polar low has, in recent years, come to connote an intense Arctic storm of at least tropical storm and often hurricane intensity. Excluded from the above definition will be those comma-shaped cloud systems that are in close proximity to major frontal boundaries (Businger, 1987).

Businger (1987), using NOAA satellite data, conducted a detailed study concerning the number of days each month in which ". . .vigorous polar lows (exhibiting a well developed spiral cloud structure and high cloud tops indicated by cold radiative cloud-top temperatures) were present. . ." over the Gulf of Alaska or Bering Sea during the period 1975–83 (Fig. 6-32). The figure indicates maximum frequency in late fall through early spring with the peak development period being November through February.

Several synoptic and subsynoptic features have been shown to be associated with polar low development in the Bering Sea and Gulf of Alaska region. Businger showed that environ-

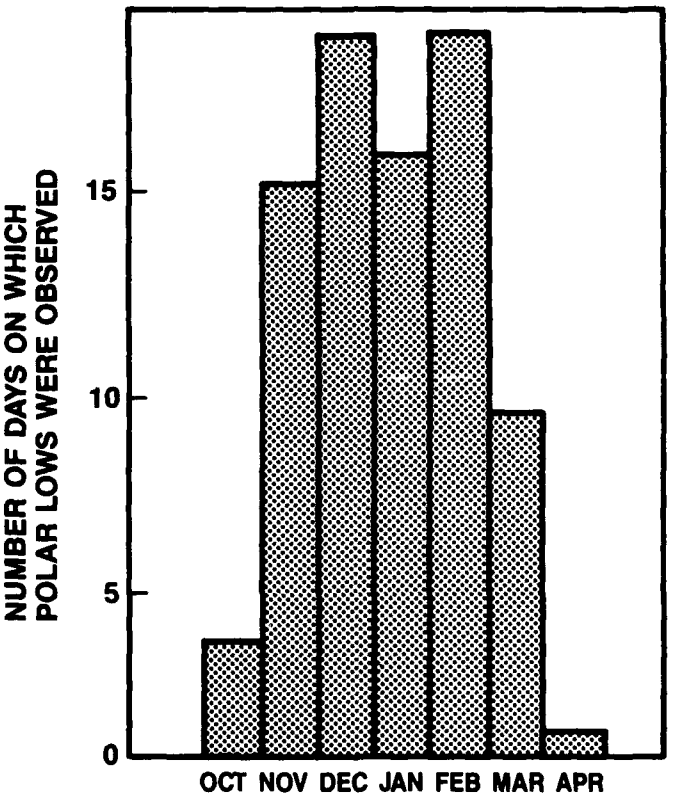

Figure 6-32. Histogram of the number of days each month in which polar lows were observed in polar-orbiting satellite imagery over the Gulf of Alaska or the Bering Sea during the period 1975–1983 (Businger, 1987).

mental factors conducive to the development of strong polar lows include (1) a deep outflow of Arctic air over open water, (2) a cold, synoptic scale closed low aloft, (3) differential PVA associated with a small, synoptic scale trough or vortex at 500 mb, and (4) significant negative height and temperature anomalies throughout the troposphere.

Brown (1986) pointed out that development of high latitude polar lows inevitably is associated with cloud street structures. The role of Arctic boundary layer fronts (the boundary between air that has been warmed on a long path over the sea and air that has just left snow-covered land or the ice pack) as a source of baroclinic instability that can lead to polar low development has been addressed by Shapiro and Fedor (1989).

6.2.1 Polar Low Development and Intensification

The conditions favorable for polar low development, as noted above, are of synoptic scale. A typical scenario includes (1) the stalling and gradual dissipation of a mature synoptic scale cyclone leaving behind a large cold vortex aloft; (2) the establishment within the synoptic regime of a subsynoptic scale baroclinic zone such as a boundary layer front (a boundary between warm air wrapping around the mature cyclone due to frontal occluding process and ambient cold air) through convergence of low level flow regimes, or any other mechanism resulting in a baroclinic zone development; and (3) for development of the more intense polar lows (dubbed "Arctic hurricanes"), the passage of a jet maximum (jet streak), typically associated with a secondary trough "spokewheeling" around the upper low and passing over the lower level baroclinic development (Emanuel and Rotunno, 1989).

Polar low development tends to be episodic because the basic forcing patterns are of synoptic "spatial" scale, whereas the temporal scale is extended because dissipating mature cyclones become nearly stationary over the Bering Sea region. It is not unusual for several polar lows to be occurring within the region at one time with the formation and dissipation processes going on for several days.

Observations in the region revealed that a favorable location for polar lows is in the western and northwestern sector of dissipating synoptic lows. Because the polar lows develop some distance away from the center of the synoptic low, they are likely to have moderate to strong steering flow over them. As a result they will move at a velocity representative of the steering flow and not with the movement of the dissipating synoptic low. The more intense the polar low and related vertical development, the higher in the atmosphere will be the representative steering level. Steering is actually an integrated result of the flow throughout the layer of the atmosphere interacting with the low, but in general, the flow near the midpoint of the vertical development of the low will be representative of the integrated or mean steering flow. Because of the suppressed atmosphere of high latitudes, even strong polar lows will likely have a representative steering level closer to 850 mb rather than the 500 mb that is generally used as a thumb rule for synoptic scale midlatitude features. A speed of advance of 30 kt (55 km/hr) is not unusual for well developed polar lows. Because of the relatively small horizontal extent of the Bering Sea and Gulf of Alaska and the tendency to dissipate rapidly once over land, the average duration of polar lows is only a day or two. Only under optimum forcing and migration path can polar lows persist for several days. Because their forcing is localized and they are small in size, polar lows can develop

rapidly, frequently reaching maximum development within 12 to 24 hr from initial development, and dissipate rapidly.

Analysis of aircraft and radiosonde data collected during field experiments has shown that some polar lows have warm cores. Satellite imagery frequently shows an "eye" similar to that seen in tropical cyclones and surrounding strong convection. The warm core configuration is likely associated with the strong convective activity. This thermodynamic structure has led to the coining of the term Arctic hurricane.

Because of their small scale and localized forcing, polar lows are usually below the resolution of existing operational numerical models. However, the models can depict the favorable synoptic scale patterns. Forecasters should closely monitor the numerical analyses and prognoses for existing and developing favorable synoptic conditions. Equally important is the utilization of satellite imagery and conventional observations. This introductory section and the examples that follow are intended to provide forecasters with the background information necessary to assist them in recognizing and forecasting polar low activity. The following features are favorable for polar low development:

- Cold air outbreak and formation of low level cloud street patterns.
- Large negative anomalies in upper level temperature and heights.
- Development of a low level baroclinic zone such as an Arctic boundary layer front due to convergence of air streams with different overwater flow length or wraparound warm air slots to the west and south of occluding frontal systems.
- Upper level short-wave trough and/or jet maximum moving over low level features.

After initial development occurs as a result of low level baroclinic conditions, the polar low clouds that are generally of convective form begin to organize into the classic comma shape. If favorable upper air conditions exist, further intensification will occur, which can result in winds reaching hurricane force. During the development process of polar lows certain sequences of cloud signatures can be seen in satellite imagery. Initial development typically occurs along Arctic fronts or other convergence or baroclinic zones that exhibit recognizable enhanced cloud development and organization.

Intensifying polar lows tend to have highly symmetric, spiral shaped cloud signatures with vigorous cumulonimbus surrounding a clear area or eye. Polar lows at this stage of development will have central pressures 4 to 8 mb below ambient SLP and winds in the 30- to 40-kt (15–21 m/s) range, and their cloud pattern will be 100 to 200 n mi (185–370 km) in diameter. To reach Arctic hurricane status increased low level convergence or upper level divergence is required, resulting in the cloud pattern becoming asymmetrical with an anticyclonically curved cirrus shield reflecting the outflow region. The cirrus shield may cover the cumulonimbus-surrounded eye. At this stage the cloud pattern will have a diameter of 300 to 400 n mi (556–741 km), the central surface pressure will be near 970 mb, and winds will be in the 40- to 60-kt (21–31 m/s) range.

During passage of an Arctic hurricane in March 1977, St. Paul Island recorded a pressure drop from 985 to 972 mb in 3 hr and then back to 985 mb 3 hr after passage. Concurrently the air temperature rose from 19 to 27 °F (−7 to −3 °C), reflecting the warm core nature of these most intense polar lows, and then back down. A Russian icebreaker caught in this same Arctic hurricane encountered winds over 60 kt (31 m/s), 30 ft (9 m) waves, lightning, snow, and sea spray, resulting in heavy superstructure icing, rapidly changing pressure and temperature, and passage through an "eyelike" calm, clear, warm area.

The following features are favorable for polar low intensification:

- Development or movement of an upper air negative height anomaly of about 200 m over an oceanic region. Over the Bering Sea and Gulf of Alaska this generation in general means 500-mb heights below 5000 m.
- Negative 500-mb temperature anomalies of -6 Celsius degrees equates to a 500-mb temperature of generally < -36°C for this area.
- Approach of an upper level jet streak or area of PVA.

Other environmental features that have been recognized in studies of polar low episodes include

- Existence of a synoptic scale low pressure trough such as the remnants of a dissipating occluded low.
- An area of enhanced sea surface temperature gradient in the vicinity of the area of potential.
- Isobar packing to the west of an area conducive to, or of already developed, polar lows.
- A steep surface temperature gradient of about 18 Fahrenheit degrees (10 Celsius degrees) over 120 n mi (222 km) to the west of the area of potential.
- A very low tropopause height on the order of 6000 m.

6.2.2 An Episodic Event of Polar Vortex and Polar Low Development

Polar vortices associated with polar low development appear in a diversity of sizes and intensities. They also exhibit a fairly wide range of speeds of advance and length of life. Other characteristics include (1) polar vortices generally develop within a synoptic scale, cold air outbreak characterized by cloud streets and open celled cumulus patterns under the influence of an upper level cold low or trough; (2) the initial development of polar vortices and lows occurs hundreds of nautical miles (kilometers) away from the synoptic scale frontal cloud band; (3) the more intense systems tend to form on lines of enhanced convective activity located some 200 to 300 n mi (370–556 km) south of the ice edge; and (4) a second regime of small, weaker appearing vortices (less vertical development, smaller in size and slower moving) tend to form near the ice edge in areas of relatively weak off-ice flow (indicated by diminished cloud street development).

In the following study three cloud features pertinent to polar low development are identified within the cold air outbreak regime: (1) the general cloud street pattern, (2) boundary layer fronts seen as lines of enhanced cumulus development, and (3) the vortices of the polar lows. Cloud bands reflecting the synoptic scale frontal features are of course also quite evident.

This study covers a 7-day period when three large polar vortices were observed to develop and track eastward at 25 to 35 kt (45–65 km/hr). These three vortices are referred to as P1, P2, and P3 in the following discussion. At least two weaker appearing vortex patterns (p1 and p2) formed near the ice edge and moved eastward at no more than 10 to 15 kt (20–30 km/hr).

4 February 1990

Figure 6-33 shows a polar vortex (P1) near 57 °N, 176 °E. A boundary layer front extending from over the ice edge southward along 170 °W to beyond the Aleutian chain is also seen in the figure. A small vortex, with no significant vertical cloud development around it, is seen just south of the ice edge and west of the boundary layer front. The surface (Fig. 6-34) and 500 mb (Fig. 6-35) analyses for 0000 GMT 4 February 1990, about 6 hr before the time of Fig. 6-33, show the synoptic scale pattern. Note that P1 is located slightly east of the closed 1008-mb contour around the small synoptic scale 1006.5-mb low centered near 56 °N, 170 °E. On subsequent surface analyses this low remained nearly stationary

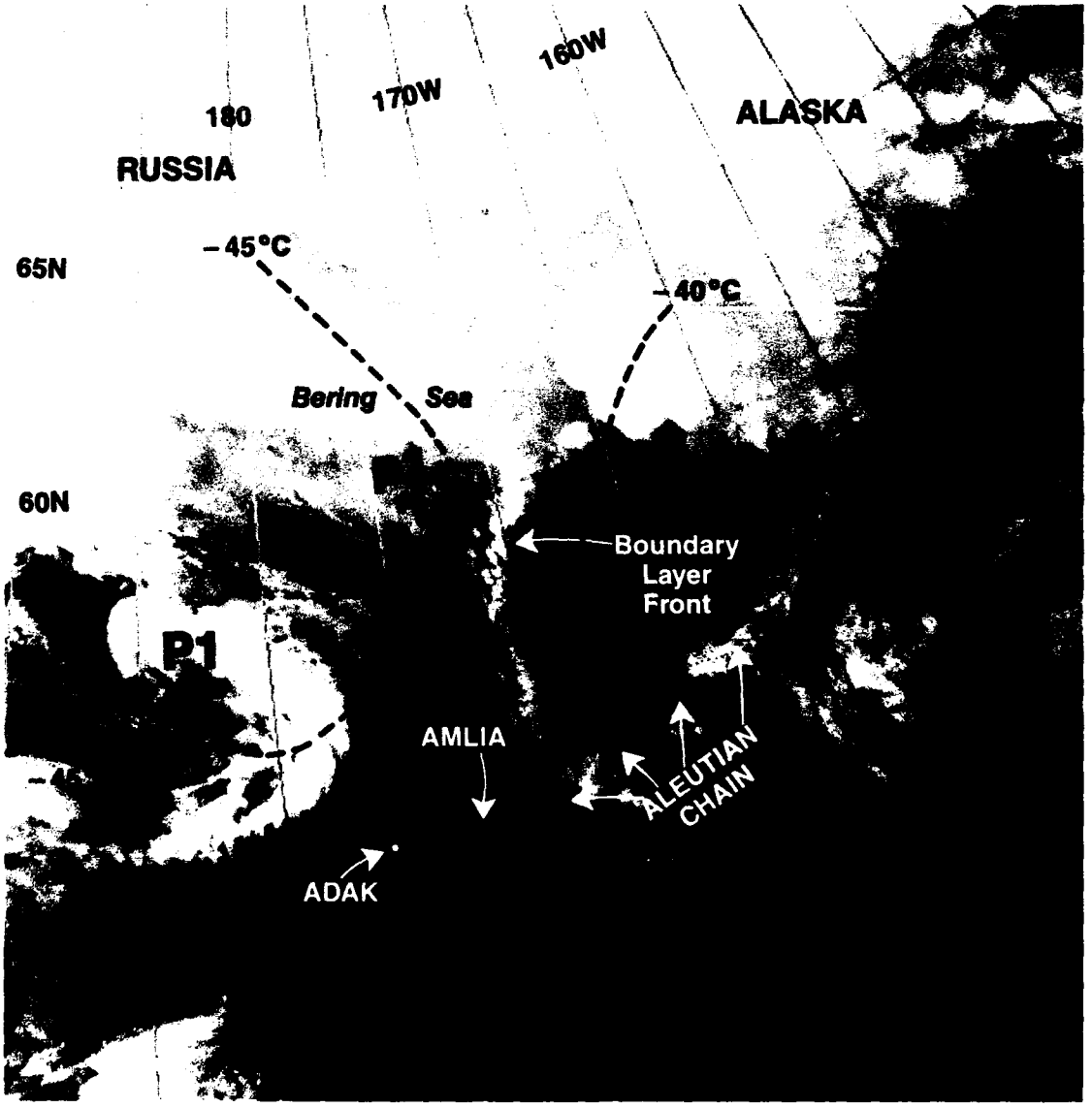

Figure 6-33. DMSP infrared imagery 0625 GMT 4 February 1990.

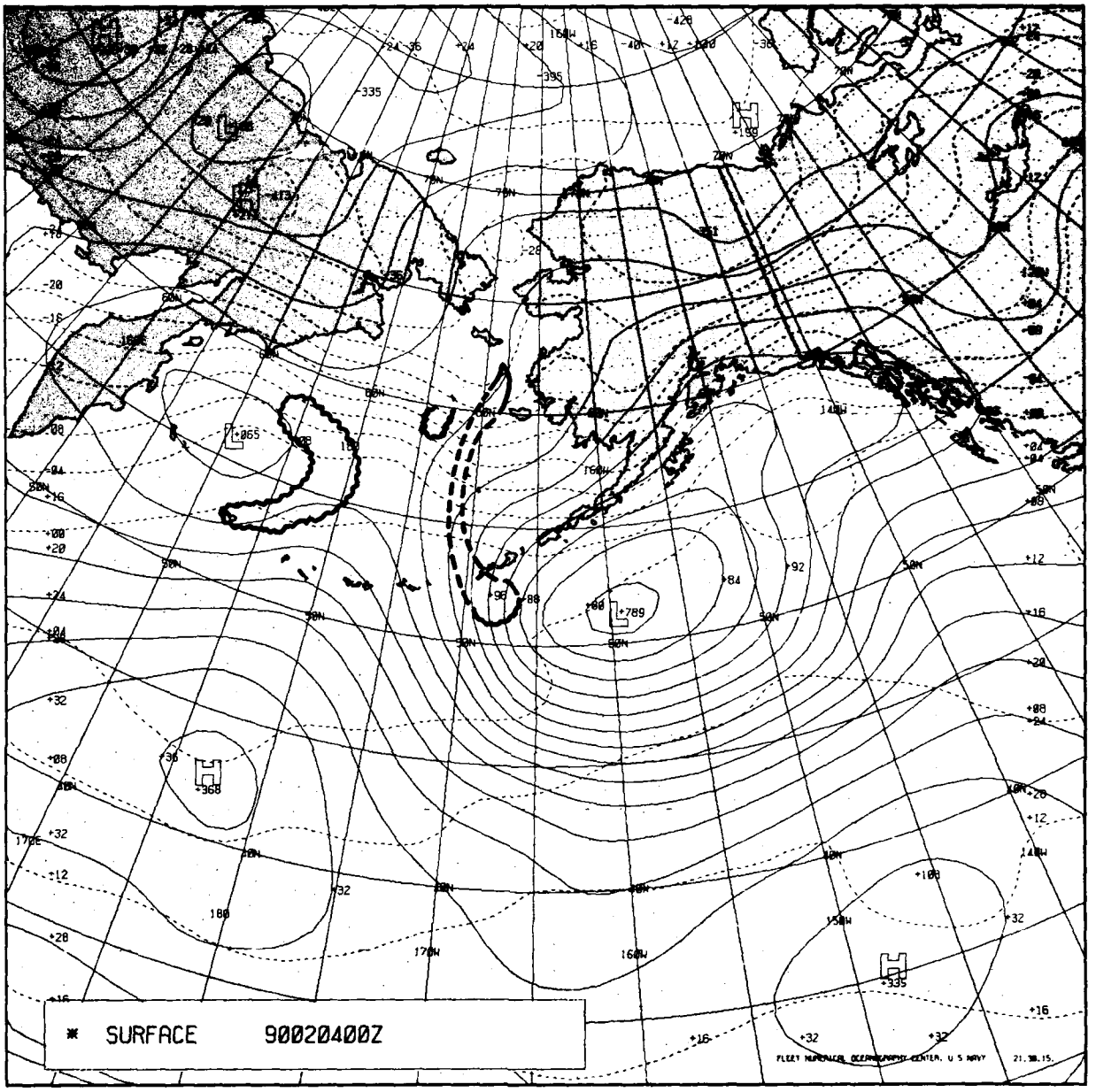

Figure 6-34. FNOC surface analysis 0000 GMT 4 February 1990.

and the polar low seen in the imagery progressed eastward. The comma head of P1 at this time is located over the southern portion of the steepest surface air temperature gradient. The 500-mb chart (Fig. 6-35) shows a pocket of −45°C air covering most of the Bering Sea. Over the position of P1 there is about a 12-Celsius-degree negative temperature anomaly and a 210-m negative 500-mb height anomaly.

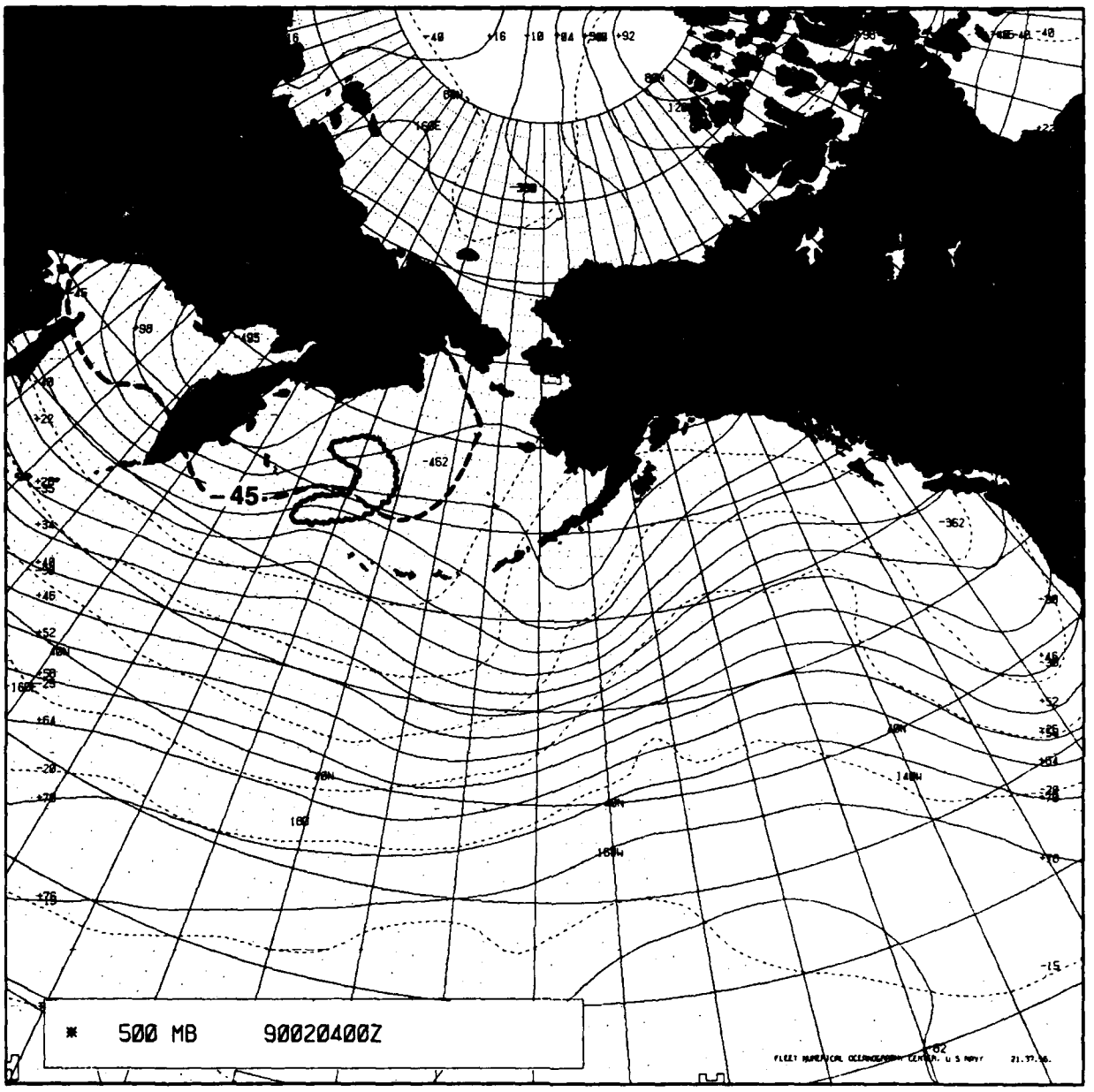

Figure 6-35. FNOC 500-mb analysis 0000 GMT 4 February 1990.

The vortex designated p1 moved eastward in phase with the boundary layer front at about 15 kt (8 m/s) over the following 30 hr before merging with and being absorbed by a synoptic scale front. P1 moved eastward across the central Bering Sea with a speed of 30 to 35 kt (55–65 km/hr) during the following 36 hr. It also merged at that time with a synoptic scale frontal system.

5 February 1990

Figure 6-36 on 5 February 1990, about 39 hr after Fig. 6-33, shows P2 forming near 58 °N, 173 °E near the same location where P1 formed. Other smaller vortices are apparent south-southwest of P2 lying along a line that might be considered a boundary layer front. P2 moved almost due east along 58 °N until it dissipated near the Alaska Peninsula as it approached the synoptic frontal system, shown stretching northeastward in Fig. 6-36 near the Aleutian chain. Note that P2 formed very near the coastline of Kamchatka in an intense cold air outbreak as evidenced by the cloud lines in that region.

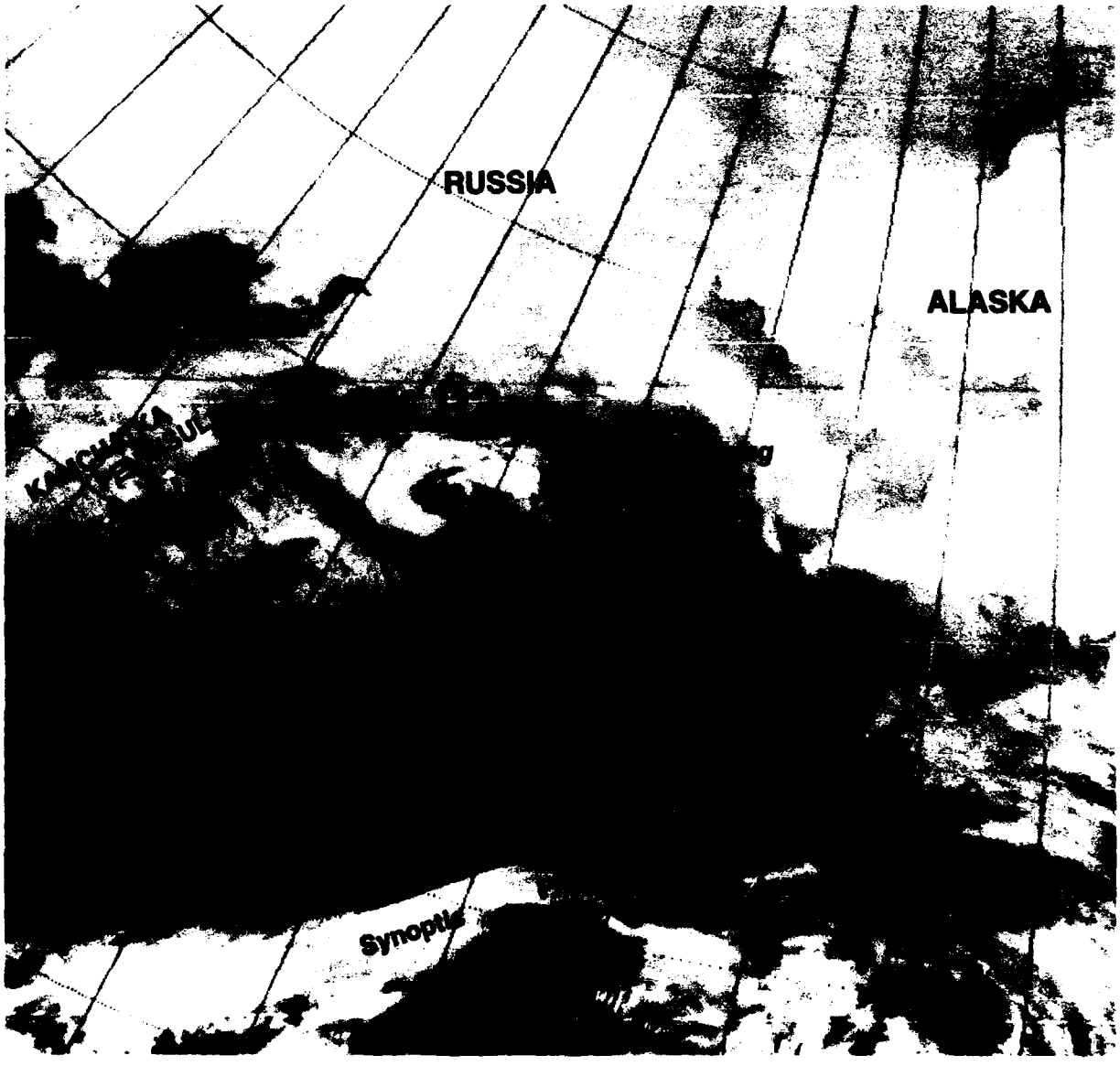

Figure 6-36. DMSP infrared imagery 2107 GMT 5 February 1990.

7–9 February 1990

Figure 6-37, on 7 February 1990, about 48 hr after Fig. 6-36, shows yet another vortex, P3, forming over the northwest Bering Sea very near the same location of development for P1 and P2. A second, weaker polar vortex (p2) is seen near the ice edge in a position reminiscent of the development of p1 (Fig. 6-33). The conclusion may be correctly drawn that these areas are especially favorable for boundary layer front, polar vortex, and polar low development.

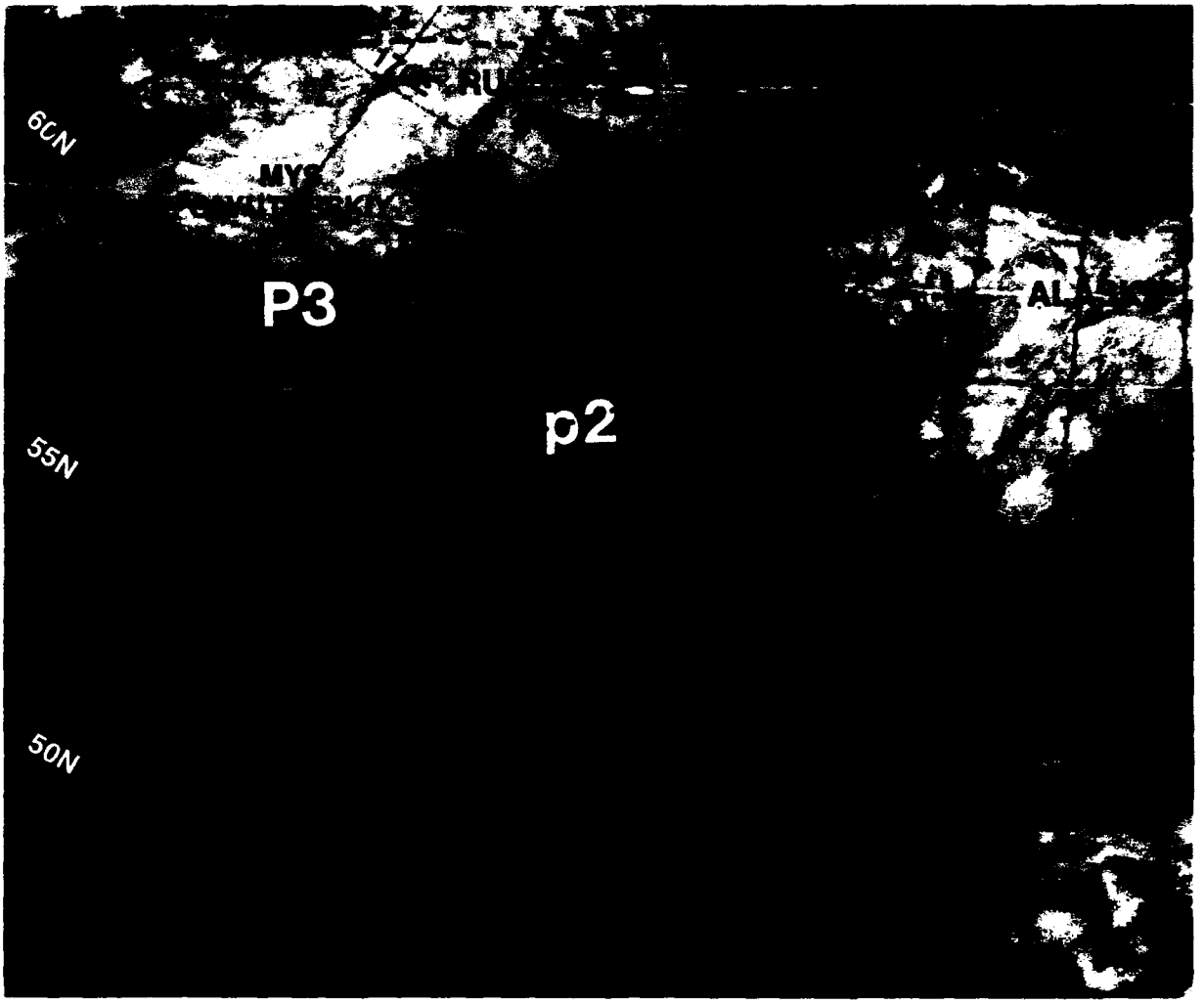

Figure 6-37. DMSP infrared imagery 2026 GMT 7 February 1990.

The FNOC surface analysis for 8 February 1990 at 0000 GMT (Fig. 6-38), about 3.5 hr after the time of the satellite imagery (Fig. 6-37), with the outlines of P3 and p2 superimposed, reveals that the systems have formed within a general trough region. From a synoptic scale point of view winds are relatively light around the vortices. However, a lack of reports close to the vortex centers prevents an assessment of intensity from a smaller scale point of view. Documented cases of similar appearing vortices such as P3 indicates that surprisingly strong winds (40–60 kt or 21–31 m/s) may sometimes be encountered even in the absence of a closed low pressure center. The forecaster should always be alert to this potential.

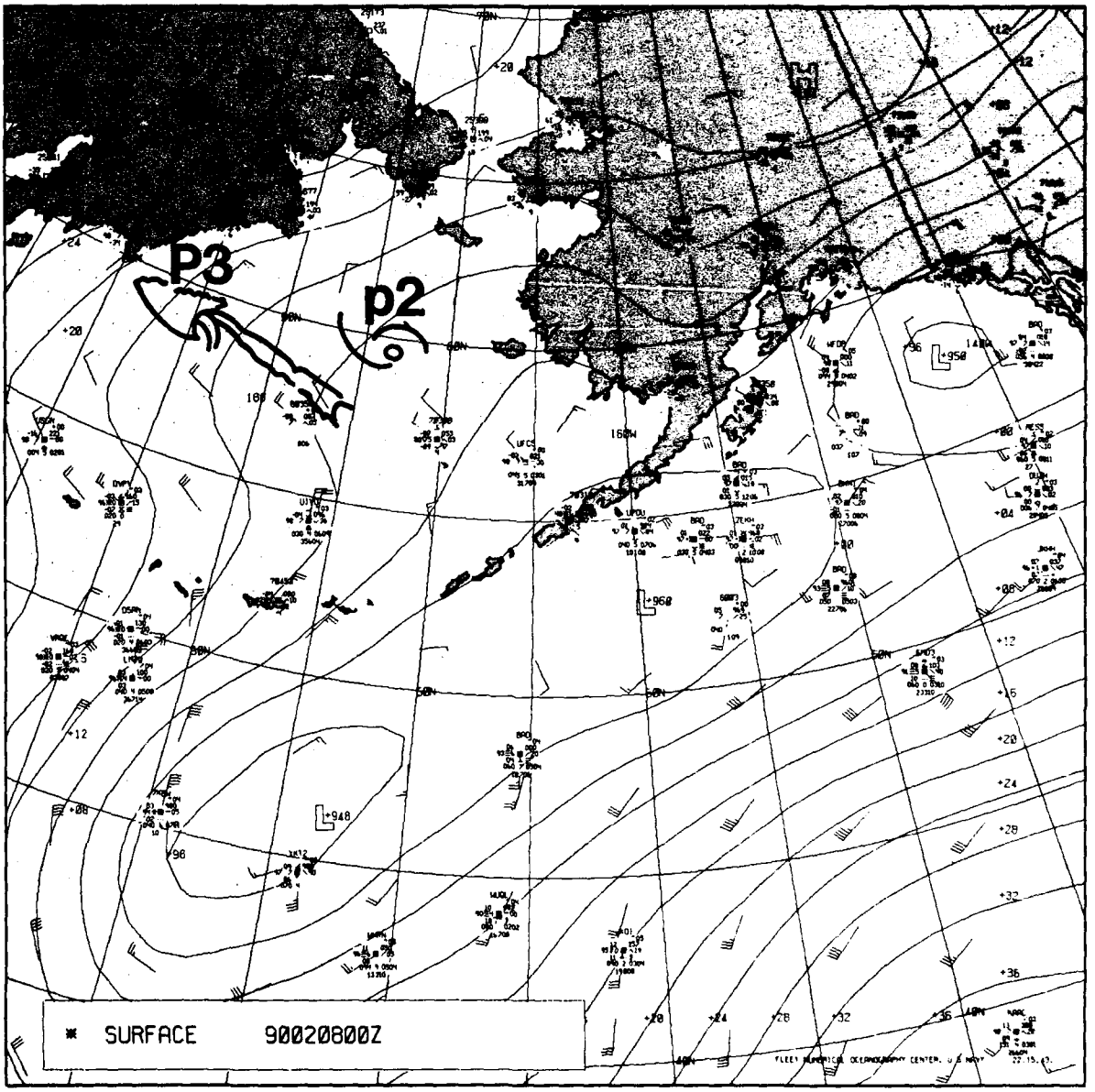

Figure 6-38. FNOC surface analysis 0000 GMT 8 February 1990.

A cold air outbreak off the Siberian coastline north of Mys Olyutorskiy is indicated by the strong northwest winds in that region blowing nearly perpendicular to the isobars and isotherms (not shown). At 500 mb (Fig. 6-39) the cold pocket, indicated by the closed −45 °C isotherm, extends over the surface location of P3. Large negative 500-mb temperature −11 °C and height −200 m anomalies have persisted. Such conditions are favorable for polar vortex and polar low development.

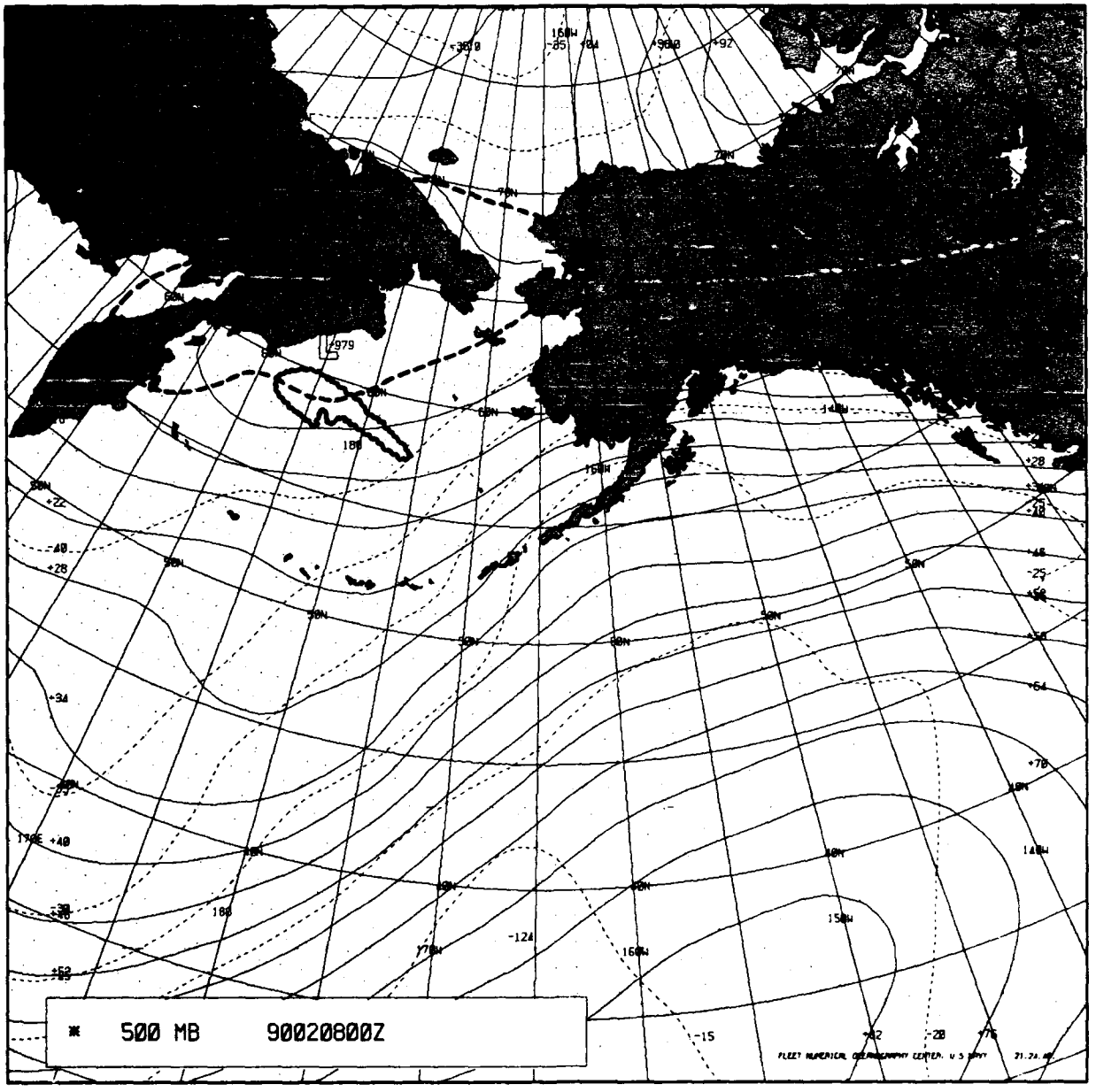

Figure 6-39. FNOC 500-mb analysis 0000 GMT 8 February 1990.

Figure 6-40 on 9 February 1990 shows P3 near 56°N, 163.5°W about to cross southward over the Aleutian chain. It had moved across the Bering Sea on a track just slightly south of east at about 25 kt (45 km/hr) during the approximately 37 hr between Figs. 6-37 and 6-40. A line of convection reflecting a boundary layer front extends westward along the Aleutian chain from P3's position. The synoptic pattern has also been progressing eastward during this period. This synoptic pattern movement has carried with it the synoptic environment most favorable for polar vortex and polar low development.

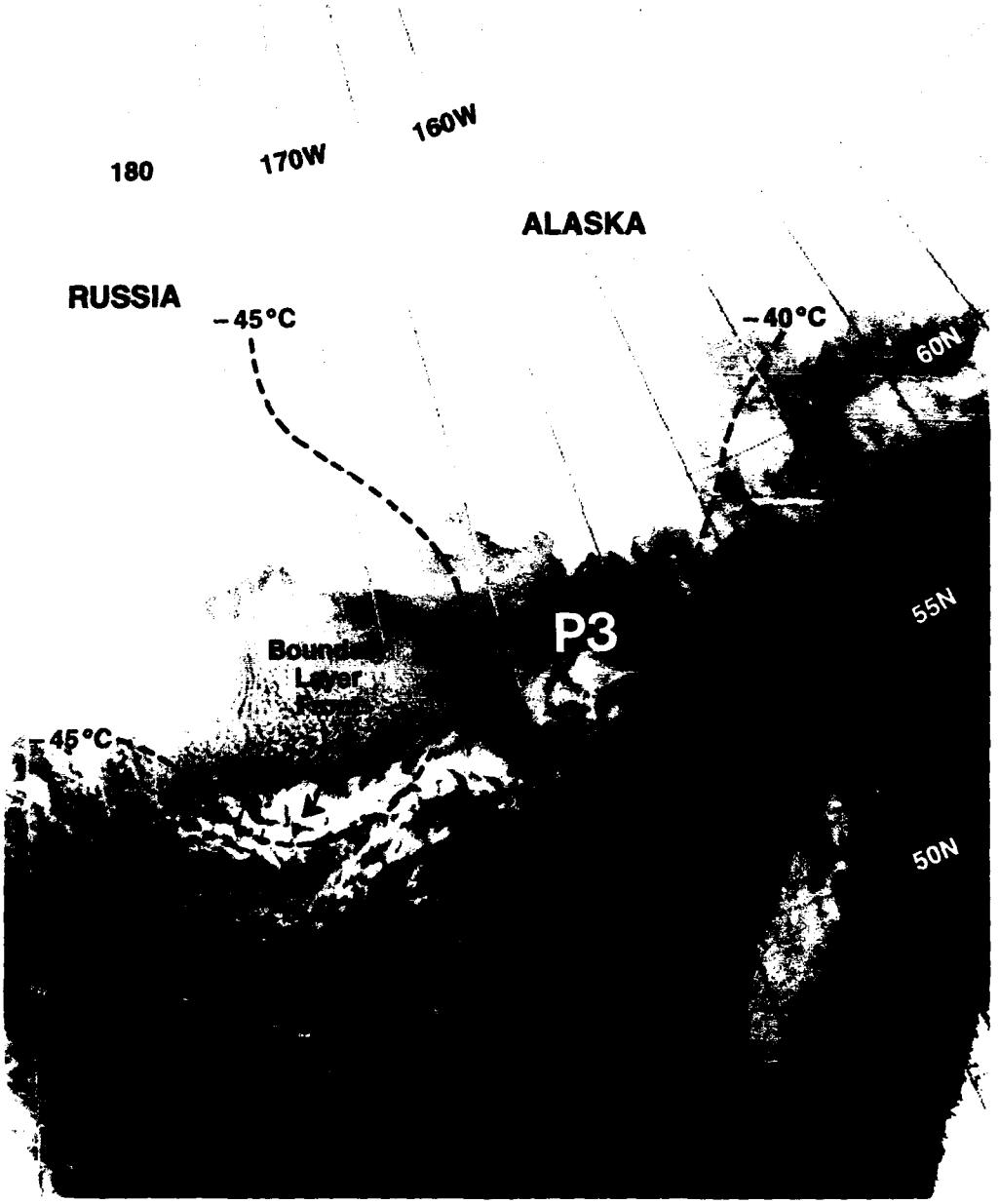

Figure 6-40. DMSP infrared imagery 0936 GMT 9 February 1990.

10 February 1990

The cloud vortex seen over the north central Gulf of Alaska on 10 February 1990 (Fig. 6-41, taken about 24 hr after Fig. 6-40), indicates that P3 has intensified significantly once over the warmer waters of the Gulf of Alaska. From its Fig. 6-40 position P3 moved slightly north of east at about 25 to 30 kt (45–55 km/hr) until near 150°W and then accelerated to about 40 kt (21 m/s) during the last 4 hr before reaching the location and

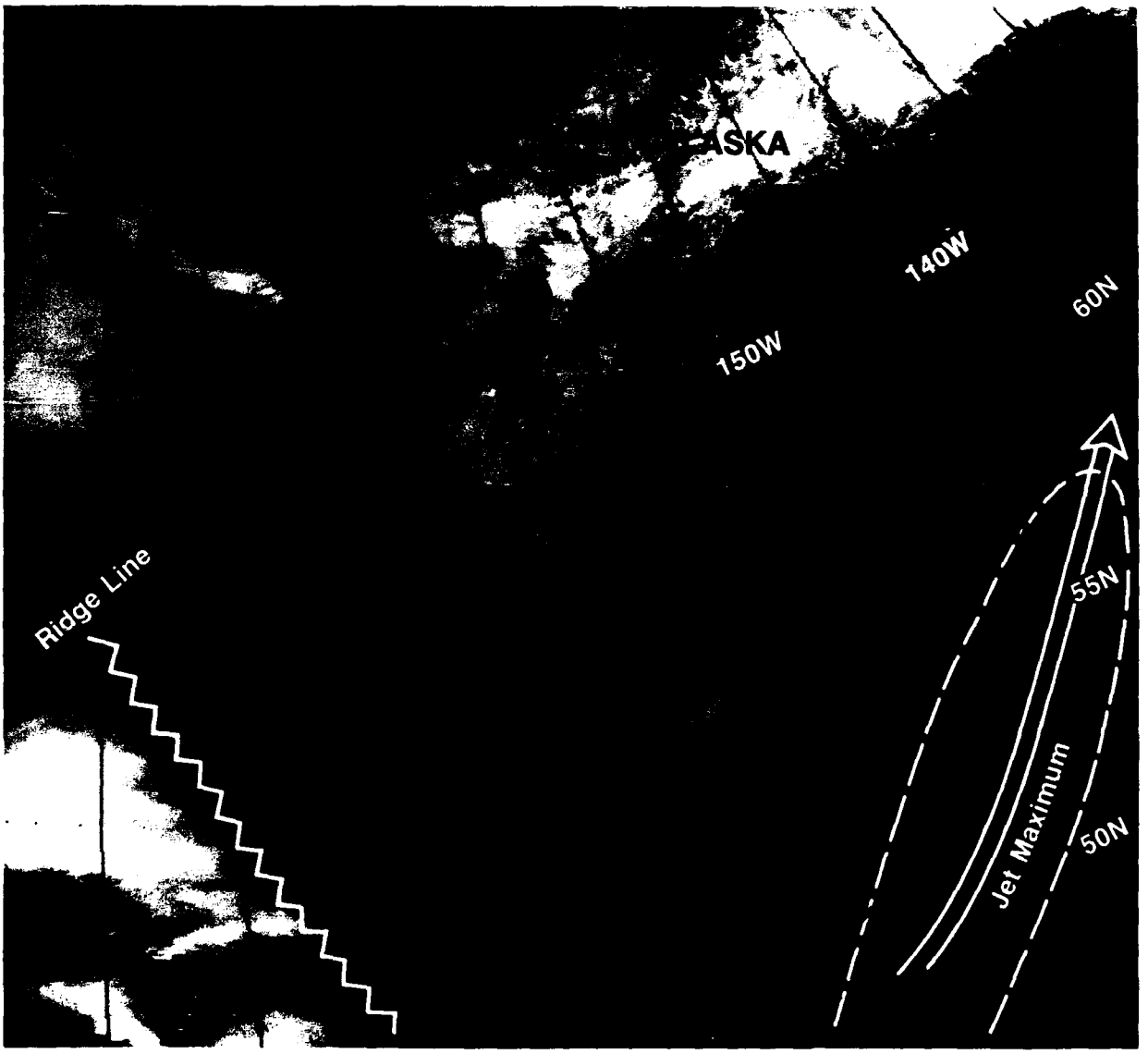

Figure 6-41. DMSP infrared imagery 0916 GMT 10 February 1990.

configuration of Fig. 6-41. The surface analysis for 1200 GMT, about 3.5 hr after the DMSP image (Fig. 6-42) shows that the vortex is located just southeast of an analyzed low pressure center. By chance there is a ship (KHJB) located just southwest of the vortex center reporting a 40 kt (75 km/hr) westerly wind. This indicates that the vortex has achieved polar low intensity and that undoubtedly a low pressure center of less than 994 mb surrounds the polar low center.

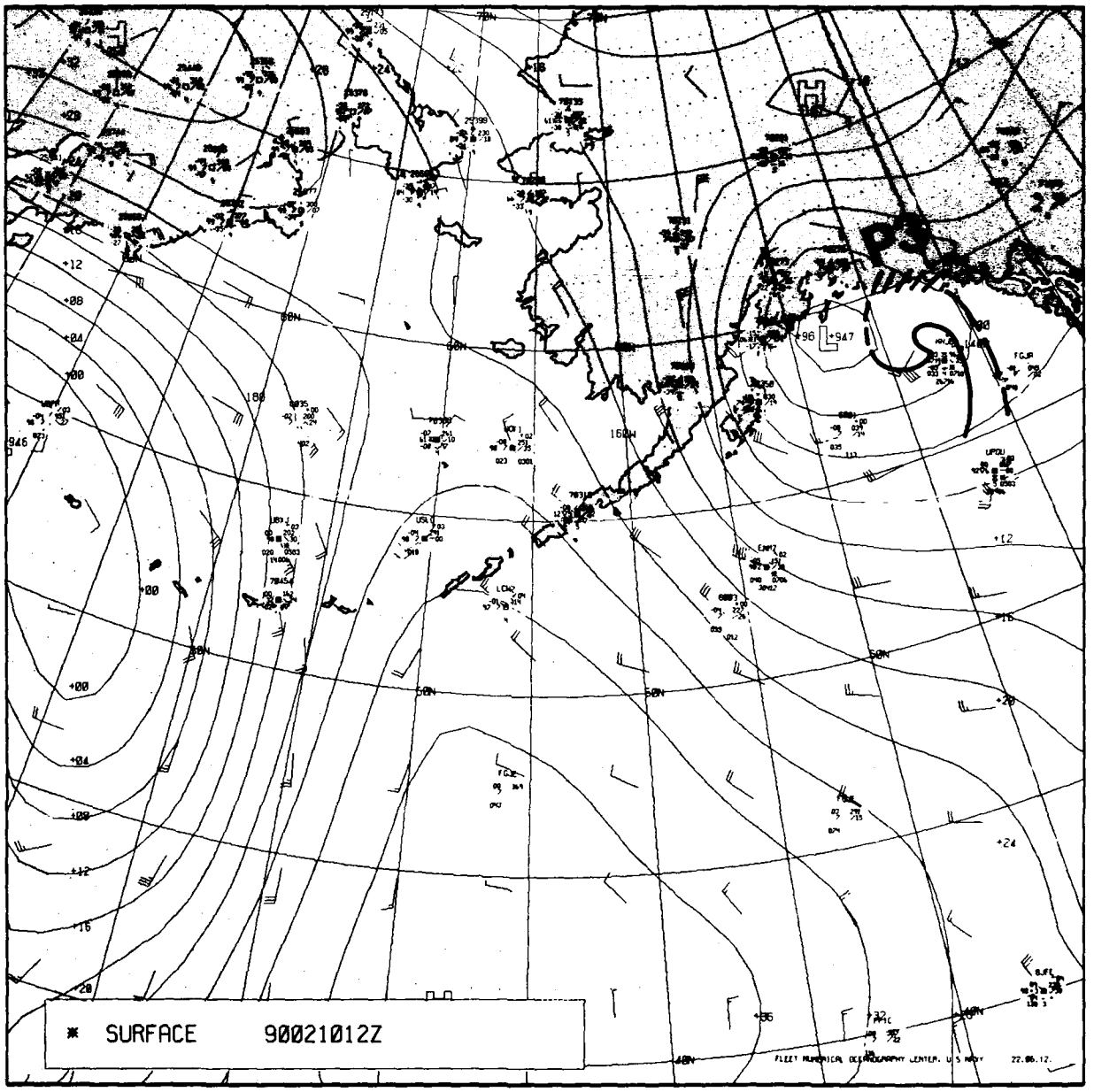

Figure 6-42. FNOC surface analysis 0000 GMT 10 February 1990.

The corresponding 500-mb analysis (Fig. 6-43) shows that an upper cold low and cold trough has accompanied the polar low development. Ridging at both the surface and 500-mb range has moved over the Bering Sea, and the cold air outbreak and cloud street pattern have shifted to the Gulf of Alaska. No further polar low activity was noted over the next week or so as the approaching synoptic low and associated frontal clouds, which cover the lower left corner of Fig. 6-41, took a northerly route into the eastern Bering Sea.

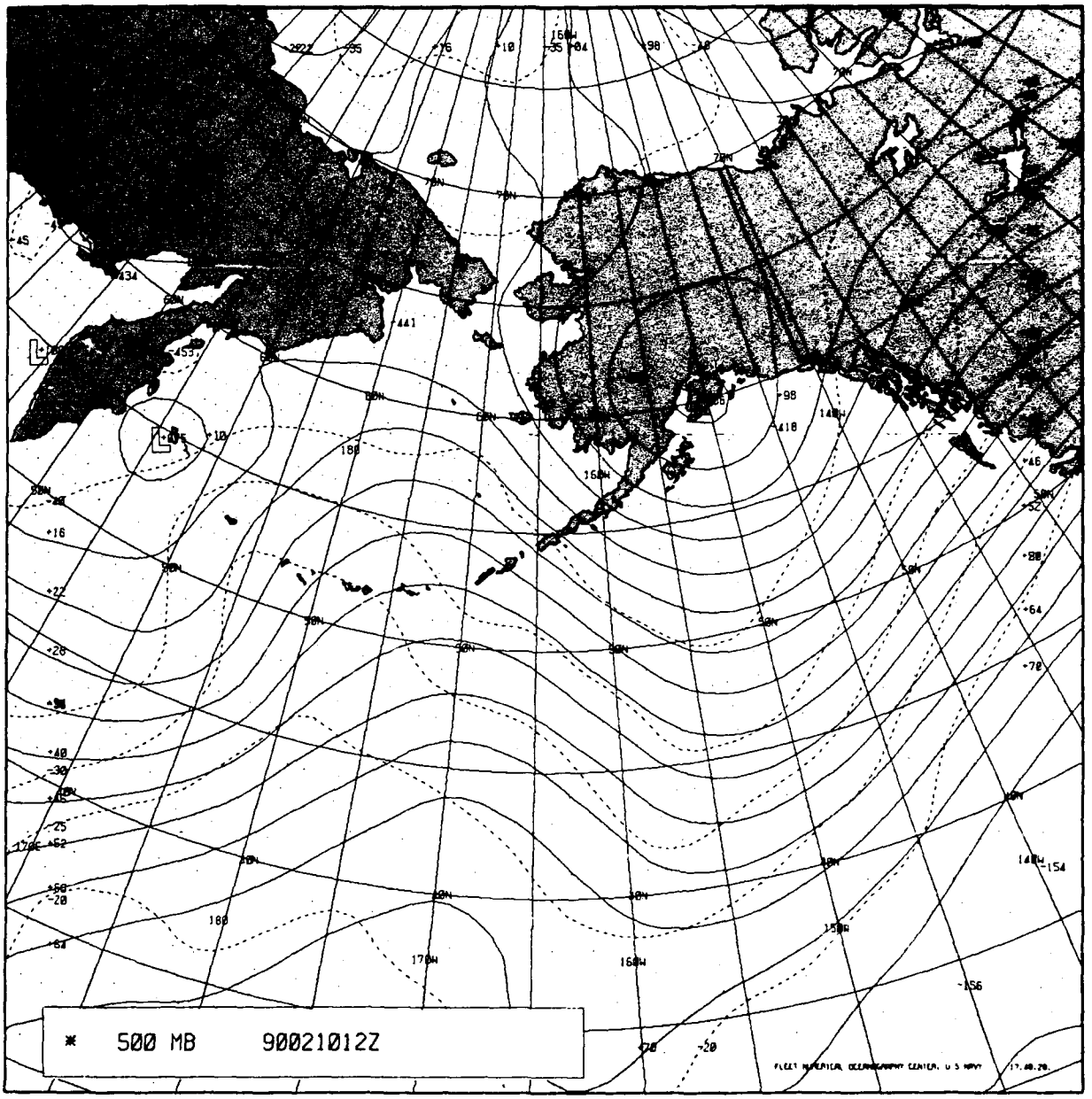

Figure 6-43. FNOC 500-mb analysis 0000 GMT 10 February 1990.

Figure 6-44 is another surface analysis for 10 February at 1200 GMT, similar to Fig. 6-42, but this time with an isotherm analysis superimposed (dotted with lines). Interestingly, the track of P3 from the eastern Bering Sea into the western Gulf of Alaska followed near the center of the steepest surface air temperature gradient, as depicted in Fig. 6-44. The region of low level cold air outbreak is now centered over the Alaska Peninsula. The cloud lines seen in this region (Fig. 6-41) clearly support the indicated cold air advection pattern.

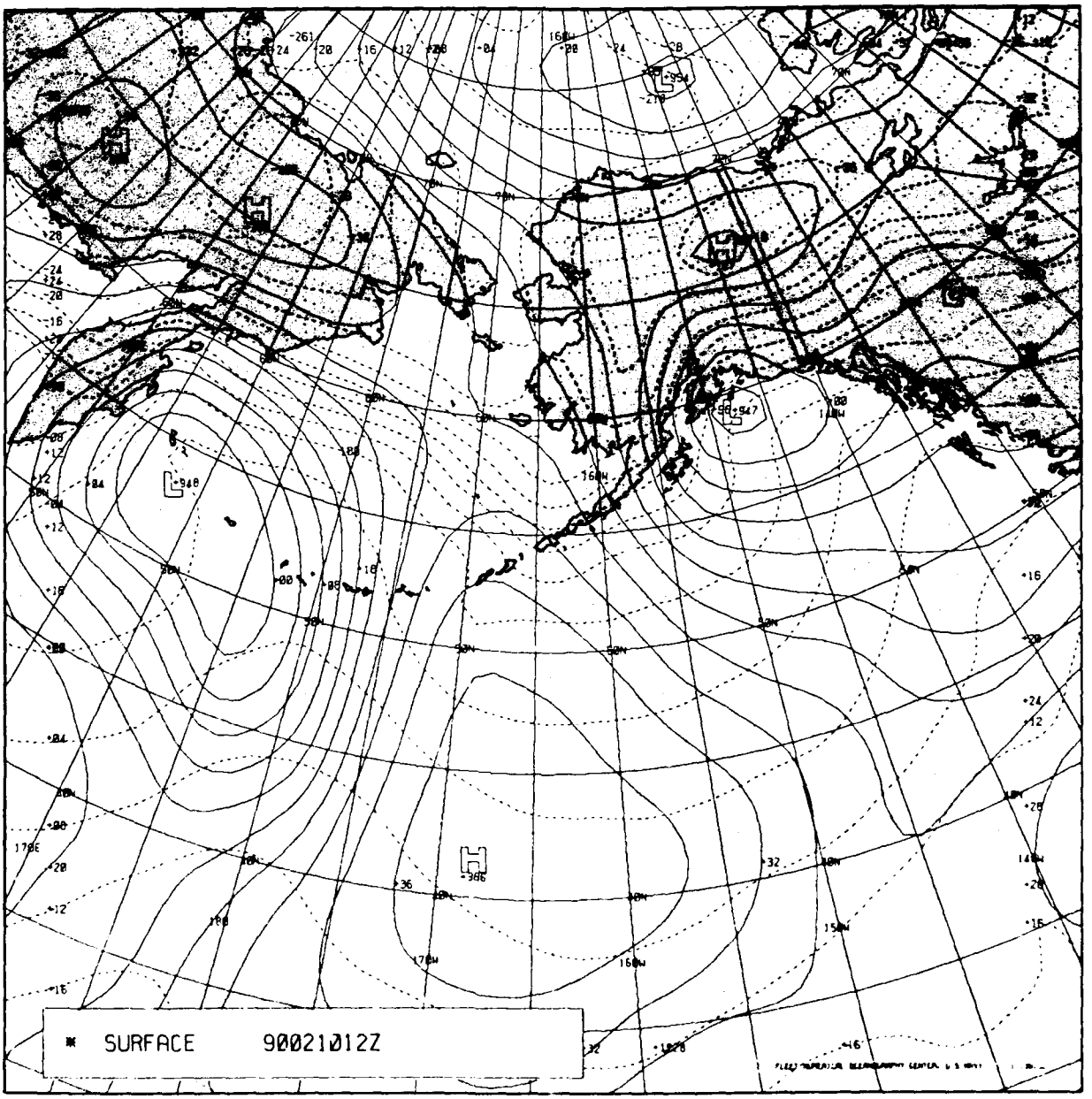

Figure 6-44. FNOC surface analysis 1200 GMT 10 February 1990.

Forecast Aids

1. Polar vortices and polar lows tend to form in preferred geographical locations. Local terrain features may channel the low level flow such that synoptic scale flow may be disturbed resulting in convergence areas, convective formation, and subsequent polar low development.
2. Polar vortices and polar lows tend to form in trough regions and usually are offset from objectively analyzed synoptic scale low pressure centers.
3. Intense polar low development is favored during periods of pronounced cold air advection that have an accompanying upper cold low or trough.

6.3 Formation of Boundary Layer Fronts

Boundary layer fronts form in the high latitudes where low level flow patterns from different directions with varying overwater path lengths converge. The western Bering Sea is a region where both synoptic and local circulation patterns exist that are conducive to formation of boundary layer fronts. In the following three-view sequence, boundary layer fronts and related vortices are seen that appear to be forced by both synoptic and local circulation patterns.

6–7 February 1990

In Fig. 6-45 a nearly east-west line of enhanced cloud development is seen, clearly indicating a cyclonic vortex near its eastern end. The fine featured cloud-line pattern to the north of the line of enhanced convection implies cold northerly flow off the Siberian landmass, typically referred to as a cold air outbreak. As this cold air flows southward it displaces relatively warm maritime air of unknown origin that is associated with the synoptic flow. The vertical displacement of the warmer maritime air results in enhanced cloud development and latent heat release. At this time a boundary layer front has developed between the low level cold flow off the land and the ambient maritime air.

Figure 6-46 (13 hr later) reflects the continued outbreak of cold air with longer and larger cloud lines implying increasing wind speeds and resulting in further intensification of the boundary layer front and associated vortices. There are now indications of vortices near both ends of the boundary layer front. Also apparent in Fig. 6-46 is a new low level, north-south aligned convergence zone or boundary layer front extending offshore along 173 °E. This new feature is interpreted as the result of local convergence between opposing northeast and northwest air flows of varying lengths over water paths. Features of this type and near this location have been noted in a number of cases. The convergence appears to focus near Mys Olyutorskiy (near 170 °E): the northwest flow to the west converging with northeast-to-southeast flow to the east. At this time the angle of convergence is small, and the developing boundary layer front is weak.

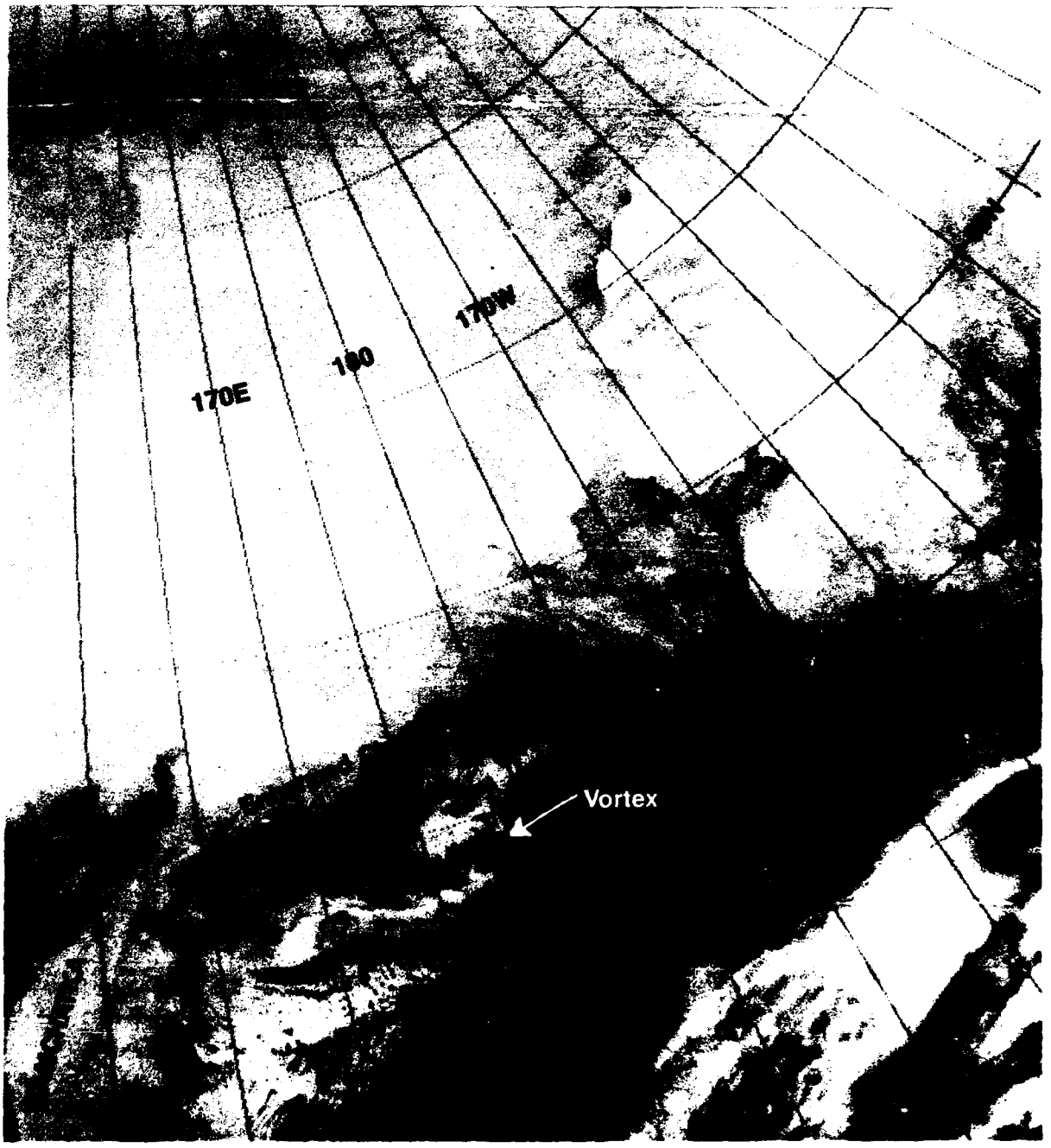

Figure 6-45. DMSP infrared imagery 0649 GMT 6 February 1990.

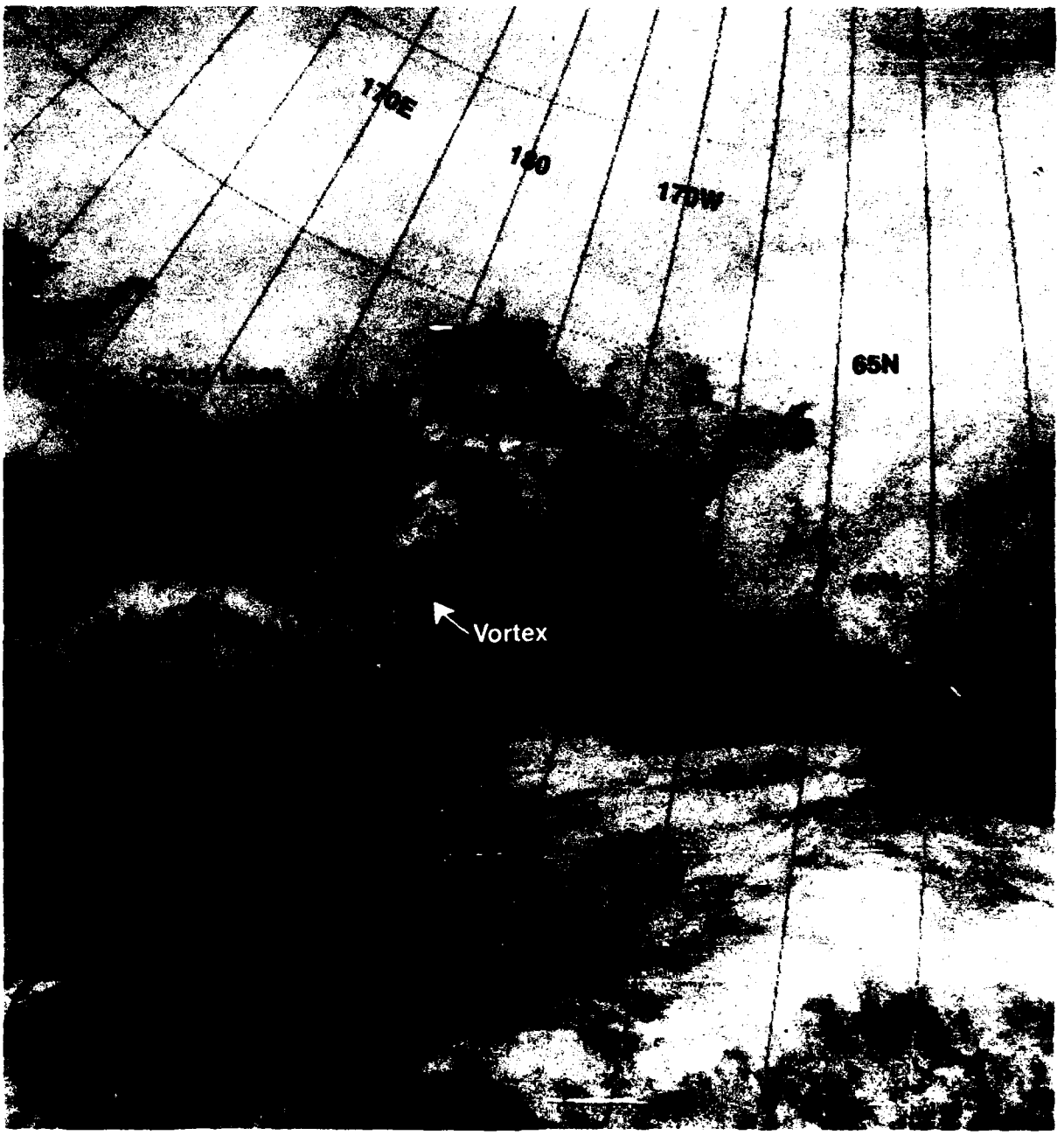

Figure 6-46. DMSP infrared imagery 1956 GMT 6 February 1990.

Figure 6-47, taken about 13.5 hr after Fig. 6-46, reflects significant weakening of the original boundary layer front between the local cold air outbreak and the synoptic circulation. The second boundary layer front that formed between local converging air flows has intensified and a distinct vortex has formed near its northern end. The cloud lines on either side of the vortex indicate nearly directly opposing flows converging into the vortex circulation.

Figure 6-47. DMSP infrared imagery 0927 GMT 7 February 1990.

The decaying original boundary layer front and its major vortex have moved eastward. The vortex now near 60 °N, 174 °W appears to have a nearly cloud-free eye, and the dark gray shade of the eye implies a warm core. The warm core is induced through subsidence as low level air within the eye is entrained into the encircling convective bands. The low level loss of air within the eye requires compensating subsidence from higher levels, thereby dissipating or preventing the formation of lower level cloudiness.

Boundary layer fronts, as implied by their name, are low level baroclinic zones. Figures 6-48, 6-49, and 6-50 show the surface, 850-mb, and 500-mb analyses, respectively, and illustrate the thermal advection pattern over the western Bering Sea during this period of boundary layer front development. Both the surface and 850-mb analyses show strong cold air advection over the western and central Bering Sea where the boundary layer fronts formed. The 500-mb pattern over this area shows the isotherms and height contours nearly parallel, implying that no thermal advection is occurring at that level. If the boundary layer front and embedded vortices were to move under a region of 500-mb cold air advection, further intensification of the vortices should be expected. Such a scenario would likely result in an outbreak of polar low development.

Forecast Aids

1. Boundary layer fronts form in the high latitudes where low level flow patterns from different directions with varying overwater path lengths converge.
2. Boundary layer fronts can develop between flows that result from either local or synoptic circulation or combinations of the two.
3. Certain geographical features and locations tend to enhance and have higher frequencies of boundary layer front formation.
4. Small scale vortices frequently form on boundary layer fronts. The convective activity that develops along these fronts is most intense in the vortex areas. This enhances low-level convergence, which, in turn, increases the vortex circulation. These low level feedback mechanisms, when further enhanced by favorable upper level conditions, can lead to development of hurricane force polar lows.
5. Boundary layer fronts that result from subsynoptic or local scale circulations can form and dissipate quite rapidly. Life cycles of a day or two are typical.
6. The conditions that are favorable for boundary layer front formation include converging air flows capped by low level inversions; this is the same environment in which polar lows are likely to develop initially. Because these conditions are to a large degree related to synoptic scale forcing, the development, movement, and persistence of areas of boundary layer front development are synoptic in nature even though the features themselves are subsynoptic.

6.4 Views of Geographical Terrain Features, Cloud Features, and Other Local Features in Satellite Imagery

Satellite imagery provides many examples of local geographical and cloud features as well as other nonpermanent local conditions such as sunglint, sea surface temperature patterns, and, in the Bering Sea region, even an occasional volcano eruption. The identification of and retention of views showing specific geographical features are important factors relative to optimizing the use of satellite imagery over areas including oceanic and land regions. Geographical features provide reference points for latitude and longitude gridding in general and for relative location and movement of image features from orbit to orbit.

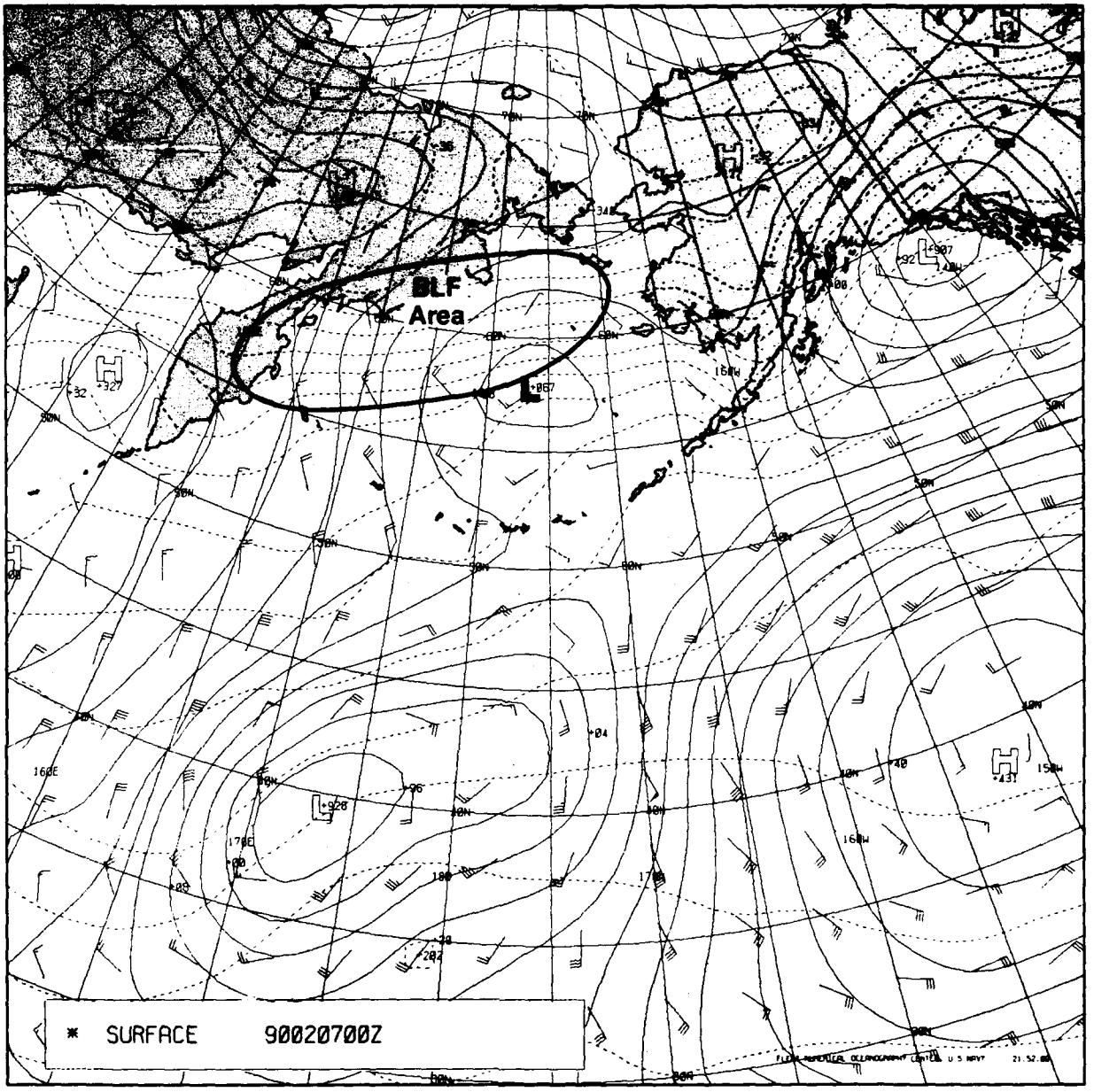

Figure 6-48. FNOC surface analysis 0000 GMT 7 February 1990.

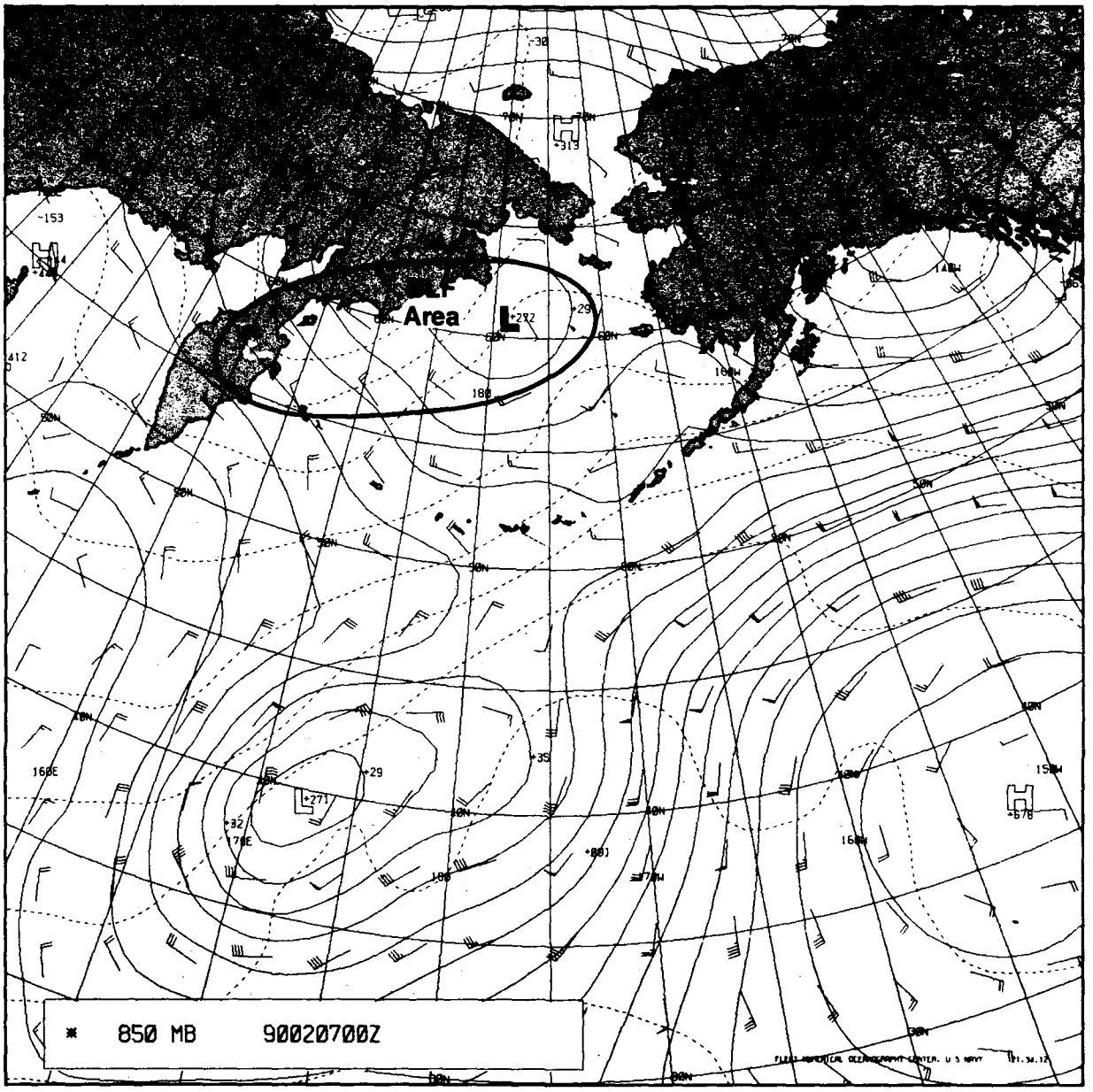

Figure 6-49. FNOC 850-mb analysis 0000 GMT 7 February 1990.

Furthermore, the interaction between terrain features and air flows are known to create unique cloud features under certain combinations of wind, moisture, and stability conditions. Readers are referred to the Navy Tactical Application Guide (NTAG) series, published by the Naval Environmental Prediction Research Facility (NEPRF), now a division of the Naval Research Laboratory, for details on interpretation techniques and local and regional phenomena and effects. Knowledge of terrain features such as mountains, islands, valleys,

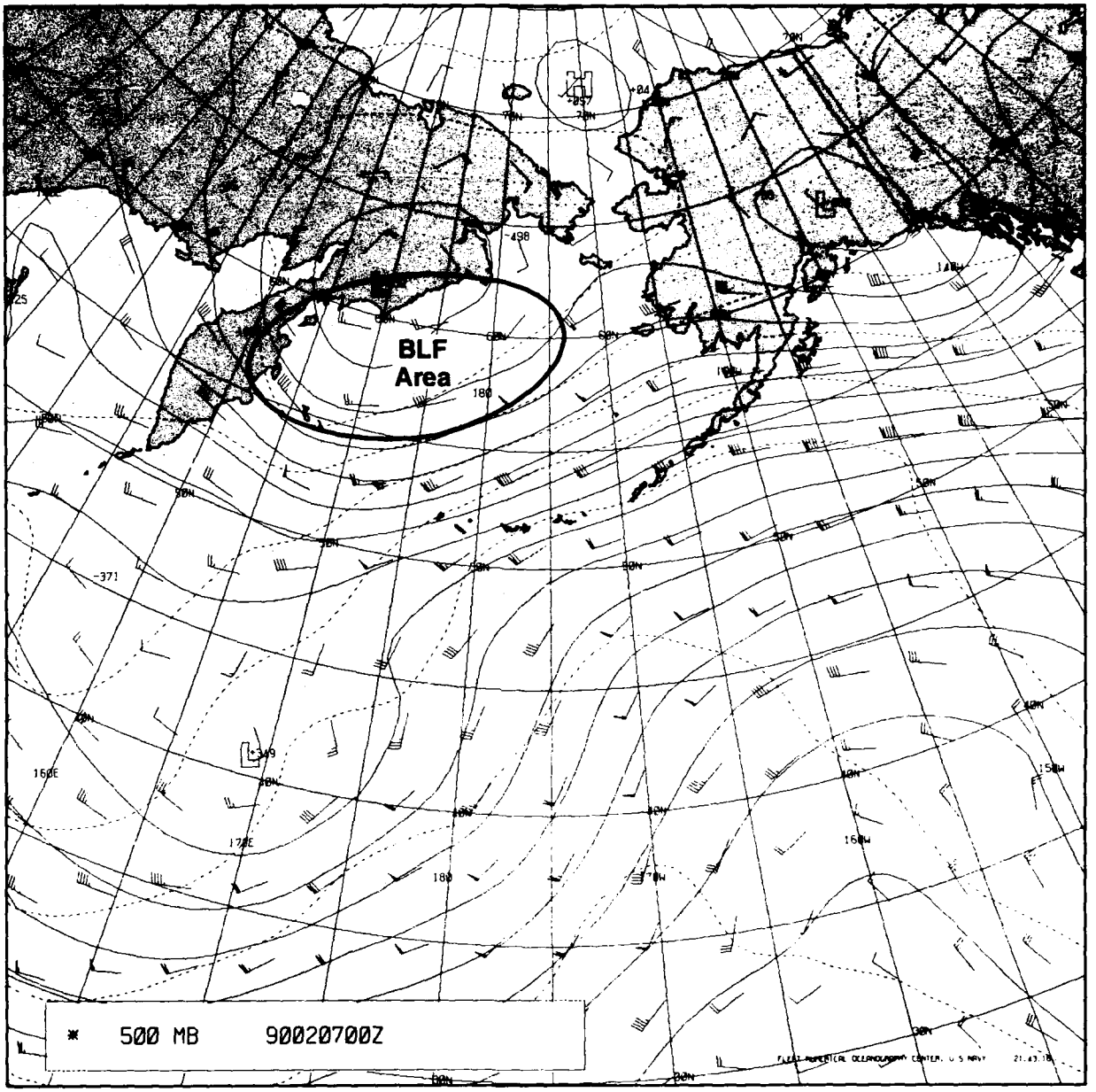

Figure 6-50. FNOC 500-mb analysis 0000 GMT 7 February 1990.

gaps, and straits, coupled with environmental effects such as cloud features and gray shade patterns, are basic aspects of satellite imagery interpretation. This section provides examples of mesoscale and local scale features seen in satellite imagery of the Bering Sea region.

6.4.1 Views of the Bering Strait and Adjacent Areas, 28 July 1990

Two views of the Bering Strait area geographical features and existing environmental conditions are shown. Figure 6-51 (2005 GMT 28 January 1990) is a midmorning visual image showing mostly clear conditions over the northern Bering Sea, Bering Strait, and southern Chukchi Sea. The cloud cover distribution seen in this view is representative of the region; on average the Bering Sea's northern region enjoys better weather and less low cloud cover and fog than its southern regions. Another climatological feature evident in this view is the northerly position of the ice edge, in the vicinity of 165 °W, seen near 73 °N at this time. The late summer-fall ice edge in the vicinity of 165 °W is typically a couple of hundred nautical miles (300–400 km) north of the edge position east of 160 °W,

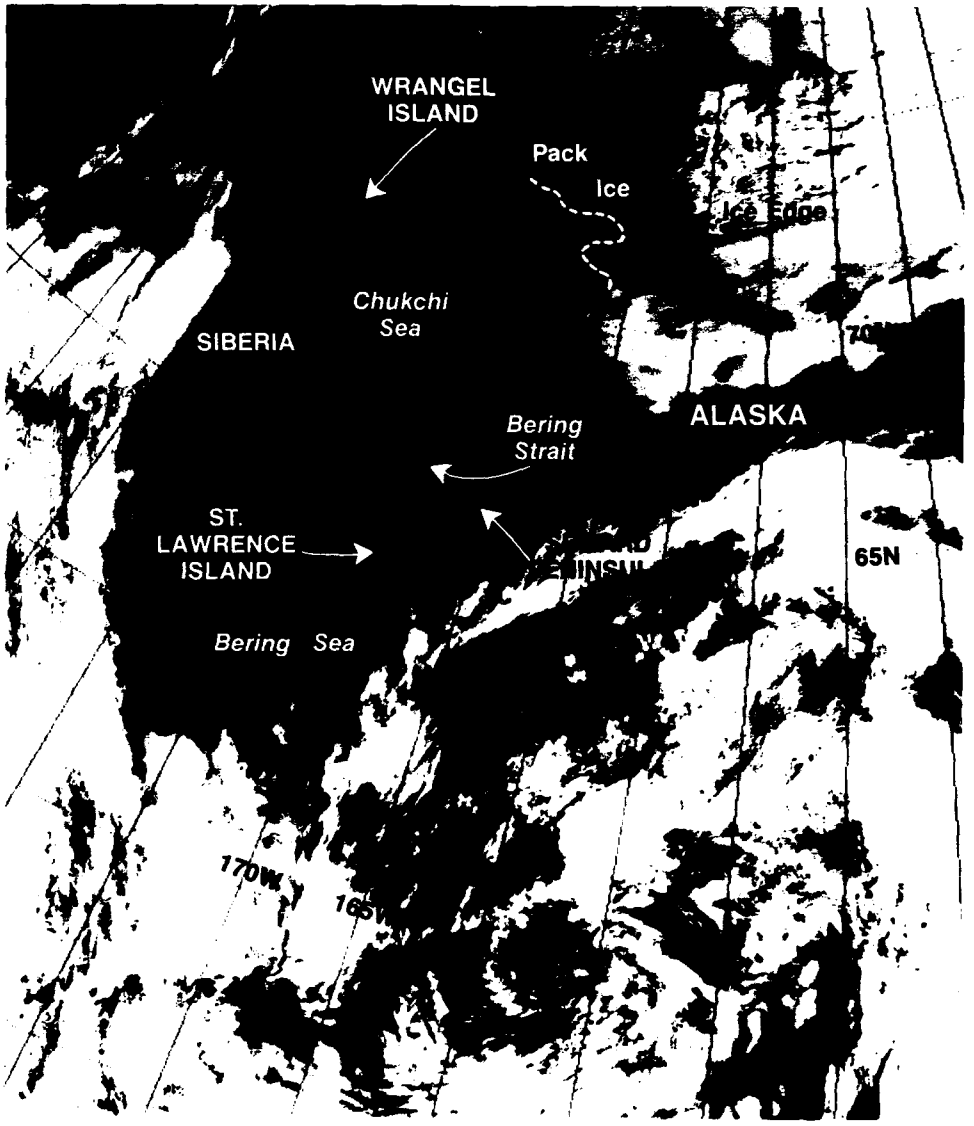

Figure 6-51. DMSP visible imagery 2005 GMT 28 July 1990.

where it tends to hug the Alaskan coastline closely. Other ice features seen include (1) an area of scattered floes north of Wrangel Island, (2) a leeside ice-free area extending 80–100 n mi (150–185 km) west-northwest from Wrangel Island, and (3) a large meandering streamer of near ten-tenths ice coverage extending north-northwestward from the southern coast of Wrangel Island and just beyond its western tip.

Figure 6-52 (1822 GMT 28 July 1990) recorded about 2 hr earlier than Fig. 6-51 shows the Bering Strait in an area of bright sunglint. This is a low sun angle, early morning local time, satellite pass. The pattern of highlighted (eastern cloud edges) and shadows (western cloud edges) are representative of morning low sun angle conditions.

The contrast between the brilliant water areas and dark terrain features in the sunglint area provide detailed views of barrier reefs and spits immediately adjacent to the coast of the Seward Peninsula extending northeastward into Kotzebue Sound. The major dark gray feature extending southward through the strait is a low cloud deck or fog bank. This cloud feature, so obvious in the sunglint area, is barely discernible in Fig. 6-51. Lee effects on the south side of the Diomede Islands, the Seward Peninsula, and St. Lawrence Island indicate a northerly surface wind through the region. This northerly wind accounts for the advection of the fog bank southward through the strait.

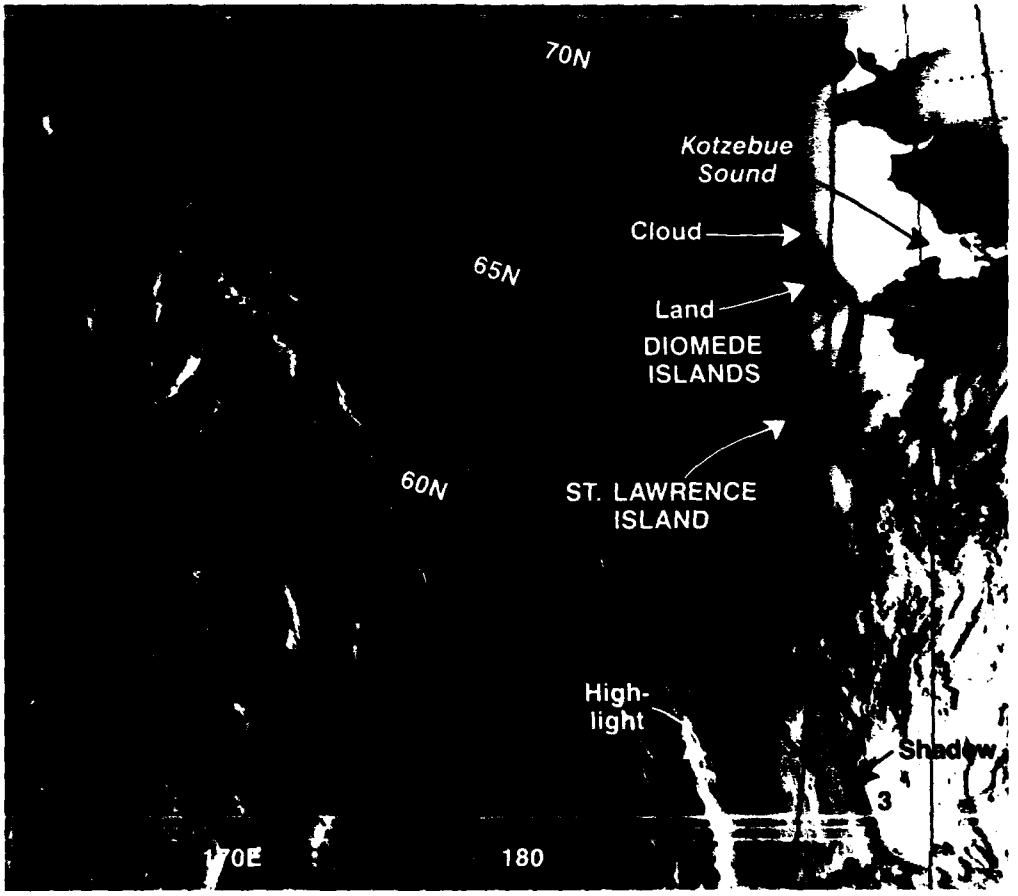

Figure 6-52. DMSP visible imagery 1822 GMT 28 July 1990.

The small scale variations of brightness over the area south of the strait reflects changing wind conditions with areas of calmest winds being the brightest. Although land areas are dark in sunglint regions because of their low reflectivity, the darkness of cloud shadow areas is simply due to the absence of sunlight reaching them to be reflected as sunglint. Note that the small dark area extending northwest from the northeast corner of St. Lawrence Island is not a terrain feature and, most likely, a cloud shadow. Over land, water areas such as lakes, rivers, and flooded lowlands may appear as bright areas in sunglint regions. Examples of these are the three bright spots seen on the Seward Peninsula. The western double spots are wide portions of the Kuzitrin River as it flows through the Imuruk Basin (65 °N, 165.3 °W). The eastern single bright spot is reflection from Imuruk Lake (65.5 °N, 163.2 °W).

Because multiple satellite passes can be received each day in the higher latitudes, including early morning and late evening ones, the cloud edge highlight and cloud shadow effect provides useful information on cloud height and existence of multiple cloud layers. In low latitude regimes the jetstream cirrus shields or areas of strong convective activity are the most common conditions in which highlight and shadow effects are evident. In the high latitudes experiencing low sun angles, only small cloud height differences are needed to result in highlight and shadow definition. The lower right-hand corner portion of Fig. 6-52 shows at least three layers of clouds based on highlight and shadow relationships. The labeled numbers 1, 2, and 3 indicate (1) a low deck of near surface-based stratus; (2) a second layer of slightly greater vertical thickness low clouds featuring a very thin shadow to the west and a highlight to the east; and (3) a thicker or higher cloud deck featuring a wider shadow along its western edge. Clouds such as those extending through the Bering Strait that exhibit neither a highlighted eastern edge nor shadow to the west are interpreted as being very thin and close to the surface. In this case, very likely, a surface based fog bank appears to have largely dissipated by the time of the Fig. 6-51 imagery, less than 2 hr after Fig. 6-52.

Forecast Aids

1. Terrain features should be identified in clear areas of satellite imagery for use both as gridding aids and interpretation factors of environmental features.
2. Sunglint (reflection off water surfaces) is most brilliant where the water surface is smoothest (lowest wind speeds) and cannot be seen from land areas or ice surfaces (unless flooded). Sunglint will occur off ice surfaces covered by water, for example, in the Arctic during the melt season (not illustrated in this case).
3. High latitude, low sun angle satellite imagery contains additional cloud height and layer information because of highlights on the edges facing the Sun and cloud shadows from the edges away from the Sun. This effect is evident for both morning and evening images with the obvious reversal of highlight and shadow sides. This case illustrates a morning pass with highlights on the eastern edges and shadows to the west.
4. Clouds or fog banks that do not exhibit edge highlights or shadows in low sun angle images are both thin and surface (fog) or very near surface based (stratus).

6.4.2 Wind Pattern in Sunglint Between Kodiak Island and the Kenai Peninsula, 3 July 1990

Dark areas within sunglint patterns have been related to local high winds (NTAG, Vol. 1, 2A-20). The entrance to Cook Inlet, located between Kodiak Island and the Kenai Peninsula to the north, has been identified as an area of strong surface winds. Macklin et al. (1990) discusses the results of a detailed analysis of a winter high wind event for this area. Figure 6-53 shows a sunglint pattern covering the Cook Inlet and entrance area. The detailed boundaries of dark land areas of Kodiak Island and the Kenai Peninsula imply a nearly cloud-free condition. Even the Barren Islands, located near the center of the entrance to Cook Inlet, can be clearly seen as small dark spots. The curved, plume shaped, medium-dark

Figure 6-53. DMSP visible imagery 1622 GMT 3 July 1990.

feature extending eastward and then curving slightly northward through the entrance is interpreted as roughened sea surface due to higher speed winds. In this situation high speed channeled winds blow through the entrance area in contrast to lighter winds in areas north and south of the eastern extent of the entrance. A similar, medium dark gray shade extends southward over Shelikof Strait, west of Kodiak Island, implying equally high winds in that area. Note that the gray shade pattern in Shelikof Strait extends to the coastline of the Alaska Peninsula. This pattern implies the lack of a blocking effect by the terrain, which, if it were in place, would result in a calmer near shore sea state. The absence of near shore lighter winds implies an unstable lapse rate with mixing down to the surface. The absence of lee blocking and a calm sea state extending eastward from the Barren Islands and Augustine Island is further indication of an unstable lapse rate over this area.

Figures 6-54, 6-55, and 6-56 are taken from Macklin et al. (1990). Figure 6-54 shows a schematic depiction of flow and terrain of the area. Figure 6-55 is a longitudinal vertical cross section from the end of Kamishak Gap on the Alaska Peninsula, across lower Cook Inlet, and eastward through the entrance. Figure 6-56 is the sea level pressure analysis for 11 February 1982 depicting a winter situation. These three figures from Macklin are shown here to aid in developing a conceptual model of wind flow in this area. The February winter wind example will, in general, show higher wind speeds and a more intense system than summer cases, such as the one seen in Fig. 6-53.

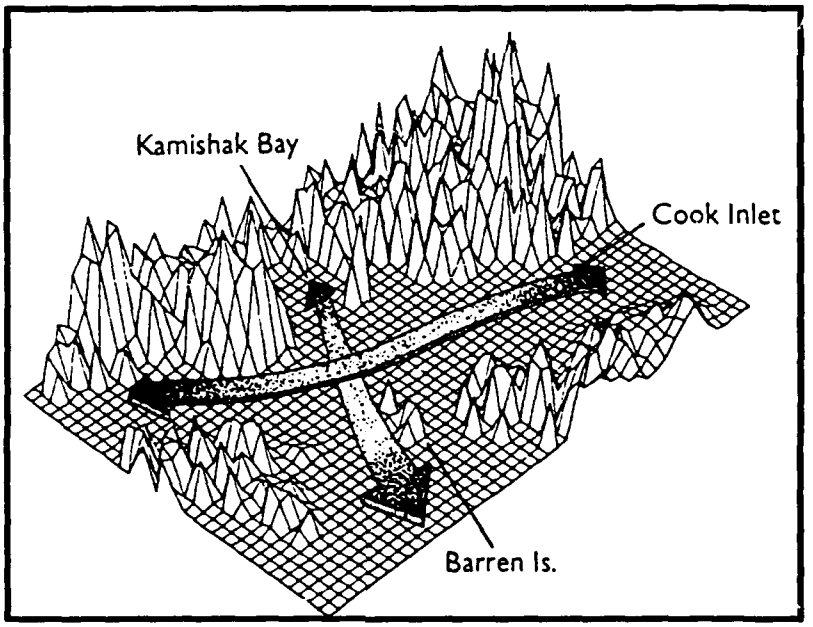

Figure 6-54. Orography of lower Cook Inlet: grid spacing is about 6 km; the vertical scale is exaggerated fortyfold. Arrows denote orographic wind channels (Macklin et al., 1990).

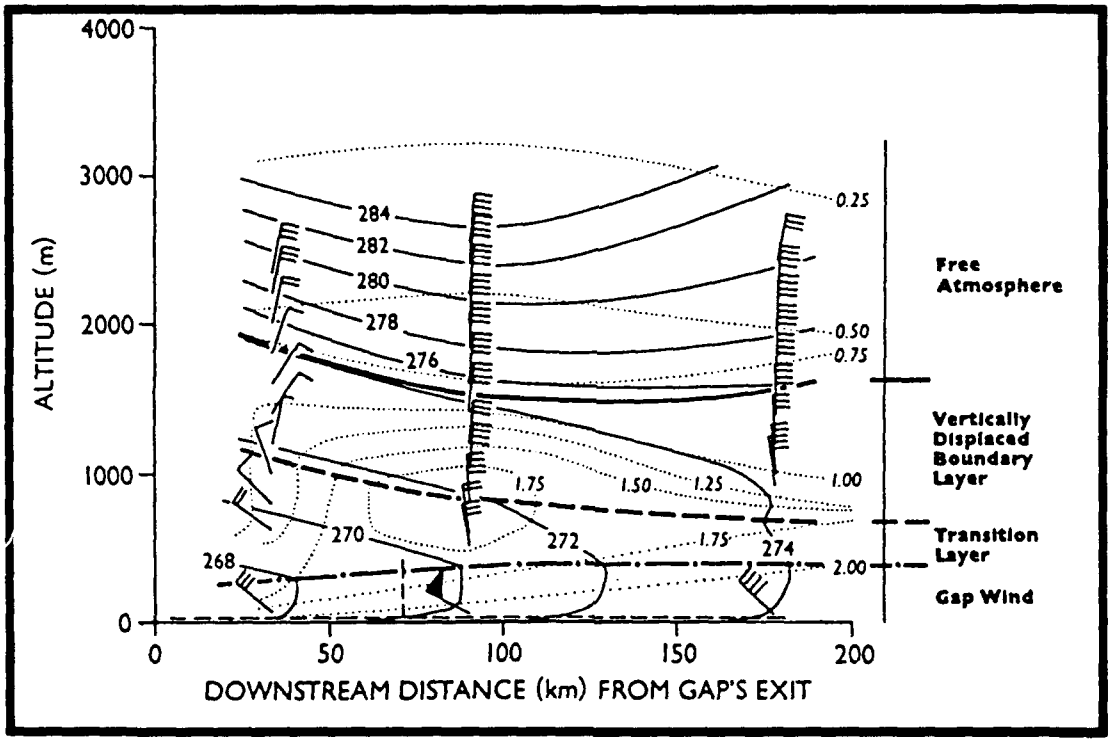

Figure 6-55. Longitudinal section of horizontal wind (full barb=5 m/s, °T), potential temperature (K) and specific humidity versus altitude (km) and distance (km) downstream from the end of Kamishak Gap. Vertical lines indicate locations of dropwindsondes; bold lines divide specific layers. Dashed lines show locations of horizontal and cross sections (Macklin et al., 1990).

Forecast Aids

1. Dark areas embedded within sunglint patterns in areas known for funneled winds imply that increased wind speeds are occurring.
2. The entrance to and region of the lower Cook Inlet and the Shelikof Strait are known areas of local low level wind enhancement. During the cold season, under certain synoptic conditions, a low level jet develops in this area and surface winds may reach 100 kt (51 m/s). Extremely hazardous surface conditions, as well as low level flight conditions, caused by high winds and seas, superstructure icing, and severe turbulence are likely to be encountered in strong winter events.
3. The synoptic pattern that results in the most intense winter wind cases will have a low in the Gulf of Alaska (this is part of the required pattern and is typical of winter conditions) coupled with high pressure ridging southward from western Alaska over the Bristol Bay area. This synoptic pattern results in a steep pressure

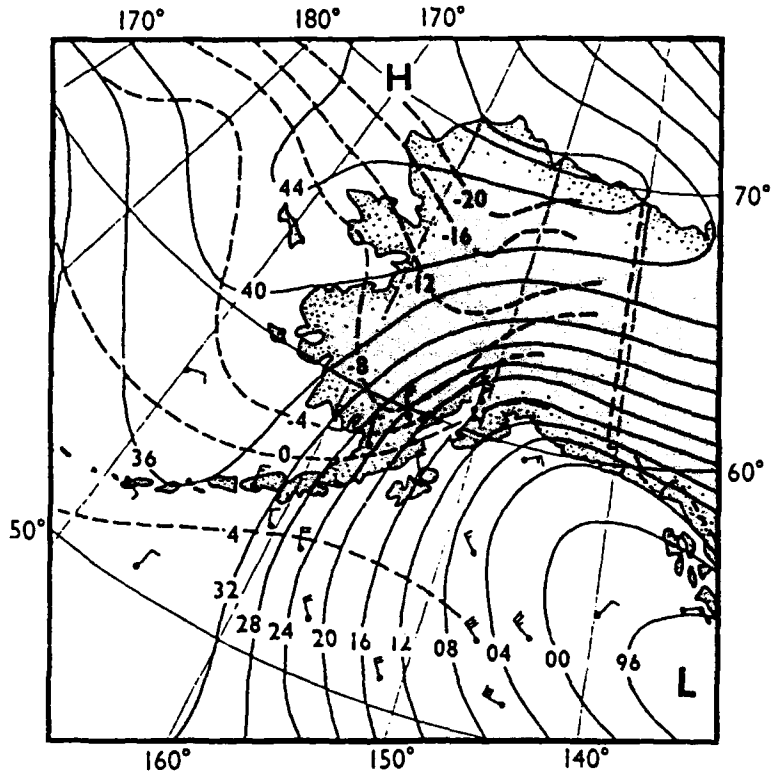

Figure 6-56. Alaska sea level pressure analysis for 0000 GMT 11 February 1982. High pressure northwest of Alaska and low pressure over the eastern Pacific Ocean caused a steep pressure gradient over Cook Inlet. A reservoir of cold air pooled west of the Aleutian Range. (Solid contours denote pressure in coded mb, dashed lines temperature in °C, full wind barb=5 m/s) (Macklin et al., 1990).

gradient over the lower Cook Inlet and entrance area. Critical to development of extreme wind conditions is that cold air flows out of Alaska and pools west of the Aleutian Range of the Alaska Peninsula. Periodically the cold air surges through mountain gaps and/or over terrain features and beyond, and then through the local straits and entrances, resulting in local extreme wind events. Winds of this type are frequently referred to as williwaws in the Aleutian area, or Kamishak Gap winds in Kamishak Bay and the Cook Inlet.

6.4.3 Local Wind-Induced Clouds and Interactions with Synoptic Scale Features

The Kamishak Gap, Cook Inlet entrance region, has been identified as a localized high wind area (Macklin et al., 1990). Cloud lines once formed have been shown to extend hundreds of miles downstream with little change in shape (Walter, 1980). The extent of the downstream persistence of cloud lines is increased when they form under synoptic scale induced low level inversions. The classic formation of a large area of cloud lines occurs where strong low level winds flow off cold land or ice surfaces over relatively warm oceanic surfaces, typically following the passage of a synoptic scale cyclone. Under such situations the cloud lines tend to evolve into open-celled cumulus as a result of the continued flux of heat from the ocean and gradual weakening of the capping inversion.

Figure 6-57, a 15 February 1990 infrared image, shows a variation of cloud-line development. A single band or line of stratus extends about 300 n mi (556 km) southeastward from the entrance to Cook Inlet, located between Kodiak Island and the Kenai Peninsula.

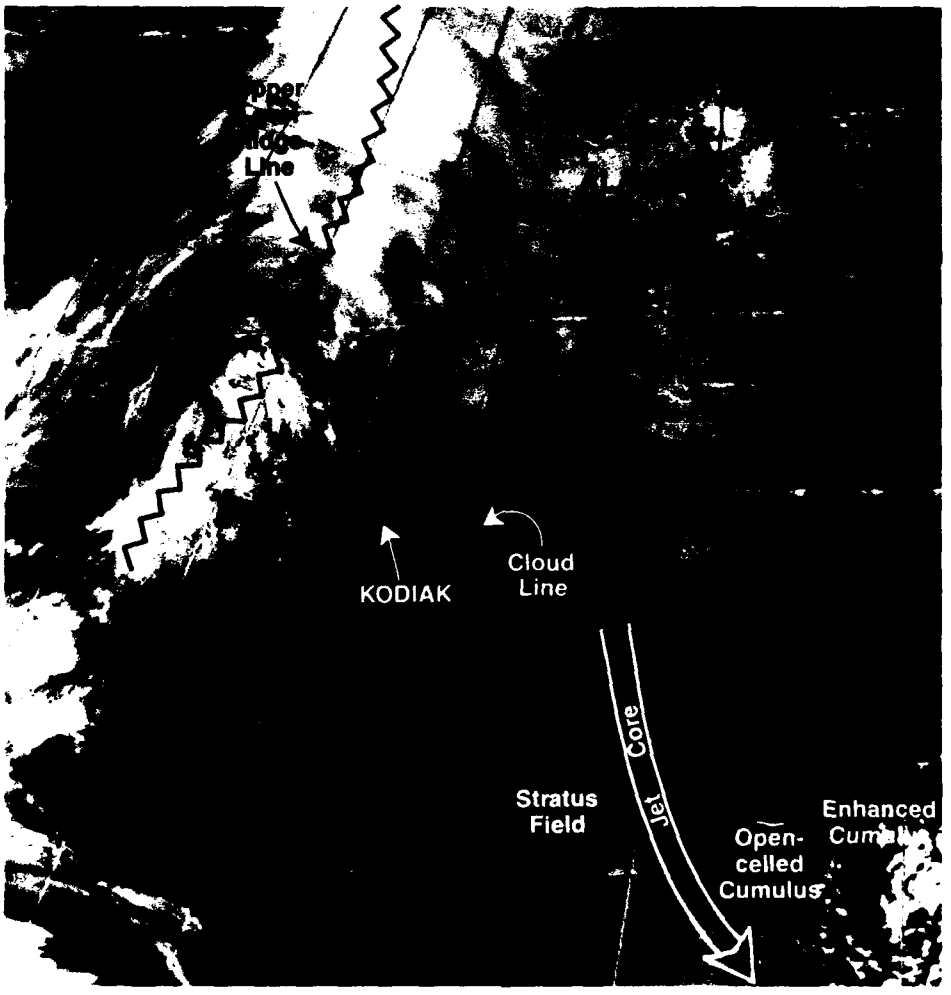

Figure 6-57. DMSP infrared imagery 1831 GMT 15 February 1990.

It merges with a synoptic scale area of stratus near 54 °N, 146 °W. This entire cloud line or stratus field feature is located east of a sharp ridge line that is evident at the surface through 250 mb and extends north-south in the vicinity of 160 °W. The cloud feature lies under an 80-kt (41 m/s) northwest jetstream level flow. Northerly winds aloft imply decreasing atmospheric layer depths, subsidence, and low level divergence. This sinking action is most pronounced on the anticyclonic side of the jet and is typically reflected in satellite imagery by areas of stratiform clouds, such as seen extending southward from the cloud-line feature. The jet core is generally located above the boundary between the stratus field and open-celled cumulus. The upper level ridge line is clearly depicted by the anticyclonically curved portion of a frontal cloud band that extends from over northwestern Alaska, southward across the Bristol Bay region and beyond over the North Pacific.

Examination of surface charts (not shown) for 1200 GMT 15 February 1990 and 0000 GMT 16 February 1990 show a 4-mb gradient across Kamishak Gap at 1200 GMT 15 February—decreasing to zero gradient by 0000 GMT 16 February. A 4-mb gradient using the Anchorage forecast rule (wind speed=gradient mb [King Salmon-Kodiak] × 6) produces a 24-kt (12 m/s) wind.

The band or cloud line extending southeast from the entrance to Cook Inlet is relatively dark gray, implying in the infrared image (Fig. 6-57) that it is a warm low level cloud and not cirrus streaming over the ridge line. Some enhanced vertical development in the synoptic scale stratus field is indicated in the area where the cloud line merges with it. The enhanced vertical development is reflected by the area of lighter gray shade (colder cloud tops).

The sequence of events resulting in this cloud-line feature starts with the evolution of a circulation pattern that results in a Kamishak Gap wind estimated at 25 kt (13 m/s). This channeled wind flow regime includes local convergence in the southern Cook Inlet resulting in development of an enhanced cloud line. Macklin et al. (1990) have recently reported on the local and synoptic scale factors related to Kamishak Gap wind events. Maintenance of the cloud band for a long distance downstream was aided by the fact that it was under the subsidence influence on the anticyclonic shear side of a strong northwesterly jet aloft, which would act to suppress diffusion of the band in relatively undisturbed straight flow over open water. On the synoptic scale increasing anticyclonic circulation was moving over the area in which the persistent cloud line evolved. The stratus field extending southeastward from the southern end of the cloud line, along with the clear area to the west, reflects a synoptic scale region of subsidence and low level inversion development under the low level high pressure regime. The maintenance of the synoptic scale stratus field, as well as the cloud line, results from the same lower atmospheric thermodynamic structure.

Forecast Aids

1. The effects of local terrain induced channeled winds are frequently evident in satellite imagery in the form of cloud lines and, in general, occur under conditions where low level synoptic scale inversions dominate.
2. The disturbance of the lower atmosphere created by local scale channeled, low level winds tend to extend downstream as far as the favorable synoptic scale conditions persist.

3. The extent and evolution of cloud lines provide insights of marine boundary layer conditions and related low level environmental conditions such as visibility, electromagnetic propagation, and low level flight conditions.

6.4.4 Redoubt Volcano Eruption

Redoubt volcano located near 60.5 °N, 152.5 °W, on the Alaskan mainland west of Cook Inlet, was erupting on 21 April 1990. The 1457 GMT DMSP infrared image (Fig. 6-58) shows an extreme bright spot near this location. Other volcanic eruptions, particularly on the Kamchatka Peninsula, were noted in DMSP infrared imagery during the review of 3 yr of imagery for use in this forecaster's handbook. Although volcanic eruptions are obviously very hot, they appear as extreme white spots (cold temperature) in the infrared imagery. Eruptions appear cold and as a singular round spot when winds aloft are essentially calm. The cold temperature results from moisture associated with the eruption being cooled as it is lifted to very high altitudes with the cloud plume radiating at such temperatures. An atomic bomb explosion would be expected to yield a similar signature.

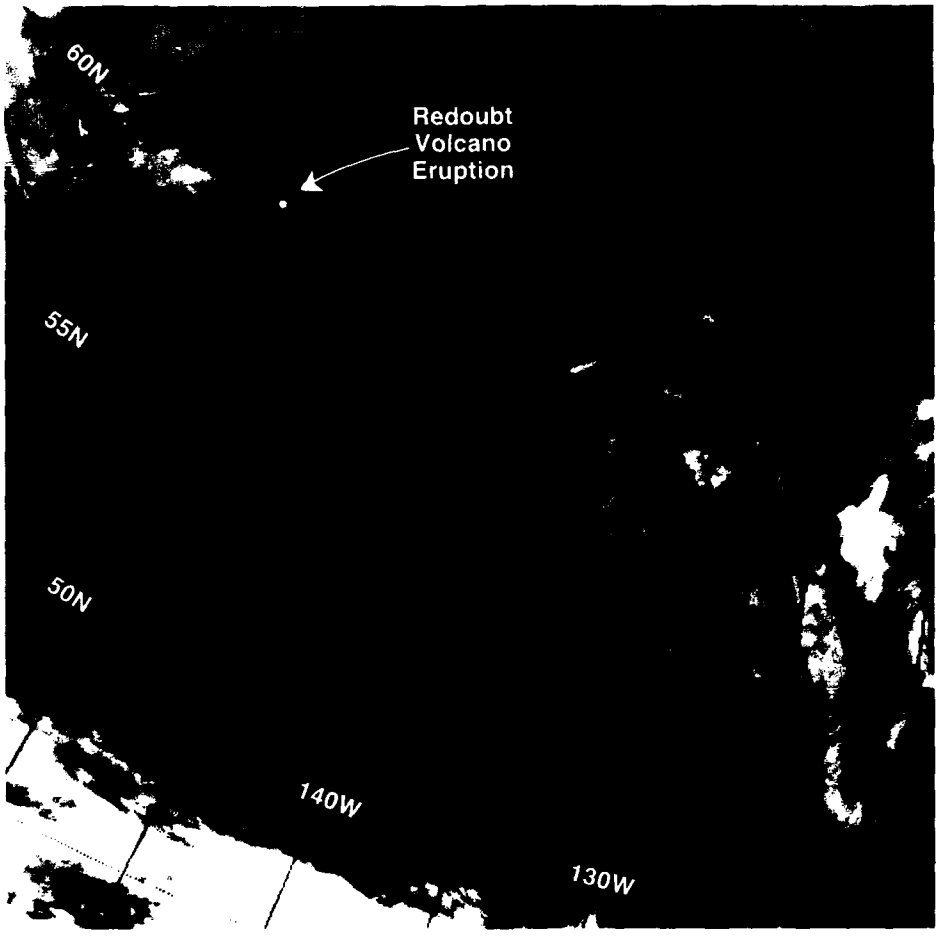

Figure 6-58. DMSP infrared imagery 1457 GMT 21 April 1990.

When the winds aloft are not calm a cold cloud plume is observed rather than a cold spot. Figure 6-59 shows the cloud plume from a Mt. Redoubt eruption on 15 December 1989. The cloud plume indicates strong southwesterly winds aloft.

It is now well known that jet engines flame out very readily when flown through such plumes. Flights are now canceled in such areas when such effects are observed.

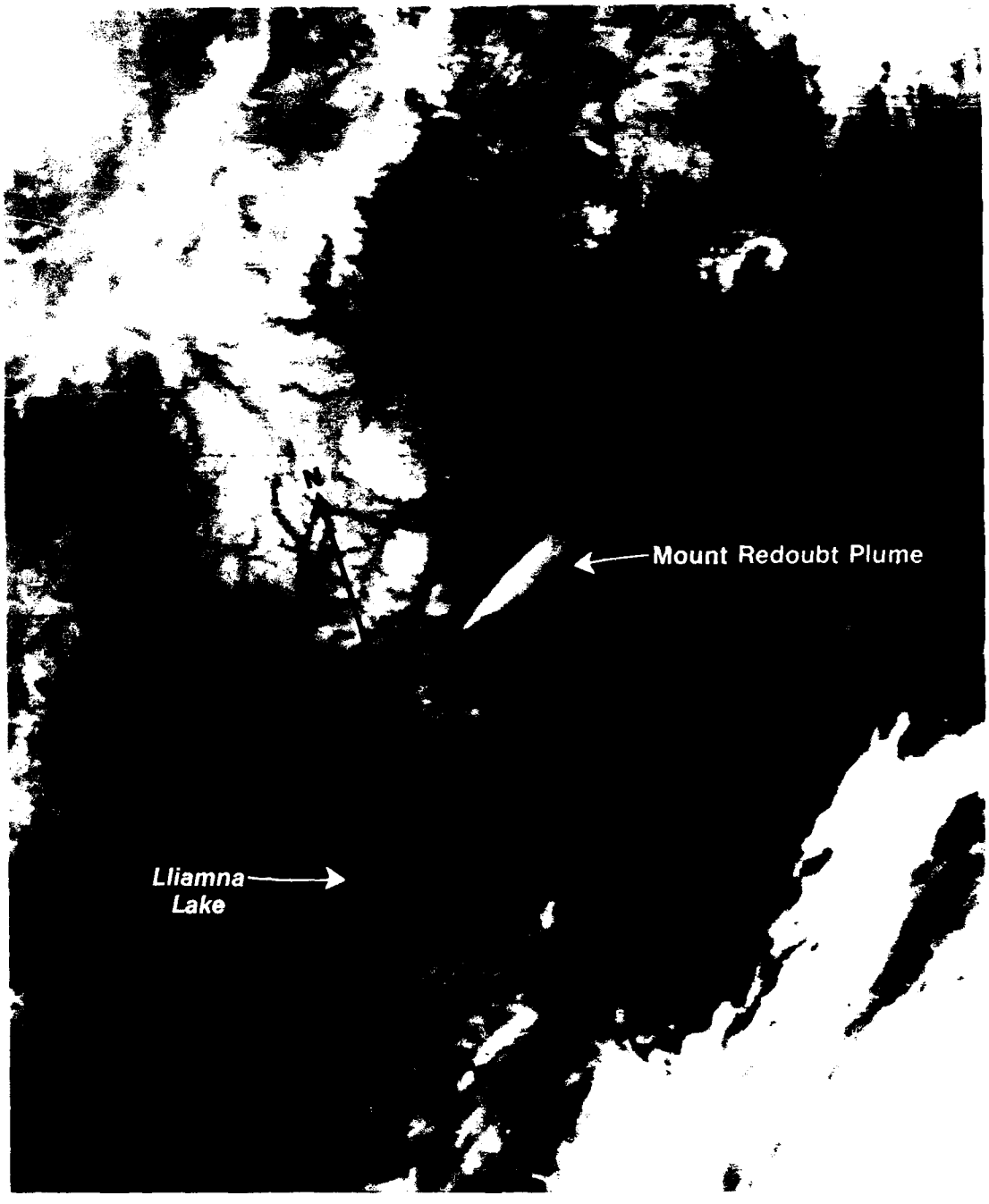

Figure 6-59. DMSP infrared imagery 0157 GMT 15 December 1989.

6.5 Sea Surface Temperature Features

Sea surface temperature gradients can influence both the synoptic and local patterns of wind, clouds, and weather through air-sea interaction. The sea surface temperature patterns themselves can be seen in infrared imagery; two such cases are discussed in this section.

6.5.1 Cold Water Southwest of Kodiak Island, April 1990

An area of cold sea surface temperature extending about 100 n mi (185 km) seaward from the southern coast of the Alaska Peninsula in the region southwestward from Kodiak Island is evident in satellite imagery on consecutive days during April 1990. The cold water area, with boundary eddies, is clearly indicated on 9 April (Fig. 6-60) by the gray shade pattern that extends from just off the northeast tip of Kodiak Island, southwestward to near 162.5 °W, where low clouds obscure the sea surface. Because sea surface temperature patterns are extremely difficult to differentiate from thin stratus or fog banks in infrared imagery,

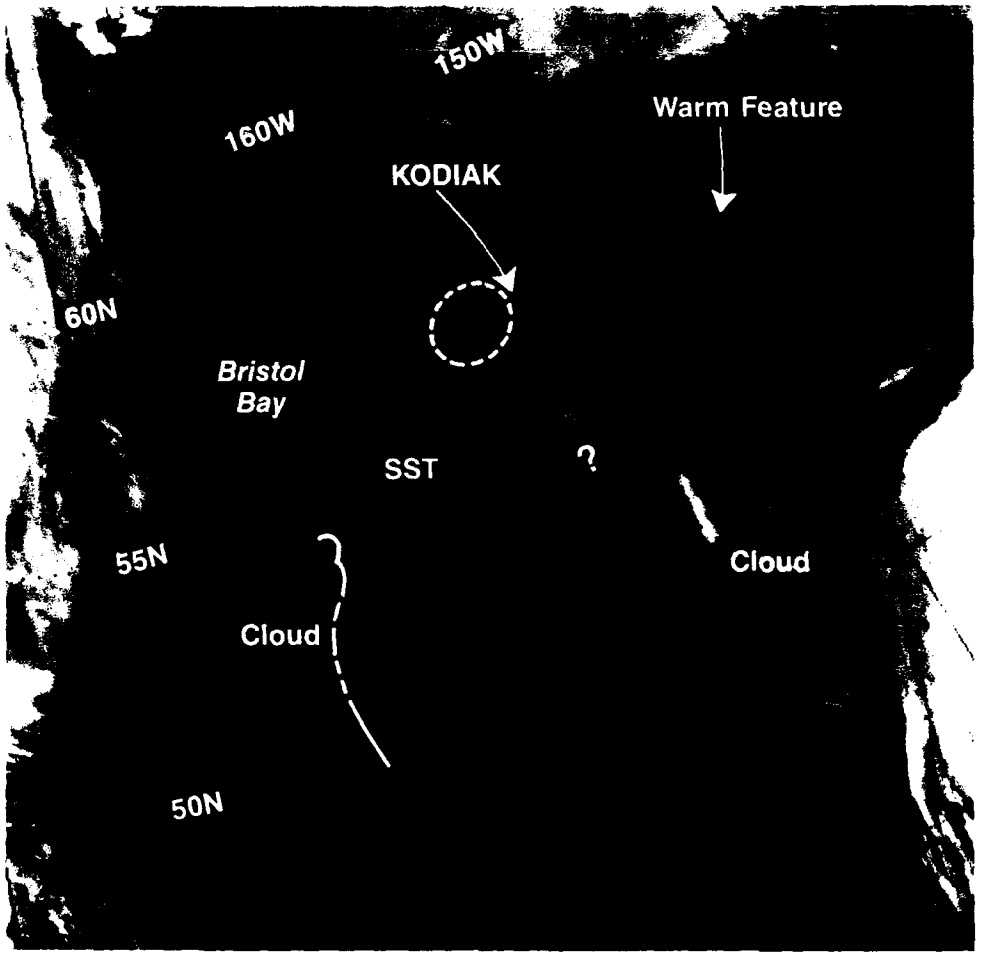

Figure 6-60. DMSP infrared imagery 0926 GMT 9 April 1990.

it is advisable to obtain more than one view of features before unequivocally classifying them as sea surface temperature features. Figure 6-61 from 10 April shows the stable feature configurations necessary to positively identify the gray shade pattern as a sea surface temperature feature. Several of the boundary eddies and plumes can be recognized from the view of April 9th on that of the 10th. This pattern is not clearly apparent in the April mean sea surface temperature chart (Fig. 6-62).

Very close inspection of individual feature elements in the Shelikof Strait west of Kodiak Island (circled area) indicates southwest movement of the sea surface temperature patterns in that area from the time of the image in Fig. 6-60 to that in Fig. 6-61. One possible explanation of the overall sea surface temperature pattern would be the counterclockwise advection of warm water by the Alaska Current around the periphery of the Gulf of Alaska. Regardless of the flow characteristics involved, knowledge of the location of ocean thermal boundaries are important for many maritime operations, certainly including seeking warm water during hazardous structural icing conditions.

The interpretation of the diffuse gray shade pattern between the sea surface temperature pattern and the obvious cloud features to the southeast is uncertain. Some day-to-day persistence is noted in the area eastward from Kodiak Island, in particular the relatively warm feature (darker gray shade) centered near 57 °N, 145 °W. This feature could be associated

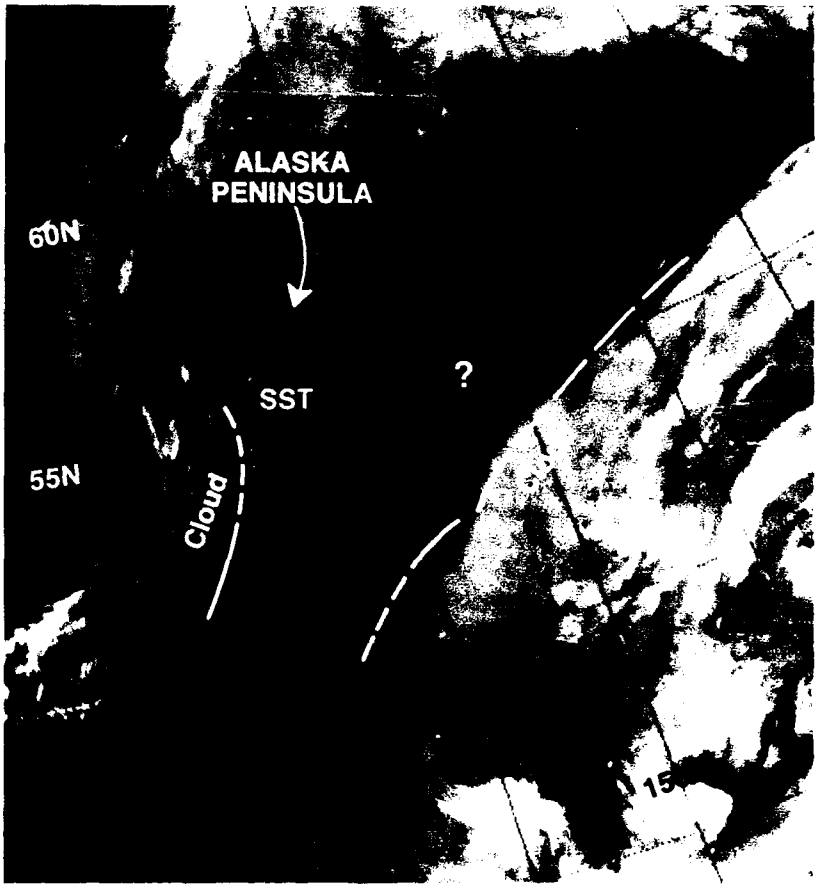

Figure 6-61. DMSP infrared imagery 0906 GMT 10 April 1990.

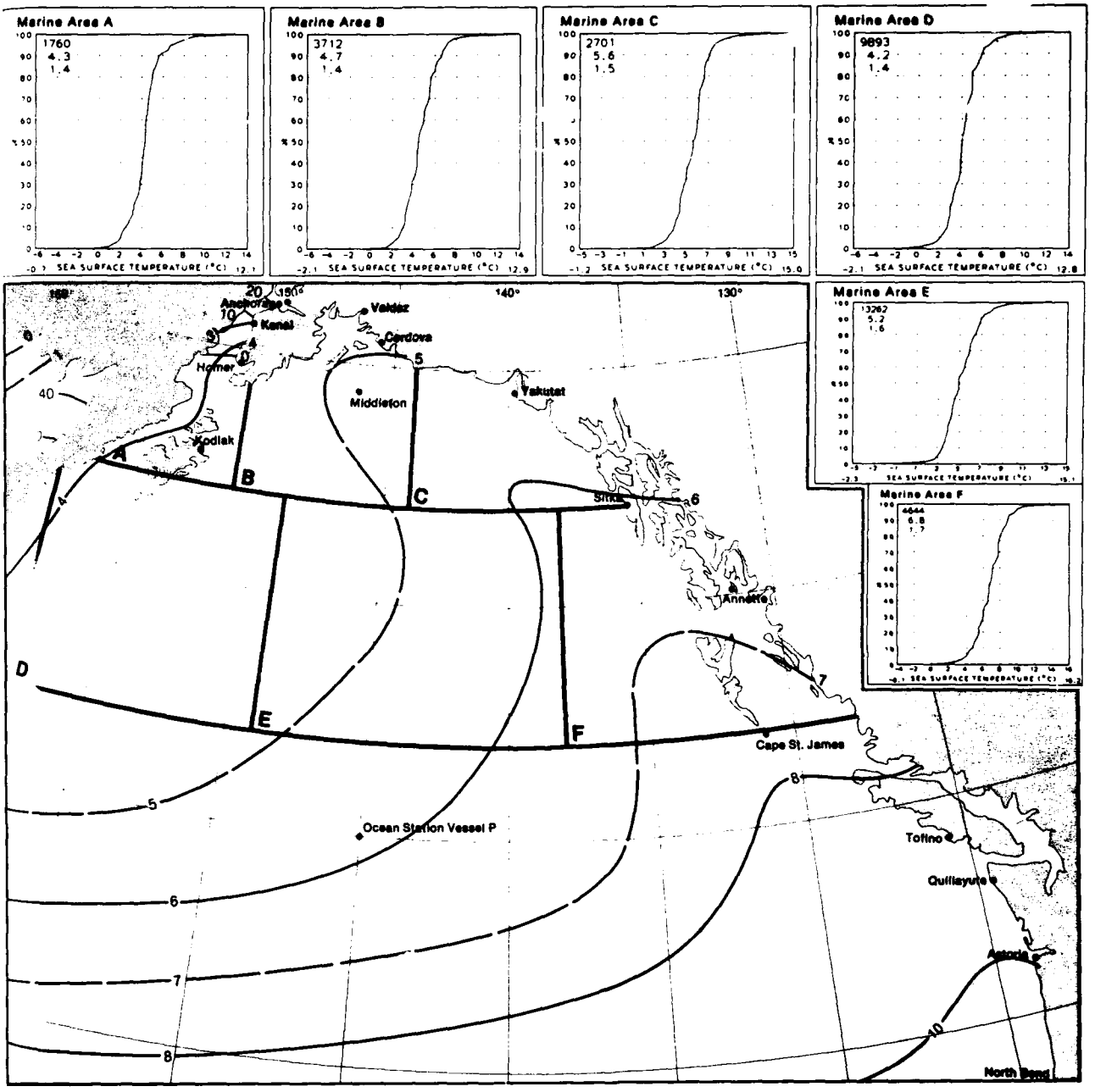

Figure 6-62. Mean sea surface temperature (°C) and ice of any kind (%)—April (Brower et al., 1988).

with the Kayak Island eddy mentioned in the "current" section of this handbook. The eddy has been identified by Brower et al. (1988) as a permanent anticyclonic eddylike feature dominating the region west of Kayak Island. However, the feature seen in Figs. 6-60 and 6-61 is on the order of 180 n mi (334 km) south of Kayak Island (near 59.8 °N, 144.2 °W) and not in close agreement with the location shown in Fig. 6-62.

Forecast Aids

1. Regions of steep sea surface temperature gradients do exist along the Aleutian chain and can be seen in DMSP infrared imagery. Knowledge of these conditions has application to ASW forecasting and fishery considerations.
2. The sea surface temperature features in this region, as elsewhere, persist for several days or longer. This characteristic is important in both differentiation of these features from low cloud or fog features and in application of persistence forecasting.

6.5.2 Cold Sea Surface Temperature Pattern Along the Aleutian Chain During September 1990

The monthly mean sea surface temperature charts for July through October show a temperature minimum along the Aleutian chain. The sea surface temperature climatology for September is shown in Fig. 6-63. The location of the minimum temperature value during the 4-month period is very near the September location shown just west of the 180th meridian.

This climatological feature can also be seen in satellite imagery. Figure 6-64 is a local night time (2239 LST) infrared image from 30 September 1990. Close inspection reflects a light gray band extending along most of the Aleutian chain. The widest area appears around Adak (about 52 °N, 176 °W) and to slightly beyond 175 °E. Figure 6-65 is another DMSP infrared image acquired over the same region on the following morning at 0637 LST. Most of the individual islands of the Aleutians are also apparent in this image, as is the subtle light gray shade surrounding the islands, indicative of slightly cooler sea surface temperatures with respect to outlying areas.

Cloud systems 1 and 2 have been indicated on both images and it can be seen that these systems have been advected eastward with time indicating a westerly flow through the region. It should also be noted that the slightly colder ocean temperatures have acted to inhibit or suppress low cloud development over those areas. The effect is most apparent in the western portion of the Aleutians in the region where the climatological temperature minimum was indicated (Fig. 6-63).

The light gray shade indicating cooler water coincides roughly with the shallow water encompassing the Aleutian Islands as shown in the bathymetry chart for that region (see Fig. 2-7 in Chapter 2). Cooler water in the wintertime over shallow ocean waters is a known phenomenon and is described in detail for the Bahama Banks by Garwood et al., 1981. In this paper the authors showed that the cooler water of the Banks could be attributed to heat loss as a result of conduction and evaporation when cold fronts pass through the area. The combination of decreased temperature and increased wind speed maximized the cooling effect apparent in satellite infrared views of the region. The effect was shown to be reversed in summertime when the Banks became warmer than the surrounding seas as shallow water heated more readily than the adjacent deep water areas.

The summer and early fall sea surface temperature minimums over the Aleutian Islands seem to be an apparent contradiction to the above study. The contradiction is resolved when considering the following facts: (1) the Bahama Banks are very shallow—only 6 to 10 ft

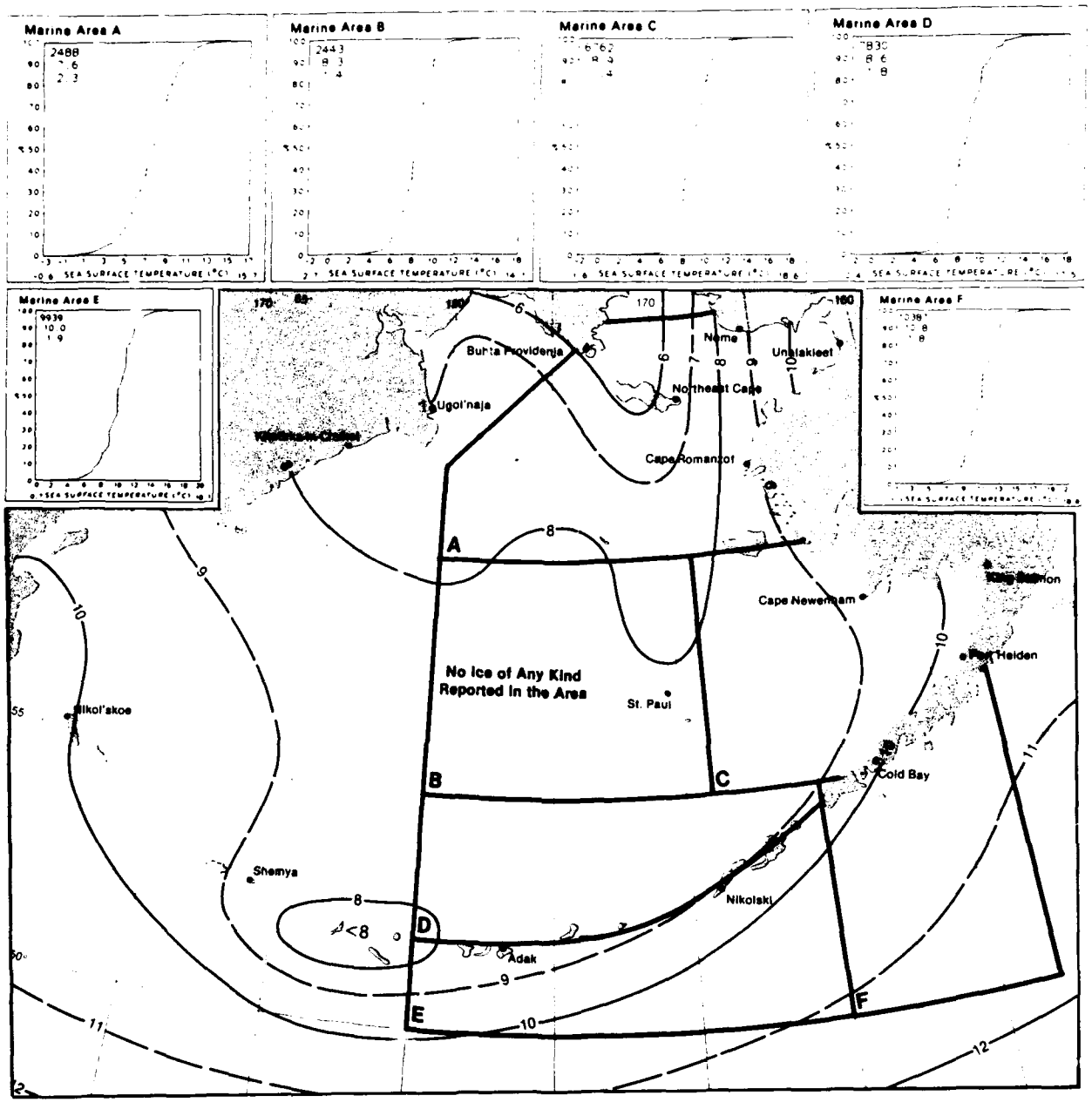

Figure 6-63. Mean sea surface temperature (°C) and ice of any kind (%)—September (Brower et al., 1988).

(2–3 m) deep over large areas, (2) residence time of water over the banks may be as long as 250 days, (3) no banks surround the Aleutian Islands—water depth increases very rapidly to over 328 ft (100 m) around most of the islands, and (4) currents flow through the straits between the Aleutian Islands consistently at speeds of 2 to 10 inches/s (5–25 cm/s) in summer and 0.4 to 2.4 inches/s (1–6 cm/s) in winter. Therefore, no long-term residence of water surrounds the islands.

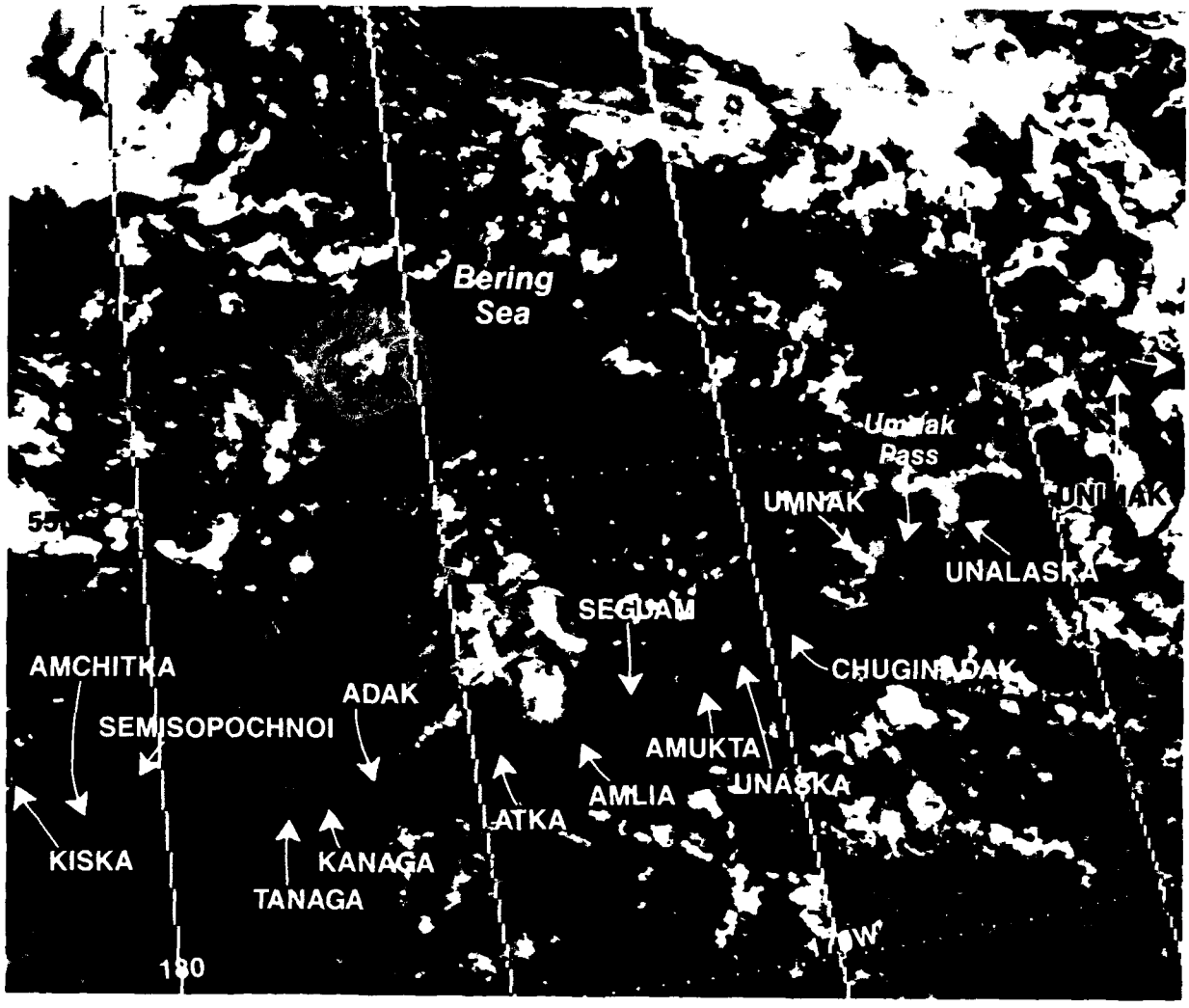

Figure 6-64. DMSP infrared imagery 0839 GMT 30 September 1990.

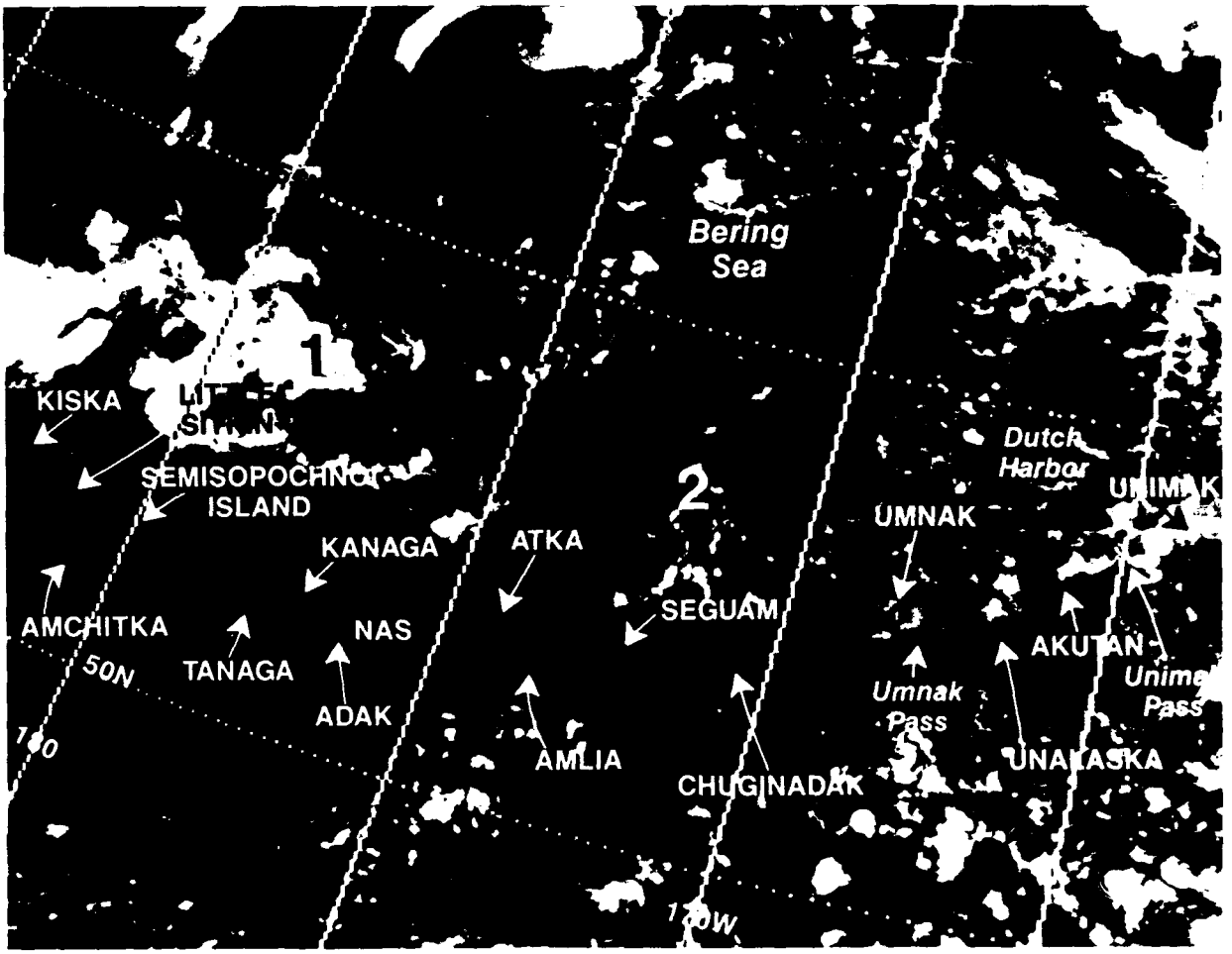

Figure 6-65. DMSP infrared imagery 1637 GMT 30 September 1990.

Because of the nature of the above facts upwelling could be ruled out as a cause for the cool water effects observed over the Bahama Islands during winter. However, upwelling, and perhaps mixing, is the only plausible explanation for the temperature minimum observed over the relatively deep water immediately surrounding the Aleutians. But why is this generally only a summer and early fall phenomenon and not observable by satellite during winter? The answer seems to lie in the nature and persistence of the two major weather regimes dominating the Aleutian region on a seasonal basis: the Aleutian Low and the North Pacific High (Fig. 6-66). During winter the Aleutian Low dominates the weather pattern and no consistent flow parallels the chain that could promote upwelling. In summer, however, the North Pacific High is the dominant weather pattern affecting the area. As can be seen in Fig. 6-66, winds tend to blow from the southwest, parallel to the chain during this period. This is precisely the necessary direction to promote the observed upwelling and the general wind direction prevailing at the time of these data (shown by the advection of cloud patterns in Figs. 6-64 and 6-65).

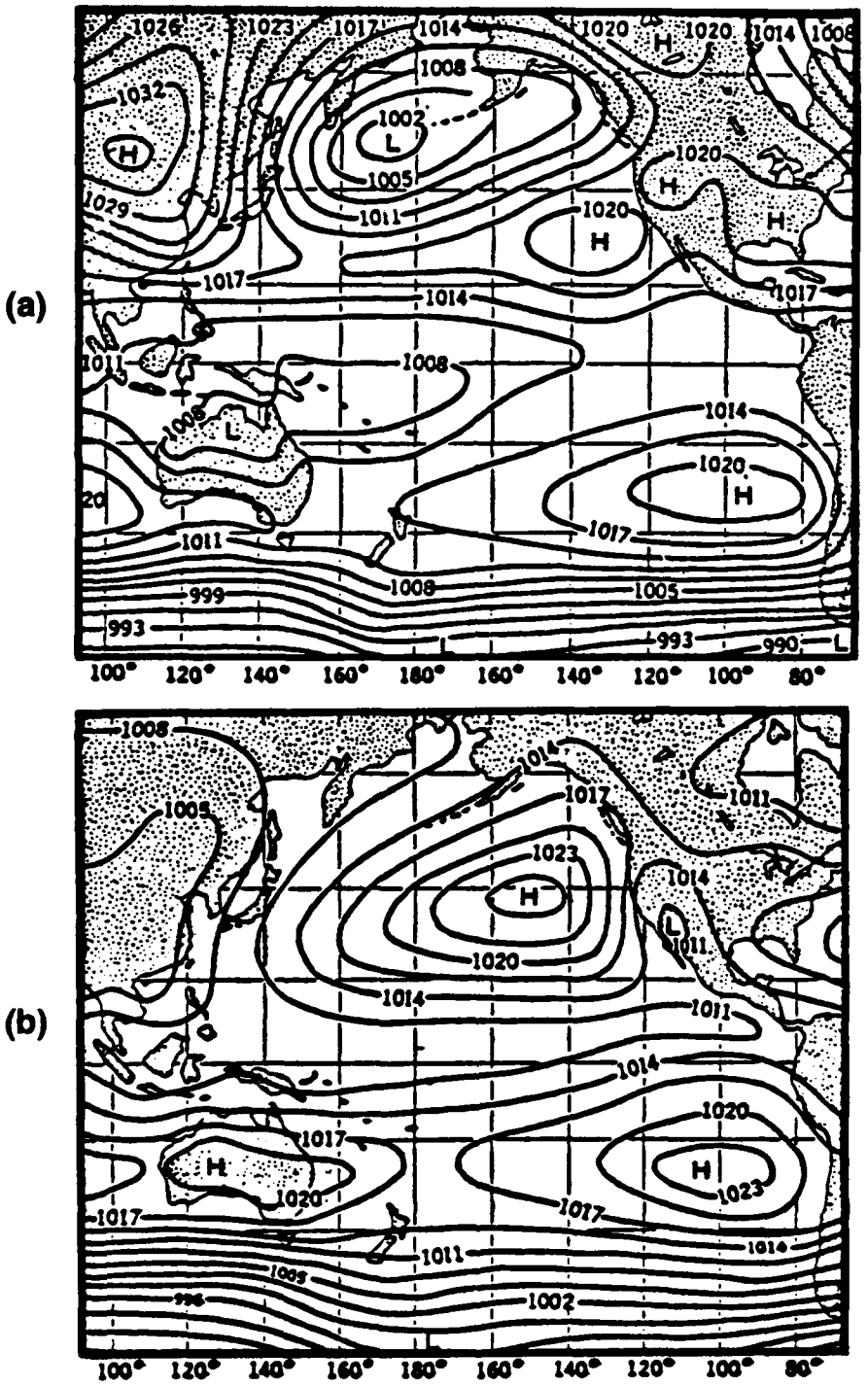

Figure 6-66. Atmospheric pressure over the Pacific; above, in northern winter (January); below, in northern summer (July) (Encyclopedia of Oceanography, 1966).

One other point is of great interest with regard to this study. The mean air temperature for islands in the western Aleutians is very close to the value of the mean sea surface temperature during the months of May through October. As an example, the October mean air temperature for Amchitka is 45.3 °F (7.4 °C) and the mean sea surface temperature surrounding the island is 45 °F (7 °C). One would therefore anticipate that there would be times during the day when the island would be invisible in remotely-sensed infrared data, even under clear sky conditions, since the island temperature and sea surface temperature could be identical. Since the mean air temperature is actually warmer than the mean sea surface temperature the island should at times appear as a warm area surrounded by colder water. Diurnal heating under clear sky conditions should further emphasize this effect. Figure 6-67 shows an example where this has happened. The DMSP infrared data are shown in this example for 30 September 1990 at 1029 LST. It can be seen that the island of Amchitka is revealed as a warm feature surrounded by colder water. Despite the prevailing clear sky conditions, most of the other islands including Kiska, Adak, Atka, and Amlia are invisible or barely perceptible because their temperatures are apparently the same as the surrounding water.

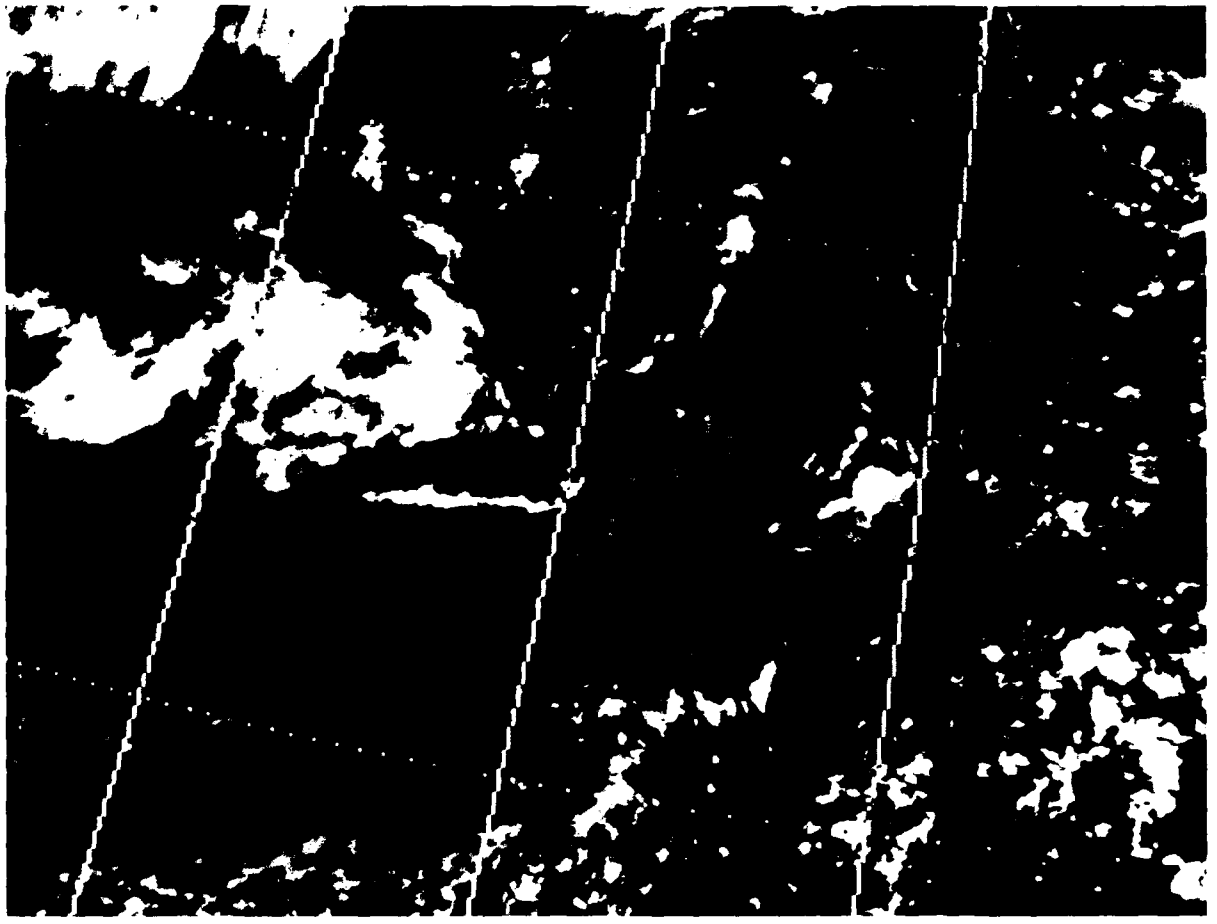

Figure 6-67. DMSP infrared imagery 2029 GMT 30 September 1990.

6.6 Pack Ice

Pack ice coverage changes in response to winds and ocean currents. In areas near the ice sheet edge waves and swells can also affect ice motion. The following case studies discuss three examples of pack ice coverage.

6.6.1 Extreme Change of Areal Ice Cover in the Eastern Bering Sea, 7–12 January 1990

The areal ice coverage of the Bering Sea had retreated northward to the vicinity of St. Lawrence Island by 9 January 1990. The retreat resulted from a period of strong, warm southerly flow on the west side of a blocking high centered over the Gulf of Alaska, with ridging northward to beyond Alaska into the Arctic basin. Temperatures above freezing were experienced at Nome and likely even further north over the water area. Southerly winds of 20 to 25 kt (10–13 m/s) prevailed for several days prior to 9 January. By late on that date the high had started breaking down and more typical zonal flow rapidly became reestablished. By 12 January cold northerly flow prevailed over the eastern Bering Sea and the ice coverage had advanced southward beyond St. Matthew Island and east-southeastward to northern Bristol Bay. The 3-day advance was on the order of 300 to 400 n mi (556–741 km).

Air temperatures at St. Paul Island (station 70308) fell from 36 °F (2 °C) on 7 and 8 January to 10 °F (−12 °C) by 11 January. Nome reached a high of above freezing on the 7th, then cooled off to −6 °F (−21 °C) by the 9th, warmed slightly to 12 °F (−11 °C) on the 10th, and then dropped to below −4 °F (−20 °C) by the 11th. The temperature change in the vicinity of St. Paul Island between 0000 GMT 10 January and 1200 GMT 11 January would have changed the superstructure icing rate from no icing to one of heavy to very heavy (0.8 to ≥2 inches/hr or 2–5 cm/hr).

Discussion

Prior to the event to be described, a long wave blocking high extending over Alaska from the northeast Pacific had resulted in strong southerly flow from south of the Aleutian Islands northward deep into the Arctic basin. Figure 6-68 illustrates the surface pattern at 0000 GMT 8 January 1989. The 500-mb pattern (not shown) reflected the same basic configuration. The 1833 GMT 7 January 1989 DMSP infrared image (Fig. 6-69) shows the meridional configuration of frontal cloud bands extending from near the Aleutian Islands and southeast Alaska well into the central Arctic basin. The anticyclonically curved cirrus shield over the central Bering Sea, together with the cyclonic flow over the Gulf of Alaska, is a likely indicator of a breakdown in the long wave meridional flow pattern. The dark

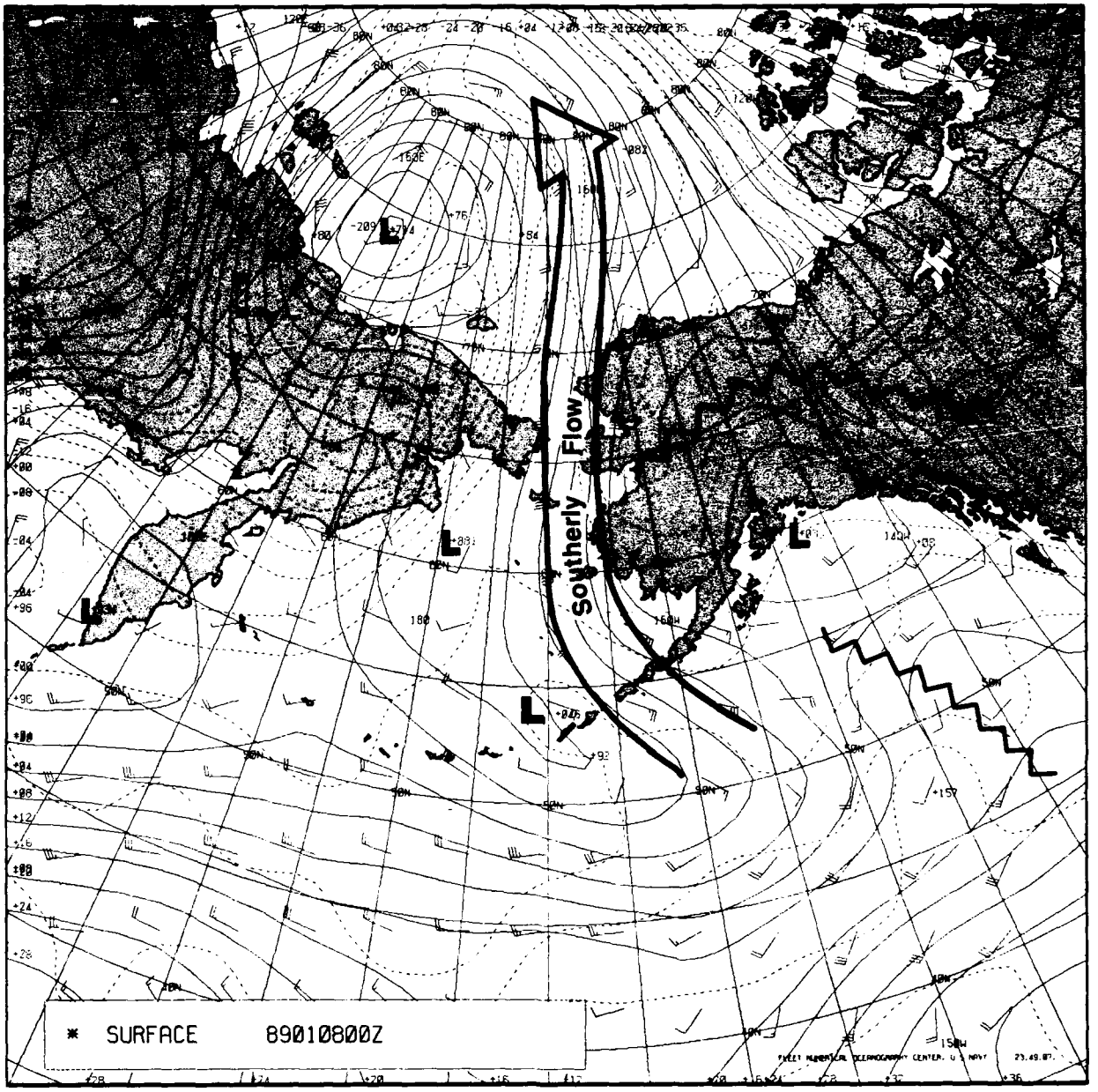

Figure 6-68. FNOC surface analysis 0000 GMT 8 January 1989.

Figure 6-69. DMSP infrared imagery 1833 GMT 7 January 1989.

shade of the Bering Sea water area between the west coast of Alaska and the approaching cloud band indicates ice-free areas of relatively warm (above freezing) sea surface. West of the cloud band ice cover along the southern coast of Siberia is seen as light gray areas. Figure 6-70 shows a DMSP infrared image 36 hr later at 0640 GMT 9 January. The eastern Bering Sea is still largely ice free and a large polynya can be seen extending northward from St. Lawrence Island. The faint gray shade over the area from eastern St. Lawrence Island southeastward to the Alaskan coast indicates a limited amount of new ice forming, but still much less and warmer (newer) than the ice west of St. Lawrence Island in the Gulf of Anadyr. This ice coverage distribution pattern is anomalous in that the area to the east of St. Lawrence Island generally has more and older ice than the area to the west of the island. An important synoptic observation at this time shows that the frontal cloud band is no longer continuous from south of the Aleutian Islands northward into the Arctic,

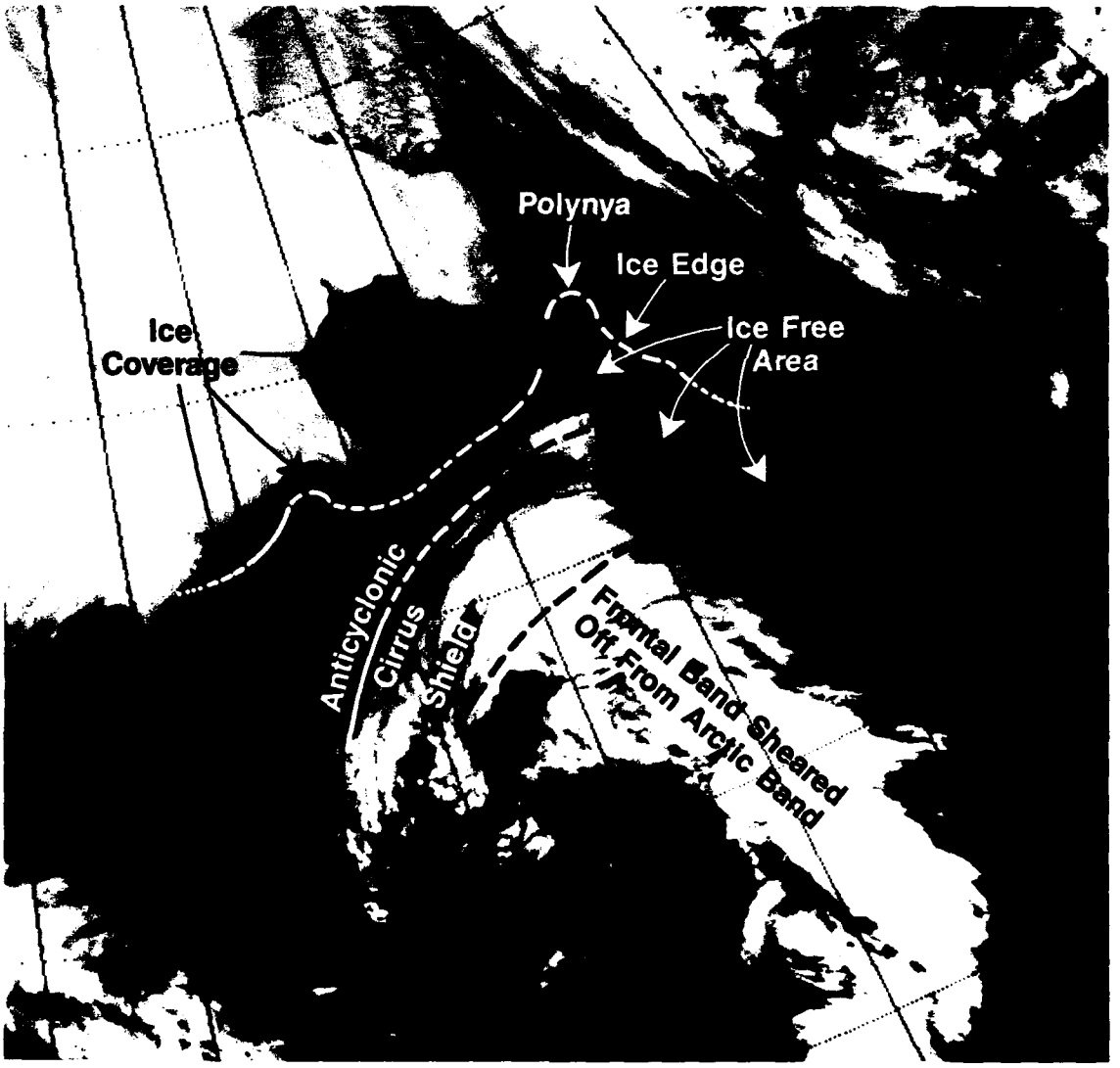

Figure 6-70. DMSP infrared imagery 0640 GMT 9 January 1989.

which indicates a breakdown in the long wave meridional flow pattern. Both surface (Fig. 6-71) and 500-mb analyses (not shown) of 1200 GMT 9 January 1989 indicate the return of zonal flow and end of the blocking pattern, and resulting extensive southerly flow and warm air advection northward from the midlatitudes over the eastern Bering Sea and beyond. Synoptic scale southerly flow in advance of the central Bering Sea Low is, however, still occurring.

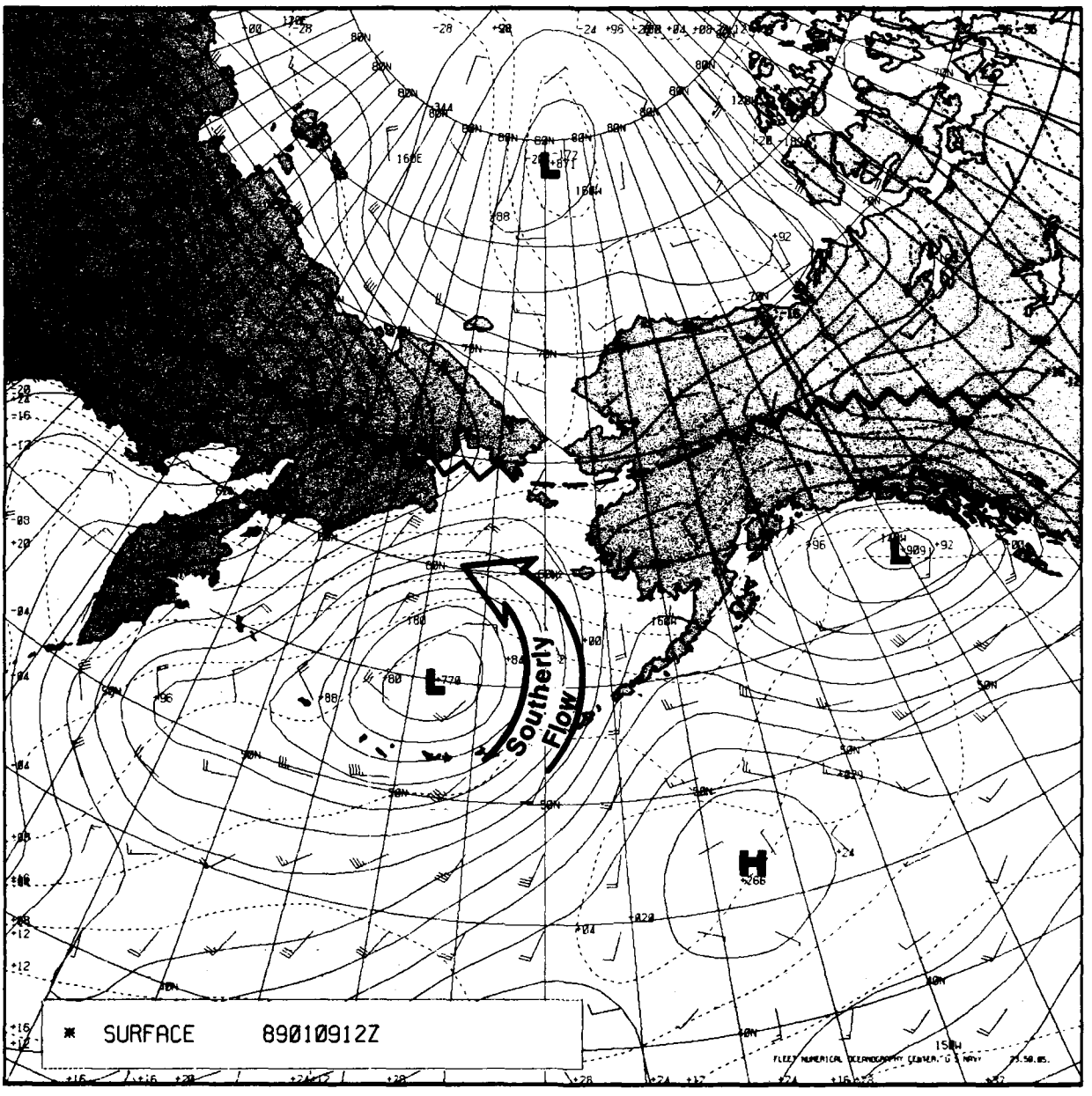

Figure 6-71. FNOC surface analysis 1200 GMT 9 January 1989.

The rapid return of the ice cover over the eastern Bering Sea, through combined refreezing and wind advection, is clearly shown in the 1614 GMT 12 January 1989 infrared DMSP image (Fig. 6-72). Ice now covers most of the eastern Bering Sea from St. Matthew Island east-southeastward to northern Bristol Bay. Further evidence of the magnitude of change is reflected in the configuration of polynyi. The open water or newly formed ice areas are now seen south of not only St. Lawrence Island but also south of the Diomede Islands in the Bering Strait, Wrangel Island in the northwest Chukchi Sea, Nunivak Island, and along the south-facing coasts of Siberia and Alaska. New ice appears darker, and in fact until it is more than a few inches (centimeters) thick, it may not be distinguishable from open water. Therefore, it is unlikely that the dark areas identified as polynyi are totally ice free. In fact, with the ocean precooled to the freezing point over the shallow shelf area and air temperatures of 5 to −13 °F (−15 to −25 °C), some form of new ice is likely throughout the "polynya" appearing areas.

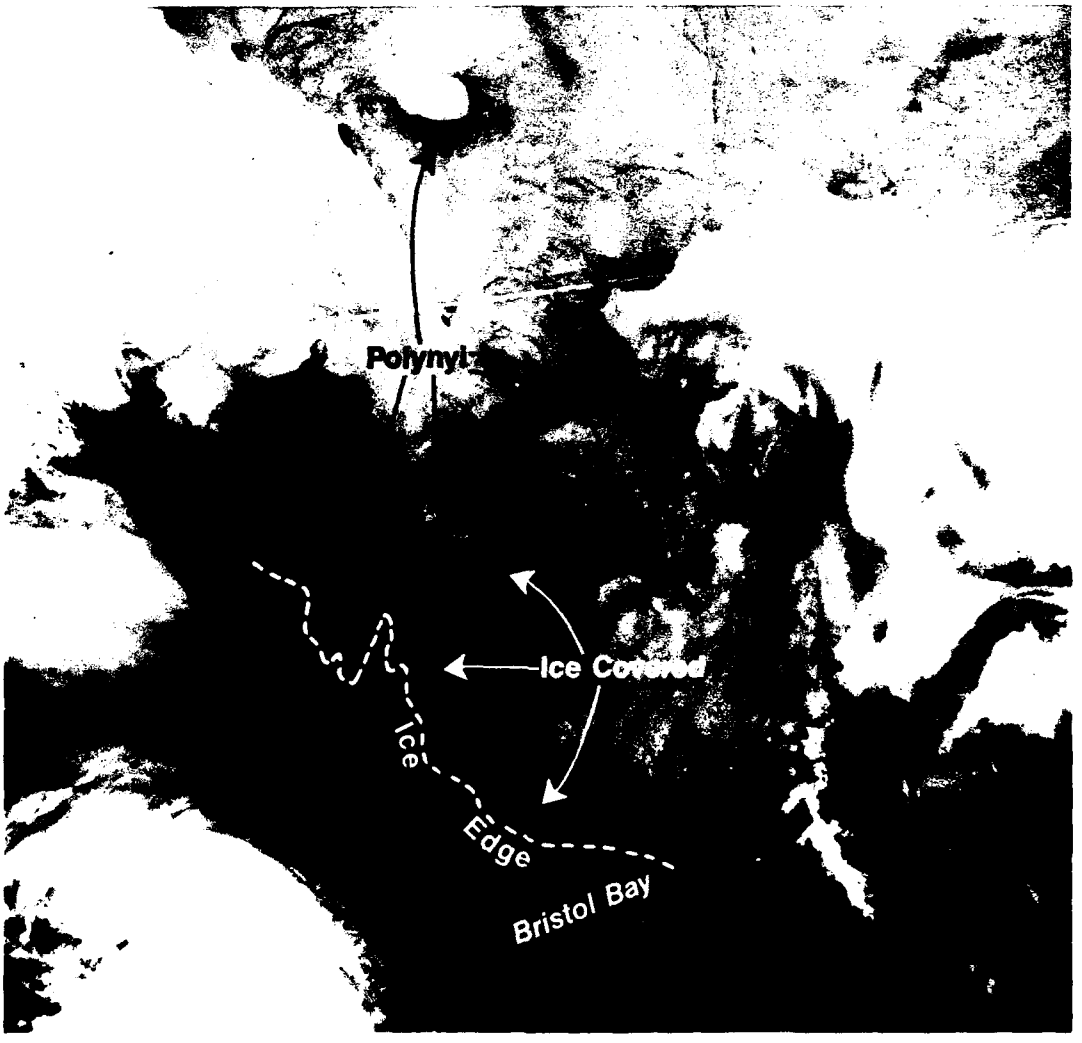

Figure 6-72. DMSP infrared imagery 1614 GMT 12 January 1989.

Forecast Factors

1. Rapid changes frequently occur over the Bering Sea. In this example a large area of open water between St. Lawrence Island and Nunivak Island became ice-covered in about 3 days.
2. During winter the ice edge and coverage area may advance at the rate of a couple hundred nautical miles (300–400 km) a day under strong, cold northerly flow, following periods of anomalous northward retreat under strong, warm southerly flow.
3. Blocking high patterns that may persist for a week or more result in marked warm air advection on their western boundary.
4. When the long wave blocking pattern breaks down, the rapid return of cold northerly flow will result in temperature drops of 59 to 68 Fahrenheit degrees (15–20 Celsius degrees) within a day or two.
5. When the circulation pattern change results in strong northerly flow (25–35 kt or 13–18 m/s, or greater) and cold temperature 14 to −13 °F (−10 to −25 °C), the superstructure icing conditions can change from no icing to heavy to very heavy icing (1–2 inches/hr or 2.5–5 cm/hr) within a day or two or less.

Forecast Aids

1. The numerical progs should be watched for indications of the configuration or breakdown of meridional flow patterns, which can result in extreme changes in environmental conditions.
2. Satellite imagery indicates the breaking down of the meridional flow by the shearing off of the midlatitude frontal cloud band from the Arctic region cloud band.
3. Appearance of anticyclonic cirrus shields across frontal cloud bands indicate a return to zonal flow rather than meridional flow at the level of the cirrus and probable breakdown of the blocking pattern.
4. The change of location of polynyi around islands and in coastal areas reflects changes in wind direction, and in the direction of ice movement.
5. Sea water freezes at about 28.8 °F (−1.8 °C); air temperatures lower than this will result in the accumulation of superstructure ice accumulation.
6. Superstructure icing rates are reduced by running vessels with the wind and/or moving to the lee of terrain barriers.
7. Polynyi form to the lee of islands and off lee coastlines and may extend 100 n mi (185 km) or so offshore in the Bering Sea. However, they are very nonpersistent and can open or close or freeze over in less than a day.
8. If, during the freezeup or winter periods, the location of the ice edge or areal coverage is well to the north of the seasonal mean location, there likely will be a period of rapid southward advance during adjustment back to a more typical atmospheric circulation pattern.

Forecast Insights

1. Ice conditions are a reflection of prior atmospheric forcing and, to some extent current conditions. Anomalous ice conditions that reflect anomalous atmospheric preconditioning can be used as insights to the expected rapid return to normal conditions once the anomalous forcing is removed.
2. Long-wave blocking patterns are quite stable and likely to persist for several days. The tendency for a late January thaw or warm period occurs often enough over the Bering Sea and Alaskan area to be noted as a singularity for that region. The return to winter conditions, being a sure thing and likely to occur rapidly, must be closely monitored by forecasters, particularly if units of concern have recently entered the region when it has been under the influence of the warm spell.
3. Areas that appear ice free in satellite imagery may be covered with a couple of inches (centimeters) of new ice.

6.6.2 Fall Pack Freezeup Patterns, 20–23 December 1989

On 20 December 1989 (Fig. 6-73) new ice formation is seen as light gray areas extending from the Bering Strait, south and eastward past St. Lawrence Island, and along the Alaskan coast beyond Nunivak Island to near 59 °N. The ice in the area from the Bering Strait to north of St. Lawrence Island is of the lightest shade of any ice in the Bering Sea, reflecting the coldest and thickest ice of the area. The small northward arching crescent in the western Bering Strait indicates some outflow from the Chukchi Sea southward through the strait. At this time, however, the lack of clouds over the northern Bering Sea indicates near calm conditions. The area westward from St. Lawrence Island across most of Anadyr Gulf, except along the Siberian coast, appears ice free. The faint gray shade near the Siberian coast indicates an area of new ice formation. The ice-free area overlies slightly deeper water (>164 ft or >50 m) than the coastal area and the areas to the east and south-southeast of St. Lawrence Island (see Fig. 2-7 in Chapter 2) where ice is forming.

By 23 December (Fig. 6-74) the off-ice flow has started to increase as evidenced by the cloud lines forming to seaward of the ice cover in the eastern portion of the image. Close inspection of the cloud lines help define the outer edge of the pack. The existence of open water along the south-facing coastlines is also indicated by cloud lines emanating from the slightly darker areas along coasts inside the leading edge of the ice. Cloud lines are seen in this image extending from the coastal areas just north of Nunivak Island and in Kuskokwim Bay. The deeper water area west of St. Lawrence Island remains mostly ice free. South of St. Lawrence and along the south-facing coast of the Seward Peninsula the typical polynya formations where new ice is constantly being formed can be seen. These are at the source areas for the conveyor belt ice formation conceptual model (discussed in Section 3.1.9). Ice bands parallel to the wind at the leading edge of the pack can be seen in the edge area south of St. Lawrence.

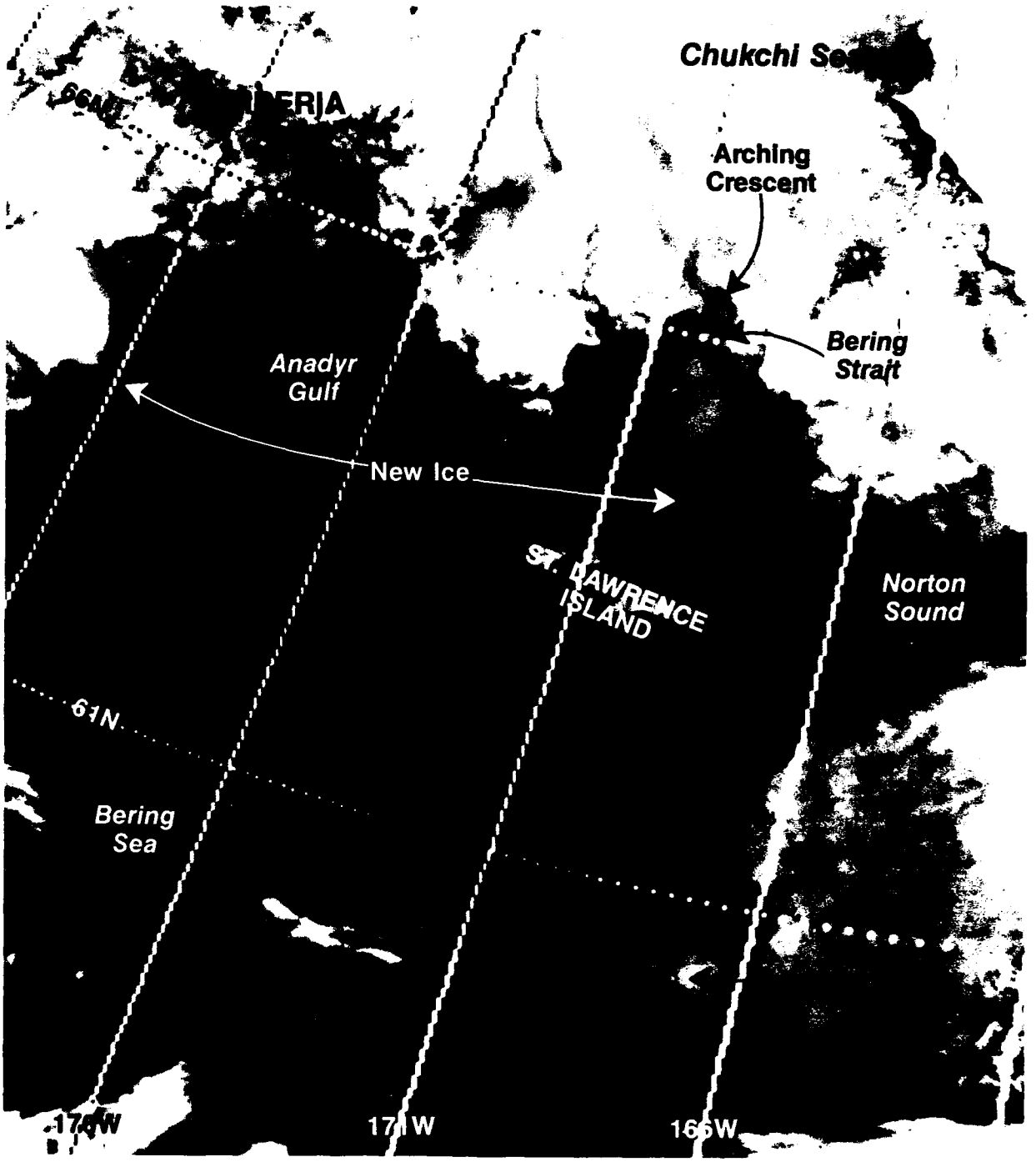

Figure 6-73. DMSP infrared imagery 1936 GMT 20 December 1989.

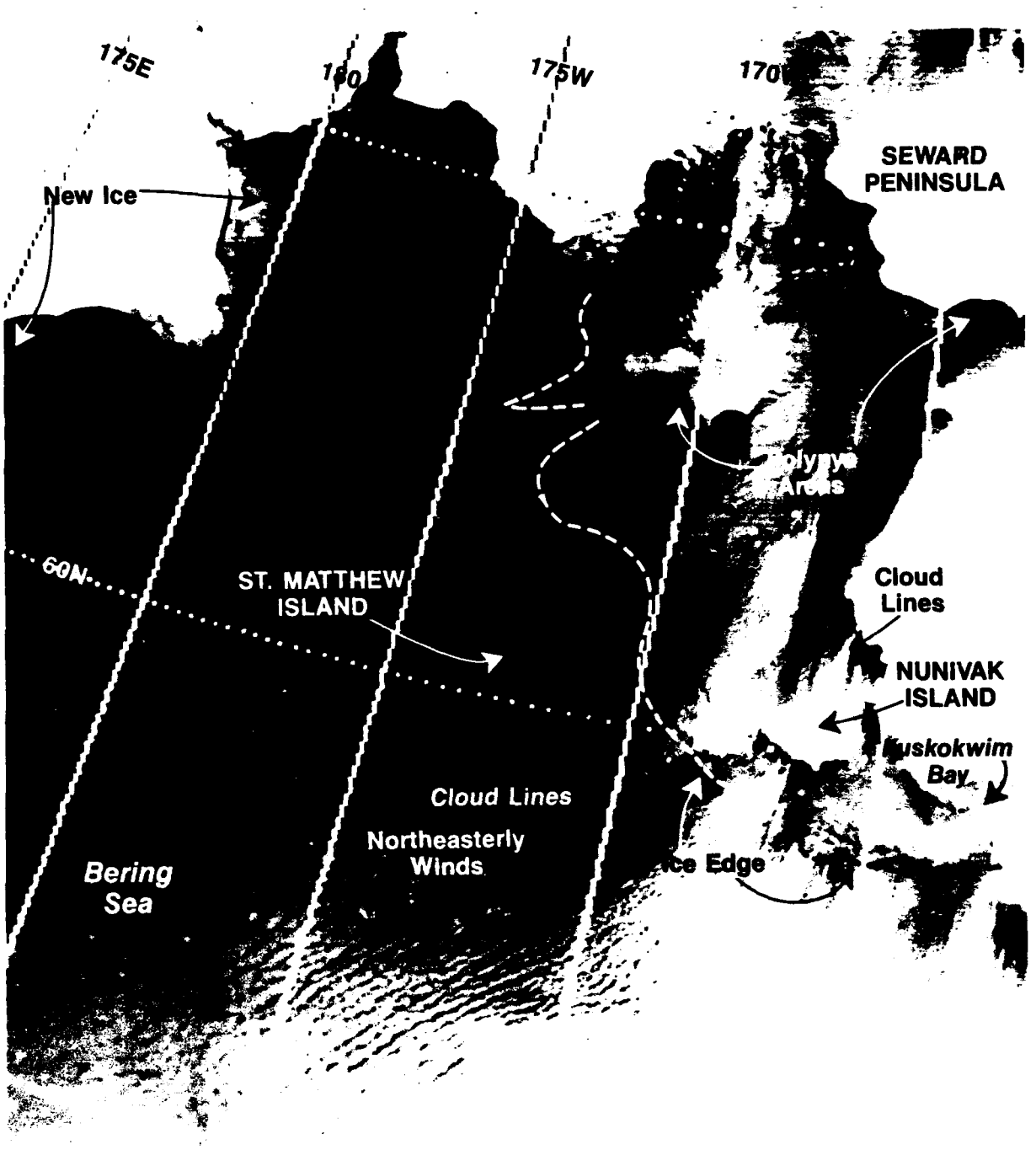

Figure 6-74. DMSP infrared imagery 1647 GMT 23 December 1989.

Satellite Imagery Forecast Aids

1. Sea ice forms first in the shallowest areas of the northern Bering Sea where the water column becomes isothermal at about 28.9 °F (−1.7 °C). In infrared imagery new ice first appears as dark gray and, if not covered by snow, gradually becomes lighter shades of gray as the ice thickens.
2. Darker areas along coastlines with lighter areas offshore (ice covered) indicate areas of offshore wind. As the new ice forms near the coast it is advected offshore resulting in the thinnest ice or open water in the near coastal areas. Under the prevailing northerly winds of the northern Bering Sea, regions of persistent polynyi include the areas of south-facing coastlines of Alaska and Siberia and to the lee (south side) of St. Lawrence, St. Matthew, and Nunivak Islands.
3. When ice flows through a restricted passage such as the Bering Strait the ice cover fractures in a crescent shape, arching against the direction of flow. Because the average ocean current is northward through the Bering Strait, crescents as seen in this case only form when strong northerly winds overcome the northward set and ice advection of the ocean current.

6.6.3 Spring Pack Ice Breakup Patterns, April 1990

The spring breakup of pack ice over the Bering Sea takes on more than one pattern. The normal pattern is for the pack ice to first clear along the Alaskan coast from Kuskokwim Bay northward through Etolin Strait to near the southern shores of Norton Sound, about 63 °N (Miller, 1973). However, it is further noted by Miller that the breakup pattern for the Bering Sea is not consistent. Sometimes the breakup pattern occurs first along the Siberian coasts. At other times the breakup may occur simultaneously along both the Alaskan and Siberian sides of the sea. This case provides illustrations of the normal pattern and the combined version showing breakup along both the Alaskan and Siberian coasts. Note that the examples are only separated by 17 days. The pack ice, in fact, responds very rapidly to changing wind patterns, often within a day or less, during the breakup season when the ice floes are free to move independently of each other. The free movement of the open pack during breakup is in contrast to the winter, large area, semi-rigid condition of frozen, consolidated large floes or nearly solid pack conditions when pack movement response is restricted.

11 April 1990, Normal Spring Breakup Pattern

Figure 6-75 from 11 April 1990 reflects the normal breakup pattern. The pack ice has cleared along the Alaskan coast from Kuskokwim Bay northward to extreme southwestern Norton Sound. Open water is also seen in eastern Norton Sound. Near ice-free areas exist both south and northwest of St. Lawrence Island. Other ice features include the coastal lead along the north coast of Siberia near 170 °W to the vicinity of 165 °E, the banding configuration of the ice edge in the central Bering Sea, and the concentration of larger floes in the area from northeast of St. Lawrence Island around its eastern end and then

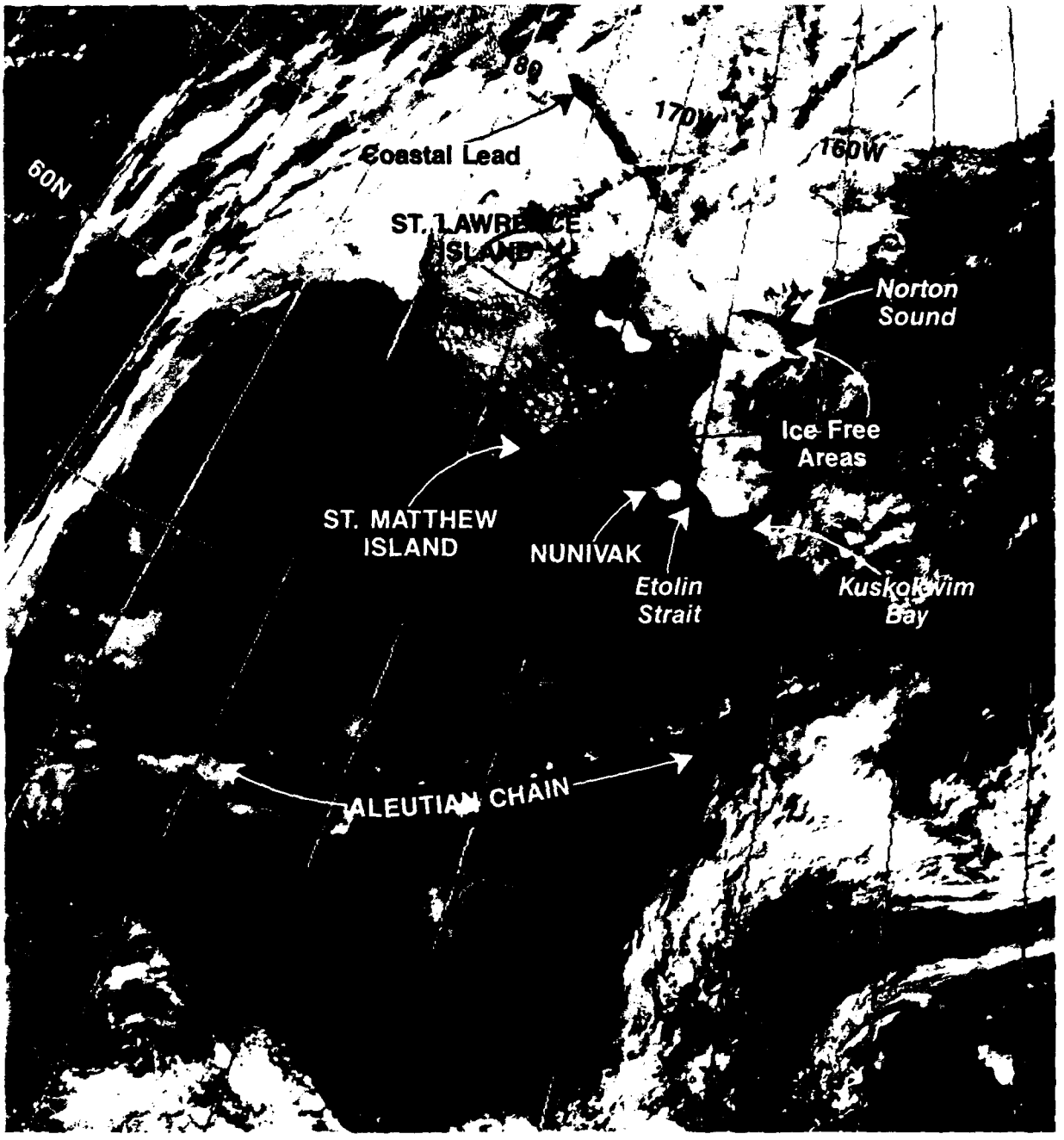

Figure 6-75. DMSP visible imagery 1944 GMT 11 April 1990.

southwestward to near St. Matthew Island. This latter area has been noted to typically contain the thickest and oldest ice floes and be the last area to clear of ice. Another notable feature in this image is the snow-capped mountains of the Aleutian chain and Alaska Peninsula, which show as bright white spots. Terrain features over land areas such as snow-covered mountains and treeless flat lands (white areas of Alaska) and rivers and tree-covered regions (dark areas of Alaska) are also apparent in this view. Recognition of various terrain features in views of opportunity will frequently be useful in gridding or checking gridding in imagery where cloud cover dominates.

28 April 1990, Combined Alaska and Siberian Coastal Breakup

The ice breakup pattern seen in Fig. 6-76 shows the combined version. The Siberian side has opened significantly since 11 April, and some closing of the Alaskan coastal lead north of about 61.5 °N has occurred. The northern Siberian coastal lead extends northwest from the Bering Strait to near 175 °W but is closed for at least 300 n mi (556 km) to near 172 °E. The open areas noted around St. Lawrence Island on the 11th now contain significant amounts of ice, and a new open area now extends southwestward from the island. Overall the total amount of ice in the Bering Sea appears to have decreased during the period as one would expect during spring. The rearrangement of the ice locations would, of course, be of operational concern for units in the northeastern Bering Sea. During the period of breakup and free moving ice, conditions can change rapidly with shifting wind patterns. Close attention must be paid to both synoptic and local wind conditions when forecasting ice conditions during the breakup period.

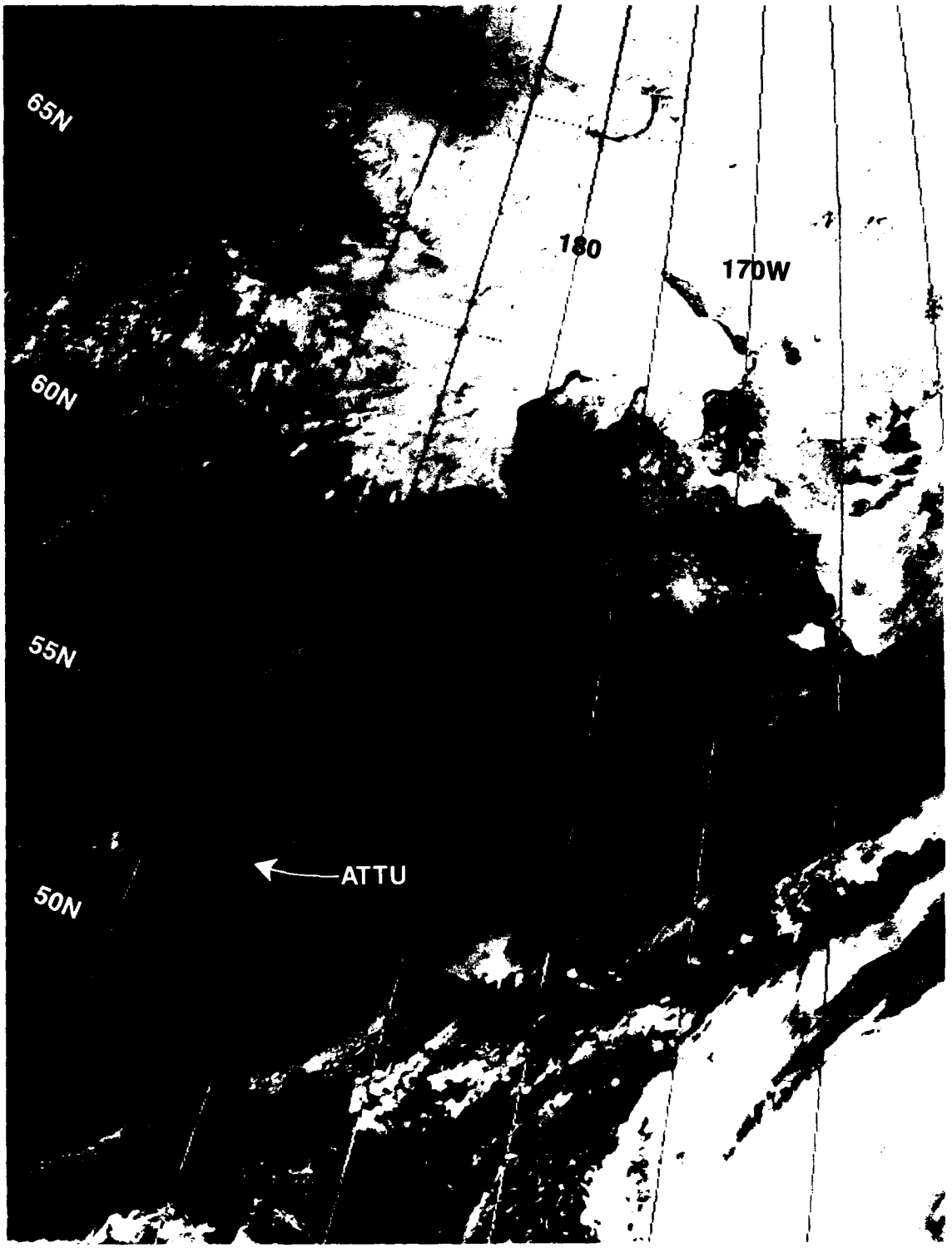

Figure 6-76. DMSP visible imagery 2125 GMT 28 April 1990.

7. ICING

The ability to forecast vessel icing is one of the more challenging tasks facing marine meteorologists in high-latitude waters. Rapid accretion on superstructures creates an extreme hazard for vessels because of the lack of stability.

7.1 Superstructure Icing

In the case of smaller ships, the added weight of the ice reduces freeboard and therefore reduces the range of stability of the vessel. Ice formed high on masts, rigging, and superstructures alters the vertical center of gravity, and the vessel may become top-heavy and capsize. For larger vessels, including warships, the primary effects of topside icing, in addition to ship systems and combat systems inoperability, are increases in the ship's displacement and vertical center of gravity. Ice accretion on the windward side of the ship, caused by spray from wind abeam of the ship, can create a shift in the ship's transverse center of gravity resulting in a list. The degree of hazard these conditions may pose is dependent on several factors: type of ship, ship's stability status, and ship's ballasting capability. Ships with relatively large superstructures and low freeboard (FF, FFG, CG, CGN, DD, DDG) are especially vulnerable. Larger aviation type ships (CV, CVN, LHA, LHD) are less vulnerable (U.S. Navy, 1988).

7.1.1 Types of Ice Accretion

Liquid particles can come from atmospheric processes or be windborne. Atmospheric sources result in the formation of frost, rime, or glaze ice, whereas spray sources can result only in the formation of rime or glaze (Minsk, 1980).

Frost is caused by water vapor sublimating on a surface that is at or below freezing. A more proper term would be "hoarfrost." Hoar is the generic term for ice crystals formed directly from the vapor phase. Hoarfrost can form only when the air is still or nearly so. The resulting bond can be very strong such as on windows, or weak such as on a snow surface. Since there is little water vapor at subfreezing temperatures, the rate of accumulation and total accumulation on exposed surfaces are small compared to other types of ice accretion.

Discrete water droplets in the atmosphere can easily become supercooled because of their small volume. When the supercooled droplets strike a surface that is at or below freezing they will freeze, forming *rime* ice. Hard rime will form when freezing is relatively slow; soft rime occurs when droplets freeze rapidly upon deposition, resulting in a granular structure. The denser, hard rime appears milky or translucent, depending on the amount of air trapped within the structure. Soft rime, because of its much lower density, is more delicate in structure and may appear fluffy.

Glaze or clear ice forms when water droplets striking a surface have sufficient time to flow in a continuous film over the surface prior to freezing. This condition creates hard, nearly homogeneous, nearly bubble-free ice, which is sometimes referred to as glare ice or black ice. Because the surface has been wetted nearly completely prior to freezing, a very strong bond results. Increasing droplet size increases the likelihood of glaze ice formation.

Droplets can be generated by breaking waves, by the shattering of trapped air bubbles as they rise to the surface of the water, and by wind forces. But the splashing of waves against an object in the water, such as a ship's hull, produces the most and largest droplets. *Spray ice* or *freezing spray* originating from seawater will generally include brine pockets, since salts must be rejected before the ice will freeze at 32 °F (0 °C). Sea spray ice, therefore, is weaker than freshwater ice, but it may adhere just as strongly to a surface when no brine pockets are present at the interface. Freezing spray is the most dangerous form of icing. It occurs when the air temperature is below the freezing temperature of the sea water, about 28 °F (−2 °C). The spray freezes on the exposed surfaces of the vessel to produce clear ice or glaze. At lower air temperatures, the ice may be opaque, which may be due to the spray being supercooled so that it partially freezes on impact and entraps air. At extremely low temperatures (1 °F or −17 °C, and below), as might be encountered in anchorages or close inshore, wind-induced spray may be frozen before it strikes the vessel, so that it does not adhere to the vessel, but may form drifts on deck. With air temperatures below 28 °F (−2 °C), freezing spray is observed in winds of 18 kt (9 m/s) or higher. The lower the air temperature and the stronger the wind, the more rapid is the accumulation of ice. A low sea temperature also increases the rate of accumulation of ice.

Once spray is produced, two other factors become important: (1) the vertical distribution and (2) the size of the droplets. These factors determine the rate of cooling of the droplets on their trajectory toward the ship. Once the spray reaches vessel surfaces, continued cooling of the ocean water from its sea temperature to the freezing point is determined by the heat flux away from the spray, a function of local wind speed and air temperature.

Sea spray usually does not extend more than about 50 ft (15 m) above peak water level. Flooding of ship decks by wave action normally does not result in ice. The huge volumes of water often accompanying wave action flooding will wash away deck ice that has not yet bonded firmly to any surface. However, deck icing could result if the water cannot be drained and becomes puddled.

Since a ship can present different aspects to the wind and spray source, it is to be expected that the amount of spray reaching the ship will vary. Observations aboard medium-sized trawlers have shown that the greatest frequency of spray, and therefore icing, occurs when a ship is heading into the wind at an angle between 15 and 45 °. Asymmetrical icing

occurs under this condition with the greater accumulation on the windward side. Lesser icing occurs with the ship headed directly into the wind, and then accumulation tends to be uniform. For a period of about 2 hr after ice formation on metal or canvas surfaces, the ice is loosely bonded and can be easily knocked or scraped off. After that time the ice becomes very tightly bonded to the surfaces and can be removed only with great difficulty (Minsk, 1977).

Sea spray generation depends on the wave height and period of waves. Waves in turn depend on the speed, duration, and fetch of the wind. Generally, the higher the wind speed for the critical temperature ranges (discussed below), the greater the ice accumulation. One factor that can reduce the effect of high wind speeds on icing is the concentration of the ice pack. Obviously, if the ice pack concentration exceeds about 50%, wave formation is sharply reduced, and freezing spray is minimized.

7.1.2 Conditions for Icing

The critical range for icing is from 0 to 32 °F (−18 to 0 °C). At temperatures below 0 °F (−18 °C) the spray striking the structure will usually be in the form of nonadhering small dry ice crystals. A Japanese study proposed a handy rule of thumb: during offshore flow of Arctic air, ship icing is likely when the 850-mb temperature is −4 °F (−18 °C) or colder (Taiyo Fishing Company, Ltd., 1972).

The critical range of sea surface temperatures are 28 to 48 °F (−2.2 to 8.9 °C). Seawater of normal salinities is generally frozen below 28 °F (−2.2 °C). The upper value of 48 °F (8.9 °C) is not an impediment to freezing since sea spray can be cooled rapidly when air temperatures are below 28 °F (−2.2 °C).

Added to the spray blown from the wave caps is the spray generated by the vessel herself. The amount of spray generated depends on the ocean wave field, the vessel length, its seakeeping ability, stability, freeboard, hull shape, and vessel heading and speed relative to the wave field. As the dominant wavelength approaches the vessel length, vessel vertical motion is enhanced. This interaction between the vessel and the sea causes an increase in the amount of spray.

It should be emphasized that an accumulation of ice will, in itself, speed up the rate of accumulation. The ice already formed increases the effective cross section of rigging, mast, rails, and antennae exposed to the spray.

7.1.3 Ice Producing Phenomena

As discussed previously, many factors affect the rate and total amount of accretion of shipboard icing: air temperature, wind velocity, water temperature, ship direction relative to the wind, and ship geometry. Atmospheric conditions and sea conditions act in concert to create icing. In subfreezing temperatures precipitation such as snow, freezing rain, or mist can result in the formation of ice layers on exposed areas of a ship. However, high winds cause particularly heavy icing due to seawater spray, and approximately 90% of all ship icing is caused by spray. In addition to spray, two other common sources will cause icing in Alaskan waters: freezing rain and Arctic sea smoke.

Freezing rain will cover a ship or small craft with freshwater glaze (clear) ice. However, the weight of the accumulated ice is unlikely to be sufficient to endanger the vessel directly because the rates of ice accretion depend on rainfall rates, which are not great in Arctic airmasses.

Arctic sea smoke occurs when the air temperature is at least 16 °F (9 °C) colder than the sea. If the air temperature is below 32 °F (0 °C), then the Arctic sea smoke is called Arctic frost smoke. This frost smoke is often confined to a layer only a few feet (centimeters) thick, and trawlermen in northern waters refer to it as "white frost" when the top of the layer is below the observer's eye level. It is referred to as "black frost" when it extends above eye level.

The small water droplets in frost smoke are supercooled. On contact with exposed surfaces on a vessel, part of the droplet freezes immediately, while the remainder stays liquid for a short time before it too freezes. The result of the instantaneous freezing of the supercooled droplets is an accretion of opaque, white rime ice with trapped air. Because rime ice is porous it is easier to remove than clear ice (glaze). In one case a ship (of unknown size) caught in air temperatures colder than 14 °F (−10 °C) and dense frost smoke, accumulated 4 inches (10 cm) of rime ice on deck and 12 inches (30 cm) on the ship's side at rail level during a 12-hr period. This represented an ice accumulation of nearly 2.5 tons/hr (2268 kg/hr).

7.1.4 Estimating Rates of Accumulation

No exact methods of ice accretion prediction exist. However, research and observations by scientists and mariners have produced some reliable indicators that can be plotted graphically. A major breakthrough in ice accretion prediction occurred in 1968, with the use of the Mertins icing diagrams. Since then, improved databases and improved methods of analysis have resulted in more accurate icing diagrams. Figure 7-1 shows the latest icing nomograms. These nomograms are endorsed by the National Oceanic and Atmospheric Administration (NOAA), and NOAA recommends that previous nomograms and the Mertins tables be disregarded (U.S. Navy, 1988).

The nomograms of Fig. 7-1 are based on small ship studies and are provided as baseline data. As the size of the ship increases, a proportional decrease in the amount of accretion can be expected. These nomograms show potential icing on the ship's superstructure for four water temperature ranges and a ship heading into the wind, or with the wind on the beam. Ships running downwind will not likely incur accretion rates as high.

These nomograms offer the best prediction method for icing available to the fleet. Laboratory experiments conducted at the Naval Applied Science Laboratory provide some further indication as to the potential weight increase that a ship may experience. A wind speed of 10 kt (5 m/s) and an air temperature of 0 °F (−18 °C) will yield an hourly accretion rate of 8 lb/sq ft (39 kg/sq m). An Oliver Hazard Perry class frigate has over 7000 sq ft (650 sq m) of exposed area on the forward one-third of the ship. Therefore, ice accretion could amount to 25 long tons/hr (25,400 kg/hr) of extra weight.

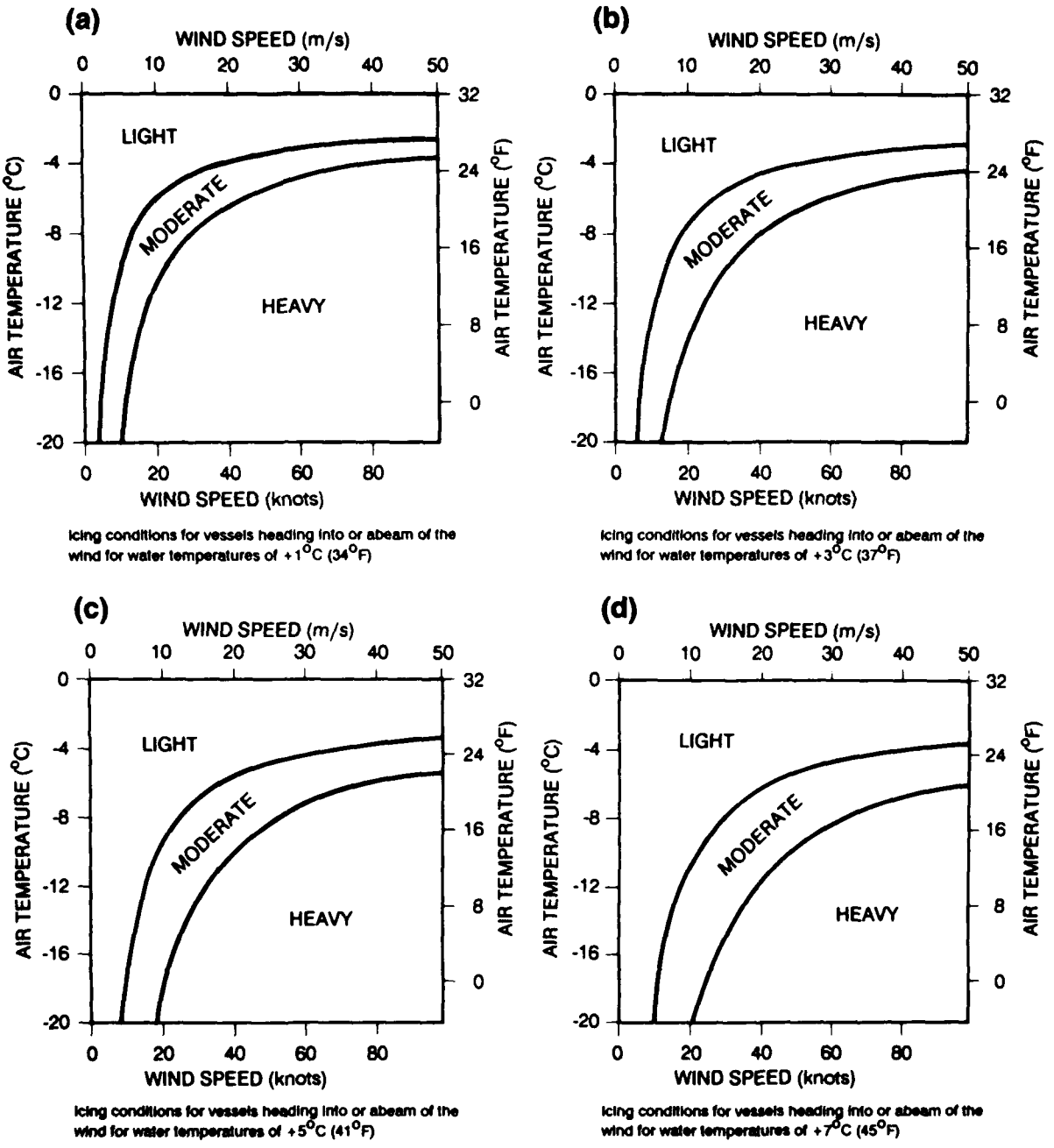

Light Icing - Less than 0.7 cm/hr (0.3 in/hr)
Moderate Icing - 0.7 cm/hr (0.3 in/hr) to 2.0 cm/hr (0.8 in/hr)
Heavy Icing - Greater than 2.0 cm/hr (0.8 in/hr)

Figure 7-1. Latest icing nomograms (U.S. Navy, 1988).

Figure 7-2 is an icing nomogram based on the four nomograms shown in Fig. 7-1. It combines the four graphs into one nomogram.

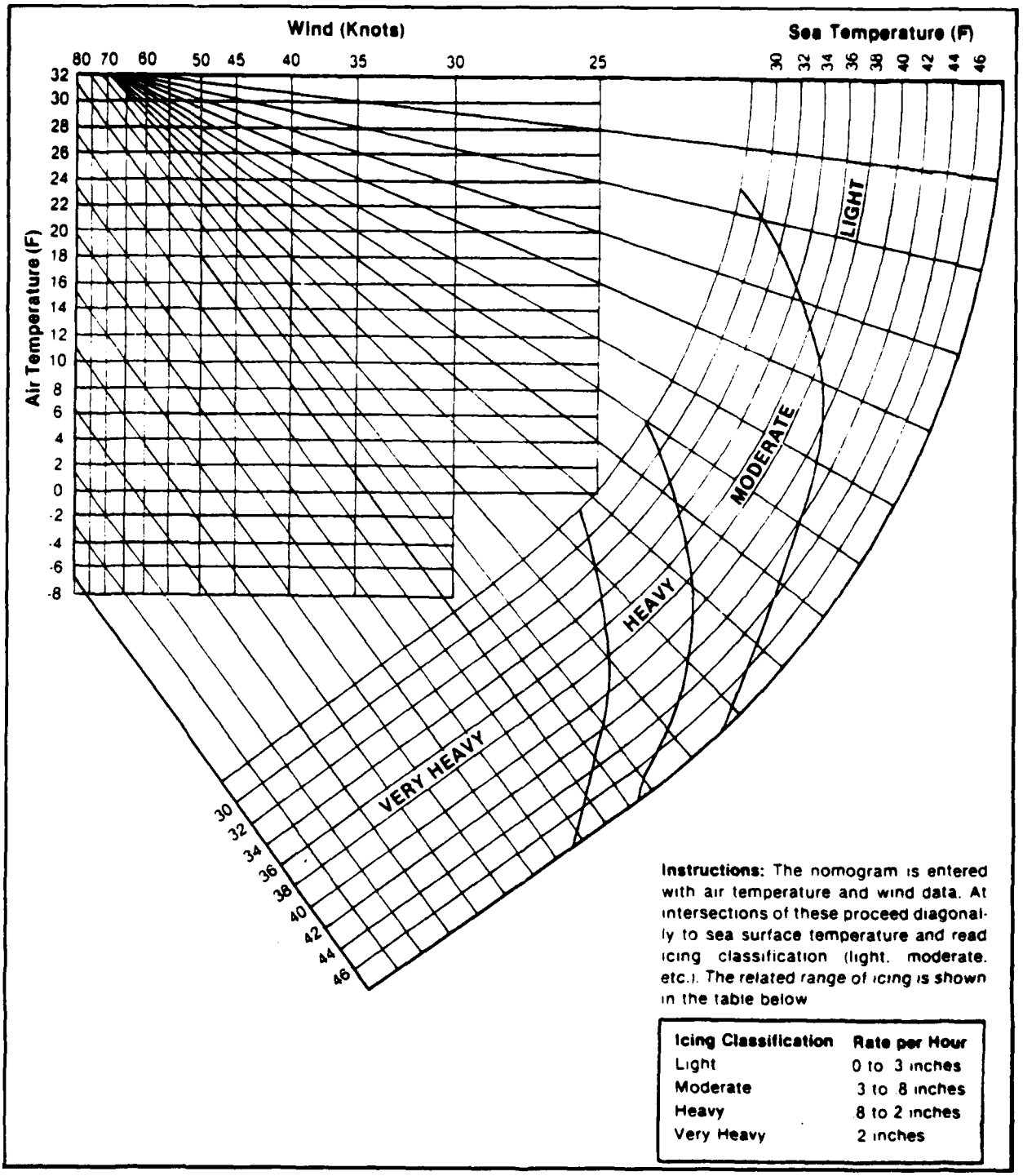

Figure 7-2. Icing rate nomogram (Brower et al., 1988).

Figure 7-3 is presented to show ice accretion versus wind velocity for six air temperatures. It is important to note, however, that icing rates vary with geometry of structure and orientation, whether horizontal or vertical.

The sea surface temperature has a direct influence on the rate of ice accretion. In addition, warmer sea temperatures frequently mean warmer air temperatures. Since the air temperature also has a strong influence on the rate of ice accretion, the benefit of warmer water may be twofold.

Vessels that seek shelter in the lee of land may still experience low air temperatures, but some reduction of wind speeds and wave heights should be observed and, therefore, less spray blown from the wave caps. Ship-generated spray in the calmer water will be greatly reduced. Furthermore, attempts to remove the ice will not be thwarted by the vessel's motion and seas sweeping the deck, as would be the case in the open sea.

In very high latitudes, however, ships should not seek shelter in the lee of the ice edge. The ice provides negligible shelter from the wind, and here the coldest air and sea

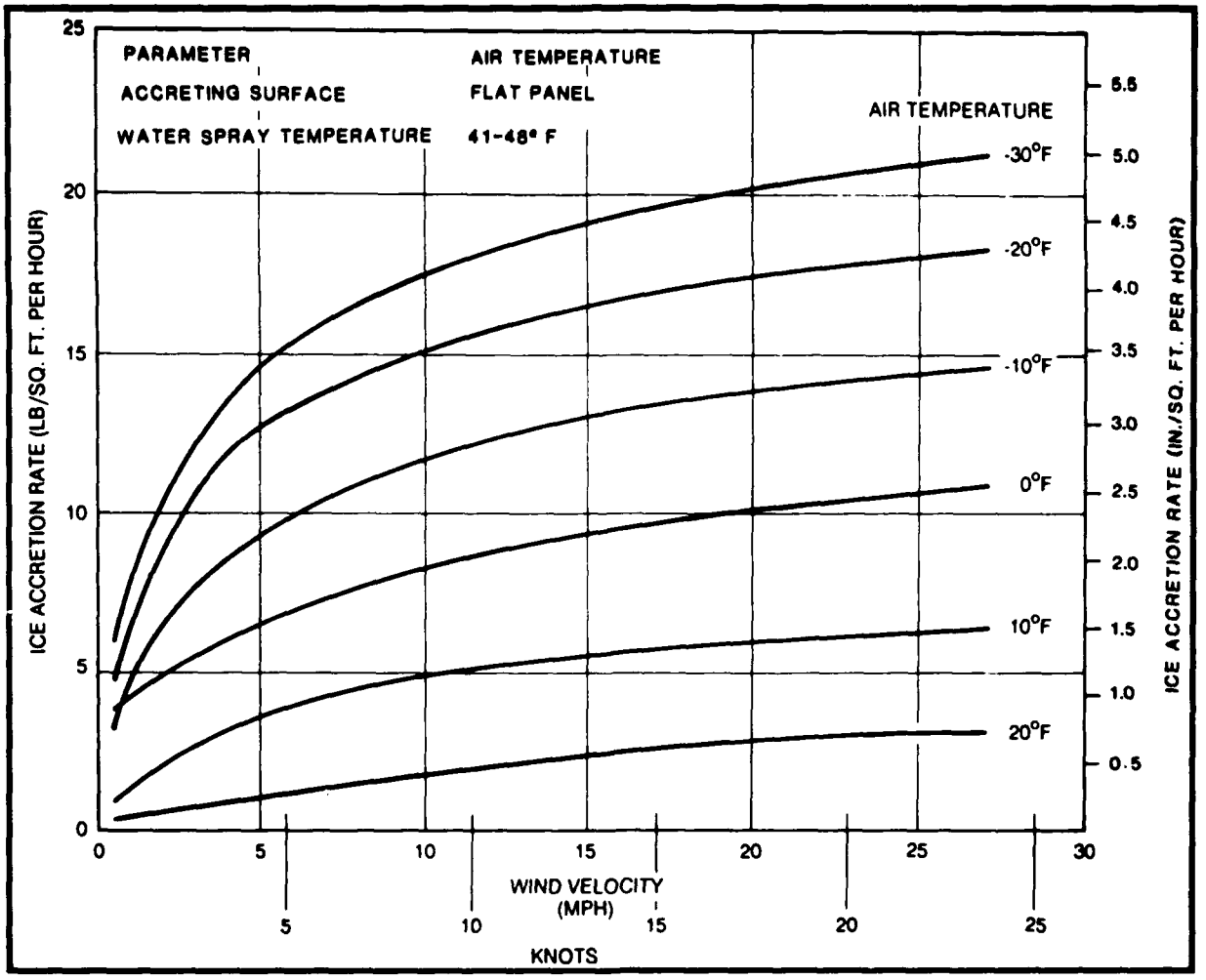

Figure 7-3. Ice accretion versus wind velocity (U.S. Navy, 1988).

temperatures are found and provide the most severe conditions for icing. If the wind backs or veers parallel to the ice edge, the air temperature remains very low and heavy seas are soon generated.

When ice accumulation reaches about 4 inches (10 cm), dangerous conditions prevail. If this accumulation occurs within 4.5 hr, the condition is one of *extreme icing*. *Heavy icing* would produce this thickness in 8 hr, and *light icing* would produce this thickness in 1 day.

7.1.5 An Example of Extreme Icing

During the week of 22 to 29 January 1989 the crabbing ship Vestfjord was making its way across the Gulf of Alaska from Cape Spencer, Alaska, to the ice edge near Dutch Harbor in the Aleutians (see locator map, Fig. 7-4). As the ship passed south of Kodiak on 28 January the strong westerly winds it had encountered on the previous day intensified significantly and impeded its forward progress. The ship's superstructure began icing from the supercooled sea spray as it encountered strong, cold air advection and 50-kt (26 m/s) winds.

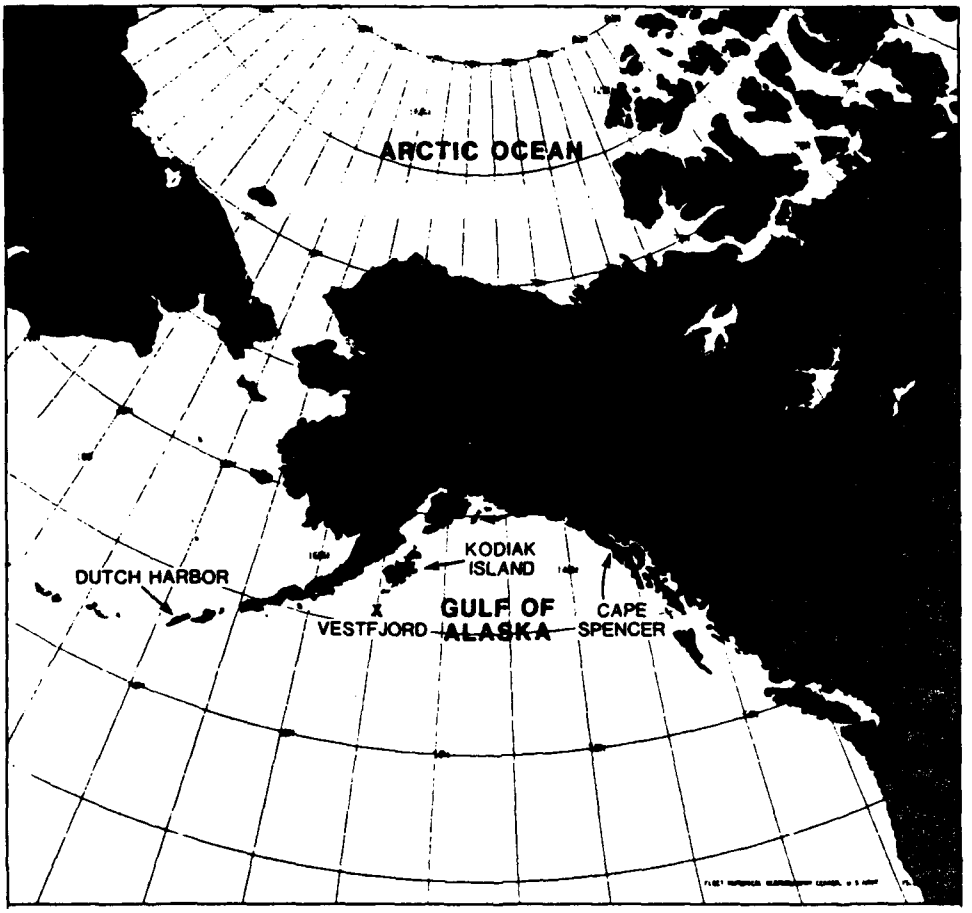

Figure 7-4. Locator map.

The severity of the situation increased on 29 January as can be gleaned from the 0600 GMT surface weather map for that date (Fig. 7-5). This surface chart shows a sharp, elongated low-pressure trough oriented nearly east-west and extending from the vicinity of Great Slave Lake, Canada, to the Alaska Peninsula. The trough terminates just east of an intense high pressure area centered over the Aleutians. Between these two systems was a very steep pressure gradient that resulted in northwest winds in excess of 50 kt (26 m/s) with 27 ft (8 m) seas. The air temperature in the northern Gulf of Alaska, meanwhile, was about 7 °F (−14 °C) and the sea surface temperature near 39 °F (4 °C).

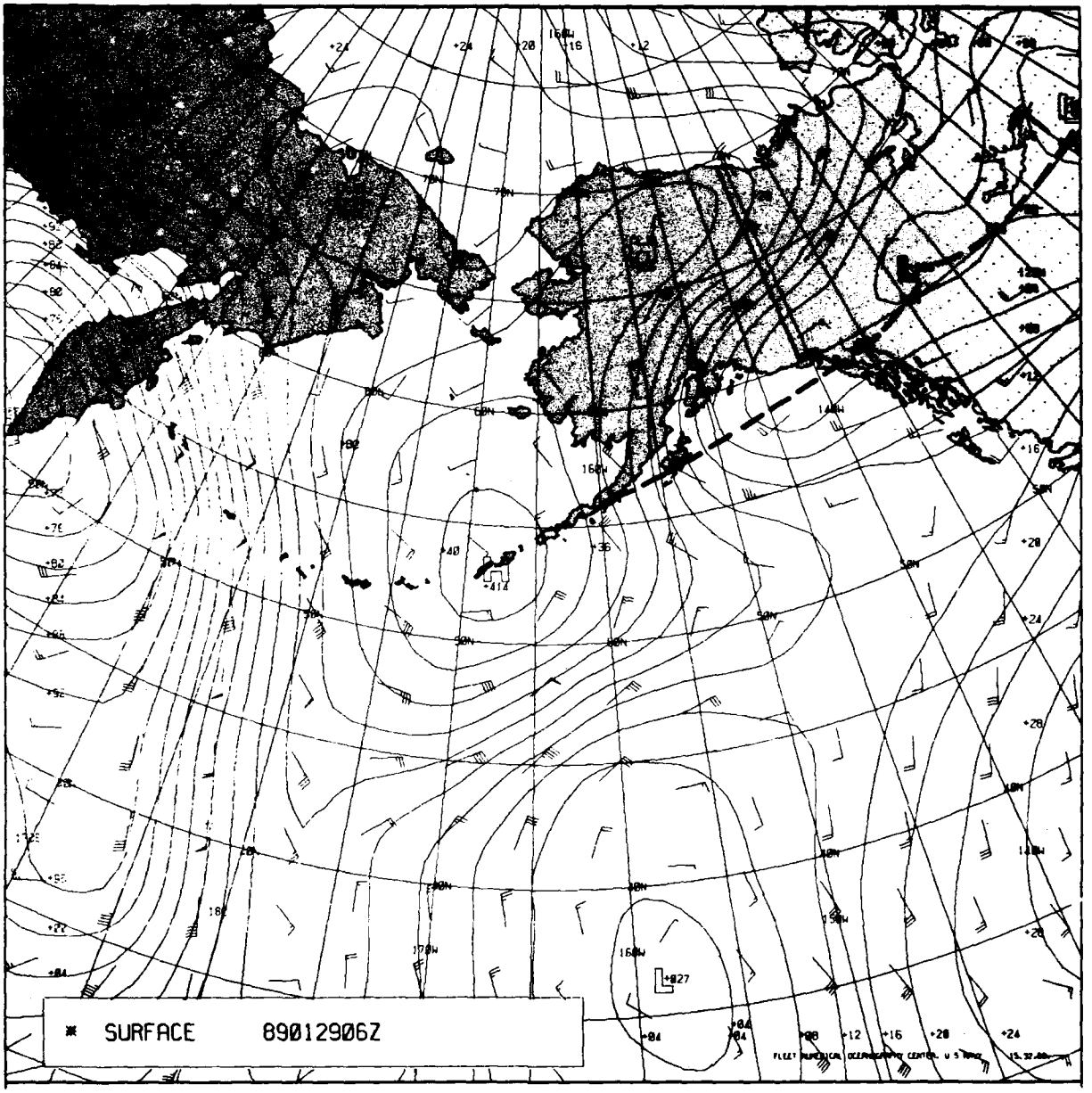

Figure 7-5. Surface chart for 0600 GMT 29 January 1989.

The intensity of the cold air advection occurring at the time of heaviest icing is best depicted on the 850-mb chart for 0000 GMT 29 January 1989, as seen in Fig. 7-6. The strongest cold advection on this chart occurred south of Kodiak Island. This is precisely the region in which the ship overturned and sank with all six hands at 1010 GMT on the 29th (last position of Vestfjord shown as an "X" in Fig. 7-4).

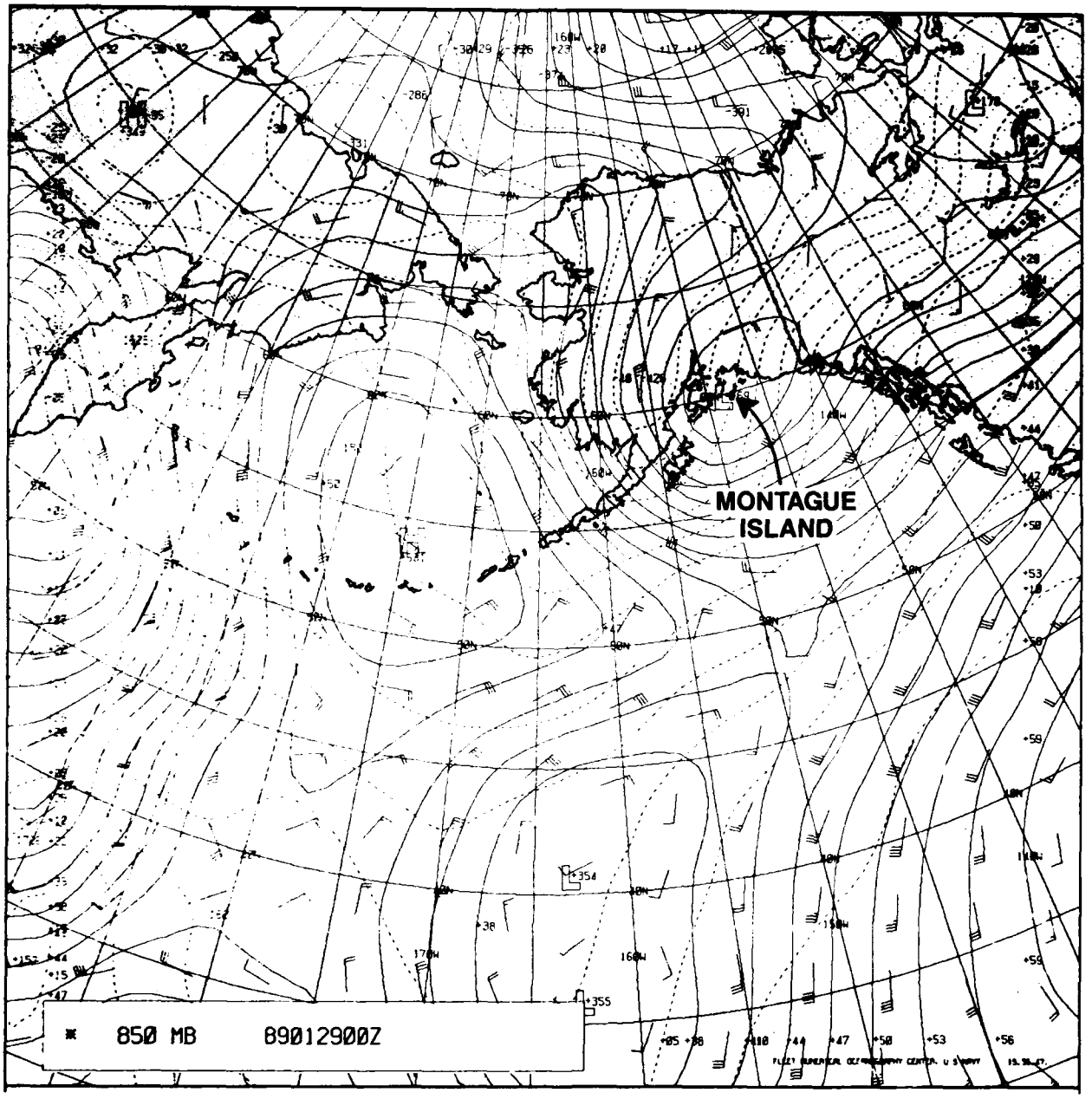

Figure 7-6. An 850-mb chart for 0000 GMT 29 January 1989.

Figure 7-7 is a satellite imagery from the DMSP satellite for 0552 GMT on 29 January 1989. An X marks the approximate location of the ship at that time. Cloud lines resulting from the cold surge are apparent in the imagery, indicating not only strong northwest flow but the likelihood of precipitation as well.

Figure 7-7. Infrared satellite imagery 0552 GMT 29 January 1989.

As Fett (1989) noted in his study of this case, icing can be heavy even with water temperatures as high as 45 °F (7 °C) if the air temperature is cold enough and wind speeds high enough. Icing is highly likely in these conditions if the ship has been "cold soaked." Cold soaking is defined as long-term exposure of the ship to subzero temperatures and near freezing seas. The ship gradually reaches thermal equilibrium with its environment after about a 2- to 3-week exposure. The ship is considered cold soaked when the heat loss rate drops to the same point as the heat production rate (U.S. Navy, 1988). A cold-soaked ship traveling into warmer water temperatures would still be cold enough to accumulate icing, if the other necessary factors are present. Fett also noted that icing conditions are especially favored in the region in advance of an approaching 500-mb trough. Figure 7-8 is the 500-mb chart for 0000 GMT 29 January 1989 that shows the trough line just east of and parallel to the Aleutians about 10 hr before the ship disappeared.

7.2 Aircraft Icing

Aircraft icing is one of the major weather hazards to aviation. Ice on the airframe decreases lift and increases weight, drag, and stalling speed. In addition, the accumulation of ice on exterior movable surfaces affects the control of the aircraft. Finally, airframe icing greatly increases fuel consumption and decreases range.

The subject of aircraft icing is complex. The following discussion outlines the basic elements of aircraft icing and makes no attempt to encompass all available knowledge on the subject.

7.2.1 The Formation of Ice on Aircraft

Two basic conditions must be met for ice to form on an airframe in significant amounts. First, the aircraft-surface temperature must be colder than 32 ° (0 °C). Second, supercooled water droplets, that is liquid-water droplets at subfreezing temperatures, must be present. Water droplets in the free air, unlike bulk water, do not freeze at 32 °F (0 °C). Instead, their freezing temperature varies from an upper limit near 23 °F (−10 °C) to a lower limit near −40 °F (−40 °C). The smaller and purer the droplets, the lower is their freezing point. When a supercooled droplet strikes an object such as the surface of an aircraft, the impact destroys the internal stability of the droplet and raises its freezing temperature. Therefore, the possibility of icing must be anticipated in any flight through supercooled clouds or liquid precipitation at temperatures below freezing. In addition, frost sometimes forms on an aircraft in clear, near saturated air if both aircraft and air are at subfreezing temperatures.

7.2.2 Icing Factors

Temperature of the cloud droplets and aircraft surface temperature are only two of the physical factors involved in aircraft icing. Also to be considered are (1) liquid water content, (2) droplet size, (3) collection efficiency, and (4) aerodynamic heating.

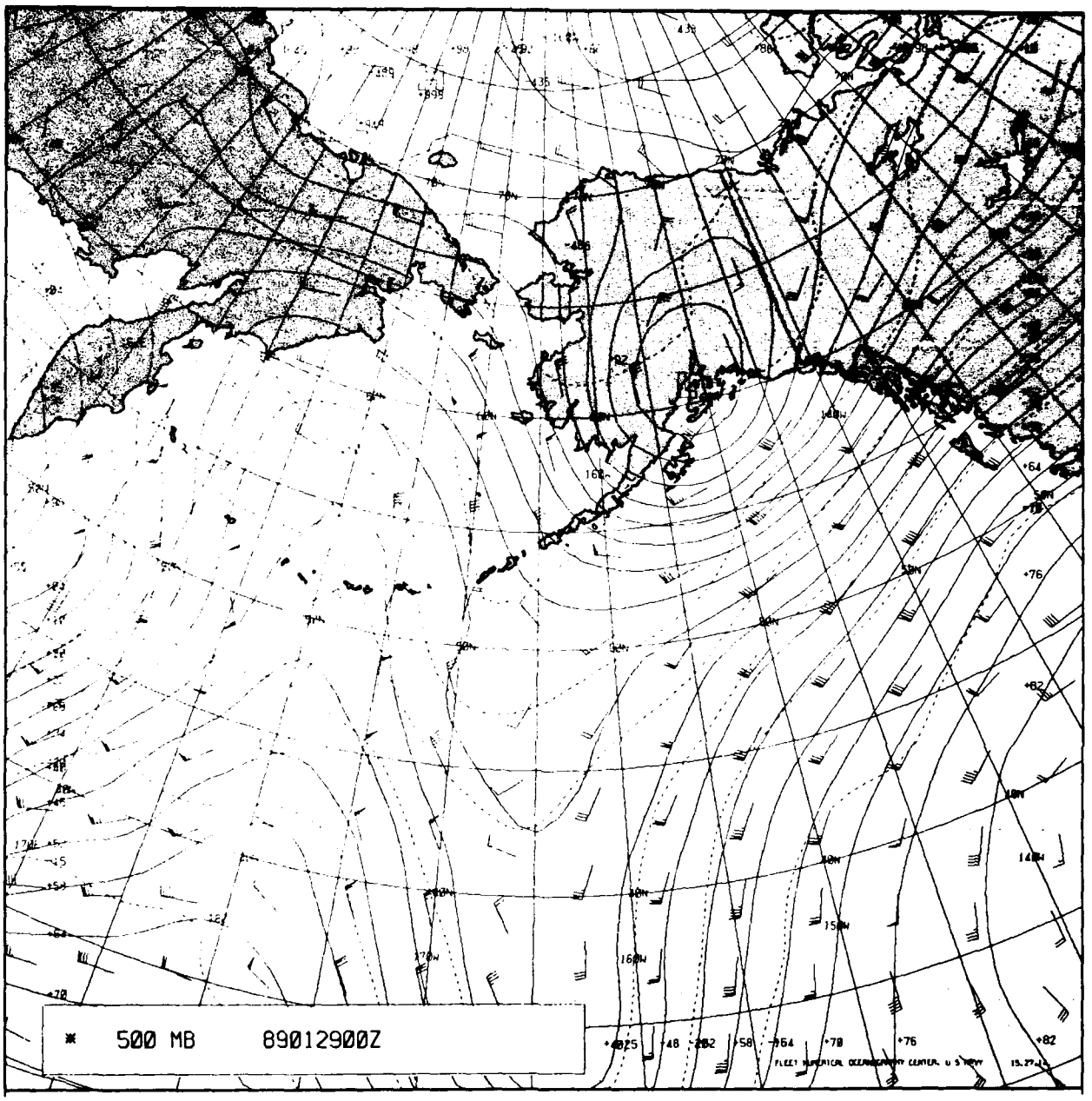

Figure 7-8. A 500-mb analysis 0000 GMT 29 January 1989.

Under icing conditions, the *liquid-water content* of the cloud is probably the most important parameter in determining the ice-accumulation rate. In general, the lower and warmer the base of the cloud, the higher is its water content. Within the cloud, the average liquid-water content increases with altitude to a maximum value and then decreases. The maximum concentration usually occurs at a lower level in stratiform than in cumuliform clouds, and the average liquid-water content of a stratiform cloud is usually less than that of a cumuliform cloud.

The *size distribution* and median size of the droplets in a cloud are related to the type, depth, and age of the cloud, to the strength of the updrafts, to the humidity of the airmass, and to other factors. Droplet size is generally greater in cumuliform clouds than other cloud types.

The icing rate depends to a large extent upon the *collection efficiency* of the aircraft component involved. Collection efficiency, or the fraction of the liquid-water collected by the aircraft, varies directly with droplet size and aircraft speed, and inversely with the size of the collecting surface. The size of an aircraft component is described in terms of the radius of curvature of its leading edge. Those components that have large radii of curvature (canopies, thick wings, etc.) collect only a small percentage of the cloud droplets, especially of the smallest droplets. Components having small radii of curvature (antenna masts, thin wings, etc.) deform the airflow less, permitting a higher proportion of droplets of all sizes to be caught. Once ice begins to form, the shape of the collecting surface is modified, with the radius of curvature nearly always becoming smaller and the collection efficiency increasing. In general, fighter-type aircraft, because of their greater speed and thinner wings, have higher collection efficiencies than do cargo aircraft.

Aerodynamic heating is the temperature rise resulting from adiabatic compression and friction as the aircraft penetrates the air. (The saturation-adiabatic laws, including the effects of fusion and evaporation, apply to flight through clouds.) The amount of heating varies primarily with the speed of the aircraft and the altitude (air density) ranging from about 34 °F (1 °C) for very slow aircraft at low altitudes to more than 122 °F (50 °C) for supersonic jets at low altitudes. Thus, although it is frequently stated that an aircraft flying through any supercooled liquid-water cloud must anticipate icing, it actually is necessary that the amount of supercooling exceed the amount of aerodynamic heating (U.S. Navy, 1985).

7.2.3 Atmospheric Distribution of Icing

The atmospheric distribution of potential aircraft icing zones is mainly a function of temperature and cloud structure. These factors, in turn, vary with altitude, synoptic situation, orography, location, and season.

Altitude and Temperature

In general, once the temperature of maximum icing is reached, the frequency of icing decreases rapidly with decreasing temperature, becoming rather rare at temperatures below °22 °F (−30 °C). The vertical temperature distribution in the Arctic atmosphere is such that icing is usually restricted to the lower 25,000 ft (7620 m) of the troposphere.

The type of icing, also, is highly dependent on temperature. Clear ice usually occurs at temperatures just below freezing, whereas rime ice predominates at lower temperatures.

Clouds

Icing in middle and low level stratiform clouds is confined, on the average, to a layer between 3000 and 4000 ft (900–1200 m) thick. The intensity of the icing generally ranges from a trace to light, with the maximum values occurring in the upper portions of the cloud. Both rime and mixed icing are observed in stratiform clouds. The main hazard lies in the great horizontal extent of some of these cloud decks. High level stratiform clouds are composed mostly of ice crystals and give little icing.

The zone of probable icing in cumuliform clouds is smaller horizontally but greater vertically than in stratiform clouds. Furthermore, icing is more variable in cumuliform clouds because many of the factors conducive to icing depend to a large degree on the stage of development of the particular cloud. Icing intensities may range from generally a trace in small supercooled cumulus to often light or moderate in cumulonimbus. Although icing occurs at all levels above the freezing level in a building cumulus, it is most intense in the upper regions in a mature cumulonimbus and in a shallow layer near the freezing level in a dissipating thunderstorm. Icing type in cumuliform clouds is usually clear or mixed.

Frontal Systems

Warm frontal icing may occur both above and below the frontal surface. Moderate or severe clear icing usually occurs where freezing rain or freezing drizzle falls through the cold air beneath the front. This condition is most often found when the temperature above the frontal inversion is warmer than 32 °F (0 °C) and the temperature below is below freezing. Icing above the warm frontal surface, in regions where the cloud temperatures are colder than freezing, is usually confined to a layer less than 3000 ft (914 m) thick. For fast-moving, active warm fronts moderate icing, usually clear or mixed, can be found 100 to 200 mi (160–320 km) ahead of the front.

Generally, over land, warm frontal icing is widespread, and icing associated with cold fronts is usually spotty. Its horizontal extent is less, and the areas of moderate icing are localized. Over water, horizontal extent is much greater. To the rear of marine fronts, extensive areas of open-celled cumulus are common. Each of these cells has the potential for icing. Clear icing is more prevalent than rime icing in the unstable clouds usually associated with cold fronts. Moderate clear icing is usually limited to supercooled cumuliform clouds to the rear of the cold front surface position and is usually most intense immediately above the frontal zone. Light icing is often encountered in the extensive layers of supercooled stratocumulus clouds that frequently exist behind cold fronts.

Orographic Influences

High or steep terrain, particularly mountains, causes icing to be more intense than is usual under identical conditions over flat terrain. Icing is greater over the ridges than over the valleys and greater on the windward side than on the leeside. Moderate icing, usually clear, is experienced in convective clouds over mountainous terrain. Windward mountainous coasts in winter are especially subject to extensive aircraft icing zones.

Geographic Distribution

A wide variation between geographic areas in aircraft icing potential is due to area-to-area variations in temperature and available moisture. Because of the comparatively small amount of moisture in winter Arctic air and the small liquid water content of clouds, icing is seldom regarded as a serious problem in the Arctic in winter. It is not surprising, therefore, that icing was reported by weather reconnaissance aircraft only 2% of the time over the Arctic Ocean at 10,000 ft (3050 m). On the other hand, at the same altitude over the northern portion of the North Atlantic Ocean, icing was reported 19% of the time. Weather reconnaissance data at 700 and 500 mb over the oceans suggest that the greatest winter icing frequency was found over the northern and western parts of the North Pacific and North Atlantic, and the least over the Arctic Ocean. These data do not imply that icing is never a hazard in the Arctic. In those instances when moisture-laden air from the North Atlantic and North Pacific invades the Arctic, conditions conducive to copious icing are established. Normally winter is the season of maximum icing, except over the Arctic Ocean, where the maximum icing occurs in summer because the temperatures and moisture amounts are much too low in winter.

8. REFRACTIVITY IN THE ARCTIC ATMOSPHERE

All electromagnetic radiation propagation through the atmosphere is affected by the atmosphere. Electromagnetic energy can be reflected, refracted, scattered, and absorbed by different atmospheric constituents. The extent of these atmospheric effects depends upon both the frequency and power of the electromagnetic source and on the state of the atmosphere through which the electromagnetic energy must propagate. This chapter summarizes the effects of the environment on electro-optical, infrared, laser, microwave, and radio wave sensor and communication systems.

In general environmental effects on communication systems are classified into three categories: *attenuation*, or loss of energy, of the radiation beam due to beam interaction with absorbing or scattering constituents in the beam path; *refraction*, or bending of the beam, due to atmospheric density variations along the beam path; and *scintillation*, or distortion of the beam, due to small scale atmospheric turbulence (Cook and Payne, 1987). Since particulate and density variations are usually greatest in the lower troposphere, it is essential to understand the nature of the atmospheric boundary layer in studying electromagnetic propagation. A brief discussion of the atmospheric boundary layer is included in Section 8.5.

8.1 Attenuation

Attenuation is the most important environmental effect on nonlaser visible and infrared systems. Small airborne particles (aerosols) and air molecules can remove energy from the radiation beam by scattering the energy out of the beam path and/or absorbing the energy and producing heat. The scattering relationship between aerosols and energy is governed by particle size and energy wavelength. Examples of scattering are the attenuation of visible light by clouds, fog, rain, haze, smoke, and snow.

Atmospheric scattering processes are difficult to quantify and forecast accurately because of the lack of appropriate measurements of particle size distributions and chemical properties. Predictions of attenuation due to scattering for visible wavelengths are operationally derived from atmospheric visibilities, which are related to meteorological conditions as shown in Table 8-1.

TABLE 8-1. INTERNATIONAL VISIBILITY CODE, VISIBILITY, AND PERCENT ATTENUATION DUE TO SCATTERING FOR 1 KM PATH

Code No.	Weather Condition	Visibility		1 km Path Attenuation (%)
		Metric	English	
0	Dense Fog	<50 m	<50 yd	100
1	Thick Fog	50 m – 200 m	50 yd – 219 yd	>99.99999 – 99.99999
2	Moderate Fog	200 m – 500 m	219 yd – 547 yd	99.99999 – 99.9
3	Light Fog	500 m – 1000 m	547 yd – 1095 yd	99.9 – 98
4	Thin Fog	1 km – 2 km	1095 yd – 1.1 n mi	98 – 86
5	Haze	2 km – 4 km	1.1 n mi – 2.2 n mi	86 – 61
6	Light Haze	4 km – 10 km	2.2 n mi – 5.4 n mi	61 – 32
7	Clear	10 km – 20 km	5.4 n mi – 11 n mi	32 – 18
8	Very Clear	20 km – 50 km	11 n mi – 27 n mi	18 – 8
9	Exceptionally Clear	>50 km	>27 n mi	<8
—	Pure Air	277 km	149 n mi	<1

Note: Scattering for moderate to heavy snowfall can be approximated by the figures for light fog.

As the table shows, attenuation at visible wavelengths is practically 100% for clouds, fog, and snow. Attenuation at infrared wavelengths shows a similar increase from pure air to dense fog, except that clear air is slightly more opaque to infrared radiation than to visible, and fog and haze generally are slightly more translucent in the infrared.

In addition to scattering by aerosols, infrared energy is strongly absorbed by atmospheric water vapor. Water vapor is such an efficient absorber of infrared energy that the multiple absorption lines overlap to the point of creating a virtual continuum—an extremely broad-band infrared absorption feature. Since water vapor is so abundant in the atmosphere, infrared

systems are normally confined to operating within two minimum absorption windows in the spectrum. The two window regions are 3–5 μm and 8–12 μm.

The attenuation in the 3–5-μm region is generally affected less by water vapor absorption than the 8–12-μm region; however, aerosol scattering and absorption by CO_2 molecules is more significant at 3–5 μm. In low latitudes with high water vapor density conditions, the 3–5-μm band is sometimes thought to provide superior transmission because of the heavy absorption of 8–12-μm radiation. Haze affects the 3–5-μm more than the 8–12-μm band, however, and long haze-free paths through humid atmospheres are rare. Therefore, the preference in hazy conditions is the 8–12-μm band. At high latitudes, the low values of water vapor density again make the 8–12-μm band the preferred choice. Since objects at ambient temperature radiate with their energy peaked in the 8–12-μm band, this window region is a logical choice for target imaging and detection. Hotter targets, such as exhaust plumes, radiate at shorter wavelengths, and when the paths are at high altitudes where the water vapor densities are very low, the 3–5-μm band is preferred.

The attenuation of electro-optical and infrared radiation by atmospheric gases and precipitation as a function of wavelength are depicted in Fig. 8-1. (Attenuation due to dry aerosols, such as pollutants and salt from sea spray, is not shown.) The visible region of the spectrum is transparent in clear air, becomes translucent in the presence of precipitation, and is virtually opaque in dense fog. The same is true for the infrared window regions. The far infrared and submillimeter wave regions of the spectrum are dominated by water vapor absorption.

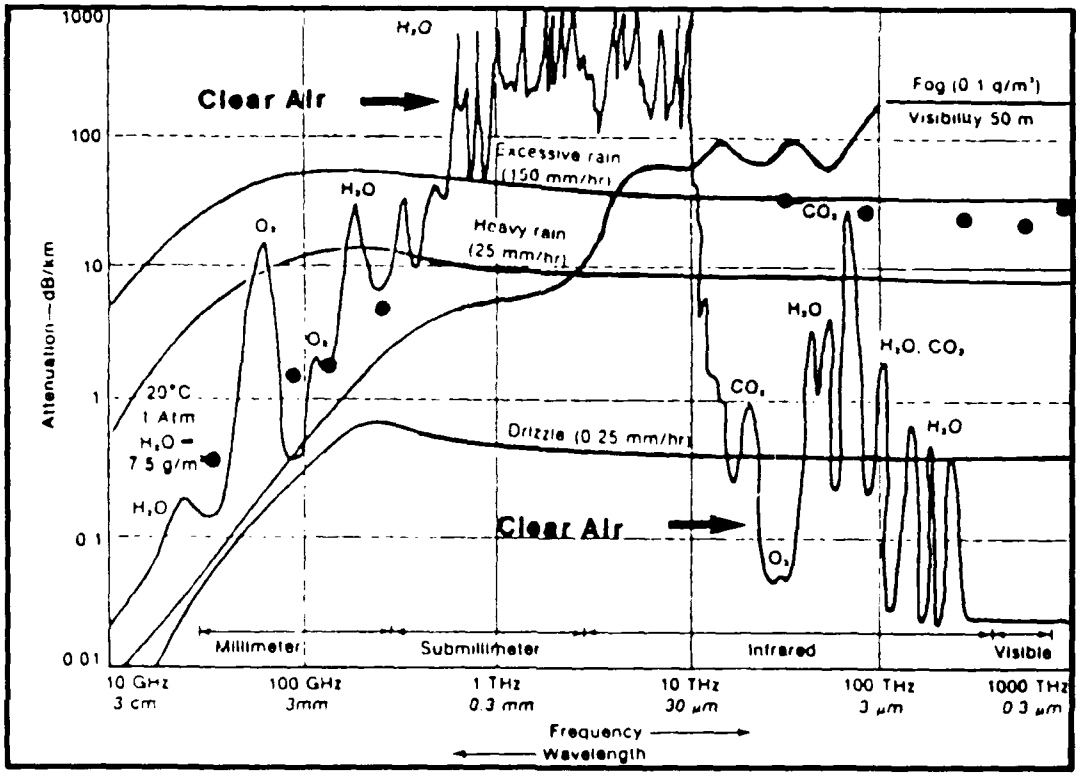

Figure 8-1. Atmospheric attenuation at sea level.

Laser beams are also subject to attenuation as previously described. The proper wave band must be chosen to minimize attenuation because other environmental factors seriously affect beam quality, spot size, and power with respect to the target.

Electromagnetic radiation (radar and communications) passing through the atmosphere is depleted by both absorption and scattering, which are caused by gaseous constituents of the atmosphere and by particles carried by the atmosphere. Molecular absorption and scattering have the greatest effect on super high frequency (SHF, 3–30 GHz) and extremely high frequency (EHF, 30–300 GHz) radiation (see Fig. 8-2). This absorption involves well-defined frequencies and thus occurs in narrow bands (or lines), primarily attributable to oxygen and water vapor. Since water vapor concentration varies significantly through the atmosphere, absorption by water vapor also varies significantly.

At microwave frequencies (300 MHz – 100 GHz), scattering and absorption by particles in the atmosphere are dominated by liquid water drops. These droplets scatter wavelengths roughly the same size as the droplets and thus scatter frequencies above about 300 MHz (ultra high frequency [UHF] and higher). Other important scattering particulates include smoke, dust, and insects, which primarily affect UHF, although smoke particles also absorb SHF and EHF.

8.2 Refraction

Refraction is the bending of light rays owing to refractive index (density) changes in the atmosphere. For visible and infrared propagation, refraction can cause image distortion, image inversion, and path length changes important for laser ranging. Refractive conditions are characterized by comparison to the refraction expected from a standard atmosphere.

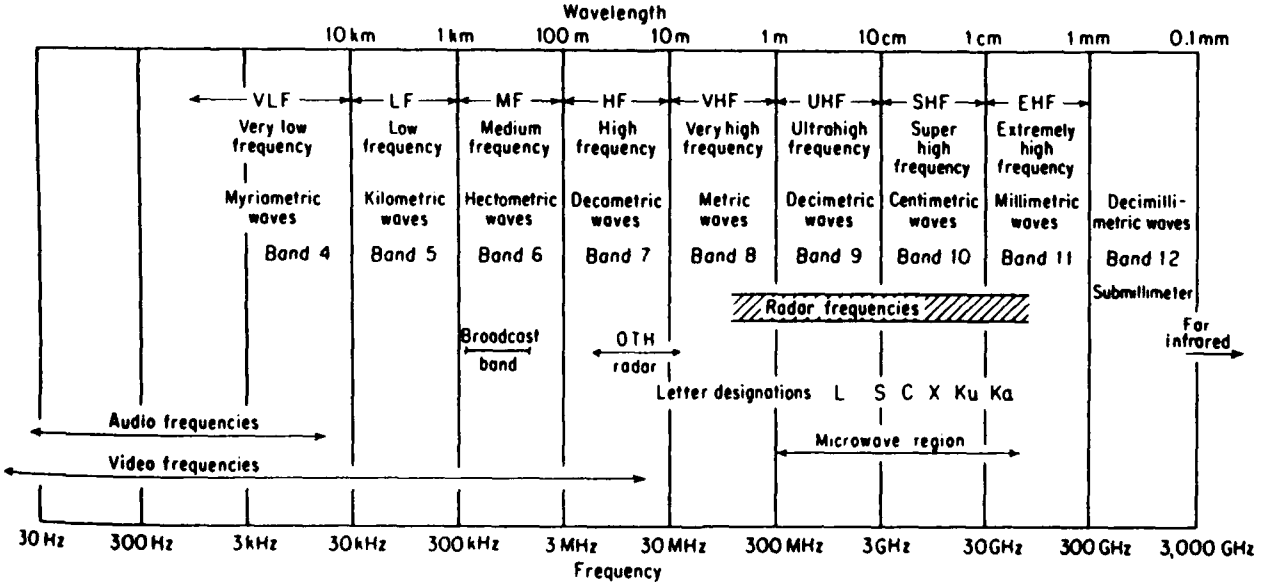

Figure 8-2. The electromagnetic spectrum.

Differences from standard conditions are due to temperature and water vapor density fluctuations. Large gradients of these parameters near the ocean surface can seriously affect surface horizontal propagation paths. Propagation over slant paths are usually not seriously affected by refraction.

The index of refraction of a medium, n, is defined by Eq. 8.1, where c is the velocity of an electromagnetic wave in free space and v is the velocity of the same electromagnetic wave in another medium.

$$n = c/v \tag{8.1}$$

For the atmosphere, the refractive index is defined to be the ratio of the velocity of propagation of an electromagnetic wave in a free space to that in the air. Since the velocity of an electromagnetic wave in free space is always faster than that in any medium, the index of refraction is always greater than one. In the standard atmosphere, a typical near sea-level value for n is approximately 1.0003 (Bean and Dutton, 1966). For convenience, the refractivity N is defined by Eq. 8.2 such that normal atmospheric values of N units range from 250 to 400.

$$N = (n\text{-}1) * 10^6 \tag{8.2}$$

As stated by Battan (1973), "In dry air the index of refraction has the same value over almost the entire range of the electromagnetic spectrum: it is the same for light and radio waves. However, when water vapor is added to the air, the value of N for the mixture becomes frequency dependent. It is well known that the water vapor molecule is polar in nature and that the dipole moment of the molecule has a different response to different frequencies of radio waves. With the extremely high frequencies of visible light, the water molecules are electronically polarized. With the lower frequencies of radar waves, the water molecules not only acquire electronic polarization, but also reorient themselves rapidly enough to follow the electric-field changes. As a result, the index of refraction of water vapor is greater for radio than for optical frequencies."

Temperature, water vapor, and pressure are the major variables of the atmosphere that determine its refractivity. Bean and Dutton (1966) express refractivity in terms of temperature T in Kelvin, pressure P, and water vapor pressure e, in millibars, as follows in Eq. 8.3:

$$N = 77.6\ P/T - 5.6\ e/T + 3.75 * 10^5\ e/T^2 \tag{8.3}$$

In an atmosphere of constant N units, no bending of an electromagnetic wave could occur regardless of the value of N. Refraction is dependent upon the gradients of N.

Since gradients of pressure, temperature, and humidity occur throughout the atmosphere, it follows that gradients of N must also exist. It can be shown (Battan, 1973) that when the gradient of N (i.e., dN/dZ) is equal to $-157\ km^{-1}$, a propagating electromagnetic wave will bend with a curvature exactly equal to that of the Earth. This would cause a horizontally propagating electromagnetic wave to remain constantly parallel to the Earth's surface always at the same height. Any value of dN/dZ less than $-157\ km^{-1}$ would cause an electromagnetic wave to bend with greater curvature than the Earth's surface. Therefore, $-157\ km^{-1}$ is the threshold for "trapping" such a wave.

Trapping, or ducting, occurs when the microwave energy is trapped in layers and propagates to greater ranges than normal because of the absence of vertical spreading of the rays. Ducting regions can be elevated or surface based. Radar propagation and coverage are affected by the refractive nature of the atmosphere. Nonstandard refractive conditions lead to anomalous propagation and can cause microwaves to be refracted less than normal (subrefraction), refracted more than normal (superrefraction), or trapped in wave-guide modes (ducted), as in Fig. 8-3.

Over the oceans, a persistent surface-ducting mechanism is the rapid, near-surface decrease in moisture due to evaporation, which creates evaporation ducts. The relation for the vertical gradient of refractivity as a function of temperature *(T)*, pressure *(P)*, and specific humidity *(q)* is given by Eq. 8.4.

$$dN/dZ = 0.3\ dP/dZ + 7.2\ dq/dZ - 1.3\ dT/dZ \tag{8.4}$$

It is sometimes convenient to portray the Earth's surface as flat and to represent the electromagnetic wave refraction in this frame of reference. This portrayal can be done simply by subtracting the Earth's curvature from the electromagnetic wave and from the Earth. A modified refractivity M has been developed to take into account the Earth's curvature and to allow for easy identification of ducting. Equation 8.5 shows the relationship of M to N (Battan, 1973).

$$M = N + (157)Z,\ Z \text{ in km} \tag{8.5}$$

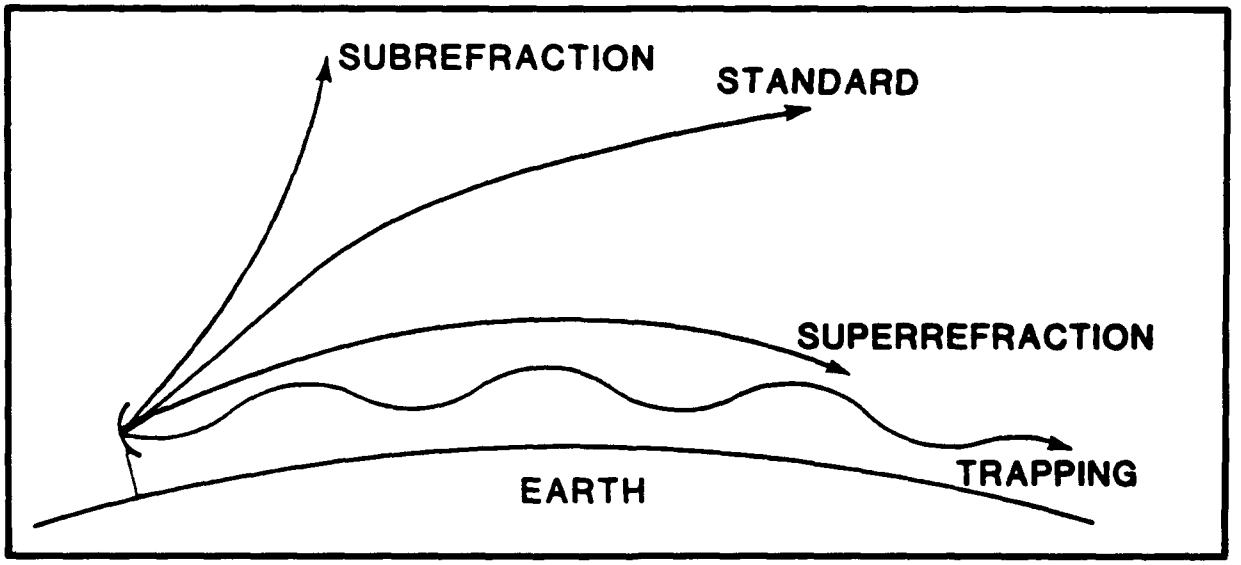

Figure 8-3. Four basic categories of refraction.

8.3 The Integrated Refractive Effects Prediction System (IREPS)

The Integrated Refractive Effects Prediction System (IREPS) is a shipboard environmental data processing and display system that is used to predict the effects of refraction on electromagnetic signals for naval surveillance, communications, electronic warfare, and weapons guidance systems. Environmental data usually obtained from radiosondes are processed on a desk-top computer, the Hewlett-Packard 9845, to derive a comprehensive assessment of refractive effects in the lower atmosphere. Knowledge of the refractive environment can be used to maximize tactical advantage. The most recent IREPS, version 2.2, is an integral part of the Tactical Environmental Support System (TESS), now being introduced into the fleet.

The IREPS uses M gradients to classify refractive conditions. Table 8-2 shows IREPS classifications of refractive conditions and the relationship of N units to M units.

TABLE 8-2. IREPS CLASSIFICATION OF REFRACTION CONDITIONS

IREPS Classification	dN/dZ km^{-1}	dM/dZ km^{-1}	Range
Subrefraction	>0	>157	Reduced
Normal	0 to -79	79 to 157	Normal
Superrefraction	-79 to -157	0 to 79	Increased
Trapping	<-157	<0	Greatly Increased

The performance of the IREPS model is directly related to the quality and timeliness of atmospheric information entered into the program. Accurate and timely data must be used if the resulting displays are to indicate the true refractive structure of the atmosphere. Knowledge of the immediate environment and its dynamical evolution are necessary for a proper interpretation of IREPS results.

By comparing the IREPS version 2.2 computed atmospheric refractivity conditions for a high resolution and degraded resolution sounding, Dotson (1987) showed the importance of high resolution data. The high resolution data were better able to define the smaller scale refractive structure of the atmosphere and, therefore, allowed IREPS to portray the ambient ducting conditions realistically. By observing the variability in ducting conditions for 120 soundings taken at irregular time intervals over a 47-day period, Dotson found that refractive conditions are in constant dynamic evolution on diurnal as well as synoptic time scales, which implies that timely data must be used to achieve accurate refractivity condition predictions.

Contrary to previous arguments that in over 85% of the time the horizontal homogeneity was not a factor in refractive considerations, Dotson found that horizontal inhomogeneity does indeed cause significant variability in radar lobe coverage at least 50% of the time when near areas of weak sea surface temperature gradients.

Ducting is of primary concern to Navy operations and is caused by trapping layers. A trapping layer is defined as the area where M decreases with height ($dM/dZ < 0$). In this region the ray is bent downward relative to the Earth's surface. A duct is defined as the region in which the energy is confined. A surface-based duct occurs when an electromagnetic wave is refracted downward at a curvature greater than the Earth's curvature and is then subsequently reflected up from the Earth's surface. It is the continuous refraction down and the reflection up that forms the duct and makes it a concern to the Navy by allowing detection by surface radars far beyond the normal horizon. The type of duct depends on the height, strength, and extent of the trapping layer.

The top of the duct is defined as the height where M reaches a minimum value. It also corresponds with the top of the trapping layer. In practice, thickness of the duct may be found by dropping a vertical line from the tip of the duct down towards the surface until it intersects the M profile. Duct strength is defined as the maximum range of M values within the limits of the duct. The optimum coupling height is the height where the dM/dZ profile changes from a positive to a negative value.

Three types of ducts commonly exist: (1) the *surface-based* duct; (2) the *elevated* duct; and (3) the *evaporative* duct. Profile (a) of Fig. 8-4 depicts an elevated duct often found when an inversion layer is present. Large temperature and humidity gradients are usually present within the inversion. The boundary layer is cool and moist relative to the overlying air, and over the ocean it is often referred to as the *marine* layer. These jumps in the vertical structure of the temperature and humidity are associated with warming and drying attributed to subsidence above the inversion and turbulent mixing in the boundary layer. In the Bering Sea-Aleutian Islands area, this type of ducting is most likely when high pressure is well established over the region.

Profile (b) of Fig. 8-4 is an example of a surface-based duct. These ducts are formed by relatively warm, dry air being advected over a cool body of water, or by strong subsidence modifying the elevated duct.

Figure 8-4(c) shows an evaporative duct. The evaporative duct can be created by two different mechanisms. First, an evaporative duct may be created by the very rapid decrease of moisture immediately above the ocean surface. The air adjacent to the ocean is saturated with water vapor, and the relative humidity is 100%. The high relative humidity decreases rapidly in the first few meters to an ambient value that depends on varying meteorological conditions. This initial rapid decrease in humidity will cause M to decrease with height to a minimum, and then M will increase with height. The second way in which an evaporative duct can be formed is independent of the decrease in humidity. This "evaporative duct" is caused by strong cooling at the surface. The cooling can cause a sufficient positive temperature gradient between the air near the surface and the air just above to create a duct. Radiation fog is often associated with this condition because the overlying air is cooled sufficiently by radiational transfer for the relative humidity to increase to the point of condensation. Evaporative ducts almost always exist over the oceans, but it is the strength and

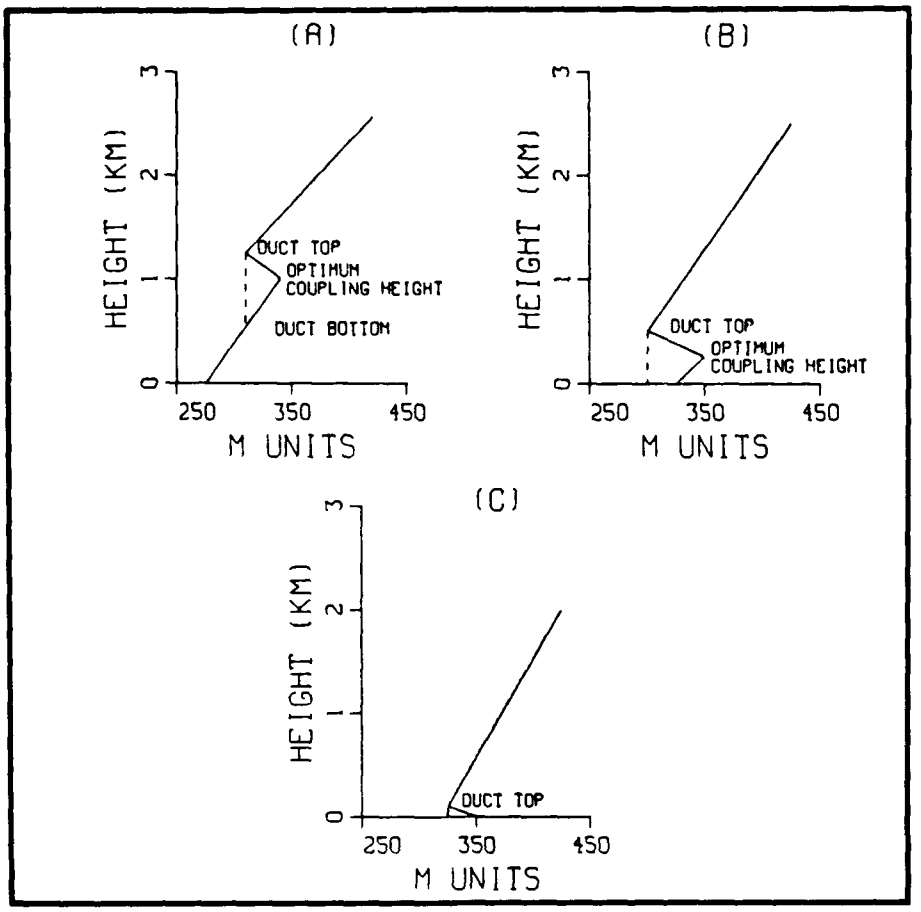

Figure 8-4. Ducting occurrences for typical M profiles.

upper boundary that are critical in determining the importance of the duct to tactical operation. The evaporative duct, although present, is generally shallow in the Bering Sea-Aleutian Islands area.

Two other important refractive effects are *subrefraction* and *superrefraction*. Subrefraction is defined as N increasing with height, as shown in Table 8-2. In this situation the rays actually bend away from the Earth's surface, and the radar range is reduced. Superrefraction is defined in Table 8-2 as N gradients having values between -79 and -157 per km. The electromagnetic wave is bent toward the Earth's surface, but not strongly enough to form a trapping layer. In this situation the radar range is increased somewhat, and the refractive conditions vary from one location to another. The variation was a function of the existing atmospheric conditions at a specific location at the time of that launch. The assumption made by IREPS that horizontal homogeneity is valid 85% of the time is *not* valid in the Bering Sea-Aleutian Islands area.

8.4 Description of Some IREPS Output Products

Figure 8-5 is a representation of one type of IREPS product. The "environmental data list" is used primarily for checking the numerical values of the input data. The IREPS computed output values of dewpoint depression, dN/dZ values, *M* units, and a single word description of the refractive conditions give an overall assessment of the atmospheric refractive conditions from each input level to the next.

The propagation conditions summary, reproduced in Fig. 8-6, is a system independent visual display and plain-language narrative assessment of expected refractive conditions. Vertical profiles of refractivity *N*, as well as modified refractivity *M*, are accompanied by a diagram showing the presence and vertical extent of any existing ducts. Evaporation duct height and surface wind speed information is given along with brief statements concerning anticipated performance of surface-to-surface, surface-to-air, and air-to-air electromagnetic systems.

Propagating radar waves experience constructive and destructive interference as direct path rays coincide with rays reflected from the sea surface. The resultant amplitude of the radar wave is a function of the phase differences among the intersecting waves. As a result, radar lobes (constructive interference) are created with shadow zones (destructive interference) appearing in between. Knowledge of where these lobes and shadow zones occur can become an immediate tactical advantage in both offensive and defensive operations. The

IREPS REV 2.2

**** ENVIRONMENTAL DATA LIST ****

LOCATION: 31 56N 118 36W
DATE/TIME: 17 JUN 0045Z

WIND SPEED 12.0 KNOTS

EVAPORATION DUCT PARAMETERS:
SEA TEMPERATURE 18.2 DEGREES C
AIR TEMPERATURE 15.1 DEGREES C
RELATIVE HUMIDITY 89 PERCENT
EVAPORATION DUCT HEIGHT 28.0 FEET

SURFACE PRESSURE = 1008.0 mB
RADIOSONDE LAUNCH HEIGHT = 60.0 FEET

LEVEL	PRESS (mB)	TEMP (C)	RH (%)	DEW PT DEP(C)	FEET	N UNITS	N/Kft	M UNITS	CONDITION
1	1,008.0	15.1	39.0	1.9	60.0	340.0	-28.2	342.9	SUPER
2	1,000.0	14.2	87.0	2.1	281.6	333.8	15.6	347.2	SUB
3	993.0	13.9	95.0	0.8	476.6	336.8	-10.9	359.6	NORMAL
4	982.0	13.3	97.0	0.5	785.3	333.4	-176.4	371.0	TRAP
5	972.0	20.4	25.0	20.8	1,071.8	282.9	27.2	334.2	SUB
6	962.0	21.5	34.0	16.6	1,364.9	290.9	-28.9	356.2	SUPER
7	949.0	21.5	27.0	19.9	1,751.3	279.7	-9.4	363.5	NORMAL
8	862.0	20.6	25.0	20.8	4,477.3	254.0	-9.5	468.2	NORMAL
9	850.0	19.7	25.0	20.7	4,873.5	250.2	-7.6	483.4	NORMAL
10	807.0	20.0	25.0	20.7	6,339.1	239.0	-6.0	542.3	NORMAL
11	726.0	14.5	34.0	15.8	9,299.4	221.2	-8.9	666.1	NORMAL
12	700.0	11.8	34.0	15.5	10,305.6	212.2	------	705.3	------

SURFACE REFRACTIVITY: 341 --SET SPS-48 TO 344

Figure 8-5. IREPS environmental data list.

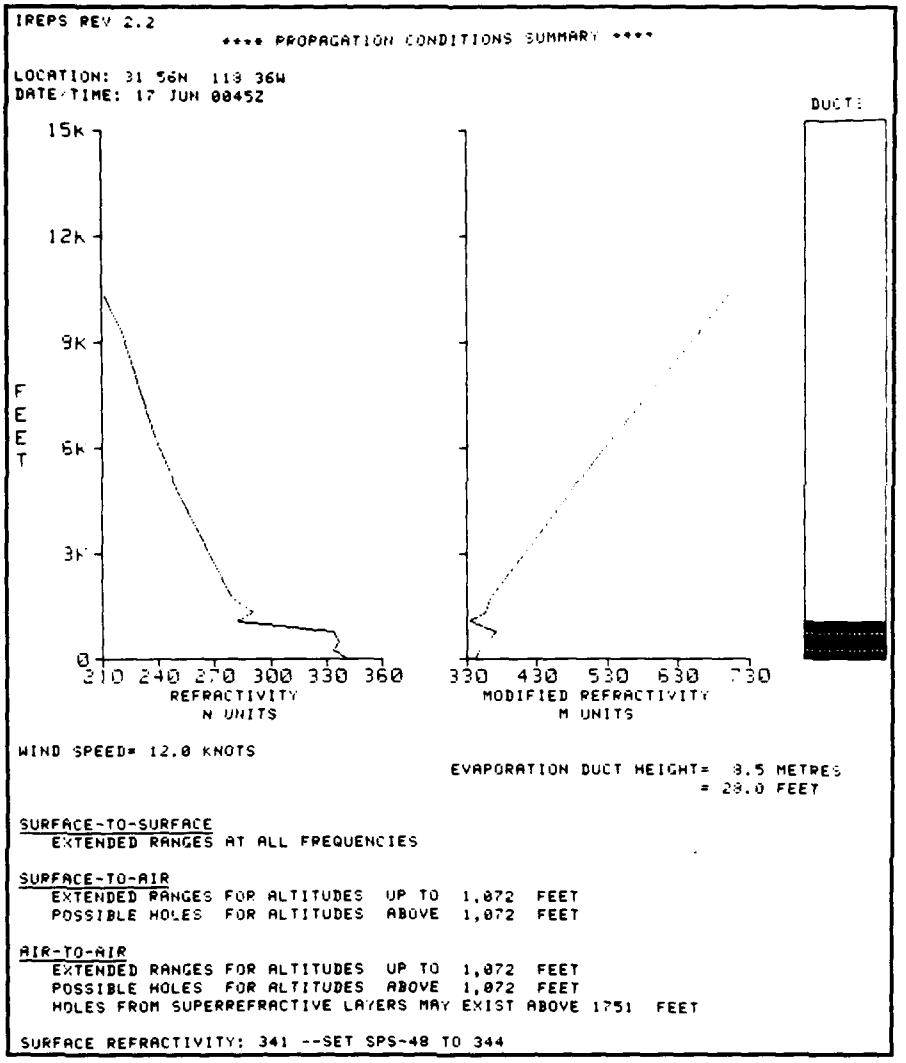

Figure 8-6. IREPS propagation conditions summary.

IREPS version 2.2 produces radar coverage diagrams that display the positions of the lobes and the shadow zones for any specified radar system and target at any desired probability of detection.

Since these lobes and shadow zones are created by reflections from the sea surface, their extent is determined by the roughness of the sea surface. Surface roughness is dependent on the sea state and wind speed, with higher wind speeds and rougher seas leading to relatively reduced coverage; low wind speeds and calm seas lead to relatively increased coverage. Wind speed changes are important indicators of changing radar conditions not dependent on refractivity.

Figure 8-7 is an example of the IREPS radar coverage display product, which also can be very useful in determining an electromagnetic system's maximum range capability. It depicts a specified electromagnetic system's area of coverage on a curved earth, range-versus-height plot. Varying probabilities of detection are indicated by variations in the shading of the lobes. A numeric listing of some of the parameters used to generate the display, along with the location, and time and date information of the profile, is included at the top and bottom of this product.

8.5 Atmospheric Boundary Layer

Propagating electromagnetic waves, unless in a completely homogeneous medium, will experience some degree of bending due to changes in the index of refraction. The Earth's atmosphere is normally a very inhomogeneous fluid. Certain regions, such as the atmospheric boundary layer, characteristically have large mean gradients in temperature and/or humidity. Rapid vertical changes in both temperature and humidity create layers that significantly refract propagating electromagnetic signals. This phenomenon is readily apparent, for example, in the evaporation duct at the base of the marine atmospheric boundary layer and in the elevated trapping layer associated with the inversion layer at the top of the atmospheric boundary layer.

The atmospheric boundary layer is defined by Stewart (1979) as the portion of the lower atmosphere that has turbulent flow and is in direct contact with the Earth's surface. The atmospheric boundary layer extends from the surface to a height of a few feet (centimeters) in conditions of strongly stable stratification and to thousands of feet (meters) in highly convective conditions. On the average, the atmospheric boundary layer extends through the lowest 3300 ft (1 km) of the atmosphere and contains 10% of the mass of the atmosphere. The boundary layer is very important to the dynamics and thermodynamics of the atmosphere because it is in this layer that all momentum, water vapor, and thermal energy exchanges between the atmosphere and the Earth's surface take place.

Physical continuity between the atmosphere and the Earth dictates that wind velocity be zero at the immediate surface over land and equal to the surface drift current over water. Above the surface, velocity increases with height in an approximately logarithmic fashion to the top of the layer. Thus, strong vertical wind shear is common in this layer. It, along with convection, produces turbulence that facilitates the transport of moisture and momentum within the layer. The relatively homogeneous mixed layer directly above the turbulent surface layer constitutes the majority of the unstable atmospheric boundary layer. Turbulence tends to continuously erode local gradients and, thus, conditions are well mixed up to the inversion layer. The final 165 to 325 ft (50–100 m) of the convective atmospheric boundary layer is usually an inversion layer. In it the kinetic energy available for mixing is damped by strong stable vertical temperature gradients. The gradients have a "capping" effect on the convection below and effectively suppress exchange of physical properties with the free atmosphere above.

If the atmospheric boundary layer is cooled from below it will be stable. Turbulence is suppressed by the resulting density structure, and generally little mixing will occur except in the surface layer. All exchanges between the atmosphere and the Earth's surface are thus greatly reduced.

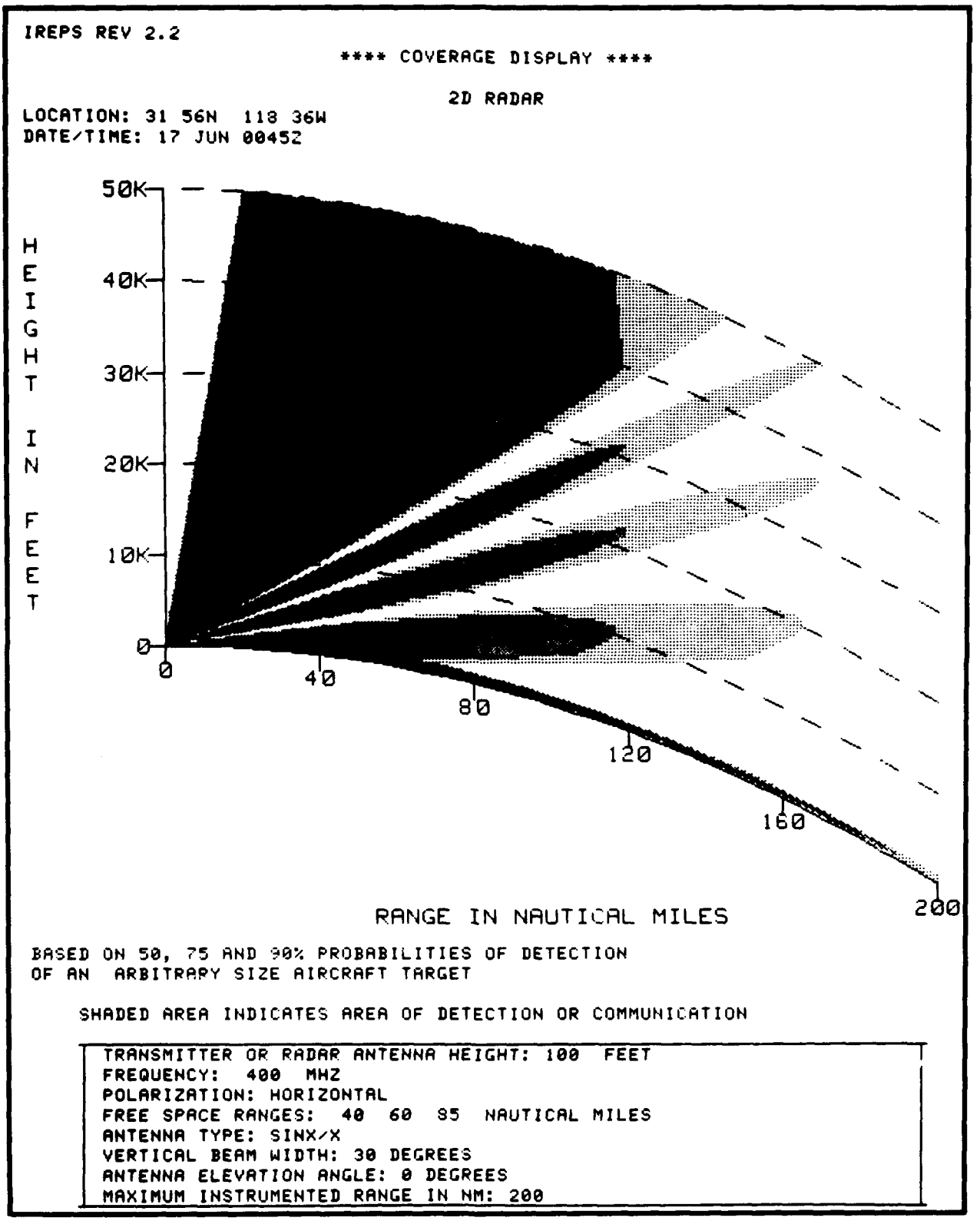

Figure 8-7. IREPS radar coverage diagram.

It is in the marine atmospheric boundary layer that the oceans and the atmosphere exchange energy directly in the form of turbulent heat, moisture, and momentum fluxes. Gases and solids are also in continuous exchange between each fluid. Wave activity can toss small water droplets directly into the lower atmosphere where they become suspended and eventually evaporate. Normally, evaporation from the sea surface creates a shallow layer of rapidly decreasing relative humidity from 100% at the sea surface to a lower value (80%-90%) directly above the sea surface. This low level feature produces an extended radar propagation phenomenon known as the evaporation duct because of its formation mechanism. The evaporation duct extends only tens of feet (meters) above the ocean's surface but is of great importance to the mariner because it occurs in varying degrees throughout all oceanic areas and results in over-the-horizon radar propagation.

The atmospheric boundary layer over land shows much more variation than the marine atmospheric boundary layer. Seasonal and diurnal changes are both more pronounced. Larger variations in the vertical temperature structure occur over land than over the ocean, but there is usually less vertical humidity variation. Radiative heating and cooling can cause large diurnal fluctuations in the height of the atmospheric boundary layer from near surface values at night to over 6500 ft (2000 m) during the day.

8.6 Arctic Refractive Conditions

Willis (1987) examined the spatial and temporal variability of the refractive structure of the lower atmosphere in the vicinity of the Fram Strait marginal ice zone (MIZ). The data used in this study were collected by four ships during the Marginal Ice Zone Experiments of 1984 (MIZEX-84). The ships operated in the pack ice, at the MIZ, and in the water adjacent to the ice edge.

The results of a spatial study showed that the refractive structure leading to elevated ducting was different over the pack ice and the MIZ from over the open water adjacent to the ice edge. The ducts were generally lower, weaker, and thinner over the pack ice with the averages of height, strength, and thickness increasing dramatically over the water as one traveled away from the ice edge. Scatter diagrams showed that the duct height, strength, and thickness exhibited a linearly increasing relationship with respect to distance from the ice. The average height, strength, and thickness values increased slightly from the pack ice to the MIZ and then dramatically increased from the MIZ to 115 n mi (210 km) from the ice edge. This linearly increasing relationship from the pack ice to the open water was strongest with the height data. These differences in the refractive structure over this relatively narrow region are tactically important. An electromagnetic wave transmitted from a source located over the ice would be affected differently than an electromagnetic wave transmitted from a source over the water. Multiple ducts were seen only at the ice edge and may have reflected the multiple inversions that were seen on sodar traces.

Willis (1987) also made a temporal study by selecting six regimes to assess the effect of the difference in synoptic flow on the refractive structure. In four of six regimes a cyclone passed over the area. When the low passed directly over all four of the ships no ducts were recorded. The greatest number of ducts was associated with the two regimes in which high

pressure dominated the period. This was the only situation in which persistence of the ducts was seen. On two separate occasions two ships reported ducts that persisted for 24 hr. However, at both these times only two of the four ships reported ducts, so once again it was seen that considerable spatial inhomogeneity existed. The longest case in which a duct persisted was 36 hr.

Shaw et al. (1989) has presented some results of refractive studies carried out during the MIZEX of 1984 and 1987. Several conclusions were drawn from that work derived from numerous summer and winter radiosonde records.

- First, substantial difficulty may be incurred in obtaining accurate refractivity profiles from rawinsondes in the Arctic if the sensors pass through subfreezing stratus clouds. Many launches from MIZEX-84 produced profiles that may indicate erroneous saturation due to frost formation on the humidity sensor.
- Second, irrespective of the frost formation problem, trapping layers in the marginal ice zone of the Arctic are in general quite weak and occur within 30 n mi (60 km) of the ice edge. Further, they occur typically 1000 to 2600 ft (300–800 m) above the surface, making them unlikely to affect surface-based microwave devices. However, there is a decidedly upward slope from ice (shallow boundary layer) to water (deeper boundary layer) of the trapping layer, which may indeed affect surface systems that are well into the ice. Trapping layers are also sporadic in extent. During the 1984 experiment the four ships making measurements never observed a trapping layer at the same time. The majority of the time (61%) only one ship observed a trapping layer, and a third of the time two ships made the observation.
- Third, horizontal homogeneity is observed less than 13% of the time in the Arctic at levels above 65,000 ft (20 km).
- Clearly, anomalous refraction will be of less consequence in the MIZ than in warmer regions of the globe. Equally clear, however, when anomalous refraction is important it will be largely attributable to horizontal variability of the refractivity field.

SPECIAL NOTE: At the time of publication of this handbook, research was being conducted which will improve on the IREPS concept. A range dependent radar propagation model, Radio Physical Optics (RPO), has been developed at the Naval Command, Control and Ocean Surveillance Center, RDT&E Division and is now being validated. Where IREPS assumes a horizontal homogeneous atmosphere using a single data point (local RAOB), RPO is coupled with a gridded atmospheric model yielding RPO output at each grid point. These data often show a horizontal inhomogeneous atmosphere.

9. NUMERICAL MODELS

The forecaster using numerical model generated weather products can benefit by acquiring some knowledge of the models and computer systems that produce the charts and data sent to the field. Each numerical model is part of a system that not only creates a forecast but also performs data assimilation, data analysis, and quality control. Many factors combine to determine the quality and usefulness of a model forecast.

A primary consideration is to keep in mind inherent limitations of numerical models in terms of resolvable spatial scales. For example, a model with 50 n mi (80 km) grid spacing should not be expected to forecast coastal sea breeze circulations on a scale of 5 to 10 n mi (8 to 16 km).

The current version of NOGAPS (Navy Operational Global Atmospheric Prediction System), introduced in August 1989 is a T79 spectral model, meaning that 79 wave numbers are represented. The system is therefore able to resolve features that are 500 km (310 mi) or more in horizontal extent (Fig. 9-1). At present, NOGAPS is the only operational atmospheric model run by the Navy that provides coverage of Arctic regions.

Typical polar lows have spatial scales on the order of a few hundred to 1000 km (620 mi), placing them at the lower limit of features that NOGAPS is able to resolve. In some cases the model forecast may be used to infer the presence or likelihood that a given small-scale feature does exist. For example, a sea breeze circulation is likely to occur when synoptic-scale winds are light and a strong contrast in temperature exists between the land surface and adjacent water surface.

Physical processes that are too small for a model to resolve are parameterized in terms of the model prognostic variables, which include temperature, winds, and moisture. The methods used to parameterize physical processes vary widely among numerical models and can lead to significant differences in forecast quality. The Naval Operational Global Atmospheric Prediction System includes parameterizations for vertical diffusion, cumulus convection, and long- and short-wave radiation. The Arakawa-Schubert cumulus parameterization used in NOGAPS is considered one of the most sophisticated used in any global model.

Four times daily NOGAPS performs data assimilation, using surface, upper air, and satellite observations. Forecasts are produced out to 120 hr from 00 UTC, and to 72 hr from 12 UTC. The model is run at the Fleet Numerical Oceanography Center (FNOC) in Monterey, California.

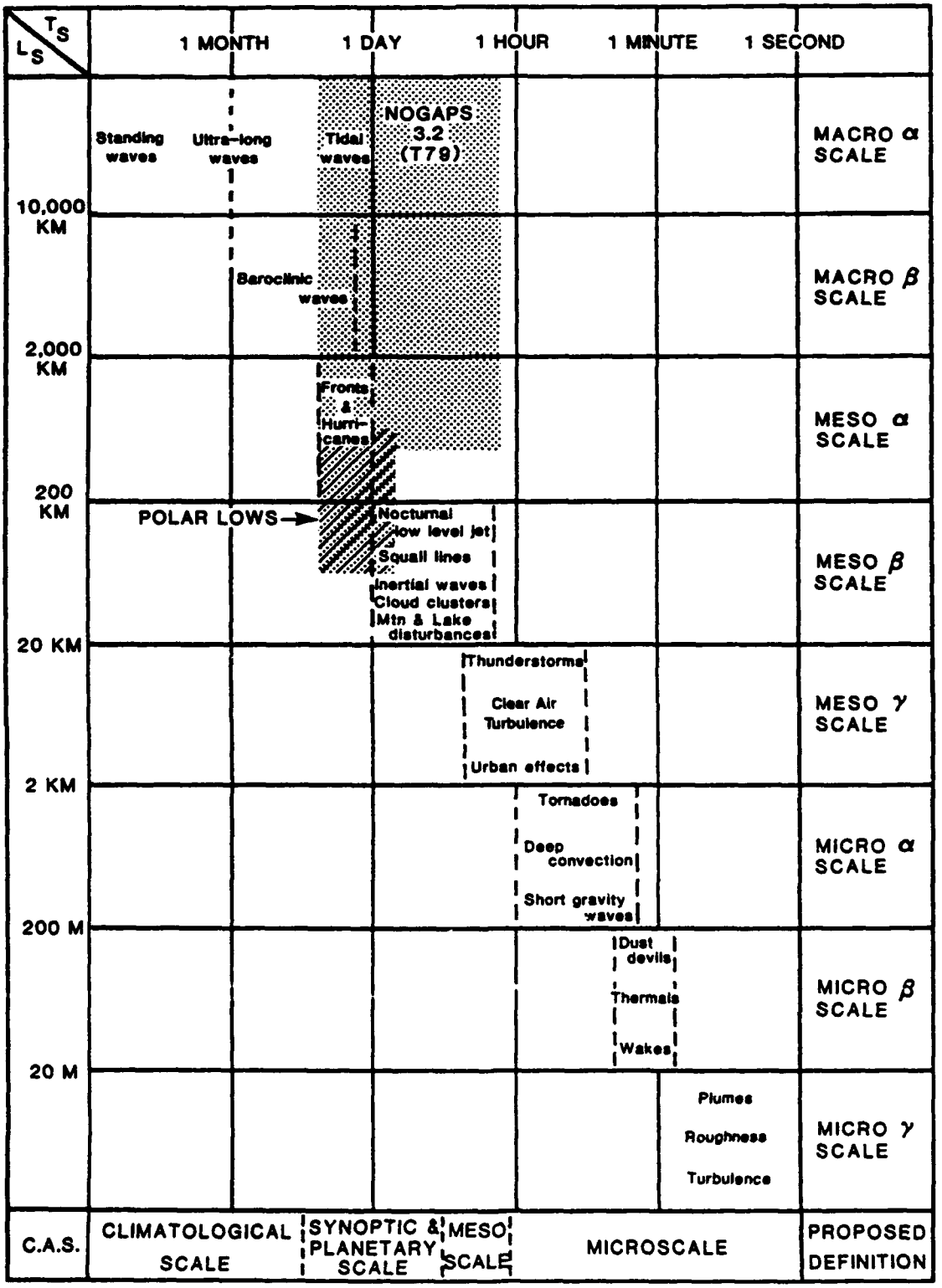

Figure 9-1. Scale definitions and various processes with characteristic time and horizontal scales.

In terms of systematic errors, NOGAPS is somewhat slow to deepen developing storms and slow to fill cyclones that are past their deepest point of development. Storm tracks tend to be poleward and lag behind the analyzed cyclone position. The system tends to perform best on deep baroclinic systems, as opposed to shallow storms driven by latent heat release close to the surface. A more complete discussion of NOGAPS, including descriptions of numerical procedures is give by Hogan and Rosmond (1991).

The FNOC products that use NOGAPS forecast fields include an ocean wave model (WAM), an ocean mixed layer model (TOPS), the Polar Ice Prediction System (PIPS), the Navy Operational Regional Atmospheric Prediction System (NORAPS), and the Optimum Path Aircraft Routing System (OPARS). The following discussion of NOGAPS forecasting models is intended only to provide an introduction and overview of basic model characteristics.

9.1 Description of the Navy Operational Global Atmospheric Prediction System

The Fleet Numerical Oceanography Center in Monterey runs two large scale numerical models on an operational basis. These are the global model NOGAPS and the regional model NORAPS. The latter system can be run over the polar regions, but the current plan calls for NOGAPS to provide primary forecast coverage of the Arctic. The operational version of NOGAPS is upgraded frequently; the description included here is accurate as of late 1991.

Until 1981 the FNOC ran a hemispheric grid point, primitive equation model having a horizontal resolution of 205 n mi (380 km). The first FNOC global model was NOGAPS 2.0, which had a resolution of 2.4° east-west and 3.0° north-south. Installed operationally in January 1988, NOGAPS 3.0 was the first spectral model. This version was a T47 spectral model with equivalent horizontal resolution of 2.5°, equivalent to about 150 n mi (275 km) in the longitudinal direction (and east-west at the Equator).

In September 1989 NOGAPS 3.2 became operational and included a significant increase in horizontal resolution—from T47 to T79 (1.5°, 90 n mi or 165 km). This version has 18 vertical levels and contains a complete set of physical parameterizations, including long- and short-wave radiation and cumulus convection (Hogan and Rosmond, 1991). The forecasts made by NOGAPS 3.2 extend to 120 hr, and the quality is considered equal or superior to the global model produced by the National Meteorological Center.

The NOGAPS 3.2 is run on the FNOC Cyber 205, taking approximately 15 min per forecast day (excluding input-output time). Planned increases in computer power may allow for an increase in resolution equivalent to 50 n mi (80 km), the current grid spacing now used in NORAPS.

The following section provides a general description of NOGAPS performance in Arctic regions. The forecaster should be aware of model biases as well as the inherent limitations of scale in the model.

9.2 Verification of Numerical Model Forecasts

Computer forecast models are in a perpetual state of update, revision, and change. For this reason, it is necessary to monitor the accuracy of the model continuously in hopes of spotting error tendencies. Although monitoring is usually performed at the center producing the forecast model, the user should still verify the model forecasts against the analyses for his or her area of responsibility. An evaluation of a particular model is not included in this handbook, since it would soon be outdated. Rather, a few simple guidelines are given to assist the forecaster in evaluating models.

The sparsity of data has always been a problem that forecasters must face every day. Sometimes a forecast can depend on one crucial observation from one observing station. Computer models are also highly dependent on observational data. Even in data poor areas, such as the tropic and polar regions, analyses must still be produced. Inevitably, schemes must be developed to handle these regions.

The most common method of performing an analysis of the existing atmospheric variables (e.g., temperature, moisture, pressure) employs a first-guess field. This is commonly the 6- or 12-hr model forecast from the previous model run. Observational data are interpolated to grid points and compared with the first-guess value at each point. If a number of observations influence a grid point, the first-guess field is essentially ignored. But in data poor areas, it is possible that no observational data are available within a reasonable distance of a grid point. In such cases, the first-guess field becomes the analysis at that particular grid point. If only a limited number of observations are found, the data are blended with the first-guess field to arrive at an analysis.

It is apparent that the first-guess field can play a large role in the analysis of the current meteorological variables. Thus, a good first-guess field is critical. Without observational data, the analysis field in certain areas is nearly a reproduction of the model's earlier forecast. The result is a catch-22 situation: a poor forecast leads to a poor analysis, which leads to a poor forecast. The Arctic forecaster needs to be aware of this possibility. Even though a computer analysis has a low pressure center at a given location and intensity, it may only be a poor forecast from 12 hr earlier.

The sources of data also need to be considered by a forecaster using a computer model. The surface and upper air observational network is fairly well established and widely known. Satellites, however, can provide large amounts of data that are usable by computer-generated analyses. These data are usually supplied in two forms: cloud track winds and vertical thickness soundings.

Cloud track wind data are largely confined to the midlatitudes. They are a man-machine mix form of data where the human determines the wind direction based on cloud motion and the computer decides on the height of the cloud based on its temperature. Vertical soundings are completely automated (i.e., no human intervention required) and can provide large amounts of data anywhere over the globe. These data are in the form of temperature or thickness soundings for a single column, similar to that of a radiosonde. However, the accuracy and vertical density of the data are much less than that of a radiosonde. Still, the value of these data in the Arctic region cannot be disputed.

Another consideration is the time of the model forecast (i.e., 0000 GMT or 1200 GMT). Surface ships often only report during daylight hours. In the Pacific Ocean, for example, the plan of operation means that more data are available for the 0000 GMT run than for the 1200 GMT run, as shown in Fig. 9-2. Obviously this data disparity would have a great effect on the surface analysis in the region. Time of day is less of a problem for upper air data such as RAOBS, AIREPS, and satellite soundings.

(a)

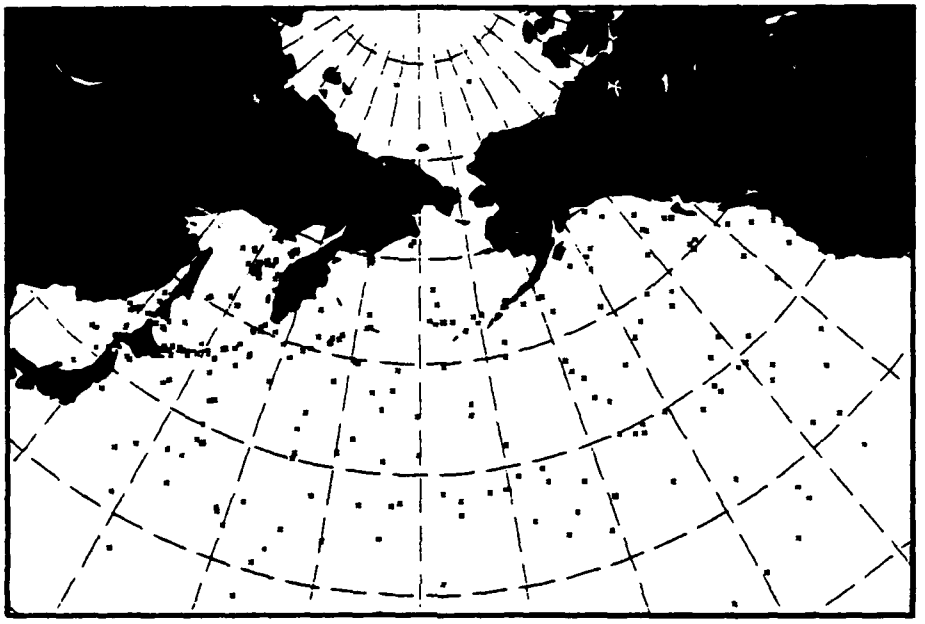

(b)

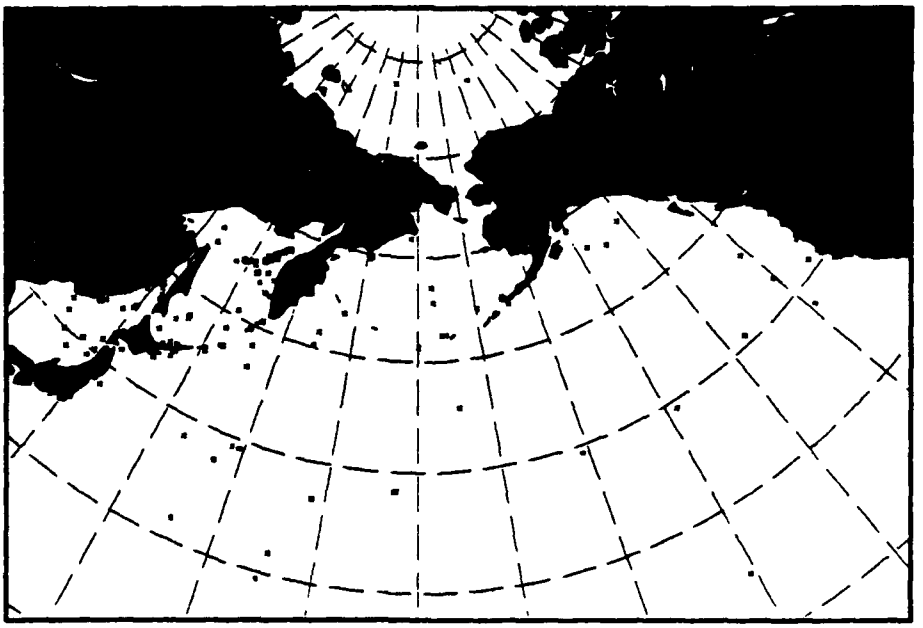

Figure 9-2. Location of surface ship observations in the North Pacific for 18 January 1989 at (a) 0000 GMT and (b) 1200 GMT.

9.2.1 Model Errors

Computer forecast models are far from perfect. Whereas, in some instances the guidance they give is very valuable, at other times they can give erroneous forecasts leading to major busts. Even in these situations, however, the information provided by the model can be useful if the error characteristics of the forecast model are known.

Random observation of a model performance can often lead to incorrect assumptions about a model's behavior. For example, a low that is underforecast 7 mb by a model on a given day does not mean that all lows in all situations are underforecast by the model. Rather, the model's performance must be evaluated daily over a period of time to understand the error pattern.

Model errors fall into two classes: model tendencies and systematic errors. The former refers to similar treatment of a situation without regard to season or location. An example would be that the model deepens lows too slowly. A systematic error refers to an error occurring in the same location and/or time more than once. Knowledge of both kinds of errors can be very useful to a forecaster.

9.2.2 Model Tendencies

A recurring model tendency (NOGAPS 3.2) in the western Aleutian Islands and Kodiak Island area is to move lows erroneously into the interior of Alaska in the winter. One possible theory for this tendency is the model's limited ability to discern the cold valley between the mountain ranges. In winter, the valley will stay very cold 14 to 22 °F (−10 to −30 °C), creating a stable high pressure area. Unless strong southerly (warming) winds aloft remain over the area for least a day or two, the high pressure will remain, blocking transitory lows. These southerly winds also act as steering flow to move lows into the interior. A series of maps from November 1991 illustrates this tendency. Figure 9-3, the surface chart for 1200 GMT 14 November 1991, shows a large low pressure center near 55 °N and the Dateline. The corresponding 500-mb chart is shown in Fig. 9-4. Note that strong southerly flow aloft does not extend into central Alaska.

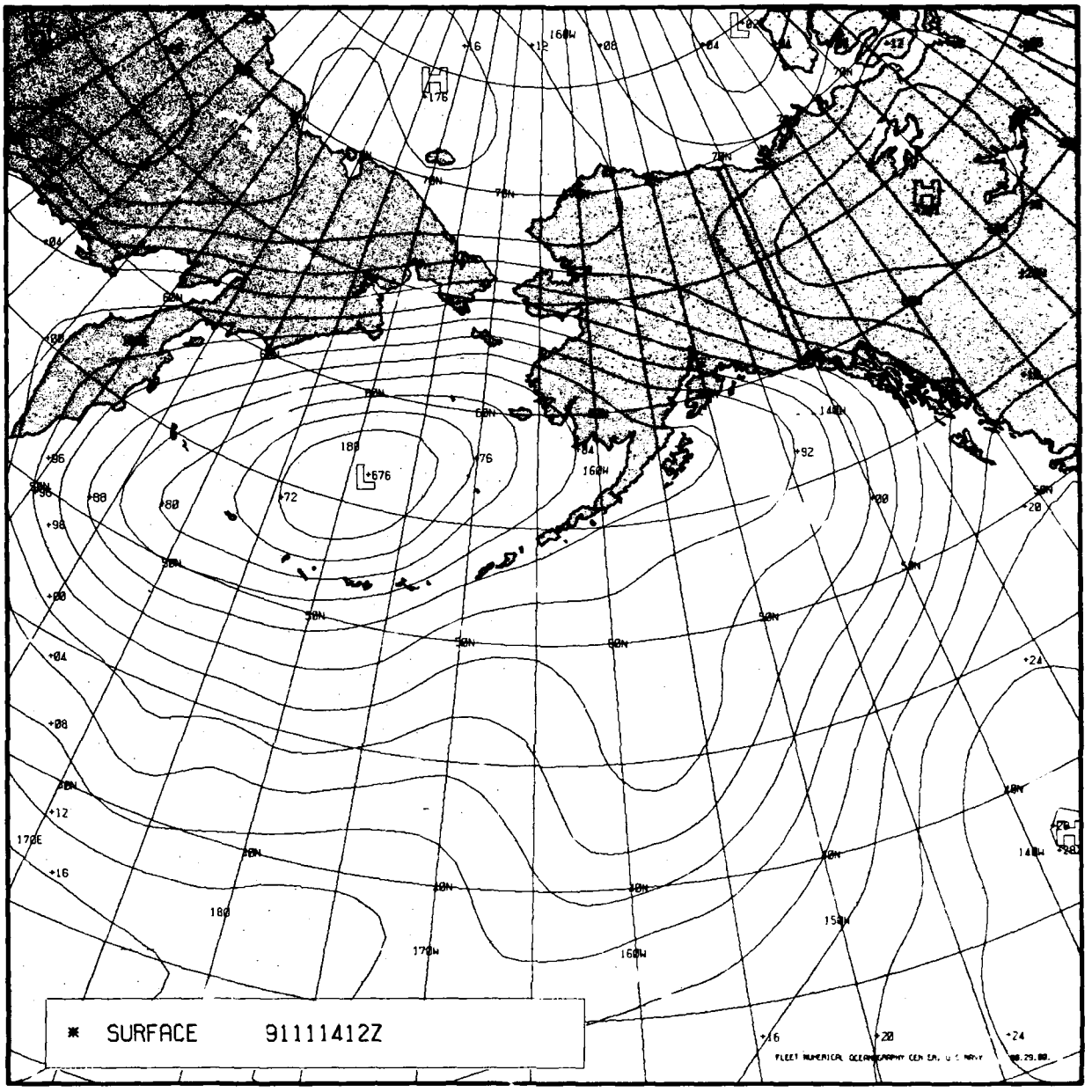

Figure 9-3. FNOC surface analysis 1200 GMT 14 November 1991.

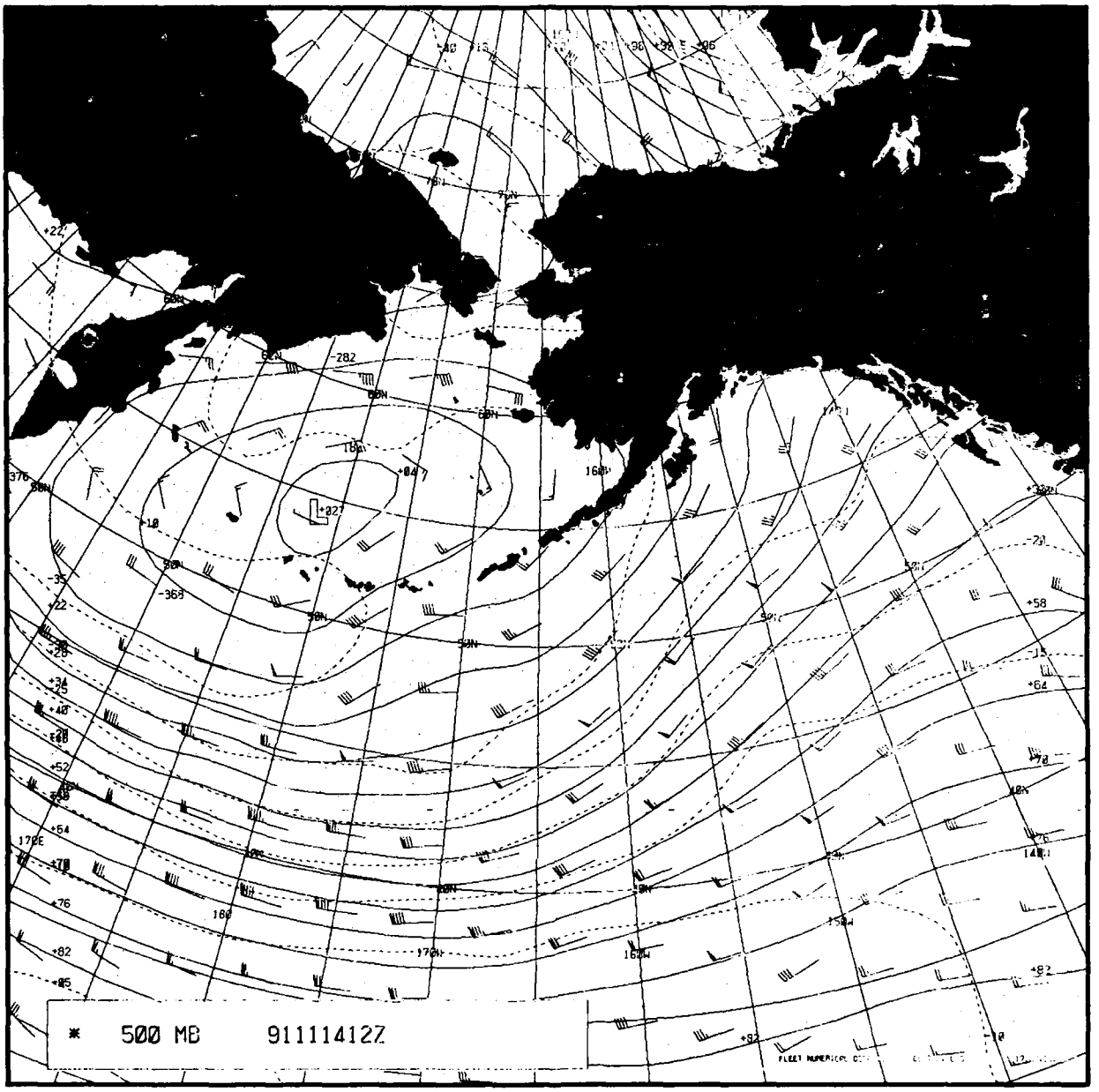

Figure 9-4. FNOC 500-mb analysis 1200 GMT 14 November 1991.

Surface forecast maps for 48 hr and 72 hr are based on 1200 GMT 14 November 1991 (Fig. 9-3). These maps are shown in Figs. 9-5 and 9-6, respectively.

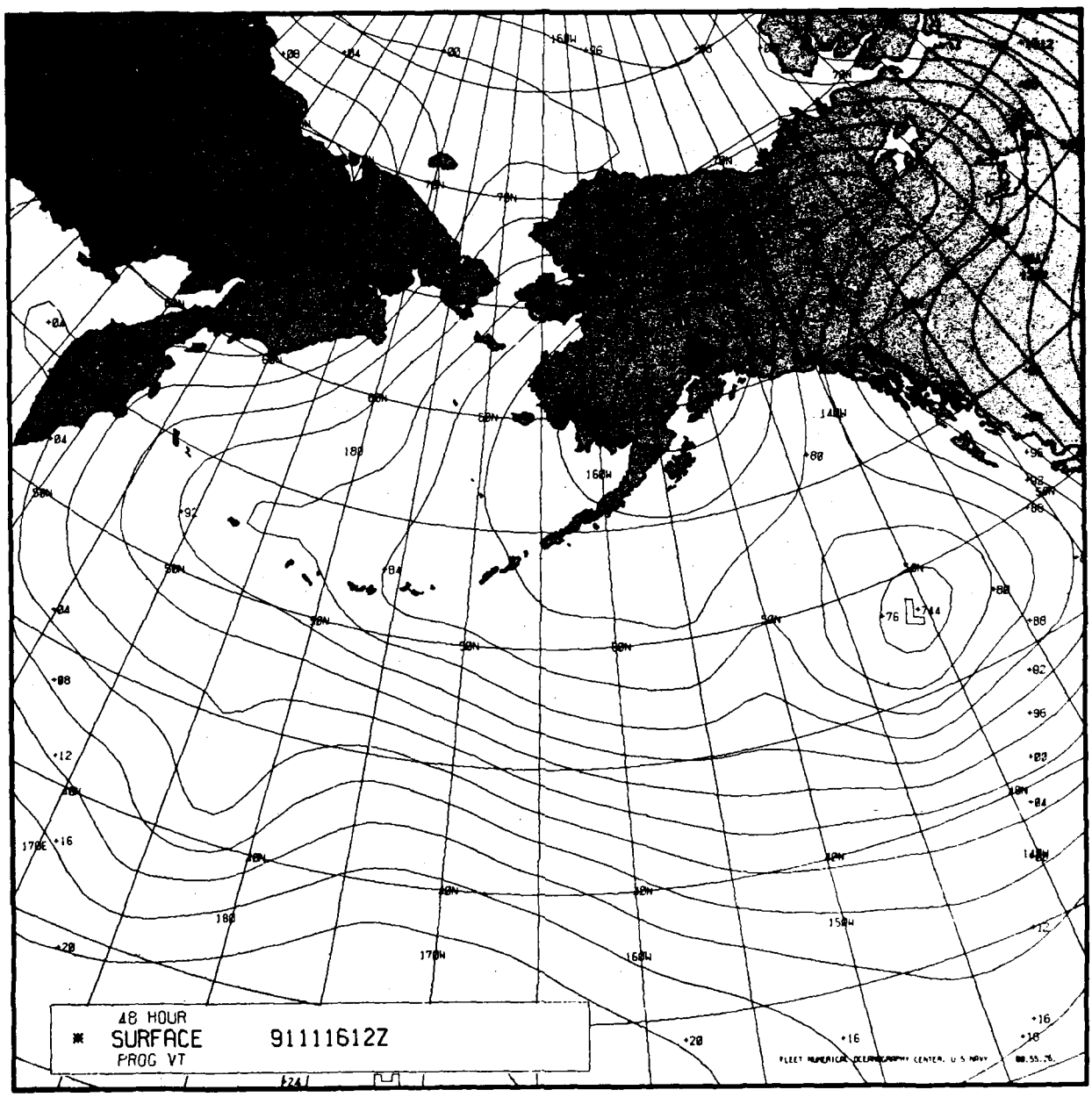

Figure 9-5. FNOC 48-hr surface forecast chart valid 1200 GMT 16 November 1991.

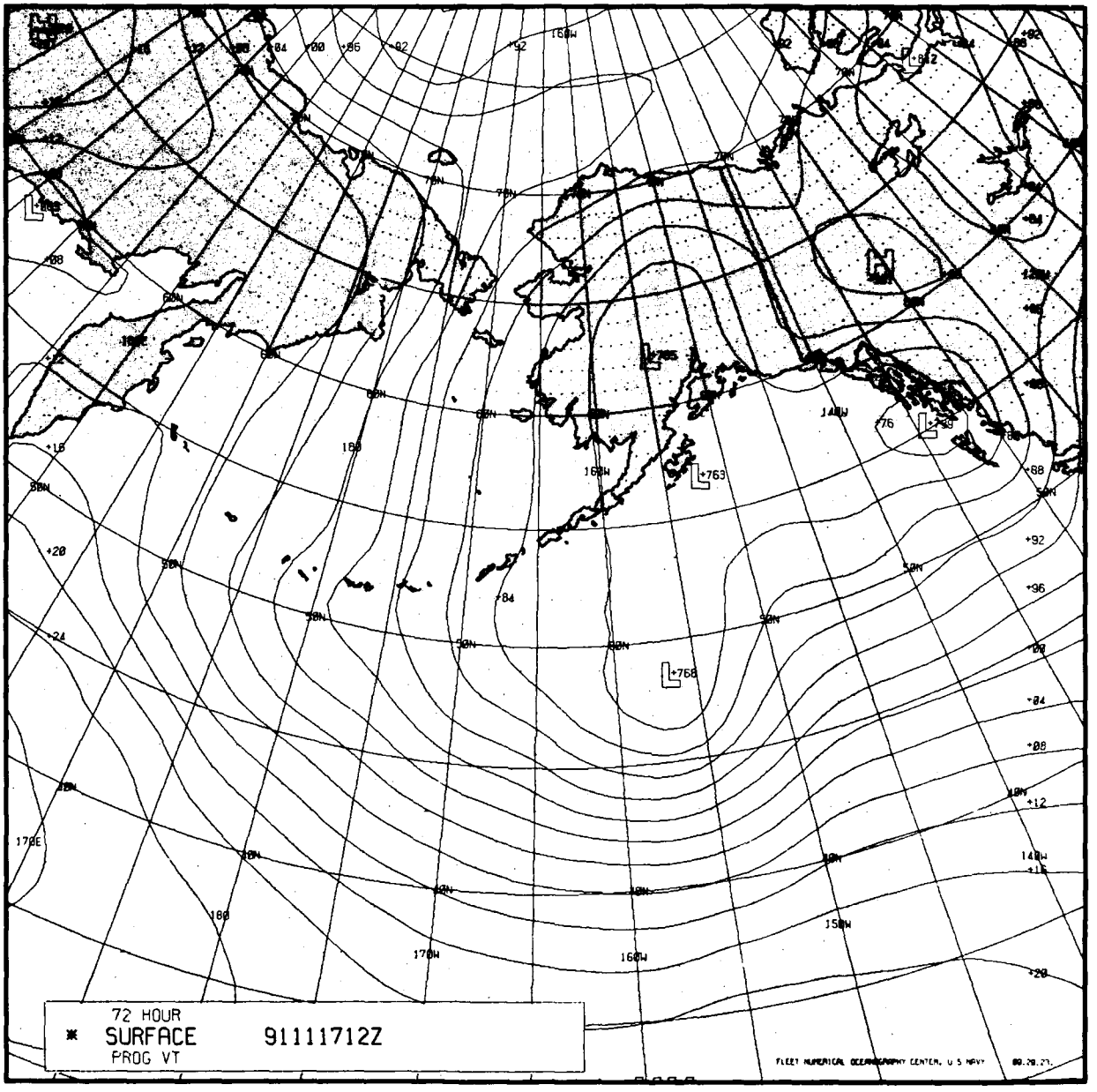

Figure 9-6. FNOC 72-hr surface forecast chart valid 1200 GMT 17 November 1991.

Interior surface temperatures at the beginning of this series (Fig. 9-3) ranged from about 3 to −8 °F (−16 to −22 °C). Remember too, at this time, the absence of strong southerly winds aloft. These two facts would lead the forecaster to believe that lows moving into the Kodiak Island area would stay south of the Alaskan interior. However, both the 48-hr prog (Fig. 9-5) and the 72- hr prog (Fig. 9-6) show lows in the interior. Throughout the period of this series of charts, temperatures stayed cold in the interior and winds aloft remained relatively weak. Subsequent surface analyses show that the lows did track south of Alaska and not into the interior. Figure 9-7 is an example valid at the time of the 48-hr forecast chart, Fig. 9-5.

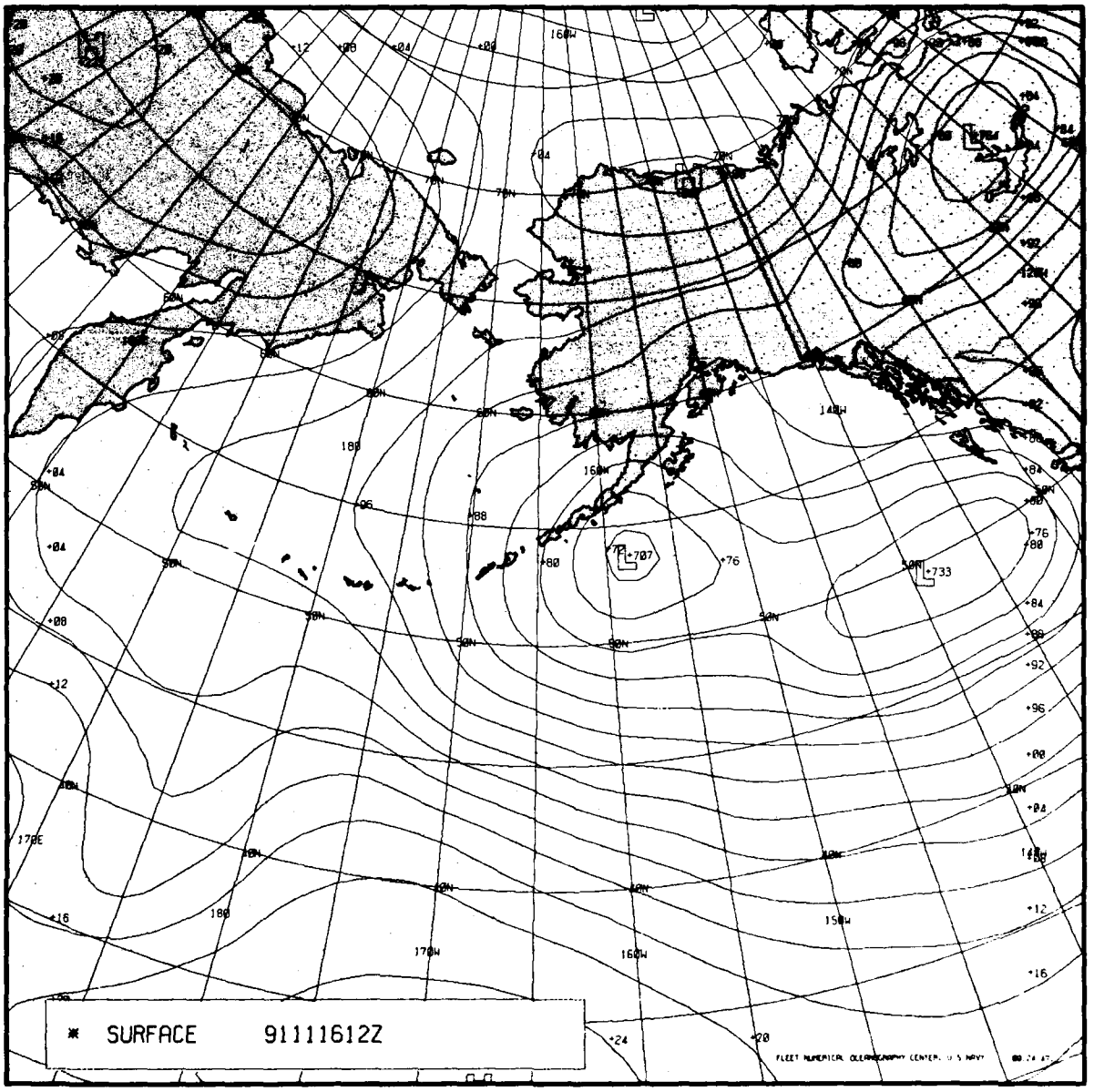

Figure 9-7. FNOC surface analysis 1200 GMT 16 November 1991.

9.3 Summary

The model tendency shown in the previous example can persist for days, appearing continuously in several forecast charts. A major pattern change will usually force the tendency to disappear, but it will most likely reappear soon. Forecasters must be alert and watch for this possibility.

Numerical models provide a great deal of information that can assist a forecaster. The Navy's numerical guidance products available to the fleet are as good as any in the world and better than most. Unfortunately, model (any model) forecasts are not always correct. It is easy to become too trusting of the computer forecasts, that is, accepting the forecasts as correct without questioning their validity. Eventually, the model has a major bust, which leads to an embarrassing situation for the forecaster. A total lack of trust in models usually results.

To avoid this complete loss of faith in model forecasts, they should be constantly scrutinized for accuracy. A working knowledge of systematic errors and model tendencies, such as the preceding example, will help prevent a forecaster from using erroneous computer guidance that could lead to large forecast errors.

SPECIAL NOTE: In the spring of 1992 an R & D version of the NORAPS model, having an entirely new physics package and 20 km grid spacing, was used in support of the Leads Experiment (LEADEX) in the Beaufort Sea area. The products generated by the model and used by LEADEX forecasters were found to be of excellent quality. This model has not yet been implemented operationally.

References

Ahlnäs, K., and G. Wendler, 1979: Sea-ice observations by satellite in the Bering, Chukchi, and Beaufort Seas. *Proc., Port and Ocean Engineering Under Arctic Conditions,* Trondheim, Norway, Vol. 1, 313–329.

Barnes, J.C., and C.J. Bowley, 1979: A five-year sea ice climatology of the Bering Sea derived from satellite observations. *Proc., Port and Ocean Engineering Under Arctic Conditions,* Trondheim, Norway, Vol. 1, 191–205.

Bascom, W., 1980: *Waves and Beaches* (update of 1964 publication), Anchor Books, Garden City, NY.

Battan, L.J., 1973: *Radar Observation of the Atmosphere.* University of Chicago Press, Chicago, IL.

Bauer, J., and S. Martin, 1980: Field observations of the Bering Sea ice edge properties during March 1979. *Mon. Wea. Rev., 108* (12), 2045–2056.

Bean, B.R., and E.J. Dutton, 1966: *Radio Meteorology.* NBS Monograph 92, U.S. Department of Commerce, National Bureau of Standards, Washington, D.C.

Brower, W.A., Jr., R.G. Baldwin, L.D. Leslie, C.N. Williams, Jr., and J.L. Wise, 1988: *Climatic Atlas of the Outer Continental Shelf Waters and Coastal Regions of Alaska.* NCDC/NESDIS/NOAA, Arctic Environmental and Data Center, University of Alaska, Anchorage, AK.

Brown, R.A., 1986: The planetary boundary precursor to the polar low. *Proc., International Conference on Polar Lows,* Oslo, 1986, Norwegian Meteorological Institute, Oslo, Norway.

Businger, S., 1987: The synoptic climatology of polar-low outbreaks over the Gulf of Alaska and the Bering Sea. *Tellus, 39A,* 307–325.

Coachman, L.K., K. Aagaard, and R.B. Tripp, 1975: *Bering Strait: The Regional Physical Oceanography,* University of Washington Press, Seattle, WA. 172 pp.

Coachman, L.K., and K. Aagaard, 1981: Reevaluation of water transports in the vicinity of the Bering Strait. *The Eastern Bering Sea Shelf: Oceanography and Resources,* Vol. 1. Office of Marine Pollution Assessment, National Oceanic and Atmospheric Administration, Washington, D.C., 95–110.

Cook, J. and S. Payne, 1987: *Summary of environmental effects on sensors and communications systems.* NEPRF Technical Report TR87-02, Naval Environmental Prediction Research Facility, Monterey, CA.

Dotson, M.E., 1987: "An evaluation of the impact of variable, temporal and spatial data resolution upon IREPS." Master's thesis, Naval Postgraduate School, Monterey, CA.

Emanuel, K.A., and R. Rotunno, 1989: Polar lows as arctic hurricanes. *Tellus, 41A,* 1–17.

Encyclopedia of Oceanography, 1966: Chapter on Pacific Ocean, R.W. Fairbridge (ed.), Reinhold Publishing Corporation, New York, p. 659.

Favorite, F., 1974: Flow into the Bering Sea through Aleutian island passes. *Oceanography of the Bering Sea, Proc., International Symposium for Bering Sea Studies, Hakodate, Japan, 1972,* D.W. Hood and E.J. Kelley (eds.), Institute Marine Science, Occasional Publication No. 2, University of Alaska, Fairbanks, AK, 900 pp.

Fett, R.W., 1992: Case 2, Ship's Icing, *Navy Tactical Applications Guide (NTAG),* Vol. 8, Part 2. NRL Publication NRL/PU/7541--92-0005, Naval Research Laboratory, Monterey, CA.

Garwood, R.W., R.W. Fett, K.M. Rabe, and H.W. Brandli, 1981: Ocean frontal formation due to shallow water cooling effects as observed by satellite and simulated by a numerical model. *J. Geophys. Res., 86* (C11), 11000–11012.

Grubbs, B.E., and R.D. McCollum, Jr., 1968: *A climatological guide to Alaskan weather* (revised in 1978 by R.H. Padgett), Elmendorf Air Force Base, AK.

Hogan, T.F., and T.E. Rosmond, 1991: The description of the Navy operational global atmospheric prediction system's spectral forecast model. *Mon. Wea. Rev., 119* (8), 1786–1815.

Kotsch, W.J., 1983: Ice Accretion—Hazard of significance to seafarers. *Weather for the Mariner,* Chapter 10, Naval Institute Press, Annapolis, MD.

Lackmann, G.M., and J.E. Overland, 1989: Atmospheric structure and momentum balance during a gap-wind event in Shelikof Strait, Alaska. *Mon. Wea. Rev., 117* (8), 1817–1833.

Macklin, S.A. N.A. Bond, and J.P. Walker, 1990: Structure of a low-level jet over the lower Cook Inlet. *Mon. Wea. Rev., 118* (12), 2568–2578.

Miller, D.R., 1973: Class notes, Ice Observers School, U.S. Navy Fleet Weather Facility, Suitland, MD.

Minsk, D.L., 1977: *Ice accumulation on ocean structures.* CRREL Report 77-17, Cold Regions Research and Engineering Laboratory, Hanover, NH.

Minsk, D.L., 1980: *Icing on structures.* CRREL Report 80-31, Cold Regions Research and Engineering Laboratory, Hanover, NH.

Nelson, C.H., D.M. Hopkins, and D.W. Scholl, 1974: Cenozoic sedimentary and tectonic history of the Bering Sea. *Oceanography of the Bering Sea, Proc., International Symposium for Bering Sea Studies, Hakodate, Japan, 1972,* D.W. Hood and E.J. Kelley (eds.) Institute Marine Science, Occasional Publication No. 2, University of Alaska, Fairbanks, AK, 900 pp.

Pease, C.M., 1980: Eastern Bering Sea ice processes. *Mon. Wea. Rev., 108* (12), 2015–2023.

Pritchard, R.S., R.W. Reimer, and M.D. Coon, 1979: Ice flow through straits. *Proc., Port and Ocean Engineering Under Arctic Conditions,* Trondheim, Norway, Vol. 3, 61–74.

Salo, S.A., J.D. Schumacher, and L.K. Coachman, 1983: *Winter currents on the eastern Bering Sea shelf.* NOAA Technical Memorandum ERL-PMEL-45, Pacific Marine Environmental Laboratory, U.S. National Oceanic and Atmospheric Administration, Seattle, WA.

Shapiro, M.A., and L.S. Fedor, 1989: A case study of an ice edge boundary layer front and polar low development over the Norwegian and Barents Seas. *Polar and Arctic Lows*, P.W. Twitchell, E.A. Rasmussen, and K.L. Davidson (eds.) A. Deepak Publishing, Hampton, VA, 257–278.

Shaw, W.J., K.L. Davidson, Z. Willis, and D. Groters, 1989: Horizontal variability of mean refractive structure in the Arctic. *Proc., Conference on Microwave Propagation in the Marine Boundary Layer,* NEPRF Technical Report TR89-02, Naval Environmental Prediction Research Facility, Monterey, CA.

Squire, V.A., and S.C. Moore, 1980: Direct measurement of the attenuation of ocean waves by pack ice. *Nature, 283,* 365–368.

Stewart, R.W., 1979: *The Atmospheric Boundary Layer.* World Meteorological Organization, Geneva.

Taiyo Fishing Company, Ltd., 1972: *Study on Preventative Measures Against Icing Induced Marine Accidents of Fishing Vessels,* Japan.

Takenouti, A.Y., and K. Ohtani, 1974: Currents and water masses in the Bering Sea: A review of Japanese work. *Oceanography of the Bering Sea, Proc., International Symposium for Bering Sea Studies, Hakodate, Japan, 1972,* D.W. Hood and E.J. Kelley (eds.) Institute Marine Science, Occasional Publication No. 2, University of Alaska, Fairbanks, AK, 900 pp.

U.S. Navy, 1985: *Aerographers' Mate 1 and C.* NAVEDTA 10362-B1, U.S. Government Printing Office, Washington, D.C.

U.S Navy, 1988: *Cold Weather Handbook for Surface Ships.* OPNAV P-03C-01-89, Chief of Naval Operations, Washington, D.C.

Walter, B.A., 1980: Wintertime observations of roll clouds over the Bering Sea. *Mon. Wea. Rev., 108* (12), 2024–2031.

Willis, Z.S., 1987: "The spatial and temporal variability of the Arctic atmospheric boundary layer and its effect on electromagnetic (EM) propagation." Master's thesis, Naval Postgraduate School, Monterey, CA.

Appendix A

Glossary of Ice Terms

The following text and photos are adapted from Sea Ice Nomenclature, WMO No. 259, TP 145.

AGED RIDGE: Ridge that has undergone considerable weathering. These ridges are best described as undulations.

ANCHOR ICE: Submerged ice attached or anchored to the bottom, irrespective of the nature of its formation.

BARE ICE: *Ice without snow cover.*

BELT: A large feature of pack ice arrangement that is longer than it is wide, from 0.5 mi to 65 mi (1–100 km) in width.

BERGY BIT: A large piece of floating glacier ice, generally showing less than 16 ft (≈ 5 m) above sea level but more than 3 ft (≈ 1 m) and normally about 120 to 360 sq yds (≈ 100–300 sq m) in area.

BESET: Situation of a vessel surrounded by ice and unable to move.

BIGHT: An extensive crescent-shaped indentation in the ice edge, formed by either wind of current.

BRASH ICE: Accumulations of floating ice made up of fragments not more than 6.5 ft (≈ 2 m) across, the wreckage of other forms of ice.

BUMMOCK: From the point of view of the submariner, a downward projection from the underside of the ice canopy; the counterpart of a hummock.

CALVING: The breaking away of a mass of ice from an ice wall, ice front, or iceberg.

CLOSE PACK ICE: Pack ice in which the concentration is seven-tenths to eight-tenths, composed of floes mostly in contact.

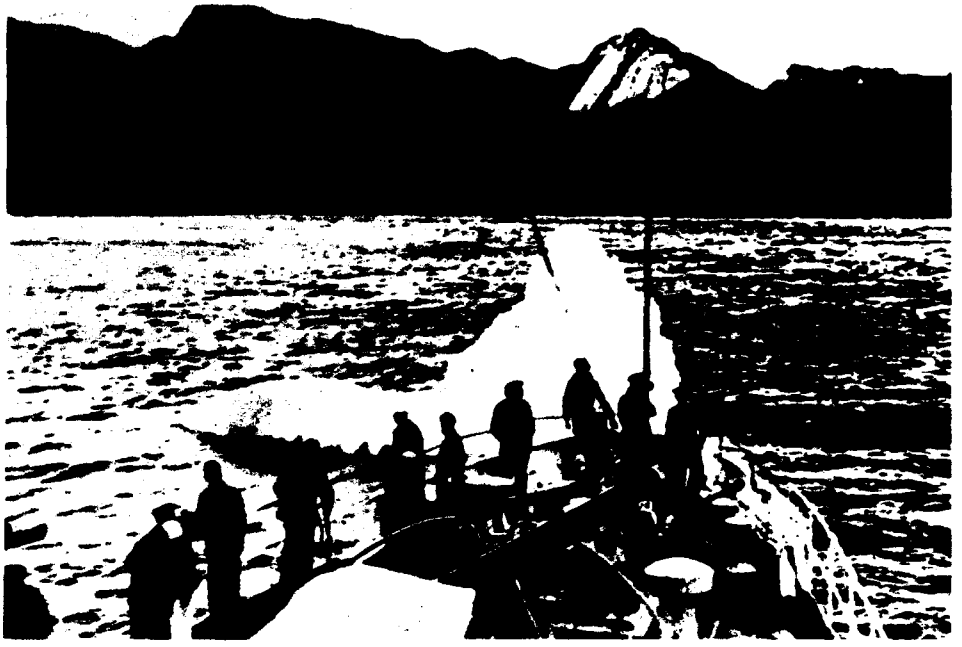

Figure A-1. Example of a Bergy Bit.

COMPACTED ICE EDGE: Close, clear-cut ice edge compacted by wind or current; usually on the windward side of an area of pack ice.

COMPACTING: Pieces of floating ice are considered to be compacting when they are subjected to a converging motion, which increases ice concentration and/or produces stresses that may result in ice deformation.

COMPACT PACK ICE: Pack ice in which the concentration is ten-tenths, and no water is visible.

CONCENTRATION: The ratio in tenths of the sea surface actually covered by ice to the total area of sea surface, both ice covered and ice free, at a specific location or over a defined area.

CONCENTRATION BOUNDARY: A line approximating the transition between two areas of pack ice with distinctly different concentrations.

CONSOLIDATED PACK ICE: Pack ice in which the concentration is ten-tenths and the floes are frozen together.

CONSOLIDATED RIDGE: A ridge in which the base has frozen together.

CRACK: Any fracture that has not parted.

DARK NILAS: Nilas that is under 2 in (5 cm) in thickness and is very dark in color.

DEFORMED ICE: A general term for ice that has been squeezed together and, in places, forced upwards (and downwards). Subdivisions are rafted ice, ridged ice, and hummocked ice.

DIFFICULT AREA: A general qualitative expression to indicate, in a relative manner, that the severity of ice conditions prevailing in an area is such that navigation in it is difficult.

DIFFUSE ICE EDGE: Poorly defined ice edge limiting an area of dispersed ice; usually on the leeward side of an area of pack ice.

DIVERGING: Ice fields or floes in an area are subjected to diverging or dispersive motion, thus reducing ice concentration and/or relieving stresses in the ice.

DRIED ICE: Sea ice from the surface of which meltwater has disappeared after the formation of cracks and thaw holes. During the period of drying, the surface whitens.

EASY AREA: (Opposite of DIFFICULT AREA listed above) Navigation is not difficult.

FAST ICE: Sea ice that forms and remains fast along the coast, where it is attached to the shore, to an ice wall, to an ice front, between shoals or grounded icebergs. Vertical fluctuations may be observed during changes of sea level. Fast ice may be formed on site from sea water or by freezing of pack ice of any age to the shore, and it may extend a few yards (meters) or several hundred miles (kilometers) from the coast. Fast ice may be more than one year old and may then be prefixed with appropriate age category (old, second-year, or multiyear). If it is thicker than about 7 ft (2 m) above sea level, it is called an ice shelf.

FAST-ICE BOUNDARY: The ice boundary at any given time between fast ice and pack ice.

FAST-ICE EDGE: The demarcation at any given time between fast ice and open water.

FINGER-RAFTED ICE: Type of rafted ice in which floes thrust "fingers" alternately over and under the other.

FIRN: Old snow that has recrystallized into a dense material. Unlike ordinary snow, the particles are to some extent joined; but, unlike ice, the air spaces in it still connect with each other.

FIRST-YEAR ICE: Sea ice of not more that one winter's growth, developing from young ice; thickness 1 to 7 ft (30 cm–2 m). May be subdivided into thin first-year ice (white ice), medium first-year ice, and thick first-year ice.

FLAW: A narrow separation zone between pack ice and fast ice, where the pieces of ice are in a chaotic state; it forms when pack ice shears under the effect of a strong wind or current along the fast ice boundary.

FLAW LEAD: A passageway between pack ice and fast ice that is navigable by surface vessels.

FLAW POLYNYA: A polynya between pack ice and fast ice.

FLOATING ICE: Any form of ice found floating in water. The principal kinds of floating ice are lake ice, river ice, and sea ice, which form by the freezing of water at the surface, and glacier ice (ice of land origin) formed on land or in an ice shelf. The concept includes ice that is stranded or grounded.

FLOE: Any relatively flat, isolated piece of sea ice 65 ft (≈ 20 m) or more across. Floes are subdivided according to horizontal extent as follows:

GIANT: over 5.5 n mi (10 km)
VAST: 1–5.5 n mi (2–10 km)
BIG: 550–2200 yd (500–2000 m)
MEDIUM: 110–550 yd (100–500 m)
SMALL: 22–110 yd (20–100 m)

FLOEBERG: A massive piece of sea ice composed of a hummock or a group of hummocks, frozen together and separated from any ice surroundings. It may float up to 17 ft (5 m) above sea level.

FLOODED ICE: Sea ice that has been flooded by meltwater or river water and is heavily loaded by water and wet snow.

FRACTURE: Any break or rupture through very close pack ice, compact pack ice, consolidated pack ice, fast ice, or a single floe resulting from deformation processes. Fractures may contain brash ice and/or may be covered with nilas and/or round ice. Length may vary from a few yards (meters) to many miles (kilometers).

FRACTURE ZONE: An area that has a great number of fractures.

FRACTURING: Pressure process whereby ice is permanently deformed, and rupture occurs. Most commonly used to describe breaking across very close pack ice, compact pack ice, and consolidated pack ice.

FRAZIL ICE: Fine spicules, or plates of ice, suspended in water.

FRIENDLY ICE: From the point of view of the submariner, an ice canopy containing many large skylights or other features that permit a submarine to surface. There must be more than ten such features per 30 n mi (56 km) along the submarine's track.

GLACIER: A mass of snow and ice continuously moving from higher to lower ground or, if afloat, continuously spreading. The principal forms of glacier are inland ice sheets, ice shelves, ice streams, icecaps, ice piedmonts, cirque (half-bowl) glaciers, and various types of mountain (valley) glaciers.

GLACIER BERG: An irregularly shaped iceberg.

GLACIER ICE: Ice in, or originating from, a glacier, whether on land or floating on the sea as icebergs, bergy bits, or growlers.

GLACIER TONGUE: Projecting seaward extension of a glacier, usually afloat.

GRAY ICE: Young ice 4 to 6 in (10–15 cm) thick. Less elastic than nilas and breaks on swell. Usually rafts under pressure.

GRAY-WHITE ICE: Young ice 6 to 12 in (15–30 cm) thick. Under pressure more likely to ridge than to raft.

GREASE ICE: A later stage of freezing than frazil ice. It occurs when the crystals have coagulated to form a soupy layer on the surface. Grease ice reflects little light, giving the sea a matte appearance.

Figure A-2. Example of Gray Ice.

Figure A-3. Example of Grease Ice on Far Right, Nilas to the Left.

GROUNDED HUMMOCK: Hummocked grounded ice formation. Single grounded hummocks occur as well as lines (or chains) of grounded hummocks.

GROUNDED ICE: Floating ice that is aground in shoal water.

GROWLER: Smaller piece of ice than a bergy bit, often transparent but appearing green or almost black in color. Usually extends less than 3 ft (1 m) above the sea surface and normally occupies an area of about 24 sq yd (20 sq m).

HOSTILE ICE: From the point of view of the submariner, an ice canopy containing no large skylights or other features that permit a submariner to surface.

HUMMOCK: A hillock of broken ice that has been forced upwards by pressure. May be fresh or weathered. The submerged volume of broken ice under the hummock, forced downwards by pressure, is termed a bummock.

HUMMOCKED ICE: Sea ice piled haphazardly one piece over another to form an uneven surface. When weathered, it has the appearance of smooth hillocks.

HUMMOCKING: The pressure process by which sea ice is forced into hummocks. When the floes rotate in the process it is termed screwing.

ICEBERG: A massive piece of ice of greatly varying shape, more than 16 ft (5 m) above sea level, which has broken away from a glacier, and which may be afloat or aground. Icebergs may be described as tabular, dome-shaped, sloping, pinnacled, weathered, or glacier bergs.

Figure A-4. Example of a Growler.

ICEBERG TONGUE: A major accumulation of icebergs projecting from the coast, held in place by grounding and joined together by fast ice.

ICE BLINK: A whitish glare on low clouds above an accumulation of distant ice.

ICE BOUND: A harbor, inlet, etc., is said to be ice bound when navigation by ships is prevented on account of ice, except possibly with the assistance of an icebreaker.

ICE BOUNDARY: The demarcation at any given time between fast ice and pack ice or between areas of pack ice of different concentrations.

ICE BRECCIA: Ice of different stages of development frozen together.

ICE CAKE: Any relatively flat piece of sea ice less than 22 yd (20 m) across.

ICE CANOPY: Pack ice from the point of view of the submariner.

ICE COVER: The ratio of an area of ice of any concentration to the total area of sea surface within some large geographic locale; this locale may be global, hemispheric, or prescribed by a specific oceanographic entity such as Baffin Bay or the Barents Sea.

ICE EDGE: The demarcation at any given time between the open sea and sea ice of any kind, whether fast or drifting. It may be termed compacted or diffuse.

ICE FIELD: Area of pack ice consisting of floes of any size that are greater than 5.5 n mi (10 km) across.

ICEFOOT: A narrow fringe of ice attached to the coast, unmoved by tides and remaining after the fast ice has moved away.

ICE FREE: No sea ice present. Some ice of land origin may occur.

ICE FRONT: The vertical cliff forming the seaward face of an ice shelf or other floating glacier varying in height from 6 to 165 ft (2–50 m) or more above sea level.

ICE ISLAND: A large piece of floating ice about 16 ft (5 m) above sea level, which has broken away from an Arctic ice shelf, having a thickness of 100 to 165 ft (30–50 m) and an area of from a few thousand square yards (meters) to 200 sq mi (500 sq km) or more, and usually characterized by a regularly undulating surface that gives it a ribbed appearance from the air.

ICE JAM: An accumulation of broken river ice or sea ice caught in a narrow channel.

ICE KEEL: From the point of view of the submariner, a downward-projecting ridge on the underside of the ice canopy—the counterpart of a ridge. Ice keels may extend as much as 165 ft (50 m) below sea level.

ICE LIMIT: Climatological term referring to the extreme minimum or extreme maximum extent of the ice edge in any given month or period based on observations over a number of years. Term should be preceded by minimum or maximum.

ICE MASSIF: A concentration of sea ice covering hundreds of square miles (kilometers) that is found in the same region every summer.

ICE OF LAND ORIGIN: Ice formed on land or in an ice shelf, found floating in water. The concept includes ice that is stranded or grounded.

ICE PATCH: An area of pack ice less than 6 n mi (10 km) across.

ICE PORT: An embayment in an ice front, often of a temporary nature, where ships can moor alongside and unload directly onto the ice shelf.

ICE RIND: A brittle shiny crust of ice formed on a quiet surface by direct freezing or from grease ice, usually in water of low salinity. Thickness to about 1 in (5 cm). Easily broken by wind or swell, commonly breaking in rectangular pieces.

ICE SHELF: A floating ice sheet of considerable thickness showing 6 to 165 ft (2–50 m) or more above sea level, attached to the coast. Usually of great horizontal extent and with a level or gently undulating surface. Nourished by annual snow accumulation and also by the seaward extension of land glaciers. Limited areas may be aground. The seaward edge is termed an ice front.

ICE STREAM: Part of an island ice sheet in which the ice flows more rapidly and not necessarily in the same direction as the surrounding ice. The margins are sometimes clearly marked by a change in direction of the surface slope but may be indistinct.

ICE UNDER PRESSURE: Ice in which deformation processes are actively occurring and hence a potential impediment or danger to shipping.

ICE WALL: An ice cliff forming the seaward margin of a glacier that is not afloat. An ice wall is aground, the rock basement being at or below sea level.

LAKE ICE: Ice formed on a lake, regardless of observed location.

LARGE FRACTURE: More than 1,640 ft (500 m) wide.

LARGE ICE FIELD: An ice field over 12 n mi (20 km) across.

LEAD: Any fracture or passageway through sea ice that is navigable by surface vessels.

LEVEL ICE: Sea ice that is unaffected by deformation.

LIGHT NILAS: Nilas that is more than 2 in (5 cm) in thickness and rather lighter in color than dark nilas.

MEAN ICE EDGE: Average position of the ice edge in any given month or period based on observations over a number of years. Other terms that may be used are mean maximum ice edge and mean minimum ice edge.

MEDIUM FIRST-YEAR ICE: First-year ice 25 to 50 in (70–120 cm) thick.

MEDIUM FRACTURE: 650 to 1,650 ft (200–500 m) wide.

MEDIUM ICE FIELD: An ice field 8 to 10 mi (15–20 km) across.

MULTIYEAR ICE: Old ice up to 10 ft (3 m) or more thick that has survived at least two summers' melt. Hummocks even smoother than in second-year ice, and the ice is almost salt free. The color, where snow free, is usually blue. The melt pattern consists of large interconnecting irregular puddles and a well developed drainage system.

NEW ICE: A general term for recently formed ice that includes frazil ice, grease ice, slush, and shuga. Theses types of ice are composed of ice crystals that are only weakly frozen together (if at all) and have a definite form only while they are afloat.

NEW RIDGE: Ridge newly formed with sharp peaks and slope of sides usually 40 degrees. Fragments are visible from the air at low altitude.

NILAS: A thin, elastic crust of ice bending easily on waves and swell. Nilas has a matte surface and is up to 4 in ($\approx$ 10 cm) thick. Under pressure it thrusts into a pattern of interlocking fingers (see FINGER-RAFTED ICE). May be subdivided into dark nilas and light nilas.

NIP: Ice is said to nip when it forcibly presses against a ship. A vessel so caught, though undamaged, is said to have been nipped.

OLD ICE: Sea ice that has survived at least one summer's melt. Most topographic features on old ice are smoother than those on first-year ice. May be subdivided into second-year ice and multiyear ice.

OPEN PACK ICE: Pack ice in which the ice concentration is four-tenths to six-tenths, with many leads and polynyas, and the floes are generally not in contact with one another.

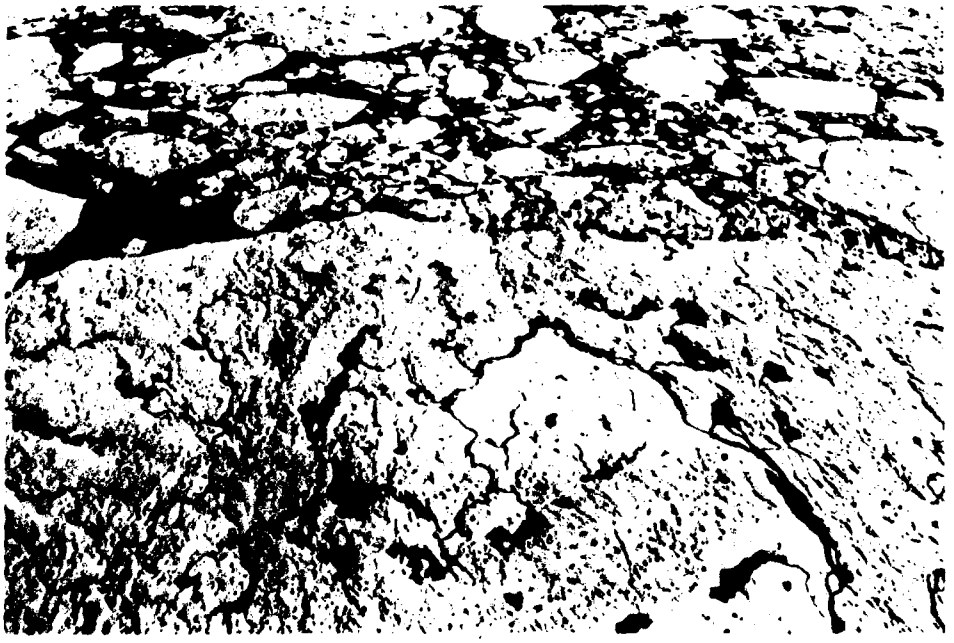

Figure A-5. Example of Multiyear Ice.

OPEN WATER: A large area of freely navigable water in which sea ice is present in concentrations less than one-tenth. When no sea ice is present, the area should be termed ice free, even though icebergs occur.

PACK ICE: Term used in a wide sense to include any area of sea ice, other than fast ice, no matter what form it takes or how it is disposed.

PANCAKE ICE: Predominantly circular pieces of ice from 1 to 10 ft (30 cm–3 m) in diameter and up to about 4 in ($\approx$ 10 cm) in thickness, with raised rims due to the pieces striking against one another. It may be formed on a slight swell from grease ice, shuga, or slush, or as a result of the breaking of ice rind, nilas, or, under severe conditions of swell or waves, of gray ice. Sometimes pancake ice forms at some depth, at an interface between water bodies of different physical characteristics, from where it floats to the surface; it may cover wide areas of water rapidly.

POLYNYA: Any nonlinear-shaped opening in the water but enclosed by ice. Sometimes the polynya is limited on one side by the coast and is called a shore polynya, or by fast ice and is called a flaw polynya. Some polynyi recur annually in the same position.

PUDDLE: An accumulation on ice of meltwater, mainly due to melting snow, but in the more advanced stages, also to the melting of ice. Initial stage consists of patches of melted snow.

RAFTED ICE: Type of deformed ice formed by one piece of ice overriding another.

RAFTING: Pressure processes whereby one piece of ice overrides another. Most common in new and young ice.

RAM: An underwater ice projection from an ice wall, ice front, iceberg, or floe. Its formation is usually due to a more intensive melting and erosion of the unsubmerged part.

RECURRING POLYNYA: A polynya that recurs in the same position every year.

RIDGE: A line or wall of broken ice forced up by pressure; it may be fresh or weathered. The submerged volume of broken ice under a ridge, forced downwards by pressure, is termed an ice keel.

RIDGED ICE: Ice piled haphazardly one piece over another in the form of ridges or walls. Usually found in first-year ice.

RIDGED-ICE ZONE: An area in which much ridged ice with similar characteristics has formed.

RIDGING: The pressure process by which sea ice is forced into ridges.

RIVER ICE: Ice formed on a river, regardless of observed location.

ROTTEN ICE: Sea ice that has become honeycombed and is in an advanced state of disintegration.

SASTRUGI: Sharp, irregular ridges formed on a snow surface by wind erosion and deposition. On drift ice the ridges are parallel to the direction of the prevailing wind at the time they were formed.

SEA ICE: Any form of ice found at sea that has originated from the freezing of sea water.

SECOND-YEAR ICE: Old ice that has survived only one summer's melt. Because it is thicker and less dense than first-year ice, it stands higher out of the water. In contrast to multiyear ice, summer melting produces a regular pattern of numerous small puddles. Bare patches and puddles are usually greenish-blue.

SHEARING: An area of pack ice is subject to shear when the ice motion varies significantly in the direction normal to the motion, subjecting the ice to rotational forces. These forces may result in phenomena similar to a flaw.

SHORE LEAD: A lead between pack ice and the shore or between pack ice and an ice front.

SHORE POLYNYA: A polynya between pack ice and the coast, or between pack ice and an ice front.

SHUGA: An accumulation of spongy white ice lumps, a few inches (centimeters) across; they are formed from grease ice or slush and sometimes from ice rising to the surface.

SKYLIGHT: From the point of view of the submariner, thin places in the ice canopy, usually less than 3 ft (1 m) thick and appearing from below as relatively light, translucent patches in dark surroundings. The undersurface of a skylight is normally flat. Skylights are called large if big enough for a submarine to attempt to surface through them, or small if not.

SLUSH: Snow that is saturated and mixed with water on land or ice surfaces, or as a viscous floating mass in water after a heavy snowfall.

SMALL ICE CAKE: An ice cake less than 7 ft (2 m) across.

SMALL ICE FIELD: An ice field 5 to 10 n mi (10–15 km) across.

SNOW-COVERED ICE: Ice covered with snow.

SNOWDRIFT: An accumulation of windblown snow deposited in the lee of obstructions or heaped by wind eddies. A crescent-shaped snowdrift, with ends pointing downwind, is known as a snow barchan.

STANDING FLOE: A separate floe standing vertically or inclined and enclosed by rather smooth ice.

STRANDED ICE: Ice that has been floating and has been deposited on the shore by retreating high water.

STRIP: Long narrow area of pack ice, about 0.5 n mi (1 km) or less in width, usually composed of small fragments detached from the main mass of ice, and run together under the influence of wind, swell, or current.

TABULAR BERG: A flat-topped iceberg. Most tabular bergs form by calving from an ice shelf and show horizontal banding.

THAW HOLES: Vertical holes in sea ice formed when surface puddles melt through to the underlying water.

THICK FIRST-YEAR ICE: First-year ice over 4 ft (120 cm) thick.

THIN FIRST-YEAR ICE (WHITE ICE): First-year ice 1 to 2 ft (30–70 cm) thick.

TIDE CRACK: Crack at the line of junction between an immovable ice foot or ice wall and fast ice, the latter subject to rise and fall of the tide.

TONGUE: A projection of the ice edge up to several miles (kilometers) in length, caused by wind or current.

VERY CLOSE PACK ICE: Pack ice in which the concentration is nine-tenths to less than ten-tenths.

VERY OPEN PACK ICE: Pack ice in which the concentration is one-tenth to three-tenths and water preponderates over the ice.

VERY WEATHERED RIDGE: Ridge with tops very rounded, slope of sides usually 20 to 30 degrees.

WATER SKY: Dark streaks on the underside of low clouds, indicating the presence of water features in the vicinity of sea ice.

WEATHERED RIDGE: Ridge with peaks slightly rounded and slope of sides usually 30 to 40 degrees. Individual fragments are not discernible.

WEATHERING: Processes of ablation and accumulation that gradually eliminate irregularities in an ice surface.

WHITE ICE: Same as thin first-year ice.

Figure A-6. Example of Thin First-Year Ice (White Ice).

YOUNG COASTAL ICE: The initial stage of fast ice formation consisting of nilas or young ice, its width varying from a few yards (meters) up to 110 to 220 yd (100–200 m) from the shoreline.

YOUNG ICE: Ice in the transition stage between nilas and first-year ice, 4 to 12 in (10–30 cm) in thickness. May be subdivided into gray ice and gray-white ice.

Appendix B

Equivalent Wind Chill Temperature

Table 10–1. The cooling power of the wind expressed as "Equivalent Chill Temperature," and the danger of freezing exposed flesh. Courtesy of USAF Air Weather Service (MAC).

Wind Speed		Cooling Power of Wind Expressed as "Equivalent Chill Temperature"																				
Knots	*MPH*	Temperature (°F)																				
Calm	Calm	40	35	30	25	20	15	10	5	0	-5	-10	-15	-20	**-25**	**-30**	**-35**	**-40**	**-45**	**-50**	**-55**	**-60**
		Equivalent Chill Temperature																				
3-6	5	35	30	25	20	15	10	5	0	-5	-10	-15	-20	**-25**	**-30**	**-35**	**-40**	**-45**	**-50**	**-55**	**-65**	**-70**
7-10	10	30	20	15	10	5	0	-10	-15	-20	**-25**	**-35**	**-40**	**-45**	**-50**	**-60**	**-65**	**-70**	-75	-80	-90	-95
11-15	15	25	15	10	0	-5	-10	-20	**-25**	**-30**	**-40**	**-45**	**-50**	**-60**	**-65**	**-70**	-80	-85	-90	-100	-105	-110
16-19	20	20	10	5	0	-10	-15	**-25**	**-30**	**-35**	**-45**	**-50**	**-60**	**-65**	-75	-80	-85	-95	-100	-110	-115	-120
20-23	25	15	10	0	-5	-15	-20	**-30**	**-35**	**-45**	**-50**	**-60**	**-65**	-75	-80	-90	-95	-105	-110	-120	-125	-135
24-28	30	10	5	0	-10	-20	**-25**	**-30**	**-40**	**-50**	**-55**	**-65**	**-70**	-80	-85	-95	-100	-110	-115	-125	-130	-140
29-32	35	10	5	-5	-10	-20	**-30**	**-35**	**-40**	**-50**	**-60**	**-65**	-75	-80	-90	-100	-105	-115	-120	-130	-135	-145
33-36	40	10	0	-5	-15	-20	**-30**	**-35**	**-45**	**-55**	**-60**	**-70**	-75	-85	-95	-100	-110	-115	-125	-130	-140	-150
Winds Above 40 Have Little Additional Effect		Little Danger					**Increasing Danger (Flesh may freeze within 1 min.)**							Great Danger (Flesh may freeze within 30 seconds)								
Danger of Freezing Exposed Flesh for Properly Clothed Persons																						

Figure B-1. Equivalent Wind Chill Temperature Chart (Kotsch, 1983).

Distribution List

NATIONAL OCEAN DATA CENTER
ATTN: G.W. WITHES
6001 EXECUTIVE BLVD. RM. 103
ROCKVILLE, MD 20852

COMFLENUMOCEANCEN
MONTEREY, CA 93943-5005

COMMANDER
TAYLOR NAVAL RSCH. CEN.
BETHESDA, MD 20084-5000

COMMANDING OFFICER
FLEET ANTI SUB WARFARE
TRAINING CENTER
ATLANTIC NAVAL STATION
NORFOLK, VA 23511-6495

COMMANDER IN CHIEF
U.S. ATLANTIC FLEET
ATTN: FLT METEOROLOGIST
NORFOLK, VA 23511-6001

COMMANDER IN CHIEF
U.S. NAVAL FORCES EUROPE
ATTN: MET. OFFICER
FPO AE 09510

COMSECONDFLT
ATTN: NSAP SCIENCE ADVISOR
APO AE 09501-6000

COMMANDER
U.S. NAVAL FORCES ICELAND
PSC 1003 BOX 7
FPO AE 09728-0307

COMMANDER
U.S. NAVAL FORCES JAPAN
FPO SEATTLE 98762-0051

COMNAVAIRPAC
ATTN: NSAP SCIENCE ADVISOR
NAS, NORTH ISLAND
SAN DIEGO, CA 92135-5100

CHIEF OF NAVAL OPERATIONS
ATTN: OP-096 OP-0961B
U.S. NAVAL OBSERVATORY
WASHINGTON, DC 20392-1808

COMMANDING OFFICER
NAVAL OCEANOGRAPHIC OFFICE
JCSSC, MS 39522-5001

SUPERINTENDENT
NAVPGSCOL
MONTEREY, CA 93943-5000

OFFICE OF NAVAL TECHNOLOGY
DR. M. BRISCOE, CODE 228
800 N. QUINCY ST.
ARLINGTON, VA 22217-5000

COMMANDER IN CHIEF
U.S. ATLANTIC FLEET
ATTN: NSAP SCIENCE ADVISOR
NORFOLK, VA 23511-6001

CINCUSNAVEUR
BOX N39
FPO AE 09510-0150

COMTHIRDFLT
ATTN: FLT METEOROLOGIST
FPO AP 96601-6001

COMMANDER NAVAL AIR FORCE
U.S. ATLANTIC FLEET
ATTN: NSAP SCIENCE ADVISOR
NORFOLK, VA 23511-5188

COMMANDER
U.S. NAVAL FORCES KOREA
APO AP 96301-0023

COMMANDER
NAVAL SURFACE FORCE
U.S. ATLANTIC FLEET
NORFOLK, VA 23511-6292

COMMANDER
SPAWARSYSCOM
WASHINGTON, DC 20363-5100

COMMANDING OFFICER
ONR BRANCH OFFICE
BOX 39
FPO AE 09510-0700

OFFICE OF NAVAL RESEARCH
ATTN: CODE 10
800 N. QUINCY ST.
ARLINGTON, VA 22217-5000

UNIVERSITY OF WASHINGTON
APPLIED PHYSICS LABORATORY
1013 NORTHEAST 4OTH ST.
SEATTLE, WA 98105

CINCPACFLT
ATTN: CODE 02M
PEARL HARBOR, HI 96860-7000

COMMANDER SECOND FLEET
ATTN: MET. OFFICER
FPO AE 09501-6000

COMSEVENTHFLT
ATTN: FLT METEOROLOGIST
FPO AP 96601-6003

COMNAVSURFLANT
ATTN: NSAP SCIENCE ADVISOR
NORFOLK, VA 23511

DR. RUSS SCHNELL
MLO NOAA P.O. BOX 275
HILO, HI 96721-0275

NAVOCEANO BOAT
ATTN: LCDR MCSHANE
NCBC BUILDING 406
GULFPORT, MS 39501

COMSUBLANT
ATTN: CODE N23
NORFOLK, VA 23511-6296

COMMANDING OFFICER
USS D. EISENHOWER (CVN-69)
ATTN: MET. OFFICER, OA DIV.
FPO AE 09532-2830

COMMANDING OFFICER
USS J.F.KENNEDY (CV-67)
ATTN: MET. OFFICER OA DIV.
FPO AE 09538-2800

COMMANDING OFFICER
USS T. ROOSEVELT (CVN-71)
ATTN: MET. OFFICER OA DIV.
FPO AE 09559-2871

COMMANDING OFFICER
USS ENTERPRISE (CVN-65)
ATTN: MET. OFFICER OA DIV.
FPO AE 09543-281O

COMMANDING OFFICER
USS RANGER (CV-61)
ATTN: MET. OFFICER OA DIV.
FPO AP 96633-2758

COMMANDING OFFICER
USS MOUNT WHITNEY (LCC-20)
ATTN: MET. OFFICER
FPO AE 09517-3310

COMMANDING OFFICER
USS BLUERIDGE (LCC-19)
ATTN: MET. OFFICER
FPO AP 96628-3300

COMMANDING OFFICER
USS INCHON (LPH-12)
ATTN: MET. OFFICER
FPO AE 09529-1655

COMMANDING OFFICER
USS SAIPAN (LHA-2)
ATTN: MET. OFFICER
FPO AE 09549-1605

COMMANDING OFFICER
USS OKINAWA (LPH-3)
ATTN: MET. OFFICER
FPO AP 96625-1630

COMSUBFORPAC
ATTN: CODE N216
PEARL HARBOR, HI 96860-6550

COMMANDING OFFICER
USS FORRESTAL (CV-59)
ATTN: MET. OFFICER OA DIV.
FPO AA 34080-2730

COMMANDING OFFICER
USS NIMITZ (CVN-68)
ATTN: MET. OFFICER OA DIV.
FPO SEATTLE 98780-2820

COMMANDING OFFICER
USS A. LINCOLN (CVN-72)
ATTN: MET. OFFICER
FPO AE 09580-2872

COMMANDING OFFICER
USS KITTY HAWK (CV-63)
ATTN: MET. OFFICER OA DIV.
FPO AP 96634-2770

COMMANDING OFFICER
USS CARL VINSON (CVN-70)
ATTN: MET. OFFICER OA DIV.
FPO AP 96629-2840

COMMANDING OFFICER
USS NASSAU (LHA-4)
ATTN: MET. OFFICER
FPO AE 09557-1615

COMMANDING OFFICER
USS GUADALCANAL (LPH-7)
ATTN: MET. OFFICER
FPO AE 09562-1635

COMMANDING OFFICER
USS IWO JIMA (LPH-2)
ATTN: MET. OFFICER
FPO AE 09561-1625

COMMANDING OFFICER
USS BELLEAU WOOD (LHA-3)
ATTN: MET. OFFICER
FPO AP 96623-1610

COMMANDING OFFICER
USS PELELIU (LHA-5)
ATTN: MET. OFFICER
FPO AP 96624-1620

COMMANDING OFFICER
USS AMERICA (CV-66)
ATTN: MET. OFFICER
FPO AE 09531-2790

COMMANDING OFFICER
USS INDEPENDENCE (CV-62)
ATTN: MET. OFFICER, OA DIV.
FPO SEATTLE 96618-2760

COMMANDING OFFICER
USS SARATOGA (CV-60)
ATTN: MET. OFFICER, OA DIV.
FPO AA 34078-2740

COMMANDING OFFICER
USS CONSTELLATION (CV-64)
ATTN: MET. OFFICER, OA DIV.
FPO AE 09558-2780

COMMANDING OFFICER
USS GUAM (LPH-9)
ATTN: MET. OFFICER
FPO AE 09563-1640

COMMANDING OFFICER
USS NEW ORLEANS (LPH-11)
ATTN: MET. OFFICER
FPO AP 96627-1650

COMMANDING OFFICER
USS TARAWA (LHA-1)
ATTN: MET. OFFICER
FPO AP 96622-1600

COMMANDING OFFICER
USS LASALLE (AGF-3)
ATTN: MET. OFFICER
FPO AE 09577-3320

NATIONAL SECURITY AGENCY
ATTN: LIBRARY 2C029
FORT MEADE, MD 20755

NAVRSCHLAB
F.M. FETTERER CODE 321
JSSC, MS 39529-5004

OIC NOCD ADAK
PSC 486 BOX 1243
FPO AP 96506-1243

COMMANDING OFFICER
USS TRIPOLI (LPH-1O)
ATTN: MET. OFFICER
FPO AP 96626-1645

COMMANDING OFFICER
31 OCEANO DEV. SODN 8-VXN-8
NAVAL AIR STATION
PATUXENT RIVER, MD 20670-5109

DET 2 HO AWS
THE PENTAGON
WASHINGTON, DC 20330

LIBRARY
NAVAL ARCTIC RESEARCH LAB
BARROW, AK 99723

NAVEASTOCEANCEN (3)
ATTN: OPS. OFFICER
MCADIE BLDG. (U117), NAS
NORFOLK, VA 23511-5399

NAVOCEANCOMFAC
ATTN: OPS. OFFICER
NAVAL AIR STATION
BRUNSWICK, ME 04011-5000

DIRECTOR OF RESEARCH
U.S. NAVAL ACADEMY
ANNAPOLIS, MD 21402

NAVPGSCOL
ATTN: LIBRARY
MONTEREY, CA 93943-5000

COMMANDING OFFICER
ATTN: USAFA (DEG)
USAF ACADEMY, CO 80840

COMMANDER
AWS DNXS
SCOTT AFB, IL 62225

U.S. ARMY RESEARCH OFFICE
ATTN: GEOPHYSICS DIV.
P.O. BOX 12211
RSCH TRI PARK, NC 27709

COMMANDANT
U.S. COAST GUARD
WASHINGTON, DC 20226

COMMANDING OFFICER
USS PUGET SOUND (AD-38)
ATTN: METEOROLOGICAL OFFICE
FPO AE 09544-2520

USCINCPAC
BOX 13
ATTN: STAFF CINCPAC J37
CAMP SMITH, HI 96861

OFFICER IN CHARGE
NAVOCEANCOMDET
NAVAL STATION
FPO SEATTLE 98791-2943

COMMANDING OFFICER
FLEET INTELLIGENCE CENTER
NORFOLK, VA 23522

NAVPOLAROCEANCEN (3)
ATTN: OPS. OFFICER
4301 SUITLAND RD.
WASHINGTON, DC 20395-5180

U.S. NAVAL ACADEMY
ATTN: LIBRARY REPORTS
ANNAPOLIS, MD 21402

NAVPGSCOL
ATTN: CODE MR
MONTEREY, CA 93943-5000

NAVAL WAR COLLEGE
ATTN: GEOPHYS. OFFICER
NAVOPS DEPT.
NEWPORT, RI 02841

AFGL LY
ATTN: MET. OFFICER
HANSCOM AFB, MA 01731

USAFETAC TS 20
ATTN: TECH. LIBRARY
SCOTT AFB, IL 62225

LIBRARY NRL COLD REGION RSCH & ENGINEERING
HANOVER, NH 03755-1290

NORTHWEST OCEAN SERV CENT
7600 SAND POINT WAY
N.E. BIN C15700
SEATTLE, WA 98115

OFFICER IN CHARGE
NAVOCEANCOMDET
AFGWC
OFFUTT AFB, NE 68113

NAVWESTOCEANCEN (3)
ATTN: OPERATIONS OFFICER
PEARL HARBOR HI 96860

U.S. NAVOCEANCOMFAC
ATTN OPS. OFFICER
PSC 1003 BOX 26
FPO AE 09728-0326

U.S. NAVAL ACADEMY
ATTN: OCEANOGRAPHY DEPT.
ANNAPOLIS, MD 21402

NAVPGSCOL
ATTN: CODE OC
MONTEREY, CA 93943-5000

SPAWARSYSCOM
ATTN: CODE PMW-165
NAT CTR NR 1
WASHINGTON, DC 20363-5100

COMMANDING OFFICER
NAVAL UNIT
ATTN: LNN/STOP 62
CHANUTE AFB, IL 61868

3350 TCHTG TTMV
CHANUTE AFB, IL 61868

DIRECTOR NMC
NWS NOAA
WWB ROOM 204
WASHINGTON, DC 20233

NATIONAL WEATHER SERVICE
WORLD WEATHER BLDG. RM. 307
5200 AUTH ROAD
CAMP SPRINGS, MD 20023

SCIENCE APPLICATIONS INTERNATIONAL SAIC
550 CAMINO EL ESTERO 102
MONTEREY, CA 93940

FEDERAL COORD. FOR METEORO. SERVS. & SUP. RSCH. (OFCM)
11426 ROCKVILLE PIKE
SUITE 300
ROCKVILLE, MD 20852

CHIEF SCIENTIFIC SERVICES
NWS NOAA WESTERN REGION
P.O. BOX 11188
SALT LAKE CITY, UT 84111

DIRECTOR NWS
NOAA ALASKA REGION
BOX 23, 701 C STREET
ANCHORAGE, AK 99513

SPACE FLIGHT METEORO GROUP
ATTN: STEVE SOKOL, CODE Z8
JOHNSON SPACE CENTER
HOUSTON, TX 77058

OCEANROUTES INC
680 W. MAUDE AVE.
SUNNYVALE, CA 94086-3518

DIRECTOR METEO & OCEANO
NATIONAL DEFENSE HDQ.
OTTAWA ONTARIO KIA OK2
CANADA

DIRECTOR INSTITUTE OF PHYSICAL OCEANOGRAPHY
HARALDSGADE 6
2200 COPENHAGEN N
DENMARK

COMMANDER IN CHIEF FLEET
ATTN: STAFF METEOROLOGIST & OCEANOGRAPHY OFFICER
NORTHWOOD MIDDLESEX HA6 3HP
ENGLAND

ICELANDIC MET OFFICE
BUSTAOAVEGUR 9
105 REYKJAVIK, ICELAND

EXECUTIVE SECRETARY CAO
SUBCOMMITTEE ON ATMOS SCI
NATIONAL SCIENCE FOUNDATION
RM. 510 1800 G. STREET
WASHINGTON, DC 20550

DIRECTOR NOAA
PACIFIC MARINE CENTER NATIONAL OCEAN SURVEY
1801 FAIRVIEW AVE. EAST
SEATTLE, WA 98102

NOAA LIBRARY, E/AI216
7600 SAND POINT WAY N.E.
BIN C15700
SEATTLE, WA 98115-0070

UNIV. OF WASHINGTON
ATMOSPHERIC SCIENCES DEPT.
SEATTLE, WA 98195

CHAIRMAN METEOROLOGY DEPT.
MCGILL UNIVERSITY
805 SHERBROOKE ST., W.
MONTREAL, QUEBEC
CANADA H3A 2K6

DIRECTOR METEOROLOGIE INST.
ZENTRALEINRICHTUNG 2 DER
FREIEN UNIVERSITAT BERLIN
1000 BERLIN 33, GERMANY

DIRECTOR OF NAVAL OCEANO & METEOROLOGY
MINISTRY OF DEFENCE
LACON HOUSE THEOBOLD ROAD
LONDON WC 1X8RY, ENGLAND

LIBRARY FINNISH METEORO INST.
BOX 503
SF 00101 HELSINKI 10
FINLAND

MARITIME METEOROLOGY DIV.
JAPAN METEORO AGENCY
OTE-MACHI 1-3-4 CHIYODA-KU
TOKYO, JAPAN

LIBRARY BIBLIOTHEQUE
ATMOSPHERIC ENVIRON SERV
4905 RUE DUFFERIN STREET
DOWNSVIEW ONTARIO
CANADA M3H 5T4

INSTITUT FOR TEORETISK METEOROLOGI
HARALDSGADE 6
DK 2280 KOBEHAVN N
DENMARK

DEPARTMENT OF METEOROLOGY
UNIVERSITY OF READING
2 EARLYGATE WHITEKNIGHTS
READING RG6 2AU, ENGLAND

DIRECTOR SWEDISH METEORO HYDROLOGICAL INSTITUTE
P.O. BOX 923
S-601 19 NORRKOPING
SWEDEN

DENNIS PERRYMAN (3)
NRL MARINE METEOROLOGY
MONTEREY, CA 93943-5006

CDR L.E. BOUNDS (ONT-228)
OFFICE OF NAVAL TECHNOLOGY
800 N. QUINCY ST.
ARLINGTON, VA 22217-5008

DR. G. WELLER
DEP. DIR. GEOPHYSICS INST.
UNIVERSITY OF ALASKA
FAIRBANKS, AK 99775-0800

GREENHORNE & O'MARA
ATTN: DR. HERCHENRODER
7500 GREENWAY CENTER DR.
SUITE 700
GREENBELT, MD 20770

USCOMSOLANT
FPO AA 34099-6001

MIC
NATIONAL WEATHER SERVICE
222 WEST 7TH AVE. NR-23
ANCHORAGE, AK 99513-7075

EILEEN MATURI
NESDIS WORLD WEA. BLDG.
RM. 601
5200 AUTH ROAD
CAMP SPRINGS, MD 20023

NRL CRREL, CODE 332
72 LYME RD.
HANOVER, NH 03755-1290

AL FISHER
NAVAL OCEAN SYS. CENTER
CODE 624
SAN DIEGO, CA 92152-5000

CARL BYERS
GEOPHYSICS INSTITUTE
U. OF ALASKA
FAIRBANKS, AK 99775-0800

MIC
NATIONAL WEATHER SERVICE
101 12th AVE., BOX 21
FAIRBANKS, AK 99701

DIRECTOR NORWEGIAN METEOROLOGICAL INST.
P.O. BOX 320, BLINDERN, N-0314
OSLO 3, NORWAY

DR. TORGNY VINJENORSK
POLARINSTITUTT, P.O. BOX 158
N-1330 OSLO LUFTHAVN
NORWAY

COMMANDING OFFICER
NAVOCEANO CODE NTTS
JCSSC, MS 39522-5001

COMMANDER 2ND FLT
ATTN CODE 323
FPO AE 09506-6000

COMMANDER
AMPHIBIOUS GROUP 2
FPO AE 09501-6007

SECRETARY
JCS THE PENTAGON
WASHINGTON, DC 20593

NAVPGSCOL (15)
ATTN: PROF. WILLIAMS
CODE MR
MONTEREY, CA 93943-5000

AWC NEIL PARKER
TWIN ATRIA BLDG/AES
4999 98TH AVE.
EDMONTON, ALBERTA
CANADA TGB 2X3

U.S. NAVY LIAISON OFFICER
U.S. COAST GUARD G ON 31
2100 SECOND ST. S.W.
WASHINGTON, DC 20593

JERRY EHRHARDT
NAVAL SEA SYSTEMS COMMAND
CODE PMS 377 J-2
WASHINGTON, DC 20362-5101

ARCTIC RESEARCH CENTER
SCRIPPS INSTITUTE
DIV. H-014
ATTN: R. WHRITNER
LA JOLLA, CA 92093

DIRECTOR, NORTH NORWAY
WEATHER CENTRAL
P.O. BOX 2760, ELVERHOY N-9001
TROMSØ, NORWAY

NAVOCEANO ATLANTIC
COMPONENT
FLEET ASW TRAINING CENTER
NORFOLK, VA 23511-6495

COMMANDING OFFICER USCG
POLAR STAR WAGB10
ATTN: ELIZABETH FANO
FPO SEATTLE, WA 98799-3920

USCOMEASTLANT
FPO AE 09510

CMDR USCG ATLANTIC AREA
GOVERNORS ISLAND
NEW YORK, NY 10004

DIRECTOR
DEFENSE NUCLEAR AGENCY
WASHINGTON, DC 20305

HANK BRANDLI
3165 SHARON DRIVE
MELBOURNE, FL 32904

DR. ROGER COLONY
APL, U. OF WASHINGTON
1013 NE 40TH STREET
SEATTLE, WA 98105-6613

NAVOCEANO PACIFIC COMP
FLT ASW TRAINING CENTER
SAN DIEGO, CA 92147-5000

MIKE HELFERT
CODE SN15
NASA JOHNSON SPACEN
HOUSTON, TX 77058

CMDR TRAINING COMMAND
U.S ATLANTIC FLEET
NORFOLK, VA 23511-6597

COMMANDING OFFICER
USS FT. MCHENRY (LSD-43)
FPO AP 9665-1781

DIRECTOR, TRS 2F
DEF. INTELLIGENCE AGENCY
WASHINGTON, DC 20301

COMMANDING OFFICER
USS TRENTON (LPD-14)
FPO AE 09588-1716

COMMANDING OFFICER
USS SHREVEPORT (LPD-12)
FPO AE 09587-1714

ASST. FOR ENV. SCIENCES
ASST. SECNAV PENTAGON
WASHINGTON, DC 20350

DIRECTOR
LIBRARY TECH. INFO. CEN.
ARMY ENG. WATERWAYS STN.
VICKSBURG, MS 39180

NAVRSCHLAB
LIBRARY CODE 7035.3
JCSSC, MS 39529-5004

JOINT SPEC. OPS COMM JI
P.O. BOX 70239
FORT BRAGG, NC 28307

COMMANDER
NAVAL OCEANOGRAPHY COMM.
JCSSC, MS 39529-5000

COMMANDING OFFICER
USS AUSTIN (LPD-4)
FPO AE 09564-1705

COMMANDING OFFICER
USS EL PASO (LKA-117)
FPO AE 09568-1704

COMMANDING OFFICER
USS CHARLESTON (LKA-113)
FPO AE 09566-1700

COMMANDING OFFICER
USS PORTLAND (LSD-37)
FPO AE 09582-1725

OCEANOGRAPHIC UNIT FIVE
FPO AE 09501-7105

U.S. LIAISON OFFICER TO SUPREME ALLIED COMMANDER
ATLANTIC
NORFOLK, VA 23511

SCRIPPS INSTITUTE LIBRARY
DOCUMENTS REPORTS SECTION
LA JOLLA, CA 92093

THE BRITISH LIBRARY
SCI. REF. LIBRARY A
25 SOUTHAMPTON BLDGS.
CHANCERY LANE
LONDON WC2A IAW, ENGLAND

HEAD OCEANO & LIMNOLOGY
SMITHSONIAN INSTITUTION
WASHINGTON, DC 20560

THE JOINT STAFF J-3 ESD
ENVIRONMENTAL SERVICES DIV.
OPERATIONS DIRECTORATE
WASHINGTON, DC 20318-3000

OFFICER IN CHARGE
NOCD FEDERAL BLDG.
ASHEVILLE, NC 29901-2696

COMMANDING OFFICER
AMPHIB. SCHOOL CREEK
NORFOLK, VA 23521

COMMANDING OFFICER
NAVAIRSYSCOM HQ.
WASHINGTON, DC 20361-0001

COMMANDING OFFICER
USS PONCE (LPD-15)
FPO AE 09582-1717

COMMANDING OFFICER
USS NASHVILLE (LPD-13)
FPO AE 09579-1715

COMMANDING OFFICER
USS PENSACOLA (LSD-38)
FPO AE 09582-1726

COMMANDING OFFICER
USS WHIDBEY ISLAND (LSD-41)
FPO AE 09591-1729

DIRECTOR
NAVSURFWEACEN WHITE OAKS
NAVY SCIENCE ASST.
SILVER SPRING, MD 20903-5000

MR. DICK GILMORE
215 N FAIRWAY CT.
OAK HARBOR, WA 98277

LIBRARY INSTITUTE OF OCEANOGRAPHIC SCIENCES
ATTN: DIRECTOR
WORMLEY, GODALMING
SURREY GU8 5UB, ENGLAND

ROBERT BLUTHNTIC
4301 SUITLAND RD.
WASHINGTON, DC 20395-5020

CHIEF OF NAVAL RESEARCH
LIBRARY CODE 01232L
BALLSTON TOWER 1
ARLINGTON, VA 22217-5800

PCO
GEO WASHINGTON (CVN-73)
SUP. OF SHIPBUILDING USN
NEWPORT NEWS, VA 23607-2787

DIRECTOR (2)
DTIC-FD, BLDG 5, CAMERON STN
ALEXANDRIA, VA 22304-6145

COMMANDING OFFICER (12)
NAVAL RESEARCH LAB
ATTN: LIBRARY CODE 5227
WASHINGTON, DC 20375-5320

INSTITUT FUR MEERESKUNDE
UNIVERSITAT HAMBURG
HEIMHUDERSTRASSE 71
2000 HAMBURG 13
GERMANY

DIRECTOR
NOCD
E-OC23 NOAA
WASHINGTON, DC 20235

DIANA MCQUESTION (3)
SCIENCE AND TECH. CORP.
101 RESEARCH DR.
HAMPTON, VA 23666-1340

CENTRO NAZIONALE DE
METEORO
E. CLIMATOLOGIA AERONAUTICA
PIAZZALE DEGLI ARCHIVI 34
00144 ROMA, ITALY

LCDR MARIO RUNCO
JOHNSON SPACE CENTER
NASA CODE CB
HOUSTON, TX 77058

FAIRWEATHER FORECASTING
ATTN: SUE ATWATER
715 L STREET NUMBER ONE
ANCHORAGE, AK 99501

USFETAC TS20
SCOTT AFB, IL 62225

BELGIAN AIR STAFF
VSD CTL MET.
EVERESTAAT 1
1140 BRUSSELS, BELGIUM

DEFENSE LOGISTIC STUDIES
INFORMATION EXCHANGE
ARMY LOGISTICS MAN. CEN.
FORT LEE, VA 23801

METEOROLGIE NATIONALE SMN
DOCUMENTATION
2 AVENUE RAPP
75340 PARIS CEDEX 07, FRANCE

NAVAL RESEARCH LAB.
CODE 7035.3
JCSSC, MS 39529-5004

DEPT. OF METEOROLOGY
UNIV. OF READING
2 EARLYGATE WHITEKNIGHTS
READING RG6 2AU, ENGLAND

DIRECTION DE LA METEOROLOG
ATTN: J. DETTWILLER MN RE
77 RUE DE SEVRES
92106 BOULOGNE BILLANCOURT
CEDEX FRANCE

DIRECTOR ENVIR. & LIFE SCI.
UNDER SECDEF E&LS
RM. 3D129 PENTAGON
WASHINGTON, DC 20301

COMMANDING OFFICER
NAVAL RESEARCH LAB.
ATTN: CODE 1221
WASHINGTON DC 20375-5320

☆ U.S. Government Printing Office: Jacket No. 786-009